Understanding host and environmental factors in the immunology and epidemiology of chytridiomycosis in anuran populations in Australia

Thesis submitted by

Laura Frances GROGAN

BVSc (Hons) Uni Syd, BSc(Vet) (Hons) Uni Syd

November 2014

for the degree of

Doctor of Philosophy

in the School of Public Health, Tropical Medicine and Rehabilitation Sciences

James Cook University

STATEMENT ON THE CONTRIBUTION OF OTHERS

My research was funded by three main sources including the Morris Animal Foundation's Wildlife grants program (MAF), the United States Fish and Wildlife Service's Wildlife Without Borders program (USFWS-WWB) and the International Union for the Conservation of Nature's Amphibian Specialist Group Seed Grants program (IUCN/ASG-seed grant). I was also awarded an Australian Postgraduate Award and a one-year Australian Research Council (ARC) linkage grant funded "PhD Scholarship".

Some of this research required use of facilities/equipment external to my organizational unit within James Cook University, as well as collaboration and consultation with colleagues at James Cook University and other institutions within Australia and overseas. The Molecular Ecology and Evolution Laboratory (MEEL) at James Cook University, Townsville campus, provided facilities and in-kind support for my RNA extractions work. Taronga Conservation Society provided facilities and extensive in-kind support for animal husbandry and exposure experiments. QIMR Berghofer Medical Research Institute provided facilities and in-kind support through my collaborator, Dr. Jason Mulvenna.

My supervisors, Drs. Lee Skerratt, Lee Berger, Rick Speare, Scott Cashins and Erica Rosenblum gave advice throughout the project on research methodology, interpretation of results and manuscript and thesis preparation. Below I have summarised the specific scientific and intellectual contributions of other individuals to each chapter of the thesis.

CHAPTER 3

PAPER 1: Phillott, A. D., **Grogan, L. F.**, Cashins, S. D., McDonald, K. R., Berger, L., Skerratt, L. F. (2013) Chytridiomycosis and seasonal mortality of tropical stream-associated frogs 15 years after introduction of *Batrachochytrium dendrobatidis*. Conservation Biology 27:1058-1068.

This published peer-reviewed paper represents original research led by Andrea Phillott, who performed the majority of field work collecting data and swabs, assisted by the field experience of Keith McDonald and the research planning of Lee Skerratt. My role in the paper involved performing all data analysis, results interpretation and manuscript write-up. Andrea Phillott, Scott Cashins, Lee Berger and Lee Skerratt provided substantial editorial input.

PAPER 2: Grogan, L. F., Phillott, A. D., Scheele, B. C., Berger, L., Cashins, S. D., Bell, S. C., Puschendorf, R., Skerratt, L. F. (in prep) Parasite aggregation and its implications for the microparasitic disease, endemic chytridiomycosis.

This manuscript in preparation represents my original data analysis, results interpretation and manuscript write-up based on an alternative, more complex analysis with a different focus, from the data reported in Phillott et al (2013). As such, similarly to the previous paper, the data was collected by Andrea Phillott. Andrea Phillott, Ben Scheele, Lee Berger, Scott Cashins, Sara Bell, Robert Puschendorf and Lee Skerratt provided substantial editorial input.

CHAPTER 4

PAPER 1: Cashins, S. D., **Grogan, L. F.**, McFadden, M., Hunter, D., Harlow, P. S., Berger, L., Skerratt, L. F. (2013) Prior infection does not improve survival against the amphibian disease chytridiomycosis. PLOS One 8:e56747.

This published peer-reviewed paper represents original research led by Scott Cashins, the primary investigator. My role in the paper included assistance with design and conduct of the experiment, animal husbandry, data collection and editorial input.

CHAPTER 5

PAPER 1: Cashins, S. D., **Grogan, L. F.**, McFadden, M., Hunter, D., Harlow, P. S., Berger, L., Skerratt, L. F. (in prep) Alpine tree frogs have variable innate immunity against chytridiomycosis with potential evolution of disease resistance.

This manuscript (prepared originally as a stand-alone manuscript, but later incorporated in part into a larger extended manuscript for publication) represents original research led by Scott Cashins, who performed the initial pilot study, contributed to preparations and the first few weeks of the experiment proper, and part of the data analysis. My role in the manuscript involved assistance with experimental study design, performing the majority of animal husbandry work, conducting the experiment, collecting data, writing the methodology section of the initial manuscript draft and performing part of the data analysis, as well as substantial input into results interpretation, and editorial input. Michael McFadden, Dave Hunter and Peter Harlow assisted with field components and on-site logistical arrangements. Lee Skerratt and Lee Berger provided substantial assistance with experimental design and wrote parts of the initial manuscript draft, and all co-authors provided substantial editorial input.

PAPER 2: Grogan, L. F., Cashins, S. D., Berger, L., Skerratt, L. F., Mulvenna, J. P. (in prep) Evolution of resistance to chytridiomycosis is associated with a robust early immune response in a wild amphibian.

This manuscript in preparation represents my original study design, conduct, sample collection and processing, data organisation, data analysis, results interpretation and manuscript write-up. Lee Skerratt, Lee Berger and Scott Cashins provided substantial assistance with experimental design. Scott Cashins assisted with conduct of the exposure experiment and sample collection. Jason Mulvenna provided substantial assistance and guidance with data organisation and analysis, and all co-authors provided editorial input.

PAPER 3: Grogan, L. F., Berger, L., Skerratt, L. F., Cashins, S. D., Trengove, R. D., Gummer, J. P. A. (in prep) Using a non-targeted metabolomics approach to investigate amphibian host responses to chytridiomycosis.

This manuscript in preparation represents my original study design, conduct, sample collection, data analysis, results interpretation and write-up. Joel Gummer performed metabolite extractions, gas chromatography-mass spectrometry (GC-MS) and data clean-up, as well as providing assistance with data analysis. Lee Berger, Lee Skerratt and Scott Cashins provided assistance with experimental design. Scott Cashins assisted with conduct of the exposure experiment and sample collection. All co-authors provided substantial editorial input.

CHAPTER 6

PAPER 1: Scheele, B. C., Hunter, D. A., **Grogan, L. F.**, Berger, L., Kolby, J., McFadden, M., Marantelli, G., Skerratt, L. F., Driscoll, D. A. (2014) Interventions for reducing extinction risk in chytridiomycosis-threatened amphibians. Conservation Biology 28(5):1195-1205.

This published peer-reviewed paper represents original review, synthesis and writing led by Ben Scheele, the primary investigator. My role in the paper included substantial assistance with the conceptual design, construction of figures and editorial input.

PAPER 2: Grogan, L. F., Berger, L., Rose, K., Grillo, V., Cashins, S. D., Skerratt, L. F. (2014) Surveillance for emerging biodiversity diseases of wildlife. PLOS Pathogens 10(5):e1004015.

This published peer-reviewed paper represents my original review, synthesis and writing. Lee Berger, Karrie Rose, Victoria Grillo, Scott Cashins and Lee Skerratt provided substantial editorial input.

APPENDIX I

PAPER 1: Bataille, A., Cashins, S. D., **Grogan, L. F.**, Skerratt, L. F., Hunter, D., McFadden, M., Scheele, B., Brannelly, L. A., Macris, A., Harlow, P. S., Bell, S., Berger, L., Waldman, B. (submitted) Susceptibility of amphibians to chytridiomycosis is associated with MHC class II conformation.

This manuscript submitted to the journal Proceedings of the National Academy of Sciences journal, represents original research led by Arnaud Bataille, the primary investigator. My role in the manuscript involved collection and shipping of tissue samples from the frog exposure experiment (in which I was involved in assisting with experimental study design, I performed the majority of animal husbandry work, conducted the experiment proper, collected data, and wrote up the experimental methodology), and I also contributed substantial editorial input to this manuscript.

STATEMENT OF ACCESS

I, the undersigned, the author of this thesis, understand that the James Cook University will make it available for use within the University Library and, by microfilm or other photographic means, allow access to users in other approved libraries. All users consulting this thesis will have to sign the following statement:

> *In consulting this thesis I agree not to copy or closely paraphrase it in whole or in part without the written consent of the author; and to make proper written acknowledgement for any assistance which I have obtained from it.*

Beyond this, I do not wish to place any restriction on access to this thesis.

Signature: Date: 26th November 2014

STATEMENT OF SOURCES DECLARATION

I declare that this thesis is my own work and has not been submitted in any form for another degree or diploma at any university or other institution of tertiary education. Information derived from the published or unpublished work of others has been acknowledged in the text and a list of references is given.

Every reasonable effort has been made to gain permission and acknowledge the owners of copyright material. I would be pleased to hear from any copyright owner who has been omitted or incorrectly acknowledged.

Signature: Date: 26th November 2014

DECLARATION ON ETHICS

The research presented and reported in this thesis was conducted in compliance with the National Health and Medical Research Council (NHMRC) Australian Code of Practice for the Care and Use of Animals for Scientific Purposes, 7th Edition, 2004 and the Qld Animal Care and Protection Act, 2001.

The proposed research study received animal ethics approval from the JCU Animal Ethics Committee:

Approval Number: A1589

Signature:

Date: 26 November 2014

ACKNOWLEDGMENTS

I am deeply appreciative of my supervisors Lee Skerratt and Lee Berger for their continued guidance, assistance, patience, support and enthusiasm for my project, especially through the many hurdles, delays and challenges I faced along the way. Lee Skerratt taught me optimism and resilience in the face of adversity. Lee Berger was an exceptional mentor and particularly helped develop my writing skills. I would like to thank co-supervisor Scott Cashins for his extensive guidance with amphibian captive husbandry and practical chytridiomycosis experimental methods. I would also like to thank associate supervisors Rick Speare and Erica Rosenblum for support and advice at the outset. Stephen Garland and Andrea Phillott also provided considerable mentorship when I was finding my feet. I am especially appreciative of the extensive assistance provided by Jason Mulvenna, who guided me with the transcriptomics part of the project, and Joel Gummer for his extensive assistance with the metabolomics side of the project - their experience has been invaluable.

I am very thankful to Taronga Conservation Society (Taronga Zoo) staff and volunteers for their extensive assistance with the logistical components of the exposure experiment aspects of the project, as well as for their guidance and support with the animal husbandry. In particular I'd like to thank Mike McFadden for his endless enthusiasm and passion; Pete Harlow for facilitating the project, for his encouragement and sense of humour; Bec Spindler for our helpful discussions; and Jo Wiszniewski for keeping us on track with the paperwork. Thanks also to Bree Keraunos and Laura Powe for being wonderful assistants with animal husbandry and swabbing. I'm also deeply indebted to Dave Hunter for always going above and beyond to support our work, including long trips to Kosciuszko National Park for field work. Thanks also to Tiggy Grillo and Karrie Rose for support and helpful discussions on the state of wildlife disease surveillance.

I would like to extend my thanks to members of the JCU One Health Research Group who provided support, collaborative assistance and friendship throughout the PhD - especially Ben Scheele, Sara Bell, Andrea Phillott, Laura Brannelly, Alex Roberts, Rebecca Webb, Gerardo Martin, Diana Mendez, Felicity Smout, Jenny Laycock, Jonathan Kolby, Robert Puschendorf and Tori Llewelyn. I am greatly appreciative of the assistance, support and friendship provided me by members of Jason Mulvenna's laboratory group during my stay at QIMR Berghofer working on proteomics and transcriptomics, especially including Jeremy Potriquet, Sidney Jia, Jarinya Khoontawad, Ponlapat Yonglitthipagon, Dhirendra Kumar, Chaad Laohaviroj, Dalia Ponce and Poojithaa Padmanaban. I am very thankful for the assistance and support of several

members of the MEEL lab at JCU while I performed RNA extractions, especially including Heather Veilleux, Roger Huerlimann and lab managers Georgia McDougall and Carolyn Smith-Keune. I also owe special thanks to Kyall Zenger for assisting me initially with planning aspects for my gene expression study. Many thanks to the administrative staff at JCU Townsville SPHTMRS, in particular Ari Gardener for assisting me with whatever needed doing, and also Michelle Moline, Sandra Burrows and Merrilee Forest. My thanks also extend to members of the Griffith Wildlife Disease Ecology Group who invited me into their midst and helped me see the PhD through to the end - especially Alison Peel, Hamish McCallum and Douglas Kerlin.

Many friends have helped me along the way, too many to name - I would however especially like to mention Marie Magnussen for her continued support and mentorship, and Ben Scheele for being an amazing sounding board for ideas. Thanks to Laura Brannelly for teaching me the true meaning of perseverance, and thanks to Sara Bell for her keen very practical outlook on life. Thank you also to Betsy Roznik for teaching me that chocolate solves all problems!

Last but definitely not least, I am vastly indebted to my amazing family who have inspired and supported me throughout my life, and for their never-ending patience with my ups and downs. I am also deeply thankful to my partner Pete for always being there for me.

DEDICATION

I wish to dedicate this thesis with love to my wonderful family,
especially my darling parents, Jenny and Joe Grogan.

You have always been there through every joyful moment to congratulate me in my successes.
And through every trial and tribulation you have been there with clear-sighted perspective,
ready encouragement, patience and enthusiasm.

You have constantly inspired me to dream, and taught me to never give up.

This thesis would not have been possible without you.

Thank you!

ABSTRACT

Emerging infectious diseases (EIDs) affecting biodiversity (hereafter 'biodiversity diseases') have tremendous and increasing social, environmental, economic and political impacts worldwide. The devastating amphibian skin disease, chytridiomycosis, caused by the fungus, *Batrachochytrium dendrobatidis* (hereafter Bd), is an example of such a disease, and has been an important driver of species declines and extinctions since its recent emergence. Bd is now considered endemic throughout most of its climatically suitable range. However this does not imply that the disease is now benign.

The aims of my research were to 1) investigate and characterize population- and individual-level impacts of endemic chytridiomycosis, 2) investigate the amphibian host immune response to Bd infection to determine the practical utility of immunization, and investigate the potential for evolution of resistance, and 3) evaluate strategies to mitigate endemic chytridiomycosis and minimize the impact of future emerging biodiversity diseases.

I performed Cormack-Jolly-Seber and Pradel analysis of an intensive two-year mark-recapture data set from two populations of the common mistfrog (*Litoria rheocola*) in the lowland wet tropics of Queensland, Australia. I found that endemic chytridiomycosis continues to have substantial seasonally fluctuating population-level effects on amphibian survival which necessitates increased recruitment for population persistence. Populations at both sites exhibited very low annual survival probabilities but high recruitment. My results suggest that similarly endemically infected amphibian populations may thus be under continued threat from chytridiomycosis, which may render them vulnerable to other threatening processes, particularly those affecting recruitment success.

Multistate Mark Recapture analysis of *L. rheocola* from the Tully population, and examination of abundance, distribution and transmission of Bd between hosts, allowed me to identify and characterize pathogen aggregation as a key feature of endemic chytridiomycosis, and evaluate its implications for study, modeling and management of the disease. Examination of transition probabilities revealed that more infections occurred in cooler months, that recoveries were frequent throughout the year, and that survival probabilities were dependent on infection intensity. In order to account for the effects of over-dispersed pathogen distributions in future studies, I recommend the quantification of individual infection burdens as well as prevalence where possible.

I performed a controlled exposure experiment of individually-housed captive-bred Bd-naïve Booroolong's frogs (*Litoria booroolongensis*) involving prior exposure and treatment with the antifungal itraconazole as a form of immunization. I compared survival and infection intensities between immunized and infection-naïve frogs, and was unable to demonstrate differences indicative of clinically protective host adaptive immunity. My results are consistent with other studies suggesting Bd-induced suppression of the host adaptive immune system, and indicate that immunization for reintroduced frogs is unlikely to be an effective management strategy in the near future.

I performed a second controlled exposure experiment instead with alpine tree frogs (*Litoria verreauxii alpina*) from multiple populations with differing long-term Bd-exposure histories. I demonstrated population, clutch and individual-level differences in susceptibility to chytridiomycosis (measured as survival and infection intensities). I found that frogs from one long-exposed population survived significantly longer when compared with frogs from two other long-exposed populations and the naïve population. My results demonstrate differences in survival and infection dynamics between populations and clutches associated with infection exposure history that are consistent with selection for disease resistance. Features of the natural history of this species, such as lack of Bd-exposure and high survival until after breeding at two years of age, may limit opportunities for natural selection of disease resistance. My finding of a more resistant population, however, holds promise for the future management of species threatened by chytridiomycosis.

I analysed skin, liver and spleen tissue samples from a subset of the frogs from this latter experiment using a systems biology approach in order to examine underlying mechanisms contributing to observed differences in population susceptibility to chytridiomycosis. Via total RNA extraction, next-generation sequencing, *de novo* transcriptome assembly, functional annotation and differential gene expression analysis, I found marked evidence for activation of gene pathways associated with immune responses in Bd-infected frogs, that differed among populations and times of sampling post exposure. I demonstrated a link between a chytridiomycosis-resistant phenotype from a long-exposed population, and evidence for a more robust early immune response at the level of gene expression compared with other populations. These differences in gene expression may putatively explain a large component of population-level differences observed in survival in the larger experiment.

In addition to gene expression analysis, via metabolite extraction, gas chromatography-mass spectrometry, and both univariate and multivariate analyses, I identified a number of key metabolites in the skin and liver tissues that predominantly differentiate moribund frogs with

chytridiomycosis from both unexposed control and subclinical frogs. I also identified metabolites related to differences in population of origin, which may be associated with variation in phenotypic resistance between populations. These findings help build our understanding of the key mechanisms and pathways involved in pathogenesis.

In a review of current and upcoming techniques, I contributed substantially to developing a conceptual framework for management of endemic chytridiomycosis. This framework consisted of interventions to guide experimental management and applied research, and involved two main approaches, 1) reducing Bd in the environment or on amphibians, and 2) increasing the capacity of populations to persist despite increased mortality from disease. In this review I recommended trialling several promising management actions including habitat manipulation, antifungal treatments, animal translocation, bioaugmentation, head starting and selection for resistance.

Finally, to help improve timely mitigation of future emerging biodiversity diseases, I reviewed and evaluated the efficacy of current surveillance approaches for these diseases. Barriers to effective surveillance include a relative lack of social and political will, and the inherent complexity and cost of implementing surveillance for multiple and diverse free-ranging populations. I synthesized recommendations to address these challenges by 1) extending global animal disease surveillance systems to emphasize diseases that could predominantly affect biodiversity, and 2) utilizing a systematic, population-based and self-evaluative approach to improve timely disease recognition and management, with the aim of reducing species loss.

In summary, I found that endemic chytridiomycosis impacts amphibian population dynamics in Australia and is characterized by high mortality rate and turnover. I found that immunization is currently an ineffective strategy. However, from clinical and systems biology data, the evolution of innate immunity is possible and hence assisted selection may be a viable management strategy among other approaches.

TABLE OF CONTENTS

CHAPTER 6: Managing wildlife disease

CHAPTER 7: Conclusions and recommendations

LIST OF APPENDICES

APPENDIX D: Additional results for MSMR modeling

APPENDIX E: Capture-Mark-Recapture methodological review

APPENDIX F: Lva clinical manuscript supporting information

APPENDIX G: Transcriptomics manuscript supporting information

APPENDIX H: Metabolomics manuscript supporting information

APPENDIX I: Major Histocompatibility Complex (MHC) study

LIST OF TABLES

LIST OF FIGURES

CHAPTER 1: Scope of the thesis

1.1 Objectives and context for the research

The broad objectives of my research were to 1) investigate and characterize population- and individual-level impacts of endemic chytridiomycosis, 2) investigate the amphibian host immune response to *Batrachochytrium dendrobatidis* (Bd) infection to determine the feasibility of immunization, and investigate the potential for evolution of resistance, and 3) evaluate strategies to mitigate endemic chytridiomycosis and minimize the impact of future emerging biodiversity diseases.

My research was largely driven by concerns for amphibian biodiversity conservation in the face of unprecedented disease-associated declines and extinctions that have occurred across the globe in recent years, predominantly due to the fungal skin disease, chytridiomycosis.

Many factors, including globalization and the industrial revolution, have led to increasing emergence of infectious diseases in humans and domestic animals, with the majority of those receiving attention constituting zoonoses that have spilled over from wildlife hosts. Although the subject of much less attention, infectious diseases have similarly been emerging in wildlife species. These diseases sometimes have the potential to extirpate populations with severe consequences for biodiversity, however their potential impact was for a long time overlooked.

In the last decade and a half, the devastating implications of emerging wildlife diseases have become overtly apparent. In the most extreme example, research has revealed the unparalleled loss of amphibian populations and species due to anthropogenically mediated spread of the pathogen *Batrachochytrium dendrobatidis* (hereafter Bd), aetiological agent of chytridiomycosis.

Research in the field of amphibian diseases has since greatly expanded, however unfortunately, mitigation attempts have been unable to contain the spread of the pathogen Bd. Chytridiomycosis is now considered endemic in most climatically suitable regions and host-appropriate amphibian species around the world including the majority of Australia (with a few select areas still remaining naïve including the World Heritage Area in Tasmania, and the island of Madagascar).

With pathogen endemism, the contextual background for amphibian disease research has necessarily changed in recent years, with a shift in focus from preventing spread to attempting to maintain and assist wild populations that have been or continue to be affected by disease. The goal now is longer-term population persistence of threatened amphibians.

Broader research priorities thus currently involve 1) establishing the ongoing impact of chytridiomycosis within Australia and around the globe in endemically infected populations, and 2) identifying strategies for mitigating the impact of the disease on threatened populations.

My research project was designed to address these priorities. I firstly set out to retrospectively investigate the impact of chytridiomycosis on endemically infected populations of the common mist frog (*Litoria rheocola*) in the wet tropics of Australia, from mark-recapture encounter data collected by a colleague some years earlier. I also analysed these data to better understand and characterize the dynamics of infection and disease within endemically infected populations.

Secondly, given the priority for longer-term solutions to the disease problem (to potentiate the successful repatriation of captive colonies, and long-term wild population persistence), I focused on investigating the host immune response to infection and disease. I aimed to identify the potential for two main management techniques involving the host response, 1) immunization of booroolong's frogs (*Litoria booroolongensis*) (harnessing the adaptive immune system within the life of an individual, akin to vaccination), and 2) assisted selection for disease resistance (harnessing heritable resistance mechanisms of the innate immune system). This latter focus required first establishing the mechanisms by which evolved disease resistance may manifest, hence I investigated multiple populations of alpine tree frogs (*Litoria verreauxii alpina*) with varying long-term exposure histories to Bd infection.

Finally, I aimed to place this work in the broader context of wildlife disease management and mitigation strategies by 1) establishing a framework for interventions for chytridiomycosis-threatened amphibians, and 2) highlighting the issue of surveillance for diseases affecting biodiversity, in order to raise awareness and promote policies that assist in the early recognition of emerging disease threats.

1.2 Development of the research

My original research intention was to use gene expression microarrays and a systems biology approach to investigate and characterise both adaptive and innate immune mechanisms underlying the amphibian host response to chytridiomycosis infection. My research grew as an extension to a newly developed collaboration between JCU researchers, amphibian biologists

from Taronga Conservation Society Sydney, and the Department of Environment, New South Wales State Government. This collaboration was established under the Australian Biosecurity Cooperative Research Council grant scheme to answer specific questions related to managing amphibian chytridiomycosis via targeting the host immune response, including firstly, 'Does prior exposure to Bd and treatment of chytridiomycosis render subsequent disease resistance in individual adult amphibians?', and secondly, 'Is there evidence for the evolution of disease resistance in long-exposed populations of amphibians, suggesting the potential for assisted selection techniques?'. I came on board with the collaboration early during the experimental design and planning phase of this research. I was aiming to obtain experimental samples from the two large clinical experiments (projects being led by a JCU Postdoctoral Research Fellow) that might then be compared using a variety of techniques to identify underlying molecular mechanisms and correlate these with clinical outcomes between the various treatment groups.

Due to unfortunate logistical difficulties, the associated large clinical experiments were delayed in their initial progress. During this time I was involved in grant-writing to obtain funding for the wet-lab analytical parts of my project (RNA sequencing, protein and metabolite extraction and mass spectrometry analysis), and I started writing a review involving synthesizing a systematic framework for surveillance for diseases affecting biodiversity. During this time I also assumed responsibility for an additional data modeling project involving mark-recapture analysis, manuscript write-up and publication. This latter project expanded to become a major component of my research. The raw data were sourced from a colleague, Dr. Andrea Phillott, at that time finishing up her post-doctoral term at JCU. The data consisted of an intensive two-year mark-recapture field study on four species of frogs (although the majority of data related to a single species, the common mist frog) that were captured, marked, measured and swabbed (for Bd infection intensity and status) from two study sites in the wet tropics of Australia in order to investigate environmental factors influencing chytridiomycosis in the field. My analysis of this data provided a unique opportunity for me to investigate priority questions associated with the impact of chytridiomycosis on endemically infected amphibian populations, and the nature of the underlying disease dynamics. After cleaning the data set and performing initial exploratory analysis, I decided to employ Cormack-Jolly-Seber, Pradel and Multistate Mark Recapture modeling techniques. I analyzed and interpreted these results and independently wrote initial drafts for the two subsequent manuscripts.

I was closely involved from the start of the large clinical adaptive immunity experiment in Booroolong's frogs (*Litoria booroolongensis*), contributing substantially to all aspects of laboratory setup, animal husbandry, experimental exposures and data collection, as well as collecting tissue samples from my own subset of experimental animals for further mechanistic

analyses. Unfortunately, despite sufficient sampling power to detect a biological effect of ample magnitude, and an initially promising set of pilot results, the final survival and infection intensity results of this experiment did not suggest differences between previously immunized and naïve-exposed frog groups. As I was predominantly interested in understanding mechanisms contributing to observed clinical responses in the various treatment groups, obtaining clinical correlates was a crucial component of the utility of my tissue-based mechanistic analysis of host immune response, and it was therefore not worthwhile to progress further with the molecular and bioinformatics analysis of these tissue samples.

There were also unexpected delays in commencing the second large clinical experiment comparing disease responses of alpine tree frogs (*Litoria verreauxii alpina*) from populations with differing long-term exposure histories. This was due to complications in sourcing the animals that were originally intended to be wild-caught but captive-raised in an external facility. In order to facilitate the success of the project, and the collection of the necessary tissue samples for my mechanistic study, I was thus heavily involved in the day to day running of this project from laboratory setup, initial egg-mass collection, animal husbandry raising the tadpoles through metamorphosis to eight months post-metamorphosis, experimental setup, Bd exposure, and data collection. I also collected the tissue samples from my subset of animals for the mechanistic study, and was then required to assume total responsibility for conduct of and data collection from the large clinical experiment when the associated Principal Investigator left for a new position on a different project a few weeks after commencing the experiment proper. In this study I was also primarily responsible for collecting and shipping samples to a collaborator working on Major Histocompatibility Complex (MHC) analyses.

The collection of tissue samples from this second (innate immunity) experiment, with clinical results suggesting a difference between populations in survival, allowed me to progress with my mechanistic tissue analyses. These involved extracting total RNA and protein from liver, skin and spleen tissue samples, sending extracted RNA for next-generation sequencing at an external facility, and sending skin and liver tissue samples for metabolomics gas-chromatography mass-spectrometry analysis to a collaborator in Murdoch University. I also commenced wet-lab protocols to label and analyse protein expression in the various samples, however, difficulties with the protocol and mass-spectrometer led to this part of the project being delayed and thus excluded from the reported results in this thesis. Within the evolving field of transcriptomics, it became clear part-way through my research that RNA-seq rather than gene expression microarrays might yield results of higher sensitivity and utility, and thus I pursued sequencing RNA of adequate depth for the purpose of differential gene expression analyses. I formed a collaboration with a colleague at QIMR Berghofer Medical Research Institute to obtain

sufficient experiential support for the complex bioinformatics subsequently involved. I was then primarily responsible for the data analysis of both the transcriptomics and metabolomics work (involving data preparation, *de novo* transcriptome assembly, functional annotation, differential gene expression analysis, as well as univariate and multivariate statistical analyses), data interpretation and manuscript preparation from these results.

1.3 Significance of the research

This research project enabled a thorough analysis of an intensive mark-recapture field study to investigate the impacts of endemic chytridiomycosis at the population and individual levels. This led to recognition of the continued impact of chytridiomycosis on amphibian populations despite endemism, as well as an improved understanding of the role of pathogen aggregation in endemic chytridiomycosis, together with a better understanding of the occurrence of infection incidence and recovery.

The host immunity clinical exposure experiments and associated systems biology approach allowed me to establish the lack of feasibility of exposure and treatment as a form of 'vaccination' for chytridiomycosis in repatriated individuals, and led to an increased emphasis on alternative and longer-term goals for improving population persistence, in the form of considering selection for resistance to disease as a management strategy for select populations. The innate immunity experiment comparing populations and clutches revealed heritable components to the more disease resistant phenotype, likely associated with the evolution of resistance. The gene and metabolite expression work further elucidated the nature of these population and individual-level differences and immune mechanisms.

Evaluating and synthesizing conceptual frameworks for both chytridiomycosis management and biodiversity disease surveillance highlighted key gaps and strategies to approach these issues, and will benefit government departments, non-government organisations, community groups, researchers and the public.

Investigating endemic chytridiomycosis in several Bd-threatened species of amphibians from the wet tropics of north Queensland, to the Australian alps in NSW, Victoria and the ACT, as well as coastal stream environments in NSW, has improved our knowledge base regarding the impact, dynamics and host responses to endemic Bd infection both regionally and internationally.

1.4 Contribution of others to this thesis

My research involved a number of collaborations with colleagues at James Cook University and other institutions. In particular, the mark-recapture field data were collected by a colleague several years earlier, and I was granted permission to analyse, interpret and write-up the results of this study. Wet-lab analyses requiring specialized facilities and equipment, including qPCR, RNA-seq, and Gas Chromatography-Mass Spectrometry were performed by collaborators and external commercial facilities, and these are clearly identified in the thesis.

CHAPTER 2: General introduction and justification of aims

"The Living Planet Index (LPI), which measures trends in thousands of vertebrate species populations, shows a decline of 52 per cent between 1970 and 2010. In other words, vertebrate species populations across the globe are, on average, about half the size they were 40 years ago." *World Wildlife Fund, Living Planet Report, 2014; released 30th September, 2014*

2.1 Overview

This chapter provides contextual background for the research described in the ensuing thesis. It includes an up to date review of pertinent existing literature synthesizing the current state of knowledge in the field. Where appropriate I discuss motivating factors for the studies I performed, and refer to relevant sections of the thesis. However, I have also summarized concurrent and more recent research developments from the broader literature, particularly in the rapidly moving field of chytridiomycosis immunity. These additional findings are pertinent to an overall understanding of immune mechanisms and have shaped the development of my research projects as well as informing my interpretation of the results.

2.2 The biodiversity crisis and 'biodiversity diseases'

The term 'Anthropocene' has been used to describe our current geological epoch (Williams and Crutzen, 2013), lending credence to the immense global impact of humanity. Biodiversity loss is a crucial component of this impact, involving the extensive loss of faunal and floral species through extinctions, range contractions, and reductions in overall abundance as epitomized by the introductory quote above, from the recent Living Planet Report (World Wildlife Fund; Dirzo et al., 2014). Global concern over this issue has been prominent for many years - the most recent United Nations Convention on Biological Diversity called for "effective and urgent action to halt the loss of biodiversity" (cited in Normile, 2010). The extent of recent species loss relative to the fossil record has led to comparison with the five recognized mass extinction events that occurred in geological history (roughly the last 500 million years) - scientists are describing our current era as the beginning of the 'sixth mass extinction' (Barnosky et al., 2011).

Emerging infectious diseases have only recently been appreciated as proximate causes of species extinction and biodiversity loss (Scott, 1988). This may be due to the lack of a precedent, absence of baseline demographic data, difficulty separating signals of disease-associated population decline from stochastic noise, and difficulties observing signs of disease in free-ranging wildlife species (Wobeser, 2007). Passive community surveillance, the most

common means of disease detection in wildlife populations, predominantly detects indicator animals suffering highly visible morbidity or mortality from the infected portion of the population. It usually involves voluntary submission and reporting, and thus reporting bias (Stallknecht, 2007; Thulke et al., 2009).

Diseases affecting reproduction are intrinsically difficult to detect. Evidence that these diseases occur in wildlife populations was discussed in the seminal paper by Scott (1988). More recent examples include malaria in wild birds (Knowles et al., 2010), porcine reproductive and respiratory syndrome virus (PRRSV) in wild boars (Reiner et al., 2009), and bacterial infections in wild ungulates (Pioz et al., 2008). Furthermore, reproductive diseases, particularly tract infections inducing infertility, may selectively target portions of the population leading to biased effective sex ratios, which may itself lead to population decline (Dyson and Hurst, 2004; Polkinghorne et al., 2013).

Diseases causing morbidity and mortality may also be difficult to detect due to *disease factors* (short time-course of clinical disease, subtle nature of clinical signs), *host factors* (behavioural changes inhibiting detection, host-range affected by disease, species, size, taxonomic class, terrestrial vs aquatic, diurnal vs nocturnal, social vs solitary), *environmental factors* (predation of infected animals, scavenging post-mortem, carcass persistence), and finally *human-related factors* (proximity to human populations, socioeconomic status and human population size, motivation, nature and availability of pathology facilities, perceived socioeconomic impact, previously identified disease vs novel emerging disease, testing costs, and prevailing attitudes vs evidence based medicine; Merianos, 2007; Stallknecht, 2007).

In addition to difficulties observing disease, it was widely believed that disease dynamics were dominated by density-dependent transmission of infectious organisms (modeled by mass-action kinetics), which precludes host extinction by removing pathogen transmission at low host densities. This assumption completely overlooked the possibility of multiple-host, vector-borne or reservoir disease systems (de Castro and Bolker, 2005; Lafferty and Gerber, 2002). Despite this delay in acknowledgment of the potential impact of disease on wildlife populations, infectious wildlife diseases have been empirically proven capable of causing declines and extinctions in multiple instances with apparently increasing frequency (Cunningham and Daszak, 1998; Laurenson et al., 1998; Schloegel et al., 2006; Skerratt et al., 2007; Thorne and Williams, 1988; Williams et al., 2002). Through both direct species loss and an indirect cascade of trophic interactions involving co-extinctions, emerging infectious diseases are now recognized as an important contributor to global biodiversity loss (Aguirre and Tabor, 2008; Daszak, 2000; Maillard and Gonzalez, 2006; Smith et al., 2009a). Moreover, there is mounting

evidence that reduced biodiversity affects ecosystem functioning (Balvanera et al., 2006) and contributes to increased disease emergence (Chivian and Bernstein, 2008; Keesing et al., 2010).

In order to differentiate the importance of diseases predominantly affecting biodiversity, from zoonotic diseases that emerge or spillover from wildlife hosts but are mainly of interest due to their impact on human public health and agriculture (Jones et al., 2008), in this thesis (see Section 6.3; Grogan et al., 2014) I coin, define and exemplify the term 'biodiversity diseases' to encompass both the impact of concern and the host group affected. Thus a 'biodiversity disease' is 'a disease that has caused, or is predicted to cause, a decline in a wild species sufficient to worsen its conservation status'. This term is not intended to be specific either to an infectious aetiology nor wildlife species in general (among the Kingdoms Plantae and Animalia), however, in our current context, I will be focusing on one member of this subset of diseases.

2.3 Chytridiomycosis - a devastating biodiversity disease

Chytridiomycosis, a skin disease of amphibians, caused by infection with fungal pathogen *Batrachochytrium dendrobatidis* (hereafter Bd; Berger et al., 1998; Longcore et al., 1999), is an example of a disease that has caused declines and extinctions of wildlife species on an unprecedented scale. Chytridiomycosis has been described as being responsible for "the most spectacular loss of vertebrate biodiversity due to disease in recorded history" (Skerratt et al., 2007). Approximately 42% of amphibian species sampled have been found infected with the pathogen (Olson et al., 2013), and an estimated 202 species have suffered declines or extinctions due to the disease (Skerratt et al., 2007). Combining disease with other threats to amphibian biodiversity such as habitat loss, it has been suggested that not only are amphibians declining more rapidly than other vertebrate classes (Stuart et al., 2004), but that they may be leading the sixth mass extinction (Wake and Vredenburg, 2008).

Bd is thought to have emerged and been anthropogenically spread around the world through trade (Fisher and Garner, 2007; Karesh et al., 2005; Kriger and Hero, 2009; Picco and Collins, 2008; Schloegel et al., 2009), vectors, fomites and contaminated water (Garmyn et al., 2012; Johnson and Speare, 2005; Kilburn et al., 2011; McMahon et al., 2013a; Piotrowski et al., 2004; Symonds et al., 2008) in the last 30-50 years, from an unconfirmed origin (Farrer et al., 2011; Houlahan et al., 2000). Retrospective sampling of preserved amphibians and analysis of the fungal genome suggests Bd was present in Africa and Japan from as early as 1933 and 1902 respectively, with low prevalence suggesting regional endemnicity (Goka et al., 2009; Soto-Azat et al., 2010; Weldon et al., 2004).

In Australia, the earliest record of chytridiomycosis was from 1978, corresponding with regional amphibian declines and extinctions (Berger et al., 1998; Hines et al., 1999; Murray et al., 2010a; Speare, 2006). While there is difficulty in accurately classifying extinction status of species due to short observation windows (Connors et al., 2014; McKelvey et al., 2008), it is believed that at least six amphibian species were extirpated in Australia in association with the initial emergence of chytridiomycosis, including *Litoria nyakalensis* (nyakala frog), *Taudactylus acutirostris* (sharp-snouted torrent frog; Schloegel et al., 2006), *T. rheophilus* (tinkling frog), *T. diurnus* (Mt Glorious torrent frog), *Rheobatrachus silus* (southern gastric-brooding frog) and *R. vitellinus* (northern gastric-brooding frog) (pers. comm. D. Hunter and B. Scheele). Although the nature of any continuing impact of chytridiomycosis in Australia was unclear at the start of this research project, many remaining species have been found to occur at much lower densities and with smaller distributions than previously and there is now evidence that some populations continue to decline (Hunter et al., 2010; Vredenburg et al., 2010). A further seven Australian species have recently been identified as being most threatened by chytridiomycosis, including *Pseudophryne corroboree* (southern corroboree frog), *P. pengilleyi* (northern corroboree frog; Hunter et al., 2010), *Philoria frosti* (baw baw frog), *L. spenceri* (spotted tree frog), *L. lorica* (armoured mistfrog), *L. burrowsae* (Tasmanian tree frog; Zhang et al., 2014), and *T. pleione* (Kroombit tinker frog or Pleione's torrent frog) (pers. comm. D. Hunter and B. Scheele).

2.3.1 Chytridiomycosis endemism and pathogen virulence

Many studies investigating declining populations have recorded epidemic outbreaks of disease and mass mortality when the fungus first invaded an amphibian community assemblage (Lips, 1999; Woodhams et al., 2008b). Since Bd was first discovered and characterized in 1998 (Berger et al., 1998; Longcore et al., 1999), it has been recorded in wild amphibians from every continent except Antarctica (Berger et al., 1998; Bosch et al., 2001; Fisher et al., 2009b; Goka et al., 2009; Hanselmann et al., 2004; Lips et al., 2006; Olson et al., 2013; Schloegel et al., 2006; Weldon et al., 2004; Yang et al., 2009), and it is so ubiquitous it is now considered endemic in most climatically suitable regions around the world (Fisher et al., 2009b; Kinney et al., 2011; Murray et al., 2011a; Murray et al., 2009; Retallick and Miera, 2007). Endemism (where the basic reproductive number of the pathogen, R_0 is approximately equal to 1; Real and Biek, 2007; Stallknecht, 2007), does not, however, imply a benign state, absence of host morbidity/mortality, or stable host population dynamics, but instead suggests maintenance of the pathogen through time in a population without external inputs (Real and Biek, 2007).

There is a perceived trend in the research community towards belief in pathogen avirulence associated with host-pathogen co-evolution and endemism (Ewald, 2004). Virulence is a

complex, combinatorial, heritable and conserved trait (Odds et al., 2001; Ron, 2010; Steenbergen and Casadevall, 2003) of a pathogen in the context of its host and their shared environment, which describes the severity of disease or compromise within an infected host (Thomas and Elkinton, 2004). Conventional wisdom until the 1980s favoured pathogen progression from transitory maladaption expressing high virulence during emergence in new hosts to avirulence and equilibrium (Ewald, 2004). The most widely theorized current hypothesis is that of virulence-transmission trade-off, favouring intermediate virulence through the interplay of pathogen replication and transmissibility (Alizon et al., 2009).

Two further models are described by Adiba et al. (2010) to include within-host selection and coincidental evolution. While these hypotheses are not necessarily mutually exclusive and attempts have been made to conjoin them (Alizon et al., 2009), there is as yet no overarching model with conclusive empirical support (Brunner and Collins, 2009). Choisy and de Roode (2010) describe one possible reason for the lack of empirical support to be the mismatching of single-generational empirical studies with theoretical analyses which tend to investigate multi-generational stabilizing equilibria. In the absence of widespread empirical support for pathogen avirulence with endemism (Brunner and Collins, 2009), it is unclear whether the many populations infected with endemic Bd are still being threatened by chytridiomycosis, decades post emergence (despite research speculation; Retallick et al., 2004), nor what the nature of any continuing impact might be. Section 3.2 of this thesis examines this question in the context of two endemically Bd-infected populations of a stream-associated frog (*Litoria rheocola*) in the wet tropics of Queensland, Australia.

2.3.2 Overview of chytridiomycosis - host, pathogen, environment, pathogenesis, diagnosis and treatment

When considered at the level of the individual host, chytridiomycosis conforms well to the classic epidemiologic triad model of infectious disease, based on interactions between the host, pathogen, and a conducive environment (see Figure 2.1; Engering et al., 2013). Although the global panzootic lineage of Bd (BdGPL) is considered highly virulent, in the absence of a susceptible host and suitable environment it fails to produce disease (Farrer et al., 2011). Many host, pathogen, and environmental factors (or component causes) have been found to be associated with the degree of severity of resulting Bd infection and chytridiomycosis disease. These factors will be discussed in more detail below.

Figure 2.1. The host-pathogen-environment epidemiologic triad model applied to chytridiomycosis, highlighting factors found to be important for manifestation of disease.

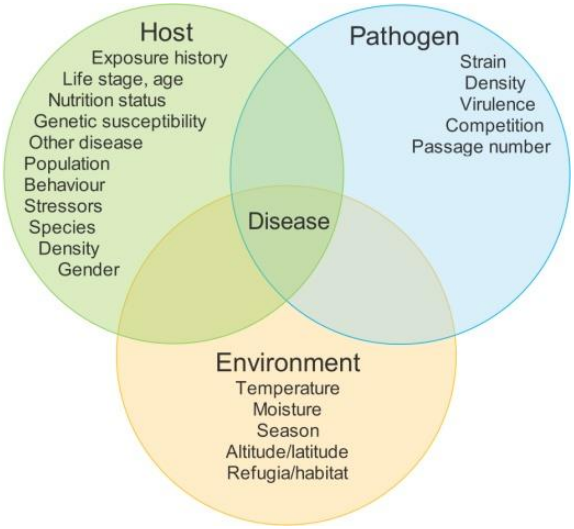

2.3.2.1 Host factors

Considerable variation in susceptibility to chytridiomycosis has been observed between hosts at the individual, population and species levels, indicating the importance of both genetic and phenotypic factors in the development of disease (Blaustein et al., 2005; Pilliod et al., 2010; Searle et al., 2011; Tobler and Schmidt, 2010). At the broad scale, population declines appear strongly linked to species' distribution and habitat use. Declines have been particularly severe among tropical high-altitude, stream-associated anurans, although in many cases of field observation, susceptibility and population declines are likely associated with environmental suitability for the fungus than necessarily indicating variations in host-specific factors between species (Fisher et al., 2009b; Lips et al., 2006). Even amongst syntopic species, however, habitat use may differ which may explain some degree of variation in perceived susceptibility to chytridiomycosis (Rowley and Alford, 2007b).

The *Atelopus* genus of Neotropical toads from Central and South America appears to have been most severely affected (La Marca et al., 2005), although Bd-associated declines and extinctions have been recorded in numerous other amphibian taxa, particularly other anurans (Fisher et al., 2009b). Recent evidence suggests many salamanders may also have been significantly affected (Cheng et al., 2011; Rovito et al., 2009). There are several host species that are predominantly resistant to or tolerant of infection and may serve as reservoirs or carriers of infection. These species may have been responsible for the widespread dissemination of the fungus and include for example *Pseudacris regilla*, *Rana catesbeiana*, *R. pipiens*, *Xenopus laevis*, *Eleutherodactylus coqui*, *Litoria lesueuri complex*, *Litoria ewingii* and *Crinia signifera* (Beard

and O'Neill, 2005; Obendorf, 2005; Reeder et al., 2012; Retallick et al., 2004; Ricardo, 2006; Schloegel et al., 2010; Weldon et al., 2004).

Intrinsic host factors associated with signalment (life-stage, age and larval body size) have been found to differentiate susceptibility to chytridiomycosis between individuals in laboratory experiments and field observations. Despite interspecific variation, metamorphosis from larval to adult form and the immediate post-metamorphic phase appear to be the most susceptible periods (Berger et al., 1998; Lamirande and Nichols, 2002). Infections are limited to the keratinized mouthparts of larval anurans, and are typically not fatal during this stage (Berger et al., 1998; Fellers et al., 2001; Pessier et al., 1999; Rachowicz and Vredenburg, 2004), however the tadpoles of some species may suffer significant mortality (Blaustein et al., 2005). Prevalence and intensity has been found to increase with larval development (Smith et al., 2007), and any infected tadpoles may provide a potential fungal reservoir for metamorphosing frogs (Rachowicz and Vredenburg, 2004). There is little evidence from experimental infections to suggest an intrinsic difference between sexes in susceptibility to chytridiomycosis, suggesting that any observed variation from field studies may be more likely associated with extrinsic factors such as differences in behaviour, and hence fungal exposure or infection development (Johnson and Hoverman, 2014). Other putative intrinsic determinants of susceptibility may include previous exposure history, concurrent infection, nutritional level, and the presence of stressors (Kindermann et al., 2012; Murphy et al., 2011; S. Young, unpublished). Variations in susceptibility due to immune mechanisms are reasonably well characterized and will be discussed in more detail later in Section 2.6.

Behaviour that increases exposure to the pathogen may constitute an important extrinsic host factor contributing to variation in susceptibility. This may be through rates and types of host contact with conspecifics, contaminated water and environmental substrates containing Bd (Rowley and Alford, 2007a). Importantly, however, other general movement patterns, including thermoregulatory behaviours such as basking, and the use of retreat sites, may also play a role by altering existing infection intensities or pathogen growth rates due to the optimal thermal range of the fungus (Daskin et al., 2011; Puschendorf et al., 2011; Richards-Zawacki, 2010; Rowley et al., 2007). Behaviour may differ particularly between life-stages due to aquatic versus terrestrial or arboreal habitats, as well as between male and female adults due to their seasonal utilisation of different environments for reproduction (Duellman and Trueb, 1994). Other autecologic factors may include the density of individuals within the population (higher densities may increase environmental zoospore load; Hudson and Dobson, 1998), the age-structure of the population (where tadpoles may act as reservoir hosts, or dispersal patterns and

habitat use differ between stages; Rachowicz and Vredenburg, 2004), and the presence of and interactions with any syntopic species and vectors (Reeder et al., 2012; Rivas, 1964).

2.3.2.2 Pathogen features

Batrachochytrium dendrobatidis (Bd), first characterized in 1999 (Longcore et al., 1999), is one of only two known species of the fungal genus *Batrachochytrium* (the other, *B. salamandrivorans*, was only recently described and also causes syndromic chytridiomycosis; Martel et al., 2013). Bd is also one of the only species of the predominantly saprophytic *Chytridiomycota* that is known to parasitize vertebrates (Fisher et al., 2009b). Bd has two lifecycle stages, including the aquatic, motile, free-living, flagellated zoospore (2-4 µm diameter), and the asexually reproductive zoosporangium stage (7-15 µm; Berger et al., 2005a; Longcore et al., 1999; Pessier et al., 1999). The infectious zoospore has been described to respond to nutritional cues, chemotaxing with the use of the flagellum towards suitable substrates including amphibian skin, and away from antifungal metabolites (Lam et al., 2011; Moss et al., 2008). Upon encystment on the amphibian keratinized epithelial surface (Berger et al., 2005a), a germ tube is extended through multiple host cell layers to the epidermal stratum granulosum (Greenspan et al., 2012; Van Rooij et al., 2012), and the germling contents are transferred inside a host cell, where a thallus produces the subsequent zoosporangium intracellularly (Berger et al., 2005a). As the epidermal cells mature and differentiate, migrating towards the stratum corneum, the sporangium anchors inside the host cell via rhizoids and clonally replicates, producing a discharge tube (typically directed to the skin surface) through which zoospores are then released (Berger et al., 2005a). In culture, the Bd lifecycle takes approximately 4-5 days at 22 °C (Berger et al., 2005a). Outside the host, zoospores are able to survive for up to three months in moist river sand, and 3-4 weeks in sterile water (Johnson and Speare, 2003; Johnson and Speare, 2005), although Bd is considered incapable of long-term saprobity (Briggs et al., 2010; Johnson and Speare, 2003; Lips et al., 2006).

Several pathogen-related factors are important to the development of chytridiomycosis, and these include strain or passage-history related virulence factors, and ecological factors unrelated to Bd strain. Pathogenicity combines both virulence and transmissibility, (Thomas and Elkinton, 2004 proposed that pathogenicity = virulence x infectivity), hence virulence itself is independent of the ability to transmit between or infect hosts. Bd virulence within equivalent hosts has been shown to differ with isolate (strain) and *in vitro* passage history (Berger et al., 2005b; Berger et al., 1999a; Fisher et al., 2009b; Retallick and Miera, 2007). These variations have been characterized in terms of genetic diversity between strains, proteomic profiles and phenotypic traits including strain fecundity and sporangial morphology (Farrer et al., 2011; Fisher et al., 2009a; Voyles, 2011). *In vitro* studies have identified inhibitory factors from Bd

culture supernatants that impair proliferation and induce apoptosis in lymphocytes (Fites et al., 2013), and work is currently underway to characterize these factors (A. Roberts, unpublished data). Non-strain-related characteristics may also be important in defining the disease outcome in amphibian hosts including initial and continuing exposure dose, and competition with other pathogens/microbes (Austin, 2000; Bustamante et al., 2010; Harris et al., 2006).

2.3.2.3 Environment factors

Field studies have identified a number of environmental factors typically associated with chytridiomycosis outbreaks, including tropical latitude, high altitude montane and temperate environments, and the winter season (Becker et al., 2012; Berger et al., 1998; Fisher et al., 2009b). Many of these factors operate through variations in two major mechanisms - the effects of temperature and moisture on pathogen growth. The degree of canopy closure, for instance, is likely to affect both temperature and moisture in the amphibian microenvironment (Becker et al., 2012), leading to variations in susceptibility of populations to disease. Ultraviolet light was not found to significantly affect the survival of Bd in culture (Johnson et al., 2003).

The thermal optimum for the fungus in culture has been identified as 17-25 °C at pH 6-7, although it is able to grow and reproduce at 4-25 °C, with growth ceasing above 28 °C and mortality over 30 °C (Johnson et al., 2003; Piotrowski et al., 2004; Woodhams et al., 2008a). As amphibians are ectotherms, these temperatures within the host due to climate, microhabitat and thermoregulatory behaviour have a similar effect on Bd growth, as has been demonstrated in several experimental and field studies (Andre et al., 2008; Berger et al., 2004; Bustamante et al., 2010; Forrest and Schlaepfer, 2011; Murphy et al., 2011; Rowley and Alford, 2013). Indeed, high temperatures have been used successfully as a treatment for infected amphibians (Chatfield and Richards-Zawacki, 2011; Geiger et al., 2011). Thermal variability has been linked with increased host susceptibility (Raffel et al., 2006), and lower temperatures have been shown to have a modulating effect on the host immune response (Andre et al., 2008; Ribas et al., 2009).

As chytrids are essentially aquatic organisms, the availability of moisture has been found to be the other major limiting factor for Bd growth and survival. Although humidity was not found to significantly affect infection intensities or survival outcomes of the host, contact with water and the presence of moisture are important not only for Bd survival and growth *in vitro* but for host infection (Bustamante et al., 2010; Johnson et al., 2003; Murphy et al., 2011).

2.3.2.4 Pathogenesis of chytridiomycosis

Pathogenesis of disease is the culmination of the epidemiologic triad whereby a suitable dose of a virulent strain of Bd infects a susceptible host in a conducive environment. It describes the

mechanisms in the development of the disease, including both the replication of the pathogen, and the immune and physiological responses of the host. Chytridiomycosis in amphibians is limited to epidermal infection of keratinized regions (hence precluding all but the keratinized mouthparts of tadpoles; Fellers et al., 2001), with no evidence for pathogen invasion of other host tissues, although host responses are often systemic (Berger et al., 1998; Longcore et al., 1999). Typically the ventral abdomen, pelvic 'drink patch', thighs and digits of frogs are most heavily infected, likely due to location of exposure and constant contact with moist surfaces maintaining a suitable environment for Bd (Berger et al., 1998).

Development during the subclinical infection stage is relatively slow, and infections can take several weeks to progress to clinical signs (Longcore et al., 1999; Nichols et al., 2001). Histologic examination of infected skin revealed localisation of the immature thalli intracellularly within the deeper layers of the stratified epidermis (including the stratum granulosum), with zoosporangia and host cells maturing and differentiating synchronously as they migrate towards the skin surface (Berger et al., 2005a; Berger et al., 1998). Histopathological signs of infection include hyperkeratosis and regions of ulceration and erosion of the stratum corneum, together with the presence of the Bd sporangial patches or clusters within the skin (Berger et al., 1998).

Clinical signs typically occur only in the final stages of disease progression (a few days to a few hours prior to death), and include peripheral hyperaemia (reddening of the extremities), abnormal and excessive skin sloughing, lethargy, inappetance, and neurological signs including abnormal posture and loss of righting reflex (Berger et al., 1998; Berger et al., 2004; Berger et al., 1999a; Nichols et al., 2001; Parker et al., 2002). Chytridiomycosis causes mortality in amphibians by asystolic cardiac arrest due to disrupted electrolyte transport in the skin and associated abnormal electrolyte homeostasis (Voyles et al., 2007; Voyles et al., 2009).

2.3.2.5 Diagnosis of chytridiomycosis

Diagnosis of chytridiomycosis or Bd infection is made by one of several means, although the current gold standard utilizes molecular methods and involves quantitative polymerase chain reaction (qPCR). Quantitative PCR permits relative quantification of conserved Bd 18S and 28S ribosomal DNA from skin swabs down to a resolution of one genomic zoospore equivalent from as soon as seven days post infection (Annis et al., 2004; Boyle et al., 2004; Hyatt et al., 2007; Kriger et al., 2006). There has been some debate about the distinction between the presence of Bd zoospore DNA and the presence of either infection or disease (Smith, 2007), as well as the biological relevance of low or indeterminant positive results from the qPCR method. In counter to this concern, the qPCR technique has been found highly sensitive and specific, both with *in*

vitro samples and field samples (Hyatt et al., 2007; Skerratt et al., 2011b), and while not able to distinguish between infection and disease, qPCR provides rapid non-invasive and quantitative diagnostic information that is of high value to researchers and conservation managers (Kriger et al., 2007a; Skerratt et al., 2011b). Furthermore, results should be considered carefully in the context in which the samples are taken, and qPCR results, while providing relative quantification of infection intensity, are typically a gross under-estimate of true Bd loads (Kriger et al., 2007a). Several improvements have also since been made to the qPCR technique to increase efficiency, remove inhibition and improve detection from sediments and water (Kirshtein et al., 2007; Kosch and Summers, 2013; Ruthig and DeRidder, 2012).

Other techniques that have been described for diagnosis, detection and characterization of Bd infection and chytridiomycosis include histology, which reveals patches of Bd sporangia particularly within the ventral skin, as well as histological signs of infection including epithelial hyperkeratosis, hyperplasia, spongiosis, disordered cell layers, ulcerations and erosions with mild inflammation as described above (Berger et al., 1998; Berger et al., 2005c; Bosch et al., 2001; Green and Sherman, 2001; Kriger et al., 2006; Pessier et al., 1999). Other methods for diagnosis include immunohistochemistry and immunoperoxidase techniques which enhance visual recognition of Bd within histologic skin samples (Berger et al., 2002; Van Ells et al., 2003). Scanning and transmission electron microscopy permit examination of tissue ultra-structure (Berger et al., 2005a).

2.3.2.6 Treatment of chytridiomycosis in captivity

There is currently no universally accepted treatment available for chytridiomycosis in captive amphibians, owing to the vast number of different host species affected, and their differing tolerances for particular treatments Berger et al., 2010. A number of different treatments have been trialled using differing dosing regimens, with variable success in eliminating Bd and clinical signs, and varying degrees of side effects including mortality among different species and life stages. These treatments include disinfectants (malachite green and formaldehyde [Parker et al., 2002], benzalkonium chloride [Berger et al., 2009b], steriplantN, and PIP Pond Plus [Woodhams et al., 2012c], Virkon Aquatic and General Tonic [Geiger and Schmidt, 2013]), antifungals (itraconazole [Berger et al., 2010; Brannelly et al., 2012; Garner et al., 2009; Jones et al., 2012; Nichols et al., 2001; Tamukai et al., 2011; Taylor et al., 1999; Woodhams et al., 2012c], fluconazole [Berger et al., 2009b; Berger et al., 2010], amphotericin B [Martel et al., 2011], voriconazole [Martel et al., 2011], mandipropamid [Woodhams et al., 2012c]), an antibiotic (chloramphenicol; Poulter et al., 2007; Young et al., 2012b), antimicrobial peptides (from *Pelophylax esculentus*; Woodhams et al., 2012c), bioaugmentation (application of symbiotic skin bacteria *Pedobacter cryoconitis*; Woodhams et al., 2012c), as well as heat

(Berger, 2001; Berger et al., 2004; Chatfield and Richards-Zawacki, 2011; Geiger et al., 2011; Retallick and Miera, 2007; Woodhams et al., 2003; Woodhams et al., 2012c; Young et al., 2012b), electrolyte solutions (Berger et al., 2010; Young et al., 2012b) and drying treatments (L. Brannelly, unpublished data). Itraconazole and heat treatments have been most widely used with the greatest success, however at certain concentrations itraconazole may be hepatotoxic to tadpoles and cause depigmentation (Garner et al., 2009), and heat treatments may not be tolerated by alpine or temperate zone amphibians, and particularly tadpoles (Berger et al., 2010).

2.4 Management of chytridiomycosis in the field

Ensuring the persistence of amphibian populations and species in the wild is the main aim of managing chytridiomycosis in the field. Unfortunately, disease mitigation in the wild presents a markedly different scenario to the controlled captive *ex situ* environment, so treatments that may work in captivity can typically not be effectively applied at the broader scale (Scheele et al., 2014). The current global distribution of Bd is so vast that eradication is virtually impossible (Fisher et al., 2009b), and regional or local extirpation of the fungus is impractical in view of the inability to control reintroduction (Woodhams et al., 2011). The majority of management effort thus far has been aimed towards reducing the spread of Bd to naïve regions and establishing amphibian *ex situ* captive assurance colonies (Department of the Environment and Heritage, 2006; Gagliardo et al., 2008; Mendelson et al., 2006; Woodhams et al., 2011). With regards to endemically infected populations, no single strategy has thus far been broadly applied, however targeting the reduction of disease based on the epidemiologic triad model described above may provide guidance for the range of techniques available. Research and trials are currently underway on numerous potential management strategies, however these are largely still in the experimental research phase (outlined in Fig. 2.2). In Section 6.2 of this thesis I explore many of these issues regarding management strategies for chytridiomycosis-threatened amphibians.

Figure 2.2. Schematic application of the host-pathogen-environment epidemiologic triad model to identify management techniques for reducing the manifestation of disease in endemically infected wild amphibian populations.

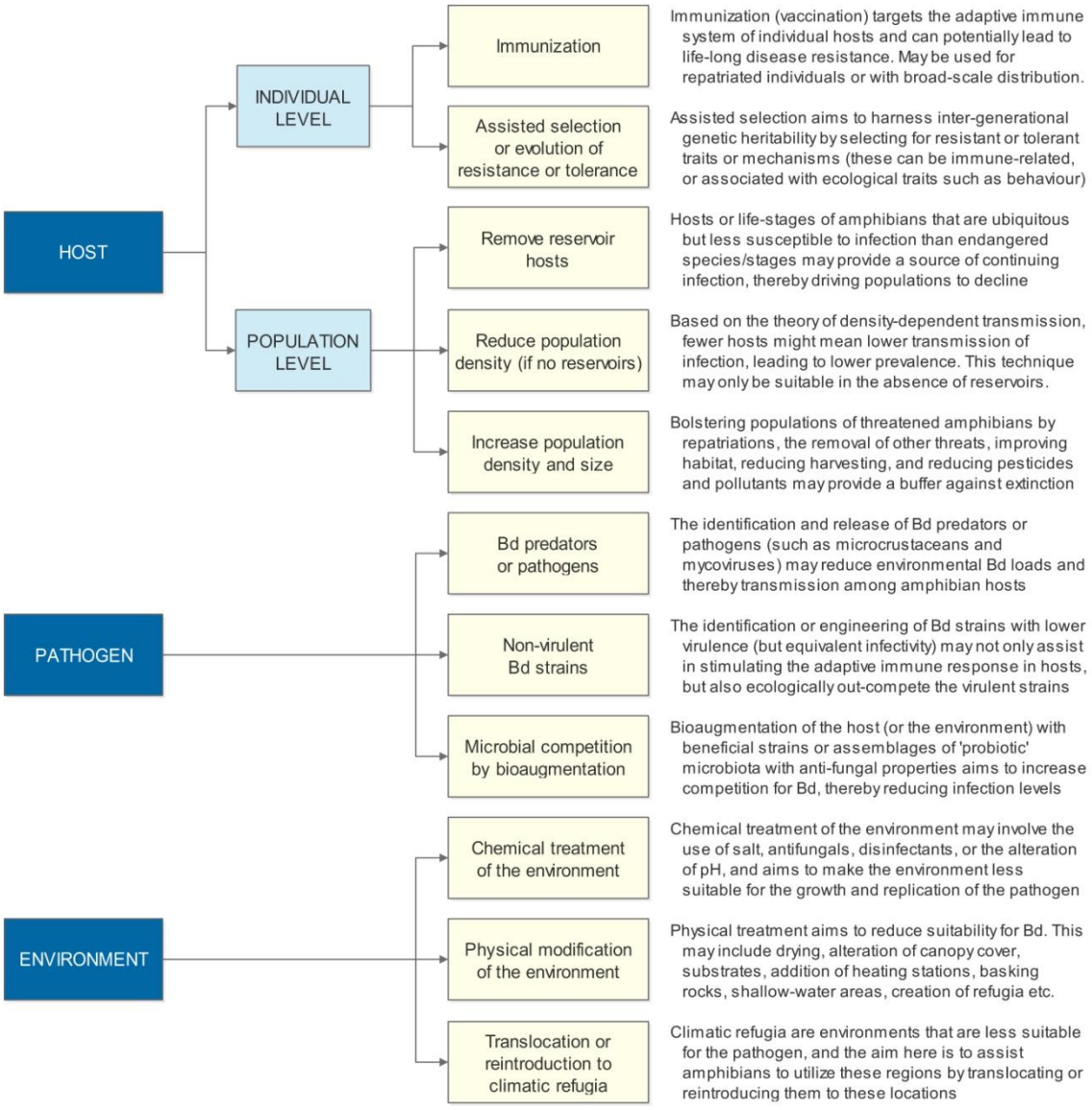

2.4.1 Host immunologic research and associated management techniques

Research into immunologic mechanisms is one of the most promising avenues for developing new techniques to manage emerging biodiversity diseases. Manipulation of the host adaptive and innate immune response (via immunization and assisted selection for disease resistance) is a proven strategy in humans and domestic animals, with considerable potential to reduce the impact of chytridiomycosis in the field (the classic human example is the eradication of smallpox via immunization and systematic surveillance; Henderson and Klepac, 2013).

Immunization (commonly known as 'vaccination') may provide life-long resistance to disease in the individual host, but has rarely been applied to wildlife diseases. The aerially distributed oral rabies bait vaccine is a good example of a cost-effective and sustainable disease control strategy for wildlife species (Holmala and Kauhala, 2006; Niin et al., 2008). Immunization may be utilized with captively-bred or -raised amphibians that are repatriated to endemically Bd-harbouring wild habitats with the potential to improve survival rates post-release. In the absence of host immune manipulation, reintroductions and translocations have had variable success, with the continued presence of the pathogen in the environment leading to eventual mortality of all reintroduced individuals (Dreitz, 2006; Stockwell et al., 2008). Immunization may be of particular value for maintaining population size, improving reproductive potential and slowing the rate of decline in species with longer natural life spans. For example, the southern corroboree frog (*Pseudophryne corroboree*) has a longevity of 6-10 years in the absence of chytridiomycosis (Major, 2009). Another potential benefit of immunization may be the protective effect of herd immunity, where the density-dependent nature of transmission dynamics render the unvaccinated portion of the population 'safe' from infection if the vaccinated portion is above a certain threshold (Fine, 1993). This may apply in particular to species with small home ranges, and minimal contact with syntopic reservoirs (McCallum, 2012). In addition, although adaptive immunity is not heritable and hence may be perceived as a short-term approach, it may assist in providing a population size buffer for the natural evolution of innate immunity.

The innate immune system is generally considered responsible for the evolution of inter-generational immunity, and disease resistance or tolerance may be up-regulated within a population via assisted selection for less susceptible individuals (Venesky et al., 2012; Venesky et al., 2013). Comparative techniques (for example, marker-assisted selection and estimated breeding values) have been widely and successfully used for breeding of disease resistance in plant and domestic animal agriculture (Heringstad et al., 2007; Leeds et al., 2010; Miedaner and Korzun, 2012; Ragimekula et al., 2013). Harnessing the heritability of innate immunity may be especially beneficial as a long-term sustainable approach for repatriating the numerous amphibian species that are now extinct in the wild and only persist in *ex situ* captive programs (Gagliardo et al., 2008). Despite the controversies surrounding these programs (Griffiths and Pavajeau, 2008; Williams and Hoffman, 2009), assisted selection may permit successful reintroduction sooner than is currently envisaged (Mendelson et al., 2006).

Two main approaches that might be feasible in practice for promoting disease resistance include 1) direct selection via exposure of post-metamorphic individuals to Bd, then breeding from those with lower observed susceptibility, and 2) identifying molecular markers of resistance to

advance selection to earlier life stages, removing the need to regularly expose individuals to infection (Woodhams et al., 2011). If suitable markers for resistance are found, straightforward molecular techniques such as PCR might be used to detect alleles conferring resistance at the egg or tadpole stage, leading to more ethically acceptable and accelerated selection for captive breeding and release programs.

Successful and long-term sustainable management is the primary motivation for the studies I undertook on host immunity which will be described in more detail below (Section 2.6), and are covered in chapters 4 and 5 of this thesis. The first research step towards selection as a management technique is establishing whether evolution can occur in the wild, and what mechanisms render populations more resistant. At the commencement of this project, little progress had been made towards these objectives, although variations in susceptibility between amphibian species observed during controlled laboratory experiments (Searle et al., 2011) were promising for the ability to identify resistance mechanisms. Since that time, minor progress has been made in this regard via a study of the major histocompatibility complex (MHC; Savage and Zamudio, 2011), however, in another study, Woodhams et al. (2010) were unable to demonstrate evidence for evolved resistance in terms of antimicrobial peptide responses.

2.4.2 Non-immunologic host management strategies

Non-immunologic host management strategies aim to break the host component of the epidemiologic triad for chytridiomycosis, making the host less susceptible or transmission less probable. These strategies include the removal of reservoir hosts or life stages (often by culling, but sometimes by translocation or exclusion; McCallum, 2012), the reduction of population density in the absence of Bd reservoirs (Beeton and McCallum, 2011; McCallum et al., 2001; Woodhams et al., 2011), or the bolstering of overall population size as a buffer against disease-associated mortality. This latter strategy draws into play a broad range of applicable conservation techniques in order to remove other threatening processes from small and declining populations such as improving habitat suitability and extent for amphibians (combating habitat loss; Stuart et al., 2004), reducing harvesting (Choisy and Rohani, 2006), excluding competitors and introduced pests (Vredenburg, 2004), reducing the impacts of pesticides and pollutants (Relyea and Diecks, 2008; Schiesari et al., 2007), increasing the population size through reintroductions, and minimizing the effect of early predation by head-starting larval stages through metamorphosis in captivity (Hunter et al., 1999).

2.4.3 Pathogen manipulation for management

Preliminary research is underway examining Bd ecology on the host and in the environment in order to break the pathogen component of the epidemiologic triad. Potential management

strategies include manipulating microbial competition via bioaugmentation of the host or environment with probiotic bacteria that express antifungal metabolites (Becker et al., 2009; Muletz et al., 2012; Vredenburg et al., 2011), dissemination of Bd predators (microcrustacea; Buck et al., 2011; Hamilton et al., 2012) and pathogens (such as mycoviruses; Woodhams et al., 2011), and the identification or engineering and release of non-virulent strains of Bd (Woodhams et al., 2011).

2.4.4 Environmental manipulation for management

One group of potential management techniques that has perhaps been underutilized to date is that of altering the environmental suitability for infection and disease. A number of chemical treatments have been proposed or trialled in the field, including the application of salt (Stockwell et al., 2012) and agricultural fungicides (Johnson et al., 2003; Lilley and Inglis, 1997; Woodhams et al., 2011), however there may be negative consequences for other components of wetland ecosystems by their widespread use. Physical modifications of the environment might be used on a local scale for critically threatened amphibians *in situ* and may render the habitat less suitable for Bd. These include drying, drainage or alteration of waterflow, provision of shallow warm-water areas, reduction in canopy cover to increase temperature (Becker et al., 2012; Skelly et al., 2002), or the addition of basking sites or artificial heat. Section 6.2 of this thesis (Scheele et al., 2014) was prompted by the absence of immediate on-the-ground techniques for mitigating the effects of chytridiomycosis in the field and investigates these strategies in greater detail by providing a decision-making framework and real-world examples for managers.

2.5 Endemic disease and population dynamics

Although many studies have investigated the impact of overt chytridiomycosis outbreaks on amphibian populations, particularly associated with spread of the fungus to naïve communities (Lips et al., 2006), the impact and dynamics of *endemic* chytridiomycosis are relatively less well understood (Briggs et al., 2010; Murray et al., 2009).

Several factors render it difficult to accurately assess the impact of endemic diseases such as chytridiomycosis on free-ranging wildlife species. Epidemic mass mortalities are not typically a feature of endemic infections (unless environmental factors play a significant role in determining disease manifestation) because no spatial or temporal point source of infection is involved (Porta et al., 2008; Real and Biek, 2007; Wobeser, 2007). Other factors that make chytridiomycosis detection in frogs less likely include the remoteness of the locations from human populations, the small and cryptic (often nocturnal and aquatic or arboreal) nature of the amphibians themselves, the long durations of subclinical Bd infection outweighing the short

window of overt clinical disease, and the high likelihood for predation of sick animals (Merianos, 2007; Morner et al., 2002; Stallknecht, 2007). Small carcasses such as those of frogs may be quickly scavenged or degrade post mortem, making detection less probable. As an example, in an artificially manufactured field experiment, Wobeser and Wobeser (1992) found that only 20% of bird carcasses could be relocated 24 hours after placement.

At a population level in epidemic outbreaks of chytridiomycosis, population declines have been associated with an average infection intensity threshold of 10,000 zoospores (Briggs et al., 2010; Kinney et al., 2011; Vredenburg et al., 2010). However, these intensities may not be observed with endemic disease (Briggs et al., 2010), either due to a change in the nature of disease manifestation, or simply due to the staggered temporal course of endemic infections. Despite a potential inability to correlate either infection intensity or prevalence with population impact in endemically infected populations, endemic Bd may continue to cause individual frog mortality (Murray et al., 2009). Both direct (contact) and indirect (environmental) transmission have been found to apply with chytridiomycosis (Rachowicz and Briggs, 2007), and transmission is likely influenced by host behaviour and pathogen distribution both spatially and through time. Recoveries from chytridiomycosis have also been observed in the field, however it is not clear whether these are associated with host immune mechanisms or environmental factors such as increased temperature (Briggs et al., 2010).

Key elements necessary for understanding population dynamics in relation to disease include measuring infection or disease abundance and transmission within the population, and relating these findings back to basic population parameters including survival, reproduction (or recruitment), immigration/emigration as well as overall population size or density. For the reasons described above, obtaining reasonable estimates for these parameters in order to examine their potential relationships can be very difficult. Capture-mark-recapture (CMR) refers to both a set of field techniques and statistical models to investigate population parameters in the event of imperfect detection of individuals, which have been particularly applied in the study of wildlife ecology (Burnham and Anderson, 2002; Cormack, 1964; Jolly, 1965; Lebreton et al., 1992; Pollock et al., 1990; Seber, 1965). CMR studies permit the estimation of survival and recapture probabilities, along with a suite of other parameters depending on the specific model type employed (such as multi-state mark recapture for transitions between disease states; Cooch et al., 2012). CMR studies may provide less confounded survival estimates than the often used measure of 'return rate' (Kriger and Hero, 2006b; Retallick et al., 2004).

I chose to employ CMR techniques in the analysis of an intensive two-year mark-recapture field study on common mist frogs (*Litoria rheocola*) in the wet tropics of Australia, as I wished to obtain the most appropriate estimates possible for population and disease parameters. Chapter 3 describes the analyses I performed in order to elucidate the population dynamics of endemic chytridiomycosis. I also provide a detailed outline and synthesis of the complex methodology behind CMR studies and the necessary steps in analysis in Appendix E, including current best reporting practices.

2.5.1 Pathogen abundance and prevalence

A first essential step in examining the dynamics of disease is the ability to measure and report its abundance in a meaningful and comparable way. Since the development of qPCR for Bd detection (see above), this has been the gold standard for reporting chytridiomycosis, however it is limited to measuring the presence of Bd DNA rather than true disease or necessarily infection (discussed by Kriger et al., 2007a; Smith, 2007). This then has the potential to confound the often reported measure of prevalence as it is no longer disease or infection prevalence that is reported, but pathogen presence. This is particularly concerning when prevalence is used as a proxy for population impact of disease in place of estimated parameters of survival or population size/density.

Prevalence, or the proportion of infected individuals in a population (Porta et al., 2008), is a widely used summary measure for describing and comparing infection abundance of microparasitic diseases in wild animal populations. As such it necessarily replaces individual-level data with a scalar proportion based on a binary infection variable (where individuals are defined as either infected or uninfected, diseased or healthy). The prevalence measure is defined to either fluctuate over time (point prevalence) or remain static over a period (period prevalence). There are some cases, however, where adopting a binary definition (that assumes an underlying normal parameter distribution) of infection and disease may be misleading in the absence of contextual information, and hence prevalence may be an inappropriate summary measure and incomparable between studies. The range in infection prevalence reported for Bd in the literature is unfortunately too broad to be particularly informative or comparable due to a number of underlying confounding factors associated with often misguided study design and reporting (Lindberg, 2012).

Prevalence and other binary disease classifications are insensitive to and have poor predictive value for population dynamics with changes in underlying host, spatial or temporal pathogen aggregation especially where pathogenicity depends on infectious burdens, as is the case with Bd (Voyles et al., 2009; Vredenburg et al., 2010). Parasite aggregation implies that most

infected individuals have low infectious burdens, while only a few hosts have high burdens (Hudson and Dobson, 1998). Prevalence neither indicates the degree of aggregation, nor the characteristics of any low-burden class (which may be newly infected, recovering, tolerant, resistant, or represent a spurious result). Additionally, prevalence measures are strongly influenced by the time-course of infection, as well as mortality and recovery rates, and can hence lead to spurious inferences about population dynamics where external variables (such as seasonal and stochastic fluctuations in temperature as occurs with Bd) are largely responsible for driving infections, recoveries, and mortalities. In Section 3.3 of this thesis I investigate the concept of parasite aggregation as one reason why prevalence may be an insufficient measure to characterize chytridiomycosis infection abundance, despite its frequent use in the literature. In doing so, I compare chytridiomycosis dynamics with those of macroparasites (including helminths and arthropods), a concept introduced by Briggs et al. (2010).

2.5.2 Population impacts

Ultimately, observational and modeling studies investigating chytridiomycosis dynamics in the field are driven by concerns for the population impact of Bd infection and disease. Mortality induced by chytridiomycosis is therefore of considerable importance in relation to threatened populations, however survival probabilities are just one component of the population equation. Due to the extent of larval mortality, amphibians as a group have relatively large reproductive potential, with clutch sizes ranging between tens and thousands of eggs (Duellman and Trueb, 1994). In years past, the reproductive strategies of this group would have characterized it as a predominantly r-selected taxon (Reznick et al., 2002). This high reproductive potential means that recruitment into the population may compensate for adult mortality in all but the most extreme circumstances, leading to relatively stable annual population sizes (Muths et al., 2011).

However other factors in addition to population size may also be important for determining disease impact. Examples include the buffering capacity of the population and the ability to recover from severe stochastic events (such as droughts or cyclones), alterations in age structure of the population (which may lead to years with no reproduction due to age at sexual maturity and the absence of particular age classes), and changes in evolutionary reproductive strategy (such as shifts in the timing of breeding). All of these factors may contribute to rendering the population more vulnerable despite apparently stable dynamics during good years. These factors should be considered in the design of management strategies (Murray et al., 2011b).

2.6 Host immunity

As described above (Section 2.4.1), immunologic management strategies may provide a long-term and sustainable approach to minimizing the impact of chytridiomycosis on threatened

amphibians in the wild. For this reason, one of my major research objectives focused on investigating the amphibian host immune response to Bd infection. In particular, I separated the objective into two component parts according to the somewhat blurred distinction between the vertebrate adaptive and innate immune systems (see Chapters 4 and 5 of this thesis respectively). In the following sections I describe the typical amphibian host immune response to an invading infectious organism, and compare it with the observed response to Bd infection as described in the literature (see also Fig. 2.3), highlighting current gaps in our knowledge.

2.6.1 Similarities of the amphibian immune system to other vertebrates

The larval and adult immune system of *Xenopus spp.* (South African clawed frog) has undergone extensive investigation as a transitional non-mammalian model organism for comparative and evolutionary immunology and studies of immune ontogeny (Robert and Ohta, 2009). The adult anuran immune system is fundamentally similar to other jawed vertebrates (Du Pasquier et al., 1989), however there are some differences. Anurans lack the lymph nodes of mammals (Flajnik, 2002), and instead the major lymphoid organs include the thymus (differentiation of T lymphocytes) and spleen (lymphocyte accumulations), with leukocyte aggregations additionally occurring in the liver, kidneys and intestine (Marr et al., 2007). Innate immune cell types are morphologically similar to those of mammals and include polymorphonuclear cells (neutrophils, eosinophils and basophils), as well as monocytes, macrophages and natural killer cells (Robert and Ohta, 2009). Many innate immune genes and gene pathway homologues have been identified in *Xenopus spp.* (Robert and Ohta, 2009). These include receptors (polymorphic major histocompatibility class I and II genes, toll-like receptors; Ishii et al., 2007), cytokines (interferon-γ, interleukins, tumor-necrosis factor α), and complement (classical, alternative and lectin pathways; Fujita et al., 2004). The amphibian innate immune system is remarkable in the production of potent antimicrobial peptides in granular (serous) glands of the skin (Rollins-Smith, 2009).

Anuran adaptive immune cells and receptor pathways are also orthologous to other vertebrates, including antigen-presenting dendritic cells as well as B and T lymphocytes. Unlike mammalian lymphocytes, many differentiated B cells have phagocytic capabilities (Li et al., 2006). The process of affinity maturation of lymphocytes via somatic hypermutation and class switch recombination (IgM to IgY) is less well developed in comparison with mammals (Flajnik, 2002; Marr et al., 2007; Robert and Ohta, 2009). The antibody responses of adult amphibians also differ slightly from mammals and consist of IgM, IgX (mucosal expression) and IgY (splenic expression induced via T-cell dependent responses), the latter two of which are functionally analogous to IgA and IgG of mammals (Flajnik, 2002). Recently, two further isotypes have been discovered, IgD and IgF (Ohta and Flajnik, 2006; Zhao et al., 2006b).

The immune system of tadpoles, while competent, is functionally less well developed compared with that of adult anurans, and undergoes substantial remodeling accompanied by immunosuppression during metamorphosis, through until about six months post-metamorphosis (Robert and Ohta, 2009; Rollins-Smith, 1998). Of particular note, the immunoglobulin repertoire is typically smaller and less specific in tadpoles, the thymus involutes and is re-formed during metamorphosis, and the expression of MHC class I and II molecules greatly expands (Du Pasquier et al., 1989; Flajnik et al., 1987; Robert and Ohta, 2009). In the research undertaken in this thesis I have focused exclusively on adult anurans (> 6 months post metamorphosis).

2.6.2 Characteristics of the amphibian immune response to Bd infection

While the amphibian immune response to Bd infection has been relatively widely studied to date, there are many areas that are still not well understood, likely owing to the complexity of the system and the vast range in species' responses to infection. The expression and function of various components of both the innate and adaptive immune systems have been found important for differentiating susceptible and resistant individuals. While predisposing immunosuppression is not necessary for epidemics to occur (Berger et al., 1999a), apparent immunosuppression has been observed in Bd-infected individuals (detected via skin histopathology, and corroborated via gene expression and *in vitro* immune studies (Berger et al., 2005c; Ribas et al., 2009; Rollins-Smith et al., 2011; Rosenblum et al., 2012b). Thus is appears that Bd may either have low inherent antigenicity (perhaps due to intracellular localization), or may suppress immune pathways in susceptible hosts. In light of this trend, below I provide an overview of the expected adult amphibian immune response in a susceptible individual, accompanied by a sequential schematic illustration of anuran skin (see Fig. 2.3), which I compare with evidence from the literature of what has actually been observed in a typical Bd infection, thus highlighting the current gaps in our knowledge for further research.

Figure 2.3. Amphibian host immunity schematic, demonstrating a histological section through the skin (the site of infection), with the main cellular components of the expected immune response to Bd infection illustrated.

(A) Normal skin: Layers of uninfected frog skin including, from deepest to most superficial, the basal lamina, stratum germinativum, stratum spinosum, stratum granulosum, stratum corneum and the superficial mucus layer. Also illustrated are a dermal capillary with the nucleated red blood cells of amphibians, an immune dendritic cell, and an example complement of naïve B and T lymphocytes waiting quiescent in the spleen (not illustrated). **(B) Early infection:** Expected immune mechanisms upon initial exposure to Bd. Zoospores are illustrated penetrating the mucus layer, and early thalli with zoosporangia developing are illustrated inside deeper host cells. Non-specific pathogen recognition is expected to lead to the infiltration of innate immune cells illustrated here to include macrophages and granulocytes. **(C) Intermediate infection:** Expected response at an intermediate stage of infection includes the recognition of antigens by dendritic cells which then differentiate into antigen presenting cells and migrate to the spleen enabling antigen-specific selection of lymphocytes. Simultaneously, membrane-bound immunoglobulin on naïve B lymphocytes is exposed to extracellular Bd antigens, and with the assistance of T helper cells, these B cells are activated to respond to infection. **(D) Late infection:** The late adaptive response involves lymphocyte clonal expansion, differentiation into plasma cells and activated T cells (including helper and cytotoxic T cells), as well as the production of antibodies by plasma cells. **(E) Recovery:** If the frog is cleared of infection (perhaps by topical antifungals or heat), the skin might be expected to return to normal, however, a cohort of selected memory lymphocytes should remain. **(F) Re-exposure:** If the frog is then later re-exposed to Bd, the memory lymphocytes (produced during the previous clonal expansion) are activated and induced to replicate and differentiate, leading to a much more rapid and effective adaptive immune response on re-exposure. This is the concept of immunization (vaccination).

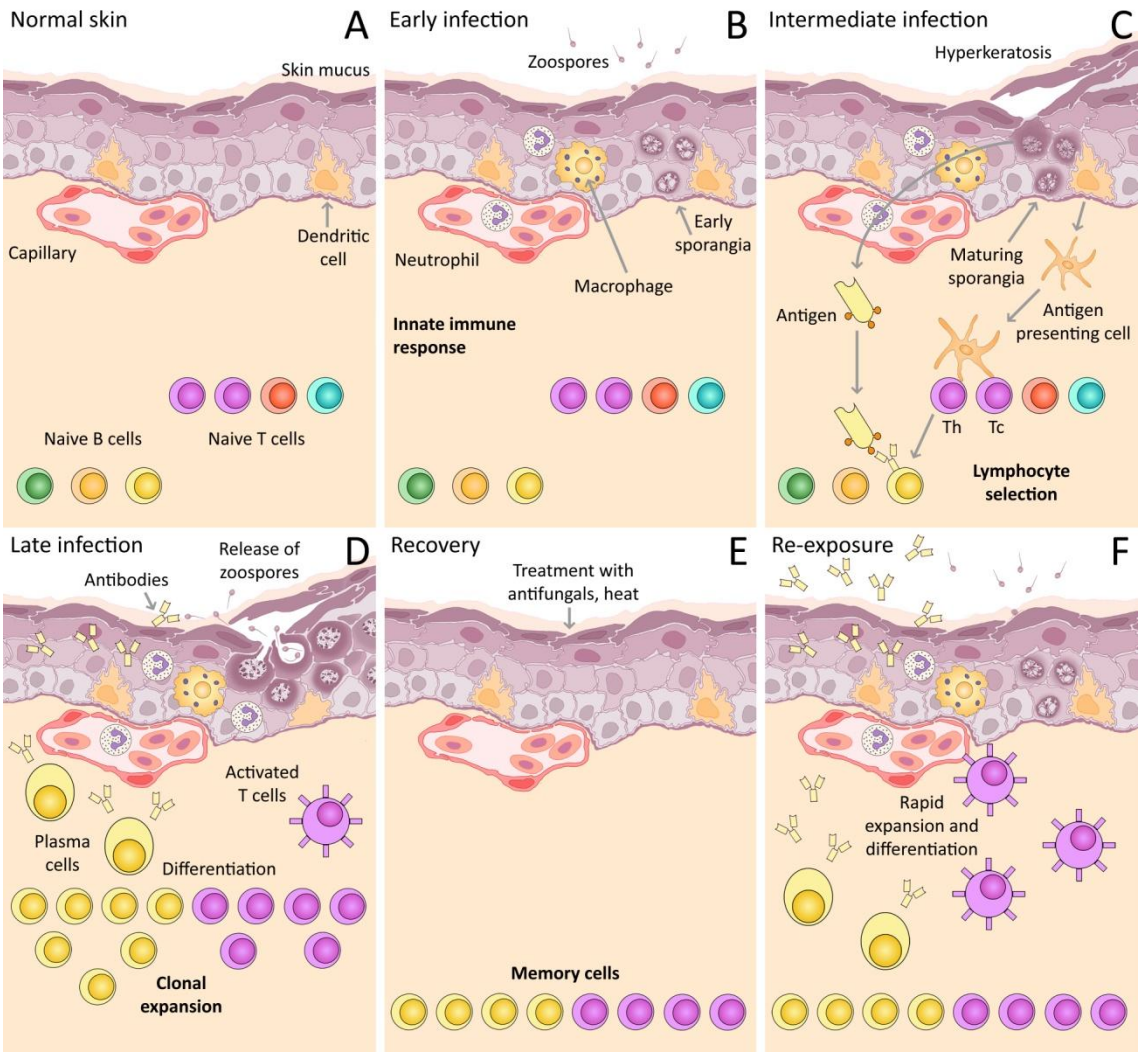

2.6.2.1 The immunocompetent uninfected state

Normal uninfected integument of an immunocompetent amphibian host consists of epidermal and deeper dermal layers (Fig. 2.3A). The epidermis constitutes an immediate innate physical defense barrier against pathogen invasion and consists of a number of cell layers or strata that differ in their maturation stage, from the roughly cuboidal or columnar-shaped germinal cells of the stratum germinativum above the basal lamina (basement membrane) through stratum spinosum and stratum granulosum to the highly differentiated keratinized squamous epithelial cells at the surface of the skin, the stratum corneum, that are joined by tight junctions (Fox, 1994; Murphy, 2012). A number of peripheral immune surveillance cells are typically also present in the epidermis, particularly Langerhans dendritic cells (that later differentiate to become antigen presenting cells; Carrillo-Farga et al., 1990). Serous and mucous glands are also present (the former more common on dorsal skin), as are pigment-bearing chromatophores, and smooth muscle fibres. Capillaries and nerves course through the highly collagenous dermis which consists of deeper stratum compactum and thicker and more superficial stratum

spongiosum, separated in some species by the substantia amorpha granular calcified layer (Berger et al., 2005c; Duellman and Trueb, 1994; Schwinger et al., 2001). On the surface of this uppermost stratum sits a layer of mucus produced by mucous glands, potentially containing antimicrobial lectins, lysozyme, secretory phospholipase A_2 produced by phagocytes and keratinocytes, and antimicrobial peptides (such as defensins, cathelicidins and histatins) secreted via serous glands, a complement of mucosal antibodies, as well as any commensal symbiotic bacterial communities together with their antimicrobial metabolites (Murphy, 2012). In the uninfected state, the repertoire of naïve B and T lymphocytes, each with a unique and specific antigen receptor combination, are quiescent within the major lymphoid organs (spleen, and other aggregations such as in the liver and intestine) (see Fig. 2.3A).

2.6.2.2 Early naïve infection and constitutive defenses

Early infection with Bd involves the chemotaxis of infectious zoospores towards the skin surface (Moss et al., 2008; illustrated in Fig. 2.3B), whereupon they encounter the skin mucus and any associated constitutive defenses such as antimicrobial peptides, enzymes or antibodies that may reduce their numbers and inhibit colonization. Naïve frogs that have not previously been exposed to Bd are unlikely to express specific mucosal antibodies to bind to and inhibit zoospores, however 'natural antibodies' directed against highly conserved pathogen epitopes may be present prior to pathogen exposure. A lysozyme from amphibian skin secretions has been isolated and characterized to have potent bactericidal activity (Zhao et al., 2006a). Although typically considered an antibacterial enzyme, lysozyme has long been known to also possess antifungal properties (Anil and Samaranayake, 2002; Woods et al., 2011), so amphibian lysozymes (Ostrovsky et al., 1976) may similarly have activity against pathogens such as Bd as well as pathogenic bacteria (Rollins-Smith et al., 2009; Rollins-Smith and Woodhams, 2012). Increased expression of lysozyme was demonstrated in a study by Rosenblum et al. (2009) in the skin of *Xenopus (Silurana) tropicalis* when exposed to Bd, however this occurred at a late stage of infection (21 days post exposure), so may instead be associated with uncharacterized secondary bacterial infection (Berger et al., 2005c).

The antimicrobial peptides of vertebrates are analogous to those of invertebrates, and have long been recognized to provide a non-specific defense against pathogenic organisms (Nicolas and Mor, 1995). In particular, the antimicrobial peptides of amphibian skin can be produced readily in large quantity and have been the target of many medical studies for use in pharmaceutical applications (for example Conlon et al., 2005; Conlon et al., 2004; King et al., 2005). The expression of antimicrobial peptides can be induced and modulated by the presence of microoganisms (Mangoni et al., 2001), and through *in vitro* growth inhibition assays, many peptides and peptide mixtures (at concentrations likely to occur *in situ*) have been found to

inhibit the growth of various pathogens including Bd as well as other fungi (Conlon et al., 2007; Gibble et al., 2008; Morton et al., 2007; Pask et al., 2012; Rollins-Smith et al., 2003; Rollins-Smith et al., 2002a; Rollins-Smith et al., 2005a; Rollins-Smith et al., 2002b; Rollins-Smith et al., 2005b; Rollins-Smith et al., 2006). Correlations between the *in vitro* peptide efficacy against Bd, concentration and number of peptides produced, and the extent of species population declines in the wild, have provided conflicting results between species (Conlon, 2011; Rollins-Smith et al., 2006; Woodhams et al., 2007a; Woodhams et al., 2006a). Attempts have been made to use these data for predictive indices for species decline in naïve regions (Woodhams et al., 2006b). *In vivo* antimicrobial peptide depletion led to increased susceptibility to Bd infection in exposure trials in resistant amphibian species *Xenopus laevis* (Ramsey et al., 2010) and *Rana pipiens* (Pask et al., 2013), however not in *Pelophylax esculentus* and *P. lessonae* (Woodhams et al., 2012b). Peptide expression was found to differ between infected and uninfected wild-caught *Litoria serrata*, with infected frogs demonstrating reduced expression (Woodhams et al., 2012a), although whether this was a cause or result of infection was not known. Antimicrobial peptide genes or precursors including preprocareulein and cathelicidin have been detected in the spleen and skin of infected frogs respectively via microarray gene expression studies, although the significance of the unexpected presence in the spleen is currently unknown (Ribas et al., 2009; Rosenblum et al., 2012b).

Commensal bacterial communities on amphibian skin may provide another mechanism of constitutive innate immunity in their ability to inhibit pathogenic microbes such as bacteria and fungi (Austin, 2000; Culp et al., 2007). Numerous epibiotic bacterial species isolated from amphibian skin have been demonstrated *in vitro* to be growth inhibitive for Bd (Harris et al., 2006). Cell-free *in vitro* bacterial metabolite screening methods for inhibitive activity against Bd have now been developed (Bell et al., 2013). There is also now *in vitro* evidence for a synergistic effect between bacteria and antimicrobial peptides for inhibiting Bd growth (Myers et al., 2012). The bacterial species *Janthinobacterium lividum* has shown particular promise for its antifungal properties (Lauer et al., 2007), and in clinical Bd exposure experiments, both frogs (*Rana muscosa*) and salamanders (*Plethodon cinereus*) inoculated with *J. lividum* demonstrated lower morbidity and mortality (Harris et al., 2009a; Harris et al., 2009b). This effect also extended to soil augmentation and environmental transfer of bacterial species to amphibian hosts, thereby inhibiting Bd infection (Muletz et al., 2012). The mechanism of inhibition is thought to involve the bacterial production of anti-chytrid metabolite violacein (Harris et al., 2009a), at a threshold concentration of 18 µM on salamander skin (Becker et al., 2009).

Despite these promising results, inoculation of Panamanian Golden frogs (*Atelopus zeteki*; extinct in the wild) with *J. lividum* bacteria resulted in only transitory colonisation, and had no

effect in delaying or preventing mortality (Becker et al., 2011). Unfortunately, other experimental bacterial inoculation trials have thus far proved ineffective (Woodhams et al., 2012c), with no significant effect on amphibian survival. Clinical Bd exposure experiments demonstrated that bacterially-depleted salamanders (*P. cinereus*) had lower body mass and displayed more behaviours linked with infection (limb-lifting), however there was no significant difference in Bd infection loads between bacterially-depleted and intact salamander groups, and all individuals cleared Bd infection spontaneously by 28 days post Bd-exposure (Becker and Harris, 2010). Preliminary results involving repetition of this experiment with *Rana sphenocephala* resulted in a positive association between bacterial depletion and higher Bd intensities (Holden and Rollins-Smith, 2014). There is some evidence for a population-level correlation between the presence of (and proportion of individuals harbouring) anti-Bd bacterial species and population declines (Lam et al., 2010; Woodhams et al., 2007c), however, conflictingly in another study, amphibian species found infected with Bd also harboured bacterial species with the highest anti-Bd activity (Flechas et al., 2012). A controlled preliminary field mark-recapture bioaugmentation trial of a rapidly declining frog (*Rana sierrae*) population with *J. lividum* suggested promising results, with bacterially-inoculated frogs having higher recapture rates and lower infection intensities than control frogs (Vredenburg et al., 2011). These results have yet to be corroborated.

2.6.2.3 Induced innate immune defenses

If the invading Bd zoospores are not contained with constitutive host immunity, they then encyst upon the keratinized skin surface (Berger et al., 2005c), send germination tubes through one or more cell layers (Greenspan et al., 2012; Van Rooij et al., 2012), and inject their contents into deep cells of the host epidermis, including the stratum spinosum and stratum granulosum (Berger et al., 1998; Fig. 2.3B). The intracellular location and process of injecting zoospore contents into deep cells may permit Bd evasion of host immune surveillance, as has been described with other fungal pathogens (Woods, 2003).

In the absence of targeted immune evasion, an invading infectious organism should prompt host recognition thereby inducing firstly innate then adaptive immune responses in the host via antigens that are either secreted or expressed on the pathogen cell surface. These antigens often contain epitopes of widely recognised pathogen-associated molecular patterns (PAMPs) that are common to many different micro-organisms. These PAMPs bind to host pattern recognition receptors (PRRs) expressed within or on cells of the innate immune system (such as resident macrophages within the skin, keratinocytes or dendritic Langerhans cells). These PRRs may include toll-like receptors, mannose receptors, scavenger receptors, glucan receptors, C-type lectin receptors, and NOD-like receptors among others (Murphy, 2012). In addition, cellular

stress and the release of cell contents through trauma produce damage associated molecular patterns (DAMPs) that are similarly recognised by host immune cells. Furthermore, there are many secreted extracellular and plasma proteins that also recognise characteristics of antigens, including receptors of the alternate and lectin complement pathways (such as mannose-binding lectin [MBL]), pentraxins (such as C-reactive protein and serum amyloid), collectins, peptidoglycan recognition proteins (PGRs), and ficolins.

Binding of PAMPs by PRRs leads to an innate amplifying inflammatory cascade that varies depending on the initial signaling pathways involved. The alternative and lectin complement pathways may be activated in a variety of ways, for instance, and in combination with MBL-associated serine proteases (MASPs), ultimately form the membrane attack complex (MAC). The MAC functions to agglutinate pathogens and lyse their cell membranes, as well as attract phagocytes to the locality and enhance their phagocytosis of pathogens via opsonization. Binding of other PRRs may induce signalling pathways and the release of cytokines (pathways such as nuclear factor kappa-light-chain-enhancer of activated B cells [NFκB], and mitogen-activated protein [MAP] kinase). Binding may also stimulate endocytosis and destruction of microorganisms, or apoptosis of infected host cells.

Gene expression studies in Bd-infected frogs have demonstrated mixed results on the expression of various PRRs. Rosenblum et al. (2009) and Rosenblum et al. (2012b) found no evidence for increased expression of toll-like receptors in either the skin or liver tissues of *Xenopus (Silurana) tropicalis*, *Rana muscosa* or *R. sierrae*, although there was mild increase in spleen tissues in *X. tropicalis* of the associated myd88 gene at 3 days post exposure. They also reported the predominantly decreased expression of many complement pathway genes in all three species, and the up-regulation of inhibitory genes associated with NFκB. They were unable to report on other PRRs. Ribas et al. (2009) also reported decreased expression of complement pathway genes in infected *X. tropicalis*, however they found increased expression of fucose binding lectin that may be involved in pathogen recognition, as well as seven genes related to serine proteases. In contrast, Ellison et al. (2014) reported the increased expression of seven toll-like receptor genes in infected *Atelopus zeteki*, as well as numerous complement pathway genes and greatly upregulated expression of serine proteases.

Cytokines are endogenous inflammatory mediators and include lymphokines (such as macrophage activating factor [MAF]), interleukins (ILs), tumour necrosis factors (TNFs), interferons (IFNs), transforming growth factors (TGFs), chemokines, colony stimulating factors (CSFs), polypeptide growth factors (GFs) and stress proteins (including heat shock proteins [HSPs]). While some of these cytokines act in an autocrine fashion (on adjacent cells), others

are distributed through the systemic circulation and attract leukocytes to the site of infection, among other functions (Murphy, 2012). In addition, inflammatory mediators activate pathways involved in blood coagulation and tissue repair.

The Bd gene expression results for cytokines were similar to those above, with little evidence for expression in exposed frogs except for mild increase in a small number of cytokine genes. These included interleukin 17A/F-like gene, calcineurin interleukin 2 inducible gene, tumour necrosis factor associated factor (TRAF) and guanylate binding protein interferon inducible gene in spleens of *X. tropicalis* (Ribas et al., 2009; Rosenblum et al., 2009), and some interferon and interleukin-associated genes in *Rana Spp.* (Rosenblum et al., 2012b). Several heat shock proteins were found to be upregulated in *X. tropicalis* tissues (Rosenblum et al., 2009) but the response was inconsistent (Rosenblum et al., 2012b). In contrast, Ellison et al. (2014) demonstrated increased expression of numerous cytokines including interferons, interleukins, and tumour necrosis factors. These discrepant results may be associated with differences in dynamic range and sensitivity of gene expression microarray technologies in comparison with next-generation sequencing (RNA-seq; Wang et al., 2009). Alternatively, they may also be due to possible confounding associated with the presence of secondary bacterial infections that typically accompany late stages of infection (Berger, 2001; Berger et al., 1998) and that could not be ruled out in the study by Ellison et al. (2014).

2.6.2.4 Leukocyte recruitment and infiltration

Recruitment of leukocytes to the site of infection is a key part of the inflammatory cascade, and is typically reflected by circulating white blood cell numbers (when examined by systemic haematology). Innate immune leukocytes include monocytes that differentiate into macrophages at the site of infection, polymorphonuclear phagocytes including neutrophils, eosinophils and basophils, as well as natural killer cells and mast cells. These leukocytes contribute to amplifying the inflammatory cascade, they destroy extracellular pathogens via phagocytosis, and trigger apoptosis of damaged or infected host cells (Murphy, 2012).

Haematological (circulating) and histopathological (tissue) results of leukocyte numbers from comparisons between Bd-infected and uninfected control frogs have suggested that cellular inflammation in chytridiomycosis is inconsistent but generally only mild or decreased across species. Woodhams et al. (2007a) found decreased circulating neutrophils and eosinophils, and increased numbers of basophils in infected adult *Litoria chloris* frogs, while Davis et al. (2010) and Peterson et al. (2013) found increased neutrophils and fewer eosinophils in infected *Rana catesbeiana* tadpoles and *Litoria caerulea* adults respectively. Young et al. (2014) found lower total white blood cell counts in chronically infected adult *L. caerulea*, with overall impairment

of responses on immune stimulation. Histological results have revealed an inconsistent mild inflammatory response in 10-40% of skin sites, involving foci with macrophages and few neutrophils, often near areas of ulceration suggesting a possible association with secondary bacterial infections (Berger et al., 2005c; Nichols et al., 2001; Pessier et al., 1999). Rosenblum et al. (2009) found a mild increase in neutrophil-associated genes in the spleen of infected *Xenopus (Silurana) tropicalis* frogs, while Ellison et al. (2014) found increased expression of several macrophage and neutrophil associated genes.

2.6.2.5 Activation of the adaptive immune response

In a typical immune response to an infectious organism, the adaptive immune system is dependent on initial activation and co-stimulation by receptors and mediators of the innate immune system. However, the adaptive response is characterized uniquely by somatic recombination (V[D]J recombination) of T and B cell receptors (TCR, BCR) yielding a large lymphocyte pathogen receptor repertoire, and also by somatic hypermutation and class switch of B cell receptors during affinity maturation. Through lymphocyte selection, affinity maturation and the production of memory lymphocytes, the adaptive immune system *adapts* to an infectious agent during the course of an infection and the life of an individual (with multiple pathogen exposures; Murphy, 2012). Thus the adaptive immune response increases in efficacy with exposure to an infectious agent during an individual host's lifetime (unlike the innate immune response), leading to the concept of immunization (or vaccination). The adaptive response typically takes longer to manifest than the innate immune response, and pathogen-specific antibody expression has been reported to peak around 14 days post exposure in amphibians (Gantress et al., 2003).

Pathogen antigens are detected by PRRs expressed by dendritic cells (as well as some macrophages and B cells) which stimulates endocytosis and degradation of the pathogen or peptide, and differentiation of the dendritic cell into an antigen presenting cell (APC; see Fig. 2.3C). Major histocompatibility complex genes (MHC) are involved in presenting components of the antigens on the cell surface to T cells in combination with co-stimulatory molecules in order to activate them. MHC evolution has been widely demonstrated to occur under selection by infectious diseases (Meyer and Thomson, 2001). Hereafter I classify MHC components to bridging elements between the innate and adaptive immune systems due to their inter-generational heritability (unlike the somatic hypermutation and recombination that characterizes T and B cell receptors). MHC diversity is important for appropriate antigen presentation (by MHC classes I and II) and is generated by polygeny (the presence of multiple interacting genes), allele codominance, and gene polymorphism. Tumour necrosis factor alpha (TNF-α) then stimulates APC migration via the lymph sacs or circulatory system to the spleen (and other

leukocyte conglomerates such as in the liver), where the APC will contact circulating CD4 T helper cells.

There are many thousands of naïve T and B lymphocytes in the body, each bearing unique cell surface receptors which together constitute the unique lymphocyte receptor repertoire of the host. Lymphocytes that encounter antigen for which they have a specific receptor are activated in the presence of co-stimulation. This includes MHC and additional co-stimulatory molecules in the case of T lymphocytes, and MHC-antigen binding with a specific TCR of T helper cells in the case of B lymphocytes (Murphy, 2012). Co-stimulatory molecules are expressed on APCs in response to mediators of the innate immune system (such as TLRs and NFκB). They are essential for the activation of the naïve CD4 T lymphocytes, which are important for initiating downstream adaptive immune pathways. B cells typically require this co-stimulation by CD4 T cells for activation and ensuing proliferation, receptor somatic hypermutation, and differentiation into plasma cells, which are the effector form that produce and secrete antibodies (immunoglobulins; see Fig. 2.3C and D). T lymphocytes proliferate by clonal expansion, differentiate into their effector forms (such as cytotoxic T cells) and migrate to the site of infection.

Antibodies are the main adaptive components of humoral immunity and they target and destroy extracellular pathogens by several means. Antibodies bind specifically with the epitope of the antigen and cause the antigens to agglutinate, inactivating them. Antibodies also activate the classical complement cascade, leading again to the membrane attack complex, and they also tag the antigen for destruction by phagocytic cells. In contrast, cell-mediated immunity is likely to be especially important for intracellular pathogens such as Bd (Rollins-Smith et al., 2009). It involves the differentiation of T lymphocytes into cytotoxic T cells which recognise and stimulate apoptosis of infected host cells, or phagocytosis by cells of the innate immune system.

There is little evidence from the literature to suggest the effective activation of the adaptive immune response to chytridiomycosis. Circulating numbers of lymphocytes were found to be greatly reduced in exposed infected *L. caerulea* (Peterson et al., 2013; Young et al., 2014), and results from histopathology of the skin showed either only a mild response with foci of lymphocytes associated with regions of ulceration, or no evidence of lymphocytes (Berger et al., 2005c; Nichols et al., 2001; Pessier et al., 1999). In terms of gene expression results, Rosenblum et al. (2009) found decreased expression of the classical complement pathway, increased NFκB and no change in T cell markers or MHC genes in *X. tropicalis*. Results were similar in their second study on *Rana spp.* (Rosenblum et al., 2012b) however there was some mild evidence for an adaptive immune response in the spleen with activation of complement, interferons and

interleukins, and increased IL-1 and MHC class II genes in the skin during late-stage infection. Ribas et al. (2009) found that adaptive immune genes were generally down-regulated in the spleen of *X. tropicalis*. Again in contrast, in *A. zeteki* frogs at the late stage of infection, Ellison et al. (2014) found the upregulation of numerous genes and receptors associated with both B and T lymphocytes, including immunoglobulins and MHC genes.

2.6.2.6 Memory lymphocytes and re-exposure (the concept of immunization)

If time is sufficient for the adaptive immune response to develop prior to host mortality (including both lymphocyte clonal expansion and differentiation), or if the infected individual recovers (either spontaneously or through treatment as discussed above in Section 2.3.2.6, Fig. 2.3E) and is re-exposed to the same pathogen some time later, the ensuing adaptive response is both more rapid and effective than the initial response (see Fig. 2.3F). This occurs due to the production of memory lymphocytes during clonal expansion that are similarly antigen-specific, but longer lived and in higher number than the original naïve lymphocytes with receptor specificity for the pathogen antigens. This gives rise to the concept of immunization (vaccination).

At the time of commencing this project there was little knowledge of the potential for immunization against Bd to be an effective management strategy, although it had been suggested as such (Kurtz and Scharsack, 2007) and appeared a promising approach, given the highly successful examples from human and domestic animal agriculture (Robbins et al., 1998). Studies reported by Rollins-Smith et al. (2009) and Ramsey et al. (2010) attempted to immunize *Xenopus laevis* frogs against chytridiomycosis via an intraperitoneal injection with heat-killed Bd. They found promising results of a high-titer IgY antibody response in the immunized frogs at 14 days post immunization. Furthermore, X-irradiation of frogs to reduce splenic leukocytes led to increased Bd infection loads in *X. laevis* (Ramsey et al., 2010). In contrast, a repeat experiment with killed-Bd injections into the dorsal lymph sac (days 0 and 14) and peritoneum (day 28) followed by splenocyte culture with phytohaemagglutinin (PHA) showed generally weak lymphocyte proliferation. In another experiment, boreal toads (*Bufo boreas*) were immunized following a similar protocol and then exposed to Bd, however there was no evidence for a difference in survival between the immunized and sham-injected exposed frogs, suggesting that the immunization had not been successful in stimulating protective adaptive immunity (Rollins-Smith et al., 2009).

In discussions amongst collaborators at the time (pers. comm. L. Skerratt, L. Berger) it was considered that the route of immunization (injection either into the dorsal lymph sac or intraperitoneally) may play a role in preventing clinically relevant protection upon exposure or

re-exposure to Bd due to the required specificity of the mucosal immune response (Rollins-Smith et al., 2009). Hence a topical application or a regimen involving prior exposure followed by treatment may yield greater success. In addition, small sample sizes and low statistical power of these preliminary studies described above would likely have precluded the detection of infection rate differences between groups of less than 40%. When considering critically endangered species where the wild population consists of fewer than 50 animals (for example, the southern corroboree frog, *Pseudophryne corroboree*), and the goal of reintroduction programs is to release 500 individuals, an improvement in survival of as little as 10% would be considered highly biologically relevant as it would more than double the existing wild population. In Chapter 4 of this thesis I describe a controlled clinical exposure trial to investigate this question of immunization by using the technique of clinical Bd exposure, treatment with itraconazole, followed by re-exposure of individual adult booroolongs frogs (*Litoria booroolongensis*) to Bd.

Since the beginning of this project (and benefiting from the work described in Chapter 4 of this thesis) further studies have been published investigating the question of adaptive immunity and the potential for immunization. It has become generally more apparent that Bd in some way either evades or compromises the host adaptive immune response (Ellison et al., 2014). Stice and Briggs (2010) immunized *Rana muscosa* with formalin-killed Bd in combination with adjuvants by injection into the dorsal lymph sac and found no differences in the proportion of frogs infected nor time to infection. An unpublished study by a colleague in James Cook University (S. Young, unpublished) found that prior infection (followed by treatment with chloramphenicol) increased the likelihood of re-infection and subsequent infection intensities with Bd re-exposure. In contrast, a study of prior infection in *B. boreas* by Murphy et al. (2011) found that previously exposed frogs survived longer if they were provided a dry habitat option upon re-exposure. Most recently, a study by McMahon et al. (2014) found a mild protective effect against chytridiomycosis from multiple prior exposures to Bd. In keeping with these results suggesting a relatively poor adaptive immune response, *in vitro* experiments involving the proliferation of splenic lymphocytes in culture, found that soluble factors released by Bd inhibited proliferation and caused apoptosis of T cells (from *X. laevis* and *R. pipiens*; Fites et al., 2013). These factors were found to be resistant to heat, acid and protease, were absent in Bd zoospores and were reduced by nikkomycin Z, suggesting they may be cell-wall components. Further work is currently underway characterizing these factors.

2.7 Project aims

To summarize, in response to concerns over the loss of amphibian biodiversity due to chytridiomycosis-associated species declines and extinctions, I developed a multifaceted

research agenda aiming to address key priorities and knowledge gaps related to 1) the continued impact of endemic Bd on amphibian populations, and 2) the potential for immunologic management strategies to provide long-term and sustainable mitigation of chytridiomycosis.

Thus the aims of my research included 1) to investigate and characterize population- and individual-level impacts of endemic chytridiomycosis, 2) to investigate the amphibian host immune response to Bd infection to determine the practical utility of immunization, and investigate the potential for evolution of resistance, and 3) to evaluate strategies to mitigate endemic chytridiomycosis and minimize the impact of future emerging biodiversity diseases. Fig. 2.4 provides a schematic guide to these aims and their associated chapters and publications or manuscripts in this thesis.

Figure 2.4. Project aims, indicating division into thesis chapters and manuscripts/papers.

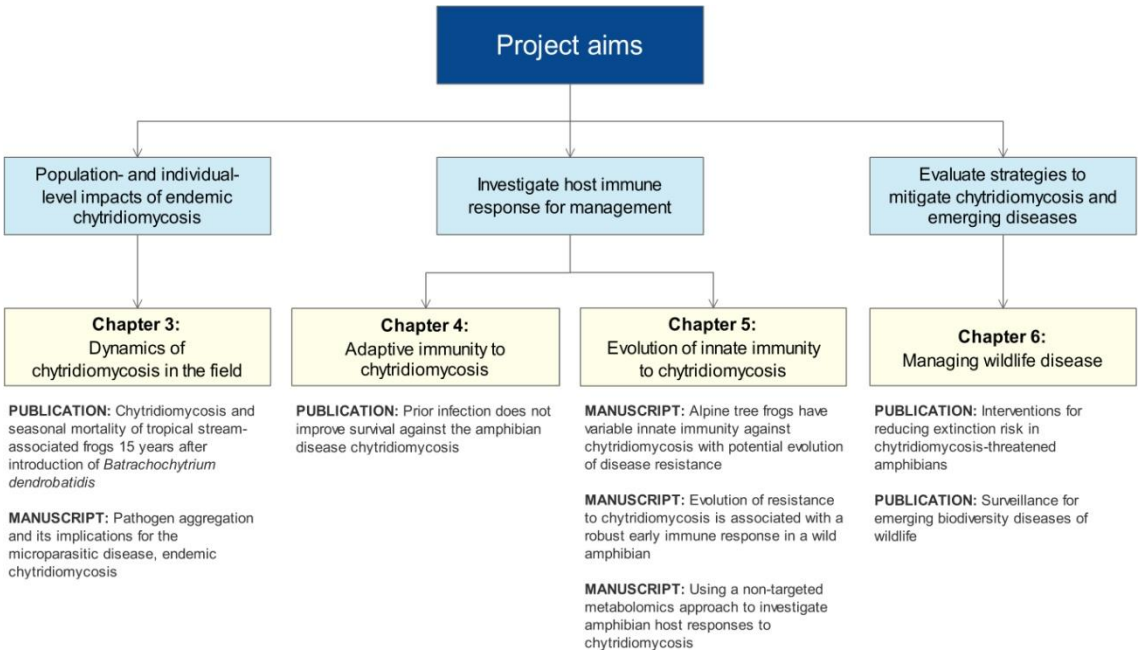

CHAPTER 3: Dynamics of chytridiomycosis in the field

3.1 Introduction

The fungal pathogen, *Batrachochytrium dendrobatidis* is now endemic in amphibian populations throughout the world, however the impact and dynamics of endemic chytridiomycosis are still relatively poorly understood. The potential for chytridiomycosis to cause ongoing amphibian population declines and extinctions once established in a region is of particular concern given the existing distribution of the fungus. Furthermore, an improved understanding of within-population and within-host pathogen distribution and the dynamics underlying infection transmission and recovery could assist in the management of vulnerable populations.

In this chapter I investigated an intensive two-year mark-recapture field study data set of the common mist frog (*Litoria rheocola*) from two populations in the wet tropics of Australia. I aimed to better understand the impact of endemic chytridiomycosis on amphibian populations, as well as characterize aspects of the underlying infection dynamics. This chapter addresses my first aim, to investigate population- and individual-level impacts of endemic chytridiomycosis (see Fig. 3.1).

This chapter consists of 1) a published peer-reviewed paper investigating host survival and recruitment probabilities using Cormack-Jolly-Seber and Pradel modeling, and 2) a manuscript in preparation using Multi-State Mark-Recapture modeling incorporating infection as a time-varying individual covariate, to investigate infection abundance and dynamics.

Figure 3.1. Project aims, highlighting Chapter 3: Dynamics of chytridiomycosis in the field.

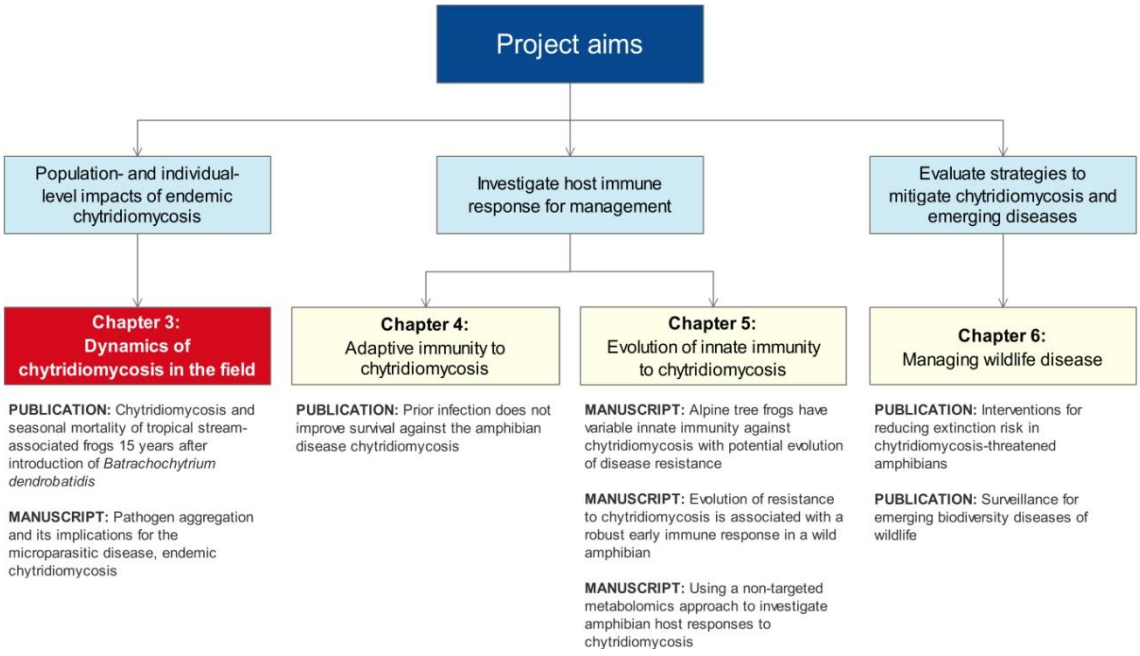

3.2 PAPER 1: Chytridiomycosis and seasonal mortality of tropical stream-associated frogs 15 years after introduction of *Batrachochytrium dendrobatidis*

This published peer-reviewed paper represents original research led by Andrea Phillott, who performed the majority of field work collecting data and swabs, assisted by the field experience of Keith McDonald and the research planning of Lee Skerratt. My role in the paper involved performing all data analysis, results interpretation and manuscript write-up. Andrea Phillott, Scott Cashins, Lee Berger and Lee Skerratt provided substantial editorial input.

The full reference for the published paper is:
Phillott, A. D., **Grogan, L. F.**, Cashins, S. D., McDonald, K. R., Berger, L., Skerratt, L. F. (2013) Chytridiomycosis and seasonal mortality of tropical stream-associated frogs 15 years after introduction of *Batrachochytrium dendrobatidis*. Conservation Biology 27:1058-1068.

The following text is a word for word copy of the manuscript published in the journal Conservation Biology. Section, table and figure numbering has been added or reformatted for this thesis for ease of reference. Since the journal uses American English, the spelling follows this convention.

3.2.1 Front matter

Chytridiomycosis and Seasonal Mortality of Tropical Stream-Associated Frogs 15 Years after Introduction of *Batrachochytrium dendrobatidis*

Running head: Seasonal mortality in chytridiomycosis

Andrea D. Phillott[1], Laura F. Grogan[1*], Scott D. Cashins[1], Keith R. McDonald[2], Lee Berger[1], Lee F. Skerratt[1]

Keywords: amphibian declines, *Batrachochytrium dendrobatidis*, endemic, mark-recapture, survival, population growth, recruitment

[1]One Health Research Group, School of Public Health, Tropical Medicine and Rehabilitation Sciences, James Cook University, Townsville, Queensland 4811, Australia
[2]Environment Protection Agency, Queensland Parks and Wildlife Service, PO Box 975, Atherton, Queensland 4883, Australia

[*] Address correspondence to L. F. Grogan, email laura.f.grogan@gmail.com

3.2.2 Abstract

Assessing the effects of diseases on wildlife populations can be difficult in the absence of observed mortalities, but it is crucial for threat assessment and conservation. We performed an intensive capture-mark-recapture study across seasons and years to investigate the effect of chytridiomycosis on demographics in 2 populations of the threatened common mist frog (*Litoria rheocola*) in the lowland wet tropics of Queensland, Australia. Infection prevalence was the best predictor for apparent survival probability in adult males and varied widely with season (0-65%). Infection prevalence was highest in winter months when monthly survival probabilities were low (approximately 70%). Populations at both sites exhibited very low annual survival probabilities (12-15%) but high recruitment (71-91%), which resulted in population growth rates that fluctuated seasonally. Our results suggest that even in the absence of observed mortalities and continued declines, and despite host-pathogen co-existence for multiple host generations over almost 2 decades, chytridiomycosis continues to have substantial seasonally fluctuating population-level effects on amphibian survival, which necessitates increased recruitment for population persistence. Similarly infected populations may thus be under continued threat from chytridiomycosis which may render them vulnerable to other threatening processes, particularly those affecting recruitment success.

3.2.3 Introduction

It is crucial to understand the effect of endemic disease (disease constantly present in a region; Andre and Day, 2005; Porta et al., 2008) on wildlife populations for threat assessment and conservation but this is difficult to achieve in the absence of mass mortalities and census information (Wobeser, 2007). Endemic disease can have insidious effects on population persistence because it can cause slow declines, suppress population densities, or render populations more vulnerable to stochastic events and other threatening processes (e.g., gradual decline of the southern corroboree frog [*Pseudophryne corroboree*]; Hunter et al., 2010). Subtle individual-level effects of endemic disease can range from decreased reproduction to morbidity and mortalities that may be unobservable due to their sporadic occurrence and acute course; increased predation of morbid individuals; rapid carcass decomposition, and scavenging (Stallknecht, 2007). Difficulties detecting population-level effects may be compounded where compensatory mechanisms confound effects on population growth rates, such as where increased recruitment compensates for reduced survival (Muths et al., 2011).

The recently emerged global pandemic of chytridiomycosis, a fungal skin disease of amphibians (*Batrachochytrium dendrobatidis*, hereafter Bd), has caused the decline and extinction of approximately 200 species of frogs worldwide (Skerratt et al., 2007). *Batrachochytrium dendrobatidis* has now become endemic in many climatically suitable environments around the world (Fisher et al., 2009b; Kinney et al., 2011; Murray et al., 2011a). Although much research has focused on overt epidemics or disease-induced declines in critically endangered species, there are potentially many more species globally that continue to be threatened by endemic chytridiomycosis. It is crucial to understand the population-level effect of endemic diseases such as chytridiomycosis so that populations at greatest risk of future collapse can be identified.

To better understand the nature of population effects of endemic chytridiomycosis, we performed an intensive capture-mark-recapture (CMR) study in 2 endemically infected populations of the common mist frog (*Litoria rheocola*) in the lowland wet tropics of northeast Queensland, Australia. The common mist frog is a suitable model for investigating endemic chytridiomycosis because individuals are susceptible to Bd and active in streams throughout the year, and they share habitat with at least 6 other species of obligate stream-associated frogs that similarly have undergone severe population declines in Queensland since 1985 (McDonald and Alford, 1999). Populations of the common mist frog disappeared from upland protected areas (>400 m asl) from 1989-1994, but they persisted in anecdotally stable populations at lower elevations (McDonald and Alford, 1999; Richards et al., 1993). These declines were due to the arrival of Bd, which has been detected in frogs collected from the region since 1989 (Murray et

al., 2010a). We sought to assess the overall effect of endemic chytridiomycosis on populations approximately 15 years after introduction.

Results of previous empirical studies suggest that due to thermal tolerance limits of Bd, infection prevalence in common mist frogs should vary seasonally (Forrest and Schlaepfer, 2011; McDonald et al., 2005). In addition, endemic infection may continue to cause individual frog mortality, as demonstrated by Murray et al. (2009) in southeast Queensland 30 years after disease emergence. On the basis of these results, we hypothesize that overall survival probabilities vary seasonally in our populations, where lowest survival correlates with highest prevalence and occurs during winter months. This scenario does not elucidate the effect of endemic chytridiomycosis on populations however, for which it is necessary to understand population responses to putatively lowered survival rates of infected individuals. Such populations may persist and appear stable over the long term if overall population abundance is reduced, if infection prevalence is very low, if other regulatory mechanisms compensate for chytridiomycosis-induced mortalities (e.g., predation mostly of sick individuals), or if mechanisms for compensating recruitment are invoked. Alternatively, consistent with the finding of recent upland recolonization, 15 years of co-evolution at our study sites may have altered the host-pathogen interaction and led to the expression of effective innate immunity or reduced pathogen virulence (McDonald et al., 2005). This second scenario implies a declining effect of chytridiomycosis on the population and favors long-term persistence through survival of reproductive adults.

We investigated whether in a long-term endemically infected tropical system Bd may still have an important seasonal effect on overall apparent survival probabilities at the population level.

3.2.4 Methods

3.2.4.1 Species ecology and study sites

The common mist frog is a nocturnal rainforest and wet sclerophyll forest specialist with an obligate association to creeks and streams for breeding. Males are present throughout the year and exhibit territorial inter-male spacing along stream banks or rocks, whereas females are present from March-July (Hodgkison and Hero, 2002; McDonald and Alford, 1999). Females and juveniles spend less time along the stream; likely, they favor terrestrial foraging sites (Hodgkison and Hero, 2002).

From November 2005 to October 2007 we surveyed a 150-m-long transect of an unnamed creek in lowland wet tropical rainforest of Tully Gorge National Park (hereafter Tully) (145°38'E

17°46'S, 130 m asl) for a total of 26 sampling trips. Each sampling trip to Tully consisted of 1-3 consecutive sampling nights. The interval between trips averaged 28 days (range 6-88). Similarly, a transect 200 m in length along the creek from Bridge 7 in Murray Upper National Park (hereafter Kirrama) (145°52'E 18°11'S, 206 m asl) was surveyed during 18 sampling trips that consisted of 1-4 sampling nights. The interval between trips averaged 31 days (range 9 to 139). We selected study sites and transect lengths in accordance with breaks in habitat to minimize expected frog migration out of the site (a large waterfall and the Tully River bounded the Tully site) and for logistical reasons. Both populations could migrate relatively freely through the rainforest to adjacent streams, however dispersal lessened during the drier winter months, and frogs were rarely encountered in the Tully River downstream of the Tully site.

The creek beds at the 2 sites were composed of granite rocks of variable size; water flow was generally fast in the wet summer months and there were small waterfalls and riffles (> 5 cm/second^2). Slower-flowing connected pools formed in winter when rainfall decreased. Surrounding vegetation was characterized by mesophyll to notophyll vine forest on moderately fertile granite and rhyolite that had patches of remnant vegetation including pink bloodwood (*Corymbia intermedia*) and red stringybark (*Eucalyptus pellita*) (Department of Environment and Resource Management, 2011).

Tully Gorge and Murray Upper National Parks are in the monsoonal Austral tropics and have warm, moist summers with high rainfall from December to March. Spatially interpolated weather values were obtained from the SILO climate database (Jeffrey et al., 2001). At Tully average maximum temperature and rainfall for summer over the study period were 31.6 °C and 1066 mm respectively, and for winter were 24.7 °C and 220 mm. At Kirrama average maximum temperature and rainfall for summer were 28.1 °C and 712 mm respectively, and for winter were 20.2 °C and 148 mm (Bureau of Meteorology, 2008).

3.2.4.2 Mark-recapture sampling

Frogs were observed after dusk with spotlights and captured by hand by experienced workers. Workers wore a new pair of plastic gloves for each frog they caught (Phillott et al., 2010b). Snout-urostyle length (SUL) was measured with Vernier calipers, and clinical signs of disease were recorded if observed (peripheral erythema and skin shedding). Gender and breeding characteristics were also recorded (Hodgkison and Hero, 2002).

We examined adult frogs for previous identifying toe-tip marks or missing digits. If not previously marked, we made a unique toe-tip mark by removing the toe-disc of up to 5 digits with disinfected dissection scissors (Phillott et al., 2010a; Phillott et al., 2007). The toe-tipping

scheme has been used with the Tully population since 1992 (McDonald et al., 2005). Juvenile frogs (< 24 mm SUL) were not marked and were excluded from analyses.

We swabbed each frog caught with a sterile dry swab following standard protocols (Hyatt et al., 2007). Swabs were stored dry at 4 °C and were analyzed within 6 months of collection for the presence of Bd DNA with the TaqMan real-time PCR protocol (Hyatt et al., 2007). Individual swabs were analyzed in triplicate, and each run included an internal positive control. A single positive result of one zoospore equivalent (ZSE) or greater was considered positive for optimized sensitivity (Murray et al., 2009; Skerratt et al., 2011b).

3.2.4.3 Capture-Mark-Recapture modeling

We sought to quantify unbiased estimates of demographic parameters in combination with infection data to explore the population-level effect of endemic chytridiomycosis. Hence, we used capture-mark-recapture (CMR) (Cooch et al., 2012; Lindberg, 2012) and performed stochastic modeling on the basis of maximum likelihood and the information theoretic approach (Burnham and Anderson, 2002). Capture-mark-recapture methods supply relatively robust estimates of population demographic parameters and provide promising techniques for assessing the effects of endemic disease on populations. In these analyses, we assumed that the chance of encountering an individual on a particular occasion was a product of 2 or more apparent probabilities (survival φ, recapture ρ, population growth λ, and recruitment f), which may be affected by predictor variables (e.g., infection status or environmental, linear, or individual covariates).

Analysis included defining biological questions, *a priori* hypotheses and estimable parameters; determining biologically plausible predictor variables; testing goodness of fit from general mark-recapture assumptions for the most parameterized models to determine an overdispersion parameter $\hat{c}$; specifying candidate model sets; selecting parsimonious models using small sample size and overdispersion-corrected quasi-Akaike's information criterion ($QAIC_c$); and performing multimodel inference via model averaging. We specify parameter and unconditional precision estimates (95% CIs), relative factor importance, evidence ratios of support between models for inference about certain hypotheses, and the model averaged effect sizes of infection status groupings where applicable.

We sought to determine the growth rates of the populations, and the importance of Bd and other covariates (environmental or individual) on survival and recruitment probabilities. These questions are associated with hypotheses that relate to estimable parameter probabilities (adult local apparent survival probability [φ] confounded by permanent emigration, recapture

probability[ρ], population growth [λ], and recruitment probability [*f*] confounded by permanent immigration) and biologically plausible predictor variables, including infection status at first capture (binary grouping variable, *g*), seasonally varying environmental covariates (temperature, rainfall, relative humidity, and radiation), linear variables (apparent trip prevalence; cyclical seasonal linear trend; noncyclic linear trend, and capture effort [*d*]), and a static individual covariate (snout-urostyle length as proxy for age) (Dochtermann and Jenkins, 2011) (Appendix A). We performed mark-recapture modeling with Program Mark (version 6, build 6002) (White and Burnham, 1999). We used the Cormack-Jolly-Seber (CJS) open population live-recaptures only approach for basic analysis and reverse time Pradel models (Pradel, 1996) to determine realized population growth rate (λ) and recruitment (*f*). We performed single imputation of population means for missing values. Females and juveniles were excluded from CMR analyses due to infrequent presence at the stream. A monthly temporal scale was used for data input; hence, parameters were estimated as monthly probabilities (where 1 month $= \frac{365}{12} \approx 30.42$ days). Candidate model sets for CJS and Pradel analyses for each study site were separately constructed *a priori* via a restricted form of the all subsets approach and tested systematically (Doherty et al., 2012; Hegyi and Garamszegi, 2011; Lukacs et al., 2010) (Appendices A, B and E). The number of variables was small relative to sample size to avoid Freedman's paradox (Lukacs et al., 2010). Fixed-effects models demonstrated superior parsimony to random effects models and hence were used exclusively in these analyses.

Several assumptions must be fulfilled for CMR analyses to be applied without bias (Lebreton et al., 2009; Lindberg, 2012). Toe-tip marks were permanent in adults for the study duration, and every effort was made to identify them correctly. Sampling time was negligible relative to sampling intervals. Two further assumptions relate to individual heterogeneity (in capture and survival probabilities), and these were formally addressed with goodness-of-fit tests on the most general model in the candidate set, from which the overdispersion parameter $\hat{c}$ was calculated ($\hat{c}$ = 1.145, 1.098 for Tully and Kirrama CJS analyses respectively [Appendix A]).

3.2.5 Results

3.2.5.1 Population and disease summary statistics

The observable population of adult common mist frogs was larger at Tully (302 frogs) than at Kirrama (88 frogs; Table 3.1). However, in both populations only 23 females were observed (Table 3.2). At Tully, although statistical significance was precluded by few captures, infection trends in captured females suggested higher infection prevalence (59% compared with 37% of males infected at first capture) and higher infection intensity than in males (mean zoospore load

of 415 zoospore equivalents compared with 40 zoospore equivalents in males). In addition, 3 of the 4 clinically infected frogs that died on capture during the study period were females. No amplexing pairs were observed; however, males were calling and possessed nuptial pads year round, and females were observed at the stream May-August.

Chytridiomycosis infection prevalence for each trip varied seasonally in both populations with highest prevalence during winter months (Table 3.3). There was a strong negative correlation between apparent prevalence and mean daily maximum temperature of the 28 days preceding each trip at Tully (Spearman's correlation coefficient -0.894, $p \leq 0.0005$, $n = 21$ sampling trips for CMR analyses) (Fig. 3.2). At Kirrama infection prevalence had low precision due to infrequent captures, but it varied seasonally (Table 3.3). Adult males appeared to maintain territories at both sites and rarely migrated within the study site; location for recaptured frogs (mean first recapture interval 72.3 days, median 45.5 days for Tully; mean interval 101.9 days, median 90 days for Kirrama) correlated strongly with location at initial capture (Spearman's correlation coefficient 0.877, $p \leq 0.0005$, $n = 128$ for Tully; 0.807, $p \leq 0.0005$, $n = 37$ for Kirrama).

3.2.5.2 Mark-recapture modeling

Model-averaged parameter estimates revealed clear seasonality in apparent survival, population growth, and recruitment probabilities (Figs. 3.3, 3.4 and Appendix B). Evidence ratio support for seasonal effects was strong at Tully (in a comparison of most parsimonious models of temporal constancy dot [.] or nonseasonal *d* models with seasonal effects models, ratios were 1134.3, 40614, and 35329 for survival, population growth, and recruitment respectively), which correlated with limited to moderate support at Kirrama (1.8306, 25.580, and 1.0379 for survival, population growth, and recruitment respectively) (Lukacs et al., 2007). There was no evidence for a seasonal effect on recapture probability at either site (most parsimonious models contained the variable capture effort *d* but not seasonal effects).

Apparent infection prevalence at each trip correlated negatively with and was the most important predictor variable for survival at Tully (relative predictor variable importance, reporting only those > 0.1, was prevalence 0.6287, temperature 0.1688, and seasonal trend 0.1262) (Fig. 3.3a). Sparse data at Kirrama precluded the usefulness of prevalence as a variable with that population (low precision) (Table 3.3); however, apparent survival estimates followed a similar seasonal trend to those at Tully (relative importance of predictors for survival were seasonal trend 0.2215, temperature 0.1707, rainfall 0.1217 and prevalence 0.1176) (Fig. 3.4a). There was predictor selection uncertainty for recapture at Tully (*d* 0.2891, relative humidity 0.2154, and radiation 0.1283) (Fig. 3.3b); however, the number of capture nights per trip was an

important predictor for recapture probability at Kirrama (d =0.9060) (Fig. 3.4b). Population growth at Tully was best described by a positive association with relative humidity at Tully (relative humidity 0.8376 and prevalence 0.1187) (Fig. 3.3c) and a seasonal linear trend in which spring was considered equivalent to autumn, at Kirrama (seasonal trend 0.6301 and temperature 0.2327) (Fig. 3.4c).

Despite seasonality, average annual survival probability over the study period (derived from daily model-averaged estimates interpolated via third-order piecewise polynomial) was 0.12 (95% CI 0.02-0.30) for Tully and 0.15 (95% CI 0.00-0.60) for Kirrama (from CJS candidate model sets). Annual recruitment was similarly 0.91 (95% CI 0.83-0.96) for Tully and 0.71 (95% CI 0.31-0.98) for Kirrama. Population growth fluctuated seasonally during the study period (Figs. 3.3c and 3.4c). The values above and the equation $\lambda = \varphi + f$ indicate that annual population growth was 1.03 (95% CI 0.84-1.26) for Tully and 0.85 (95% CI 0.31-1.58) for Kirrama, which suggests equivocal results for gradual decline in the latter. There was little apparent effect of Bd infection status at first capture on survival or recapture at both Tully and Kirrama (model-averaged effect size 95% CI for difference between group parameter estimate means contained zero).

Table 3.1. Encounter distribution summary of adult common mist frogs grouped by study site.

Study site	Capts[a]	Frogs[b]	Frogs captured > 1[c]	Range of capts per trip[d]	Max encounters[e]	Max period (days)[f]
Tully	535	302	128	7-53 (May 2007)	10	309
Kirrama	151	88	37	3-22 (May 2006)	5	506

[a]Total number of captures. [b]Total number of frogs captured. [c]Number of frogs captured more than once. [d]Month and year when highest number of frogs were observed in parentheses. [e]Maximum number of encounters recorded for any frog. [f]Maximum period over which an individual frog was observed.

Table 3.2. Number of male, female, and gender indeterminate adult common mist frogs captured.

Study site	Male (% total)[a]	Female (% total)	Unknown (% total)[b]	Total
Tully	284 (94.0)	16 (5.3)[c]	2 (0.7)	302
Kirrama	73 (83.0)	7 (8.0)[d]	8 (9.1)	88
Total	357	23	10	390

[a]Numbers in parentheses are percentages of total frogs per site. [b]Gender undetermined. [c]One female was recaptured. [d]No females recaptured.

Table 3.3. *Batrachochytrium dendrobatidis* (Bd) infection prevalence (prev) in adult common mist frogs.

Study site	Prev range (%)[a]	Lowest prev[b]	Highest prev[c]	Positive PCR tests (total tests)	Mean zoospore load (range)	SD[d]	Median[e]
Tully	5.3-65.4	February 2006	August 2007	193 (530)	28 (0-4028)	210.2	0
Kirrama	0.0-59.3	many[f]	July 2006	46 (148)	65.88 (0-4232)	479.0	0

[a]Range in point Bd infection prevalence measured per trip as percentages (Appendix A). [b]Month and year when the lowest prevalence was recorded. [c]Month and year when the highest prevalence was recorded. [d]Standard deviation of common mist frog zoospore loads. [e]Median common mist frog zoospore load. [f]Across-species trip prevalence at Kirrama was recorded as 0.0 during 4 of 18 sampling trips.

Figure 3.2. Apparent chytridiomycosis infection prevalence of adult male common mist frogs in Tully Gorge National Park.

Apparent chytridiomycosis infection prevalence of adult male common mist frogs (Appendix A), daily maximum temperatures (Temp Max) over the study period (from the end of the first survey interval), and mean daily maximum temperature for the 28 days preceding each trip (Temp Mean) at an unnamed creek in Tully Gorge National Park. Prevalence error bars are the 95% confidence interval of a proportion from the binomial distribution (dependent on sample size).

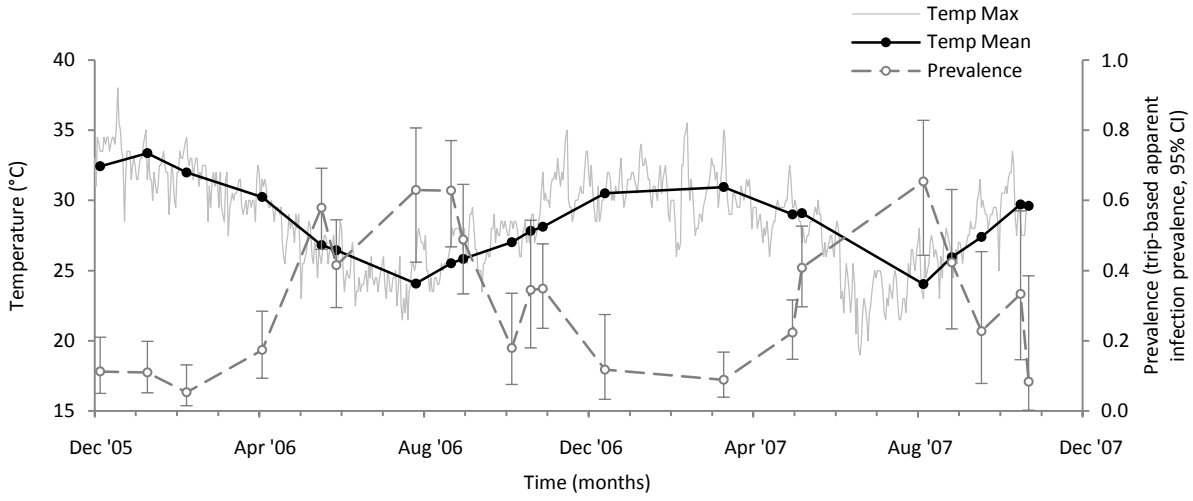

Figure 3.3. Model-averaged estimates for monthly (a) survival probability, (b) recapture probability, and (c) population growth rate and recruitment probabilities in Tully Gorge National Park.

Model-averaged estimates for monthly (a) survival probability, (b) recapture probability, and (c) population growth rate and recruitment probabilities with unconditional 95% confidence intervals from the Cormack-Jolly-Seber and Pradel analyses respectively for adult male common mist frogs at an unnamed creek in Tully Gorge National Park. The respective most highly supported predictor variables accompany each parameter probability curve for comparison (prevalence, apparent chytridiomycosis prevalence; capture effort, capture effort per trip; relative humidity, mean relative humidity 28 days preceding each sampling trip [Appendix A]). Points on the graph for trip sessions have been staggered horizontally where necessary for clarity, initial values correspond temporally with the end of the first survey interval, and a straight-line interpolation has been added between estimates for visual comparison of trends.

(a)

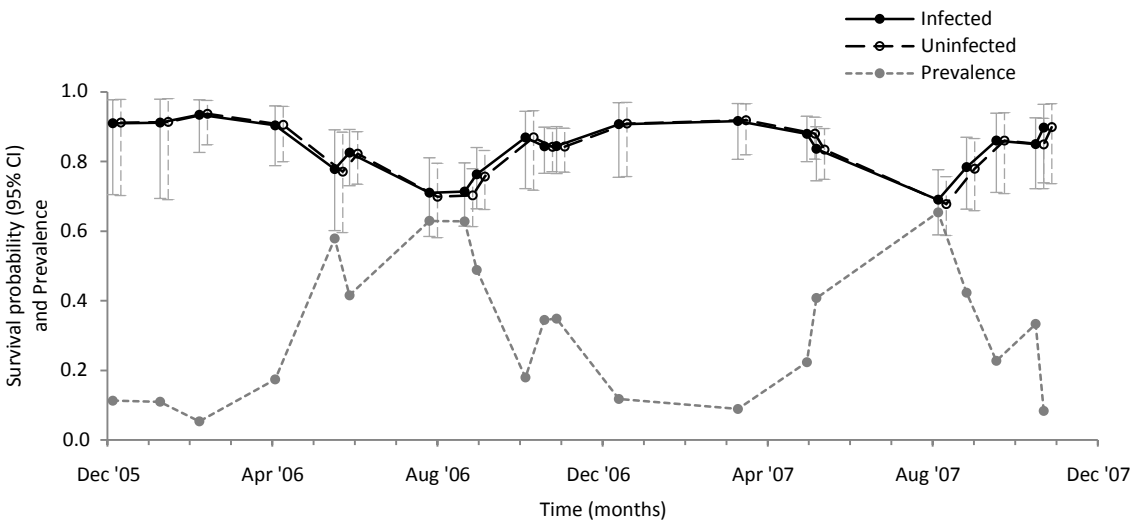
Infected
Uninfected
Prevalence
Survival probability (95% CI) and Prevalence
1.0
0.8
0.6
0.4
0.2
0.0
Dec '05
Apr '06
Aug '06
Dec '06
Apr '07
Aug '07
Dec '07
Time (months)

(b)

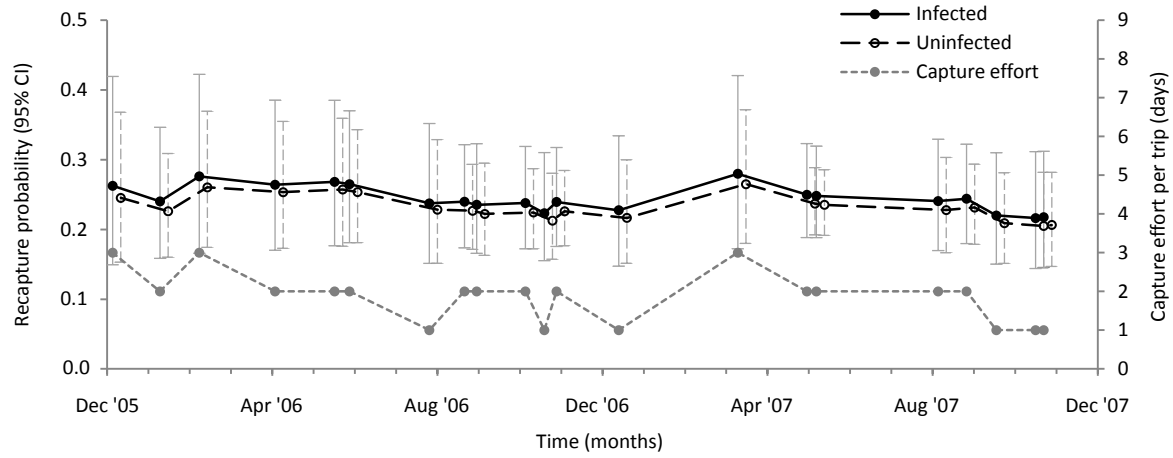
Infected
Uninfected
Capture effort
Recapture probability (95% CI)
Capture effort per trip (days)
0.5
0.4
0.3
0.2
0.1
0.0
9
8
7
6
5
4
3
2
1
0
Dec '05
Apr '06
Aug '06
Dec '06
Apr '07
Aug '07
Dec '07
Time (months)

(c)

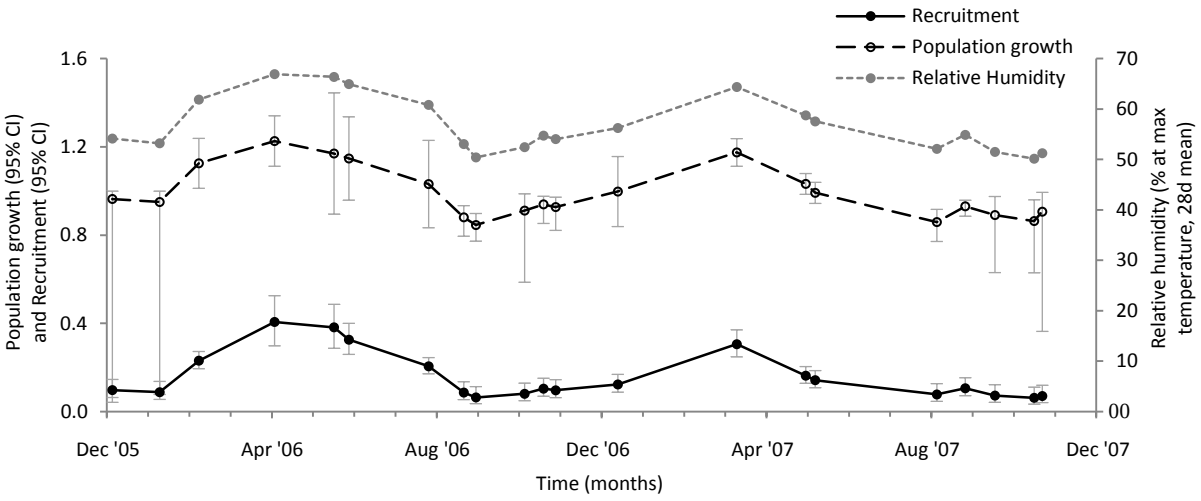
Recruitment
Population growth
Relative Humidity
Population growth (95% CI) and Recruitment (95% CI)
Relative humidity (% at max temperature, 28d mean)
1.6
1.2
0.8
0.4
0.0
70
60
50
40
30
20
10
00
Dec '05
Apr '06
Aug '06
Dec '06
Apr '07
Aug '07
Dec '07
Time (months)

Figure 3.4. Model averaged estimates for monthly (a) survival probability, (b) recapture probability, and (c) population growth rate and recruitment probabilities in Murray Upper National Park near Kirrama.

Model averaged estimates for monthly (a) survival probability, (b) recapture probability, and (c) population growth rate and recruitment probabilities with unconditional 95% confidence intervals from the Cormack-Jolly-Seber and Pradel analyses respectively for adult male common mist frogs at Bridge 7 in Murray Upper National Park near Kirrama. The respective most highly supported predictor variables accompany each parameter probability curve for comparison (temperature, mean daily maximum temperatures of 28 days preceding each trip; seasonal trend, cyclical seasonal trend [spring considered equivalent to autumn]; capture effort, capture effort per trip [Appendix A]). Points on the graph for trip sessions have been horizontally staggered where necessary for clarity, initial values correspond temporally with the end of the first survey interval, and a straight-line interpolation has been added between estimates for visual comparison of trends.

(a)

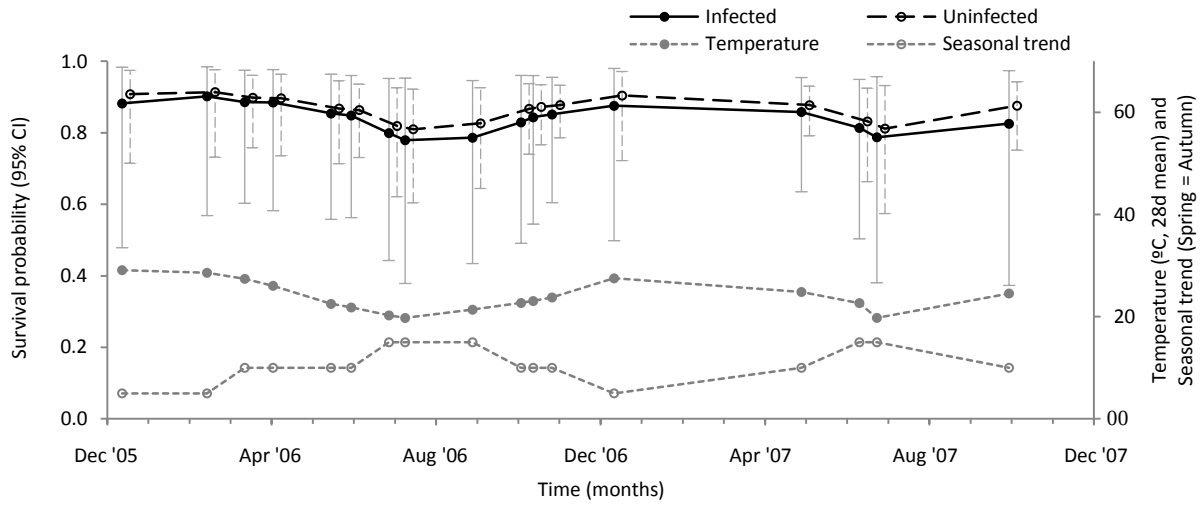
Infected
Uninfected
Temperature
Seasonal trend
Survival probability (95% CI)
Temperature (ºC, 28d mean) and Seasonal trend (Spring = Autumn)
1.0
0.8
0.6
0.4
0.2
0.0
60
40
20
00
Dec '05
Apr '06
Aug '06
Dec '06
Apr '07
Aug '07
Dec '07
Time (months)

(b)

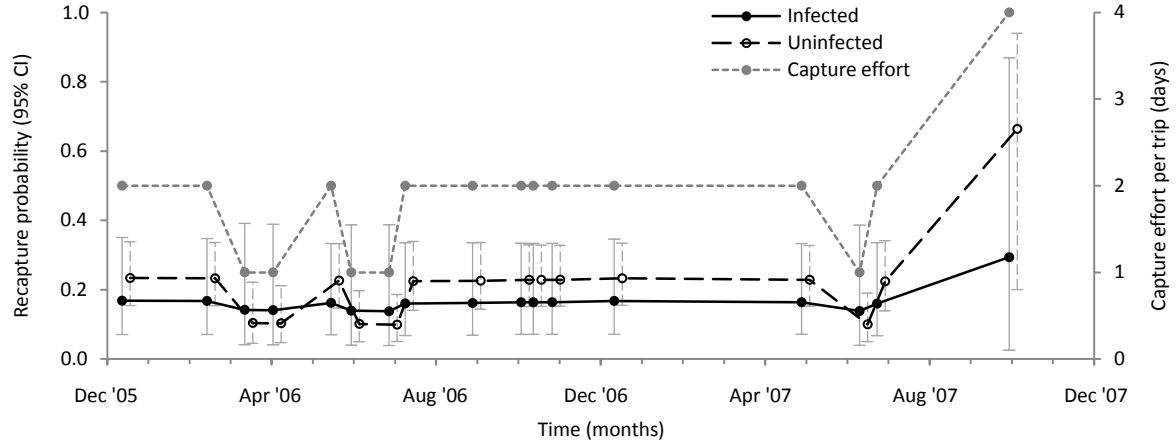
Infected
Uninfected
Capture effort
Recapture probability (95% CI)
Capture effort per trip (days)
1.0
0.8
0.6
0.4
0.2
0.0
4
3
2
1
0
Dec '05
Apr '06
Aug '06
Dec '06
Apr '07
Aug '07
Dec '07
Time (months)

(c)

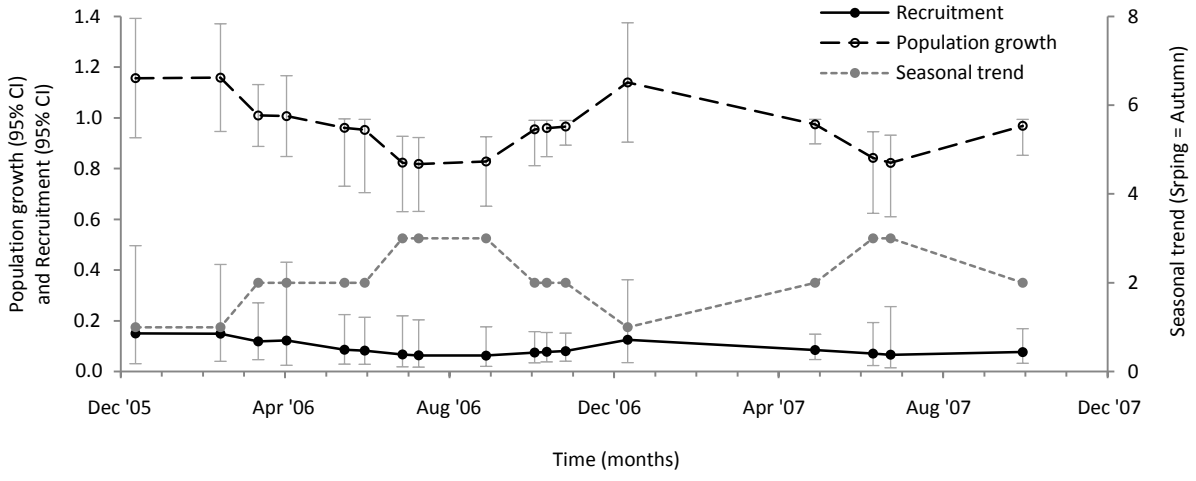
Recruitment
Population growth
Seasonal trend
Population growth (95% CI) and Recruitment (95% CI)
Seasonal trend (Srping = Autumn)
1.4
1.2
1.0
0.8
0.6
0.4
0.2
0.0
8
6
4
2
0
Dec '05
Apr '06
Aug '06
Dec '06
Apr '07
Aug '07
Dec '07
Time (months)

3.2.6 Discussion

Our results suggest that more than 15 years after the arrival of Bd in the region, chytridiomycosis continued to be an important cause of frog mortality at the population level. At our lowland study sites, however, high recruitment appeared to compensate for this high apparent annual adult mortality and resulted in population growth rates that fluctuated seasonally during the study period. The necessity for increased recruitment (or immigration) to maintain populations at their current size potentially renders these populations vulnerable to stochastic events and other threatening processes. Thus, these populations may still be threatened by endemic chytridiomycosis.

3.2.6.1 Chytridiomycosis prevalence and apparent survival

Apparent annual male survival probabilities were low at both study sites. Our results were limited to the male subpopulation for logistical reasons; thus, gender differences may contribute to biased interpretation, particularly if female survival has more effect on population persistence than male survival. Our occasional observations of females, however, suggested non significant trends in survival similar to, if not greater in effect than those of the male subpopulation. Our results suggested chytridiomycosis was the cause of high apparent winter mortality in both years despite infrequent detection of dying frogs. Linking population-level measures throughout and between years, Bd infection prevalence was the best predictor of apparent survival probability. Apparent Bd prevalence at Tully was almost 4 times as well supported as temperature and the other putative predictors including environmental covariates and snout-urostyle length. Although the results for Kirrama were not similarly clearly linked to prevalence, we suggest that limited recaptures reduced precision of the prevalence measure in this population and led to lower model parsimony, although the general trends in apparent survival were similar.

Our findings are consistent with those of previous studies conducted in other bioregions, which indicates the negative effect of endemic chytridiomycosis on frog populations. These studies demonstrate reduced individual survival probability due to infection (Murray et al., 2009), and that infected populations can have lower growth rates than comparable naïve populations (Pilliod et al., 2010).

3.2.6.2 Seasonality and breeding season

Seasonality of both infection prevalence and various demographic parameters (such as survival) at our sites is consistent with results of previous studies on chytridiomycosis (Kriger and Hero, 2006a) and was likely driven by climate (Altizer et al., 2006). Seasonal weather changes drive patterns in resource availability, host factors (behavior, immune function and contact rates) (Rachowicz and Vredenburg, 2004; Ribas et al., 2009; Rowley and Alford, 2007a), and pathogen factors (abundance, distribution and growth rates) (Piotrowski et al., 2004). Our

finding of a strong negative correlation between prevalence and temperature is consistent with previous evidence that suggests an optimal range of temperatures for Bd growth (17-25°C) (Forrest and Schlaepfer, 2011). The correlations between temperature, prevalence, and survival we found are consistent with the loss of high-elevation populations of common mist frogs that coincided with the regional emergence of Bd (McDonald and Alford, 1999). Temperature is likely an important mechanistic driver of infection prevalence in our susceptible range-contracted but currently nondeclining endemic system, and in turn, prevalence was an important driver of seasonal adult mortality.

The presence of transient females and high male abundance at the stream during May-August (autumn and winter) suggests this was the breeding season, and the correlated capture locations of resident males between sampling trips was consistent with the maintenance of territories (Hodgkison and Hero, 2002). In a separate but related study, common mist frog tadpoles were observed at the stream year-round, but predominantly May-January (S. Cashins. unpublished data). We also identified high-capture deviance residuals during early winter (Appendix B), which suggests the presence of transient individuals during the breeding season (although these sampling trips were necessarily excluded from CMR analyses). The higher winter prevalence could thus also be caused by the increased potential for infection transmission due to higher host densities during the breeding season.

3.2.6.3 Management implications

Understanding the effect of endemic Bd on demographic parameters has important implications for short-term management strategies and the longer-term potential for evolution of host resistance, particularly where apparent annual host survival is low. We speculate that if reproduction during the breeding season occurs prior to or during the subclinical phase of infection and is followed by high adult mortality, then selection for resistance to Bd may have less opportunity to manifest between generations. Despite evidence for species, population, and individual differences in susceptibility to chytridiomycosis (Searle et al., 2011; Tobler and Schmidt, 2010), to date only one study has demonstrated evidence for intergenerational selection for resistance to infection (Savage and Zamudio, 2011). Population dynamics such as those described above may contribute to slowing the evolution of resistance to chytridiomycosis, particularly where infection is not vertically transmitted and juveniles favor terrestrial foraging sites, which reduces their prebreeding infection risk (Hodgkison and Hero, 2002).

High apparent mortality of the reproductive subpopulation additionally forces dependence on seasonal recruitment of juvenile or immigrating males (consistent with high recruitment found

here). Without baseline demographic data (due to the absence of Bd-naïve populations), we speculate that these infected populations may be facing physiological boundary thresholds for their reproductive capacity, as demonstrated by Pilliod et al. (2010) and Muths et al. (2011), and may be at lower abundance than if the disease were absent. Depending on meta-population connectivity, resource quality, and the presence of other synergistically acting threatening processes, these populations may have increased vulnerability to stochastic perturbations (such as drought and cyclones). We suggest use of adaptive management strategies to improve understanding of the degree of threat imposed by endemic chytridiomycosis (Woodhams et al., 2011). Comparing demographic responses between sites where active management has been undertaken and untreated sites may elucidate the capacity of these populations to recover from infection pressure or accommodate additional stressors. Reducing seasonal mortality may relieve the necessity for high recruitment or increase baseline population abundance.

3.2.6.4 Study uncertainties

We were unable to quantify mortality attributable to chytridiomycosis in this study because there was no apparent effect of infection status at first capture on survival or recapture probability. This was not unexpected because in the field the infection is frequently gained and lost through time (consistent with Briggs et al., 2010). The use of time-varying individual covariates and multistate designs (Murray et al., 2009) is currently precluded for Pradel analyses, although methods may soon be developed (Lebreton et al., 2009). In addition, the use of highly sensitive diagnostic tests and the short time course and high mortality of clinical disease meant that ill individuals comprised only a small proportion of the captured subpopulation (moribund frogs were rarely observed) (Cooch et al., 2012). Inference was thus limited to the observable population which in this case largely excluded the moribund class and females and juveniles. Additional limitations of the study include our use of spatially interpolated climatic variables, which meant we could not account for small-scale habitat factors (Bureau of Meteorology, 2008; Jeffrey et al., 2001), and possible effects of toe-tipping on both survival and recapture probabilities (Phillott et al., 2010a).

Apparent survival probabilities are confounded with permanent emigration in mark-recapture studies (Murray et al., 2010b). However, our study extended across years, and we found high site fidelity in recaptured males (45% of the male population). This finding reduced the likelihood of emigration confounding. Moreover, periods of lowest apparent survival corresponded with the influx (or higher visibility) of transient males during the breeding season, so confounding of survival by emigration is a less plausible explanation. In addition, we speculated that predominantly subclinical infection prevalence is unlikely to be a good predictor

of emigration probability due to the absence of marked physiological changes, although further research into effects of subclinical chytridiomycosis on frog behavior is warranted.

3.2.6.5 Conclusions

Our results suggest that even in the absence of observed mortalities and continued declines, endemic chytridiomycosis may have important seasonally fluctuating population-level effects on amphibian survival. The low apparent survival probability of adult common mist frogs necessitates increased annual recruitment for population persistence. Seasonal mortality of reproductive adults may also have implications for the long-term evolution of resistance to chytridiomycosis. We found that seasonal increases in prevalence negatively affected survival, despite host-pathogen coexistence for multiple host generations, and this finding suggests that these and similar endemically infected populations may be under continued threat from chytridiomycosis and thus may be vulnerable to other threatening processes, particularly those affecting recruitment success.

3.2.7 Acknowledgments

We thank H. Ricardo and volunteers for assistance in the field, S. Garland and R. Campbell for PCR testing, and B. Scheele for helpful comments on the manuscript. This study was conducted with approval by the James Cook University Animal Ethics Committee (certificate A970) and Queensland Environmental Protection Agency (fauna permit WISP033606305). The Department of Environment Heritage provided funding via the tender 42/2004, Experimental Research to Obtain a Better Understanding of the Epidemiology, Transmission and Dispersal of Amphibian Chytrid Fungus in Australian Ecosystems.

3.2.8 Supporting information

Detailed information about predictor variables, goodness-of-fit testing, construction of candidate model sets and abbreviated tables of results are available in Appendices A and B. The authors are solely responsible for the content and functionality of these materials. Queries (other than absence of the material) should be directed to the corresponding author.

3.3 PAPER 2: Parasite aggregation and its implications for the microparasitic disease, endemic chytridiomycosis

This manuscript in preparation represents my original data analysis, results interpretation and manuscript write-up based on an alternative more complex analysis with a different focus, from the data reported in Phillott et al (2013). As such, similarly to the previous paper, the data was collected by Andrea Phillott. Andrea Phillott, Ben Scheele, Lee Berger, Scott Cashins, Sara Bell, Robert Puschendorf and Lee Skerratt provided substantial editorial input.

The full reference for the manuscript is:
Grogan, L. F., Phillott, A. D., Scheele, B. C., Berger, L., Cashins, S. D., Bell, S. C., Puschendorf, R., Skerratt, L. F. (in prep) Parasite aggregation and its implications for the microparasitic disease, endemic chytridiomycosis.

The following text was prepared for submission to the Journal of Applied Ecology. Section, table and figure numbering has been added or reformatted for this thesis for ease of reference. Since the journal uses American English, the spelling follows this convention.

3.3.1 Front matter

Parasite aggregation and its implications for the microparasitic disease, endemic chytridiomycosis

Authors:
Laura F. Grogan[1*], A. D. Phillott[1,2], Benjamin C. Scheele[3], Lee Berger[1], Scott D. Cashins[1], Sara C. Bell[1], Robert Puschendorf[4], Lee F. Skerratt[1]

Author affiliations:
[1]One Health Research Group, School of Public Health, Tropical Medicine and Rehabilitation Sciences, James Cook University, Townsville, Queensland 4811, Australia
[2]Biological Sciences, Asian University for Women, Chittagong 4000, Bangladesh
[3]Fenner School of Environment and Society, College of Medicine, Biology & Environment, Australian National University, Forestry Building 48, Linnaeus Way, Canberra, ACT 0200, Australia
[4]School of Biological Sciences, Plymouth University, Drake Circus, Plymouth, Devon, PL4 8AA, United Kingdom

Author email addresses:
Laura F. Grogan laura.grogan@my.jcu.edu.au

A. D. Phillott andrea.phillott@auw.edu.bd
Benjamin C. Scheele ben.scheele@anu.edu.au
Lee Berger lee.berger@jcu.edu.au
Scott D. Cashins scashins@gmail.com
Sara C. Bell saracbell@gmail.com
Robert Puschendorf robert.puschendorf@plymouth.ac.uk
Lee F. Skerratt lee.skerratt@jcu.edu.au

Running title: Parasite aggregation in chytridiomycosis

* **Corresponding author**
Name: Laura Grogan
Address: One Health Research Group, School of Public Health, Tropical Medicine and Rehabilitation Sciences, James Cook University, Townsville, Queensland 4811, Australia
Tel: (+61 4) 0225 5204
Email: laura.grogan@my.jcu.edu.au

Key index words:
Parasite aggregation, multistate, microparasite, mark-recapture, chytridiomycosis, endemic

3.3.2 Summary

Parasite aggregation is a central tenet of macroparasitic disease ecology, and implies that while few hosts harbor heavy parasite burdens, light infections are common. In contrast, the distribution of microparasites among hosts is rarely examined. We used the multistate mark recapture framework to study the abundance, distribution and transmission of *Batrachochytrium dendrobatidis* (the microparasitic fungal agent of the devastating amphibian disease chytridiomycosis) between individual common mist frogs (*Litoria rheocola*) in tropical Australia to investigate the effects of pathogen aggregation on disease dynamics. For the first time, three infection states were analyzed (uninfected, low and higher infectious burdens). We describe a highly over-dispersed pathogen distribution and differential state transition dynamics and survival probabilities between the three infection states. We found that 1) infections establish more in winter, consistent with temperature dependent effects on fungal growth; 2) recoveries (loss of infection) occur frequently in the field throughout the year but are less likely in winter; and 3) survival probabilities depend on infection burden. Our results suggest that pathogen aggregation is important in endemic chytridiomycosis, and that intensity of infection determines disease impact. We recommend quantifying individual infectious burdens as well as prevalence where possible in microparasitic diseases.

3.3.3 Introduction

Features of endemic chytridiomycosis suggest that using standard microparasite approaches for both modeling infection dynamics and interpreting field data, which neglect examination of underlying parasite distribution among hosts, may be inappropriate and instead macroparasitic approaches should be considered. This has implications for chytridiomycosis and more broadly for our understanding of microparasite disease ecology. *Batrachochytrium dendrobatidis* (hereafter Bd), the cause of the devastating amphibian fungal skin disease chytridiomycosis, has been described as possessing characteristics typical of macro- as well as microparasites (Briggs et al., 2010; Skerratt et al., 2007). Fungal pathogens are classified as microparasites both taxonomically and for the purposes of modeling their disease dynamics (Anderson and May, 1981), however Bd infections demonstrate a number of features more common to larger parasites such as helminths and arthropods (Briggs et al., 2010; Hudson and Dobson, 1998). Bd is a small, single-celled fungal organism and has a short life cycle within a single host involving two forms (infectious zoospore and reproductive sporangium; Berger et al., 2005a). In contrast to typical microparasites it appears to suppress an effective adaptive immune response in hosts (Cashins et al., 2013; Fites et al., 2013; Rosenblum et al., 2012b). While it is able to multiply asexually at a moderate rate on individual hosts, duration of infection can be long, and pathogenicity relies on high infectious burdens, a feature typical of macroparasites (Voyles et al., 2009; Vredenburg et al., 2010). Infectious burden also appears to be strongly dependent on external factors affecting the life cycle of the pathogen, such as temperature and moisture (Voyles et al., 2012), similar to macroparasitic diseases, and hence population infections often display highly seasonal dynamics and spatiotemporal distribution patterns consistent with environmental determinants (Murray et al., 2013; Phillott et al., 2013). Parasite aggregation, another feature common to macroparasites, occurs with chytridiomycosis (Skerratt et al., 2011b), but its effects on disease dynamics have not been investigated. Aggregation may help explain the inability to detect a difference in survival probability between two disease states (infected and uninfected) in the multistate mark-recapture study by Briggs et al. (2010), because the effects of a small proportion of highly infected frogs may be unobserved when grouped with low infection results.

Parasite aggregation involves most infected individuals having low infectious burdens, while few hosts have high burdens, and is an important component in understanding macroparasite disease ecology (Hudson and Dobson, 1998). Parasite aggregation means that the infection intensity pattern (described by the intensity-frequency curve) between hosts within a population tends to be highly positively skewed - thus infectious organisms are both spatially and temporally aggregated among hosts (Wilson et al., 2002). Chytridiomycosis provides a unique opportunity to examine the phenomenon of parasite aggregation with a microparasite (Hudson

and Dobson, 1998; Skerratt et al., 2011b). Unlike typical microparasitic infections, the epidermal localization of chytridiomycosis and the use of real time PCR enable the relative quantification of burdens between hosts (Hyatt et al., 2007). Given parasite aggregation is a feature of endemic chytridiomycosis, and infection intensity affects both survival and infection transmission probabilities, examining its effects on disease dynamics could have important implications for our understanding of the disease ecology of microparasites.

We used the Multi-State Mark Recapture framework to investigate transmission and recovery dynamics of endemic chytridiomycosis in the common mist frog (*Litoria rheocola*) in tropical north Queensland, Australia, as a function of individual-level infection status, population-level apparent prevalence, and environmental covariates. The study aimed to firstly, characterize the presence of Bd parasite aggregation in the context of a wild population of endemically Bd infected amphibians, and secondly, to investigate infection and recovery state transition dynamics throughout seasons and years. In particular, we wanted to determine whether defining infection as a binary variable (two infection states: uninfected and infected) or tertiary variable (three states: uninfected, and two discrete levels of infectious load which takes into account parasite aggregation) affects our understanding of infection dynamics.

3.3.4 Materials and methods

3.3.4.1 Species, site and sampling

We collected mark-recapture encounter data (via toe-tip marks) for adult male common mist frogs (*Litoria rheocola*) from a 150 m stream transect in lowland tropical rainforest of Tully Gorge National Park (145° 38' E 17°46' S, 130 m above sea level), Queensland, Australia over 22 trips between November 2005 and October 2007 (see Phillott et al., 2013 for further details of field work at this site). Bd is suspected to have arrived at this site around 1989. Although annual survival rates are low (12%) there is high recruitment (91%) and the population appears stable (Phillott et al., 2013). *L. rheocola* is an obligate stream-breeder, and the breeding season for this population occurs from May to August (coinciding with the dry winter season; Bureau of Meteorology, 2008) however adult males maintain calling territories at the stream throughout the year (Hodgkison and Hero, 2002; Phillott et al., 2013). Individual frogs were skin-swabbed at every capture (maintaining strict hygiene, and following standard protocols; Phillott et al., 2013; Phillott et al., 2010b), and swabs were analyzed for the presence of Bd DNA via quantitative PCR (qPCR; one well, one zoospore equivalent [*zse*] considered positive; Hyatt et al., 2007; Skerratt et al., 2011b).

3.3.4.2 Multi-State Mark-Recapture (MSMR) modeling

Multi-State Mark-Recapture analysis (MSMR; Lebreton et al., 2009) has recently emerged as a unified framework for capture-mark-recapture field studies (CMR; Lebreton et al., 1992). In this framework the chance of encountering an individual on a particular occasion is a product of its probability of recapture (ρ), conditional on its probability of surviving the interval (*S*), and its probability of making one of a number of defined transitions between states (ψ). The state concept enables investigation of time-varying individual categorical variables, such as mass, site, breeding status or disease status (see Lebreton et al., 2009 for review and synthesis), and has thus expanded CMR studies to the investigation of individual-level disease dynamics (Cooch et al., 2012). The advantage of CMR for studying wildlife disease is that it accounts for imperfect detection, compared with traditional epidemiological cohort near-census follow-up. Multistate modeling is increasingly being used for the study of disease in wild animals (see for example Conn and Cooch, 2009; Rossi et al., 2011; Senar and Conroy, 2004). MSMR has been applied to the study of chytridiomycosis in several ecological systems to date (Briggs et al., 2010; Murray et al., 2009), and provides less confounded parameter estimates (Jennelle et al., 2007) than the previously used measure of 'return rate' (Kriger and Hero, 2006b).

We applied the Information Theoretic approach (IT-AIC, following the steps outlined in Phillott et al., 2013) to explore state-specific endemic chytridiomycosis infection dynamics using the MSMR framework. We hence performed two- and three-state multistate modeling with program MARK (version 6.0; White et al., 2006) to elucidate the individual-level effect of chytridiomycosis infection on survival probability in the field by assigning frogs to an infection state at each capture via qPCR results. We particularly wanted to determine the probabilities for infection and recovery transitions, in order to understand the nature of infection dynamics *in situ* (Cooch et al., 2012; Murray et al., 2009).

We investigated the best predictors (several, due to model uncertainty) from the Cormack-Jolly-Seber (CJS) analysis for existing survival and recapture parameters for this data set (Phillott et al., 2013) in the new context of state transition probabilities. Hence we investigated survival as a function of infection status (*g*), apparent trip prevalence (*prev*), mean daily maximum temperature (°C) for the 28 days preceding each trip (*temp*), and a cyclical seasonal linear trend variable (*Ts*, where autumn is considered equivalent to spring). Recapture probability was investigated as a function of infection status (*g*), mean daily relative humidity (%) at maximum temperature for the 28 days preceding each trip (*rh*), mean daily radiation (MJ/m^2) over 28 days preceding each trip (*rad*), and capture effort (in days per trip *d*). Weather variables were obtained from the SILO climate database which provides spatially interpolated values from regional meteorological stations (Bureau of Meteorology, 2008; Jeffrey et al., 2001).

We defined infection status (g) as a time-varying individual covariate categorized into either two or three states on the basis of infection intensity (*zse*) at each capture. In two-state analysis A = Bd negative (uninfected) and B = Bd positive (infected). In three-state analysis, Bd load was discretized into groups: A = Bd negative, B = 1-4 *zse* "low", C > 4 *zse* "high". This low-burden group of hosts is the most poorly defined in terms of disease processes; individuals may be newly infected, recovering, resistant, their burdens may represent background contamination, or they may contain unaccounted sampling or laboratory error (McClintock et al., 2010). The chosen threshold between infection states (4 *zse*) allowed us to separately model the transmission dynamics of this low-burden group and eliminated potential confounding from the high-infected host group. In addition, multistate analysis methods have high data requirements, and this threshold permitted Bd positive results to be split evenly between states B (low intensity) and C (higher intensity) providing sufficient power for analysis (66 samples *zse* ≤ 4; 64 samples *zse* > 4; Fig. 3.5). We acknowledge that by artificially discretizing the continuous variable *zse* into low and high categories of intensity of infection there is some loss of information and some potential misclassification of infection levels close to the cutoff value (although the repeatability of the quantitative PCR at James Cook University is very high; Hyatt et al., 2007). However, the results will remain interpretable in terms of the effects of comparative levels of infection. The sample size was not sufficient for categorization into additional levels of infection intensity, such as a moderate group.

The state transition parameter ψ_i^{rs} defines the probability that an individual in state *r* at time *i* will be in state *s* at time *i + 1*. Importantly where there are more than two states, this includes the probability of transitions from each state in the MSMR Jolly-Movement Model (JMV; Lebreton et al., 2009), including the probability of remaining in the same state ψ_i^{rr}, and the outgoing probabilities for each state must sum to one (Fig. 3.5). States in this study represent discrete infection conditions (defined by *zse* infection intensities) in which the marked individual may potentially be encountered, conditional on being in that state and alive. Following the results in Phillott et al. (2013), and to incorporate both individual and population-level effects, we hypothesized that state transition probabilities are influenced by infection status (g), apparent prevalence (*prev*) and seasonal environmental covariates such as temperature (*temp*). As an example of how these effects might influence the transitions between states, recoveries should be associated with increased ambient temperature to reduce Bd growth (Voyles et al., 2012) and promote host thermoregulatory immunomodulation (Richards-Zawacki, 2010). Similarly, recoveries should also be associated with reduced prevalence as they require an absence of re-infection.

We applied the bootstrap and median $\hat{c}$ goodness of fit tests with the general model $S(g)\rho(g)\psi(g)$ (further details on goodness of fit testing and modeling assumptions can be found in Appendix C). Bootstrapping yielded p = 0.61 ($\hat{c}$ = 1.028), and median $\hat{c}$ yielded $\hat{c}$ = 1.110 (95% CI 0.925 - 1.295; 1000 simulations) for two state multistate data set, hence the most conservative estimate of $\hat{c}$ = 1.110 was used. Similarly for the three-state analysis, bootstrapping yielded p = 0.64 ($\hat{c}$ = 1.026), and median $\hat{c}$ gave $\hat{c}$ = 1.097 (95% CI 0.944 - 1.250; 1000 simulations), hence $\hat{c}$ = 1.097 was employed. Candidate model sets for two and three-state analyses were constructed separately *a priori* using a restricted form of the all subsets approach, and tested systematically (Appendices C, D and E; Doherty et al., 2012; Hegyi and Garamszegi, 2011; Lukacs et al., 2010). We constructed models using the intercept design matrix coding format and the logistic (logit) link function. Where numerical convergence was suspect, we employed the alternate optimization routine from within MARK, and assessed each model individually for estimable parameter count, adjusting as necessary (Cooch et al., 2012; Lebreton et al., 2009). We used $QAIC_c$ to rank model parsimony (Burnham and Anderson, 2002), model averaging to reduce selection bias (Lukacs et al., 2010), and we estimated monthly parameter probabilities ($1\ month = \frac{365}{12} \approx 30.42\ days$), reporting unconditional 95% Confidence Intervals (95% CI; Burnham and Anderson, 2002). Akaike weights were used to determine relative variable importance from entire candidate model sets (Doherty et al., 2012), and we report evidence ratios and model averaged effect sizes where appropriate for comparisons between states (Burnham and Anderson, 2002). Model averaged effect sizes were based on model averaged real parameter estimates and confidence intervals were unbounded on the real probability scale using the delta method for difference between two variances with the model averaged variance-covariance matrix. We additionally performed a discrete time simulation for a population of adult frogs employing the model-averaged trip-based parameter estimates from the three state multistate mark-recapture analysis over the study period to demonstrate the impact of estimated state transition and survival parameters on actual population numbers. Detailed methods and results from this simulation are available in Appendices C and D.

3.3.5 Results

3.3.5.1 Infection pattern summary

We made 424 captures of 243 uniquely marked adult male *L. rheocola* frogs throughout the study period (109 frogs were caught more than once). Forty-seven frogs (43% of those caught more than once) changed infection state at least once (became infected or recovered), and 13 frogs (28% of those caught more than twice) changed state two or more times (although only three of these, 23%, were re-infected after recovery). State transitions were approximately even with 28 infection and 34 recovery transitions. Two frogs gained and lost infection several times.

The highest infection intensity recorded prior to recovery was 123 *zse*. The intensity-frequency histogram for qPCR swab results for the whole study period was highly positively skewed (Fig. 3.6; 291 records for Bd negative, and 21 high *zse* records truncated for visualization; N = 421, range 0 to 4028 *zse*). The variance to mean ratio of infectious organisms per host (s^2/m) was 2227.47 (very much higher than one, indicative of parasite aggregation). The Weibull distribution ($\alpha = 0.46901$, $\beta = 15.259$) and negative binomial distribution were fit to the data (Fig. 3.6), and the corrected moment estimate of k (of the negative binomial distribution) was 0.0069, indicating a high degree of parasite aggregation (Wilson et al., 2002).

3.3.5.2 Multi-State Mark Recapture results

Model averaged parameter estimates revealed marked seasonality in survival and transition probabilities in both analyses (monthly model averaged estimates for state-dependent survival, recapture and state transition probabilities are reported with unconditional 95% confidence intervals in Figs. 3.7 and 3.8 for two- and three-state multistate analyses, respectively; see Appendix D for ranked tables of model results). While survival differed between infected and uninfected frogs in the two-state analysis, apparent survival probability estimates for the infected group were incongruously higher than those for the uninfected group, except during one winter trip session. Confidence intervals for the infected group were considerably wider, however, and overlapped those for the uninfected group for all trip sessions (Fig. 3.7a). In comparison, when the infected group was separated into two infection categories (group B with 1-4 zse, group C > 4 zse) in the three-state analysis, frogs with differing levels of infectious burden had differing survival probabilities (frogs with > 4 zse had consistently lower survival; Fig. 3.8a). While recapture probabilities were relatively stable throughout the study period in both analyses, in the two-state analysis both uninfected and infected frogs had similar recapture probabilities (Fig. 3.7b), whereas in the three-state analysis the low-burden group had low recaptures compared with the high-burden group (although confidence margins were wide in the three-state analysis; Fig. 3.8b).

Parameter estimates revealed marked seasonality in state transition probabilities between infection states. In the two-state analysis, frogs were much more likely to become infected in winter (correlating with prevalence), while there was a moderate reduction in the probability for recovery transitions during this period in the infected group (Fig. 3.7c). The three-state analysis further highlighted these trends with some exceptions despite overlapping confidence margins (transitions constituting the gain of or increase in infectious burden shown in Fig. 3.8c; reduction of infectious load or loss of infection transitions shown in Fig. 3.8d). The highest probability for infection transitions occurred during winter from the uninfected (group A) to low-burden frogs (group B). Recovery transition (loss of infection) probabilities were seasonal,

peaking during summer and autumn, and similar between both high and low-burden groups. Stationary transition probabilities (shown in Fig. D.2, Appendix D) were derived from the aforementioned model-averaged transition probabilities and probability theory which states that the sum of the probabilities of leaving each state must equal one. Hence throughout most of the year, among those surviving a sampling interval, frogs were most likely to either remain in the uninfected state, or return to that state through infection recovery (Fig. D.2, Appendix D). Low-burden frogs (group B) were observed to increase their infectious load (to group C) at a relatively low and stable rate throughout the study (Figs. 3.8c, D.2b, Appendix D). Hypothetical population dynamics (including variation in total population size) based on these transition and survival probabilities are exemplified in a series of three population dynamics simulation models illustrated in Fig. D.1 (Appendix D).

Despite model selection uncertainty, the most parsimonious models in both analyses modeled apparent survival and state transition probabilities as a function of a multiplicative interaction between individual-level infection state and population-level infection prevalence (the models $S(g \times prev)\rho(d)\psi(g \times prev)$ and $S(g \times prev)\rho(g + rad)\psi(6g \times prev)$, with 9.1% and 20.4% support for two- and three-state analyses respectively). Ranked relative predictor variable importance (reporting only those > 0.1) for two-state analysis were *prev* 0.6228, *temp* 0.3400 for survival; *d* 0.36301, *rad* 0.29044, *rh* 0.24491 for recapture; and *prev* 0.9254 for transition. For three-state analysis these were *prev* 0.8700, *temp* 0.1298 for survival; *rad* 0.5109, *rh* 0.2632, *d* 0.1674 for recapture; and *prev* 0.9264 for transition.

The model averaged effect size as a mean across trips for the survival difference between infected and uninfected groups in the two-state analysis was 0.1070, with the infected group demonstrating higher apparent survival overall (95% CI -0.0577 to 0.2717). Similarly, the model averaged effect sizes for survival in the three state analysis were as follows: B-A 0.1184 (95% CI -0.0448 to 0.2815), B-C 0.2610 (95% CI -0.1573 to 0.6794) and A-C 0.1427 (95% CI -0.2086 to 0.4940). While there was limited support for an effect of individual infection status on apparent survival in the two-state analysis (the evidence ratio comparing most parsimonious models with and without *g* was 2.8222), there was correspondingly strong support in the three-state analysis (evidence ratio 695.20), and strong support in both analyses for an effect of infection status on state transition probability (evidence ratios > 918.90 and 319.36 for the two- and three-state analyses, respectively; Lukacs et al., 2007).

Figure 3.5. Example schematic illustrating state transition probabilities (ψ) and survival probabilities (S) for the respective infection states at capture session six (drawn from the three state multistate analysis).

The notation ψ^{rs} indicates the monthly state transition probability from state *r* to state *s* from time (capture session) *i* to *i+1*, and S^t represents survival probability from time *i* to time *i+1*, for individuals in state *t*. Circle sizes are representative of the relative expected population size (from the simulation), and arrow line thicknesses represent the relative magnitude of the respective probabilities.

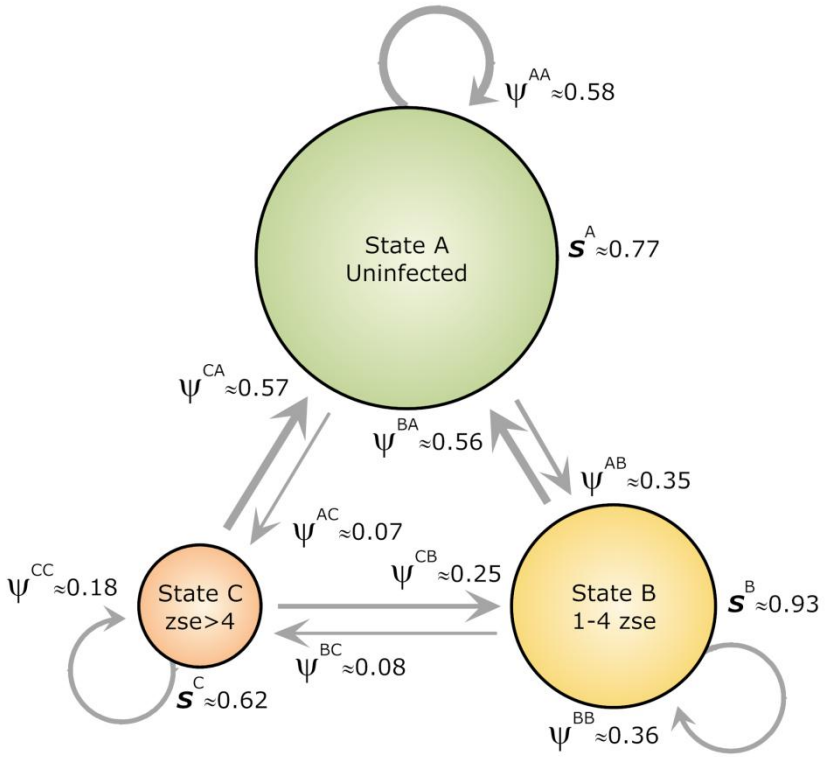

Figure 3.6. Intensity-frequency histogram showing highly aggregated infectious organism distribution between individual hosts (highly positively skewed).

Fitted Weibull and negative binomial distributions are displayed. N = 421; 291 Bd negative records and 21 high zoospore records were truncated for visualization; original data range 0 to 4028.

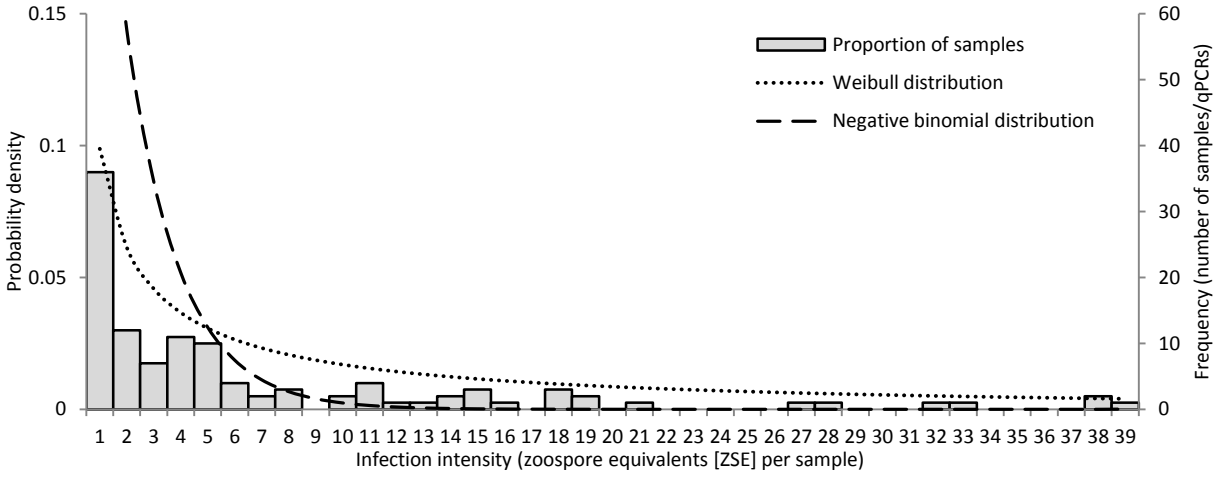

Figure 3.7. Model averaged estimates for monthly (a) survival probability, (b) recapture probability, and (c) state transition probability with unconditional 95% confidence intervals from the two-state multistate analysis for male adult *L. rheocola* at Tully.

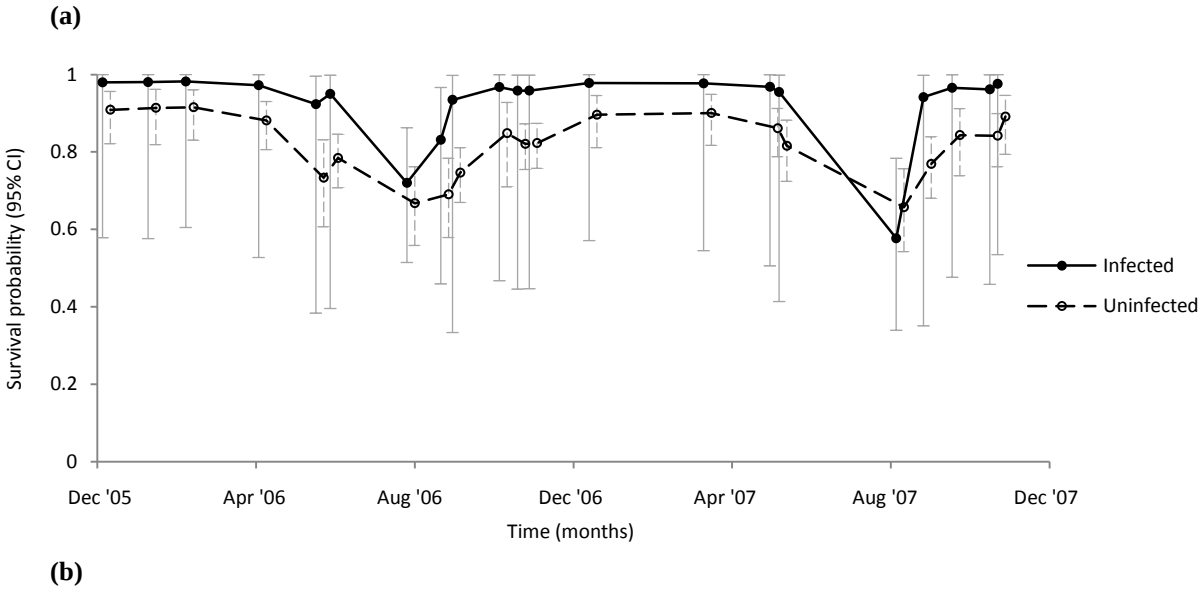

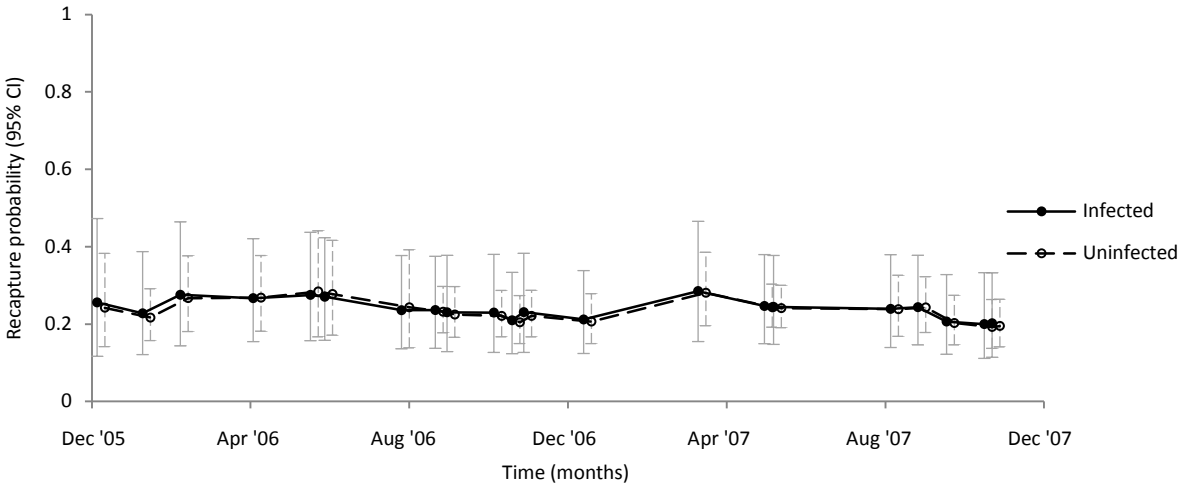
Recapture probability (95% CI)
1
0.8
0.6
0.4
0.2
0
Dec '05
Apr '06
Aug '06
Dec '06
Apr '07
Aug '07
Dec '07
Time (months)
Infected
Uninfected

(c)

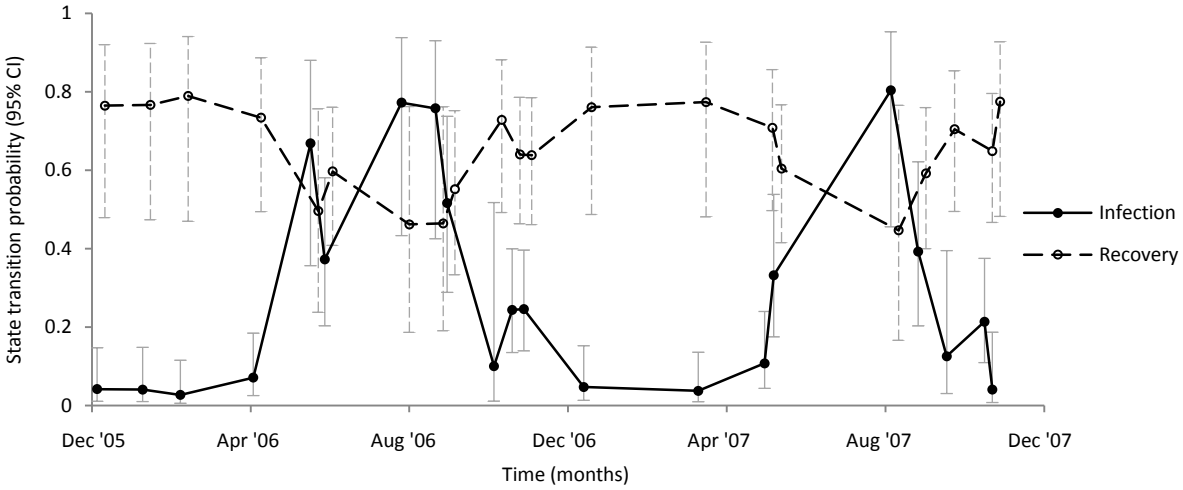
State transition probability (95% CI)
1
0.8
0.6
0.4
0.2
0
Dec '05
Apr '06
Aug '06
Dec '06
Apr '07
Aug '07
Dec '07
Time (months)
Infection
Recovery

Figure 3.8. Model averaged estimates for monthly (a) survival probability, (b) recapture probability, (c) infection transition probabilities, and (d) recovery transition probabilities at Tully.

Model averaged estimates for monthly (a) survival probability, (b) recapture probability, (c) infection transition probabilities, and (d) recovery transition probabilities at Tully with unconditional 95% confidence intervals from the three-state multistate analysis for male adult *L. rheocola* at Tully. States are defined as: state A = Bd negative (uninfected), state B = 1-4 *zse*, state C > 4 *zse*.

(a)

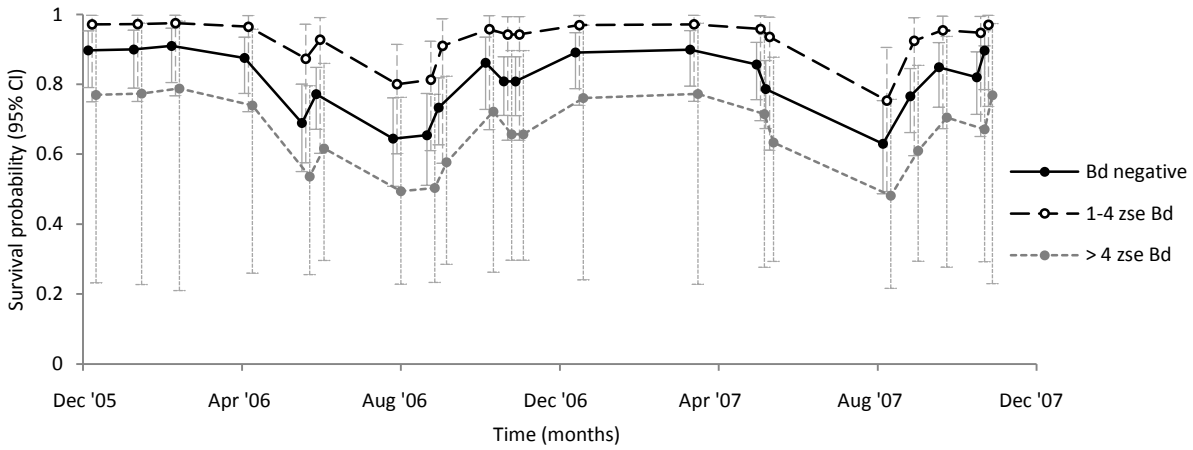

(b)

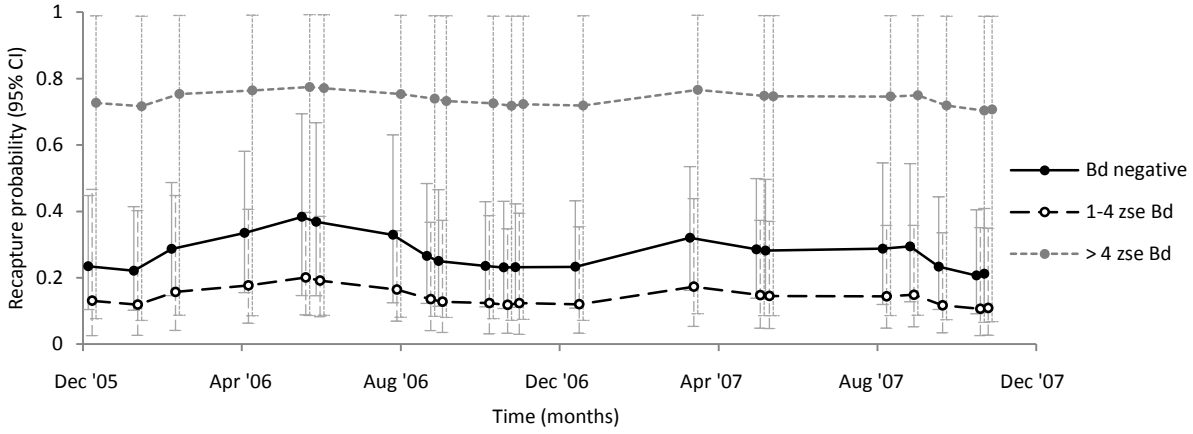

(c)

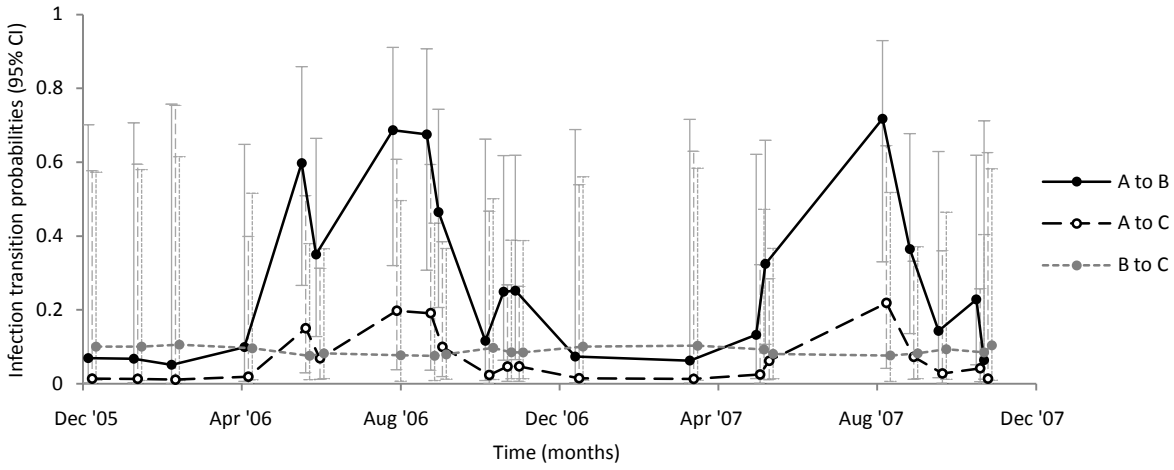

(d)

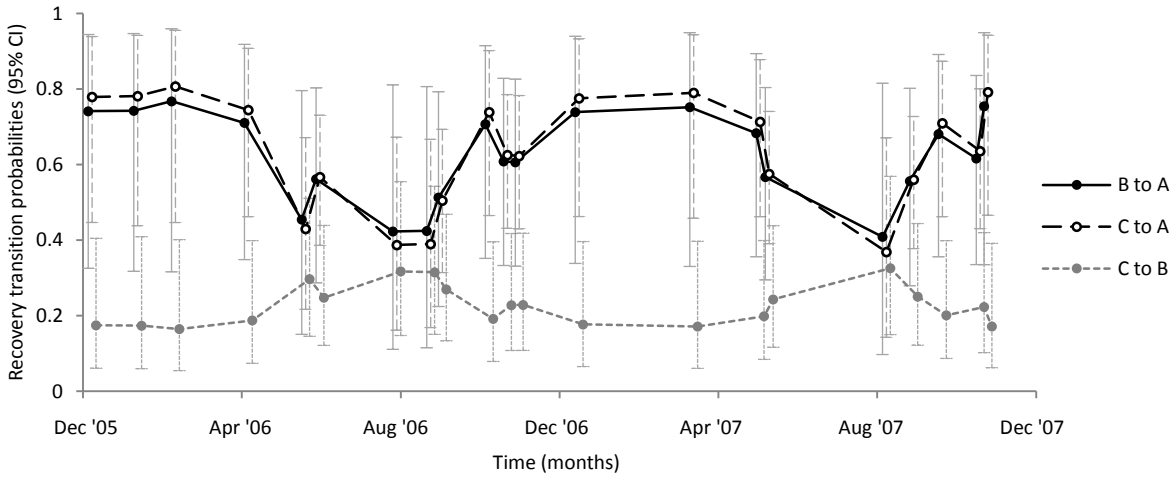

3.3.6 Discussion

We found marked spatiotemporal aggregation of Bd within our endemically infected wild amphibian population, as demonstrated by a highly over-dispersed intensity-frequency distribution curve (Fig. 3.6). Thus, while most infected individuals had low burdens, a few hosts had high burdens. Categorizing infectious burdens into low or high groups based on qPCR swab results allowed us to partially resolve paradoxical results from our two-state analysis which were similar to those reported by Briggs et al. (2010). The model averaged estimates from our two-state analysis revealed a lower apparent survival probability for uninfected frogs compared with infected frogs, although confidence intervals for the infected state were wide (Fig. 3.7a). After taking parasite aggregation into account, apparent survival probability of infected frogs fell to either side of the uninfected group, with high-burden frogs having the lowest survival estimates (Fig. 3.8a). The reason for a difference between the two and three state analyses is the high degree of parasite aggregation and its differential effects; approximately half the infected frogs were classed in the low-burden group (Fig. 3.6). In addition, infection intensity was found

to be seasonally associated with survival as well as transmission and recovery probabilities. Our results are consistent with previous field work showing aggregation (Skerratt et al., 2011b), and linking reduced survival with higher Bd infection intensities (Murray et al., 2009), and also demonstrates that quantifying infectious burdens is key to understanding the ecology of chytridiomycosis.

We used the Multi-State Mark-Recapture (MSMR) framework to provide dynamic estimates of first-order Markov infection state transition probabilities and state-dependent survival estimates from field data whilst accounting for imperfect detection (Cooch et al., 2012; Murray et al., 2009). Compared with the single-state Cormack-Jolly-Seber model (Phillott et al., 2013), the MSMR framework permits reassessment of individual disease status at each capture, which is essential for examining individual-level infection dynamics and survival probabilities in a system where infection status fluctuates. Most disease studies utilizing MSMR analyses to date have categorized individuals on the basis of their infection status (uninfected versus infected states; Briggs et al., 2010; Murray et al., 2009). This binary definition in the presence of parasite aggregation can greatly diminish our understanding of survival and state transition probabilities, and here we demonstrate the importance of this effect through comparisons of two and three state analyses.

In our study, frogs gained and lost infection frequently, consistent with previous field data on mountain yellow-legged frogs (*Rana muscosa* and *R. sierrae*) in temperate USA (Briggs et al., 2010), and some individuals demonstrated numerous state transitions. Comparing two- and three-state analyses helped resolve the nature and magnitude of transition probabilities between disease states (Figs. 3.7c, 3.8c and 3.8d), separating those frogs observed with low infectious burdens from those with higher burdens. As expected from previous studies on the temperature dependence of Bd (Voyles et al., 2012), we found that frogs were most likely to become infected during winter months (June to August in the southern hemisphere), with the transition to a low infectious burden (1-4 *zse*) being most probable (Fig. D.2a, Appendix D). Alternatively, recovery from both low and high infectious burdens was equally probable and high throughout most of the year, dropping moderately during winter (Figs. D.2b and D.2c, Appendix D).

A relatively long incubation period (roughly 3-8 weeks between exposure and clinical signs; Berger et al., 2005b; Voyles et al., 2009) in an environmentally responsive pathogen means more chance for pathogen-adverse environmental conditions (such as temperature spikes) to favor host recovery and survival. Thus, recovery transitions may be favored over infection transitions throughout most of the year in areas with higher temperatures such as at low

elevation. A long incubation period also artificially inflates point prevalence measures and deflates mortality measures compared with pathogens that have short incubation periods. This is also likely to lead to a highly over-dispersed intensity-frequency distribution because most of the infected population is in the subclinical phase of the disease at any point in time (in endemically infected populations, unlike propagating epidemics which can rapidly lead to widespread mortality). Re-infection transitions were comparatively uncommon, however (only three of the 13 frogs that were observed to change state two or more times), possibly suggesting the presence of adaptive immunity in the field. However, our third simulation scenario (Fig. D.1c, Appendix D) assumed no effect of adaptive immunity and resulted in population dynamics consistent with our expectations and dynamics observed in the wild.

Finding that uninfected frogs had lower apparent survival probabilities than those in the low-burden state (Fig. 3.8a) was unexpected. The difference in apparent survival between these infection states was small to moderate (11% for two-state analysis, 12-26% for three-state analysis), and in all cases the 95% confidence margins for the effect size on the real probability scale included zero. Perhaps this small survival discrepancy, and part of the cause for the high level of parasite aggregation, is due to the low infection group representing more resistant individuals. Under laboratory conditions conducive to disease progression, infections occur only at low levels for about a week post-exposure (Hyatt et al., 2007) suggesting low infections in susceptible wild individuals would only be maintained if conditions for the disease were suboptimal or if individual frogs were resistant. In comparison, the uninfected group would contain susceptible individuals that eventually become exposed and die from the disease but are not re-caught prior to death. Similarly, the lower winter survival probabilities in the low burden and uninfected frogs compared with other seasons (given that pathogenicity relies on high infectious burdens; Voyles et al., 2009) is likely due to mild violation of the third mark-recapture assumption (see Appendix C) whereby frogs that die are assumed to be in the last measured infection state, whereas transition to another state is possible.

It is also possible that the above discrepancy may be due to emigration confounding in Capture-Mark-Recapture studies (Murray et al., 2010b; Schmidt, 2010). For example, differential permanent emigration rates between the two states may lead to different apparent survival probabilities. We have no *a priori* reason to suspect higher emigration in uninfected frogs or in those with high zoospore burdens compared with those having low burdens. Rather, frogs appeared to maintain calling territories on the stream year-round suggesting site fidelity (Phillott et al., 2013). We suggest future implementation of tracking studies to confirm emigration and survival rates. Regardless, utilizing three-state analysis helped to resolve apparent survival discrepancies between uninfected and high-burden states.

Implications of parasite aggregation for endemic chytridiomycosis can be separated into two categories; those that affect the way we study, model and report this disease; and those that affect actual disease dynamics. In the first instance, we have demonstrated empirically that failing to account for different levels of infectious burden between hosts can lead to errors in understanding of population dynamics (for example, through mark-recapture state categorizations, or ecological modeling). In addition, we highlight that the commonly reported measure of disease abundance, population infection prevalence, is particularly susceptible to errors in interpretation when used to compare populations with differing levels of parasite aggregation. In the second instance, parasite aggregation impacts population dynamics where infectious burden affects 1) pathogenicity, 2) the rate of production of the infectious stage released to the environment, or 3) the degree of host resistance or immunity (May and Anderson, 1979). The first two conditions occur in chytridiomycosis, based on this study and past work (Hyatt et al., 2007; Murray et al., 2009).

The specific effects of aggregation on populations will likely depend on the degree and predominant causes of the observed aggregation, and elucidating these may assist with predicting long-term population outcomes. There are three main potential causes of observed aggregation including 1) heterogeneous exposure, 2) variable multiplication within the host, and 3) sampling artifact (Hudson and Dobson, 1998). In the context of chytridiomycosis, exposure varies with the nature of transmission (direct or indirect transmission, both of which apply in chytridiomycosis; Rachowicz and Briggs, 2007), which is influenced by pathogen and host behavior and distribution both spatially and through time. Territorial, seasonal breeding and foraging behavior differs with gender and life stage in frogs leading to heterogeneous habitat use (Rowley and Alford, 2007a), and pathogen growth varies with temperature (Voyles et al., 2012). Secondly, variation in pathogen replication on the host may be caused by both differences in host susceptibility and pathogen virulence (Berger et al., 2005b; Tobler and Schmidt, 2010), although the latter would be more pronounced between populations. Variation in host susceptibility may be associated with past exposure history, genetic, physiological, morphological and immunologic characteristics, and there is some evidence for each of these, although their specific importance remains uncharacterized (Savage and Zamudio, 2011; Tobler and Schmidt, 2010). Pathogen replication may also vary between hosts as body temperature and metabolic rate fluctuate with ambient conditions (Rowley and Alford, 2013). Thirdly, sampling biases due to differences in capture probability are likely to occur to some degree (Cooch et al., 2012). In populations demonstrating parasite aggregation, the pattern of pathogen distribution is often heavily influenced by the small number of heavily burdened hosts, and small sample sizes may fail to identify these individuals.

Marked parasite aggregation may imply the relative absence of homogenizing mechanisms such as intensity-dependent parasite mortality as well as intensity-dependent host immunity (Luong et al., 2011). This is consistent with the previous finding that infectious burdens follow an exponential growth curve until host mortality (Carey et al., 2006), however, there is little evidence to suggest that host immunity is associated with infectious burden in chytridiomycosis (Fites et al., 2013). In addition, the mechanisms contributing to aggregated parasite distributions often tend to stabilize host-pathogen interactions and may contribute to pathogen persistence in endemically infected populations (Wilson et al., 2002). Importantly, however, if parasite aggregation is predominantly caused by environmental factors as described above, we hypothesize that natural selection for disease resistance may be slower than if host factors are the major determinants. In the former case, the population would remain vulnerable to stochastic events which favor the pathogen, such as longer periods of optimal environmental conditions. We thus suggest it is important to identify the predominant cause of parasite aggregation where it occurs as this may provide an indication of potential long-term persistence of the population.

In conclusion, we have shown that parasite aggregation is an important feature of a microparasitic disease, in this case endemic chytridiomycosis. Overlooking non-random parasite distributions in microparasitic diseases may lead to paradoxical interpretations of disease dynamics. In future studies prevalence measures should be accompanied by other quantitative information about infectious burdens in individual hosts. We also show that Bd infections occur seasonally and that recoveries are common and likely important for population persistence. Hence, future management of chytridiomycosis might focus on environmental manipulation to favor host recoveries. Understanding the predominant causes of parasite aggregation will indicate whether other disease control interventions should be targeted towards improving host resistance or reducing exposure.

3.3.7 Acknowledgments

We thank H. Ricardo and volunteers for assistance in the field, and S. Garland and R. Campbell for PCR testing. This study was conducted with approval by the James Cook University Animal Ethics Committee (Certificate no. A970) and Queensland Environmental Protection Agency (Fauna permit no. WISP033606305). Funding was provided by the Department of Environment Heritage via the tender 42/2004 “Experimental research to obtain a better understanding of the epidemiology, transmission and dispersal of amphibian chytrid fungus in Australian ecosystems” and the Australian Research Council grants FT100100375, LP110200240 and DP120100811.

3.3.8 Data accessibility

Detailed information about predictor variables, construction of candidate model sets, goodness of fit testing and MSMR assumptions, and population dynamics simulation methods are available in Appendix C. Abbreviated tables of MSMR two and three-state results, population dynamics simulation results and figures, and a description of transition probabilities as a function of state subpopulation size are available in Appendix D. The authors are solely responsible for the content and functionality of these materials. Queries (other than absence of the material) should be directed to the corresponding author.

CHAPTER 4: Adaptive immunity to chytridiomycosis

4.1 Introduction

Immunologic research is a promising avenue for novel management techniques to address emerging biodiversity diseases by rendering individuals resistant to the effects of disease. The adaptive immune system of the amphibian host, similar to that of other vertebrates, should be capable of immunologic memory via the clonal amplification and selection for memory lymphocytes during an initial exposure to a pathogen. This repertoire of memory T and B cells may potentially provide life-long resistance to disease upon re-exposure in an individual host, similar to the concept of immunization (or vaccination) that has been extensively and successfully applied in humans and domestic animal agriculture. Immunization may assist the repatriation of amphibians in captive assurance colonies, and may provide a population buffer or even herd immunity (in reservoir-free disease systems) for wild populations.

In this chapter I investigated the potential efficacy of immunization via prior exposure and treatment of booroolongs frogs (*Litoria booroolongensis*). I compared survival and infection intensities between individuals that had been previously exposed, with those that were naïve to the fungal pathogen, upon exposure (or repeat exposure) to Bd. I aimed to establish whether this technique would provide protective immunity for subsequent exposures, and whether it might be applicable to current reintroduction programs. This chapter addresses the first part of my second aim, to investigate the host adaptive immune response, and whether immunization would be a feasible strategy (see Fig. 4.1).

This chapter consists of a published peer-reviewed paper detailing a large clinical exposure experiment in booroolongs frogs.

Figure 4.1. Project aims, highlighting Chapter 4: Adaptive immunity to chytridiomycosis.

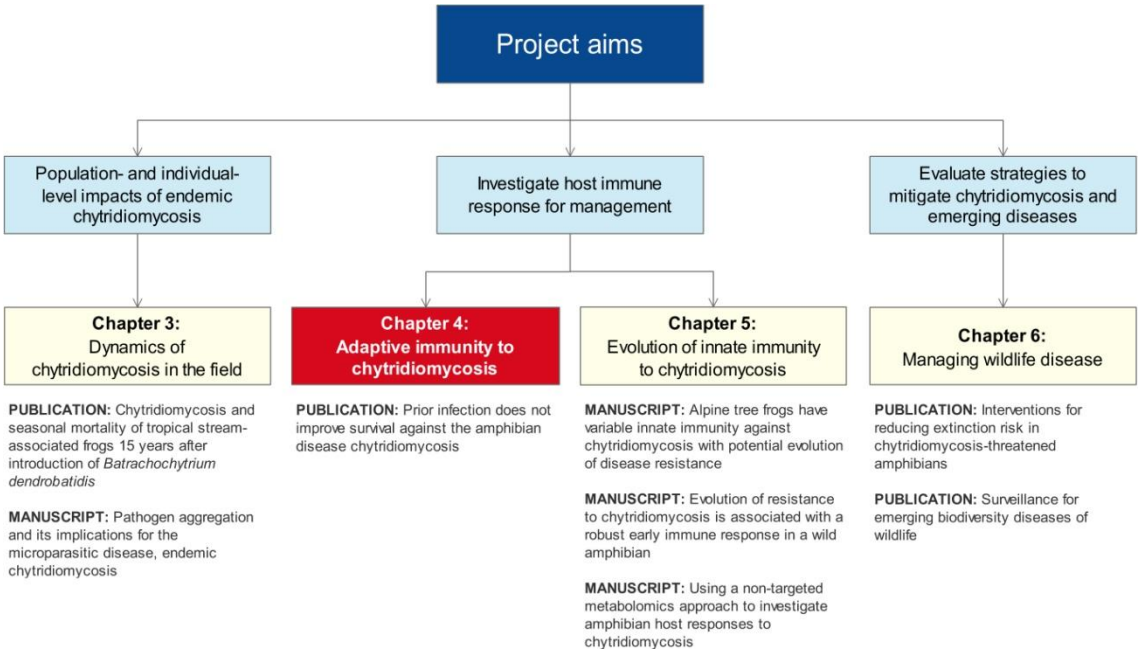

4.2 PAPER 1: Prior infection does not improve survival against the amphibian disease chytridiomycosis

This published peer-reviewed paper represents original research led by Scott Cashins, the primary investigator. My role in the paper included assistance with design and conduct of the experiment, animal husbandry, data collection and editorial input.

The full reference for the published paper is:
Cashins, S. D., **Grogan, L. F.**, McFadden, M., Hunter, D., Harlow, P. S., Berger, L., Skerratt, L. F. (2013) Prior infection does not improve survival against the amphibian disease chytridiomycosis. PLOS One 8:e56747.

The following text is a word for word copy of the manuscript published in the journal PLOS One. Section, table and figure numbering has been added or reformatted for this thesis for ease of reference. Since the journal uses American English, the spelling follows this convention.

4.2.1 Front matter

Title: Prior Infection does not Improve Survival against Chytridiomycosis

Running Title: Inoculation fails to protect against *Bd*

Keywords: *Batrachochytrium dendrobatidis*, immunization, *Litoria booroolongensis*, chytridiomycosis, adaptive immunity

Authors: Scott D. Cashins[1], Laura F. Grogan[1], Michael McFadden[2], David Hunter[3], Peter S. Harlow[2], Lee Berger[1], and Lee. F. Skerratt[1].

1: James Cook University, School of Public Health, Tropical Medicine and Rehabilitation Sciences, Townsville, QLD 4811, Australia.
2: Taronga Conservation Society Australia, Herpetofauna Division, Mosman, NSW 2088, Australia
3: New South Wales Department of Environment and Heritage, Queanbeyan 2620, Australia

Corresponding author: E-mail: scashins@gmail.com

4.2.2 Abstract

Many amphibians have declined globally due to introduction of the pathogenic fungus *Batrachochytrium dendrobatidis* (Bd). Hundreds of species, many in well-protected habitats, remain as small populations at risk of extinction. Currently the only proven conservation strategy is to maintain species in captivity to be reintroduced at a later date. However, methods

to abate the disease in the wild are urgently needed so that reintroduced and wild animals can survive in the presence of Bd. Vaccination has been widely suggested as a potential strategy to improve survival. We used captive-bred offspring of critically endangered booroolong frogs (*Litoria booroolongensis*) to test if vaccination in the form of prior infection improves survival following re-exposure. We infected frogs with a local Bd isolate, cleared infection after 30 days (d) using itraconazole just prior to the onset of clinical signs, and then re-exposed animals to Bd at 110 d. We found prior exposure had no effect on survival or infection intensities, clearly showing that real infections do not stimulate a protective adaptive immune response in this species. This result supports recent studies suggesting Bd may evade or suppress host immune functions. Our results suggest vaccination is unlikely to be useful in mitigating chytridiomycosis. However, survival of some individuals from all experimental groups indicates existence of protective innate immunity. Understanding and promoting this innate resistance holds potential for enabling species recovery.

4.2.3 Introduction

Over the past 40 years, amphibians across the globe have rapidly declined and are now the most threatened class of vertebrates, with at least one third of all species threatened with extinction (Stuart et al., 2004). Apart from habitat loss, the main cause of these declines is the emergence of the disease chytridiomycosis caused by the pathogenic fungus, *Batrachochytrium dendrobatidis* (Bd; Berger et al., 1998; Longcore et al., 1999). Multiple lines of evidence indicate Bd has recently spread worldwide from an unknown origin via human-mediated transport into naïve populations (Fisher et al., 2009b; James et al., 2009; Morgan et al., 2007; Skerratt et al., 2007). As a result, hundreds of susceptible species are feared extinct or have been reduced to small and vulnerable populations, often in well-protected and intact habitat.

Conservation biology aims to maintain or restore biodiversity, often by protecting the overall health of ecosystems. However, when specific threats to biodiversity occur in otherwise healthy ecosystems (e.g. chytridiomycosis), it is prudent to abate these threats directly (Lindenmayer and Hunter, 2010). Unfortunately, few tools are currently available to abate chytridiomycosis in the wild (Woodhams et al., 2011), limiting the options of wildlife managers to the captive management of species to prevent extinction (Gagliardo et al., 2008; Hunter et al., 2010). Where reintroduction programs have been attempted most struggle or completely fail due to the ongoing impact of chytridiomycosis (Soorae, 2010; Stockwell et al., 2008). This is a familiar issue facing animal relocations, and reintroduction efforts in other taxa have been unsuccessful due to the failure to address the processes causing decline (Fischer and Lindenmayer, 2000; Viggers et al., 1993).

A vaccination that provides protective immunity against Bd or reduces infectious burdens to a sublethal level could be used to improve survival rates in reintroduced frogs and important wild populations. Intensive vaccination could buy time for the evolution of resistance or tolerance to infection by maintaining population size and genetic diversity in the face of extirpation due to small population bottlenecks (Rollins-Smith et al., 2009; Woodhams et al., 2011). Manipulating adaptive immunity through vaccination or inoculation has been successful in combating numerous diseases of domestic and wild animals as well as humans. Well-known examples of vaccination in wildlife include the control of sylvatic plague in black-footed ferrets (Rocke et al., 2008) and the control of rabies in mammals (Robbins et al., 1998). It has been suggested that similar methods could be used to help control chytridiomycosis. Although there are no fungal vaccines yet approved for any animal, antibodies to various human fungal pathogens can be protective and promising trials are underway for Candida and Cryptococcus (Cassone, 2008).

Amphibians, like all vertebrates, have a complex immune system, consisting of both innate and adaptive components (Du Pasquier et al., 1989). Recent evidence suggests adaptive responses may be important in fighting chytridiomycosis (Richmond et al., 2009; Savage and Zamudio, 2011). The African clawed frog (*Xenopus laevis*) produced a higher concentration of mucosal antibodies following exposure to Bd, however, it remains unknown, whether this is effective in controlling infection and improving survival and whether the response is heightened with re-exposure. Experimental elimination of splenic lymphocytes (via X-irradiation) of *X. laevis* resulted in greater infection intensities and decreased weight suggesting that the adaptive immune system may be important in controlling infection (Ramsey et al., 2010). However, subcutaneous injection of heat (host: *X. laevis*) or formalin-killed (host: mountain yellow-legged frog; *Rana muscosa*) Bd did not control infection or improve survival even though it induced a systemic response in *X. laevis* resulting in circulating antibodies to Bd (Ramsey et al., 2010; Stice and Briggs, 2010).

Route of exposure and the nature of the antigen may be important in inducing an effective adaptive response to chytridiomycosis. Subcutaneous or intraperitoneal injection less effectively stimulate epidermal antigen presenting cells leading potentially to a systemic immune response, rather than targeting the skin where Bd infection naturally occurs (Rollins-Smith et al., 2009). Stimulating this epidermal response may require topical exposure to live Bd to stimulate the normal route of infection and ensure appropriate epitopes are available to be recognized by the immune system (Kurtz and Scharsack, 2007). Alternatively, if Bd is able to evade (Chai et al., 2009) or suppress (Ribas et al., 2009; Rosenblum et al., 2009) the host immune response then a prior infection will likely have little effect on survival and development of an effective vaccination strategy will be more complex. Although exposure to a live pathogen is a crude form of vaccination, it is inexpensive and could be applied immediately to species urgently requiring interventions to survive. In this study we test the hypothesis that a real infection followed by treatment to clear Bd will provide immunity and increase survival following a second exposure. We investigate this in captive-bred individuals of the critically endangered booroolong frog (*Litoria booroolongensis*), which is thought to have declined due to chytridiomycosis in areas of New South Wales (NSW), Australia (Hero et al., 2011).

4.2.4 Materials and methods

4.2.4.1 Ethics statement

The research protocols were approved by the James Cook University (A1408) and Taronga Conservation Society (5a/07/09) animal ethics committees.

4.2.4.2 Captive husbandry

To ensure all animals involved in this study had no prior exposure to Bd, we raised all experimental frogs from the captively bred spawn of confirmed Bd negative wild collected adults. Mature *L. booroolongensis* were collected from a 3 km section of the Retreat River in Abercrombie River National Park (34° 7' 18.13" S, 149° 38' 4.98" E) on the central west slopes of NSW with the permission of the New South Wales Office of Environment and Heritage. Egg masses were raised in gently aerated 32 L plastic tubs. At 14 d post-hatching, five groups of 40 tadpoles from each spawn were transferred to individual trays, flushed every 4 hr with filtered water. Water temperature was 20–21°C and each tray had one UVB emitting fluorescent tube and one daylight fluorescent tube set to a 10:14 h light:dark cycle. We fed tadpoles frozen endive and a fish food flake mix *ad libitum.* At metamorphosis groups of 20 individuals were transferred to 20 L plastic aquariums flushed with fresh water daily. Frogs were fed calcium and multivitamin dusted crickets twice and once per week respectively and kept on a 12:12 h light:dark cycle in addition to natural light through windows until they were 6 mo old when we randomly assigned each frog to a treatment group, waited 7 d to allow acclimation, and began the experiment.

4.2.4.3 Culture of Batrachochytrium dendrobatidis

We isolated Bd from an adult *L. booroolongensis* captured along the same stretch of the Retreat River in Abercrombie National Park where the founding captive colony animals were sourced (AbercrombieNP-*L.booroolongensis*-09-LB-P7) with the permission of the New South Wales Office of Environment and Heritage. The culture was maintained at 20°C on TGHL agar plates (Longcore et al., 1999). To harvest zoospores for exposures, we flooded plates with 10 ml dilute salts solution (in mMol: KH2PO4 1.0, CaCl2.H2O 0.2, MgCl2.2H2O 0.1) for 20 minutes. Three separate counts were made with a haemocytometer and averaged, and the stock zoospore solution diluted with the dilute salts solution to 150,000 zoospores/ml.

4.2.4.4 Diagnostic Polymerase Chain Reaction (PCR)

Throughout the experiment, frogs were swabbed with sterile, dry cotton tipped swabs (Medical Wire & Equipment Co MW100-100), and analysed following established protocols with a quantitative PCR TaqMan Assay that estimates the number of Bd zoospores present on the swab (Boyle et al., 2004; Garland et al., 2009; Hyatt et al., 2007). PCR reactions were run in triplicate and we considered a sample positive if at least one well returned a positive reaction to maximize sensitivity and maintain specificity (Skerratt et al., 2011b). Following swabbing, the mass (0.1 g) of each frog was recorded.

4.2.4.5 Experimental design

We established four experimental groups to investigate the effect of vaccination via pre-infection (Fig. 4.2). Group 1 (inoculated) was exposed to and infected with Bd, then cleared of infection with itraconazole and re-exposed to Bd 80 d post-treatment. Group 2 (treated) controlled for any residual antifungal effects of itraconazole and were not initially exposed to Bd, but were treated with itraconazole, then exposed to Bd for the first time. Group 3 (naïve) were not exposed, not treated and then exposed to Bd for the first time. Group 4 (control) were never exposed to Bd nor treated with itraconazole.

Figure 4.2. Flow chart of experimental treatment groups

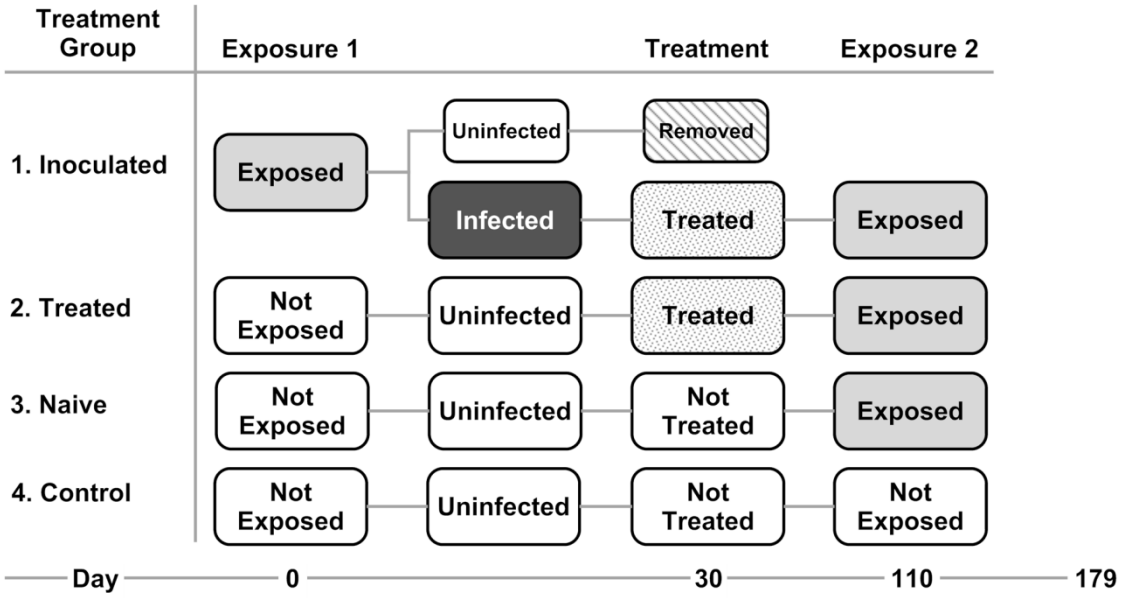

4.2.4.6 Initial exposure

We individually exposed 59 frogs to 750,000 zoospores in 5 ml dilute salts solution (sufficient to immerse the ventral surface of the frog) in 50 ml polyethylene tubs for 3 hrs on three consecutive days. At the end of each 3 hr exposure period and for 4 d following the last exposure, we transferred each frog and their inoculation broth to a 1000 ml polyethylene box containing 10 ml water (enough to cover the bottom of the container) that was replaced daily. We treated unexposed frogs similarly, but sham exposed with only dilute salts solution. After 7 d, frogs were moved from the small exposure boxes to individual 10 L plastic aquariums fitted with a false bottom (plastic egg crate wrapped in shade cloth) for drainage, a hide, and a 250 ml polyethylene tub containing water. Room temperature was maintained at 20 ± 2 °C, the same temperature at which the Bd cultures were grown, and within the temperature range when *L. booroolongensis* are most active in the wild. Sprinklers sprayed the inside of each aquarium

with water for 1 min every 4 hr and water tubs were replenished daily. This setup maintained high humidity, but allowed frogs the choice to avoid standing water and partially dry. Frogs were swabbed at 0, 2, and 3 wks post-exposure. At 3 wk, 43/59 (73%) frogs were infected. One frog died with clinical signs of chytridiomycosis between weeks 3 and 4. We removed the 16 exposed frogs that did not become infected from the experiment as we were interested in the protective effect of a prior active infection, not just prior exposure, on subsequent exposure to the pathogen.

4.2.4.7 Antifungal treatment

At 4 wk, we began treatment to clear infection. Studies in the model amphibian *X. laevis* indicate T-cell mediated responses begin approximately 14 d post exposure (Rollins-Smith et al., 2009). Therefore 4 wks was considered sufficient time for priming an adaptive response via clonal expansion. We placed all 43 infected frogs (inoculated) and 11 unexposed frogs (treated) in individual 50 ml polyethylene tubs and poured 5 ml (enough to immerse the ventrum) 0.01% itraconazole (Sporanox) over the dorsal surface (Nichols and Lamirande, 2000). Frogs were kept in the treatment solution for 5 min daily for 7 d, before being returned to their aquaria. All frogs survived and cleared infection as indicated by three negative PCR results at 2, 5 and 11 wks following the end of treatment.

4.2.4.8 Second exposure

At 80 d post-treatment (109 d post 1st exposure) we exposed frogs in the inoculated, treated and naïve groups to 750,000 zoospores in dilute salts solution daily for 3 d as described previously. The control group was sham-exposed to dilute salts solution alone. We swabbed all frogs at 2, 3, 5 and 9 wk post exposure and at death. At 70 d following the second exposure (179 d post 1st exposure) all surviving frogs were euthanized with an overdose of MS-222 (2 g/L in water).

4.2.5 Results

Prior Bd infection or prior treatment with itraconazole had no significant effect (a = 0.05, 2-sided Fisher's exact test) on survival (p = 1.0), infection status (p = 0.058), proportion of infected individuals that cleared infection (p =0.924) or the proportion of survivors that were infected at the end of the experiment (p = 0.487). Approximately half of the infected frogs in each treatment group successfully cleared infection and approximately 85% of frogs in each treatment group survived (Table 4.1).

A Kaplan-Meier survival curve using days survived as the response variable and censoring individuals that survived until the end of the experiment revealed no significant difference among groups using either the log-rank or Wilcoxon tests (Fig. 4.3, p.0.22 for both tests), and a Cox proportional hazards regression showed that neither experimental group, sex nor mass had

a detectable effect on survival. All experimental groups continued to feed normally and increased in body mass following the second exposure. A one-way analysis of variance (ANOVA) revealed no significant difference in change of body mass among treatments between the second exposure and the end of the experiment (ANOVA; df =3, F= 2.34, p= 0.083) indicating lack of a strong sublethal effect on body condition.

All frogs that died during the experiment were infected (Table 4.1) and their mean intensity of infection was significantly higher at each sampling period than in infected frogs surviving to the end of the experiment (Fig. 4.4). In infected survivors, mean infection intensity increased rapidly within the first 2 wks following the second exposure and then plateaued (Fig. 4.4). Possible differences in infection intensity over time (beginning 2 wks post re-exposure) among treatments were analysed with a factorial, repeated measures ANOVA using Log10 transformed PCR results of frogs that were infected at least once during the experiment but did not die. Degrees of freedom were corrected using Greenhouse-Geisser estimates as the data violated the assumption of sphericity. Neither the interaction of treatment and time ($F(4.5,67.7) = 1.9$, $p= 0.113$) nor time ($F(3,67.7)= 0.82$, $p = 0.457$) or treatment alone ($F(2,30) =2.76$, $p = 0.079$) had a significant effect on intensity of infection (Fig. 4.4).

Table 4.1. Infection, clearance and survival rates of each treatment group (excluding unexposed controls) following exposure to *Batrachochytrium dendrobatidis* (Bd).

	Inoculated	Treated	Naïve	Fisher's exact test (p value)
Bd infection rate (overall)	20/32 (63%)	10/11 (91%)	14/28 (50%)	0.058
Bd clearance rate	11/20 (55%)	5/10 (50%)	6/14 (43%)	0.924
Survival rate	27/32 (84%)	9/11 (82%)	24/28 (86%)	1.000
Bd infection rate (survivors)	4/27 (15%)	3/9 (33%)	4/24 (17%)	0.487
Bd infection rate (non survivors)	5/5 (100%)	2/2 (100%)	4/4 (100%)	

"Inoculated" frogs were previously exposed and infected with Bd and cleared of infection with itraconazole prior to exposure, "Treated" frogs were not initially exposed to Bd but were treated with itraconazole prior to exposure, "Naïve" frogs were not exposed nor treated prior to exposure.

Figure 4.3. Kaplan-Meier curve depicting the proportion of frogs surviving in each treatment group over the days post Bd exposure.

"Inoculated" frogs were previously exposed and infected with Bd and cleared of infection with itraconazole prior to exposure. "Treated" frogs were not initially exposed to Bd but were treated with itraconazole prior to exposure. "Naïve" frogs were not exposed nor treated prior to exposure. "Control" frogs were never exposed nor treated at any point during the experiment.

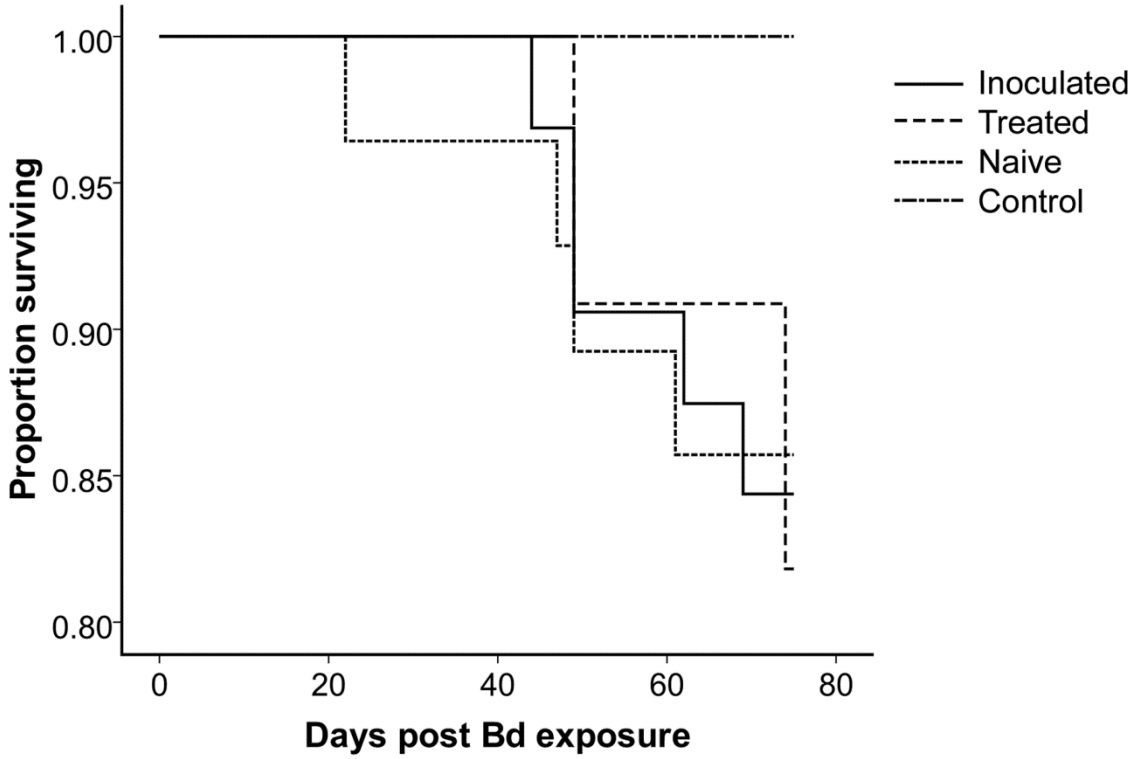

Figure 4.4. Mean intensity of *Batrachochytrium dendrobatidis* infection over time.

a) Initial exposure of and treatment of "inoculated" frogs and treatment of "treated" frogs. b) Second exposure of all frogs except unexposed controls (controls not shown). Frogs that died of chytridiomycosis are from across treatment groups. All other lines depict only frogs that survived.

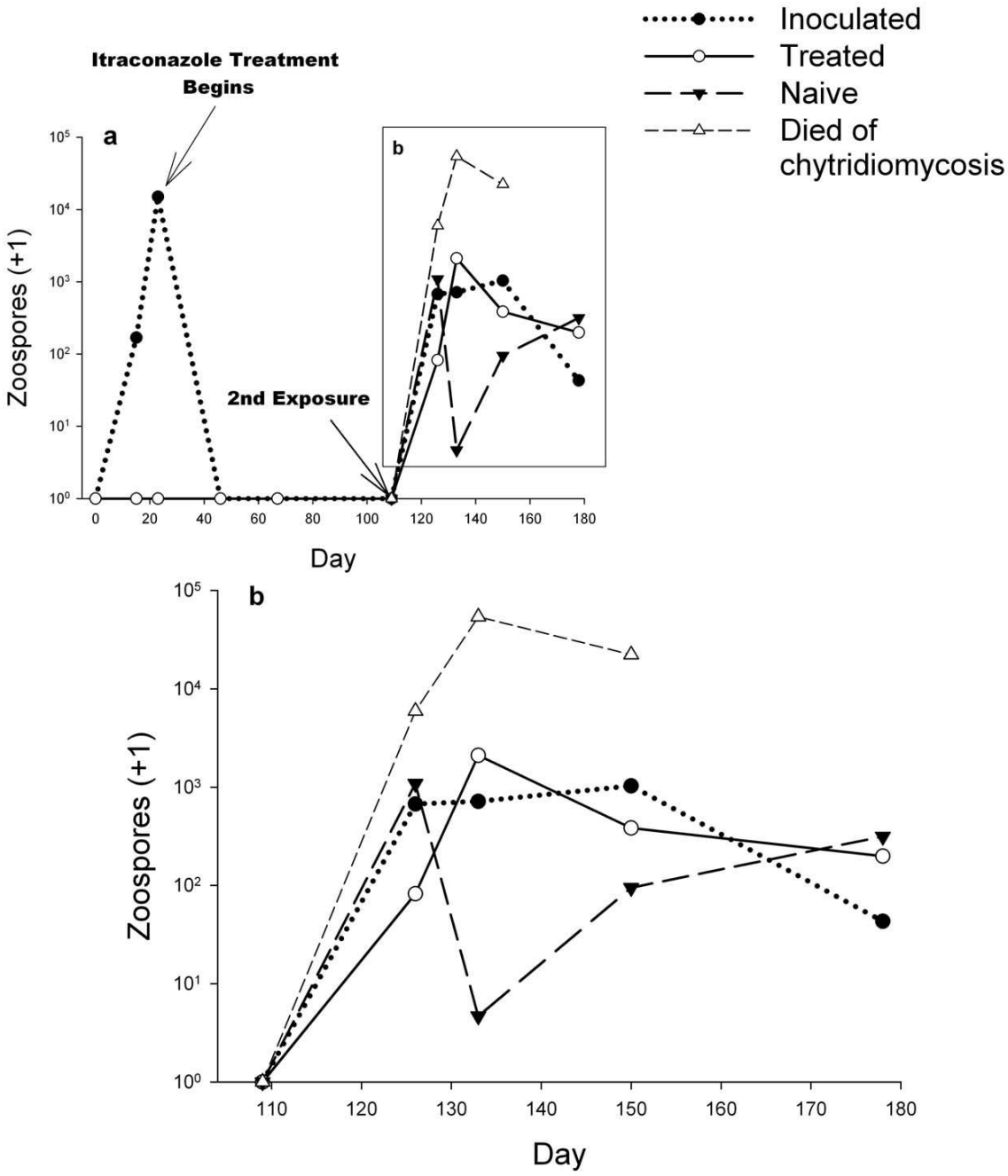

4.2.6 Discussion

We found no evidence for increased protective immunity following infection with *Batrachochytrium dendrobatidis*. Prior exposure and treatment of Bd has been widely promoted as a straightforward and inexpensive, but untested vaccination method to improve the survival of susceptible species (Kurtz and Scharsack, 2007; Richmond et al., 2009; Rollins-Smith et al., 2011). Our results show, however, that prior infection and treatment is unlikely to be an effective management strategy for *L. booroolongensis*, and possibly other species threatened by chytridiomycosis worldwide. While the relatively high survival and moderate cure rates indicate many of the frogs in this study had some form of resistance, the inability of a prior infection to increase protective immunity is striking, and a major blow to conservation efforts.

Although we found a near significant effect of treatment on prevalence (Fisher's exact test: $p = 0.058$) and intensity of infection (Repeated Measures ANOVA: $F(2,30) = 2.76$, $p = 0.079$), the direction of the effect for both results was opposite what would be expected with a successful vaccination. If prior infection provides a benefit, the 'inoculated' frogs should have lower prevalence and mean intensity of infection than the other experimental groups. Instead, prevalence was similar between the 'inoculated' and 'naïve' groups but higher in the 'treated' group (Table 4.1), and intensity of infection was similar across all treatments and time periods, but lower in the 'naïve' group 3 wk post re-exposure (Fig. 4.4). Neither of these unexpected and marginally significant results has a clear biological explanation, thus we decline from further speculation about their cause.

It remains unclear why prior exposure was ineffective against Bd. It is possible that Bd avoids and down regulates the adaptive immune response. Fungal diseases of amphibians typically incite strong inflammatory reactions observed microscopically (Berger et al., 2009a), but this response is not observed in skin infected with Bd (Berger et al., 2005c). Berger et al. (1999b) suggested that sporangia (the reproductive phase of Bd) may effectively evade recognition by the host due to their location inside cells of the superficial epidermis. Intracellular and epithelial sites of infection are both features in common with other fungi that can hide from phagocytes (Chai et al., 2009). In addition to evading the amphibian immune system, recent evidence suggests Bd may also actively suppress an immune response. In the clawed frog *Xenopus (Silurana) tropicalis*, infection results in down regulation of genes associated with toll-like receptors (which could assist pathogen recognition), complement pathways, and B and T-lymphocytes (Ribas et al., 2009; Rosenblum et al., 2009). This is possibly due to the release of soluble factors inhibitory to B and T-cells as demonstrated by *in vitro* lymphocyte proliferation assays (J. Ramsey et al., unpublished in Rollins-Smith et al. [2011]). General mechanisms of fungal evasion and suppression include shielding surface antigens, inducing anti-inflammatory

cytokines, decreasing inflammatory cytokines and phenotypic switching. The ability to evade or inhibit the immune system is a feature of other highly virulent diseases that, like chytridiomycosis, can kill previously healthy hosts and are difficult to control, e.g. malaria.

Although potential remains to develop a targeted Bd vaccine that overcomes possible evasion and inhibition of the adaptive immune response, it will likely be too expensive and lengthy an exercise to help critically threatened amphibian populations in the near future. For example, it has taken two decades and $300 million in investment to develop an effective malaria vaccine that cuts the risk of infection in infants by 56% (Agnandji et al., 2011; Waters, 2011). Despite the current unsuitability of prior exposure as a vaccination strategy, our findings contribute to a broader understanding of the ecology of chytridiomycosis. The lack of an observable adaptive response to Bd (absence of an 'immune' state) helps explain the dynamics observed in the field, such as the regular re-infection of individuals (Briggs et al., 2010; Murray et al., 2009) and annual seasonal outbreaks (Berger et al., 2009a; James et al., 2009; Longcore et al., 1999; Longcore et al., 2007; Vredenburg et al., 2010). Although we found no evidence that prior infection elicits an effective adaptive immune response, the majority of booroolong frogs in this study clearly had some form of resistance.

Despite inoculation with 750,000 zoospores for 3 d (a dose higher than would be experienced in the wild), 38% of frogs never developed a detectable infection. Of the 62% that were infected, mortality rates were relatively low (25%) across experimental groups, and in surviving frogs infection intensity peaked 3 wk post exposure before stabilising or declining for all treatments. Overall, 50% of all infected frogs successfully cleared infection, 25% maintained a sublethal infection until the end of the experiment and 25% were unable to control pathogen replication and died with elevated zoospore burdens.

Mortality from chytridiomycosis in the field has been reported to occur once the infectious burden increases above a mean threshold of 10^4–10^5 zoospore equivalents (Briggs et al., 2010; Vredenburg et al., 2010). A similar fatal threshold was found in this study and individuals able to eliminate or maintain infection below 10^4–10^5 zoospores survived. Frogs were housed in optimal conditions for the pathogen (20 °C and high humidity; Piotrowski et al., 2004) throughout the experiment, eliminating the possibility of experimental conditions alone causing clearance of infection. However, frogs were given the freedom to avoid direct contact with standing water (as would occur in the wild for this species) which could help limit pathogen proliferation and reinfection.

As observed resistance was unrelated to prior exposure, innate immune responses are likely responsible for limiting pathogen replication below the threshold. Interestingly, this resistance was not apparent when we exposed booroolong frogs to the same Bd zoospore dose in groups of 10 (750,000 zsps/10 frogs) and 100% of frogs died due to chytridiomycosis (compared with 100% survival in unexposed controls; S. Cashins, unpublished data), suggesting defenses are overwhelmed with constant re-exposure from nearby hosts. This supports field studies identifying population density as an important predictor of Bd infection intensity and impact (Briggs et al., 2010; Vredenburg et al., 2010) and may help explain why *L. booroolongensis* have declined in the wild despite their moderate susceptibility in captivity.

Vaccination via live infection has been a commonly proposed solution to mitigate the impact of chytridiomycosis on amphibian biodiversity (Woodhams et al., 2011). Although our study did not support this as an effective strategy, a number of potential management solutions remain which are aimed at either the pathogen or the host. Pathogen-focused strategies involve intensive site management such as the manipulation of water chemistry or natural chytrid predators to reduce pathogen survival and density in the environment (Buck et al., 2011; White, 2006). These strategies hold the most promise at select, discrete pond sites of high conservation value where ongoing and intensive human involvement is available to maintain conditions inhospitable for Bd.

Host-focused strategies seek to promote the factors responsible for host persistence. Some species that suffered range contractions due to Bd are now recolonising previously inhabited areas, suggesting one or more of three possibilities 1) resistance is evolving naturally, 2) Bd is becoming less virulent, and 3) lower density populations are able to survive in areas were higher population densities were extirpated (McDonald et al., 2005; Retallick et al., 2004). Species at high risk of extinction may thus be effectively managed if the underlying mechanisms of host resistance, pathogen virulence and disease dynamics are identified.

The potential for manipulating pathogen virulence has yet to be explored and while limiting host-density may provide a short term solution to species survival it is counterproductive to conservation in the long-term. Increasing the reproductive fitness or distribution of individuals with more robust innate immunity through head starting, translocation of survivors, or reintroduction programs that select for resistance currently holds the most promise for long term mitigation of disease in species threatened with chytridiomycosis. Differences in susceptibility between and within species have been described in this and other studies (Searle et al., 2011; Tobler and Schmidt, 2010), and have been correlated with individual aspects of innate immunity such as antimicrobial peptides (Woodhams et al., 2007a), MHC diversity (Savage and Zamudio,

2011) or competitive skin bacteria (Lam et al., 2010). However, Bd is an unusual pathogen (as the only member of the *Phylum Chytridiomycota* to cause disease in vertebrates and as a fatal cutaneous fungus) and so host immune mechanisms may also be unusual and complementary. Studies that adopt a broad, exploratory approach and investigate multiple components of innate immunity through immunologic, genetic and post-genomic analyses are needed to begin identifying the most important mechanisms of observed resistance.

Many endangered amphibian species threatened by chytridiomycosis exist as small populations that are unsustainable. We have found that vaccination via pre-exposure with live Bd is unlikely to be of assistance.

4.2.7 Acknowledgments

We thank J. Ashenden and P. McLachlan for their assistance in care of the experimental frogs, and all the Herpetofauna staff at Taronga Zoo, especially A. Skidmore for their assistance. R. Speare and L. Rollins-Smith provided helpful advice and planning and S. Garland, R. Webb and S. Bell performed PCR analyses. We acknowledge SITA Australia's funding to amphibian conservation which helped enable this research.

4.2.8 Author contributions

Conceived and designed the experiments: SDC LFG MM DH PSH LB LFS. Performed the experiments: SDC LFG. Analyzed the data: SDC. Contributed reagents/materials/analysis tools: SDC MM DH LB. Wrote the paper: SDC LFG MM DH PSH LB LFS.

CHAPTER 5: Evolution of innate immunity to chytridiomycosis

5.1 Introduction

The evolution of amphibian host innate immunity against Bd infection may provide long-term sustainable inter-generational resistance to chytridiomycosis within wild populations and repatriated individuals. Susceptibility to chytridiomycosis has been shown to vary between species, populations and individuals, and where this variation is attributable to heritable mechanisms such as innate immunity, evolution of resistance may be possible. Direct or marker-assisted selection for disease resistance are two potential management techniques that harness the heritability of the innate immune system, and have been successfully applied in domestic animals and plant agriculture. The latter approach has the benefit of allowing accelerated and more ethically acceptable selection between individuals, however it relies on understanding and identifying genetic and molecular mechanisms and pathways of the innate immune system that confer resistance.

In this chapter I investigated both the potential for the evolution of resistance to chytridiomycosis in alpine tree frogs (*Litoria verreauxii alpina*), as well as putative underlying genetic and molecular mechanisms. I compared survival and infection intensities between Bd-exposed individuals from both long-exposed populations (> 20 years) and a naïve population of frogs. I also collected tissue samples and performed both transcriptomics and metabolomics analyses to investigate differences in gene and metabolite expression between populations and times since Bd exposure (including uninfected control samples). I aimed to establish firstly whether evolution of resistance may be possible in order to determine the feasibility of the above-mentioned management strategies, and secondly to characterize underlying mechanisms to improve our understanding of the immune response to chytridiomycosis as well as potentially identify resistance markers (see Fig. 5.1).

This chapter consists of 1) a manuscript in preparation outlining a large clinical exposure experiment in alpine tree frogs, 2) a manuscript in preparation detailing an extensive transcriptomics analysis undertaken on tissue samples collected from the clinical experiment, and 3) a manuscript in preparation detailing metabolomics analysis from similar tissues.

Figure 5.1. Project aims, highlighting Chapter 5: Evolution of innate immunity to chytridiomycosis.

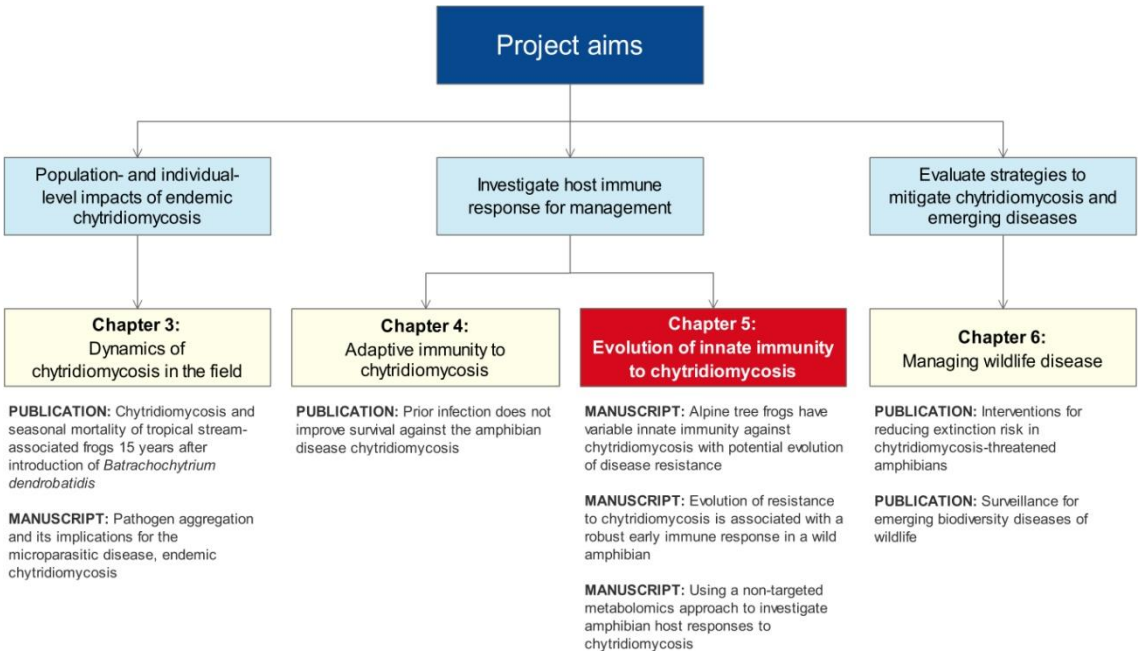

5.2 PAPER 1: Alpine tree frogs have variable innate immunity against chytridiomycosis with potential evolution of disease resistance

This manuscript (prepared originally as a stand-alone manuscript, but later incorporated in part into a larger extended manuscript for publication) represents original research led by Scott Cashins, who performed the initial pilot study, contributed to preparations and the first few weeks of the experiment proper, and part of the data analysis. My role in the manuscript involved assistance with experimental study design, performing the majority of animal husbandry work, conducting the experiment, collecting data, writing the methodology section of the initial manuscript draft and performing part of the data analysis, as well as substantial input into results interpretation, and editorial input. Michael McFadden, Dave Hunter and Peter Harlow assisted with field components and on-site logistical arrangements. Lee Skerratt and Lee Berger provided substantial assistance with experimental design and wrote parts of the initial manuscript draft, and all co-authors provided substantial editorial input.

The full reference for the manuscript is:
Cashins, S. D., **Grogan, L. F.**, McFadden, M., Hunter, D., Harlow, P. S., Berger, L., Skerratt, L. F. (in prep) Alpine tree frogs have variable innate immunity against chytridiomycosis with potential evolution of disease resistance.

The following text is a copy of the manuscript prior to its abbreviation and incorporation into another manuscript, currently submitted to Proceedings of the National Academy of Sciences (detailed in Appendix I). Section, table and figure numbering has been added or reformatted for this thesis for ease of reference. Since the journal uses American English, the spelling follows this convention.

5.2.1 Front matter

Alpine tree frogs have variable innate immunity against chytridiomycosis with potential evolution of disease resistance

Running head: Variable innate immunity to chytridiomycosis

Scott D. Cashins[1], Laura F. Grogan[1*], Michael S. McFadden[2], David A. Hunter[3], Peter Harlow[2], Lee Berger[1], Lee F. Skerratt[1]

Keywords: amphibian declines, innate immunity, *Batrachochytrium dendrobatidis*, chytridiomycosis, evolution, resistance

[1]One Health Research Group, School of Public Health, Tropical Medicine and Rehabilitation Sciences, James Cook University, Townsville, Queensland 4811, Australia
[2]Taronga Conservation Society Australia, Mosman, NSW 2088, Australia.
[3]NSW Office of Environment and Heritage, Queanbeyan, NSW 2620, Australia.

[*] Address correspondence to L. F. Grogan, email laura.f.grogan@gmail.com

5.2.2 Abstract

The recent global spread of the fungal skin disease, chytridiomycosis, into multiple amphibian species provides a rare opportunity to examine evolution of host immunity after pathogen introduction. In a controlled exposure experiment we investigated frog survival and infection intensity in 352 captive-raised and infection-naïve adult endangered Alpine tree frogs (*Litoria verreauxi alpina*) sourced from multiple clutches from an infection-naïve site and three long-exposed sites (> 20 years after introduction) in Kosciuszko National Park, Australia. We hypothesized that frogs from long-exposed populations would be more resistant to chytridiomycosis infection than frogs from the naïve population. We found that frogs from one long-exposed population survived significantly longer when compared with frogs from two other long-exposed populations and the naïve population. Infection intensity peaked later (five weeks) and the peak was lower in longer lived frogs compared with those that died within five weeks post exposure, and infection load then declined briefly before recrudescence and death. Six exposed frogs survived the duration of the experiment (86 days, approximately 12 weeks), and their infections peaked earlier than non-survivors at 3-4 weeks, and then declined, suggesting immune-mediated recovery and disease resistance. Five of these frogs were from one long-exposed population, and one was from the naïve site. We found inherent variability in survival between clutches within the naïve site and one long-exposed site. Our results demonstrate significant differences in survival and infection dynamics between populations associated with infection exposure history that are consistent with the evolution of host immunity, although this was not demonstrated across all long-exposed populations. The high level of overall mortality within the experiment suggests that there has not been strong selection for direct disease resistance, and the species is still highly susceptible to chytridiomycosis. Increased population resilience in the wild may thus be due to evolution of other factors. Features of the natural history of this species, such as high survival until after breeding at one year of age, may limit opportunities for natural selection of disease resistance. Our finding of a more resistant population holds promise for the future management of species threatened by chytridiomycosis, however, and we recommend utilizing assisted selection for more resistant individuals in *ex situ* programs.

5.2.3 Introduction

The recent global spread of *Batrachochytrium dendrobatidis* (Bd) across different environments and into multiple species (Skerratt et al., 2007) provides a rare opportunity to examine if immunity and/or virulence changes after introduction, and how different conditions influence this evolution. The best studied example of changes in host/pathogen dynamics after arrival of an exotic disease is myxomatosis, where rapid evolution led to more resistant rabbits and moderately virulent virus (Fenner, 2000). Studying evolutionary changes in immunity to chytridiomycosis may identify whether assisted selection for disease resistance could be a feasible management strategy for Bd-threatened amphibian species.

Chytridiomycosis emerged in the 1970s and continues to spread into naïve populations worldwide causing such high mortality rates that over 100 species have disappeared, including six Australian species from pristine locations (Murray et al., 2010a; Skerratt et al., 2007). In endemically infected regions, many endangered species now occur at much lower abundance with smaller distributions than previously and some populations continue to decline (Hunter et al., 2010; Vredenburg et al., 2010).

Managing invasive diseases that threaten biodiversity is a global challenge, and eradication of the causative pathogens from natural habitats is often impossible. A number of strategies hold promise for management of species threatened by chytridiomycosis including small scale environmental manipulation, population buffering, translocations, bioaugmentation, and manipulation of the host immune response to disease (Bletz et al., 2013; Scheele et al., 2014; Venesky et al., 2013).

We have previously examined the potential to manipulate the adaptive immunity to improve survival of animals reintroduced to the wild. Consistent with related studies (Rollins-Smith et al., 2009; Stice and Briggs, 2010), we found that immunization against Bd by prior infection and treatment was ineffective at rendering clinically protective immunity upon re-exposure in an Australian frog species (booroolongs frog, *Litoria booroolongensis*; Cashins et al., 2013). A potentially more promising approach, particularly for the long-term persistence of species threatened by chytridiomycosis, involves the evolution of inter-generational host immunity (Savage and Zamudio, 2011).

The evolution of disease resistance has been demonstrated in wild populations in other disease systems (Bonneaud et al., 2011; Bonneaud et al., 2012), and has also been widely utilized in domestic animal and plant agriculture. For example, marker-assisted selection (MAS) is a prominent technique in plant agriculture for the selection of disease resistance (Miedaner and

Korzun, 2012; Ragimekula et al., 2013). The use of estimated breeding values (EBVs) in vertebrates is another strategy to select for disease resistance and has been widely applied in aquaculture and livestock, particularly the dairy industry (Heringstad et al., 2007; Leeds et al., 2010). Similar techniques may be possible with *ex situ* captive assurance colonies of amphibians and may help improve their survival probability upon reintroduction.

A first step towards evaluating assisted selection for use in management is identifying resistant phenotypes, and associated genetic markers with high predictive values. Field data suggests evolution of resistance to chytridiomycosis has occurred in the wild – there are reports of population recovery with increased frog abundance in some populations which have been exposed to Bd for several years (McDonald et al., 2005; Newell et al., 2013). Large differences in susceptibility to chytridiomycosis have been observed among individuals, populations and species (Tobler and Schmidt, 2010). Such variation, particularly when observed in the field, may be associated with many factors, however, such as exposure, environment, host signalment, behaviour, immunologic history, physiological, morphological and nutritional characteristics, as well as genetic immune mechanisms (Lamirande and Nichols, 2002; Rowley and Alford, 2007a; Rowley and Alford, 2013; Savage and Zamudio, 2011; Searle et al., 2011; Tobler and Schmidt, 2010; Wells, 2007; Woodhams et al., 2006b). Our understanding of resistance heritability may be confounded by the interaction of these factors. Furthermore, observed differences in Bd virulence, *in vitro* protein expression, and culture growth suggest that despite evidence that Bd is a pandemic clone, it is adapting to new climates and hosts, and this may also contribute to observed variations in disease susceptibility (Berger et al., 2005b; Fisher et al., 2009a).

The innate immune system is generally the basis for the evolution of immunity and is the first line of defense against infectious agents (Murphy, 2012). Innate immunity consists of both constitutive and induced defenses. Constitutive defenses are continuously present within and on the host and may assist in the prevention of initial colonization of infectious organisms, as well as reducing overall infectious loads. Constitutive defenses include natural physical barriers (such as mucus and keratinized skin cells), symbiotic microbiota and their antifungal metabolites (Harris et al., 2009a), and antimicrobial peptides in skin secretions (some of which may also be inducible; Mangoni et al., 2001). In contrast, the expression of induced innate defenses increases substantially with exposure to a pathogen via the action of multiple signalling pathways and mediators. Constituents of the induced innate immune system of amphibians include numerous cell types (phagocytes and granulocytes such as macrophages, neutrophils and natural killer cells), pattern recognition receptors (such as toll-like receptors and mannose receptors), inflammatory mediators (including cytokines such as interleukins), and signalling pathways (such as NFκB and MAP kinase; Murphy, 2012; Robert and Ohta, 2009).

While the amphibian immune system has been relatively well characterized (Robert and Ohta, 2009), resistance to chytridiomycosis remains poorly understood. Amphibian skin peptides and bacteria that produce antifungal metabolites show activity against Bd *in vitro*, and have been associated with survival of some frog species (Myers et al., 2012; Woodhams et al., 2007a). The identification of genetic markers for antimicrobial peptide concentration and complement is still in its infancy (Mechkarska et al., 2012; Robertson and Cornman, 2014), while the complement of skin microbiota is likely predominantly linked with environmental factors.

There appears to be minimal histological inflammatory response in susceptible infected individuals (Berger et al., 2005c), likely due to Bd-secreted immunosuppressive factors affecting cellular immunity, although this doesn't explain the absence of a cellular innate response (Fites et al., 2013; Rosenblum et al., 2009). For the purpose of identifying resistant phenotypes and genetic markers the results are still unclear regarding the presence and expression of immune genes between susceptible and resistant frog species, at different stages during infection, and under different environmental conditions. In a microarray study of two susceptible species, *Rana muscosa* and *R. sierrae*, Rosenblum et al. (2012b) found limited or decreased expression of normal immune pathways except IL1, MHC and the antimicrobial peptide cathelicidin. These results were also consistent with their earlier work in the susceptible species *Xenopus (Silurana) tropicalis* (Rosenblum et al., 2009). In a larger study in the latter species, however, Ribas et al. (2009) identified the up-regulation of several genes in the spleen associated with a serine-protease inflammatory response at host-optimal temperatures that were reduced in a colder environment, as well as genes associated with the production of skin peptide preprocareulein.

The most promising study to date identifying potential genetic immune markers for the evolution of chytridiomycosis resistance (Savage and Zamudio, 2011) investigated correlations between survival and MHC alleles of 99 experimentally exposed frogs from five populations of the lowland leopard frog (*Lithobates yavapaiensis*) in North America. They found an association suggesting positive selection and that MHC heterozygosity was associated with clinical survival in an exposure experiment. A similar study in *Bufo calamita* (May et al., 2011) identified MHC variation with population-level Bd-infection status, and suggested that infection may be associated with the presence of specific MHC alleles. It is unknown, however, whether MHC heterozygosity or the presence of specific MHC alleles confer survival advantages across host species.

As yet there is no clear, controlled example comparing survival of uniformly-challenged frogs between long-exposed populations and geographically-related Bd-naïve populations in order to phenotype animals for chytridiomycosis resistance. Such a comparison may also indicate the propensity for natural evolution of resistance within a reasonable time-frame for management approaches that select for more resistant individuals. Until recently, we were fortunate to have access to a confirmed Bd-naïve site (hereafter Grey Mare) that had remained negative for chytridiomycosis infection despite the introduction and long exposure of all surrounding sites (that were first infected approximately 20 years ago), and the presence of susceptible frog species. This site in Kosciuszko National Park, Australia, remained uninfected with an extraordinary abundance of frogs until late in 2012 (pers. comm. B. Scheele) due to its geographic isolation. The arrival of Bd at Grey Mare has been catastrophic with few frogs seen since. Clearly, this naïve population was highly susceptible in the wild.

The alpine tree frog (*Litoria verreauxi alpina*), is an endangered subspecies endemic to the alpine regions of Victoria and New South Wales in southern Australia, and occurred in high numbers at Grey Mare until the population collapsed. Declines occurred in surrounding populations since the early 1980s when Bd is believed to have arrived (pers. comm. D. Hunter). Current long-exposed population distributions are up to 95% smaller but appear stable, despite a high prevalence of chytridiomycosis (up to 80%; pers. comm. D. Hunter). To investigate if persisting long-exposed populations have evolved disease resistance, and potentiate the characterization of resistant phenotypes, we compared susceptibility to chytridiomycosis via laboratory exposures using clutches raised from wild-caught eggs collected in 2010 from the naïve site and three long infected sites. We hypothesized that frogs from long-exposed populations would be more resistant to chytridiomycosis infection than frogs from the naïve population.

5.2.4 Methods

5.2.4.1 Study subjects and husbandry

Alpine tree frogs (*Litoria verreauxii alpina*) were obtained from wild-caught egg-masses (with possible multiple paternity; collected in 2010 under Scientific Licence number: S12848, D. Hunter), and were raised in Bd-negative quarantine conditions at Taronga Conservation Society, Sydney, Australia, until approximately eight months post-metamorphosis (in 2011). Adult frogs were transferred to individual tubs several weeks prior to commencement of the exposure experiment to allow for acclimatization. Prior to and during the exposure experiment, frogs were maintained at constant 19ºC (± 2ºC) in individual plastic containers (arranged randomly on shelves with respect to population, clutch and treatment group) with permeable gauze lids,

pebble substrate, and water drainage holes down one end of the tub (Supporting information in Appendix F, Figs. F.1-F.3). Containers were placed at a slight angle (10º) to facilitate water drainage, and provide wet and dry areas. Frogs were fed multivitamin and calcium dusted crickets alternately twice weekly *ad libitum*. Individual frogs were observed daily by an experienced animal handler and veterinarian for health status and clinical signs of disease. Tubs were flushed daily for 15 seconds with filtered water until the water ran clear and debris was removed.

5.2.4.2 Experimental design

A total of 355 chytridiomycosis-naïve adult alpine tree frogs (*Litoria verreauxii alpina*) were prepared for the exposure experiment. These frogs were originally sourced from four geographically distinct populations. The populations are hereafter designated Kiandra, a Bd long-exposed site (35.872°S 148.500°E 1356 m above sea level [asl]), Eucumbene, a Bd long-exposed site (36.152°S 148.563°E 1451 m asl), Ogilvies, similarly a Bd long-exposed site (36.036°S 148.322°E 1307m asl), and Grey Mare, a Bd-naïve site (36.317°S 148.260°E 1525 m asl). The experimental design, involving the utilization of frogs from each population and clutch together with details of the blind randomized block design used for allocation of treatment groups is outlined in Table 5.1. Numbers of frogs available for utilization was subject to original clutch size and natural attrition during growth and development. An unexposed negative control group was defined to ascertain the presence and nature of any cross-contamination in the experimental setup. As our question of greatest interest involved comparison of infected frogs between populations, we attempted to maximize the sample size of exposed frogs by randomly selecting up to 20 frogs from each block (clutches within populations) to be exposed to Bd. Some clutches where few frogs were available were of insufficient sample size to permit the allocation of negative control individuals (Eucumbene clutch B, Grey Mare clutches A and D, Ogilvies clutches A and C). Two frogs died during the acclimatization period pre-exposure, and another frog died from a condition considered unrelated to chytridiomycosis (anasarca and cloacal prolapse) and the data from these three frogs was hence removed from analyses, leaving a total of 352 experimental animals.

Table 5.1. Experimental design for *Litoria verreauxi alpina* innate immunity experiment. Numbers of *L. v. alpina* frogs from each population and clutch, and details of blind randomized block design used for allocation of treatment groups (exposed frogs versus sham-exposed negative control frogs).

Population (total number frogs)[a]	Clutch (total number frogs)[a]	Exposure group[b]	Total number of frogs	Number of males[g]	Number of females[g]	Number with undetermined gender
Eucumbene (99)	A (30)	E	20	7	13	0
		C	10	6	4	0
	B (19)	E	19	10	9	0
		C	0	0	0	0
	C (29)	E	20	10	10	0
		C	9	4	5	0
	D (21)	E	19	11	8	0
		C	2[c]	0	1	1
Grey Mare (80)	A (14)	E	14	7	6	1
		C	0	0	0	0
	B (26)	E	20	10	10	0
		C	6	3	3	0
	C (29)	E	20	11	9	0
		C	9	6	3	0
	D (11)	E	11	9	2	0
		C	0	0	0	0
Kiandra (100)	A (25)	E	20	9	11	0
		C	5	1	4	0
	B (25)	E	20	12	8	0
		C	5	1	4	0
	C (25)	E	20[d]	8	10	2
		C	5	3	2	0
	D (25)	E	20	11	9	0
		C	5	1	4	0
Ogilvies (76)	A (19)	E	19	13	6	0
		C	0	0	0	0
	B (40)	E	20	7	13	0
		C	20	6	14	0
	C (17)	E	16	9	7	0
		C	1[e]	0	0	1
Total	355		E (278) C (77)[f]	175	175	5

[a]Total number of frogs in parentheses for each group; [b]E represents exposed frogs, C represents control frogs; [c]Includes one frog that died pre-exposure and was excluded from further analyses; [d]This number includes the frog

that died of anasarca post-exposure, unrelated to chytridiomycosis; [e]This frog died pre-exposure and was excluded from analyses; [f]Total frogs grouped by exposure (E) and control (C); [g]Gender as determined by post-mortem coelomic examination.

5.2.4.3 Exposure experiment

Frogs were confirmed negative to Bd (via qPCR, see below) prior to the commencement of the exposure experiment. A Bd strain isolated roughly two years earlier was used for inoculations (AbercrombieNP-*L.booroolongensis*-09-LB-P7) on 20th September, 2011. The strain was maintained, and infectious zoospores collected and counted, as described previously (Cashins et al., 2013). A total of 278 animals (including the aforementioned anasarca frog that was removed from the experiment and subsequent analyses) were individually exposed to 750,000 zoospores in 25ml dilute salts solution (in mMol: KH2PO4 1.0, CaCl2.H2O 0.2, MgCl2.2H2O 0.1) with tubs held flat without pebble substrate for 18 hours. Following exposure, tubs were held horizontally for a further two days, however, the water was replaced daily, before having pebbles added and being placed on a mild angle (10º) for ease of drainage. Seventy-five unexposed frogs were treated similarly, but were instead sham-exposed with only dilute salts solution. Animal experiments were approved by Taronga Conservation Society Australia Animal Ethics Committee (4c/01/10).

5.2.4.4 Infection intensities and other measurements

Bd infection intensity data (in zoospore equivalents, ZSE) was collected via swabbing using new gloves and a new sterile dry swab per frog (MW 100-100; Medical Wire and Equipment, Bath, UK). Swabbing was conducted weekly from week two post-exposure onwards including the day each frog died as well as the final day of the experiment (15th December, 2011; total experimental length 86 days). Swabs were stored dry at 4 °C and were analyzed for the presence or absence of Bd DNA with the TaqMan real-time qPCR protocol following Hyatt et al. (2007). Individual swabs were analyzed in triplicate and each run included an internal positive control. Samples which recorded only one or two of the three wells as a low positive were considered indeterminate positives and were still used in analyses. Frogs showing marked clinical signs for chytridiomycosis were euthanised throughout the experiment using tricaine methanesulfonate (MS-222). Immediately prior to euthanasia, frogs were swabbed to confirm infection status and to quantify Bd infection intensity (via qPCR as above), and had their mass recorded. Gender was ascertained post-mortem via observation of coelomic reproductive organs (sexual dimorphism in frogs of this age was not consistent).

5.2.5 Results

5.2.5.1 Summary statistics

Adult *L. v. alpina* sourced from different populations had significantly different body masses (one-way ANOVA, $F(3, 273) = 8.48$, $p < 0.001$; Fig. F.4), and mass was strongly correlated with snout-urostyle length at the commencement of the experiment (Pearson correlation coefficient $r = 0.81$; Fig. F.5). However, there was no evidence for a correlation between body mass and the length of survival during the experiment (Pearson correlation coefficient $r = -0.03$; Fig. F.6). There was no significant difference in the numbers of male or female frogs between populations (Chi-squared $p = 0.74$, $N = 274$), as determined by intra-coelomic examination post-mortem. Summary results including group averages for mass, snout-urostyle length, overall survival, number of days survived, as well as ZSE average and median per group at frog death can be found in Appendix F, Table F.1.

5.2.5.2 Survival and infection intensity

Survival curves differed significantly among frogs from different populations (Kaplan-Meier $p < 0.001$, Fig 5.2). Kiandra frogs (a long-exposed population) survived for longer compared with the other two long-exposed populations and the naïve population, and Eucumbene (a long-exposed population) survived for longer compared with Ogilvies (a long-exposed population) (Multiple Comparisons Holm-Sidak method $p < 0.02$). Clutches of frogs varied in survival within two populations of origin, Grey Mare (the naïve population) and Ogilvies (Kaplan-Meier $p < 0.004$, Fig. 5.3).

The intensity of infection increased over time following a typical S curve (sigmoid function) in all frogs that died within five weeks post exposure (Fig. 5.4). For frogs that survived past five weeks but eventually died, infection followed the same pattern but after five weeks remained stable or decreased slightly for two weeks. Five of these frogs, two from Eucumbene and three from Ogilvies, died before week seven despite stable or declining infection loads. For the remaining survivors, infection intensity began to increase exponentially again after week seven until death by ten weeks post exposure and hence followed a double logistic function (Fig. 5.4). Three of these longer lived frogs were from Kiandra, three from Grey Mare and one from Eucumbene.

Six of 277 frogs included in the analyses (excluding the anasarca frog) survived exposure to chytridiomycosis until the end of the experiment at 86 days (roughly 12 weeks). For these six, intensity of infection increased similarly to frogs that died but by 3-4 weeks post exposure

started to decline gradually towards zero indicating loss of infection (Fig. 5.5). Five of the six were from Kiandra and one from Grey Mare.

5.2.5.3 Control frogs

Forty-five of 75 initially unexposed control frogs survived the duration of the experiment (60%), with 40 being recorded as uninfected (0 ZSE) at the time the experiment concluded. The number of days survived during the experiment between control and exposed frog groups was significantly different (Wilcoxon W = 20379.5, $p < 0.001$). Comparison of a mortality frequency curve for exposed frogs (all populations) versus unexposed control frogs (Fig. 5.6) clearly demonstrates a time shift in the onset of mortality between these groups. The duration of infection prior to mortality in the exposed group of frogs was approximately 25-39 days (varying with population and clutch, Table F.1). Mortalities in unexposed control frogs commenced 43 days post exposure and continued at a low level for the duration of the experiment.

Figure 5.2. Survival curves for *L. v. alpina* frogs from four different populations of origin.

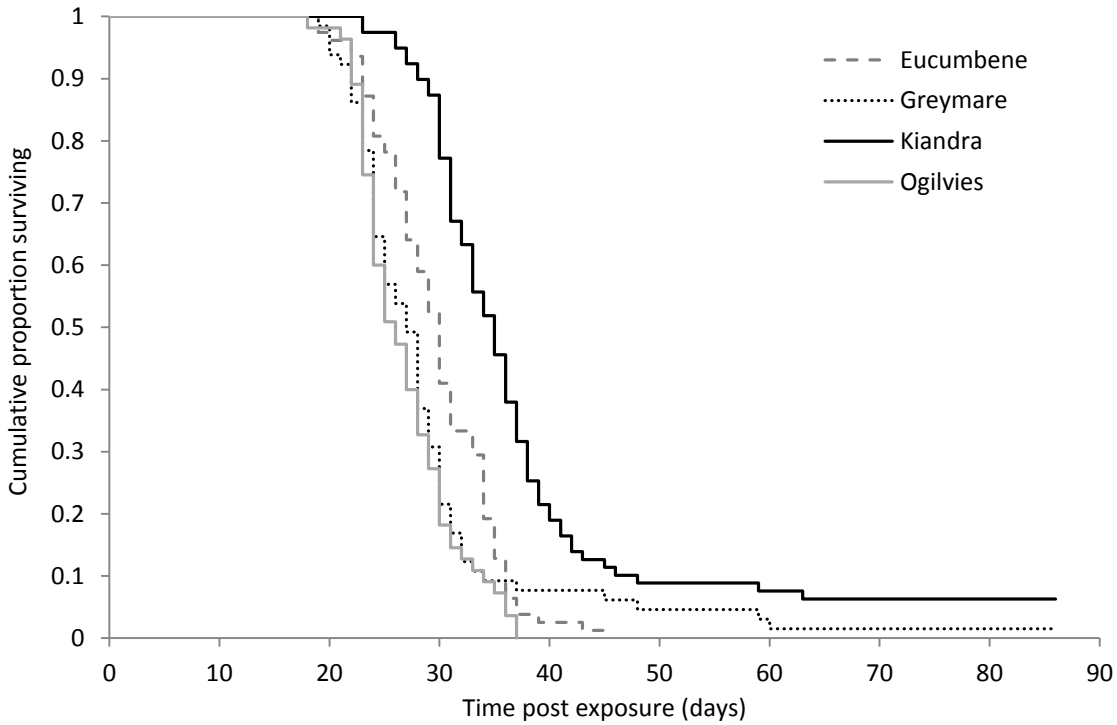

Figure 5.3. *Litoria verreauxi alpina* population survival curves by clutch.

Eucumbene (a), Grey Mare (b), Ogilvies (c) and Kiandra (d). The horizontal axis indicates days survived post exposure. The experiment was terminated at 86 days post-exposure for all groups.

(a)

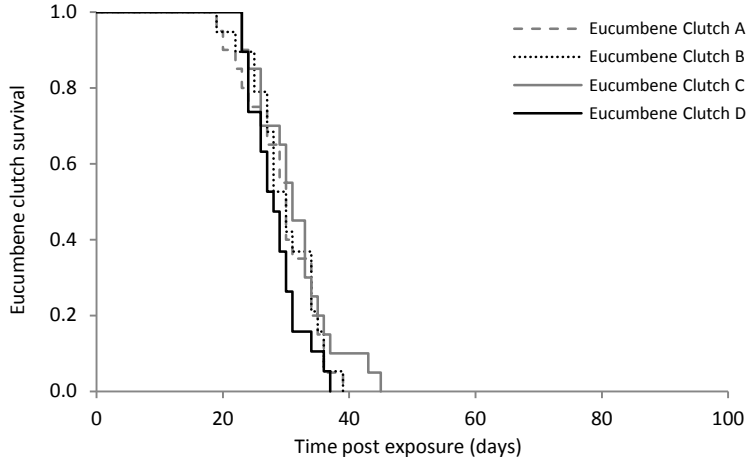

(b)

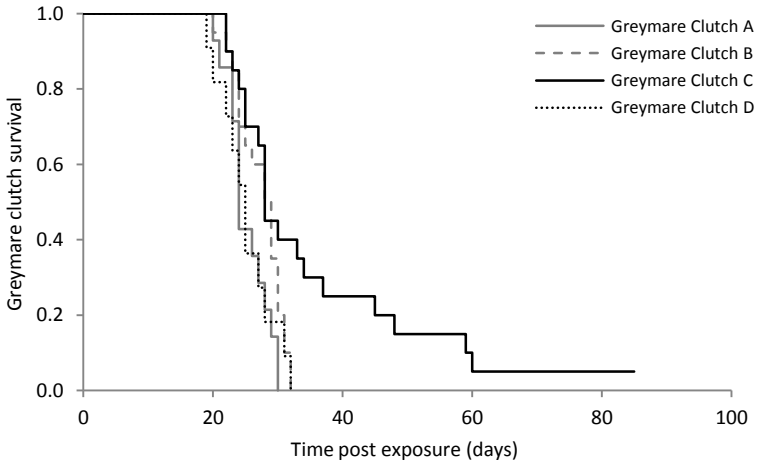

(c)

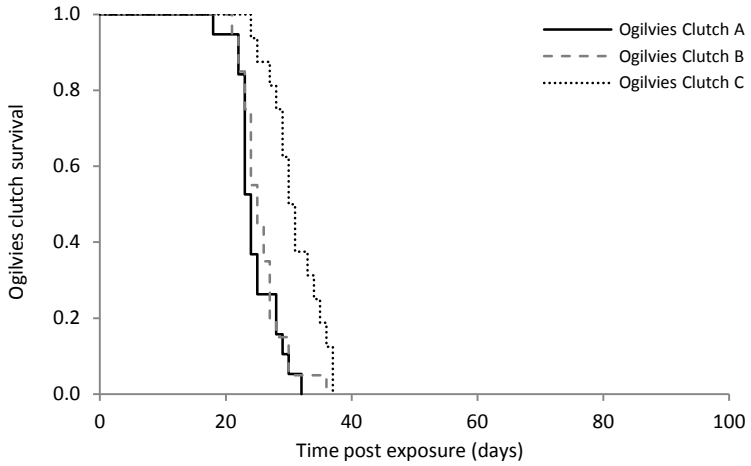

(d)

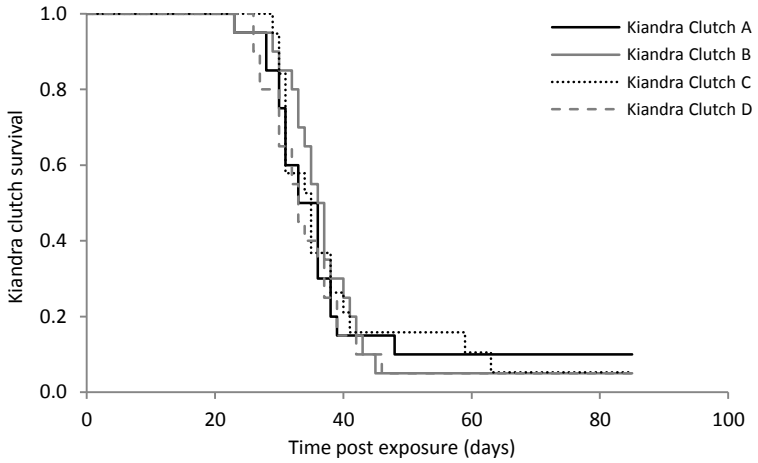

Figure 5.4. Intensity of infection (ZSE) on the log scale over time (in weeks post exposure) for *L. v. alpina* frogs from each population that died within five weeks (a) versus frogs that survived past five weeks but still died (b).

These results include the weekly swabs from a stratified random sample of up to 30 frogs from each population (stratified based on days survived). Swabs obtained on the date of death were also included in the data for the following week (except where the frog died on the day of swabbing). Error bars represent 95% Confidence Intervals.

(a)

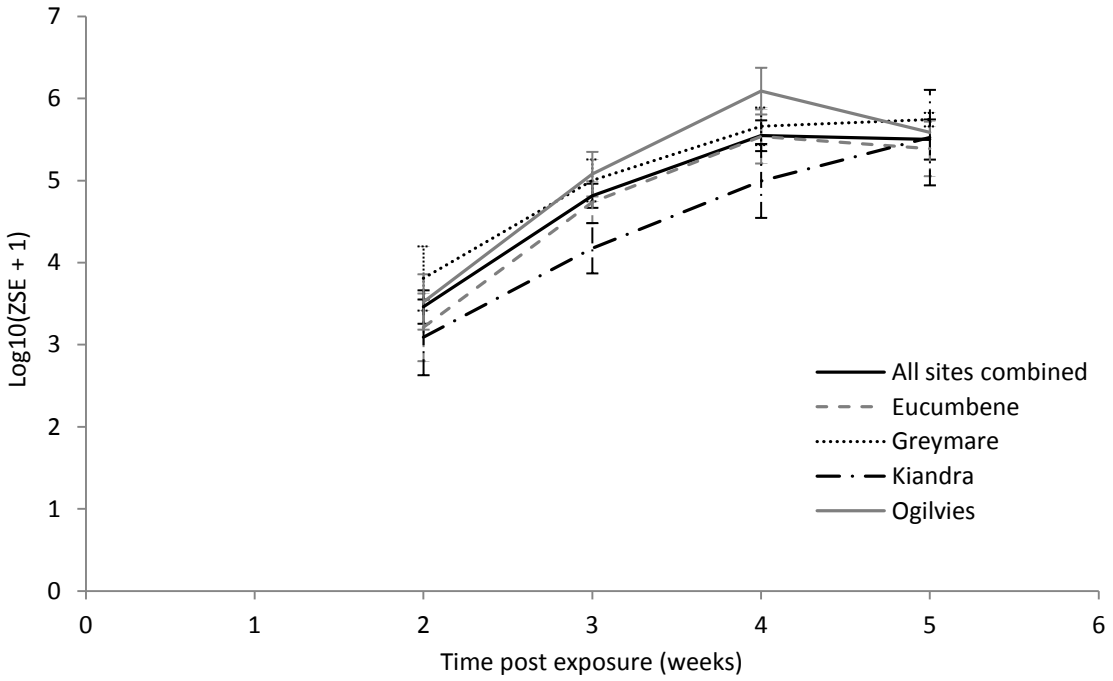
Log10(ZSE + 1)
Time post exposure (weeks)
All sites combined
Eucumbene
Greymare
Kiandra
Ogilvies

(b)

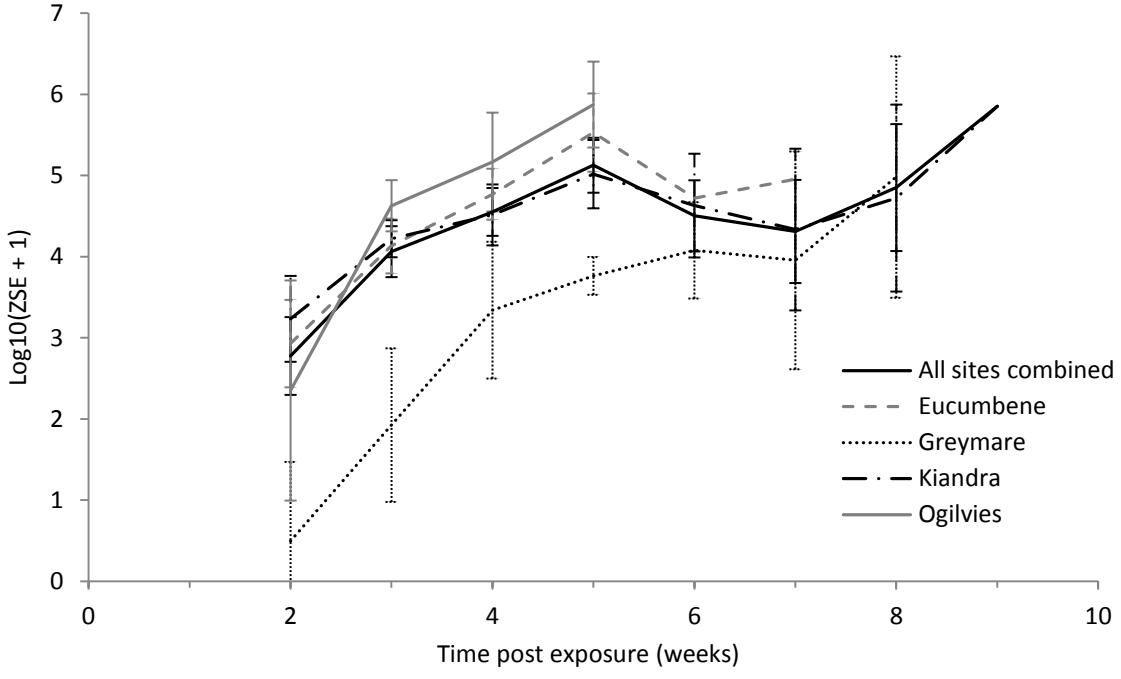
Log10(ZSE + 1)
Time post exposure (weeks)
All sites combined
Eucumbene
Greymare
Kiandra
Ogilvies

Figure 5.5. Intensity of infection on the log scale over time (in weeks) for individual *L. v. alpina* frogs identified by population, clutch and frog ID that survived the experiment.

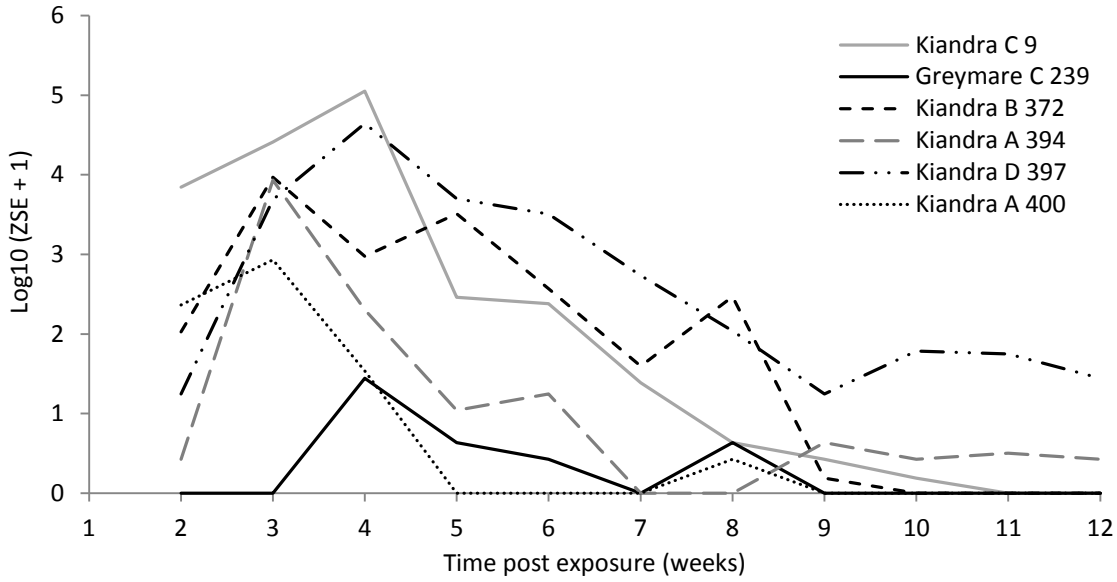

Figure 5.6. Frequency curve of *L. v. alpina* frog mortality based on days post exposure, comparing negative control and exposed frog groups (all populations pooled).

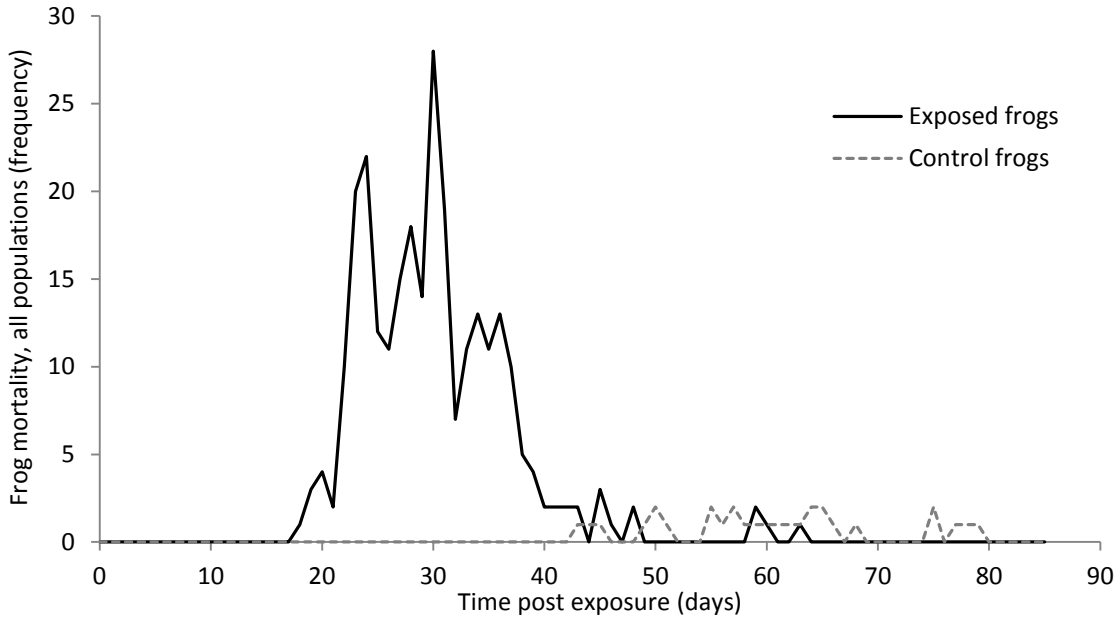

5.2.6 Discussion

The assisted evolution of disease resistance has been suggested as a possible management approach for the sustainable long-term mitigation of chytridiomycosis in threatened wild amphibian populations (Retallick et al., 2004). In order to investigate the potential for the evolution of immunologic resistance, in this study we compared susceptibility to infection with *Batrachochytrium dendrobatidis* (Bd) between three long-exposed (> 20 years) populations and a geographically associated but Bd-naïve population of alpine tree frogs (*Litoria verreauxi alpina*). Frogs were sourced from the wild as eggs and raised Bd-naïve to prevent any effects of prior Bd exposure. We found that frogs from one long-exposed population had significantly longer survival when compared with frogs from two other long-exposed populations and a naïve population, consistent with the evolution of resistance. This result is promising for the management of chytridiomycosis via assisted selection techniques.

Several features may suggest that natural selection for immunologic resistance has not been particularly strong in this species, however, despite two decades of population exposure. These features include the observed low overall survival rates (six survivors among 277 exposed frogs), high infection intensities, and the lack of a consistent difference in disease resistance between the long-exposed and the naïve population. Our experimental design eliminated many potential confounders of genetic immune resistance *a priori* by controlling the exposure environment, dose and temporal course of infection. Pathogenic fungi have previously been suggested to play a role in the evolution of life-history characteristics of amphibians (including reproductive strategies; Green, 1999). Thus persistence of the long-exposed *L. v. alpina* populations in the wild may be predominantly due to environmental factors or the evolution of life history characteristics that promote survival or population resilience, such as changes in the timing of breeding season, and increased fecundity (as has been observed anecdotally in this species; pers. comm. B. Scheele).

Increased population size post Bd-emergence in a large, subtropical Australian species, *Mixophyes fleayi*, was associated with increased longevity, which is consistent with increasing disease resistance (Newell et al., 2013). Drawing on r/K-selection theory, *M. fleayi* tends to have characteristics of a K-selected organism, as it matures relatively slowly, lives longer and reproduces more slowly than *L. v alpina*, which is more typical of an r-selected species with faster and more rapid turnover (Reznick et al., 2002). As species with naturally high mortality rates typically mature earlier and have higher fecundity, perhaps in highly susceptible species, chytridiomycosis can cause a shift more towards r- selected characteristics.

An alternative explanation for improved population persistence at the long-exposed sites in the field may involve a reduction in pathogen virulence of the local Bd strain (that would not be detected in an exposure experiment with a non-local Bd isolate) (Berger et al., 2005b; Farrer et al., 2011). However, this explanation is less likely as there have been reports of mass mortalities and a marked drop in frog abundance when Bd emerged in the previously naïve site in late 2012 (pers. comm. B. Scheele, D. Hunter). This suggests that the local Bd strains are still highly virulent for naïve populations.

We also identified significant between-clutch differences in chytridiomycosis susceptibility in frogs from two sites, including one long-exposed site (Ogilvies) and the naïve site (Grey Mare). Frogs from one clutch of the naïve population demonstrated relatively high overall survival, and one of these frogs survived the duration of the experiment. Although the population-level results from Grey Mare contradict our original hypothesis of greater susceptibility in the naïve population, the clutch-level results are consistent with greater baseline diversity at this site which might be expected to decrease with the emergence of Bd. This underlying diversity (and our findings of a clutch with much greater survival) may permit the Grey Mare population to survive the emergence of Bd, possibly with the natural selection for resistance. Characterizing any change in genetic diversity at this site since the emergence of Bd may help elucidate the nature of the impact of Bd on naïve populations.

An analysis of changes in phylogenetic diversity associated with the emergence of chytridiomycosis in central Panama (Crawford et al., 2010) indicated that amphibian loss reduced amphibian evolutionary diversity by 33%. Smith et al. (2009b) similarly investigated phylogenetic diversity and found that the pattern of amphibian loss and extirpations was associated with homogenization both in genetic diversity at the family level and with regards to habitat use and reproductive mode. Presumably these trends in the reduction of genetic diversity also occur at the within-species level between populations, and this may suggest that Bd emergence in a naïve region may be associated with a severe drop in amphibian abundance (including possibly extirpation) with an overall reduction in genetic diversity. This would be consistent with our finding of greater between-clutch variation in survival demonstrated by our experimental frogs from the naïve Grey Mare site. It does not explain, however, the variation observed between clutches from the long-exposed population Ogilvies. However, the frogs from Ogilvies had very low overall survival in our experiment, which may suggest that the persistence of this population in the wild is associated instead with environmental factors, and that frogs from Ogilvies were subject to the least disease-associated selection. The observed intrinsic variation between clutches may be utilized to investigate mechanisms of innate

immunity, and may permit selection for resistance in captive breeding and reintroduction programs.

We found that Bd infection intensities followed a typical logistic growth curve for frogs that died within five weeks post exposure, and a double logistic curve in longer lived frogs that died after five weeks. Exponential *in vivo* growth of Bd has previously been observed during epidemics (Vredenburg et al., 2010). A possible cause for the second trend of increase in infection intensities may be the presence and subsequent removal, or evasion of a Bd growth-limiting host factor between five and seven weeks. In the six frogs that survived, infection intensities peaked at three to four weeks, and then gradually declined. Given that most of these longer surviving frogs came from a long-exposed population, this finding may be consistent with the evolution of genetic disease resistance. Alternatively, the observed second increase in infection intensities may be associated with unintentional cross-contamination in the exposure experiment.

Despite all efforts to minimize cross-contamination during the experiment (involving strict accordance with stringent hygiene protocols [Phillott et al., 2010b], single use of gloves and regular decontamination of equipment), we identified unexpected levels of infection and Bd-associated mortality in frogs from the unexposed control group. Analysis of the results from control frogs demonstrated, however, a distinct time-shift in the peak mortality period between control and exposed frogs, suggesting that any cross-contamination occurred during the peak infection period for the exposed frogs (approximately 32 days post exposure). This finding is likely to be associated with the supremely high infection intensities recorded from exposed frogs which were among the highest intensities ever reported (up to an uncapped eight million ZSE were recorded from an individual swab sample). We suspect that infectious zoospores from highly infected frogs may have been aerosolized during the daily water change. This finding of cross-contamination is unlikely to greatly affect interpretation of our survival results however, as all frogs were exposed similarly (with blinded and random bench assignment). It is possible, however, that exposed frogs recorded as dying > 45 days post exposure may in fact have been re-exposed through cross-contamination, and may have alternatively survived. This finding may underlie the observed double logistic curve in Fig. 5.4.

In summary, we found a significant difference in survival between frogs from one long-exposed population and the remaining three populations (including two other long-exposed sites and the naïve site). This finding is consistent with the evolution of resistance in these frogs. The low overall survival and high infection intensities observed in this study raise the potential for non-immune mechanisms to play a large role in population persistence in the field (such as changes

in life-history characteristics), which is consistent with anecdotal observations from this species. Thus promoting disease resistance through assisted selection may help overcome lack of opportunity for natural selection in the field. Due to experimental difficulties, we cannot confidently draw conclusions about the cause for the observed double logistic curve of infection intensities, and suggest this finding warrants further research. However, our results are promising for the future use of immunologic management strategies involving assisted selection for disease resistance.

5.2.7 Acknowledgments

We thank volunteers at Taronga Zoo (B. Keraunos and L. Powe), R. Spindler, K. Rose, S. Bell, R. Webb and members of the Taronga Conservation Society Herpetofauna Department for facilitating and assisting in this study. This study was conducted with approval by the Taronga Conservation Society Australia Animal Ethics Committee (4c/01/10), and under the Scientific Licence number: S12848 (D. Hunter). Funding was provided by the Biosecurity CRC and the Australian Research Council grants FT100100375, LP110200240 and DP120100811.

5.2.8 Supporting information

Additional supporting figures and tables are providing in Appendix F. The authors are solely responsible for the content and functionality of these materials. Queries (other than absence of the material) should be directed to the corresponding author.

5.3 PAPER 2: Evolution of resistance to chytridiomycosis is associated with a robust early immune response in a wild amphibian

This manuscript in preparation represents my original study design, conduct, sample collection and processing, data organisation, data analysis, results interpretation and manuscript write-up. Lee Skerratt, Lee Berger and Scott Cashins provided substantial assistance with experimental design. Scott Cashins assisted with conduct of the exposure experiment and sample collection. Jason Mulvenna provided substantial assistance and guidance with data organisation and analysis, and all co-authors provided editorial input.

The full reference for the manuscript is:
Grogan, L. F., Cashins, S. D., Berger, L., Skerratt, L. F., Mulvenna, J. P. (in prep) Evolution of resistance to chytridiomycosis is associated with a robust early immune response in a wild amphibian.

The following text is a word for word copy of the manuscript in preparation for PLOS Pathogens. Section, table and figure numbering has been added or reformatted for this thesis for ease of reference. Since the journal uses American English, the spelling follows this convention.

5.3.1 Front matter

Evolution of resistance to chytridiomycosis is associated with a robust early immune response in a wild amphibian

Running head: Gene expression and chytridiomycosis

Laura F. Grogan[1*], Scott D. Cashins[1], Lee Berger[1], Lee F. Skerratt[1], Jason Mulvenna[2]

Keywords: amphibian declines, RNA-seq, *Batrachochytrium dendrobatidis*, chytridiomycosis, next generation sequencing, resistance, transcriptomics, gene expression

[1]One Health Research Group, School of Public Health, Tropical Medicine and Rehabilitation Sciences, James Cook University, Townsville, Queensland 4811, Australia.
[2]QIMR Berghofer Medical Research Institute, Infectious Disease and Cancer, Brisbane, Queensland 4006, Australia.

[*] Corresponding author
Address: One Health Research Group, School of Public Health, Tropical Medicine and Rehabilitation Sciences, James Cook University, Townsville, Queensland 4811, Australia

Tel: (+61 4) 0225 5204
Email: laura.f.grogan@gmail.com

5.3.2 Abstract

The fungus, *Batrachochytrium dendrobatidis* (Bd), aetiological agent of the devastating amphibian skin disease chytridiomycosis, is now considered endemic in most climatically suitable regions around the world. In the face of continuing declines and extinctions, the evolution of or assisted selection for host immune resistance to chytridiomycosis may be a promising avenue for ensuring sustainable long-term persistence of Bd-threatened wild amphibians. For such a strategy to succeed it is essential to understand the mechanisms by which such resistance manifests. Here we examined transcriptomic responses of alpine tree frogs (*Litoria verreauxii alpina*) to subclinical Bd infection, comparing long-exposed populations to a naïve population. We performed a blinded, randomized and controlled exposure experiment, collecting skin, liver and spleen tissues at 4, 8 and 14 days post-exposure from 51 frogs for transcriptome assembly and differential gene expression analyses. We analysed our results in conjunction with data on infection intensities and the results of a large clinical survival experiment run concurrently in the same species. We identified a large number of significantly dysregulated transcripts (1043 in liver, 8165 in skin and 1665 in spleen) in the tissues from subclinically infected individuals versus unexposed negative control frog tissue, including the predominant up-regulation of numerous transcripts associated with the host immune response (dysregulation of 132 unique immune-associated transcripts in liver, 645 in skin, and 216 in spleen samples). Our comparison between populations highlighted variations in response to subclinical infection associated with long-term population Bd exposure history as well as clinical evidence of survival. Individuals from the longest-surviving population demonstrated a larger complement of differentially expressed immune-associated genes in the skin at 4 days post exposure than frogs from the two more susceptible populations, consistent with a robust early innate and adaptive immune response. Our results suggest that an insufficient early immune response to infection may contribute to the susceptibility of this non-model species to chytridiomycosis. They also provide supporting proof of concept for the evolution of resistance against chytridiomycosis, as well as suggesting possible molecular and genetic targets for future studies and management involving marker-assisted selection. We recommend that further studies investigating evolved resistance mechanisms to chytridiomycosis focus more on the early immune response to infection.

5.3.3 Introduction

The emergence of biodiversity diseases that negatively impact the conservation status of one or more species is of increasing global concern (Grogan et al., 2014). Chytridiomycosis, a skin disease caused by fungal pathogen *Batrachochytrium dentrobatidis* (Bd), has devastated amphibian species around the world (Skerratt et al., 2007), but is now considered endemic in most climatically suitable regions (Fisher et al., 2009b; Kinney et al., 2011; Murray et al., 2011a). Despite endemism, many populations continue to be threatened by chytridiomycosis (Murray et al., 2009; Muths et al., 2011; Phillott et al., 2013). Development and implementation of *in situ* interventions for managing these populations are still in their infancy (Scheele et al., 2014). Selection for evolved resistance or tolerance to disease has been suggested as a possible strategy for promoting long-term population persistence, and assisting the successful repatriation of *ex situ* captive colonies (Venesky et al., 2012; Woodhams et al., 2011). The evolution of resistance against disease has been demonstrated in other wild species and disease systems such as bacterial infection with *Mycoplasma galliseptum* in the North American house finch (*Carpodacuc mexicanus*; Bonneaud et al., 2011).

Considerable evidence exists for individual, population and species-level differences in susceptibility to chytridiomycosis that suggest promise for immunologic management strategies (Gervasi et al., 2013; Scheele et al., 2014; Searle et al., 2011; Tobler and Schmidt, 2010; Woodhams et al., 2011). However, many non-immune factors also determine disease manifestation, and particularly in field observational studies, may remain uncontrolled between study subjects (factors such as variations in autecology, behaviour, environment and pathogen strain; Berger et al., 2005b; Koprivnikar et al., 2011; Murray and Skerratt, 2012; Rowley and Alford, 2007a). In addition, the large host range of chytridiomycosis makes it difficult to draw parallels across species and systems (Olson et al., 2013).

The amphibian immune response to infectious organisms, similar to other vertebrates, is enormously complex, involving numerous cell types and hundreds of interacting molecular pathways (Murphy, 2012; Robert and Ohta, 2009). This complexity makes it difficult not only to isolate the effects of individual components, but to relate these effects back to their relative importance within the system as a whole, which is crucial for prioritizing genetic targets for immunologic management strategies such as assisted selection for resistance (Rollins-Smith et al., 2011; Voyles et al., 2011). Thus, although a number of immune determinants of susceptibility have been identified, studies to date have largely focused on these variables in isolation. These studies include the expression and characterization of anti-microbial skin defense peptides, examination of symbiotic skin bacteria and their anti-fungal metabolites, skin histopathology, systemic haematology, targeted assays of infection-associated stress markers,

investigation of MHC expression, immunization studies, and various experiments on adaptive immune components *in vitro* (Berger et al., 2005c; Cashins et al., 2013; Holden and Rollins-Smith, 2014; McMahon et al., 2014; Pask et al., 2013; Ramsey et al., 2010; Rollins-Smith et al., 2011; Savage and Zamudio, 2011; Young et al., 2014).

With regards to the potential for the evolutionary development of resistance to chytridiomycosis, the most promising work thus far has been done by Savage and Zamudio (2011). They examined major histocompatibility (MHC) genes and correlated the level of heterozygosity with survival both in a clinical experiment and in the wild populations, indicating likely evolution of resistance at the MHC locus. While this targeted approach can yield important information about the potential evolution of resistance, especially at highly polymorphic loci that have been recognized to demonstrate selection in response to infectious diseases (Meyer and Thomson, 2001), it may fail to reveal the complex and potentially multifactorial and multiple-gene nature of the immune interactions involved in a protective or resistant response to infection with Bd.

High-throughput transcriptomics (via RNA-seq) is a relatively recent functional genomics approach that can be used to examine global snapshots of messenger RNA expressed within cells, tissues and whole animals at various stages of infection. Thus it allows non-targeted comparison of genes that differ in their expression levels (differential gene expression; DGE), underlying physiological and immune mechanisms, between individuals that differ in infection status, and other covariates such as time since exposure, population or species of origin, and gender, etc. The benefits of RNA-seq for DGE analysis over traditional methods such as microarray analysis are manifold, and include low and repeatable poisson-distributed technical variation (Marioni et al., 2008), high dynamic range (Wang et al., 2009), and lack of requirement for *a priori* gene targets (Wang et al., 2009) which is especially beneficial in non-model species without reference genomes available. Gene expression in response to chytridiomycosis has been examined in a few studies thus far (Ellison et al., 2014; Ribas et al., 2009; Rosenblum et al., 2012b; Rosenblum et al., 2009), however none have examined the potential for evolution of resistance and characterized underlying resistance mechanisms. Comparing populations with differential exposure histories and differing survival in response to Bd by utilizing a transcriptomics approach might yield differences in gene expression that indicate heritable resistance, and markers that may be used for assisted selection.

The goals of this study were to characterize differential gene expression among two experimental group comparisons; 1) uninfected negative control individuals and subclinically infected individuals at different time points post-exposure, and 2) subclinically infected

individuals between long-exposed populations and an evolutionarily naïve population. To achieve these aims we performed a rigorous, block-randomized, blinded and controlled clinical exposure experiment to the fungal pathogen Bd using 51 naïve wild-caught but quarantine captive-raised alpine tree frogs (a non-model, but highly susceptible species; *Litoria verreauxii alpina*). Frogs were derived from three different populations (two long-exposed to the pathogen in the wild, and one naïve at the time of sampling), and we extracted total RNA from three immune-related tissues (spleen, skin and liver) at three different time points post exposure (four, eight and 14 days post exposure, hereafter DPE) from both exposed-infected and unexposed control frogs. We assembled and annotated tissue-specific transcriptomes for the species based on all sequence information, then characterized differential gene expression between experimental groups (controls and time series post exposure, and population). In addition, we examined the infection intensities at time of euthanasia for each frog sampled, and compared our results with survival curves from a large clinical survival experiment undertaken concurrently with frogs from the same clutches and populations.

5.3.4 Methods

5.3.4.1 Study subjects and husbandry

Fifty-one Bd-naïve adult Alpine Tree frogs (*Litoria verreauxii alpina*) from three geographically distinct populations were raised in Bd-negative quarantine conditions from wild-caught egg-masses until eight months post-metamorphosis (Scientific License number: S12848). The populations are hereafter designated Kiandra, a Bd long-exposed site (35.872°S 148.500°E 1356 m above sea level [asl]), Eucumbene, a Bd long-exposed site (36.152°S 148.563°E 1451 m asl), and Grey Mare, a Bd-naïve site (36.317°S 148.260°E 1525 m asl). Frogs were transferred to individual tubs several weeks prior to commencement of the exposure experiment to allow for acclimatization. Prior to and during the exposure experiment, frogs were maintained at constant 19ºC (± 2ºC) in individual plastic take-away containers with gauze covered lids, pebble substrate, and water drainage holes down one end of the tub. Containers were placed at a slight angle to facilitate water drainage, and provide wet and dry areas. Frogs were fed multivitamin and calcium dusted crickets alternately twice weekly *ad libitum*. Individual frogs were observed daily by an experienced animal handler and veterinarian for health status and clinical signs of disease. Tubs were each flushed daily for 15 seconds with filtered water until the water ran clear and debris was removed.

5.3.4.2 Exposure experiment

Frogs were confirmed negative to Bd prior to the commencement of the exposure experiment (via qPCR – see below). The exposure experiment consisted of a total of 51 experimental animals, 18 frogs from each of Eucumbene and Kiandra populations (including 6 negative

control animals from each population), and 15 frogs from Grey Mare (including 3 negative control animals; Table 5.2). A Bd strain isolated roughly two years before was used for inoculations (AbercrombieNP-*L.booroolongensis*-09-LB-P7), being maintained as described previously (Cashins et al., 2013). Thirty-six experimental animals were individually exposed to 750,000 zoospores in 25ml dilute salts solution (in mMol: KH2PO4 1.0, CaCl2.H2O 0.2, MgCl2.2H2O 0.1) with tubs held flat without substrate pebbles for 18 hours. Following exposure, tubs were kept horizontal for a further two days but the water was replaced daily, before having pebbles added and being placed on a mild angle (10º) for ease of drainage. Unexposed frogs were treated similarly, but were sham exposed with only dilute salts solution. Animal experiments were approved by James Cook University Animal Ethics Committee (A1589).

Table 5.2. Experimental design outlining the number of frogs from each population and treatment group (Bd exposed or unexposed control) sampled at each time point post exposure.

Populations	Exposure – Day 0 Total # exposed (total # control)[a]	Day 4 # exposed sampled (# control sampled)[b]	Day 8 # exposed sampled (# control sampled)[b]	Day 14 # exposed sampled (# control sampled)[b]
Grey Mare (clutch B)	12 (3)	4 (1)	4 (1)	4 (1)
Eucumbene (clutch D)	12 (6)	4 (2)	4 (2)	4 (2)
Kiandra (clutch B)	12 (6)	4 (2)	4 (2)	4 (2)
Total	36 (15)	12 (5)	12 (5)	12 (5)

[a]Total number of unexposed control frogs shown in parentheses; [b]Number of unexposed control frogs sampled shown in parentheses.

5.3.4.3 Euthanasia and sampling

Three sampling sessions were performed at 4, 8 and 14 days post exposure, and a randomized block design was used to select 17 frogs for each sampling session (evenly spread amongst populations and exposed versus control animals). The timing of sampling sessions was designed to correspond with subclinical infections, and no frogs exhibited clinical signs of chytridiomycosis (muscle weakness, lethargy, peripheral erythema or inability to maintain normal upright posture) or mortality within the duration of the experiment. Immediately prior to euthanasia, frogs were swabbed to confirm infection status and to quantify Bd infection intensity (via qPCR see below), and had their mass and snout-urostyle length recorded. Frogs were then humanely euthanized via double pithing, and a routine midline coeliotomy was performed for tissue collection. Tissues collected included ventral abdominal and thigh skin, liver and spleen, and these were immediately transferred to RNAlater (Qiagen) and refrigerated overnight at 4 °C before being stored longer-term at -80 ºC. Gender was also ascertained via

examination of forelimb nuptial pads on males and observation of coelomic reproductive organs.

5.3.4.4 Infection intensities

Bd infection intensity data (in zoospore equivalents, ZSE) was collected via swabbing using a new sterile dry swab per frog (MW 100-100; Medical Wire and Equipment, Bath, UK). Swabs were stored dry at 4 °C and were analyzed for the presence or absence of Bd DNA with the TaqMan real-time qPCR protocol following Hyatt et al. (2007). Individual swabs were analyzed in triplicate and each run included an internal positive control. Samples which recorded only one or two of the three wells as a low positive were considered indeterminate positives.

5.3.4.5 RNA extractions

Total RNA was isolated from skin, liver and spleen tissue samples following the protocol for 5-Prime PerfectPure RNA Tissue kits for liver and skin samples and Qiagen RNeasy mini kits for spleen samples (the spleens were considerably smaller in volume), by first removing tissues from RNAlater, and lysing using a rotor-stator homogenizer. Liver and skin lysates were treated with DNase to remove genomic DNA, and skin lysates were subject to an additional proteinase K step to digest keratin, remove excess proteins, and inactivate nucleases. Pure total RNA was eluted in nuclease free water. RNA quantity was determined with a Nanodrop 1000 spectrophotometer, the absorption ratios 260/280 (~ 2.0) and 260/230 (2.0-2.2) were assessed, and the spectral pattern was evaluated in order to determine RNA integrity and purity. RNA stable plates (Biomatrica) were used to ship total RNA samples dry and at room temperature to Minnesota BioMedical Genomics Centre, USA.

5.3.4.6 RNA-Seq using the Illumina platform

Total RNA samples were reconstituted with nuclease-free water, were quantified with a fluorimetric RiboGreen assay, and had their quality assessed with capillary electrophoresis (Agilent BioAnalyzer 2100). Samples containing > 1ug total RNA and having an RNA Integrity Number (RIN) > 8 passed quality control. cDNA Illumina sequencing libraries were created from each of the samples following the manufacturers specifications (Illumina Truseq RNA Sample Preparation Kit), and up to 12 samples were individually indexed by the ligation of adaptors for multiplexing on each flow cell lane. Indexed libraries were gel-size selected to 320 base pairs (bp) +/- 5%, and hybridized to a paired end flow cell, before being clonally amplified by bridge amplification, and sequenced with the Illumina HiSeq 2000 (Illumina, San Diego, CA). Base call data for paired end reads from each sample were analyzed and de-multiplexed with CASAVA software 1.8.2 (Illumina, San Diego, CA), producing .fastq files for each sample.

5.3.4.7 Transcriptome assembly and annotation

The 100 bp paired end read sequences from each sample were examined for read quality using FastQC (www.bioinformatics.babraham.ac.uk/projects/fastqc/). Trimmomatic 0.30 (Bolger et al., 2014) was run in paired end mode and used to trim TruSeq adapter sequences, crop Illumina's random hexamers (Hansen et al., 2010), perform sliding window trimming (window size 4, required quality 15), head and tail quality trimming (required quality 3), and ensure minimum length of resultant reads was at least 75 bases. Widowed reads were retained as unpaired forward and reverse read files. Paired and unpaired files were concatenated by tissue type using custom in-house scripts, and paired reads for each sample were interleaved using shuffleSequences_fastq.pl (Velvet Package; Zerbino and Birney, 2008). We digitally normalized the file to reduce overall data set size and remove read redundancy using DigiNorm (Brown et al., 2012) with the -p flag for the paired read files. We then used Bowtie (Langmead et al., 2009) to filter reads aligning to the Bd genome. The resulting read files (one interleaved paired read file and two unpaired read files for each tissue type) were assembled *de novo* using Trinity (using the --run_as_paired flag; Haas et al., 2013). The output Trinity.fasta file for each tissue type contained all assembled transcripts, which were translated into coding amino acid sequences *in silico* using TransDecoder (Trinity). The resulting .pep files were functionally annotated by using BLASTx against an anuran database (consisting of *Xenopus spp.* and *Rana spp.*) from the non-redundant database at the National Center for Biotechnology Information (NCBI; http://www.ncbi.nlm.nih.gov).

5.3.4.8 Differential gene expression analysis

The R package RSEM (Li and Dewey, 2011) was used to quantify the abundance of genes and isoforms in individual frog tissue samples in combination with the above-described tissue-specific assembled transcriptomes, generating tables of transcript count data. EdgeR from the Bioconductor suite (Robinson et al., 2010a) was then used to identify differentially expressed genes between experimental groups. We first filtered out reads with very low counts (see Appendix G, Table G.1 for details). Significantly dysregulated transcripts were identified as those with a false discovery rate (FDR) of < 0.05 using Benjamini-Hochberg multiple testing correction. We first performed a batch analysis (based on time of sampling) on unexposed control frog samples from the three tissue types to identify any underlying systematic differences between sampling sessions. We then compared the within-population pooled unexposed control frog samples with respective exposed frog samples taken at 4, 8 and 14 days post exposure within the three populations, in order to identify genes that were either up- or down-regulated relative to the control baseline. BLASTx alignment to the NCBI non-redundant protein database, InterProScan (Jones et al., 2014) and Gene Ontology (GO) Term annotations

for identified differentially expressed genes from each comparison were then examined in detail using BLAST2GO version 2.7.2 (Conesa et al., 2005).

We manually extracted and curated a list of genes of particular interest for each time-series comparison within population and tissue type, associated with expected immune functions by comparing a list of immune-related search terms with gene name (as returned by BLASTx) and GO term descriptions. We also performed Euclidean distance clustering on differentially expressed gene sets (by population within tissue type) for genes with FDR < 0.05 and fold change (FC) > 1 (varying by population to obtain optimum clustering; using Trinity and custom scripts) and plotted heatmaps by first ordering samples (columns of the heatmaps) by infection intensity within sampling period groups in time-series fashion, then manually partitioning clusters via the gene-element dendrogram based on visual inspection ('heatmap.3' from R package GMD; Zhao and Sandelin, 2012). We then performed GO functional enrichment analysis (using Fisher's exact test and a p-value of < 0.05 to identify subtle changes consistent with the subclinical nature of our study) on each cluster against an annotated reference genome of *Xenopus (Silurana) tropicalis* to identify over-represented GO terms (Gotz et al., 2011). We used *X. tropicalis* for the reference set because the majority of top-hit BLASTx results were derived from that species.

5.3.5 Results

5.3.5.1 Experimental results

All 51 frogs survived for the duration of the experiment without demonstrating clinical signs. Detailed demographic data on the sampled frogs including infection intensities assessed via qPCR at time of sampling (pre-euthanasia) are listed in Table 5.3. There was no evidence for a significant difference between frogs from different populations in terms of the mean mass, snout-urostyle length (SUL), or uncapped ZSE at time of sampling (one-way ANOVA, $F = 0.938$, $p = 0.398$, 2 df; $F = 2.423$, $p = 0.099$, 2 df; and $F = 1.876$, $p = 0.164$, 2 df for mass, SUL and ZSE respectively; Table 5.3). Unexposed control group frogs remained uninfected for the duration of the experiment except for one indeterminate result (one well positive, < 2 ZSE). Exposed frogs became infected (with one indeterminate result and one negative result), demonstrating variable but increasing Bd intensities through time. Mean capped intensities were 34, 2,200 and 11,161 ZSE for 4, 8 and 14 DPE respectively (several samples taken at the final session were above the highest qPCR standard and without truncating for this standard, the final uncapped average was 21,482 ZSE). These infection intensities are comparable to those observed from wild alpine tree frogs (pers. comm. D. Hunter). A non-significant trend was observed indicating lower infection intensities throughout the three sampling sessions within the

Kiandra group (box and whisker plots showing log_{10}-transformed ZSE data by population and sample period is shown in Fig. 5.7).

Table 5.3. Demographic characteristics of study subjects (including sample size, treatment group, gender ratios, mean mass at death, mean snout-urostyle length at death and mean and median infection intensity at death).

	Kiandra		Eucumbene		Grey Mare		F value[a]	P value[a]	df[a]
	Exposed	Control	Exposed	Control	Exposed	Control			
Sample size	12	6	12	6	12	3			
Gender[b]	2M, 4F, 6U	2M, 4U	4M, 5F, 3U	5F, 1M	4M, 6F, 2U	1M, 2F			
Mean mass at death	2.99	3.02	3.02	4.05	3.51	3.19	0.938	0.398	2
Mean SUL at death[c]	29.97	30.72	28.80	32.1	32.27	32.03	2.423	0.099	2
Mean ZSE at death[d]	2158.82	0.28	9442.36	0.00	12114.72	0.00	1.876	0.164	2
Median ZSE at death	290.00	0.00	715.00	0.00	910.00	0.00			

[a]Statistics comparing means between populations (pooling exposed and control frog values) using one-way ANOVA, P value and df degrees of freedom; [b]Genders represented by M for males, F for females and U for unknown gender; [c]SUL is snout-urostyle length measured with Vernier callipers; [d]ZSE is zoospore equivalents as measured by qPCR.

Figure 5.7. Box and whisker plot (with data points overlaid) of log_{10}-transformed zoospore equivalent values (Bd infection intensity) for all 51 frogs at time of sampling in days post exposure, by population.

Data from uninfected control frogs has been plotted as 'zero' days post exposure (regardless of actual sampling date), for ease of comparison. Group outliers have been labeled with frog ID.

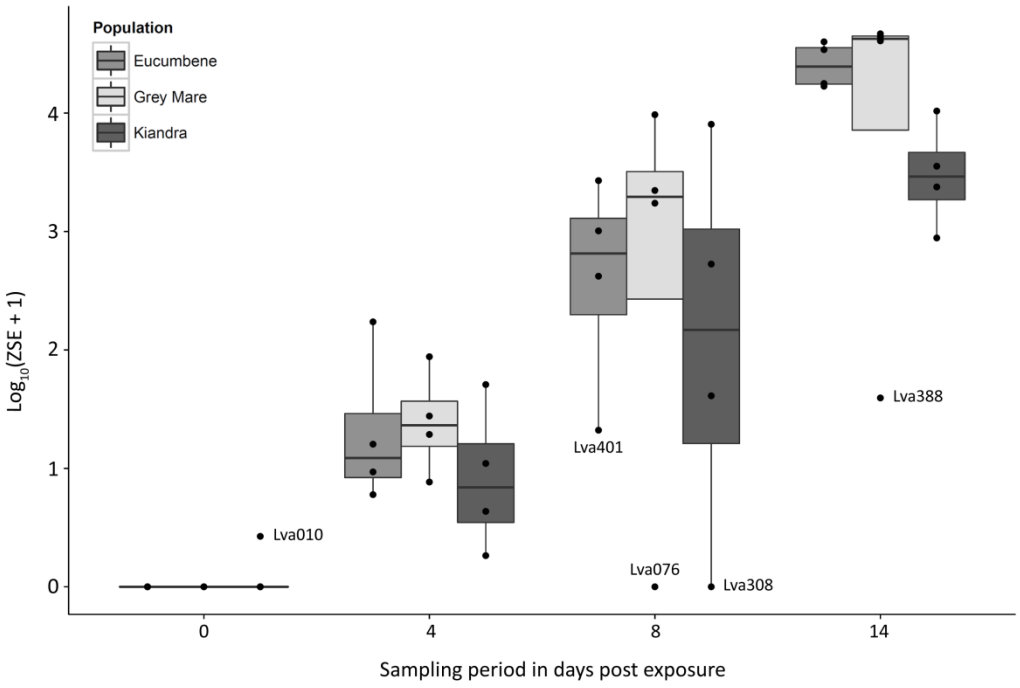

Survival results for the larger clinical experiment (Section 5.2 of this thesis) corresponding to frogs from identical clutches and populations to those sampled in this experiment (also performed concurrently), demonstrated an increasing trend in survival in frogs from populations Grey Mare, Eucumbene and Kiandra, respectively (Fig. 5.8). Frogs from long-exposed population Kiandra (Clutch B; N = 20, one frog survived the duration of the experiment to 86 DPE) survived for longer when compared with the other long-exposed population Eucumbene (Clutch D; N = 19, last surviving frog died 37 DPE; $\chi^2 = 19$, df = 1, $p < 0.0001$; using the Mantel-Haenszel test; Harrington and Fleming, 1982), and the naïve population Grey Mare (Clutch B; N = 20, last surviving frog died 32 DPE; $\chi^2 = 29.9$, df = 1, $p < 0.0001$). There was no evidence for a significant difference in survival between frogs from Eucumbene and Grey Mare ($\chi^2 = 0.7$, df = 1, p =0.41).

Figure 5.8. *L. v. alpina* population survival curves by population and clutch for the larger clinical experiment.

The horizontal axis indicates days survived post exposure (the experiment was terminated at 86 days post-exposure for all groups).

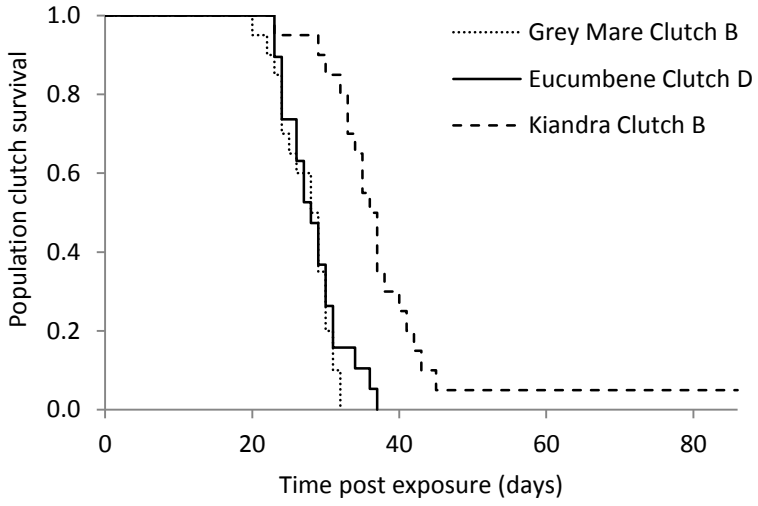

5.3.5.2 RNA-seq data, transcriptome assembly and annotation

A total of 153 tissue samples (including skin, liver and spleen tissues) were obtained from the frogs during the course of the experiment, and total RNA was successfully extracted from all samples. The amount of total RNA extracted varied by tissue type and size; mean total RNA extracted was 81.27ug for liver samples (SD 45.58ug; N = 51), 19.76ug for skin samples (SD 8.51ug; N = 51), and 5.47ug for spleen samples (SD 1.69ug; N = 50). Of these samples, 148

passed quality control with a quantity > 1ug, and RIN > 8. Shipping at room temperature using RNA stable plates did not adversely impact RNA quality or resuspended mass. All 16 Illumina HiSeq 2000 flow cell lanes generated > 160 million pass filter reads (> 10 million reads per sample). Average number of raw reads per sample for liver was 15,819,807, SD 1,940,924, N = 50; for skin was 15,220,337, SD 4,778,641, N = 51; for spleen was 16,997,724, SD 2,302,778, N = 50; and overall total number of reads = 2,417,113,729. Phred quality scores were high within individual reads and across the data set (average Q-Score = 34.7; 99.9-99.99% base call accuracy). Trinity transcriptomes were assembled *de novo* for each tissue, yielding 324,937 Trinity 'transcript clusters' (hereafter referred to as genes) for liver; 368,259 genes for skin; and 448,394 genes for spleen tissues, with average contig lengths 670, 679 and 636 bp respectively (details of the Trinity assemblies for each tissue type are shown in Table 5.4). These gene numbers are comparable with similar non-model species' *de novo* transcriptome assemblies (Ellison et al, 2014). Approximately 28% of assembled genes were able to be annotated via BLASTx against our anuran protein database from the NCBI (90,794 of 324,936 liver genes, 103,038 of 368,258 skin genes and 123,591 of 448,393 spleen genes were annotated with at least one significant hit). The majority of top BLAST hits corresponded to genes from *Xenopus (Silurana) tropicalis* (approximately 42%), and approximately 78% of genes with BLAST hits had GO terms assigned.

Table 5.4. Details of Trinity assemblies for each tissue type.

	Liver	Skin	Spleen
Total Trinity 'genes'[a]	324937	368259	448394
Total Trinity transcripts	492315	586459	722895
Percent GC	43.85	43.72	43.76
Contig N50	1016	1007	897
Median contig length	378	394	385
Average contig length	669.80	679.10	636.72
Total assembled bases	329751030	398264505	460281755

[a]Trinity labels 'transcript clusters' as roughly equivalent to 'genes'.

5.3.5.3 Differential gene expression, clustering and enrichment analyses

We compared the numbers of differentially expressed genes between control frogs (pooled between populations) sampled at 4, 8 and 14 DPE and found no evidence of a batch effect between sample sessions in the skin and spleen samples (0 differentially expressed genes for skin comparisons; and 2 differentially expressed genes for spleen comparisons between times 4 and 8 DPE, sharing one common gene with the 8 and 14 DPE comparison). However there was

some evidence for a mild batch effect between sampling sessions within the liver samples (334 differentially expressed genes identified between sampling times 4 and 8 DPE, sharing 3 similar genes with the comparison between sample sessions 8 and 14 DPE, for a total of 5 differentially expressed genes; see Appendix G, Fig. G.1).

Comparison of gene expression levels between control (uninfected) and exposed frog groups revealed distinct grouping by population for all three tissue types using multi-dimensional scaling plots (Robinson et al., 2010a; populations are represented by colour groups in Fig. 5.9). There was mild evidence for grouping by infection status in both skin and spleen samples (circles represent Bd-exposed samples, triangles represent controls; Figs. 5.9B and 5.9C), however liver samples from control frogs appeared relatively divergent in both Eucumbene and Grey Mare population samples (Fig. 5.9A).

Figure 5.9. Multi-dimensional scaling plots comparing gene expression levels between uninfected negative control frog samples (triangles) and Bd-exposed frog samples (circles). Grouping is predominantly demonstrated by source population (colour groups: Eucumbene = blue, Grey Mare = red, Kiandra = gold). (A) Liver samples, (B) skin samples, and (C) spleen samples. Group outliers have been labeled with frog ID.

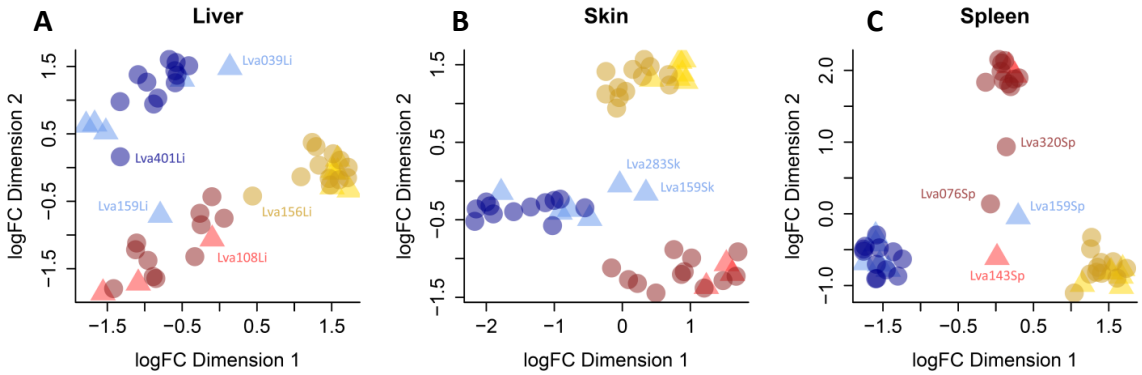

When we compared exposed with control samples on a time-series basis (comparing samples from 4, 8 and 14 DPE with controls within population and tissue type respectively), we found the highest levels of differential gene expression at the late subclinical infection time point (14 DPE), with the strongest response to infection in the skin samples at 14 DPE (high numbers of genes both up- and down-regulated; Fig. 5.10), likely associated with the severity of infection, tissue damage, and possible secondary bacterial infection in the skin. We observed a trend in levels of gene expression between populations in the skin samples at 14 DPE. Frogs from the naïve Grey Mare population had the highest levels of differentially expressed genes in the skin

at 14 DPE; long-exposed Eucumbene population had intermediate gene dysregulation; and long-exposed Kiandra population had the lowest levels of gene dysregulation respectively among the three populations compared.

Figure 5.10. Numbers of up and down regulated genes comparing uninfected negative control frog samples and Bd-exposed frog samples within-population at sampling periods post exposure, for all populations and tissues.

Gene expression in skin samples from all three populations at 14 days post exposure were most highly dysregulated.

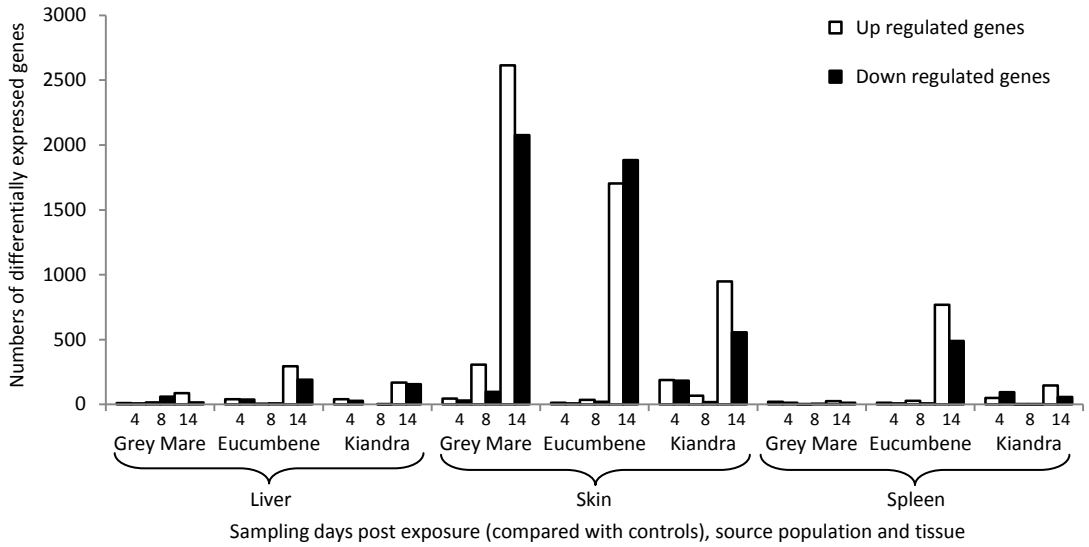

We found little overlap between populations in terms of the genes that were differentially expressed (including those between controls and 4, 8 and 14 DPE) in both the liver and spleen tissues, with greatest number of genes shared between the two long-exposed populations Eucumbene and Kiandra (Figs. 5.11A and 5.11C; Micallef and Rodgers, 2014). Many differentially expressed genes were found to be shared between populations in the skin samples, however, particularly between samples from Grey Mare and Eucumbene (total of 1564 genes shared between Grey Mare and Eucumbene samples; Fig. 5.11B). Venn diagrams for shared differentially expressed genes between populations separated by sampling time post exposure can be found in Appendix G (Figs. G.2-G.4).

Figure 5.11. Venn diagrams comparing overlap in genes that were differentially expressed. Venn diagrams compare uninfected negative control frog samples and Bd-exposed frog samples within-population at sampling periods post exposure between populations among (A) liver, (B) skin, and (C) spleen tissue samples.

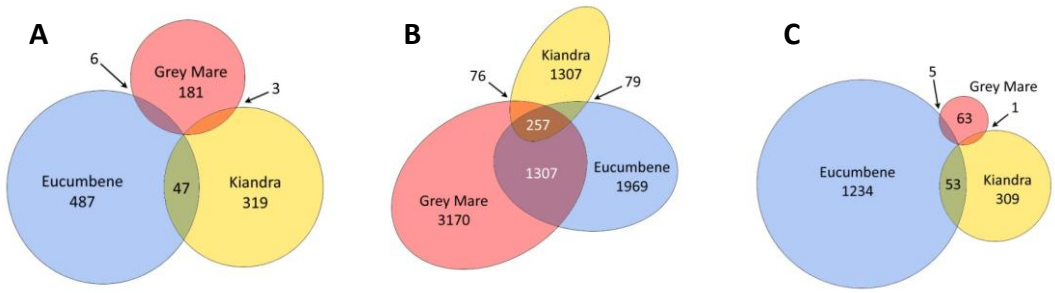

We clustered differentially expressed gene sets (within population and tissue) by Euclidean distance and visually inspected the resultant heatmaps for manual partitioning into biologically relevant clusters (skin tissue heatmaps are shown in Fig. 5.13). We identified two clusters for each of Eucumbene and Grey Mare skin samples (SkEuc1, SkEuc2, SkGre1, SkGre2 respectively; see Fig. 5.13A, 5.13B; FDR < 0.001, FC > 4), and four clusters for skin samples from Kiandra (SkKia1-4; see Fig. 5.13C; FDR < 0.001, FC > 1). Cluster plots using $\log_2$ transformed, median-centered expression values revealed an approximately increasing time-series trend in SkEuc2 and SkGre1, and a decreasing trend in SkEuc1 and SkGre2 (Figs. 5.12A and 5.12B). A more distinct jump in expression between control and 4 DPE was observed for skin samples from Kiandra (Fig. 5.12C), whereby expression of genes in cluster SkKia1 increased, and in cluster SkKia3 decreased at 4 DPE relative to controls. Genes in SkKia2 peaked in samples from 4DPE relative to controls and other exposed samples, and SkKia4 consisted only of a single gene (due to the nature of clustering).

Figure 5.12. Log_2 transformed, median-centered expression value plots for clusters defined manually from Euclidean distance clustering for differentially expressed genes (comparing exposed with control groups) identified within skin samples from each population.

(A) Eucumbene, (B) Grey Mare, (C) Kiandra. The frog ID for individual samples is listed along the horizontal axis, from left to right in order of increasing infection intensity within sample groups (Control, and 4, 8 and 14 DPE respectively), corresponding with the sample order shown in the heatmaps (Fig. 5.13).

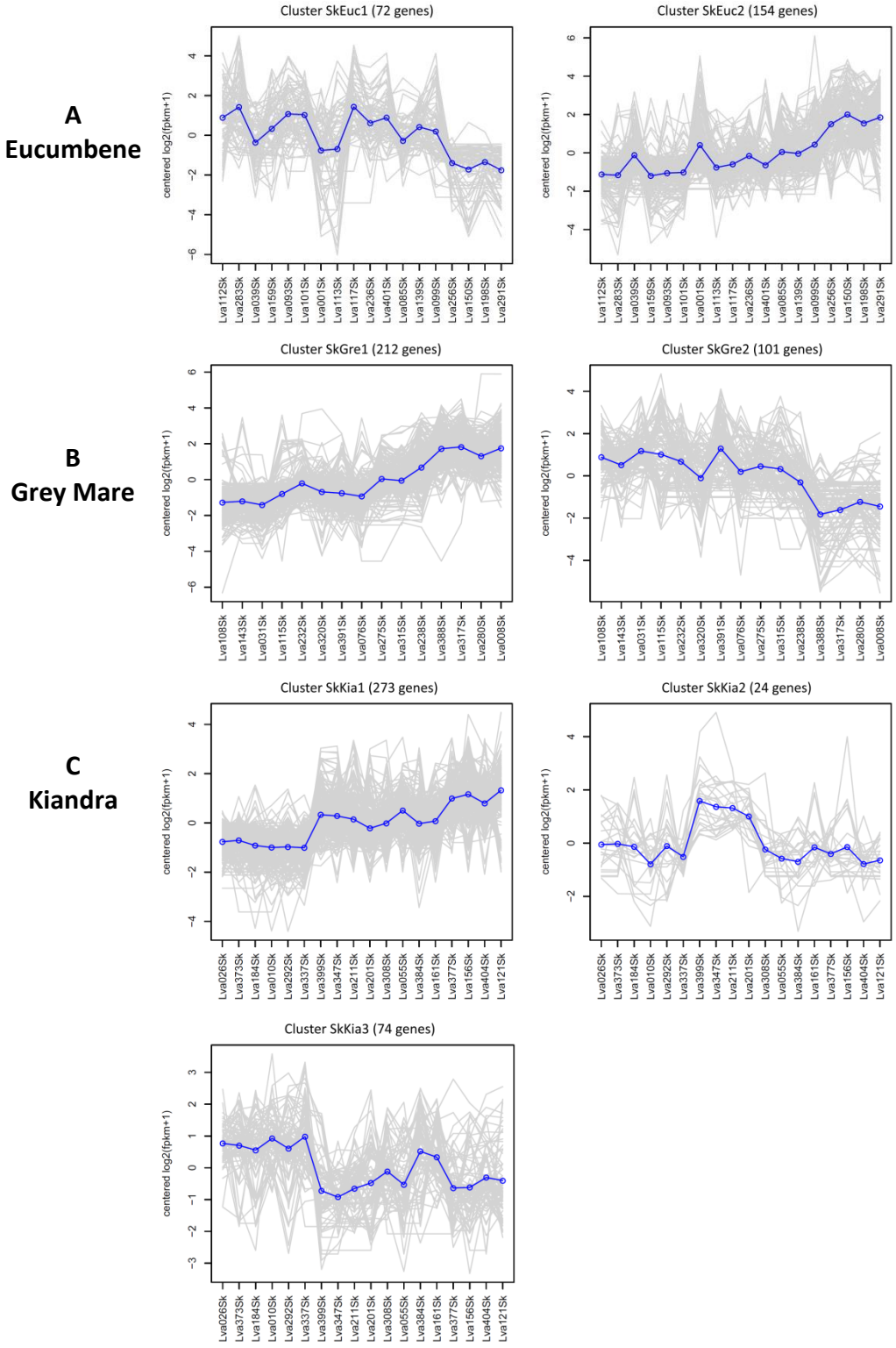

Figure 5.13. Heatmaps summarizing clusters of differentially expressed genes (vertical axis) between sample groups.

Sample groups are arranged as a time-series along the horizontal axis, accompanied by over-represented GO terms for each cluster on the right (GO term metabolic process, function or cellular component, and p-value compared with *Xenopus (silurana) tropicalis* reference annotation set). (A) skin Eucumbene (p-value 0.001, $\log_2$ FC 4), (B) skin Grey Mare (p-value 0.001, $\log_2$ FC 4), (C) skin Kiandra (p-value 0.001, $\log_2$ FC 1).

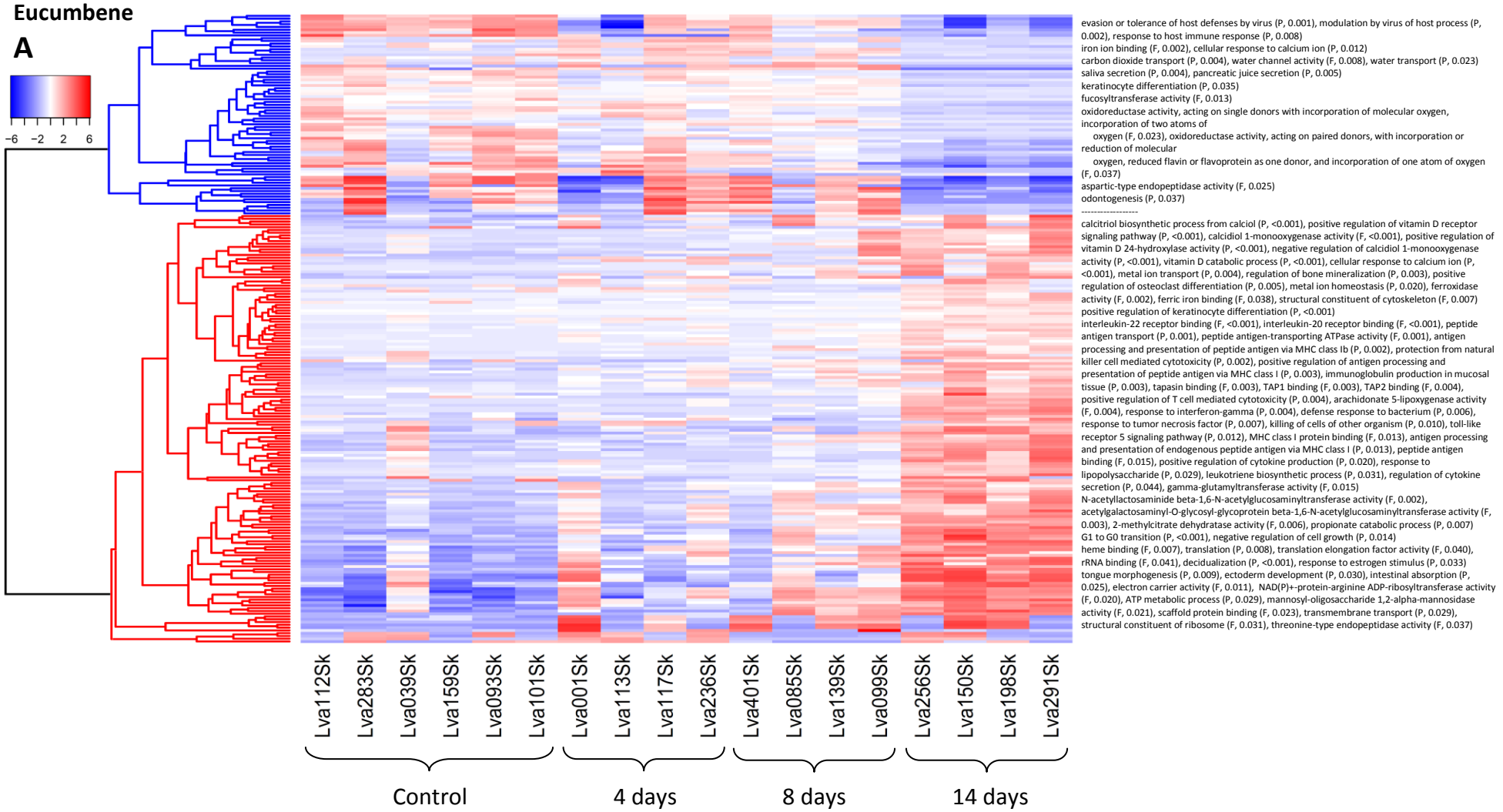

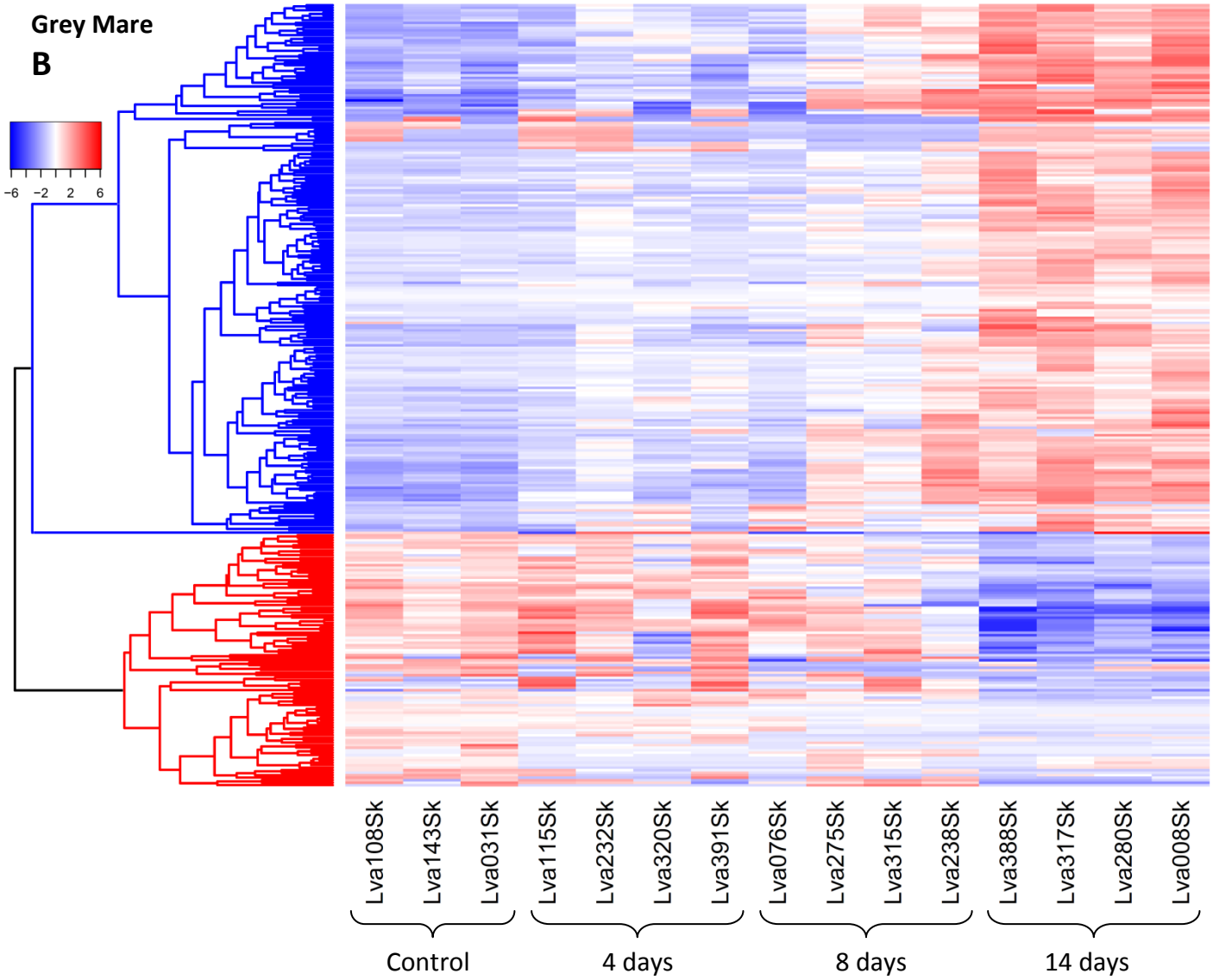

calcitriol biosynthetic process from calciol (P, <0.001), positive regulation of vitamin D receptor signaling pathway (P, <0.001), calcidiol 1-monooxygenase activity (F, <0.001), positive regulation of vitamin D 24-hydroxylase activity (P, <0.001), negative regulation of calcidiol 1-monooxygenase activity (P, <0.001), vitamin D catabolic process (P, <0.001), growth plate cartilage chondrocyte proliferation (P, 0.004), regulation of bone mineralization (P, 0.006), growth plate cartilage chondrocyte differentiation (P, 0.006), positive regulation of osteoclast differentiation (P, 0.007) positive regulation of keratinocyte differentiation (P, <0.001), collagen catabolic process (P, <0.001), iron ion binding (F, <0.001), cellular response to calcium ion (P, 0.001), receptor guanylyl cyclase signaling pathway (P, 0.028), sodium:iodide symporter activity (F, 0.005), iodide transport (P, 0.014), iodide transmembrane transporter activity (F, 0.014), cell wall macromolecule catabolic process (P, 0.035), response to interferon-gamma (P, <0.001), interleukin-22 receptor binding (F, 0.001), interleukin-20 receptor binding (F, 0.001), interleukin-10 receptor binding (F, 0.001), larval lymph gland hemopoiesis (P, 0.001), positive regulation of complement activation (P, 0.001), hemocyte differentiation (P, 0.002), heme binding (F, 0.003), positive regulation of B cell apoptotic process (P, 0.002), negative regulation of cytokine secretion involved in immune response (P, 0.002), antigen processing and presentation of exogenous peptide antigen via MHC class II (P, 0.003), response to lipopolysaccharide (P, 0.006), leukocyte migration (P, 0.006), positive regulation of killing of cells of other organism (P, 0.007), complement activation, alternative pathway (P, 0.010), response to tumor necrosis factor (P, 0.013), negative regulation of B cell proliferation (P, 0.014), toll-like receptor 5 signaling pathway (P, 0.016), nitric-oxide synthase activity (F, 0.017), peptidyl-cysteine S-nitrosylation (P, 0.009), lysozyme activity (F, 0.017), negative regulation of viral genome replication (P, 0.018), cellular response to cytokine stimulus (P, 0.027), negative regulation of interleukin-6 production (P, 0.033), chemokine activity (F, 0.036), cystine:glutamate antiporter activity (F, 0.004), positive regulation of vasodilation (P, 0.033), platelet aggregation (P, 0.048), defense response to Gram-negative bacterium (P, 0.048), response to virus (P, 0.029), receptor biosynthetic process (P, 0.035), G1 to G0 transition (P, <0.001), negative regulation of cell growth (P, 0.025), 3'-5'-exodeoxyribonuclease activity (F, 0.007), DNA integration (P, 0.021), 2-methylcitrate dehydratase activity (F, <0.001), propionate catabolic process (P, <0.001), decidualization (P, <0.001), ovarian follicle cell development (P, 0.005), cellular response to gonadotropin stimulus (P, 0.020), blastoderm segmentation (P, 0.027), tongue morphogenesis (P, 0.013), imaginal disc morphogenesis (P, 0.025), peptide hormone receptor binding (F, 0.021), sex determination (P, 0.023), cellular response to estrogen stimulus (P, 0.038), establishment of ommatidial planar polarity (P, 0.001), urea cycle (P, <0.001), positive regulation of cGMP biosynthetic process (P, 0.015), endopeptidase inhibitor activity (F, <0.001), tetrahydrobiopterin binding (F, 0.017), negative regulation of peptidase activity (P, 0.024), protein homodimerization activity (F, 0.025), scaffold protein binding (F, 0.032), negative regulation of membrane protein ectodomain proteolysis (P, 0.008), arginase activity (F, 0.004), argininosuccinate synthase activity (F, 0.006), arginine binding (F, 0.015), arginine biosynthetic process (P, 0.018), arginine catabolic process (P, 0.019), electron carrier activity (F, 0.025)

---

iron ion binding (F, <0.001), cellular response to calcium ion (P, 0.015), cation channel activity (F, 0.02816062), carbon dioxide transport (P, 0.005), water channel activity (F, 0.009), water transport (P, 0.028), iron ion transport (P, 0.038), cellular iron ion homeostasis (P, 0.041), copper ion binding (F, 0.044), activation of phospholipase A2 activity by calcium-mediated signaling (P, 0.005), activation of phospholipase C activity (P, 0.043), Fc-epsilon receptor signaling pathway (P, <0.001), heme binding (F, <0.001), evasion or tolerance of host defenses by virus (P, 0.001), modulation by virus of host process (P, 0.003), nitric-oxide synthase regulator activity (F, 0.009), response to host immune response (P, 0.010), positive regulation of nitric oxide biosynthetic process (P, 0.020), regulation of nitric-oxide synthase activity (P, 0.024), aromatase activity (F, 0.002), protein-glutamine gamma-glutamyltransferase activity (F, 0.013), oxidation-reduction process (P, 0.009), saliva secretion (P, 0.005), pancreatic juice secretion (P, 0.006), actin filament binding (F, 0.002), visceral muscle development (P, 0.003), atrial cardiac muscle tissue morphogenesis (P, 0.005), cardiac muscle fiber development (P, 0.008), actin-dependent ATPase activity (F, 0.012), regulation of ATPase activity (P, 0.029), adult heart development (P, 0.012), regulation of the force of heart contraction (P, 0.012), regulation of heart rate (P, 0.018), regulation of heart growth (P, 0.019), sarcomere organization (P, 0.020), microfilament motor activity (F, 0.020), ventricular cardiac muscle tissue morphogenesis (P, 0.022), muscle filament sliding (P, 0.033), negative regulation of epidermal growth factor receptor signaling pathway (P, 0.035), epidermal growth factor-activated receptor activity (F, 0.005), keratinocyte differentiation (P, 0.042), odontogenesis (P, 0.045), structural constituent of muscle (F, 0.036), positive regulation of catenin import into nucleus (P, 0.007), protein insertion into membrane (P, 0.012), peptide cross-linking (P, 0.026), negative regulation of protein catabolic process (P, 0.031), positive regulation of protein kinase B signaling cascade (P, 0.032), ribonuclease H activity (F, 0.005), positive regulation of DNA repair (P, 0.024), positive regulation of DNA replication (P, 0.035), response to UV-A (P, 0.006), positive regulation of cyclin-dependent protein serine/threonine kinase activity involved in G1/S transition of mitotic cell cycle (P, 0.010), MAP kinase kinase kinase activity (F, 0.011), electron carrier activity (F, 0.018) one-carbon metabolic process (P, 0.020), carbonate dehydratase activity (F, 0.020)

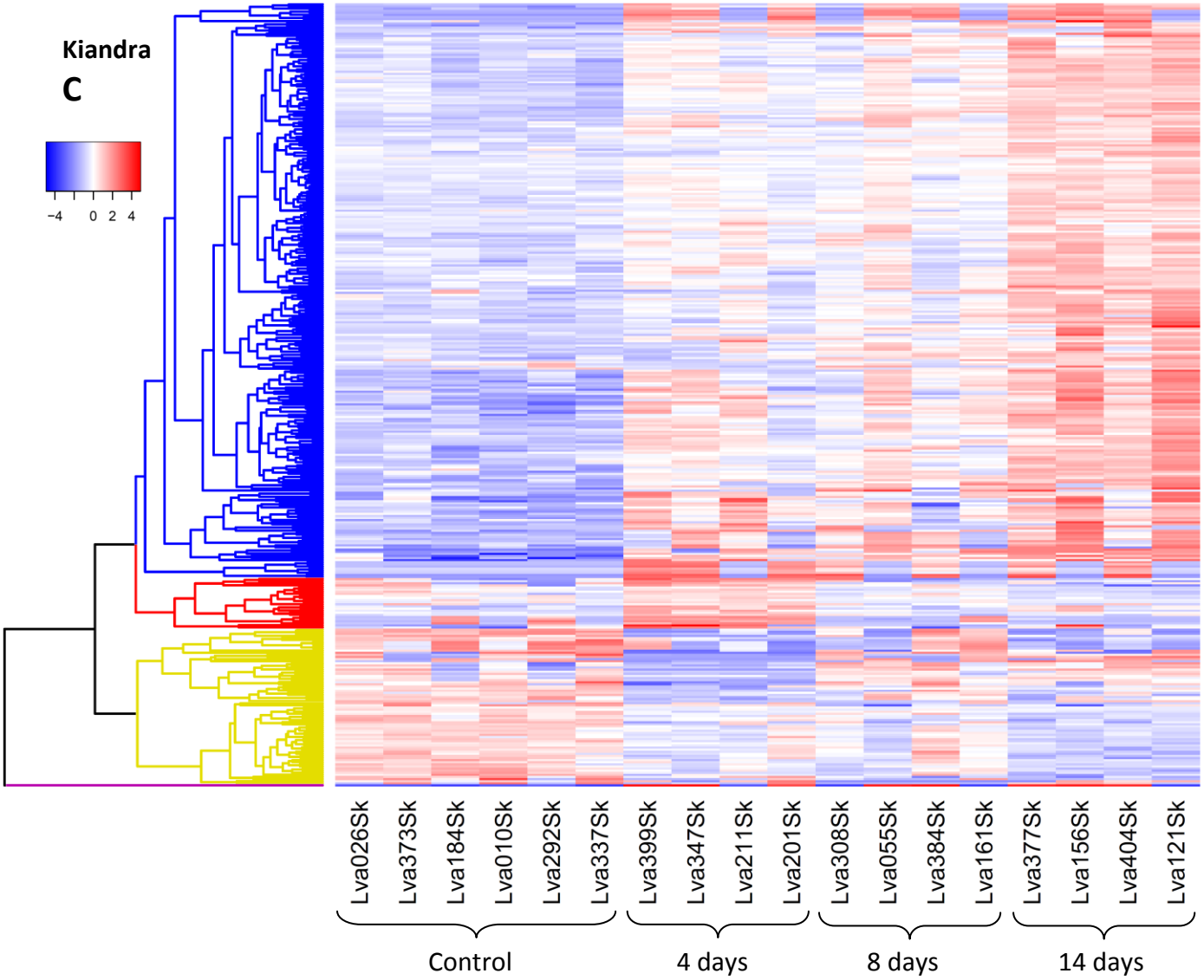

cerebellum structural organization (P, <0.001), cerebellar Purkinje cell layer development (P, <0.001) ER overload response (P, <0.001), regulation of protein folding in endoplasmic reticulum (P, 0.003) cellular response to interleukin-4 (P, <0.001), acute-phase response (P, 0.003), defense response to bacterium (P, 0.003), leukocyte tethering or rolling (P, 0.007), interleukin-1, Type II, blocking receptor activity (F, 0.009), positive regulation of cytokine production (P, 0.015), complement activation, alternative pathway (P, 0.017), toll-like receptor 5 signaling pathway (P, 0.027), killing of cells of other organism (P, 0.024), negative regulation of viral genome replication (P, 0.031), chemokine-mediated signaling pathway (P, 0.032), interleukin-1 receptor binding (F, 0.034), negative regulation of transforming growth factor beta receptor signaling pathway (P, 0.007), cytokine activity (F, 0.018), heterophilic cell-cell adhesion (P, 0.041), MyD88-dependent toll-like receptor signaling pathway (P, 0.018), negative regulation of nitric oxide biosynthetic process (P, 0.019), positive regulation of receptor internalization (P, 0.039), positive regulation of autophagy (P, 0.047), response to stilbenoid (P, 0.002), cystine:glutamate antiporter activity (F, 0.007), erythrocyte maturation (P, 0.010), thromboxane receptor activity (F, 0.012)
calcitriol biosynthetic process from calciol (P, 0.002), positive regulation of vitamin D receptor signaling pathway (P, 0.003), calcidiol 1-monooxygenase activity (F, 0.003), positive regulation of vitamin D 24-hydroxylase activity (P, 0.015), negative regulation of calcidiol 1-monooxygenase activity (P, 0.015), vitamin D catabolic process (P, 0.017)
purine-specific nucleoside:sodium symporter activity (F, 0.002), pyrimidine- and adenine-specific:sodium symporter activity (F, 0.002), neurotransmitter:sodium symporter activity (F, 0.008), pyrimidine nucleoside transport (P, 0.007), purine nucleoside transmembrane transport (P, 0.007), 3'-5'-exodeoxyribonuclease activity (F, 0.012), purine ribonucleoside monophosphate metabolic process (P, 0.045), methionyl-tRNA aminoacylation (P, 0.010), methionine-tRNA ligase activity (F, 0.010), negative regulation of transcription elongation from RNA polymerase II promoter (P, 0.010), nucleoside diphosphate phosphorylation (P, 0.034), nucleoside diphosphate kinase activity (F, 0.034), 2',3'-cyclic-nucleotide 3'-phosphodiesterase activity (F, 0.005), metalloendopeptidase inhibitor activity (F, <0.001), mitochondrial iron ion transport (P, 0.005), iron ion transmembrane transport (P, 0.015), iron ion transmembrane transporter activity (F, 0.020), copper ion transmembrane transport (P, 0.037), copper ion transmembrane transporter activity (F, 0.047), receptor guanylyl cyclase signaling pathway (P, 0.047), regulation of chondrocyte differentiation (P, 0.004), growth plate cartilage chondrocyte proliferation (P, 0.007), growth plate cartilage chondrocyte differentiation (P, 0.010), ossification (P, 0.043), keratan sulfate biosynthetic process (P, 0.007), positive regulation of keratinocyte differentiation (P, 0.029), collagen catabolic process (P, 0.045), cardiac left ventricle morphogenesis (P, 0.042), UDP-galactose:glucosylceramide beta-1,4-galactosyltransferase activity (F, 0.009), positive regulation of cGMP biosynthetic process (P, 0.026), AMP deaminase activity (F, 0.026), GTP biosynthetic process (P, 0.03388005), CTP biosynthetic process (P, 0.04217106), NAD(P)+-protein-arginine ADP-ribosyltransferase activity (F, 0.047), UTP biosynthetic process (P, 0.047), urea cycle (P, <0.001), 2-methylcitrate dehydratase activity (F, <0.001), propionate catabolic process (P, <0.001), phospholipase binding (F, 0.047), positive regulation of lipid storage (P, 0.049), misfolded protein binding (F, <0.001), activation of signaling protein activity involved in unfolded protein response (P, 0.023), positive regulation of embryonic development (P, <0.001), hormone activity (F, 0.001), peptide hormone receptor binding (F, 0.036), amino acid transmembrane transport (P, 0.001), negative regulation of endopeptidase activity (P, 0.044), peptide YY receptor activity (F, 0.012), strictosidine synthase activity (F, 0.005), vitamin K metabolic process (P, 0.019), ribosome binding (F, 0.007), cellular response to glucose starvation (P, 0.007), oligosaccharide binding (F, 0.029), G1 to G0 transition (P, 0.007), arginase activity (F, 0.007), arginine biosynthetic process (P, 0.031), argininosuccinate synthase activity (F, 0.010), sialic acid binding (F, 0.024), decidualization (P, 0.024)

---

regulation of blood volume by renal aldosterone (P, <0.001), regulation of systemic arterial blood pressure by renin-angiotensin (P, 0.007), sodium ion transport (P, 0.047), iron ion binding (F, 0.001), sodium:potassium-exchanging ATPase activity (F, 0.003), glucocorticoid metabolic process (P, 0.005), steroid binding (F, 0.025), response to food (P, 0.015), ATP biosynthetic process (P, 0.02305467), NAD binding (F, 0.031), 11-beta-hydroxysteroid dehydrogenase [NAD(P)] activity (F, 0.001), oxidation-reduction process (P, <0.001), oxidoreductase activity, acting on paired donors, with incorporation or reduction of molecular oxygen, reduced flavin or flavoprotein as one donor, and incorporation of one atom of oxygen (F, 0.025), heme binding (F, 0.004), female pregnancy (P, 0.034)

---

collagen fibril organization (P, <0.001), intramembranous ossification (P, 0.002), skin morphogenesis (P, <0.001), cartilage development involved in endochondral bone morphogenesis (P, 0.004), endochondral ossification (P, 0.005), bone trabecula formation (P, 0.005), tooth mineralization (P, 0.006), collagen biosynthetic process (P, 0.016), collagen catabolic process (P, 0.008), extracellular matrix disassembly (P, 0.012), cellular response to mechanical stimulus (P, 0.023), extracellular matrix structural constituent (F, <0.001), extracellular space (C, 0.007), negative regulation of cell-substrate adhesion (P, 0.017), positive regulation of epithelial to mesenchymal transition (P, 0.014), face morphogenesis (P, 0.015), embryonic skeletal system development (P, 0.041), positive regulation of canonical Wnt receptor signaling pathway (P, 0.025), ethanolamine-phosphate phospho-lyase activity (F, <0.001), alcohol dehydrogenase activity, zinc-dependent (F, 0.006), ethanol oxidation (P, 0.010), SMAD binding (F, <0.001), transforming growth factor beta receptor signaling pathway (P, 0.002), protein binding, bridging (F, 0.003), D-aspartate import (P, 0.004), L-glutamate import (P, 0.005), Rho protein signal transduction (P, 0.008), transaminase activity (F, 0.016), cellular response to retinoic acid (P, 0.038), response to cAMP (P, 0.041), protein heterotrimerization (P, <0.001), identical protein binding (F, 0.013), cellular response to amino acid stimulus (P, <0.001), platelet-derived growth factor binding (F, <0.001), blood vessel development (P, 0.002), glutamate:sodium symporter activity (F, 0.001), regulation of blood pressure (P, 0.002), sodium:dicarboxylate symporter activity (F, 0.008), regulation of vasoconstriction (P, 0.032)

GO enrichment analysis on SkEuc2, SkGre1 and SkKia1 (generally increasing expression through time with infection) revealed over-representation of a relatively large group of immune-associated processes and functions including responses to interferon-γ, tumor necrosis factor, interleukin binding, complement activation (classical and alternative pathways), antigen processing and presentation of exogenous peptide antigen via MHC class I, Ib and II, leukocyte migration, positive regulation of killing of cells of other organism, toll-like receptor pathway signaling, lysozyme activity, cellular response to cytokine stimulus, chemokine activity, immunoglobulin production in mucosal tissue, positive regulation of T cell mediated cytotoxicity, peptide antigen binding, response to lipopolysaccharide, and leukotriene biosynthetic process (see annotated heatmaps in Fig. 5.13). These clusters were also enriched for processes associated with calcium homeostasis and vitamin D metabolism (calcitriol biosynthetic process from calciol, positive regulation of vitamin D receptor signaling pathway, positive regulation of vitamin D 24-hydroxylase activity, negative regulation of calcidiol 1-monooxygenase activity, cellular response to calcium ion, vitamin D catabolic process). Positive regulation of keratinocyte differentiation was also a feature of these clusters. Notable over-represented processes and functions in the clusters SkEuc1 and SkGre2 (decreasing expression with infection) included evasion or tolerance of host defenses by virus, modulation by virus of host process, and response to host immune response. SkGre2 was additionally enriched for GO terms relating to muscle development such as actin filament binding, visceral muscle development, atrial cardiac muscle tissue morphogenesis, regulation of the force of heart contraction, regulation of heart rate, and regulation of heart growth. Cluster SkKia2 (peaked at 4 DPE in Kiandra) was enriched with processes related to blood volume and pressure, ion transport and energy production. Cluster SkKia3 (generally decreased expression from 4 DPE onwards in samples from Kiandra) was over-represented by structural processes including collagen fibril organization, intramembranous ossification, skin morphogenesis, cartilage development involved in endochondral bone morphogenesis, endochondral ossification, and bone trabecula formation.

5.3.5.4 Differential expression of immune-associated genes

We found a large number of genes with putative functions associated with the immune response to be differentially expressed in our time-series analysis comparing samples from control (unexposed) frogs with those from Bd-exposed frogs sampled at 4, 8 and 14 DPE, particularly within the skin tissue samples at 14 DPE (approximately 132 unique genes in liver, 645 in skin, and 216 in spleen samples using our search term list; see Fig. 5.14 and Appendix G, Tables G.2-G.4, GO enrichment results for skin samples are in Table G.5). BLASTx and assignation of GO terms resulted in gene functional homologies to all major recognized components of both the innate and adaptive vertebrate immune systems. We found genes associated with B and T

lymphocytes and associated molecules, receptors and pathways including immunoglobulins, major histocompatibility complex, Fc receptors and NF-κB. We identified differentially expressed antimicrobial peptide cathelicidin. We found genes associated with the classical, alternative and lectin complement pathways as well as lysozyme. We also identified many genes related to antigen-presenting, phagocytic and cytotoxic cells including macrophages, natural killer cells and neutrophils, as well as major groups of pattern recognition receptors including toll-like receptors, mannose-receptors, scavenger receptors, C-type lectin receptors, and NOD-like receptors. There were also examples of differentially expressed eicosanoid inflammatory mediators including leukotrienes and prostaglandins, nitric oxide, as well as cytokines and chemokines including interferons, interleukins, and tumor necrosis factors. Many more immune-associated genes were found to be up-regulated than down-regulated in comparison with unexposed control frogs (approximately two to three times, for example, 178 down-regulated compared with 473 up-regulated immune-associated genes in the skin; see Fig. 5.14), and it is important to note that many of these down-regulated genes were functionally negative regulators for immune processes (leading to an overall positive effect on the immune response).

Figure 5.14. Numbers of up and down regulated immune-associated genes comparing uninfected negative control frog samples and Bd-exposed frog samples within-population at sampling periods post exposure, for all populations and tissues.

Major immune-associated gene groups have been labeled (using gene search terms; see Appendix G, Tables G.2-G.4 for more details), with numbers of differentially expressed genes in parentheses (where > 10 genes). Immune-associated genes were predominantly up regulated, particularly in skin samples from all three populations at 14 days post exposure.

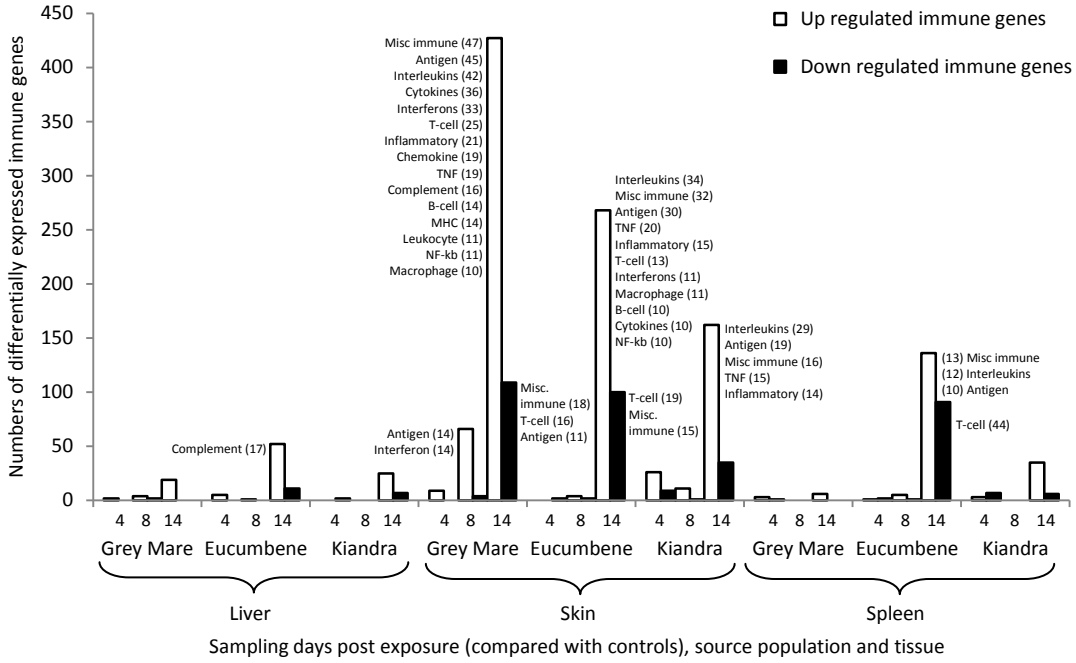

The range of log_2 FC values varied between -11 and 11 for all differentially expressed genes from all tissue types, and log_2 FC values for immune-associated genes varied similarly (log_2 FC of ±6 for skin, ±7 liver and from -6 to 10 for spleen samples). Of particular note, the immune-associated genes with highest log_2 FC values in the skin (highly up-regulated compared with controls; those with log_2 FC > 4) were found only in the two more susceptible populations, Eucumbene and Grey Mare (> 50 genes). These included genes with functional homology to interferon-induced very large gtpase 1-like genes in other species (highly up-regulated throughout infection time-series in frogs from Grey Mare; log_2 FC >6). Genes coding proteins with functional homology to cd109 antigen were up-regulated in all three populations, but particularly in late subclinical stages of infection in frogs from Eucumbene (log_2 FC > 5). Three pro-inflammatory interleukins were also highly up-regulated at late stages of subclinical infection in Eucumbene and Grey Mare (Interleukin 17f, 18 and 20). In contrast, only four immune-related genes had log_2 FC values of < -4, and these included immunoglobulin heavy chain v j region (Grey Mare 14 DPE, log_2 FC -6.1), andersonin-9 antimicrobial peptide (Kiandra

14 DPE, $\log_2$ FC -5.16), ly6 plaur domain-containing protein 2 (Eucumbene 14 DPE, $\log_2$ FC -4.76) and cd48 antigen-like (Grey Mare 14 DPE, $\log_2$ FC -4.11).

We also compared gene expression in the skin samples at 4 DPE between populations. Examination of immune-associated genes in these sets revealed 88 up-regulated and 18 down-regulated immune-associated genes differentially expressed in samples from Kiandra relative to Eucumbene, and 137 up-regulated, 26 down-regulated immune-associated genes in samples from Kiandra relative to Grey Mare.

5.3.6 Discussion

Despite the progression towards endemism of the fungal pathogen *Batrachochytrium dendrobatidis* around the world, the skin disease chytridiomycosis continues to cause declines and extinctions of amphibian species (Hunter et al., 2010; Murray et al., 2009; Muths et al., 2011; Phillott et al., 2013). The use of immunologic strategies such as assisted selection for disease resistance has been suggested as a possible long-term sustainable management approach for threatened populations (Scheele et al., 2014; Venesky et al., 2012; Woodhams et al., 2011). Two key outstanding elements of this approach involve firstly, the proof of concept for the evolution of resistance in amphibian populations, and secondly, the identification of molecular and genetic targets for marker-assisted selection (MAS), which has been successfully used for selecting disease resistance in plant and domestic animal agriculture (Heringstad et al., 2007; Leeds et al., 2010; Ragimekula et al., 2013). Savage and Zamudio (2011) made initial progress towards these goals through their targeted investigation of major histocompatibility (MHC) genes. Here we extended this work through a non-targeted transcriptomics approach, and showed that a long-exposed population of the alpine tree frog (*Litoria verreuxii alpina*) with a more disease-resistant phenotype (Kiandra), displayed a more robust early (4 days post exposure; DPE) immune response (at the level of gene expression) in comparison with a susceptible Bd-naïve population (Grey Mare), and a susceptible long-exposed population (Eucumbene). Components of this early immune response may be vital for conferring chytridiomycosis resistance.

The main purpose of our study was to investigate early subclinical immune responses to infection and to compare these between populations of known differing long-term exposure histories, survival rates on clinical exposure to Bd, and infection intensities post-exposure. From the large clinical experiment (reported in Section 5.2 of this thesis) we found that frogs from the long-exposed population Kiandra (anecdotally a large and stable population in the wild), survived significantly longer than the two other populations (Fig. 5.8). We also found that frogs from Kiandra demonstrated a non-significant trend of lower infection intensities than frogs from

the other two populations from 4 DPE onwards (Fig. 5.7). With the recognized associations between infection intensity and survival (Vredenburg et al., 2010), this trend may suggest the early manifestation of resistance mechanisms operating in the Kiandra population as early as from 4 DPE.

We investigated the subclinical immune response to chytridiomycosis (at 4, 8 and 14 DPE) at the site of infection (skin), as well as in two immune-related organs (spleen and liver) in order to ensure that our observations were relevant to the time course and survival outcomes of disease in a dynamic system. Overall, we found the transcriptional response to be highly divergent between the three populations (Fig. 5.9), with frogs from Kiandra differing substantially from those from the other two sites. Kiandra samples demonstrated lower levels of differential gene expression overall (when comparing subclinical time points post exposure with control samples; Fig. 5.10), and more divergent gene expression at the site of infection in the skin (fewer differentially expressed genes were shared between Kiandra and the other two populations).

As expected from previous studies (Ellison et al., 2014; Rosenblum et al., 2009), our gene expression results in the skin from the late subclinical stage of infection (14 DPE) were the most highly dysregulated. However, they were negatively associated with survival and infection intensity results between populations. Frog skin samples from Grey Mare, the Bd-naïve and most susceptible population (exhibiting poorest survival and highest infection intensities), demonstrated the highest levels of differentially expressed genes at the late subclinical time point, including the greatest numbers of both up and down regulated immune-associated genes. In contrast, skin samples from Kiandra, the most resistant and one of the long-exposed populations (with longest survival and a trend indicating lowest infection intensities from 4 DPE), demonstrated the lowest levels of differentially expressed genes (and immune-associated genes) at 14 DPE. These unintuitive findings suggest that results from the late subclinical time point (14 DPE) may yield poor association with survival and infection intensity trends. Indeed, Ellison et al. (2014) found a marked transcriptional response of immune-associated genes in moribund frogs even in the highly susceptible species, *Atelopus zeteki*. We hypothesize that the observed highly dysregulated gene expression at 14 DPE, particularly in Grey Mare and Eucumbene populations, may either represent immunopathology (a dysregulated and damaging immune response), or a protective immune response to secondary bacterial infection. This latter possibility is consistent with the common finding of inflammatory foci surrounding secondary bacterial infections associated with skin ulcerations and erosions (previously described from histopathology; Berger, 2001; Berger et al., 1998), which may also be the case with samples examined from moribund animals (Ellison et al., 2014).

Clustering differentially expressed genes on the basis of expression levels revealed a gradual time-series trend in clusters for both Eucumbene and Grey Mare populations (gene expression either increasing or decreasing gradually through time post exposure). Gene expression levels for clusters from Kiandra changed more noticeably from 4 DPE indicating an earlier response consistent with our trend of lower infection intensities from the early subclinical time point (Figs. 5.12 and 5.13). GO term enrichment analysis and manual examination of differentially expressed genes at 4 DPE revealed that frogs from Kiandra demonstrated evidence for activation of a robust immune response involving genes putatively coding proteins with functional homologies to all major components of the vertebrate immune system, in comparison with frogs from the other two populations (where there were few immune genes identified as differentially expressed compared with controls; Fig. 5.14). Comparisons of gene expression at 4 DPE confirmed that between populations, frogs from Kiandra had higher levels of immune-associated gene expression than both Eucumbene and Grey Mare (with 4.8 and 5.2 times the number of immune genes up regulated in Kiandra respectively). Taken together, these results suggest that the long-exposed and more resistant population of frogs from Kiandra demonstrates an earlier and more robust immune response to Bd infection than frogs from the other long-exposed population, Eucumbene, and the Bd-naïve population, Grey Mare. This early immune response may serve to limit or reduce early Bd infection intensities, leading to improved overall survival, and may be a result of evolved resistance through long-term exposure to the pathogen in the wild.

Immune-associated genes that were up regulated (relative to control samples) in the skin of frogs from the Kiandra population in the early subclinical stages of infection (4 DPE) included representatives of a functioning innate immune system including members of the alternative complement pathway (complement factor b) and the membrane attack complex (complement component c7), cytokines and chemokines related to leukocyte migration and adhesion (cystine glutamate transporter, lymphocyte antigen 6 complex, TNF superfamily 12A, p-selectin glycoprotein ligand, tubulointerstitial nephritis antigen), phagocytosis (stabilin 2), tumor necrosis factor superfamily (TNF superfamily 12A and 25), interleukins (interleukin 17c, 17e and interleukin 18 receptor 1) and pathogen recognition receptors (c-type lectin domain g, beta-galactosyltransferase). The adaptive immune system also appeared to be functioning, with the up regulation of genes related to secreted immunoglobulins (heavy and light chains), membrane-bound immunoglobulin (loc 398774), the classical complement pathway (complement c4), and genes related to assisting lymphocyte homing and adhesion, increasing B cell proliferation, promoting apoptosis and endocytosis/phagocytosis (cd 44). Of interest, the expression of TNF receptor superfamily member 25 (TNFRS25) is typically higher in activated

and antigen-experienced T lymphocytes than naïve T cells, likely indicating that in our experiment T lymphocytes had undergone differential selection in response to the fungal pathogen (part of cell-mediated immunity; LARD is an alternative name for TNFRS25; Screaton et al., 1997). Several immune-regulatory genes (anti-inflammatory) were also down regulated in the skin, including gremlin-1, epstein barr nuclear antigen, noggin1, NADP-dependent leukotriene B412 hydroxydehydrogenase and lymphocyte antigen 75, leading to an overall positive effect on the immune response. In the spleen, anthrax toxin receptor and IL 13 receptor subunit α were up regulated, while the response gene to complement 32 was down regulated, together having an overall positive effect on the immune response. The up regulation of TNF receptor-associated factor 2 (TRAF2) in the spleen signals normal antibody isotype switching from IgM to IgG in other vertebrates (Jabara et al., 2009), and may hence retain an homologous function in amphibians, switching isotype from IgM to IgY. This finding likely indicates the early maturation of a humoral response to Bd in the frogs from Kiandra, that might be expected to peak over the ensuing two weeks (Gantress et al., 2003).

There was some evidence of negative regulation of the immune response in frogs from Kiandra that may be associated with immunomodulatory Bd-secreted factors, and might explain the almost complete absence of differentially expressed immune-associated genes observed at 8 DPE. Interleukin 1 type 2 receptor found to be up regulated in skin of Kiandra frogs at 4 DPE is a decoy receptor for inhibiting IL1A and IL1B and is closely related to viral proteins that function to assist viral immune evasion (Smith and Chan, 1991; Symons et al., 1995). Complement factor H-related protein C functions to regulate the alternative complement pathway by protecting host cells from the potentially deleterious effects of uncontrolled and misdirected complement activation (Skerka et al., 2013). As the reproductive form of Bd is intracellular, we speculate that Bd sporangia may modulate their containing host cells to prevent their destruction perhaps by reducing innate signals for apoptosis via decoys for complement, and by inducing the down regulation of the adaptive arm of the immune response. Consistent with this latter idea, several genes coding proteins that negatively regulate T lymphocytes were found to be up regulated including protein btg3 with antiproliferative properties, monoglyceride lipase regulating effector T cells, and protein nlrc3 with a role in modulating T cell stimulation. This peripheral dampening of the cell-mediated immune response was also accompanied by the down regulation of several T cell associated genes in the spleen including grb2 involved in T cell co-stimulation, T cell surface glycoprotein cd8 involved in T cell mediated killing, and T cell receptor γ responsible for recognising antigens bound to MHC. The observed up regulation of cis-aconitate decarboxylase-like protein, and down regulation of Ig superfamily 10 and symmetrical lectin genes would also serve to limit the extent of the immune response. Of particular interest, down-stream processes of interferon gamma (IFN-γ) also appeared to be

markedly down-regulated (including interferon-induced very large GTPase in both spleen and liver, and multiple proteasome subunits in both spleen and liver).

In contrast to the immune response of frogs from Kiandra, transcriptomes from exposed Grey Mare frogs exhibited evidence of infection by an enterobacteria phage (98.95% sequence similarity and a min. eValue of 0, with BLASTx hit for capsid protein F which has a role in disassembly of parental virus and assembly in progeny virus, and is a coat protein found in ssDNA viruses; Air, 1976; Hafenstein and Fane, 2002). In all three tissues examined at 4 DPE, there was evidence for the significant up regulation ($\log_2$ FC > 7) of interferon-induced very large GTPase 1-like genes (involved in cell autonomous resistance with antiviral properties; Kim et al., 2012; Klamp et al., 2003; Kochs and Haller, 1999; Li et al., 2009), accompanied by interferon-induced helicase c domain gene in the skin (reported as an innate immune receptor which acts within the cytoplasm to detect viral infection and activate antiviral responses; Cocude et al., 2003), and rho GTPase-activating protein in the liver. These results suggest the marked dysregulation of interferon likely associated with bacteriophage infection of the host. Bacteriophage penetration in vertebrates is not uncommon, and may possibly play a role in enhancing Bd infection (Dabrowska et al., 2005). Interestingly, these genes were found to be up regulated in all three time points post exposure in comparison with unexposed control frogs from Grey Mare, suggesting there may be synergistic effects between Bd and the bacteriophage. It is unlikely that Bd-exposed Grey Mare frogs were infected with the bacteriophage exclusive of control Grey Mare frogs unless it was introduced during inoculation, however this is also unlikely, as the study was performed as a randomised and blinded clinical trial with no systematic differences between populations and experimental groups. Frogs from Grey Mare exhibited minimal evidence of other immune response, including up regulation of IL 17c, cd109 antigen (negatively modulates tumor growth factor beta [TGF-β] signaling, an anti-inflammatory cytokine, thereby promoting inflammation), c-c motif chemokine 20 and IL 4 receptor in the skin, and the down regulation of Ig-like receptor 2 precursor in the spleen (involved in the development of tolerance).

Frogs from Eucumbene exhibited minimal evidence of an early immune response to Bd infection, including up regulation of B cell differentiation antigen cd72 in the spleen, and evidence for an early classical pathway complement response involving complement c1q, venom factor 1 (an analog of complement c3b) and complement c1r in the liver, modulated by the down regulation of complement component c6 (part of the membrane attack complex) and lymphocyte antigen 6e in the spleen.

In summary, in this study we demonstrated a link between a chytridiomycosis-resistant phenotype from a long-exposed population (with longer survival and lower infection intensities from 4 DPE), and evidence for a more robust early immune response at the level of gene expression compared with other populations. This is the first study to identify underlying immune mechanisms at the early subclinical stage of infection that may be related to evolved resistance to Bd. This study highlights the difficulties in separating gene expression representing a protective immune effect from the presence of immunopathology (a dysregulated and damaging immune response), and any response to secondary bacterial infections. These results suggest not only the importance of examining clinical evidence of survival and infection intensity (phenotypic degree of resistance) concurrent with gene expression results, but also the importance of examining the temporal course of infection.

5.3.7 Acknowledgments

We thank P. Harlow, M. McFadden, D. Hunter and B. Scheele for assistance with logistics for the clinical experiment and species' insights. This study was conducted with approval by the James Cook University Animal Ethics Committee (Certificate no. A1589) and Scientific License number: S12848 (D. Hunter). This work was jointly funded by Morris Animal Foundation and US Fish and Wildlife Service - Wildlife Without Borders program. The funders had no role in study design, data collection and analysis, decision to publish, or preparation of the manuscript.

5.3.8 Supporting information and data accessibility

Detailed tables of results for immune-associated differentially expressed gene annotations and enrichment analyses, as well as additional figures including Venn diagrams for time-series comparisons, are available in Appendix G. The authors are solely responsible for the content and functionality of these materials. Queries (other than absence of the material) should be directed to the corresponding author.

5.4 PAPER 3: Using a non-targeted metabolomics approach to investigate amphibian host responses to chytridiomycosis

This manuscript in preparation represents my original study design, conduct, sample collection, data analysis, results interpretation and write-up. Joel Gummer performed metabolite extractions, GC-MS and data clean-up, as well as providing assistance with data analysis. Lee Berger, Lee Skerratt and Scott Cashins provided assistance with experimental design. Scott Cashins assisted with conduct of the exposure experiment and sample collection. All co-authors provided substantial editorial input.

The full reference for the manuscript is:
Grogan, L. F., Berger, L., Skerratt, L. F., Cashins, S. D., Trengove, R. D., Gummer, J. P. A. (in prep) Using a non-targeted metabolomics approach to investigate amphibian host responses to chytridiomycosis.

The following text is a word for word copy of the prepared manuscript. Section, table and figure numbering has been added or reformatted for this thesis for ease of reference. Spelling follows the American English convention.

5.4.1 Front matter

Using a non-targeted metabolomics approach to investigate amphibian host responses to chytridiomycosis

Running head: Metabolomics and chytridiomycosis

Laura F. Grogan[1*], Lee Berger[1], Lee F. Skerratt[1], Scott D. Cashins[1], Robert D. Trengove[2,3], Joel P. A. Gummer[2,3]

Keywords: amphibian declines, metabolomics, *Batrachochytrium dendrobatidis*, chytridiomycosis, GC-MS

[1]One Health Research Group, School of Public Health, Tropical Medicine and Rehabilitation Sciences, James Cook University, Townsville 4811 QLD, Australia
[2]Separation Science Laboratory, Murdoch University, Perth 6150WA, Australia
[3]Metabolomics Australia, Murdoch University, Perth 6150WA, Australia

[*] Corresponding author
Laura Grogan

Address: One Health Research Group, School of Public Health, Tropical Medicine and Rehabilitation Sciences, James Cook University, Townsville, Queensland 4811, Australia
Tel: (+61 4) 0225 5204
Email: laura.f.grogan@gmail.com

5.4.2 Abstract

Chytridiomycosis is a globally devastating emerging disease of amphibians that has caused the decline or extinction of roughly 200 species of frogs worldwide. While much research has been done on the disease and the fungal pathogen *Batrachochytrium dendrobatidis*, the host tissue metabolic response to disease remains poorly understood. We used a gas chromatography-mass spectrometry (GC-MS) metabonomic approach for non-targeted examination of metabolic perturbations to investigate physiological changes associated with time since exposure, and population variation in response to chytridiomycosis. We sampled both skin (site of infection) and liver tissues of 61 alpine tree frogs (*Litoria verreauxii alpina*) from four populations (three long-exposed and one naïve to the fungus) at various time points (4, 8, 14 days post exposure and moribund) during an exposure experiment involving both exposed (infected) and negative control individuals. Relative metabolite expression within these samples was analysed using univariate and multivariate analysis techniques. We found a total of 162 analytes, of which 72 were putatively identified by matching retention times and spectral patterns with available library databases. We found that metabolite profiles diverged between Bd-infected moribund frogs and both uninfected control and subclinically infected groups in both skin and liver tissues. We also found mild differences in metabolite expression between populations. We identified several key metabolites that were predominantly responsible for these differences. Metabolites contributing significantly to differentiating tissues by sampling period included α-ketoglutaric acid (high in controls), L-threonine and serine (both with no time-series association) in the skin samples; putrescine (high in moribund), citric acid (high in controls), γ-aminobutyric acid and D-fructose-6-phosphate (both with no time-series association), and L-glutamic acid (high in controls) in liver samples. Differences between populations in terms of metabolite expression were less pronounced, with pantothenic acid (high in Eucumbene, low in Kiandra population) being found consistently across analyses as significantly differentially expressed in the skin samples. This study is the first to identify metabolic changes in the skin and liver associated with both pathophysiology of chytridiomycosis, as well as potentially associated with the host immune response.

5.4.3 Introduction

Chytridiomycosis is an often fatal fungal skin disease of amphibians, affecting approximately 42% of species examined (Olson et al., 2013), and causing declines and extinctions around the world (Skerratt et al., 2007). While the proximate cause of mortality due to the pathogen, *Batrachochytrium dendrobatidis* (hereafter Bd) has been recognized as the alteration of electrolyte balance, leading to cardiac arrest (Voyles et al., 2009), the associated metabolic phenotype has not been well characterized. An improved understanding of the molecular basis underlying the pathophysiology of chytridiomycosis is fundamental to improving management techniques and hence population outcomes by using targeted approaches for species under continued threat from chytridiomycosis (Scheele et al., 2014). In addition, comparing the metabolome of populations with differing exposure histories to Bd and known differences in their clinical susceptibility, may help elucidate possible immune mechanisms associated with more resistant phenotypes.

Non-targeted metabolomics (or metabonomics when undertaken to investigate and compare disease states) measures the relative expression pattern of low molecular weight molecules (< 1,500 daltons; including amino acids, organic acids, sugars and nucleotides) within a biological sample (Gummer et al., 2009; Jones and Cheung, 2007). Uni- and multivariate statistical analyses can then help identify patterns of metabolite expression that may provide insight into biochemical perturbations induced by disease. There are numerous examples in the literature of where such insights have led to the development of assays for screening biomarkers of disease, particularly in human populations (Ni et al., 2014; Wang et al., 2014; Zhao et al., 2014), and metabolomics approaches have also been widely used in toxicological and pharmacological studies (Bo et al., 2014; Kell and Goodacre, 2014).

Systemic electrolyte imbalances and alterations in tissue gene expression have been implicated in the pathophysiology of morbidity and mortality in Bd-infected amphibians (Ellison et al., 2014; Ribas et al., 2009; Rosenblum et al., 2009; Voyles et al., 2009). Low plasma levels of sodium and potassium are considered proximate causes of cardiac arrest leading to mortality in the final stages of the disease (Voyles et al., 2009), which has been corroborated by evidence from gene expression studies (Rosenblum et al., 2012b). A number of metabolic pathways and processes have been associated with end-stage physiology including increased expression of genes associated with cellular stress and disruption of skin homeostasis, detoxification, proteases, antimicrobial peptides, as well as decreased expression of cytochrome p450 genes and genes associated with blood coagulation and the immune response, although recent evidence suggests degree and efficacy of immune response may differ with species (Ellison et al., 2014; Ribas et al., 2009; Rosenblum et al., 2012b; Rosenblum et al., 2009).

Targeted and non-targeted metabolomics methods have been used in investigation of secreted factors of the fungal pathogen, amphibian urinary markers of stress, epidermally secreted antimicrobial peptides, and antifungal metabolites produced by symbiotic skin bacteria (Becker et al., 2009; Fites et al., 2013; Kindermann et al., 2012; Lam et al., 2011; Peterson et al., 2013; Woodhams et al., 2007b). These studies have assisted in improving our understanding of the interaction between Bd and the amphibian host, particularly in identifying compounds on the skin that may be associated with resistance to disease. Thus far, however, no study has attempted to examine the overall metabolic phenotype (including intracellular and multiple cell types) associated with key tissues involved in the disease at various time points during pathogenesis, comparing this with normal healthy control frogs. Moreover, no study has thus far examined differences in metabolic phenotype among different populations of the one species with varying exposure histories and susceptibilities to disease.

We used a non-targeted gas chromatography-mass spectrometry (GC-MS) metabonomics approach to compare the metabolic phenotype of infection at various time points post exposure, as well as to compare the metabolome of different populations of the same species with differing long-term Bd-exposure histories and survival responses. We analyzed skin tissues at the site of infection, as well as liver tissues from exposed and negative control frogs at multiple subclinical time points (4, 8 and 14 days post exposure), and shortly prior to death from chytridiomycosis.

5.4.4 Methods

5.4.4.1 Study subjects, exposure experiment and sampling

We individually exposed 46 chytridiomycosis-naïve adult alpine tree frogs (*Litoria verreauxii alpina*) from four geographically distinct populations to Bd using the identical isolate and exposure protocol outlined in Section 5.2 of this thesis. The populations will hereafter be designated Kiandra, a Bd long-exposed site (35.872°S 148.500°E 1356 m above sea level [asl]), Eucumbene, a Bd long-exposed site (36.152°S 148.563°E 1451 m asl), Ogilvies, a Bd long-exposed site (36.036°S 148.322°E 1307m asl), and Grey Mare, a Bd-naïve site (36.317°S 148.260°E 1525 m asl). A further 15 frogs (unexposed negative control group) were sham-exposed with dilute salts solution (see Table 5.5 for details of experimental design). Three subclinical-infection stage sampling sessions were performed at 4, 8 and 14 days post exposure using a randomized block design (each session sampled a total of 17 animals, including all control frogs stratified between sessions and populations of origin). In addition to the 51 frogs already described in Section 5.2 of this thesis, the remaining 10 exposed frogs were sampled

between 28 and 30 days post exposure when they began to exhibit clinical signs of chytridiomycosis and were hence in the final moribund stages of disease. These additional frogs included two from each of Kiandra, Eucumbene, and Ogilvies populations, and four frogs from Grey Mare. Frogs were swabbed to quantify Bd infection intensity via qPCR, and examined and measured before being humanely euthanized for tissue sample collection (as described in Section 5.2 of this thesis). Tissues collected included ventral abdominal skin and liver, and these were immediately transferred to 500 µL 100% methanol, and stored at -80ºC. The ventral abdominal and thigh skin of frogs are common sites for Bd infection (Berger et al., 1998; Berger et al., 2005c). The liver is an important organ for many physiological functions including several associated with both immunity and pathogenesis of infectious disease (such as detoxification of antigens, removal of debris, breakdown of the products of apoptosis, and assimilation of energy).

5.4.4.2 Isolation of metabolites from skin and liver samples

Tissue samples were transferred from methanol to fresh microcentrifuge tubes on ice, and the methanol was vacuum concentrated (Eppendorf Concentrator Plus vacuum concentrator; Eppendorf, USA) to < 50 µL before being diluted with the addition of 100 µL water, and having the tissue sample replaced. Samples were then submerged in liquid nitrogen for drying by lyophilisation in a LABCONCO Freezone 2.5 Plus freeze-dryer (Labconco Corp., USA). We then added approximately 30 x 1.4 mm ceramic beads (Precellys, France) to each dried sample and homogenized the tissue via six 20 second rounds of vigorous agitation at 6,500 *rpm* in a Precellys 24 lysis cryo-mill (bertin technologies, France), and 15 minutes mixing at 1,400 rpm in an Eppendorf Thermomixer (Eppendorf, USA), before transferring to ice. Cell debris and precipitate were collected by centrifugation at 16,100 *g* for 30 minutes at 4 ºC, and the supernatant was transferred to a fresh 1.5 ml microcentrifuge tube. This process was repeated a further two times, first with 500 µL of ice cold methanol, and then with 300 µL of water, and the supernatants were combined. Half of the liver extract volume and the entire volume of the skin extracts were dried in preparation for derivatisation. Methanol was evaporated from the metabolite extracts by vacuum concentration for 60 minutes, and 400 µL of water was added before the sample was frozen in liquid nitrogen and dried again by lyophilisation.

5.4.4.3 MEOX-TMS Derivatization of metabolites

We derivatized the metabolites by a combination of oximation (MEOX) and silylation (TMS) as previously described (Gummer et al., 2013). The metabolite lyophilisates were dissolved in 20 µL of pyridine (20 mg ml^{-1} methoxylamine HCl; Sigma-Aldrich) and incubated at 30 ºC with agitation at 1,400 *rpm* for two hours, followed by the addition of 40 µL MSTFA (Sigma-Aldrich) and incubation at 37 ºC with agitation at 650 *rpm* for one hour. The derivatized

metabolites were transferred to a 200 µL glass vial insert within a 1.5 ml glass amber vial. Five µL of hexane containing n-decane, n-dodecane, n-pentadecane, n-nonadecane, n-docosane and n-octacosane at 6.25 µg ml^{-1}, and n-dotriacontane and n-hexatriacontane at 13.5 µg ml^{-1} was added to samples as an instrument standard, and for calculation of retention indices.

5.4.4.4 GC-MS Analysis of metabolites

Derivatized metabolites (1 µl) were analysed via GC-MS (Shimadzu QP2010 Ultra, Kyoto, Japan) equipped with an Agilent FactorFour VF-5ms column (30m x 0.25mm x 0.25µm + 10m EZ-Guard). The injection inlet temperature was 230 °C, with an interface temperature of 300 °C, and an ion source temperature of 230 °C. Helium was used as the carrier gas at a flow of between 0.8 and 1.0 ml min^{-1}. The inlet pressure was adjusted to elute mannitol (6-TMS) at 30.6 minutes. The temperature gradient consisted of an initial temperature of 70 °C, increasing at 1°C per minute for 5 min before increasing to a final temperature of 320 °C at an oven ramp rate of 5.6 °C min^{-1} with a 10 minute hold at maximum temperature. Ionisation was by electron ionization (EI) at 70 eV. The MS was operated in scan in the range m/z 40 – 600, at a scan rate of 5,600 amu sec^{-1}. For selected ion monitoring (SIM), ions were scanned at 0.38 second intervals.

5.4.4.5 Data acquisition and analysis

GC-MS data were acquired and analysed using GCMSsolution 2.61 (Shimadzu Corporation, Kyoto, Japan). From a preliminary GC-MS analysis of skin and liver metabolites using a scan mode of acquisition, a library of tentatively identified metabolites and their respective EI mass spectra were determined. A SIM method was assembled using 71 characteristic ions from the preliminary data set and the remaining sample set analysed by GC-MS with the included SIM ions. Chromatograms were deconvoluted by background subtraction of partially co-eluting ions. Metabolite identities were assigned by comparison to authentic metabolite standards, requiring a similarity index of 80% or higher MS match and a retention index of ± 3. Putative identifications were determined by match to an external MS library: Massbank, National Institute of Standards and Technology (NIST) or Wiley Registry™. Metabolites assigned "like" identities were so named by close identity to known spectra, but without a match to the RI of the known compound. Tentative identifications were assigned to metabolites with a library match of 70 – 80%. All metabolites were assigned a mass-spectral tag (MST; Desbrosses et al., 2005) identifier derived from its analytical characteristics of the format 'name_retention time_retention index_base peak'.

5.4.4.6 Data processing and interpretation

Analytes of non-biological origin were determined by comparison of no-tissue control extractions and were subsequently removed from data matrices. Peak areas were normalized to

total signal (De Livera et al., 2012), subsequently log transformed ($log_{10}(x + 1)$; van den Berg et al., 2006) and pareto-scaled (mean-centered values are divided by square root of the standard deviation; Ivosev et al., 2008). Statistical analyses were performed with SPSS (IBM, USA), R (Bell Laboratories), and Metaboanalyst 2.0 (Xia et al., 2012). Univariate analyses included Analysis of Variance with post-hoc Tukey's Honestly Significant Difference tests, a t-test template matching approach (Pavlidis, 2003), and Significance Analysis of Microarrays (SAM; Tusher et al., 2001). In all cases, an alpha error level of 0.05 corrected for multiple testing via Bonferroni correction was considered acceptable (corresponding to a false discovery rate FDR < 0.05). Multivariate analyses included unsupervised Principal Components Analysis (PCA) and supervised Partial Least Squares Discriminant Analysis (PLS-DA) providing Variable Importance in Projection scores (VIP) with model quality assessed by 10-fold cross-validation based on Q^2 and goodness of fit evaluated with permutation testing using 2000 iterations. Population comparisons excluded data on the two frogs from Ogilvies due to small sample size, however, these were included in the sample-period based analysis (in the 'moribund' class, group 4). In the latter analysis, negative control frogs were pooled into a single group despite being sampled throughout the experimental period (called group '0' to indicate that they were not exposed to infection). We also compared our findings with the gene expression results from a concurrent transcriptomics study utilizing the same tissues and frogs (Section 5.3 of this thesis, Supplementary Information Appendix G, Table G.5), by searching for identified important metabolites among Gene Ontology (GO) enrichment pathway data.

5.4.5 Results

5.4.5.1 Clinical characteristics and summary results

All 61 experimental animals survived the duration of the experiment until they were euthanized for sampling. Detailed demographic data on the sampled frogs including infection intensities assessed via qPCR can be found in Table 5.6. Gas Chromatography Mass Spectrometry (GC-MS) data on skin samples was unable to be obtained for seven frogs (five from Kiandra, one from Eucumbene and one from Grey Mare) due to the production of a precipitate during metabolite extraction. Overall, 23868 retention-time-exact mass pairs were determined (including internal reference standards and manually identified ions of saturated metabolites), with a total of 2177 zero values and no missing values, for a total of 162 analytes, 72 of which were able to be putatively identified based on their spectral pattern and retention times. Dynamic range of identified metabolite ions exceeded the detection range of the detector. Mild instrumental batch effects were observed in the skin tissue samples (batch clustering observed on PCA, Appendix H Figs. H.1 and H.2). Following normalization via Total Area Under Chromatogram (TAUC), log transformation and pareto scaling, skin and liver samples from

frog Lva259 from the Grey Mare population were consistently found to be marked outliers in the PCA results (across analyses; see for example Figs. H.3, H.4), and hence were removed from further analysis. Due to the rapid clinical course of disease and difficulty anticipating morbidity, frog Lva259 was recorded as sampled when 'fresh dead'. This is likely to have caused necrosis of both liver and skin tissues post-mortem altering the metabolic profile relative to other samples. The metabolic profile of skin tissue samples varied considerably from liver samples, demonstrating distinctly separated clusters on the PCA scores plot (Fig. H.5), with the exception of one liver sample (Lva232LiG11), consistent with the differential physiology underlying the different tissue types both in health and disease.

5.4.5.2 Sampling period comparisons

Univariate analyses

One-way ANOVA of skin samples identified 33 analytes as differing significantly between sampling periods (including 9 unknown metabolites; Table 5.7 summarizes key metabolites identified in this study, and Appendix H Table H.1 lists analytes from the ANOVA), however, on examination of Tukey's HSD post-hoc tests, most of these were associated with differences between the moribund group of frogs (group 4) and the control and subclinical groups (negative control animals were pooled and labeled group zero). The most significantly different metabolites obtaining a match to our library database were identified as α-ketoglutaric acid, serotonin, 5-hydroxyindole-3-acetic acid, L-isoleucine, glutamic acid, DL-ornithine, DL-tartaric acid, urea, serine, and fumaric acid. Identifiable metabolites that differed significantly between subclinical and control groups included DL-ornithine, urea, serine, L-threonine, and L-lysine (Table H.1). The t-test pattern matching approach using a time-series pattern (control, 4, 8, 14 days post exposure, moribund) yielded some differences to the above list (Table H.2). The most significantly different metabolites identified included α-ketoglutaric acid, putrescine, adenine, L-threonine, DL-tartaric acid, L-glutamic acid, gallic acid, L-pyroglutamic acid, adenosine and cellobiose. SAM identified the following metabolites as highly significantly differentially expressed between sampling periods (ranked in the top 10): α-ketoglutaric acid, serotonin, 5-hydroxyindole-3-acetic acid, urea, serine, glutamic acid, L-threonine, DL-ornithine, L-isoleucine, and L-lysine (Table H.3).

Liver samples grouped by sampling period and analyzed with one-way ANOVA identified 80 analytes as differing significantly (36 unknowns with two likely artifact). Similarly to the skin samples grouped by time post exposure, the majority of these analytes were significant due to differences between the moribund group of frogs and the other sampling periods (as identified by Tukey's HSD, Table H.4). The top 10 identifiable most significantly different metabolites included L-isoleucine, L-glutamic acid, gallic acid, L-pyroglutamic acid, L-leucine, putrescine,

citric acid, fumaric acid, D-fructose-6-phosphate and D-glucose-6-phosphate. Top identifiable metabolites that differed significantly between subclinical and control groups included L-isoleucine, L-leucine, γ-aminobutyric acid (GABA), serine, sucrose, and cellobiose. Searching for patterns matching the time-series of sampling periods (similar to above) yielded the following top 10 identifiable metabolites as being highly significant: L-glutamic acid, L-pyroglutamic acid, gallic acid, putrescine, L-isoleucine, L-leucine, γ-aminobutyric acid, citric acid, fumaric acid, and serine (Table H.5). SAM presented different rankings, including the following as the 10 most significant identifiable metabolites 5-hydroxyindole-3-acetic acid, citric acid, putrescine, α-ketoglutaric acid, mannitol, creatine, D-(+)-galactose, D-fructose-6-phosphate, D-glucose-6-phosphate and L-isoleucine (Table H.6).

Multivariate analyses

There was mild separation of the moribund samples cluster in the skin tissue PCA analyses by sampling period as seen from the scores plot (Fig. 5.15), which was more pronounced in the liver analysis. Supervised PLS-DA served to accentuate that separation between sample period clusters, particularly with the moribund group, although there was some consistency in the order of cluster alignment, which was roughly consistent with the time post-exposure, and this was most pronounced in the skin samples (Fig. 5.15). The top 20 metabolites ranked by VIP scores based on component one for skin samples grouped by sampling period revealed the following known metabolites: α-ketoglutaric acid, L-threonine, mannitol, putrescine, adenine, serine, and aspartic acid (in addition to 8 unknown metabolites; Table H.7, Fig. H.6). VIP scores on liver samples grouped by sampling period yielded the following metabolites as important: putrescine, 5-hydroxyindole-3-acetic acid, D-(+)-galactose, citric acid, α-ketoglutaric acid, creatine, γ-aminobutyric acid, D-fructose-6-phosphate, and L-glutamic acid (together with 6 unknown metabolites; Table H.8, Fig. H.7).

5.4.5.3 Population comparisons

Univariate analyses

One-way ANOVA of skin samples grouped according to population identified 10 analytes as differing significantly between populations based on Tukey's honestly significant difference post-hoc tests, 6 of which were unable to be matched to our library database (see Table H.9). Those able to be identified included pantothenic acid, myo-inositol, L-leucine and L-isoleucine. The t-test template matching approach with the pattern Eucumbene-Grey Mare-Kiandra yielded the following significant metabolites: pantothenic acid, L-isoleucine, L-leucine, L-proline, creatine and D-(-)-ribose with correlations as shown in Table H.10. SAM results included only pantothenic acid and myo-inositol as identifiable with significant differences between

populations (Table H.11). There were no metabolites identified as significantly differently expressed in the liver tissue between populations with a FDR < 0.05.

Multivariate analyses

Considerable overlap was identified in both the skin and liver PCA scores plots grouping samples by population. Mild separation of population clusters became evident with supervised PLS-DA, which was more pronounced with the liver samples, and consistently demonstrated the Grey Mare cluster lying between the Kiandra and Eucumbene clusters (Fig. 5.16). VIP scores for skin samples grouped by population included pantothenic acid as the seventh-ranked metabolite sorted on component one (preceded by six unknown metabolites; Table H.12, Fig. H.8). Other high-ranked metabolites identified included aspartic acid, L-threonine, L-methionine, serotonin, and guanine. VIP scores for liver samples grouped by population included D-(+)-turanose, urea, thymine, L-lysine, myo-inositol, D-fructose-6-phosphate, and sucrose (Table H.13, Fig. H.9).

5.4.5.4 Associations with differentially expressed gene pathways

A number of the metabolites we identified as contributing importantly to the differentiation between experimental groups were also found to be related to enriched gene expression pathways identified in a concurrent transcriptomics study (Section 5.3 of this thesis) from the same tissues and frogs. The accompanying GO identification numbers and terms have been listed in Table H.14, alongside their putative function with regards to chytridiomycosis pathophysiology.

Table 5.5. Experimental design outlining the number of frogs from each population and treatment group (Bd exposed or unexposed control) sampled at each time point post exposure.

Populations	Exposure – Day 0 Total # exposed (total # control)[a]	Day 4 # exposed sampled (# control sampled)[b]	Day 8 # exposed sampled (# control sampled)[b]	Day 14 # exposed sampled (# control sampled)[b]	Moribund (Day 28+) # exposed sampled
Grey Mare	16 (3)	4 (1)	4 (1)	4 (1)	4
Eucumbene	14 (6)	4 (2)	4 (2)	4 (2)	2
Kiandra	14 (6)	4 (2)	4 (2)	4 (2)	2
Ogilvies	2	-	-	-	2

[a]Total number of unexposed control frogs shown in parentheses; [b]Number of unexposed control frogs sampled shown in parentheses.

Table 5.6. Demographic characteristics of study subjects (including sample size, treatment group, gender ratios, mean mass at death, mean snout-urostyle length at death and mean and median infection intensity at death).

	Kiandra		Eucumbene		Grey Mare		Ogilvies	P value[a]	df[a]
	Exposed	Control	Exposed	Control	Exposed	Control	Exposed		
Sample size	14	6	14	6	16	3	2		
Gender[b]	4F, 3M, 7U	2M, 4U	6F, 3M, 5U	5F, 1M	7F, 5M, 4U	2F, 1U	1F, 1M		
Mean mass at death	3.21	3.02	2.95	4.05	3.43	3.19	3.29	0.917	3
Mean SUL at death[c]	30.29	30.72	28.79	32.10	32.01	32.03	31.80	0.150	3
Mean ZSE at death[d]	429122.80	0.28	145852.98	0.00	148017.50	0.00	614937.50	0.697	3
Median ZSE at death	705.83	0.00	185.83	0.00	5955.83	0.00	614937.50		

[a]Statistics comparing means between populations (pooling exposed and control frog values) using one-way ANOVA, P value and df degrees of freedom; [b]Genders represented by M for males, F for females and U for unknown gender; [c]SUL is snout-urostyle length measured with Vernier callipers; [d]ZSE is zoospore equivalents as measured by qPCR.

Table 5.7. Key identifiable metabolites in both skin and liver tissues discriminating between experimental groups (including sampling periods post exposure and populations), demonstrating overlap between univariate (ANOVA, t-test pattern matching and SAM) and multivariate analyses (PLS-DA).

This table includes only the top ten most significant identifiable metabolites that were identified as significant (with FDR < 0.05) in at least two of the three univariate analyses, or within the top 20 PLS-DA VIP scores ranked on component 1. Comparisons that were found to be significant with post-hoc Tukey's HSD tests are listed, as are the respective correlations for the pattern matching approach (with the following patterns: by time-series: controls, 4, 8, 14 days post exposure and moribund are represented by the groups 0, 1, 2, 3 and 4 respectively; and by population [site]: Eucumbene, Grey Mare, Kiandra are represented by E, G and K respectively). Where metabolites were not found to be significantly different with a particular test, values have been omitted.

Group	Tissue	Metabolite name/identification	m/z	ANOVA FDR	Tukey's HSD	Pattern matching FDR	Correlation	SAM FDR	PLS-DA VIP comp. 1
Time-series	Skin	α-Ketoglutaric acid, x TMS, 23.95, 1578	198	0.0000	4-0; 4-1; 4-2; 4-3	0.0056	-0.5098	0.0000	2.2391
		L-Threonine, 2 TMS, 17.37, 1298	117	0.0227	3-0; 3-2	0.0343	-0.3980	0.0026	2.0136
		Mannitol, 6 TMS, 30.6, 1915_saturated	320					0.0383	1.9965
		Putrescine, x TMS, 22.45, 1506_putative	174			0.0107	0.4839	0.0080	1.9353
		Adenine, 2 TMS, 29.74, 1869	264			0.0109	0.4717		1.8514
		Serine, 2 TMS, 16.43, 1260	116	0.0222	3-0; 3-2	0.0420	-0.3627	0.0026	1.7681
		Aspartic acid, 2 TMS, 20.54, 1428	160						1.7173
		L-Threonine, 3 TMS, 19.59, 1387	218						1.6906
		Putrescine, 4 TMS, 27.09, 1739_saturated	175			0.0355	0.3716	0.0195	1.6304
		Serotonin, x TMS, 39.11, 2470	174	0.0020	4-0; 4-1; 4-2; 4-3			0.0005	
		5-Hydroxyindole-3-acetic acid, 3 TMS, 35.49, 2212	290	0.0020	4-0; 4-1; 4-2; 4-3			0.0005	
		L-Isoleucine, 2 TMS, 17.32, 1295	158	0.0032	4-0; 4-1; 4-2; 4-3			0.0038	
		Glutamic acid, 3 TMS, 24.79, 1623	246	0.0037	4-0; 4-1; 4-2; 4-3	0.0355	-0.3851	0.0026	
		DL-Ornithine, 3 TMS, 24.71, 1623	174	0.0093	2-1; 3-2; 4-2			0.0026	

		DL-Tartaric acid 4TMS-like	189	0.0157	4-0; 4-1; 4-2	0.0214	-0.4411	0.0053	
		Urea, 2 TMS, 16.14, 1249	189	0.0218	1-0; 3-1			0.0015	
		L-Glutamic acid, 2 TMS, 22.7, 1519_saturated.1	157	0.0222	4-0; 4-2	0.0263	-0.4283	0.0099	
	Liver	Putrescine, x TMS, 22.45, 1506_putative	174	0.0000	4-0; 4-1; 4-2; 4-3	0.0000	0.6063	0.0000	2.5617
		5-Hydroxyindole-3-acetic acid, 3 TMS, 35.49, 2212	290	0.0009	4-0; 4-1; 4-2; 4-3	0.0033	0.4329	0.0000	2.4829
		D-(+)-Galactose, 5 TMS, MEOX, 29.94, 1880	205	0.0483	4-0; 4-1	0.0347	-0.3352	0.0016	2.4324
		Citric acid, 4 TMS, 28.69, 1817	273	0.0000	4-0; 4-1; 4-2; 4-3	0.0006	-0.4893	0.0000	2.0435
		α-Ketoglutaric acid, x TMS, 23.95, 1578	198	0.0001	4-0; 4-1; 4-2; 4-3	0.0021	-0.4483	0.0010	2.0414
		Putrescine, 4 TMS, 27.09, 1739	175	0.0000	4-0; 4-1; 4-2; 4-3	0.0001	0.5630	0.0014	2.0064
		Creatine. x TMS, 23.39, 1551	115	0.0001	4-0; 4-1; 4-2; 4-3	0.0011	0.4673	0.0016	1.9413
		γ-Aminobutyric acid, 3 TMS, 22.9, 1526	174	0.0000	3-0; 4-0; 4-1; 3-2; 4-2	0.0002	-0.5217	0.0029	1.8831
		D-Fructose-6-phosphate 6TMS, MEOX, 36.72, 2300-putative.2	387	0.0000	4-0; 4-1; 4-2; 4-3	0.0084	-0.4007	0.0016	1.7552
		Putrescine, 4 TMS, 27.13, 1738_saturated	175	0.0018	4-0; 4-1; 4-2; 4-3	0.0131	0.3808	0.0038	1.6111
		L-Glutamic acid, 2 TMS, 22.7, 1519_saturated	157	0.0000	4-0; 4-1; 4-2; 4-3	0.0000	-0.6410	0.0058	1.5740
		L-Isoleucine, 2 TMS, 17.32, 1295	158	0.0000	4-0; 2-1; 4-1; 3-2; 4-2; 4-3	0.0001	0.5536	0.0019	
		Gallic acid, x TMS, 22.73, 1520_saturated	157	0.0000	4-0; 4-1; 4-2; 4-3	0.0000	-0.6403	0.0058	
		L-Pyroglutamic acid, 2 TMS, 22.76, 1520_saturated	157	0.0000	4-0; 4-1; 4-2; 4-3	0.0000	-0.6409	0.0058	
		L-Leucine, 2 TMS, 16.74, 1274	158	0.0000	4-0; 4-1; 3-2; 4-2; 4-3	0.0001	0.5520	0.0080	
		Glutamic acid, 3 TMS, 24.79, 1623	246	0.0000	4-0; 4-1; 4-2; 4-3	0.0003	-0.5137	0.0058	
		Fumaric acid, 2 TMS, 18.29, 1357	245	0.0000	4-0; 4-1; 4-2; 4-3	0.0006	-0.4868	0.0035	
		D-Glucose-6-phosphate, 6 TMS, MEOX, 37.23, 2332	387	0.0000	4-0; 4-1; 4-2; 4-3	0.0279	-0.3472	0.0016	
Site	Skin	Pantothenic acid, O,O,O-TMS-putative	103	0.0104	G-E; K-E	0.0091	-0.5252	0.0069	2.1491
		Aspartic acid, 2 TMS, 20.54, 1428	160						2.0434

	L-Threonine, 2 TMS, 17.37, 1298	117						1.9310
	L-Methionine, 1 TMS, 20.27, 1416_putative.2	104						1.8389
	Serotonin, x TMS, 39.11, 2470_saturated	174						1.7514
	saturated_Guanine manual	367						1.6956
	Myo-Inositol, 6 TMS, 33.38, 2081	305	0.0187	K-E; K-G			0.0406	
	L-Leucine, 2 TMS, 16.74, 1274	158	0.0208	K-E; K-G	0.0091	0.4929		
	L-Isoleucine, 2 TMS, 17.32, 1295	158	0.0232	K-E	0.0091	0.4935		
Liver	D-(+)-Turanose, 7 TMS, 42.29, 2702	361						2.7651
	Urea, 2 TMS, 16.14, 1249	189						2.5120
	Thymine, 2 TMS, 19.94, 1403	255						2.4853
	L-Lysine, 3 TMS, 26.54, 1712	84						2.0561
	Myo-Inositol, 6 TMS, 33.38, 2081.1	217						1.8950
	D-Fructose-6-phosphate 6TMS, MEOX, 36.72, 2300-putative	459						1.7481
	Sucrose, 8 TMS, 41.32, 2630.1	361						1.7421

5.4.6 Discussion

In this study we compared whole-metabolome expression profiles between unexposed control frog samples and samples obtained at various time points post exposure (4, 8, 14 days post exposure, and moribund frogs at approximately 28-30 days post exposure). We also compared metabolite expression among populations of frogs with differential long-term exposure histories to the fungal pathogen *Batrachochytrium dendrobatidis* (Bd). To our knowledge this is the first non-targeted metabolomic study of amphibian host skin and liver tissue responses to chytridiomycosis. Overall we identified a total of 162 unique metabolites among the skin and liver of the 61 frogs sampled. We found that the metabolome of skin (site of Bd infection) and liver tissues differed substantially, consistent with the underlying differential physiology of the tissues both in health and disease. Several key metabolites were identified that were predominantly responsible for discriminating between exposure groups and populations. These included α-ketoglutaric acid, L-threonine and serine differentiating time since exposure in the skin samples; putrescine, citric acid, γ-aminobutyric acid, D-fructose-6-phosphate and L-glutamic acid differentiating time since exposure in the liver samples; and pantothenic acid differentiating populations in the skin samples (see Table 5.7 for summary of key identifiable important metabolites).

The expressed metabolome was distinctly divergent between moribund frogs and both control and subclinical frog groups, likely associated with end-stage pathophysiological changes occurring in the tissues shortly prior to death (Voyles et al., 2009). Identified metabolites found to be consistently most significantly different in the skin samples between moribund and remaining frog groups included α-ketoglutaric acid, serotonin, 5-hydroxyindole-3-acetic acid, L-isoleucine, glutamic acid, DL-ornithine, DL-tartaric acid, urea, serine, and L-threonine (supported as highly significant by at least two of the three univariate analyses performed). Of these, α-ketoglutaric acid (high in controls), L-threonine (no time-series association), and serine (no time-series association) were also identified as highly important for contributing to clustering in the PLS-DA VIP scores. Other metabolites contributing to clustering included mannitol, putrescine, and adenine (all high in moribund frogs), and aspartic acid (no time-series association).

Alpha-ketoglutaric acid (or 2-oxoglutarate) is an important intermediate in the tricarboxylic acid cycle (Krebs cycle), produced by the transamination of glutamate for energy generation within eukaryotic mitrochondria. As such, it is ubiquitous among tissues, and is also involved in a number of other metabolic pathways (Kanehisa and Goto, 2000). Although it is difficult to speculate the cause, decreased expression of α-ketoglutaric acid in moribund frogs may indicate

energy dysregulation in frogs at the late stages of infection relative to controls. Threonine and serine are small, closely related, polar, pH neutral, nucleophilic amino acids bearing a hydroxyl group. Although these two amino acids were found to be consistently significantly differentially expressed between sampling periods, this was not clearly associated with a time-series trend, and expression peaked at 8 days post exposure. When we examined enriched GO terms from the alpine tree frog transcriptome for related pathways, we found 22 unique GO terms that were associated with serine and threonine in the skin, suggesting their integral involvement in the early stages of infection and host response. In particular, identified pathways involved serine and threonine biosynthesis and catabolism, transport, kinase activity and protease activity (serine-type endopeptidase and carboxypeptidase, threonine-type endopeptidase) and may indicate involvement in inflammation (Pham, 2006). These findings are consistent with previous chytridiomycosis studies reporting the increased expression of genes related to serine and threonine proteases by amphibian hosts (Ellison et al., 2014; Ribas et al., 2009). We also cannot rule out, however, that these ubiquitous amino acids are not instead associated with the fungal pathogen, as has previously been demonstrated (Moss et al., 2010; Rosenblum et al., 2012a).

In the liver analyses, metabolites that were differentially expressed with end-stage physiology from the univariate analyses included L-isoleucine, L-glutamic acid, gallic acid, L-pyroglutamic acid, L-leucine, putrescine, citric acid, fumaric acid, D-fructose-6-phosphate, and D-glucose-6-phosphate (highly significant by at least two of the three analyses performed). Of these, putrescine (high in moribund), citric acid (high in controls), γ-aminobutyric acid and D-fructose-6-phosphate (both with no time-series association), and L-glutamic acid (high in controls) were also identified as important via PLS-DA VIP scores. Other metabolites contributing to clustering included 5-hydroxyindole-3-acetic acid (high in moribund), D-(+)-galactose (high in controls), α-ketoglutaric acid (high in controls), and creatine (high in moribund).

Putrescine is a polyamine breakdown product of amino acids so named for its foul odour and association with decaying flesh (Yeoman et al., 2013). Although putrescine could potentially be associated with post-mortem autolysis during tissue collection, this cause is unlikely for two reasons. Firstly, we identified putrescine as significantly over-expressed in both liver (FDR < 0.0001 in all three univariate analyses) and skin tissues (FDR ≈ 0.01 for both pattern-matching and SAM), with positive correlations to the time-series of sampling periods (expression increasing with time since exposure, correlation = 0.6063 in liver and 0.4839 in skin). As unexposed control frogs were sampled at 4, 8, and 14 days post exposure, there is no evidence for a sampling period batch effect. Secondly, our examination of GO enrichment results for the skin tissues revealed two up-regulated GO pathways involving putrescine directly (putrescine

biosynthetic process from ornithine [GO:0033387], putrescine catabolic process [GO:0009447]), suggesting gene and enzymatic involvement. Putrescine has also been shown to play important roles in immune processes and basic homeostatic mechanisms (Girdhar et al., 2006; Hashemi et al., 2014). Increased concentrations of putrescine in the late stages of infection may be associated with differential odours between infected and control individuals (as reported anecdotally by colleagues).

Citric and L-glutamic acids were found in relatively higher concentrations in control than moribund frog liver samples. Similar to α-ketoglutaric acid as discussed above from the skin tissues, citric and L-glutamic acids are also intermediates in the tricarboxylic acid cycle (although they also have many other functional roles), and their concentrations may similarly be decreased in disease in association with energy dysregulation. A total of 18 enriched GO pathways were identified to have a direct association with glutamic acid (including glutamine, glutamate and glutamyl moieties), suggesting that these pathways are integral to pathogenesis and host response. Neither γ-aminobutyric acid (GABA) nor D-fructose-6-phosphate demonstrated a clear time-series association (both most highly expressed at 8 days post exposure) despite being consistently highly significantly differentially expressed between sampling periods in liver tissues. GABA is an inhibitory neurotransmitter at neuronal synapses, but can also be found in peripheral tissues unrelated to neurotransmission (Erdo and Wolff, 1990). D-fructose-6-phosphate is a key early monosaccharide intermediate in the glycolysis pathway for the production of energy in the form of adenosine triphosphate (ATP) and nicotinamide adenine dinucleotide (NADH) from glucose. The roles of GABA and D-fructose-6-phosphate in the pathogenesis of chytridiomycosis are unclear at this time.

Pantothenic acid, myo-inositol, L-leucine and L-isoleucine demonstrated highly significantly different concentrations in skin samples between populations in at least two of the three univariate analyses performed. The pattern of association identified was Eucumbene-Grey Mare-Kiandra, which suggests that the Bd-naïve population Grey Mare lies between the other two in terms of metabolite expression. Of these, pantothenic acid (high in Eucumbene, low in Kiandra) was also identified to contribute to clustering via the supervised PLS-DA VIP results. Other metabolites contributing to cluster separation included aspartic acid, L-threonine, L-methionine, serotonin, and guanine (all high in Eucumbene). Although univariate analyses revealed no metabolites with significantly different concentrations between populations in the liver samples, VIP scores for liver samples grouped by population included D-(+)-turanose, L-lysine, and D-fructose-6-phosphate (high in Eucumbene); urea, thymine, and myo-inositol (high in Kiandra); and sucrose (high in Grey Mare). Pantothenic acid (otherwise known as vitamin B_5) is an essential water-soluble vitamin for the synthesis of coenzyme-A (CoA) which is

principally involved in energy (tricarboxylic acid cycle) and fatty acid metabolism, however it is unclear how expression differences in pantothenic acid may relate to clinical evidence of survival between the populations.

In this study we have identified a number of key metabolites in the skin and liver tissues that predominantly differentiate moribund frogs with chytridiomycosis from both unexposed control and subclinical frogs. We also identified metabolites related to differences in population of origin, which may be associated with variation in phenotypic resistance between populations. Similar to all 'omics' pathways, the level of expression (or concentration) of metabolites in tissues is dependent not only on their rate of production (upstream processes), but also their rate of degradation, catalysis to other forms, or removal (Tan et al., 2009). Because small molecule metabolites are often the end products of metabolism, numerous upstream pathways may be involved in their production, making it difficult to determine their proximate source or relationship to gene and protein expression. Furthermore, infected or body surface tissues (mucosae or epidermis) such as the skin of frogs, may harbour metabolites resulting from not only amphibian host processes, but also metabolic pathways of the fungal pathogen as well as potentially secondary bacterial infections. The differences in metabolite expression that we have identified may be characteristic of processes involved in chytridiomycosis, and we recommend examination of the tissue metabolome of other amphibian species in future studies to confirm these findings.

5.4.7 Acknowledgments

We thank P. Harlow, M. McFadden, D. Hunter and B. Scheele for assistance with logistics for the clinical experiment and species' insights. This study was conducted with approval by the James Cook University Animal Ethics Committee (Certificate no. A1589) and Scientific License number: S12848 (D. Hunter). This work was jointly funded by the US Fish and Wildlife Service - Wildlife Without Borders program and the IUCN Amphibian Specialist Group Seed grants program. The funders had no role in study design, data collection and analysis, decision to publish, or preparation of the manuscript.

5.4.8 Supporting information

Additional figures and tables referred to in text are included in the supporting information Appendix H. The authors are solely responsible for the content and functionality of these materials. Queries (other than absence of the material) should be directed to the corresponding author.

Figure 5.15. Principal Components Analysis (PCA) scores plots of principal components one and two, for comparisons between **sampling period** in skin samples (A) and liver samples (C). Projection to Latent Structures - Discriminant Analysis (PLS-DA) scores plots of components one and two, comparing sampling periods in skin samples (B) and liver samples (D).

0 represents the control group, 1 represents samples taken at 4 days post-exposure, 2 represents samples taken at 8 days post exposure, 3 represents samples taken at 14 days post exposure and 4 represents moribund frogs (roughly at 21+ days post exposure).

A

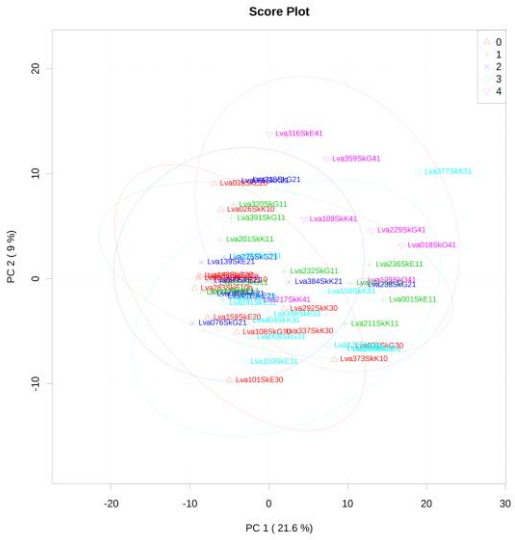

B

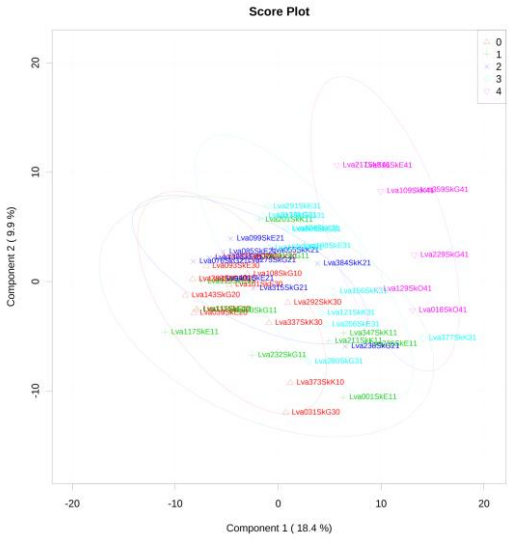

C

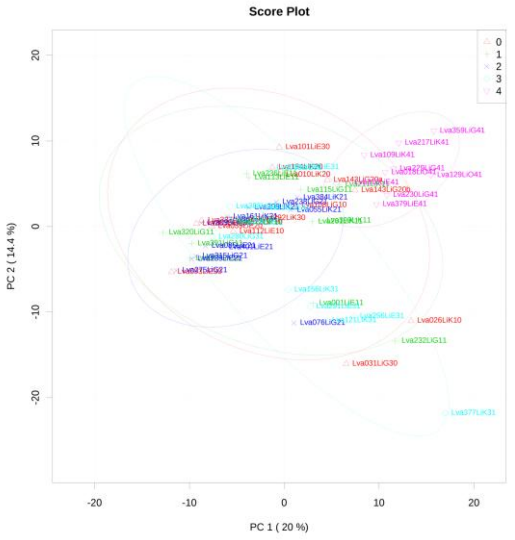

D

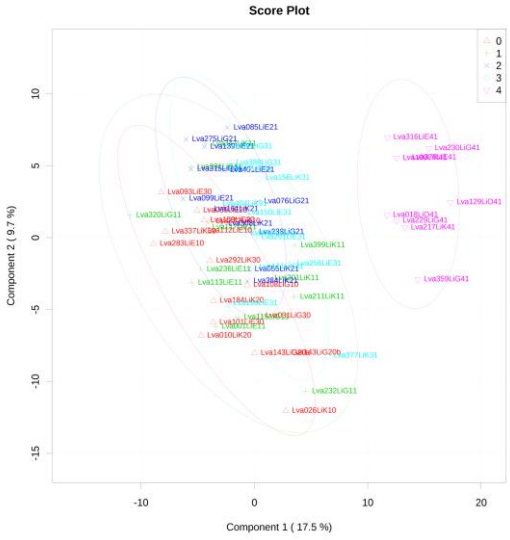

Figure 5.16. Principal Components Analysis (PCA) scores plots of principal components one and two, for comparisons between **populations** in skin samples (A) and liver samples (C). Projection to Latent Structures - Discriminant Analysis (PLS-DA) scores plots of components one and two, comparing populations in skin samples (B) and liver samples (D).

A

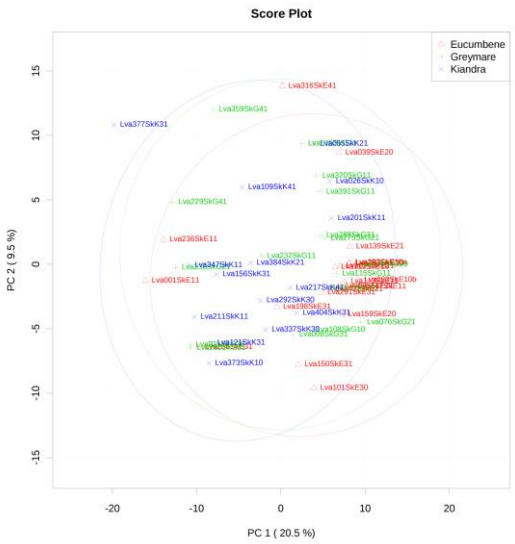

B

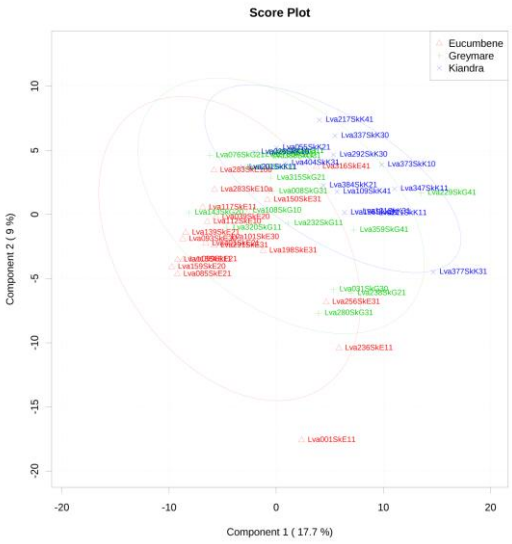

C

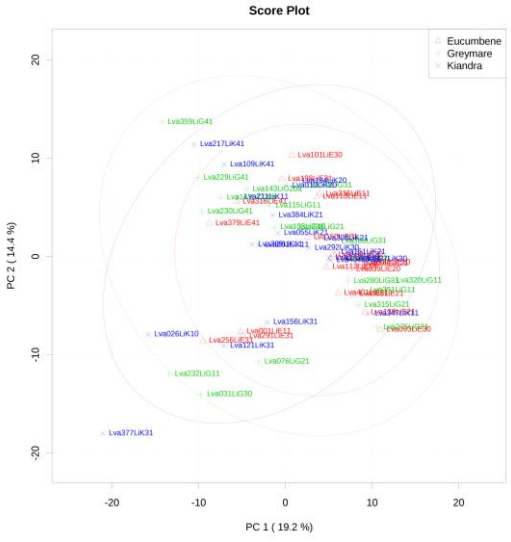

D

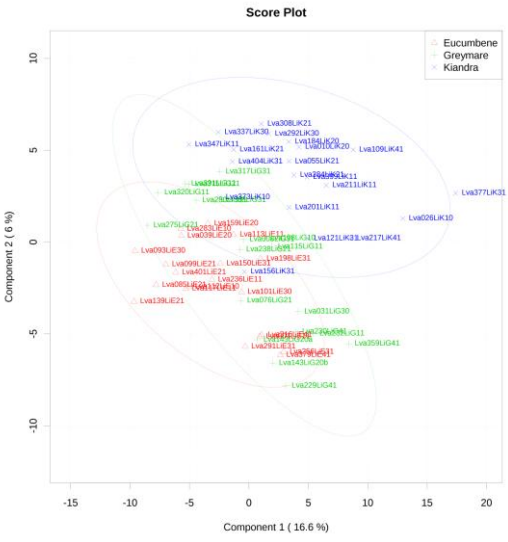

CHAPTER 6: Managing wildlife disease

6.1 Introduction

The management and mitigation of wildlife disease, although challenging, is not an intractable problem. Maintaining optimism and developing forward-thinking strategies are key for ensuring wider public and political engagement in conservation issues. We have the opportunity now to make important changes in the way we manage wildlife disease that will have far-reaching consequences for future generations. Immediate management of chytridiomycosis-threatened amphibian populations is essential to ensure their long-term persistence. Improvement in current wildlife disease surveillance techniques will help prevent a future repeat of the chytridiomycosis scenario, which has been characterized as "the most spectacular loss of vertebrate biodiversity due to disease in recorded history" (Skerratt et al., 2007).

In this chapter I developed a conceptual framework for managing endemic chytridiomycosis via two approaches; reducing Bd in the environment and on amphibians, and increasing host population persistence in the face of increased mortality. I also synthesized a systematic surveillance approach for emerging biodiversity diseases that should enable their more rapid detection and mitigation. I aimed to improve the accessibility of promising on-the-ground techniques for chytridiomycosis mitigation to assist amphibian conservation managers as well as highlight the critical need for new and better integrated wildlife disease surveillance systems (see Fig. 6.1).

This chapter consists of 1) a peer-reviewed publication describing a framework for chytridiomycosis interventions, and 2) a peer-reviewed publication outlining the challenges of biodiversity disease surveillance and recommending a systematic surveillance approach.

Figure 6.1. Project aims, highlighting Chapter 6: Managing wildlife disease.

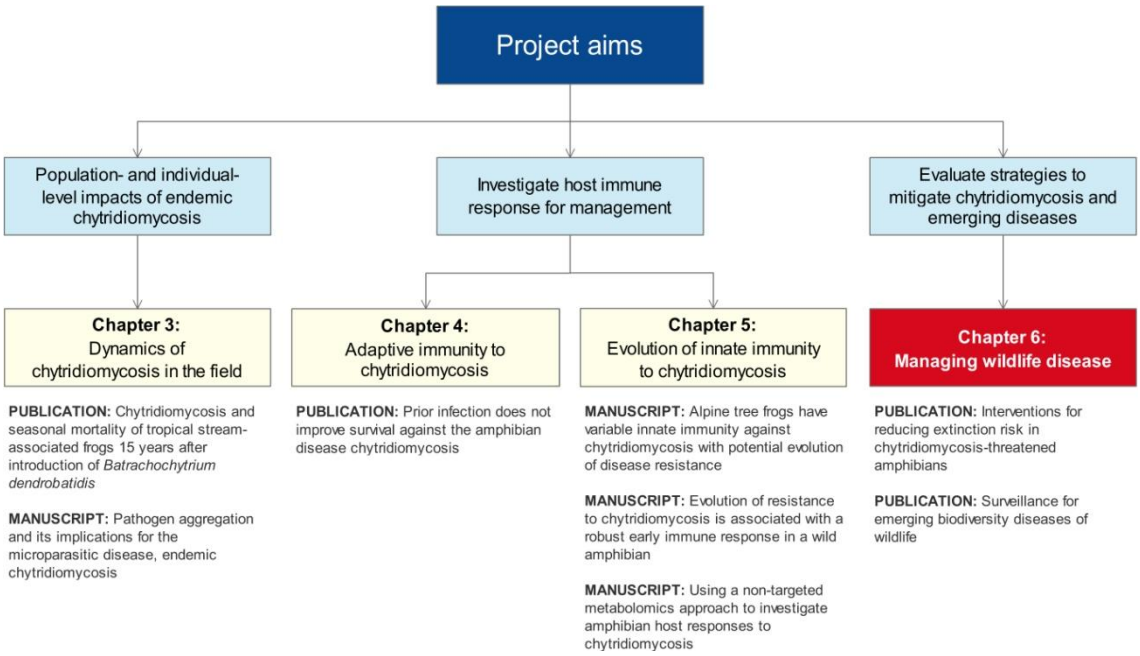

6.2 PAPER 1: Interventions for reducing extinction risk in chytridiomycosis-threatened amphibians

This published peer-reviewed paper represents original review, synthesis and writing led by Ben Scheele, the primary investigator. My role in the paper included substantial assistance with the conceptual design, construction of figures and editorial input.

The full reference for the published paper is:
Scheele, B. C., Hunter, D. A., **Grogan, L. F.**, Berger, L., Kolby, J., McFadden, M., Marantelli, G., Skerratt, L. F., Driscoll, D. A. (2014) Interventions for reducing extinction risk in chytridiomycosis-threatened amphibians. Conservation Biology 28(5):1195-1205.

The following text is a word for word copy of the manuscript published in the journal Conservation Biology. Section, table and figure numbering has been added or reformatted for this thesis for ease of reference. Since the journal uses American English, the spelling follows this convention.

6.2.1 Front matter

Interventions for reducing extinction risk in chytridiomycosis-threatened amphibians

Running title: Reducing extinction risk in amphibians

B. C. Scheele [a, b, †], D. A. Hunter [b], L. F. Grogan [c], L. Berger [c], J. E. Kolby [c, d], M. S. McFadden [e], G. Marantelli [f], L. F. Skerratt [c], D. A. Driscoll [a]

[a] ARC Centre of Excellence for Environmental Decisions, National Environmental Research Program Environmental Decisions Hub, Fenner School of Environment and Society, Forestry Building [48], Australian National University, Canberra, ACT 0200, Australia
[b] NSW Office of Environment and Heritage, Queanbeyan, NSW 2620, Australia
[c] One Health Research Group, School of Public Health, Tropical Medicine and Rehabilitation Sciences, James Cook University, Townsville, Queensland 4811, Australia.
[d] IUCN SSC Amphibian Specialist Group, Regional Co-Chair (Honduras).
[e] Taronga Conservation Society Australia, Mosman, NSW 2088, Australia.
[f] Amphibian Research Centre, PO Box 959, Merlynston, Victoria 3058, Australia.

† Address for correspondence: Australian National University,
email: ben.scheele@anu.edu.au

Key words: amphibian decline, *Batrachochytrium dendrobatidis*, chytrid, disease management, emerging infectious disease, frog, wildlife management

6.2.2 Abstract

Wildlife diseases pose an increasing threat to biodiversity and are a major management challenge. A striking example of this threat is the emergence of chytridiomycosis. Despite diagnosis of chytridiomycosis as an important driver of global amphibian declines 15 years ago, researchers have yet to devise effective large scale management responses other than biosecurity measures to mitigate disease spread and the establishment of disease-free captive assurance colonies prior to or during disease outbreaks. We examined the development of management actions that can be implemented after an epidemic in surviving populations. We developed a conceptual framework with clear interventions to guide experimental management and applied research so that further extinctions of amphibian species threatened by chytridiomycosis might be prevented. Within our framework, there are 2 management approaches: reducing *Batrachochytrium dendrobatidis* (the fungus that causes chytridiomycosis) in the environment or on amphibians and increasing the capacity of populations to persist despite increased mortality from disease. The latter approach emphasizes that mitigation does not necessarily need to focus on reducing disease-associated mortality. We propose promising management actions that can be implemented and tested based on current knowledge and that include habitat manipulation, antifungal treatments, animal translocation, bioaugmentation, head starting, and selection for resistance. Case studies where these strategies are being implemented will demonstrate their potential to save critically endangered species.

6.2.3 Introduction

In a globalizing world, emerging infectious diseases are a growing threat to biodiversity (Daszak, 2000; Fisher et al., 2012) and can have a rapid and widespread impact on wildlife, driving species to extinction (Berger et al., 1998; Joseph et al., 2013). Despite the rise of disease as a key conservation challenge, the management of wildlife diseases affecting biodiversity, especially non-mammals, remains in its infancy (Joseph et al., 2013).

Chytridiomycosis, caused by the pathogenic skin fungus *Batrachochytrium dendrobatidis* (Bd), has devastated amphibian communities globally and is considered the worst recorded wildlife disease (Berger et al., 1998; Skerratt et al., 2007). Infection with Bd has been detected in 516 of 1240 (42%) amphibian species sampled (Olson et al., 2013), and a conservative estimate suggests that chytridiomycosis has caused the severe decline or extinction of over 200 species (Skerratt et al., 2007). Amphibians are a functionally important group, and their loss is likely to have major ramifications throughout ecosystems (Whiles et al., 2013).

Although experimental management strategies are underway (Woodhams et al., 2011), there are few studies on the *in situ* management of species threatened by chytridiomycosis (Joseph et al., 2013; Zippel et al., 2011). To date, amphibian disease management has generally targeted mitigating disease spread and securing captive assurance colonies rather than restoring populations after an epidemic. Existing literature is largely directed toward policy makers, regional managers, and researchers rather than on-the-ground wildlife managers (see Department of the Environment and Heritage, 2006; Mendelson et al., 2006; Woodhams et al., 2011). We devised a framework to guide management that includes experimental strategies that directly target reduction of chytridiomycosis in host populations and outline strategies to improve population buffering capacity against disease-induced mortality, which is only briefly covered in previous disease management recommendations (Department of the Environment and Heritage, 2006; Woodhams et al., 2011). We summarize new and updated strategies aimed at mitigating the impact of chytridiomycosis to assist wildlife managers to select interventions.

Although populations of some species that declined have recovered (Newell et al., 2013), other species remain at low abundance or continue to decline and face increased risk of extinction (Hunter et al., 2010; Vredenburg et al., 2010). One of the main reasons for this elevated extinction risk is on-going mortality and restricted recruitment caused by endemic chytridiomycosis (Murray et al., 2009; Muths et al., 2011; Phillott et al., 2013). In addition, many remnant populations have limited connectivity, occur in suboptimal habitat, and are likely to have increased vulnerability to stochastic events and other threatening processes (Murray et al., 2009; Puschendorf et al., 2011).

A huge research effort over the last decade has resulted in Bd becoming one of the most studied wildlife pathogens. The ecology and pathogenesis of chytridiomycosis is relatively well understood, Bd distribution has been mapped and modeled, high-risk species have been identified, biosecurity protocols have been implemented, captive assurance colonies have been established, and antifungal treatments and disinfectants (including chemical, physical, and biological treatments) have been developed for implementation in controlled environments (e.g., Murray et al., 2011b; Woodhams et al., 2011). However, a major gap remains in translating research into post-epidemic, *in situ* management actions. It is crucial that we overcome a fear of in-field interventions and use existing knowledge to test novel solutions such as those suggested in Table 6.1 (Berger and Skerratt, 2012).

Here we propose a new framework to provide greater clarity for setting conservation objectives and to highlight approaches to practical management of species threatened by chytridiomycosis. In the framework, management strategies are grouped into 2 broad approaches and within each approach, we classified management strategies into 3 action classes based on whether strategies are implemented *in situ*, involve amphibian introductions, or are *ex situ*. We then provide a scientific underpinning for novel management strategies that hold considerable promise, including habitat manipulation, *in situ* antifungal treatment, animal translocations, bioaugmentation, head starting, and *ex situ* selection for resistance. We considered examples where researchers are implementing these strategies in conjunction with conservation agencies. Given the limited application of interventions to date, we hope that showcasing techniques currently being tested will inform and stimulate the development and implementation of conservation strategies for Bd threatened species.

Table 6.1. A framework for action to maintain populations of amphibians threatened by *Batrachochytrium dendrobatidis* (Bd) when the short-term goal is to secure these populations in captivity and in the wild.

Action classes	Reduce Bd in the environment or on host	Increase population buffering capacity
Environmental manipulation	Manipulate habitat (shallow warm water for tadpoles, decrease shading to create open basking sites for adults and metamorphs) - Artificial heat sources (all life stages) - Exclude Bd reservoir host species (McCallum, 2012; Woodhams et al., 2011) - Introduce Bd inhibitors (salts, fungicides) (Stockwell et al., 2012; Woodhams et al., 2011) - Bioaugmentation with commensal bacteria (Bletz et al., 2013; Muletz et al., 2012) - Alter water flow or pond drying regime	Minimize human impacts (e.g., hunting, collection, habitat degradation) - Manage other threatening processes (e.g., invasive species, sympatric competition, predation) - Prevent introductions and reduce impacts of other diseases (e.g., Ranaviruses) - Modify habitat to minimize mortality from climatic extremes (Shoo et al., 2011)
Amphibian introductions	Identify environmental refugia where Bd is absent (mountain tops, small islands) or refugia where environmental suitability for Bd is low (lower elevation, drier habitat) and translocate - Avoid recipient sites with Bd reservoir host species - Identify life stages where Bd is threatening population viability and temporarily bring individuals into captivity to clear infection and return to the wild (chemical or heat treatment)	Head start wild or captive bred progeny to minimize natural mortality from predators, competition, and insufficient hydroperiod length - Population augmentation from captive bred progeny - Create new habitat with a high buffering capacity against climate variability and other species-specific threats and translocate
Ex situ conservation	Treatments to clear Bd infection (e.g., chemical and physical treatments; Baitchman and Pessier, 2013; Woodhams et al., 2011) - Selection for resistance or other traits in captive colonies	Establish *ex situ* populations in biosecure facilities (Mendelson et al., 2006; Zippel et al., 2011) - Biobanking of genetic resources (Kouba et al., 2013)

6.2.4 Time frames defining the scope of management objectives

A key challenge to managing species affected by chytridiomycosis is the difficulty of developing long-term solutions. Thus, we divided this challenge into 2 separate goals based on time frames: the short-term goal of establishing robust holding populations of Bd-threatened species in response to immediate threats in the wild (Table 6.1) and the long-term goal of establishing self-sustaining wild populations. Because these goals operate on different time frames, they often require different approaches and techniques. Intensive and expensive options are acceptable as short-term emergency measures, whereas long-term sustainable measures need

to be more cost effective and take into account that species may remain reliant on conservation management, to various degrees, into the future.

We focused on developing actions that can be implemented immediately to achieve the first goal of securing populations that have experienced major declines. Predicting and mitigating disease spread and determining "trigger points" for intervening when chytridiomycosis does spread have been addressed elsewhere (Berger and Skerratt, 2012; Department of Primary Industries, 2010; Murray et al., 2011b). It is important that robust holding populations of chytridiomycosis-threatened species are secured both in captivity and in the wild to facilitate the establishment of self-sustaining wild populations. Although long-term solutions remain elusive, achieving short-term goals will provide a platform for research into long-term goals such as natural or assisted evolution of resistance and behavioral modification (e.g., Richards-Zawacki, 2010; Savage and Zamudio, 2011; Venesky et al., 2012).

6.2.5 Managing Bd-threatened species

Our conceptual framework (Table 6.1) provides a summary of different management options to help managers identify appropriate conservation actions. We identified 2 management approaches: reducing Bd in the environment or on the host and increasing population buffering capacity against Bd-induced mortality, emphasizing that intervention need not focus directly on reducing disease. Within these 2 approaches, there are 3 action classes: environmental manipulation, amphibian introductions, and *ex situ* conservation (Table 6.1). Thus far, the management of Bd-threatened species has focused on establishment of *ex situ* captive colonies (Mendelson et al., 2006; Zippel et al., 2011). This is a critical first stage and the only option for some species. However, where possible we propose that this should be combined with techniques to maintain species *in situ* to reduce costs, avoid negative consequences associated with captive breeding (e.g., reduced fitness; Araki et al., 2007), and facilitate the natural evolution of host resistance. This is where environmental manipulation and introductions can contribute.

6.2.6 Environmental manipulation

6.2.6.1 Manipulation to reduce Bd

In remnant populations of Bd-threatened species, environmental manipulation can be implemented to decrease infection rates and burdens and hence improve host survival. Environmental manipulation is an *in situ* method that has been successfully used to combat wildlife diseases and can be implemented across a wide range of scales (Wobeser, 2007). For example, decreased shading and improved drainage of nesting sites minimized avian cholera, and creating artificial watering points lowered harmful trematode infections in moose (*Alces*

alces; Wobeser, 2002). Environmental and biological factors can exert a strong influence on infectious diseases; therefore, manipulating environmental conditions can influence disease development (Wobeser, 2007). The thermal preference of Bd is relatively well understood; optimal growth is from 17 to 25 °C (Piotrowski et al., 2004; Stevenson et al., 2013). On either side of this range (5–17 °C and 25–28 °C) growth is slow. Above 30 °C Bd dies (Piotrowski et al., 2004), and mortality is rapid at higher temperatures (4 h at 37 °C; Johnson et al., 2003). The fungus is not tolerant of desiccation and is killed within 1 h of drying (Johnson et al., 2003). Field studies and models are consistent with these results and suggest that factors affecting Bd growth (particularly temperatures above 25 °C during the month prior to sampling) are key limiting factors for chytridiomycosis dynamics (Murray et al., 2013; Richards-Zawacki, 2010; Rowley and Alford, 2013). Furthermore, high climatic variability, especially unusually low temperatures, increases the impact of chytridiomycosis (Rohr et al., 2013).

Warm water (> 30 °C) provides an important refuge from Bd for aquatic amphibians (Forrest and Schlaepfer, 2011; Savage et al., 2011). Because overhanging vegetation lowers the water temperature of amphibian breeding ponds (Freidenburg and Skelly, 2004), the strategic removal of patches of vegetation, particularly over shallow, nearshore locations is likely to create warm water refuges for infected individuals (Geiger et al., 2011). Field evidence suggests that decreased shading of ponds is linked to lower Bd infection intensities (Heard et al., 2013; Raffel et al., 2010). Water temperature may also be increased through the creation of nearshore, shallow water areas that warm up rapidly or by changing substrate color or texture. For example, *Bufo americanus* tadpoles can aggregate in shallow pockets of warm water adjacent to scrap sheet metal in breeding ponds (Beiswenger, 1977).

Environmental manipulation may also be used to increase temperature in terrestrial habitats. Many riverine species bask to raise body temperature, and increasing the amount of solar radiation reaching basking sites through vegetation removal could clear or reduce infection (Fig. 6.2). Puschendorf et al. (2011) hypothesized that for the highly susceptible species *Litoria lorica* short term exposure to warm rock temperatures along a sunny stream section may be facilitating population persistence with endemic Bd. This is supported by a follow-up study showing that exposing Bd cultures to 33 °C for just 1 h significantly reduced fungal growth (Daskin et al., 2011).

In situations where habitat modification is not possible, artificial heat sources on land or in water could provide refuges for infected individuals to reduce or clear infection. This strategy has been suggested for protecting bat populations in North America threatened by white nose syndrome (Boyles and Willis, 2010). Artificial heat sources provide opportunities for

individuals to maintain preferred body temperatures, which are often higher than ambient air temperatures, and are likely to be particularly effective for species that display behavioral fever (Murphy et al., 2011; Richards-Zawacki, 2010).

Developing chemical treatments for environmental application is an area of important research; salt and several agricultural products clear or reduce Bd infections under laboratory conditions (Hanlon et al., 2012; McMahon et al., 2013b; Stockwell et al., 2012). For example, thiophanate-methyl, a widely used, broad-spectrum fungicide, cleared infection in tadpoles when applied 6 d after experimental inoculation, but tadpoles grew larger than controls, suggesting side effects may occur (Hanlon et al., 2012). Similarly, the addition of salt to pond environments is a promising strategy for inhibiting Bd growth; however, it may also have negative effects (Heard et al., 2013; Stockwell et al., 2012; Woodhams et al., 2011). Recently, Geiger and Schmidt (2013) used General Tonic (acriflavin/methylene blue) to reduce Bd in captivity, and further research is underway to evaluate the effectiveness of pond applications. Therefore, although use of chemicals in natural habitats holds promise, it is important to determine concentrations and rates of application and assess potential negative side effects.

Bioaugmentation could help maintain threatened populations and facilitate successful reintroductions (Joseph et al., 2013; Woodhams et al., 2011). Bioaugmentation involves inoculating amphibian hosts or habitats with microbes that produce metabolites that inhibit Bd growth and survival (reviewed in Bletz et al., 2013). Locally occurring microbes are most appropriate and Bletz et al. (2013) provide methods to identify microbes that both inhibit Bd and persist on target hosts. Because soil provides an important reservoir for beneficial microbes (Loudon et al., 2014) that can be transmitted to amphibians (Muletz et al., 2012), environmental application appears feasible. As with other interventions, research to improve understanding is needed while field applications are concurrently assessed.

Figure 6.2. Examples of environmental manipulation.

(a) The critically endangered *Litoria spenceri* is restricted to a single stream (stream 1) in Kosciuszko National Park, Australia, and is threatened by endemic chytridiomycosis. (b) Recipient stream (stream 2) in the park identified through broad-scale surveys where captive bred *L. spenceri* will be introduced. (c) Temperature profiles for representative *L. spenceri* basking sites from streams 1 and 2. Overhanging vegetation was pruned from half the locations on stream 1 at the end of January.

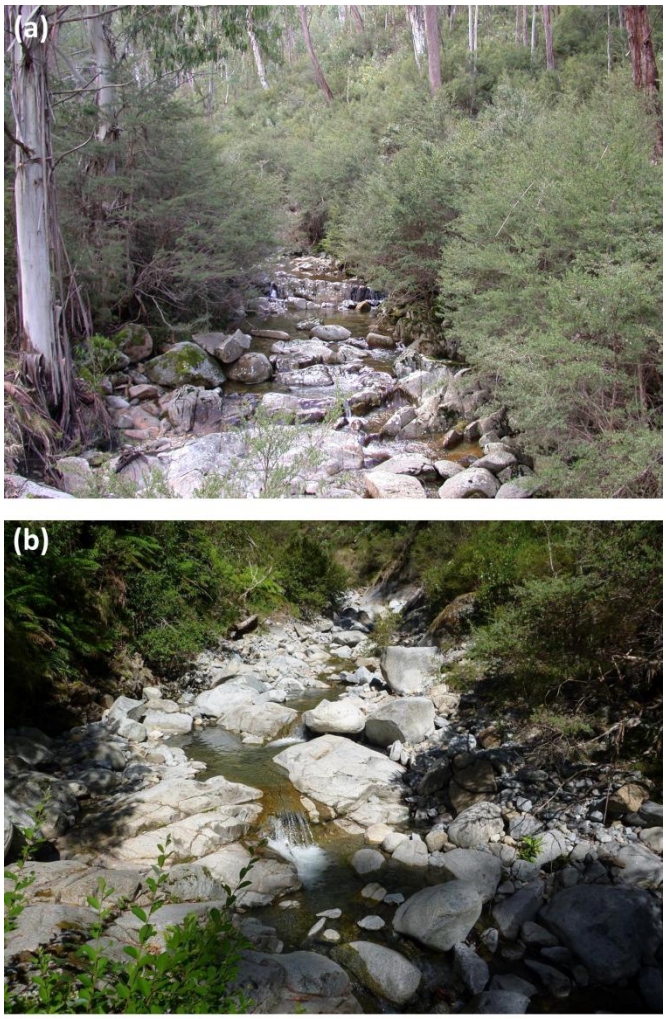

6.2.6.2 Manipulation to increase population buffering capacity

An alternative approach to directly reducing Bd pressure in disease-threatened amphibian populations is to minimize other sources of mortality. Amphibian populations can tolerate adult mortality from Bd when recruitment is sufficiently high (Muths et al., 2011; Phillott et al., 2013; Tobler et al., 2012). Habitat loss and degradation are key threatening processes for many

amphibian species (Stuart et al., 2004), and it is crucial to protect habitat for species threatened by chytridiomycosis. Introduced species can also increase juvenile and adult mortality, and their exclusion can increase population size (e.g., Vredenburg, 2004). However, increased population densities following the removal of introduced species will theoretically increase Bd transmission, and this risk should be considered against potential benefits (Briggs et al., 2010). Finally, in many amphibian populations climatic extremes are a major source of mortality (Shoo et al., 2011). To minimize drought-induced recruitment failure, amphibian breeding habitats can be manipulated to increase hydroperiod, and adult mortality can be reduced through the creation of moist refuges (see Shoo et al., 2011). When manipulating habitat, it is important to consider the relative effects of different sources of mortality because there may be trade-offs between improved survivorship and improved habitat for Bd (Murray et al., 2011b).

6.2.7 Amphibian introductions

6.2.7.1 Introductions to environments unfavorable for Bd

When Bd cannot be controlled *in situ*, translocations can be used to move animals to environments unfavorable to Bd growth or to Bd-free locations. Animal translocation can mitigate infectious disease in mammals (Wobeser, 2002), but remains untested for combating chytridiomycosis. We propose the translocation of animals into environmental refugia within or near their former range. Refugia must have suitable characteristics (Hoegh-Guldberg et al., 2008) and either occur within the physiological stress limits of the target species or be manipulated to remain within those limits. Refugia can be identified through a combination of Bd field sampling and distribution modeling (Puschendorf et al., 2009; Puschendorf et al., 2013). In general, refugia are most likely to occur at lower elevations where environmental temperatures exceed the optimum for Bd growth, or in drier areas. However, other factors, such as the absence of disease reservoir species, may be equally important in some circumstances (Joseph et al., 2013). The effectiveness of amphibian introductions to new areas is being evaluated in Kosciuszko National Park, Australia, where the critically endangered *Litoria spenceri* is restricted to a single stream (Fig. 6.2a) and is threatened by endemic chytridiomycosis. A captive breeding colony has been established and will provide offspring for reintroduction at the source site following canopy reduction as well as experimental introduction to a second stream (Fig. 6.2b) that has naturally low canopy cover, a warm microclimate (Fig. 6.2c), and no reservoir hosts or introduced predatory fish.

Although translocations have considerable promise, they can have unintended consequences, and potential benefits and risks require careful evaluation (see Hoegh-Guldberg et al., 2008; McLachlan et al., 2007). Importantly, it is crucial to follow biosecurity protocols to mitigate the

risk of disease spread and subsequent outbreaks (Department of the Environment and Heritage, 2006; Zippel et al., 2011).

6.2.7.2 Introductions to increase population buffering capacity

It may be possible to counteract the population impacts of increased mortality caused by Bd by adding captive bred individuals to wild populations. Two strategies that build on traditional reintroduction approaches are head starting and population augmentation (Fig. 6.3). Head starting involves raising wild harvested individuals, typically eggs or tadpoles, to an optimal age for release and thus enabling survival through periods of naturally high mortality (e.g., due to predation) or high Bd-induced mortality or Bd exposure. To devise effective head starting strategies for each species, it is crucial to know which life history stage has highest exposure to Bd or undergoes mortality from chytridiomycosis. For example, in upland rainforest streams in Central America chytridiomycosis causes much higher mortality in metamorphizing individuals than in adults (Kolby et al., 2010). The Honduras Amphibian Rescue and Conservation Center (HARCC) is working to address this concern and replenish the population of adult reproductive frogs. To enhance survival, late development stage tadpoles will be brought into captivity, treated for and cleared of infection, and maintained at the biosecure HARCC facility through metamorphosis (Figs. 6.3a and 6.3b). These frogs will be raised in captivity past their most Bd-vulnerable life phase and then released as young adults at their capture site. Head starting has an important benefit over *ex situ* breeding programs: individuals for reintroduction can be produced quickly, which removes the challenges and failures associated with captive breeding in species with diverse reproductive and husbandry requirements. Therefore, in systems where Bd is endemic but adults continue to produce offspring, head starting eggs or tadpoles could contribute to population survival within their natural habitat.

When recipient sites are unavailable and habitat manipulation is not possible, creating new habitat for translocated animals is likely to be useful. Human-created ponds already provide important refuges for chytridiomycosis-threatened amphibians (Heard et al., 2013). Benefits of habitat creation include a high level of control of environmental conditions and avoidance of impacts on natural habitat for non-target species. A variety of habitats should be created (Lesbarreres et al., 2010) that include warm environments where individuals can reduce or clear Bd infection. Created habitat should be designed to minimize the impacts of other threats such as fish predation or drought-induced recruitment failure (Shoo et al., 2011) because increased recruitment may compensate for chytridiomycosis-induced mortality (cf. Muths et al., 2011).

Figure 6.3. Examples of head starting programs.

(a) *Plectrohyla dasypus*, a critically endangered species that will be collected, treated for *Batrachochytrium dendrobatidis* infection, and released as part of the Honduras Amphibian Rescue and Conservation Center (HARCC) program. (b) An amphibian room at Lancetilla Botanical Gardens, Honduras, where *Batrachochytrium dendrobatidis*-free amphibians in the HARCC program will be head started and raised for future reintroductions into Cusuco National Park, Honduras. (c) Artificial ponds in natural breeding habitat in Kosciuszko National Park, Australia, where captive and wild bred eggs from the critically endangered *Pseudophryne corroboree* have been placed to prevent contact with co-occurring reservoir hosts and eliminate mortality from premature pond drying. (d) A recently metamorphosed *P. corroboree* emerging from one of the artificial ponds in (c).

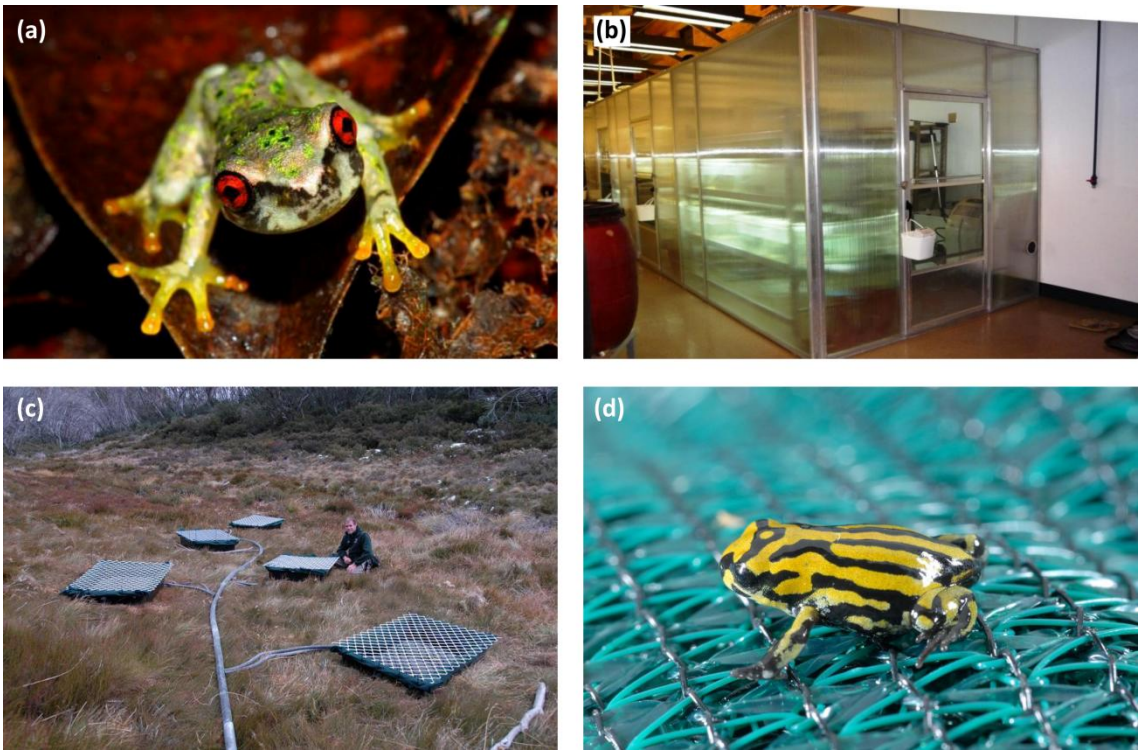

6.2.8 Ex situ conservation

6.2.8.1 Selection for resistance

For species relying on captive colonies to survive, maintaining the genetic diversity of founding individuals through generations in captivity is important because this diversity cannot be regained. However, selecting for increased disease resistance could facilitate population persistence with Bd infection and thus lead to sustainable populations (see Venesky et al., 2012; Venesky et al., 2013 for discussion on selection for increased disease resistance and tolerance).

A population of *Mixophyes fleayi* recovered naturally due to increased adult longevity, which suggests that in this species disease resistance was evolving (Newell et al., 2013). Direct selection for disease resistance in captivity involves exposing frogs to Bd and breeding from survivors or from those that survive for longer—these can be treated with antifungals to avoid mortality (Venesky et al., 2012). Alternatively genetic markers for disease resistance (Savage and Zamudio, 2011) might be used to identify resistant individuals for breeding. In addition, breeding stock should be updated with potentially resistant individuals currently surviving in the wild under natural selection. Similarly, selection for increased reproductive capacity may enable some populations to persist by offsetting chytridiomycosis-induced adult mortality (Muths et al., 2011; Phillott et al., 2013). Selection pressure should be moderate to avoid inbreeding depression for other traits by occasional outbreeding with less resistant or reproductive individuals (Frankham et al., 2011). Finally, in all *ex situ* operations it is important to develop treatments to clear Bd infection for use in emergency situations in the case of a breach in biosecurity and an outbreak of chytridiomycosis in the captive colony.

6.2.8.2 Chemical and heat treatment

Antifungal compounds and heat treatment can be used to reduce or clear Bd infection (Woodhams et al., 2011). Itraconazole is the most commonly used chemical treatment and can clear infection in a range of species (Baitchman and Pessier, 2013). Voriconazole (Martel et al., 2011), chloramphenicol (Young et al., 2012b), and terbinafine hydrochloride (Bowerman et al., 2010) can also clear infection in various species, providing alternatives to itraconazole. Species-specific optimization is needed for chemical treatments because itraconazole use has been associated with toxicity in tadpoles and adults (Baitchman and Pessier, 2013) and may lead to increased infection rates after subsequent Bd exposure (Cashins et al., 2013). Heat treatment offers an inexpensive alternative to chemical treatments (Chatfield and Richards-Zawacki, 2011). Exposure to temperatures from 27 to 37 °C has cleared infection in a variety of species (Baitchman and Pessier, 2013; Geiger et al., 2011; Woodhams et al., 2011), although it was ineffective in other species (Woodhams et al., 2012c). Chemical and heat treatments should be trialled on a small number of individuals to confirm effectiveness and safety for each species. Baitchman and Pessier (2013) provide a detailed review, including dosage rates and exposure times, for chemical and heat treatments. In populations with predictable seasonal die-offs, we suggest collecting and holding amphibians for short course treatment during times of peak burdens to improve survival. Although reducing burdens may increase survival during die-offs, failure to clear infection enables the development of drug resistance by pathogens.

6.2.9 Choosing a strategy

Assessing which management strategies are most suitable for a given species depends on a detailed understanding of Bd dynamics and species ecology. Interventions against Bd should target amphibian life history stages most affected by disease or at high risk of Bd exposure. Ecological surveys are needed to identify outbreaks, ongoing declines, and prioritize high-risk populations (Murray et al., 2011b; Skerratt et al., 2008). We provide an example illustrating how a multifaceted response can be developed to target specific life history stages from the 2 management approaches and 3 action classes (Table 6.1, Fig. 6.4). For most species, a variety of approaches implemented at different spatial scales will be necessary, such as head starting at sites where the environment has been manipulated to decrease Bd suitability (Fig. 6.4). Given the lack of proven effective strategies, all interventions should be implemented within an experimental framework. To optimize progress, research aimed at understanding the mechanisms underlying interventions should occur concurrently with their application.

Figure 6.4. Proposed timeline for management actions for *Pseudophryne corroboree* populations in Kosciuszko National Park, Australia. Management actions need to be aligned with seasonal fluctuations in climatic suitability for *Batrachochytrium dendrobatidis* growth (a and b) and the target species' life history (c).

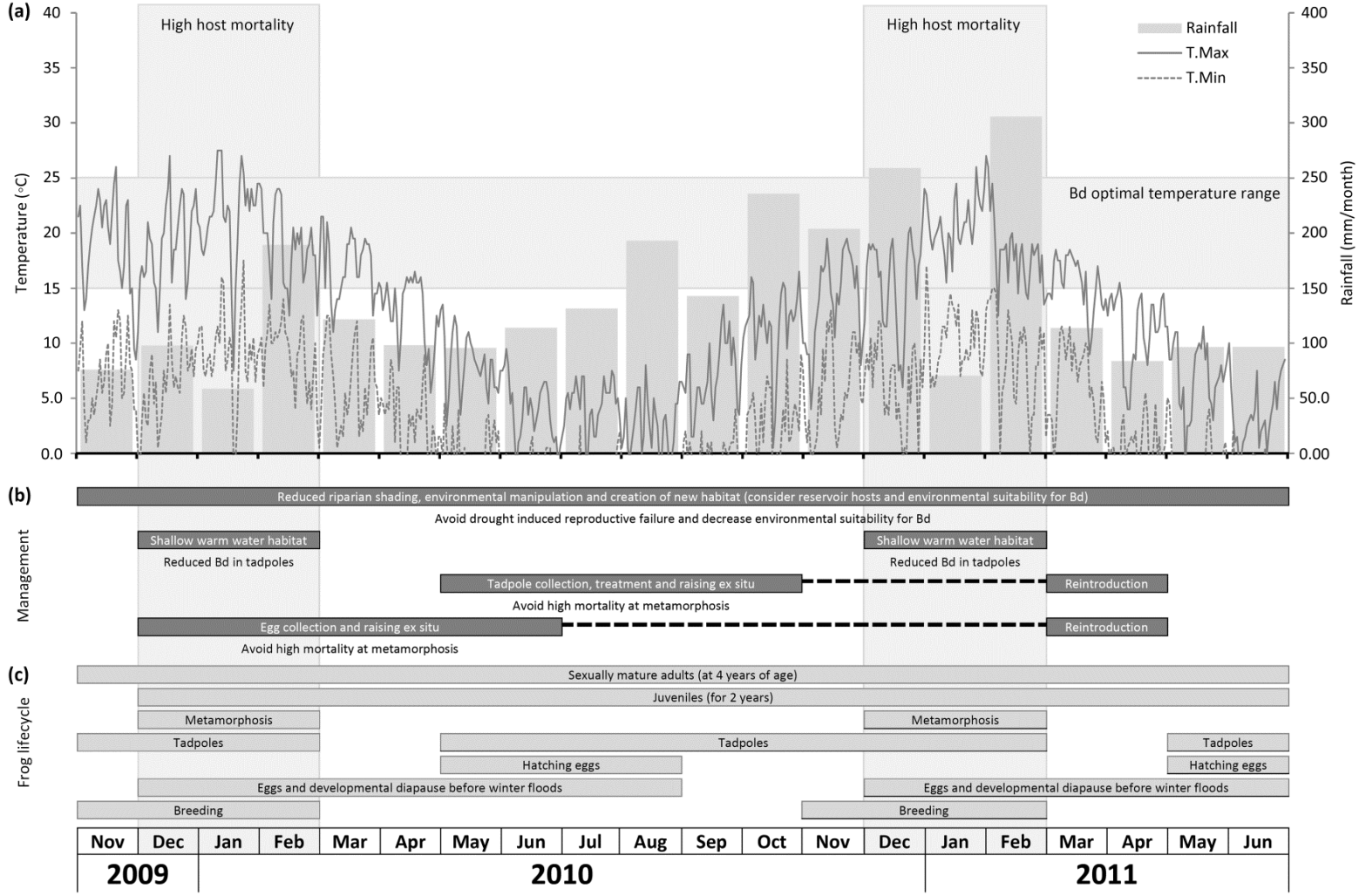

6.2.10 Conclusion

Preserving habitat is not enough to mitigate the effects of novel diseases, which require direct intervention to protect species. More amphibian extinctions are expected in the next decade (Bletz et al., 2013); thus, the consequences of not acting are likely to be more severe than conducting experimental management, such as translocations into natural or created refugia. We suggest testing relatively simple, locally adapted strategies rather than waiting for the invention of a broadly applicable solution to chytridiomycosis. Developing strategies to secure chytridiomycosis threatened species is an achievable challenge and will enable the longer-term goal of species recovery. Managers and conservation biologists in government, universities, zoos, and conservation groups must collaborate closely to identify and undertake research focused on achieving this objective (Mendelson et al., 2006). Coordination of *ex situ* responses under the Amphibian Ark umbrella provides a promising example of collaboration (Zippel et al., 2011). We hope managers and researchers investigate the ideas presented here and develop other complementary strategies. It is imperative that we act now using existing knowledge to establish *in situ* and *ex situ* populations of Bd-threatened amphibian species. Failure to do so will only increase the number of amphibian extinctions caused by chytridiomycosis.

6.2.11 Acknowledgments

We thank R. Speare for helpful discussions on chytridiomycosis management. Comments from 2 anonymous referees greatly improved the article. L.B. and L.G. were supported by Australian Research Council grants FT100100375 and LP110200240.

6.3 PAPER 2: Surveillance for emerging biodiversity diseases of wildlife

This published peer-reviewed paper represents my original review, synthesis and writing. Lee Berger, Karrie Rose, Victoria Grillo, Scott Cashins and Lee Skerratt provided substantial editorial input.

The full reference for the published paper is:
Grogan, L. F., Berger, L., Rose, K., Grillo, V., Cashins, S. D., Skerratt, L. F. (2014) Surveillance for emerging biodiversity diseases of wildlife. PLOS Pathogens 10(5):e1004015.

The following text is a verbatim copy of the manuscript published in the journal PLOS Pathogens. Section, table and figure numbering has been added or reformatted for this thesis for ease of reference. Since the journal uses American English, the spelling follows this convention.

6.3.1 Front matter

Surveillance for Emerging Biodiversity Diseases of Wildlife

Laura F. Grogan[1]*, Lee Berger[1], Karrie Rose[2], Victoria Grillo[3], Scott D. Cashins[1], Lee F. Skerratt[1]

[1] One Health Research Group, School of Public Health, Tropical Medicine and Rehabilitation Sciences, James Cook University, Townsville, Queensland, Australia,
[2] Australian Registry of Wildlife Health, Taronga Conservation Society Australia, Mosman, New South Wales, Australia,
[3] Wildlife Health Australia (formerly Australian Wildlife Health Network), Georges Heights, New South Wales, Australia

* E-mail: laura.grogan@my.jcu.edu.au

6.3.2 Main text

Effective surveillance is crucial for early detection and successful mitigation of emerging diseases (Vrbova et al., 2010). The current global approach to surveillance for wildlife diseases affecting biodiversity ("biodiversity diseases") is still inadequate as demonstrated by the slow characterization and response to the two recent devastating epidemics, chytridiomycosis and white-nose syndrome (Carmichael, 2012; Foley et al., 2011; Kuiken et al., 2011; Skerratt et al., 2007). Current surveillance for wildlife disease usually targets diseases that affect humans or livestock, not those impacting wildlife populations. Barriers to effective surveillance for biodiversity diseases include a relative lack of social and political will and the inherent complexity and cost of implementing surveillance for multiple and diverse free-ranging populations. Here we evaluate these challenges and the inadequacies of current surveillance techniques, and we suggest an integrated approach for effective surveillance.

Despite challenges in quantifying the role of disease in species declines (Smith et al., 2006), there are numerous clear examples of diseases (infectious, toxic, multifactorial, or of undetermined origin) that have caused severe population impacts; for example, avian malaria and poxvirus in Hawaii, diclofenac poisoning in Indian vultures, rinderpest in Africa, bighorn sheep pneumonia, chronic wasting disease, crayfish plague, avian trichomonosis, and Tasmanian devil facial tumor disease (Atkinson and Samuel, 2010; Besser et al., 2013; Cassirer et al., 2013; Chaudhry et al., 2012; Hawkins et al., 2006; Kozubikova et al., 2008; Robinson et al., 2010b; Vogel and Heyne, 1996; Williams, 2005).

The emergence of the amphibian fungal skin disease chytridiomycosis is a pertinent example in which a lack of effective disease surveillance contributed to global biodiversity loss (Fig. 6.5; Gagliardo et al., 2008; Pech et al., 2010; Robbins et al., 1998). Epidemiological investigation did not commence until 15 years after initial declines (Skerratt et al., 2011a). Despite recent listing of chytridiomycosis as a notifiable disease by the World Organization for Animal Health (OIE), the extended time before diagnosis very likely contributed to the decline and extinction of at least 200 species of frogs globally, helping to make amphibians the most endangered vertebrate class (Lips et al., 2006; Skerratt et al., 2007).

Figure 6.5. Chytridiomycosis: a catastrophic biodiversity disease causing amphibian declines. Chytridiomycosis emerged in the 1970s but was not detected until the 1990s. (A) An alpine tree frog (*Litoria verreauxii alpina*) with severe chytridiomycosis, showing skin reddening and an inability to maintain normal upright posture; (B) skin surface of a stony creek frog (formerly *Litoria lesueuri*). Many cells are infected with sporangia, pushing discharge tubes (arrow) to the skin surface (scanning electron micrograph). Scale bar = 10 μm.

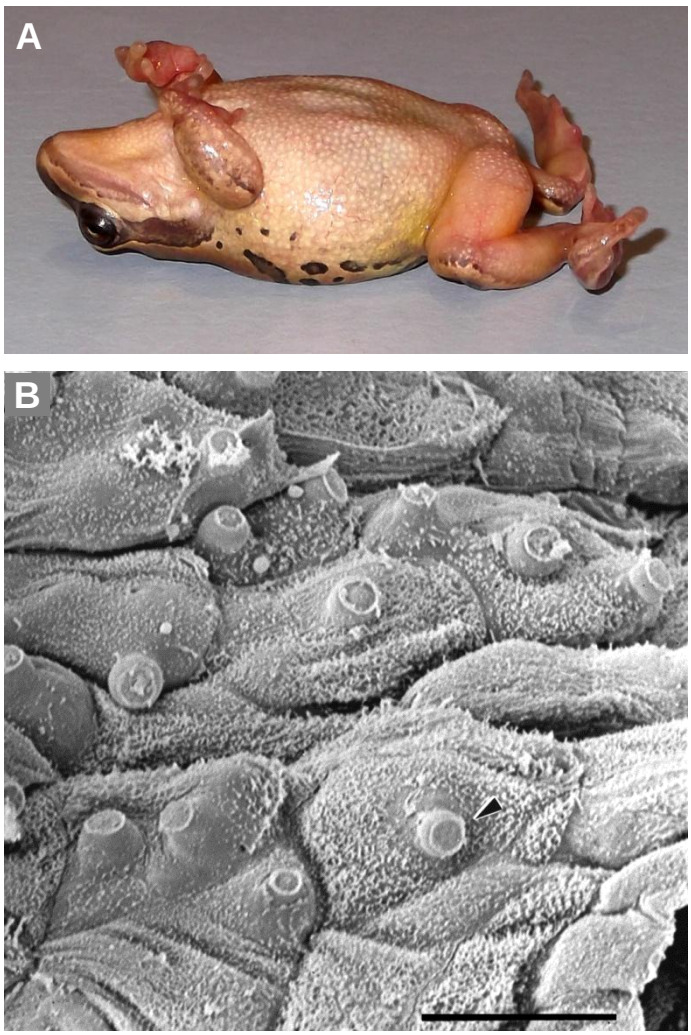

Here we define "biodiversity disease" as "a disease that has caused, or is predicted to cause, a decline in a wild species sufficient to worsen its conservation status." This term can be applied to kingdoms other than Animalia, but those are outside the scope of the current paper. Our aim is to improve wildlife biodiversity disease surveillance, which could have important socioeconomic benefits, including reducing long-term disease management costs, protecting biodiversity and ecosystem services, and contributing to pre-spillover surveillance for public health and agricultural diseases (Aguirre, 2009; Boyles et al., 2011; Childs, 2007; Childs and Gordon, 2009; Chivian and Bernstein, 2008; Jones et al., 2008; Kemere et al., 2000; Morens et

al., 2004; Tambi et al., 1999; Watson et al., 2011; Yule et al., 2013). Preventing disease-linked species extirpation will stabilize ecosystems, curtailing cascades of trophic coextinctions and global biodiversity loss (Aguirre and Tabor, 2008; Daszak, 2000; Maillard and Gonzalez, 2006). Biodiversity and ecosystem stability are also increasingly linked with decreased risk of disease emergence (Chivian and Bernstein, 2008; Keesing et al., 2010; Mills, 2006; Ostfeld, 2009; Pongsiri et al., 2009; Vaz et al., 2007).

Current funding priorities for wildlife health surveillance tend to rely on overlap with human and livestock diseases (Vrbova et al., 2010). Cost-benefit analyses applied to zoonotic and agricultural diseases in funding prioritization models, including, for example, the "willingness to pay" framework based on societal values and the concept of paying for "ecosystem services," typically do not adequately address the consequences of biodiversity loss (Carmichael, 2012; Richardson and Loomis, 2009; Spangenberg and Settele, 2010). Appropriately quantifying the value of biodiversity would assist leveraging more appropriate resource allocation.

Responsibility for wildlife health is often spread across multiple agencies, levels of government, universities, and nongovernment agencies. This fragmentation of accountability may contribute to lower prioritization of biodiversity disease surveillance and control compared with human and livestock health threats, which are managed by specific departments.

To promote effective implementation of surveillance programs, a greater focus on emerging biodiversity diseases is needed in international policy and practice and more support must be given to existing regional wildlife health frameworks, recognizing their crucial role in identifying and managing biodiversity diseases. This recognition should encourage coordination at international, national, and local levels, as well as resourcing on-the-ground surveillance.

Several international bodies concerned with animal health are appropriately situated to take on this coordinating role, and collaborations between bodies such as OIE and the World Conservation Union (IUCN) may provide the necessary transdisciplinary expertise required (Skerratt et al., 2007). The OIE has already taken steps in this direction by listing notifiable and non-notifiable infectious diseases, highlighting current issues through their Working Group on Wildlife Diseases, and developing their "Training Manual on Wildlife Diseases and Surveillance" (OIE, 2010). International coordination can result in rapid disease assessments, prioritization of resources, and targeted response via regional frameworks for wildlife health (for example, the successfully coordinated, multi-agency response to highly pathogenic avian influenza virus, H5N1; Carmichael, 2012).

A number of regional frameworks are already established, while others are new and emerging. With improved funding, regional frameworks for wildlife health will be better equipped to provide direction, facilities, and expertise for surveillance. These centers typically involve collaboration of veterinarians, ecologists, wildlife biologists, microbiologists, and molecular biologists. They require salaries for field staff, epidemiologists, and pathologists; funding for diagnostic testing; and data management systems to collect and analyze surveillance data. Agreement on methodologies, risk assessment pathways, and contingency plans for emerging infectious biodiversity diseases across these regional frameworks will support prompt responses to outbreaks (Jackson et al., 2009).

Current biodiversity disease surveillance is often ad hoc and relies on passive surveillance (data collected from community submissions) or activities that overlap with human and livestock diseases. This approach is unable to elucidate the impact of disease on the population because only the diseased subpopulation is detected, and it is less likely to detect subtle clinical signs or alterations in species fitness, such as reduced fecundity, despite potentially large population impacts (Case, 2000; Duncan et al., 2008; Knowles et al., 2010; Reiner et al., 2009; Ryser-Degiorgis, 2013; Stallknecht, 2007; Thulke et al., 2009; Wobeser, 2007; Young et al., 2012a). Some diseases may also be underrepresented due to the cryptic or noncharismatic nature of the hosts, the remote nature of the location, or apathy or acceptance of consequences once a diagnosis has been reached (Kuiken et al., 2005; Merianos, 2007; Morner et al., 2002; Stallknecht, 2007).

Considering the potential deficiencies of current approaches to detect emerging biodiversity diseases, a new, transdisciplinary, *systematic surveillance* approach is needed. Essential elements of this approach are established in many countries, but are not specifically being utilized to detect biodiversity diseases. The following aspects could be incorporated into this approach:

1. **Combine current strategies** (integrate passive and active or general and targeted techniques with outbreak investigations that characterize emerging pathogens or multifactorial disease pathways to enable implementation of effective control; Kane and Morley, 1999). Surveillance techniques in use for human and domestic animal diseases that may be adapted include:
    a. *Disease-specific screening* for incursions of important pathogens.
    b. Use of *sentinel species* or individuals at *sentinel locations* (such as key wildlife trade sites; Aguirre, 2009; Aguirre and Tabor, 2004; Kuiken et al., 2005). Species could be ranked for use as sentinels by evaluating:

i. *Species value* based on conservation status, taxonomy, ecosystem representation, and phylogenetic uniqueness.
ii. *Sentinel value* based on ecological role (keystone species and predators/scavengers), ease of observation and representative sampling, current level of study, and probability as a disease-emergence host (Halliday et al., 2007).

2. **Target both known and unknown pathogens and hosts and regions predicted to be at high risk for disease emergence through predictive modeling.** Retrospective and risk factor analyses show correlations between the incidence of disease emergence in general and socioeconomic and ecological factors (for example, highly biodiverse developing regions constitute infectious disease emergence hotspots which could be targeted; Daszak, 2009; Jones et al., 2008; Real and Biek, 2007; Taylor et al., 2001). Deterministic models based on general pathogen characteristics and sensitivity analysis, combined with metagenomic studies, hold potential for predicting future disease emergence (Parrish et al., 2008; Pulliam, 2008; Relman, 2013; Stephens et al., 2009).
3. **Ensure spatial and taxonomic representation** to prevent the loss of biodiversity in important taxonomic clades or small regions with high levels of endemism (Vieites et al., 2009).
4. **Focus on multiple biological levels,** such as ecosystems and species (Tompkins et al., 2011).
5. **Integrate essential baseline ecological data collection for an understanding of the *population impact* of disease**. Mark-recapture studies provide long-term data on population dynamics and are appropriate for wildlife population impact assessment, despite imperfect detection (Cooch et al., 2012). Integration of epidemiological transmission models with disease, population, and environmental data will better elucidate the roles of infectious disease, anthropogenic environmental disturbance, and other factors in driving changes in population structure, distribution, or size (Skerratt et al., 2010).
6. **Incorporate *self-evaluative* mechanisms to ensure adaptability and prioritization strategies**. Strategies should evolve as diagnostic and ecological monitoring techniques emerge, and as global circumstances change (Scholes et al., 2008; Thurmond, 2003; Vrbova et al., 2010). Frameworks for structured decision making and prioritization will ensure that surveillance approaches remain cost effective (Carwardine et al., 2012; Joseph et al., 2009).

In conclusion, we suggest that improved integration, capacity, and a systematic approach to disease surveillance in wildlife are imperative for future biodiversity conservation.

6.3.3 Acknowledgments

The authors thank A. Roberts, S. Young, R. Puschendorf, and D. Mendez for helpful comments on the manuscript. LFG and LB were supported by Australian Research Council grants LP110200240 and FT100100375.

CHAPTER 7: Conclusions and recommendations

7.1 Overview of outcomes

The research described in this thesis was driven by concerns for amphibian biodiversity conservation due to the devastating impact of the infectious disease, chytridiomycosis. This thesis represents an extensive body of work undertaken to address key knowledge gaps associated with several critical priorities in this highly applied field. These included 1) the need to understand and characterize the ongoing impact of the fungal pathogen Bd on endemically infected amphibian populations, 2) the need to better understand the host immune response to infection, thereby evaluating possible immunologic management strategies, and 3) the need to update, develop and improve currently available and future interventions and surveillance techniques for chytridiomycosis and emerging wildlife diseases in general.

The outcomes from the work presented in this thesis have advanced understanding of the epidemiology and immunology of chytridiomycosis relating to the following specific areas: the impacts of endemic chytridiomycosis, the underlying dynamics of infection transmission and pathogen distribution, the feasibility of immunization via prior exposure and treatment, the potential for the evolution of resistance to chytridiomycosis in the field and underlying host immune mechanisms as potential targets for marker-assisted selection, the management options currently available for mitigating chytridiomycosis, and a systematic surveillance approach for emerging diseases affecting biodiversity.

7.2 Dynamics of chytridiomycosis in the field

Detailed analysis of an intensive mark-recapture field study enabled investigation of the impact of Bd on endemically infected common mist frog (*Litoria rheocola*) populations in the Australian wet tropics, despite the common difficulties in detecting disease impacts in remote areas, and the absence of observed mass mortalities. I performed Cormack-Jolly-Seber and Pradel analysis and found that endemic chytridiomycosis continues to have substantial seasonally fluctuating population-level effects on amphibian survival which necessitates increased recruitment for population persistence.

These results highlight the continued impact of chytridiomycosis despite endemism. Although some anuran species and populations appear to be recovering from the initial disease threat, it is highly probable that endemic Bd is still contributing to population declines of many of our threatened species, particularly those declining in pristine environments (such as the southern corroboree frog, *Pseudophryne corroboree*, in the Australian alps; Hunter et al., 2010).

Disease constitutes an additional threat to many already vulnerable species, alongside the other major threatening processes including habitat loss, introduced pests and predators, pesticides and toxins, and climate change (Blaustein and Kiesecker, 2002). Chytridiomycosis will be an important consideration for continued amphibian management in Australia however it poses a unique plethora of problems for amphibian and general biodiversity conservation as it has thus far proven difficult to mitigate in the field. Vulnerable populations will benefit from further research to characterize the exact nature of chytridiomycosis impact on a system by system basis in order to prioritize and apply efficacious management techniques.

The additional Multi-state mark recapture analysis allowed investigation of population and disease dynamics at the level of the individual frog, and identified pathogen aggregation (the presence of an underlying highly positively skewed infection distribution within the population) as an important and previously overlooked feature of endemic Bd infections. Pathogen aggregation has critical implications for the study, modeling and management of chytridiomycosis. Overlooking non-random pathogen distributions in infectious diseases may lead to inappropriate and sometimes paradoxical interpretations of disease dynamics. This work highlighted the requirement for more comparable reporting measures for evaluating trends between studies, particularly the need for quantitative infectious burden data in addition to infection prevalence measures. Future research to elucidate the predominant causes of pathogen aggregation will indicate whether other disease control interventions should be targeted towards improving host resistance or reducing exposure.

The examination of the abundance, distribution and transmission of Bd between hosts revealed novel information about the dynamics underlying endemically infected populations. I found that more infections occurred in cooler months, that recoveries were frequent throughout the year, and that survival probabilities were dependent on infection intensity. These findings improved our understanding of the epidemiologic drivers of population infections, and suggest in particular the increased utilization of environmental manipulation strategies that favour host recoveries by rendering the environment less suitable for Bd.

7.3 Amphibian host immune response to chytridiomycosis

I performed two large clinical exposure trials in amphibians that allowed for a rigorous examination of host responses to chytridiomycosis in a controlled environment, hence eliminating many confounders that are often present in observational field studies.

In the adaptive immunity study I was unable to demonstrate differences in survival and infection intensity (in booroolongs frogs, *Litoria booroolongensis*) indicative of clinically

protective host adaptive immunity despite sufficient study power and promising pilot results. This finding provides clear evidence that current techniques for immunization via prior exposure and treatment will unlikely be an effective strategy for managing susceptible captive and reintroduced amphibians. Recently published studies have corroborated this finding with the discovery of Bd secreted immunosuppressive factors that inhibit the adaptive immune response *in vitro* (Fites et al., 2013).

Apparently contrasting results from another recent study (McMahon et al., 2014) indicated only very mild improvement in survival after numerous prior exposures, reinforcing our conclusion that the adaptive immune response is not clearly protective, and that immunization is likely to be ineffective and impractical in the short term for managing amphibians threatened by chytridiomycosis. With sufficient funding and future research, however, it is possible that an immunization strategy may be developed to provide a more consistent and protective host adaptive immune response.

It is important to note, however, that the longevity of many amphibian species is relatively short, and that the immunization technique does not provide heritable resistance, limiting the feasibility and long-term sustainability of this approach for use in mitigating the effects of chytridiomycosis in the field. This consideration promotes a shift towards focusing on longer-term evolutionary management strategies such as assisted selection for disease resistance.

The large clinical innate immunity trial examined differences in population and clutch responses of the alpine tree frog (*Litoria verreauxii alpina*) to Bd infection depending on long-term Bd exposure history in order to investigate the potential evolution of resistance that may have occurred over multiple generations in the field, and any underlying mechanisms. The results of this experiment revealed variation in susceptibility to disease (survival rates and infection intensities) that was consistent with the evolution of resistance in at least one of the three long-exposed populations examined. Marked differences between clutch survival results within some populations (despite a blinded and randomized block experimental design) further emphasized the likely presence of heritable immune mechanisms contributing to a more resistant phenotype.

These results demonstrate differences in susceptibility between populations and clutches associated with long-term population exposure history that are consistent with selection for disease resistance. This corroborates the potential for the evolution of resistance and is promising for the future utilization of marker-assisted selection for captive breeding and release programs. With sufficient time and conducive conditions, wild amphibians may also develop

some degree of immunologic resistance in the field, provided that their populations remain at a viable size for sufficient genetic diversity.

The high level of overall mortality within the experiment suggests that any selection for resistance has been relatively weak as the species is still highly susceptible to chytridiomycosis. Thus any observed increase in population resilience in the wild may be due to evolution of other factors. This work highlights that features of the natural history of amphibian species (such as a lack of Bd-exposure, and high survival until after the first breeding season), may limit opportunities for natural selection to occur. Artificial promotion of disease resistance through assisted selection may help counter this problem. Thus continued intensive management of Bd-threatened wild amphibian populations is still essential to ensure their long-term persistence.

The non-targeted systems biology molecular analyses (transcriptomics and metabolomics) provided considerable data on the mechanisms underlying the observed clinical response to Bd infection comparing both populations of alpine tree frogs (*L. v. alpina*) and sampling times post exposure.

In the analysis of subclinical differential gene expression I found marked evidence for immune-associated gene pathway activation in Bd-infected frogs which may explain population-level differences observed in the large survival experiment. In combination with a non-significant trend of lower infection intensities from four days post exposure and consistent gene clustering trends, individuals from the longest-surviving population (data from the survival experiment) also demonstrated a larger complement of differentially expressed immune-associated genes when compared with frogs from two more susceptible populations. These immune-associated genes included major representatives of both the innate and adaptive immune systems, and were predominantly up-regulated or had a pro-inflammatory effect at the site of infection (skin) at four days post exposure, consistent with the activation of a robust early innate and adaptive immune response. This was the first study to identify underlying immune mechanisms at the early subclinical stage of infection that may be related to evolved resistance to Bd.

With regards to the observed high overall susceptibility of *L. v. alpina* frogs in the clinical experiment, my results indicate that the host immune response even in the longest surviving population was still insufficient in preventing development of chytridiomycosis. Indeed, I observed evidence for modulation of host T cell responses consistent with the current evidence for Bd-secreted immunosuppressive factors affecting lymphocytes (Fites et al., 2013).

These results also highlighted the potentially confounding effects of immunopathology (a dysregulated and damaging immune response), and possible responses to secondary bacterial infections that often co-occur in late-stage chytridiomycosis (Berger, 2001; Berger et al., 1998; Ellison et al., 2014). Immune dysregulation was most severe at the late subclinical time point (14 days post exposure) and in the most susceptible population, suggesting a poor association with survival and infection intensity trends. Thus it will be crucial in future studies to concurrently examine clinical evidence of survival and infection intensity with gene expression results over the temporal course of infection. I particularly recommend that further studies focus more on the early immune response.

In the non-targeted metabolomics analysis I identified metabolic perturbations related to physiological changes associated with time since exposure and variations in population response to chytridiomycosis. I identified several key metabolites that were predominantly responsible for these perturbations, and investigated their associated pathways and implications for the host response to Bd infection. This was the first study to identify metabolic changes in the skin and liver associated with chytridiomycosis. The results from this analysis help build our understanding of the key mechanisms and pathways involved in immunity and the pathogenesis of chytridiomycosis.

Importantly, however, as small molecule metabolites form some of the end products of tissue metabolic processes, any perturbations in their expression need to be considered in the light of the multiple possible pathways (from amphibian host, Bd and possible secondary bacterial infections) from which they may be derived (Tan et al., 2009). Further studies may help elucidate similarities in the metabolic profiles of infected frogs, improving our ability to determine proximate sources of resultant metabolites and functional relationships with gene and protein expression.

7.4 Managing wildlife disease

In a review of management strategies for endemic chytridiomycosis I developed a conceptual framework to assist wildlife managers to identify system-appropriate immediate interventions for promoting amphibian population persistence in the field. Two main approaches were discussed including 1) reducing Bd in the environment or on amphibians, and 2) increasing the capacity of populations to persist despite increased mortality from disease. A key aspect of these approaches involved considering the specific host, pathogen and environmental factors that interact and contribute to promoting the manifestation of disease. For example, by considering in detail the host life-stage and temporal season with greatest vulnerability to Bd infection, specific management strategies such as head-starting, and environmental manipulation may be

undertaken to greater effect. This approach is already being utilized in select populations of the declining southern corroboree frog (*Pseudophryne corroboree*), with reasonable success (pers. comm. D. Hunter, B. Scheele). I recommend further experimental trials and research into several highly-promising management techniques including habitat manipulation, antifungal treatments, animal translocation, bioaugmentation, head starting and selection for resistance.

Finally, I reviewed and evaluated the efficacy of current disease surveillance approaches in order to help improve timely mitigation of future emerging diseases affecting biodiversity. Effective surveillance is the keystone for early detection of emerging infectious diseases, and an important component of successful mitigation. I identified a number of barriers and to effective surveillance and synthesized recommendations to address these challenges including 1) extending global animal disease surveillance systems to emphasize diseases that could predominantly affect biodiversity, and 2) utilizing a systematic, population-based and self-evaluative approach to improve timely disease recognition and management, with the aim of reducing species loss. These strategies will benefit numerous stakeholders in the field of wildlife disease and conservation including government departments, non-government organisations, community groups, researchers and the public.

7.5 Conclusion

The epidemiology and pathogenesis of the devastating multiple host amphibian skin disease chytridiomycosis have been demonstrated to be highly complex and multifactorial. Although a considerable research effort has been employed thus far to characterize the impact, dynamics and host immune response to infection with the fungal pathogen *Batrachochytrium dendrobatidis* (Bd), much still remains to be understood. The sustainable long-term management of Bd-threatened wild amphibian populations will rely on transdisciplinary collaborations, as well as further research into, and experimental application of promising upcoming management techniques.

In summary of this thesis, I found that endemic chytridiomycosis continues to impact amphibian population dynamics in Australia and is characterized by seasonal mortality and pathogen aggregation. I found that immunization is currently an ineffective strategy. However, from clinical and systems biology results, the evolution of innate immunity is possible and hence assisted selection may be a viable management strategy into the future, among other approaches.

LITERATURE CITED IN THIS THESIS

Adiba, S., Nizak, C., van Baalen, M., Denamur, E. & Depaulis, F. (2010) From Grazing Resistance to Pathogenesis: The Coincidental Evolution of Virulence Factors. Plos One, **5**: 10.

Agnandji, S. T., Fendel, R., Mestre, M., Janssens, M., Vekemans, J., Held, J., Gnansounou, F., Haertle, S., von Glasenapp, I., Oyakhirome, S., Mewono, L., Moris, P., Lievens, M., Demoitie, M.-A., Dubois, P. M., Villafana, T., Jongert, E., Olivier, A., Cohen, J., Esen, M., Kremsner, P. G., Lell, B. & Mordmueller, B. (2011) Induction of *Plasmodium falciparum*-Specific CD4(+) T Cells and memory B Cells in Gabonese children vaccinated with RTS,S/AS01(E) and RTS,S/AS02(D). Plos One, **6**: e18559.

Aguirre, A. A. (2009) Wild canids as sentinels of ecological health: a conservation medicine perspective. Parasit Vectors, **2 (Suppl 1)**: S7.

Aguirre, A. A. & Tabor, G. M. (2004) Introduction: Marine vertebrates as sentinels of marine ecosystem health. EcoHealth, **1**: 236-238.

Aguirre, A. A. & Tabor, G. M. (2008) Global factors driving emerging infectious diseases impact on wildlife populations. Ann N Y Acad Sci, **1149**: 1-3.

Air, G. M. (1976) Amino-acid sequences from gene F (capsid) protein of bacteriophage-phiX174. Journal of Molecular Biology, **107**: 433-443.

Akaike, H. (1973) Information Theory and an Extension of the Maximum Likelihood Principle. In: Petrov, B. N. & Csaki, F. (Eds.) *Second International Symposium on Information Theory.* Budapest, Akademiai Kiado.

Alizon, S., Hurford, A., Mideo, N. & Van Baalen, M. (2009) Virulence evolution and the trade-off hypothesis: history, current state of affairs and the future. Journal of Evolutionary Biology, **22**: 245-259.

Aljanabi, S. M. & Martinez, I. (1997) Universal and rapid salt-extraction of high quality genomic DNA for PCR-based techniques. Nucleic Acids Research, **25**: 4692-4693.

Altizer, S., Dobson, A., Hosseini, P., Hudson, P., Pascual, M. & Rohani, P. (2006) Seasonality and the dynamics of infectious diseases. Ecology Letters, **9**: 467-484.

Altschul, S. F., Madden, T. L., Schaffer, A. A., Zhang, J. H., Zhang, Z., Miller, W. & Lipman, D. J. (1997) Gapped BLAST and PSI-BLAST: a new generation of protein database search programs. Nucleic Acids Research, **25**: 3389-3402.

Anderson, D. R. & Burnham, K. P. (2002) Avoiding pitfalls when using information-theoretic methods. Journal of Wildlife Management, **66**: 912-918.

Anderson, D. R., Burnham, K. P., Gould, W. R. & Cherry, S. (2001) Concerns about finding effects that are actually spurious. Wildlife Society Bulletin, **29**: 311-316.

Anderson, R. M. & May, R. M. (1981) The population dynamics of microparasites and their invertebrate hosts. Philosophical Transactions of the Royal Society B-Biological Sciences, **291**: 451-524.

Andre, J.-B. & Day, T. (2005) The effect of disease life history on the evolutionary emergence of novel pathogens. Proceedings of the Royal Society B: Biological Sciences, **272**: 1949-1956.

Andre, S. E., Parker, J. & Briggs, C. J. (2008) Effect of temperature on host response to *Batrachochytrium dendrobatidis* infection in the mountain yellow-legged frog (*Rana muscosa*). Journal of Wildlife Diseases, **44**: 716-720.

Anil, S. & Samaranayake, L. P. (2002) Impact of lysozyme and lactoferrin on oral Candida isolates exposed to polyene antimycotics and fluconazole. Oral Diseases, **8**: 199-206.

Annis, S. L., Dastoor, F. P., Ziel, H., Daszak, P. & Longcore, J. E. (2004) A DNA-based assay identifies *Batrachochytrium dendrobatidis* in amphibians. Journal of Wildlife Diseases, **40**: 420-428.

Antao, T., Lopes, A., Lopes, R. J., Beja-Pereira, A. & Luikart, G. (2008) LOSITAN: A workbench to detect molecular adaptation based on a F(st)-outlier method. Bmc Bioinformatics, **9**.

Araki, H., Cooper, B. & Blouin, M. S. (2007) Genetic effects of captive breeding cause a rapid, cumulative fitness decline in the wild. Science, **318**: 100-103.

Atkinson, C. T. & Samuel, M. D. (2010) Avian malaria *Plasmodium relictum* in native Hawaiian forest birds: epizootiology and demographic impacts on 'apapane *Himatione sanguinea*. Journal of Avian Biology, **41**: 357-366.

Austin, R. M. (2000) Chapter 25 Cutaneous microbial flora and antibiosis in *Plethodon ventralis* - Inferences for parental care in the Plethodontidae. In: Bruce, R. C., Jaeger, R. G. & Houck, L. D. (Eds.) *The biology of plethodontid salamanders.* New York, Kluwer Academic/Plenum Publishers.

Baitchman, E. J. & Pessier, A. P. (2013) Pathogenesis, diagnosis, and treatment of amphibian chytridiomycosis. Veterinary Clinics of North America Exotic Animal Practice, **16**: 669-85.

Balvanera, P., Pfisterer, A. B., Buchmann, N., He, J. S., Nakashizuka, T., Raffaelli, D. & Schmid, B. (2006) Quantifying the evidence for biodiversity effects on ecosystem functioning and services. Ecology Letters, **9**: 1146-1156.

Barnosky, A. D., Matzke, N., Tomiya, S., Wogan, G. O. U., Swartz, B., Quental, T. B., Marshall, C., McGuire, J. L., Lindsey, E. L., Maguire, K. C., Mersey, B. & Ferrer, E. A. (2011) Has the Earth's sixth mass extinction already arrived? Nature, **471**: 51-57.

Barribeau, S. M., Villinger, J. & Waldman, B. (2008) Major Histocompatibility Complex Based Resistance to a Common Bacterial Pathogen of Amphibians. PLoS One, **3**: Article No.: e2692.

Bataille, A., Fong, J. J., Cha, M., Wogan, G. O. U., Baek, H. J., Lee, H., Min, M.-S. & Waldman, B. (2013) Genetic evidence for a high diversity and wide distribution of endemic strains of the pathogenic chytrid fungus *Batrachochytrium dendrobatidis* in wild Asian amphibians. Molecular Ecology, **22**: 4196-4209.

Beard, K. H. & O'Neill, E. M. (2005) Infection of an invasive frog *Eleutherodactylus coqui* by the chytrid fungus *Batrachochytrium dendrobatidis* in Hawaii. Biological Conservation, **126**: 591-595.

Beaumont, M. A. & Nichols, R. A. (1996) Evaluating loci for use in the genetic analysis of population structure. Proceedings of the Royal Society B-Biological Sciences, **263**: 1619-1626.

Becker, C. G., Rodriguez, D., Longo, A. V., Talaba, A. L. & Zamudio, K. R. (2012) Disease risk in temperate amphibian populations is higher at closed-canopy sites. Plos One, **7**: 7.

Becker, M. H., Brucker, R. M., Schwantes, C. R., Harris, R. N. & Minbiole, K. P. C. (2009) The bacterially produced metabolite violacein is associated with survival of amphibians infected with a lethal fungus. Applied and Environmental Microbiology, **75**: 6635-6638.

Becker, M. H. & Harris, R. N. (2010) Cutaneous bacteria of the redback salamander prevent morbidity associated with a lethal disease. Plos One, **5**: 6.

Becker, M. H., Harris, R. N., Minbiole, K. P. C., Schwantes, C. R., Rollins-Smith, L. A., Reinert, L. K., Brucker, R. M., Domangue, R. J. & Gratwicke, B. (2011) Towards a better understanding of the use of probiotics for preventing chytridiomycosis in Panamanian golden frogs. Ecohealth, **8**: 501-506.

Beeton, N. & McCallum, H. (2011) Models predict that culling is not a feasible strategy to prevent extinction of Tasmanian devils from facial tumour disease. Journal of Applied Ecology, **48**: 1315-1323.

Beiswenger, R. E. (1977) Diel patterns of aggregative behavior in tadpoles of *Bufo americanus*, in relation to light and temperature. Ecology, **58**: 98-108.

Bell, S. C., Alford, R. A., Garland, S., Padilla, G. & Thomas, A. D. (2013) Screening bacterial metabolites for inhibitory effects against *Batrachochytrium dendrobatidis* using a spectrophotometric assay. Diseases of Aquatic Organisms, **103**: 77-+.

Berger, L. (2001) Diseases in Australian Frogs. Townsville, James Cook University.

Berger, L., Hyatt, A. D., Olsen, V., Hengstberger, S. G., Boyle, D., Marantelli, G., Humphreys, K. & Longcore, J. E. (2002) Production of polyclonal antibodies to *Batrachochytrium dendrobatidis* and their use in an immunoperoxidase test for chytridiomycosis in amphibians. Diseases of Aquatic Organisms, **48**: 213-220.

Berger, L., Hyatt, A. D., Speare, R. & Longcore, J. E. (2005a) Life cycle stages of the amphibian chytrid *Batrachochytrium dendrobatidis*. Diseases of Aquatic Organisms, **68**: 51-63.

Berger, L., Longcore, J. E., Speare, R., Hyatt, A. & Skerratt, L. F. (2009a) Fungal Diseases in Amphibians. In: Heatwole, H. & Wilkinson, J. (Eds.) *Amphibian biology, Volume 8 Amphibian Decline: Disease, Parasites, Maladies, and Pollution.* NSW, Surrey Beatty & Sons.

Berger, L., Marantelli, G., Skerratt, L. L. & Speare, R. (2005b) Virulence of the amphibian chytrid fungus *Batrachochytrium dendrobatidis* varies with the strain. Diseases of Aquatic Organisms, **68**: 47-50.

Berger, L. & Skerratt, L. (2012) Disease Strategy Chytridiomycosis (Infection with *Batrachochytrium dendrobatidis*) Version 1, 2012. Department of Sustainability, Environment, Water, Populations and Communities, Public Affairs, Commonwealth of Australia, Canberra. Available at http://www.environment.gov.au/system/files/resources/387d3e66-3cdc-4676-8fed-759328277da4/files/chytrid-fungus-manual.pdf>.

Berger, L., Speare, R., Daszak, P., Green, D. E., Cunningham, A. A., Goggin, C. L., Slocombe, R., Ragan, M. A., Hyatt, A. D., McDonald, K. R., Hines, H. B., Lips, K. R., Marantelli, G. & Parkes, H. (1998) Chytridiomycosis causes amphibian mortality associated with population declines in the rain forests of Australia and Central America. Proc Natl Acad Sci U S A, **95**: 9031-9036.

Berger, L., Speare, R., Hines, H. B., Marantelli, G., Hyatt, A. D., McDonald, K. R., Skerratt, L. F., Olsen, V., Clarke, J. M., Gillespie, G., Mahony, M., Sheppard, N., Williams, C. & Tyler, M. J. (2004) Effect of season and temperature on mortality in amphibians due to chytridiomycosis. Australian Veterinary Journal, **82**: 434-439.

Berger, L., Speare, R. & Hyatt, A. D. (1999a) Chytrid fungi and amphibian declines: overview, implications and future directions. In: Campbell, A. (Eds.) *Declines and disappearances of Australian frogs.* Canberra, Environment Australia.

Berger, L., Speare, R. & Kent, A. (1999b) Diagnosis of chytridiomycosis in amphibians by histologic examination. Zoos Print J, **15**: 184-190.

Berger, L., Speare, R., Marantelli, G. & Skerratt, L. F. (2009b) A zoospore inhibition technique to evaluate the activity of antifungal compounds against *Batrachochytrium dendrobatidis* and unsuccessful treatment of experimentally infected green tree frogs (*Litoria caerulea*) by fluconazole and benzalkonium chloride. Research in Veterinary Science, **87**: 106-110.

Berger, L., Speare, R., Pessier, A., Voyles, J. & Skerratt, L. F. (2010) Treatment of chytridiomycosis requires urgent clinical trials. Diseases of Aquatic Organisms, **92**: 165-174.

Berger, L., Speare, R. & Skerratt, L. F. (2005c) Distribution of *Batrachochytrium dendrobatidis* and pathology in the skin of green tree frogs *Litoria caerulea* with severe chytridiomycosis. Diseases of Aquatic Organisms, **68**: 65-70.

Bernatchez, L. & Landry, C. (2003) MHC studies in nonmodel vertebrates: what have we learned about natural selection in 15 years? Journal of Evolutionary Biology, **16**: 363-377.

Besser, T. E., Cassirer, E. F., Highland, M. A., Wolff, P., Justice-Allen, A., Mansfield, K., Davis, M. A. & Foreyt, W. (2013) Bighorn sheep pneumonia: Sorting out the cause of a polymicrobial disease. Preventive Veterinary Medicine, **108**: 85-93.

Blaustein, A. R. & Kiesecker, J. M. (2002) Complexity in conservation: lessons from the global decline of amphibian populations. Ecology Letters, **5**: 597-608.

Blaustein, A. R., Romansic, J. M., Scheessele, E. A., Han, B. A., Pessier, A. P. & Longcore, J. E. (2005) Interspecific variation in susceptibility of frog tadpoles to the pathogenic fungus *Batrachochytrium dendrobatidis*. Conservation Biology, **19**: 1460-1468.

Bletz, M. C., Loudon, A. H., Becker, M. H., Bell, S. C., Woodhams, D. C., Minbiole, K. P. C. & Harris, R. N. (2013) Mitigating amphibian chytridiomycosis with bioaugmentation: characteristics of effective probiotics and strategies for their selection and use. Ecology Letters, **16**: 807-820.

Bo, Y., Jin, C. Y., Liu, Y. M., Yu, W. J. & Kang, H. Z. (2014) Metabolomic analysis on the toxicological effects of TiO2 nanoparticles in mouse fibroblast cells: from the perspective of perturbations in amino acid metabolism. Toxicology Mechanisms and Methods, **24**: 461-469.

Bolger, A. M., Lohse, M. & Usadel, B. (2014) Trimmomatic: a flexible trimmer for Illumina sequence data. Bioinformatics, **30**: 2114-2120.

Bolker, B. M., Brooks, M. E., Clark, C. J., Geange, S. W., Poulsen, J. R., Stevens, M. H. H. & White, J.-S. S. (2009) Generalized linear mixed models: a practical guide for ecology and evolution. Trends in Ecology & Evolution, **24**: 127-135.

Bonneaud, C., Balenger, S. L., Russell, A. F., Zhang, J. W., Hill, G. E. & Edwards, S. V. (2011) Rapid evolution of disease resistance is accompanied by functional changes in gene expression in a wild bird. Proceedings of the National Academy of Sciences of the United States of America, **108**: 7866-7871.

Bonneaud, C., Balenger, S. L., Zhang, J. W., Edwards, S. V. & Hill, G. E. (2012) Innate immunity and the evolution of resistance to an emerging infectious disease in a wild bird. Molecular Ecology, **21**: 2628-2639.

Bonner, S. J., Morgan, B. J. T. & King, R. (2010) Continuous covariates in mark-recapture-recovery analysis: a comparison of methods. Biometrics, **66**: 1256-1265.

Bonner, S. J. & Schwarz, C. J. (2006) An extension of the Cormack-Jolly-Seber model for continuous covariates with application to *Microtus pennsylvanicus*. Biometrics, **62**: 142-149.

Bonner, S. J., Thomson, D. & Schwarz, C. J. (2009) Time-varying covariates and semi-parametric regression in capture-recapture: an adaptive spline approach. In: Thomson, D. L., Cooch, E. G. & Conroy, M. J. (Eds.) *Modeling demographic processes in marked populations.* Berlin, Springer.

Bordoli, L., Kiefer, F., Arnold, K., Benkert, P., Battey, J. & Schwede, T. (2009) Protein structure homology modeling using SWISS-MODEL workspace. Nature Protocols, **4**: 1-13.

Bosch, J. & Martinez-Solano, I. (2006) Chytrid fungus infection related to unusual mortalities of *Salamandra salamandra* and *Bufo bufo* in the Penalara Natural Park, Spain. Oryx, **40**: 84-89.

Bosch, J., Martinez-Solano, I. & Garcia-Paris, M. (2001) Evidence of a chytrid fungus infection involved in the decline of the common midwife toad (*Alytes obstetricans*) in protected areas of central Spain. Biological Conservation, **97**: 331-337.

Bowerman, J., Rombough, C., Weinstock, S. R. & Padgett-Flohr, G. E. (2010) Terbinafine hydrochloride in ethanol effectively clears *Batrachochytrium dendrobatidis* in amphibians. Journal of Herpetological Medicine and Surgery, **20**: 24-28.

Boyle, D. G., Boyle, D. B., Olsen, V., Morgan, J. A. T. & Hyatt, A. D. (2004) Rapid quantitative detection of chytridiomycosis (*Batrachochytrium dendrobatidis*) in amphibian samples using real-time Taqman PCR assay. Diseases of Aquatic Organisms, **60**: 141-148.

Boyles, J. G., Cryan, P. M., McCracken, G. F. & Kunz, T. H. (2011) Economic importance of bats in agriculture. Science, **332**: 41-42.

Boyles, J. G. & Willis, C. K. R. (2010) Could localized warm areas inside cold caves reduce mortality of hibernating bats affected by white-nose syndrome? Frontiers in Ecology and the Environment, **8**: 92-98.

Bradbury, J. (2009) Does frog body temperature affect chytridiomycosis? Frontiers in Ecology and the Environment, **7**: 513-513.

Brannelly, L. A., Richards-Zawacki, C. L. & Pessier, A. P. (2012) Clinical trials with itraconazole as a treatment for chytrid fungal infections in amphibians. Diseases of Aquatic Organisms, **101**: 95-104.

Briggs, C. J., Knapp, R. A. & Vredenburg, V. T. (2010) Enzootic and epizootic dynamics of the chytrid fungal pathogen of amphibians. Proceedings of the National Academy of Sciences of the United States of America, **107**: 9695-9700.

Brown, C. T., Howe, A., Zhang, Q., Pyrkosz, A. B. & Brom, T. H. (2012) A reference-free algorithm for computational normalization of shotgun sequencing data. arXiv e-print: 1203.4802v2 [q-bio.GN].

Browne, W. J., Subramanian, S. V., Jones, K. & Goldstein, H. (2005) Variance partitioning in multilevel logistic models that exhibit overdispersion. Journal of the Royal Statistical Society Series a-Statistics in Society, **168**: 599-613.

Brunner, J. L. & Collins, J. P. (2009) Testing assumptions of the trade-off theory of the evolution of parasite virulence. Evolutionary Ecology Research, **11**: 1169-1188.

Buck, J. C., Truong, L. & Blaustein, A. R. (2011) Predation by zooplankton on *Batrachochytrium dendrobatidis*: biological control of the deadly amphibian chytrid fungus? Biodiversity and Conservation, **20**: 3549-3553.

Bureau of Meteorology (2008) SILO climate data, Australian Bureau of Meteorology.

Burnham, K. P. & Anderson, D. R. (2002) Model selection and multi-model inference: a practical information-theoretic approach, Fort Collins, Springer.

Burnham, K. P. & Anderson, D. R. (2004) Multimodel inference - understanding AIC and BIC in model selection. Sociological Methods & Research, **33**: 261-304.

Burnham, K. P., Anderson, D. R. & Huyvaert, K. P. (2011) AIC model selection and multimodel inference in behavioral ecology: some background, observations, and comparisons. Behavioral Ecology and Sociobiology, **65**: 23-35.

Bustamante, H. M., Livo, L. J. & Carey, C. (2010) Effects of temperature and hydric environment on survival of the Panamanian Golden Frog infected with a pathogenic chytrid fungus. Integrative Zoology, **5**: 143-153.

Carey, C., Bruzgul, J. E., Livo, L. J., Walling, M. L., Kuehl, K. A., Dixon, B. F., Pessier, A. P., Alford, R. A. & Rogers, K. B. (2006) Experimental exposures of boreal toads (*Bufo boreas*) to a pathogenic chytrid fungus (*Batrachochytrium dendrobatidis*). Ecohealth, **3**: 5-21.

Carmichael, C. (2012) Coordinating an effective response to wildlife diseases. Wildl Soc Bull, **36**: 204-206.

Carrillo-Farga, J., Castell, A., Perez, A. & Rondan, A. (1990) Langerhans-like cells in amphibian epidermis. Journal of Anatomy, **172**: 39-45.

Carwardine, J., O'Connor, T., Legge, S., Mackey, B., Possingham, H. P. & Martin, T. G. (2012) Prioritizing threat management for biodiversity conservation. Conservation Letters, **5**: 196-204.

Case, T. J. (2000) An Illustrated Guide to Theoretical Ecology, New York, Oxford University Press.

Cashins, S. D., Grogan, L. F., McFadden, M., Hunter, D., Harlow, P. S., Berger, L. & Skerratt, L. F. (2013) Prior infection does not improve survival against the amphibian disease chytridiomycosis. Plos One, **8**: 7.

Cassirer, E. F., Plowright, R. K., Manlove, K. R., Cross, P. C., Dobson, A. P., Potter, K. A. & Hudson, P. J. (2013) Spatio-temporal dynamics of pneumonia in bighorn sheep. Journal of Animal Ecology, **82**: 518-528.

Cassone, A. (2008) Fungal vaccines: real progress from real challenges. Lancet Infectious Diseases, **8**: 114-124.

Chai, L. Y. A., Kullberg, B. J., Vonk, A. G., Warris, A., Cambi, A., Latge, J.-P., Joosten, L. A. B., van der Meer, J. W. M. & Netea, M. G. (2009) Modulation of toll-like receptor 2 (TLR2) and TLR4 responses by *Aspergillus fumigatus*. Infection and Immunity, **77**: 2184-2192.

Chapuis, M.-P. & Estoup, A. (2007) Microsatellite null alleles and estimation of population differentiation. Molecular Biology and Evolution, **24**: 621-631.

Chatfield, M. W. H. & Richards-Zawacki, C. L. (2011) Elevated temperature as a treatment for *Batrachochytrium dendrobatidis* infection in captive frogs. Diseases of Aquatic Organisms, **94**: 235-238.

Chaudhry, M. J. I., Ogada, D. L., Malik, R. N., Virani, M. Z. & Giovanni, M. D. (2012) First evidence that populations of the critically endangered Long-billed Vulture *Gyps indicus* in Pakistan have increased following the ban of the toxic veterinary drug diclofenac in south Asia. Bird Conservation International, **22**: 389-397.

Cheng, T. L., Rovito, S. M., Wake, D. B. & Vredenburg, V. T. (2011) Coincident mass extirpation of neotropical amphibians with the emergence of the infectious fungal pathogen *Batrachochytrium dendrobatidis*. Proceedings of the National Academy of Sciences of the United States of America, **108**: 9502-9507.

Childs, J. E. (2007) Pre-spillover prevention of emerging zoonotic diseases: What are the targets and what are the tools? (Eds.) *Wildlife and Emerging Zoonotic Diseases: The Biology, Circumstances and Consequences of Cross-Species Transmission.* Berlin, Springer-Verlag Berlin.

Childs, J. E. & Gordon, E. R. (2009) Surveillance and control of zoonotic agents prior to disease detection in humans. Mt Sinai J Med, **76**: 421-428.

Chivian, E. & Bernstein, A. (Eds.) (2008) *Sustaining Life: How Human Health Depends on Biodiversity*, Oxford, Oxford University Press, USA.

Choisy, M. & de Roode, J. C. (2010) Mixed Infections and the Evolution of Virulence: Effects of Resource Competition, Parasite Plasticity, and Impaired Host Immunity. American Naturalist, **175**: E105-E118.

Choisy, M. & Rohani, P. (2006) Harvesting can increase severity of wildlife disease epidemics. Proceedings of the Royal Society B-Biological Sciences, **273**: 2025-2034.

Choquet, R., Lebreton, J.-D., Gimenez, O., Reboulet, A.-M. & Pradel, R. (2009) U-CARE: Utilities for performing goodness of fit tests and manipulating CApture-REcapture data. Ecography, **32**: 1071-1074.

Cocude, C., Truong, M. J., Billaut-Mulot, O., Delsart, V., Darcissac, E., Capron, A., Mouton, Y. & Bahr, G. M. (2003) A novel cellular RNA helicase, RH116, differentially regulates cell growth, programmed cell death and human immunodeficiency virus type 1 replication. Journal of General Virology, **84**: 3215-3225.

Collins, J. P. (2010) Amphibian decline and extinction: What we know and what we need to learn. Diseases of Aquatic Organisms, **92**: 93-99.

Conant, G. C., Wagner, G. P. & Stadler, P. F. (2007) Modeling amino acid substitution patterns in orthologous and paralogous genes. Molecular Phylogenetics and Evolution, **42**: 298-307.

Conesa, A., Gotz, S., Garcia-Gomez, J. M., Terol, J., Talon, M. & Robles, M. (2005) Blast2GO: a universal tool for annotation, visualization and analysis in functional genomics research. Bioinformatics, **21**: 3674-3676.

Conlon, J. M. (2011) The contribution of skin antimicrobial peptides to the system of innate immunity in anurans. Cell Tissue Research, **343**: 201-212.

Conlon, J. M., Abraham, B., Sonnevend, A., Jouenne, T., Cosette, P., Leprince, J., Vaudry, H. & Bevier, C. R. (2005) Purification and characterization of antimicrobial peptides from the skin secretions of the carpenter frog *Rana virgatipes* (Ranidae, Aquarana). Regulatory Peptides, **131**: 38-45.

Conlon, J. M., Sonnevend, A., Patel, M., Al-Dhaheri, K., Nielsen, P. F., Kolodziejek, J., Nowotny, N., Iwamuro, S. & Pal, T. (2004) A family of brevinin-2 peptides with potent activity against *Pseudomonas aeruginosa* from the skin of the Hokkaido frog, *Rana pirica*. Regulatory Peptides, **118**: 135-141.

Conlon, J. M., Woodhams, D. C., Raza, H., Coquet, L., Leprince, J., Jouenne, T., Vaudry, H. & Rollins-Smith, L. A. (2007) Peptides with differential cytolytic activity from skin secretions of the lemur leaf frog *Hylomantis lemur* (Hylidae : Phyllomedusinae). Toxicon, **50**: 498-506.

Conn, P. B. & Cooch, E. G. (2009) Multistate capture-recapture analysis under imperfect state observation: an application to disease models. Journal of Applied Ecology, **46**: 486-492.

Connors, B. M., Cooper, A. B., Peterman, R. M. & Dulvy, N. K. (2014) The false classification of extinction risk in noisy environments. Proceedings of the Royal Society B-Biological Sciences, **281**: 10.

Cooch, E. G., Conn, P. B., Ellner, S. P., Dobson, A. P. & Pollock, K. H. (2012) Disease dynamics in wild populations: modeling and estimation: a review. J Ornithol, **152 (Suppl 2)**: S485-S509.

Cormack, R. M. (1964) Estimates of survival from the sighting of marked animals. Biometrics, **51**: 429-438.

Cottage, A., Yang, A. P., Maunders, H., de Lacy, R. C. & Ramsay, N. A. (2001) Identification of DNA sequences flanking T-DNA insertions by PCR-walking. Plant Molecular Biology Reporter, **19**: 321-327.

Cox, D. R. (1972) Regression models and life-tables. Journal of the Royal Statistical Society Series B-Statistical Methodology, **34**: 187.

Crawford, A. J., Lips, K. R. & Bermingham, E. (2010) Epidemic disease decimates amphibian abundance, species diversity, and evolutionary history in the highlands of central Panama. Proceedings of the National Academy of Sciences of the United States of America, **107**: 13777-13782.

Cubaynes, S., Lavergne, C., Marboutin, E. & Gimenez, O. (2012) Assessing individual heterogeneity using model selection criteria: how many mixture components in capture-recapture models? Methods in Ecology and Evolution, **3**: 564-573.

Culp, C. E., Falkinham, J. O. & Belden, L. K. (2007) Identification of the natural bacterial microflora on the skin of eastern newts, bullfrog tadpoles and redback salamanders. Herpetologica, **63**: 66-71.

Cunningham, A. A. & Daszak, P. (1998) Extinction of a species of land snail due to infection with a microsporidian parasite. Conservation Biology, **12**: 1139-1141.

Dabrowska, K., Switala-Jelen, K., Opolski, A., Weber-Dabrowska, B. & Gorski, A. (2005) Bacteriophage penetration in vertebrates. Journal of Applied Microbiology, **98**: 7-13.

Daskin, J. H., Alford, R. A. & Puschendorf, R. (2011) Short-term exposure to warm microhabitats could explain amphibian persistence with *Batrachochytrium dendrobatidis*. Plos One, **6**: e26215.

Daszak, P. (2000) Emerging infectious diseases of wildlife - threats to biodiversity and human health. Science, **287**: 443.

Daszak, P. (2009) A Call for "Smart Surveillance": A Lesson Learned from H1N1. Ecohealth, **6**: 1-2.

Daszak, P., Strieby, A., Cunningham, A. A., Longcore, J. E., Brown, C. C. & Porter, D. (2004) Experimental evidence that the bullfrog (*Rana catesbeiana*) is a potential carrier of

chytridiomycosis, an emerging fungal disease of amphibians. Herpetological Journal, **14**: 201-207.

Davidson, E. W., Parris, M., Collins, J. P., Longcore, J. E., Pessier, A. P. & Brunner, J. (2003) Pathogenicity and transmission of chytridiomycosis in tiger salamanders (*Ambystoma tigrinum*). Copeia: 601-607.

Davis, A. K., Keel, M. K., Ferreira, A. & Maerz, J. C. (2010) Effects of chytridiomycosis on circulating white blood cell distributions of bullfrog larvae (*Rana catesbeiana*). Comp Clin Pathol, **19**: 49-55.

de Castro, F. & Bolker, B. (2005) Mechanisms of disease-induced extinction. Ecology Letters, **8**: 117-126.

De Livera, A. M., Dias, D. A., De Souza, D., Rupasinghe, T., Pyke, J., Tull, D., Roessner, U., McConville, M. & Speed, T. P. (2012) Normalizing and Integrating Metabolomics Data. Analytical Chemistry, **84**: 10768-10776.

Delport, W., Poon, A. F. Y., Frost, S. D. W. & Pond, S. L. K. (2010) Datamonkey 2010: a suite of phylogenetic analysis tools for evolutionary biology. Bioinformatics, **26**: 2455-2457.

Department of Environment and Resource Management (2011) Regional Ecosystem Description Database (REDD) Version 6.0b - January 2011, Department of Environment and Resource Management. Brisbane, Queensland Herbarium.

Department of Primary Industries, P., Water and Environment, (2010) Tasmanian Chytrid Management Plan. Department of Primary Industries, Parks, Water and Environment, Tasmania, Australia. Available from http://www.dpiw.tas.gov.au/inter,nsf/Attachments/LJEM-8887K5/$FILE/Tasmanian%20Frog%20Management%20Plan.pdf (accessed January 2014).

Department of the Environment and Heritage (2006) Threat Abatement Plan: infection of amphibians with chytrid fungus resulting in chytridiomycosis, Canberra, ACT, Australian Government.

Desbrosses, G. G., Kopka, J. & Udvardi, M. K. (2005) *Lotus japonicus* metabolic profiling. Development of gas chromatography-mass spectrometry resources for the study of plant-microbe interactions. Plant Physiology, **137**: 1302-1318.

Dirzo, R., Young, H. S., Galetti, M., Ceballos, G., Isaac, N. J. B. & Collen, B. (2014) Defaunation in the Anthropocene. Science, **345**: 401-406.

Dochtermann, N. A. & Jenkins, S. H. (2011) Developing multiple hypotheses in behavioural ecology. Behavioral Ecology and Sociobiology, **65**: 37-45.

Doherty, P. F., White, G. C. & Burnham, K. P. (2012) Comparison of model building and selection strategies. Journal of Ornithology, **152 (Suppl 2)**: S317-S323.

Dreitz, V. J. (2006) Issues in species recovery: An example-based on the Wyoming toad. Bioscience, **56**: 765-771.

Drew, A., Allen, E. J. & Allen, L. J. S. (2006) Analysis of climatic and geographic factors affecting the presence of chytridiomycosis in Australia. Diseases of Aquatic Organisms, **68**: 245-250.

Du Pasquier, L., Schwager, J. & Flajnik, M. F. (1989) The immune system of *Xenopus*. Annual Review of Immunology, **7**: 251-275.

Duellman, W. E. & Trueb, L. (1994) Biology of Amphibians, Baltimore, The Johns Hopkins University Press.

Duncan, C., Backus, L., Lynn, T., Powers, B. & Salman, M. (2008) Passive, opportunistic wildlife disease surveillance in the Rocky Mountain Region, USA. Transboundary and Emerging Diseases, **55**: 308-314.

Dyson, E. A. & Hurst, G. D. D. (2004) Persistence of an extreme sex-ratio bias in a natural population. Proceedings of the National Academy of Sciences of the United States of America, **101**: 6520-6523.

Efron, B. (1979) Bootstrap Methods: Another Look at the Jackknife. The Annals of Statistics, **7**: 1-26.

Ellison, A. R., Savage, A. E., DiRenzo, G. V., Langhammer, P., Lips, K. R. & Zamudio, K. R. (2014) Fighting a losing battle: vigorous immune response countered by pathogen suppression of host defenses in the chytridiomycosis-susceptible frog *Atelopus zeteki*. G3-Genes Genomes Genetics, **4**: 1275-1289.

Ellner, S. P. & Rees, M. (2007) Stochastic stable population growth in integral projection models: theory and application. Journal of Mathematical Biology, **54**: 227-256.

Engering, A., Hogerwerf, L. & Slingenbergh, J. (2013) Pathogen-host-environment interplay and disease emergence. Emerging Microbes & Infections, **2**: 7.

Erdo, S. L. & Wolff, J. R. (1990) Gamma-aminobutyric acid outside the mammalian brain. Journal of Neurochemistry, **54**: 363-372.

Ewald, P. W. (2004) Evolution of virulence. Infectious Disease Clinics of North America, **18**: 1.

Faircloth, B. C. (2008) MSATCOMMANDER: detection of microsatellite repeat arrays and automated, locus-specific primer design. Molecular Ecology Resources, **8**: 92-94.

Farrer, R. A., Weinert, L. A., Bielby, J., Garner, T. W. J., Balloux, F., Clare, F., Bosch, J., Cunningham, A. A., Weldon, C., du Preez, L. H., Anderson, L., Pond, S. L. K., Shahar-Golan, R., Henk, D. A. & Fisher, M. C. (2011) Multiple emergences of genetically diverse amphibian-infecting chytrids include a globalized hypervirulent recombinant lineage. Proceedings of the National Academy of Sciences of the United States of America, **108**: 18732-18736.

Fellers, G. M., Green, D. E. & Longcore, J. E. (2001) Oral chytridiomycosis in the mountain yellow-legged frog (*Rana muscosa*). Copeia: 945-953.

Fenner, F. (2000) Adventures with poxviruses of vertebrates. Fems Microbiology Reviews, **24**: 123-133.

Fine, P. E. M. (1993) Herd-immunity: history, theory, practice. Epidemiologic Reviews, **15**: 265-302.

Fischer, J. & Lindenmayer, D. B. (2000) An assessment of the published results of animal relocations. Biological Conservation, **96**: 1-11.

Fisher, M. C., Bosch, J., Yin, Z., Stead, D. A., Walker, J., Selway, L., Brown, A. J. P., Walker, L. A., Gow, N. A. R., Stajich, J. E. & Garner, T. W. J. (2009a) Proteomic and phenotypic profiling of the amphibian pathogen *Batrachochytrium dendrobatidis* shows that genotype is linked to virulence. Molecular Ecology, **18**: 415-429.

Fisher, M. C. & Garner, T. W. J. (2007) The relationship between the emergence of *Batrachochytrium dendrobatidis*, the international trade in amphibians and introduced amphibian species. Fungal Biology Reviews, **21**: 2-9.

Fisher, M. C., Garner, T. W. J. & Walker, S. F. (2009b) Global emergence of *Batrachochytrium dendrobatidis* and amphibian chytridiomycosis in space, time, and host. Annual Review of Microbiology, **63**: 291-310.

Fisher, M. C., Henk, D. A., Briggs, C. J., Brownstein, J. S., Madoff, L. C., McCraw, S. L. & Gurr, S. J. (2012) Emerging fungal threats to animal, plant and ecosystem health. Nature, **484**: 186-194.

Fites, J. S., Ramsey, J. P., Holden, W. M., Collier, S. P., Sutherland, D. M., Reinert, L. K., Gayek, A. S., Dermody, T. S., Aune, T. M., Oswald-Richter, K. & Rollins-Smith, L. A. (2013) The invasive chytrid fungus of amphibians paralyzes lymphocyte responses. Science, **342**: 366-369.

Flajnik, M. F. (2002) Comparative analyses of immunoglobulin genes: Surprises and portents. Nature Reviews Immunology, **2**: 688-698.

Flajnik, M. F., Hsu, E., Kaufman, J. F. & Dupasquier, L. (1987) Changes in the immune system during metamorphosis of *Xenopus*. Immunology Today, **8**: 58-64.

Flechas, S. V., Sarmiento, C., Cardenas, M. E., Medina, E. M., Restrepo, S. & Amezquita, A. (2012) Surviving chytridiomycosis: differential anti-*Batrachochytrium dendrobatidis* activity in bacterial isolates from three lowland species of *Atelopus*. Plos One, **7**: 7.

Foley, J., Clifford, D., Castle, K., Cryan, P. & Ostfeld, R. S. (2011) Investigating and managing the rapid emergence of white-nose syndrome, a novel, fatal, infectious disease of hibernating bats. Conservation Biology, **25**: 223-231.

Forrest, M. J. & Schlaepfer, M. A. (2011) Nothing a hot bath won't cure: infection rates of amphibian chytrid fungus correlate negatively with water temperature under natural field settings. PLoS One, **6**: e28444.

Fox, H. (1994) The structure of the integument. In: Heatwole, H. & Barthalmus, G. T. (Eds.) *Amphibian Biology - Volume 1: The Integument.* Chipping Norton, Surrey Beatty & Sons.

Frankham, R., Ballou, J. D., Eldridge, M. D. B., Lacy, R. C., Ralls, K., Dudash, M. R. & Fenster, C. B. (2011) Predicting the Probability of Outbreeding Depression. Conservation Biology, **25**: 465-475.

Freckleton, R. P. (2011) Dealing with collinearity in behavioural and ecological data: model averaging and the problems of measurement error. Behavioral Ecology and Sociobiology, **65**: 91-101.

Freedman, D. A. (1983) A note of screening regression equations. American Statistician, **37**: 152-155.

Freidenburg, L. K. & Skelly, D. K. (2004) Microgeographical variation in thermal preference by an amphibian. Ecology Letters, **7**: 369-373.

Fujita, T., Endo, Y. & Nonaka, M. (2004) Primitive complement system - recognition and activation. Molecular Immunology, **41**: 103-111.

Gagliardo, R., Crump, P., Griffith, E., Mendelson, J., Ross, H. & Zippel, K. (2008) The principles of rapid response for amphibian conservation, using the programmes in Panama as an example. International Zoo Yearbook, **42**: 125-135.

Gantress, J., Maniero, G. D., Cohen, N. & Robert, J. (2003) Development and characterization of a model system to study amphibian immune responses to iridoviruses. Virology, **311**: 254-262.

Garland, S., Baker, A., Phillott, A. D. & Skerratt, L. F. (2009) BSA reduces inhibition in a TaqMan (R) assay for the detection of *Batrachochytrium dendrobatidis*. Diseases of Aquatic Organisms, **92**: 113-116.

Garmyn, A., Van Rooij, P., Pasmans, F., Hellebuyck, T., Van den Broeck, W., Haesebrouck, F. & Martel, A. (2012) Waterfowl: potential environmental reservoirs of the chytrid fungus *Batrachochytrium dendrobatidis*. Plos One, **7**: 5.

Garner, T. W. J., Garcia, G., Carroll, B. & Fisher, M. C. (2009) Using itraconazole to clear *Batrachochytrium dendrobatidis* infection, and subsequent depigmentation of *Alytes muletensis* tadpoles. Diseases of Aquatic Organisms, **83**: 257-260.

Geiger, C. C., Kupfer, E., Schar, S., Wolf, S. & Schmidt, B. R. (2011) Elevated temperature clears chytrid fungus infections from tadpoles of the midwife toad, *Alytes obstetricans*. Amphibia-Reptilia, **32**: 276-280.

Geiger, C. C. & Schmidt, B. R. (2013) Laboratory tests of antifungal agents to treat tadpoles against the pathogen *Batrachochytrium dendrobatidis*. Diseases of Aquatic Organisms, **103**: 191-197.

Gervasi, S., Gondhalekar, C., Olson, D. H. & Blaustein, A. R. (2013) Host identity matters in the amphibian-*Batrachochytrium dendrobatidis* system: fine-scale patterns of variation in responses to a multi-host pathogen. Plos One, **8**: 11.

Gibble, R. E., Rollins-Smith, L. & Baer, K. N. (2008) Development of an assay for testing the antimicrobial activity of skin peptides against the amphibian chytrid fungus (*Batrachochytrium dendrobatidis*) using *Xenopus laevis*. Ecotoxicology and Environmental Safety, **71**: 506-513.

Girdhar, S. R., Barta, J. R., Santoyo, F. A. & Smith, T. K. (2006) Dietary putrescine (1,4-diaminobutane) influences recovery of turkey poults challenged with a mixed coccidial infection. Journal of Nutrition, **136**: 2319-2324.

Goka, K., Yokoyama, J., Une, Y., Kuroki, T., Suzuki, K., Nakahara, M., Kobayashi, A., Inaba, S., Mizutani, T. & Hyatt, A. D. (2009) Amphibian chytridiomycosis in Japan: distribution, haplotypes and possible route of entry into Japan. Molecular Ecology, **18**: 4757-4774.

Gotz, S., Arnold, R., Sebastian-Leon, P., Martin-Rodriguez, S., Tischler, P., Jehl, M. A., Dopazo, J., Rattei, T. & Conesa, A. (2011) B2G-FAR, a species-centered GO annotation repository. Bioinformatics, **27**: 919-924.

Green, A. J. (1999) Implications of pathogenic fungi for life-history evolution in amphibians. Functional Ecology, **13**: 573-575.

Green, D. E. & Sherman, C. K. (2001) Diagnostic histological findings in Yosemite toads (*Bufo canorus*) from a die-off in the 1970s. Journal of Herpetology, **35**: 92-103.

Greenspan, S. E., Longcore, J. E. & Calhoun, A. J. K. (2012) Host invasion by *Batrachochytrium dendrobatidis*: fungal and epidermal ultrastructure in model anurans. Diseases of Aquatic Organisms, **100**: 201-210.

Griffiths, R. A. & Pavajeau, L. (2008) Captive breeding, reintroduction, and the conservation of amphibians. Conservation Biology, **22**: 852-861.

Grogan, L. F., Berger, L., Rose, K., Grillo, V., Cashins, S. D. & Skerratt, L. F. (2014) Surveillance for emerging biodiversity diseases of wildlife. Plos Pathogens, **10**: e1004015.

Grueber, C. E., Nakagawa, S., Laws, R. J. & Jamieson, I. G. (2011) Multimodel inference in ecology and evolution: challenges and solutions. Journal of Evolutionary Biology, **24**: 699-711.

Gummer, J., Banazis, M., Maker, G., Solomon, P., Oliver, R. & Trengove, R. (2009) Use of mass spectrometry for metabolite profiling and metabolomics. Australian Biochemist, **40**: 5-16.

Gummer, J. P. A., Trengove, R. D., Oliver, R. P. & Solomon, P. S. (2013) Dissecting the role of G-protein signalling in primary metabolism in the wheat pathogen *Stagonospora nodorum*. Microbiology-Sgm, **159**: 1972-1985.

Guthery, F. S., Brennan, L. A., Peterson, M. J. & Lusk, J. J. (2005) Information theory in wildlife science: Critique and viewpoint. Journal of Wildlife Management, **69**: 457-465.

Haas, B. J., Papanicolaou, A., Yassour, M., Grabherr, M., Blood, P. D., Bowden, J., Couger, M. B., Eccles, D., Li, B., Lieber, M., MacManes, M. D., Ott, M., Orvis, J., Pochet, N., Strozzi, F., Weeks, N., Westerman, R., William, T., Dewey, C. N., Henschel, R., Leduc, R. D., Friedman, N. & Regev, A. (2013) *De novo* transcript sequence reconstruction from RNA-seq using the Trinity platform for reference generation and analysis. Nature Protocols, **8**: 1494-1512.

Hafenstein, S. & Fane, B. A. (2002) phi X174 genome-capsid interactions influence the biophysical properties of the virion: Evidence for a scaffolding-like function for the genome during the final stages of morphogenesis. Journal of Virology, **76**: 5350-5356.

Hall, T. A. (1999) BioEdit: a user-friendly biological sequence alignment editor and analysis program for Windows 95/98/NT. Nucleic Acids Symposium Series, **41**: 95-98.

Halliday, J. E. B., Meredith, A. L., Knobel, D. L., Shaw, D. J., Bronsvoort, B. & Cleaveland, S. (2007) A framework for evaluating animals as sentinels for infectious disease surveillance. J R Soc Interface, **4**: 973-984.

Hamilton, P. T., Richardson, J. M. L. & Anholt, B. R. (2012) *Daphnia* in tadpole mesocosms: trophic links and interactions with *Batrachochytrium dendrobatidis*. Freshwater Biology, **57**: 676-683.

Hanlon, S. M., Kerby, J. L. & Parris, M. J. (2012) Unlikely remedy: fungicide clears infection from pathogenic fungus in larval southern leopard frogs (*Lithobates sphenocephalus*). Plos One, **7**: 8.

Hanselmann, R., Rodriguez, A., Lampo, M., Fajardo-Ramos, L., Aguirre, A. A., Kilpatrick, A. M., Rodriguez, J. P. & Daszak, P. (2004) Presence of an emerging pathogen of amphibians in introduced bullfrogs *Rana catesbeiana* in Venezuela. Biological Conservation, **120**: 115-119.

Hansen, K. D., Brenner, S. E. & Dudoit, S. (2010) Biases in Illumina transcriptome sequencing caused by random hexamer priming. Nucleic Acids Research, **38**: 7.

Harrington, D. P. & Fleming, T. R. (1982) A class of rank test procedures for censored survival-data. Biometrika, **69**: 553-566.

Harris, R. N., Brucker, R. M., Walke, J. B., Becker, M. H., Schwantes, C. R., Flaherty, D. C., Lam, B. A., Woodhams, D. C., Briggs, C. J., Vredenburg, V. T. & Minbiole, K. P. C. (2009a) Skin microbes on frogs prevent morbidity and mortality caused by a lethal skin fungus. Isme Journal, **3**: 818-824.

Harris, R. N., James, T. Y., Lauer, A., Simon, M. A. & Patel, A. (2006) Amphibian pathogen *Batrachochytrium dendrobatidis* is inhibited by the cutaneous bacteria of amphibian species. Ecohealth, **3**: 53-56.

Harris, R. N., Lauer, A., Simon, M. A., Banning, J. L., Alford, R. A., Harris, R. N., Lauer, A., Simon, M. A., Banning, J. L. & Alford, R. A. (2009b) Addition of antifungal skin bacteria to salamanders ameliorates the effects of chytridiomycosis. Diseases of Aquatic Organisms, **83**: 11-6.

Hashemi, S. M., Loh, T. C., Foo, H. L., Zulkifli, I. & Bejo, M. H. (2014) Effects of putrescine supplementation on growth performance, blood lipids and immune response in broiler chickens fed methionine deficient diet. Animal Feed Science and Technology, **194**: 151-156.

Hauswaldt, J. S., Stuckas, H., Pfautsch, S. & Tiedemann, R. (2007) Molecular characterization of MHC class II in a nonmodel anuran species, the fire-bellied toad *Bombina bombina*. Immunogenetics, **59**: 479-491.

Hawkins, C. E., Baars, C., Hesterman, H., Hocking, G. J., Jones, M. E., Lazenby, B., Mann, D., Mooney, N., Pemberton, D., Pyecroft, S., Restani, M. & Wiersma, J. (2006) Emerging disease and population decline of an island endemic, the Tasmanian devil *Sarcophilus harrisii*. Biological Conservation, **131**: 307-324.

Heard, G. W., Scroggie, M. P., Clemann, N. & Ramsey, D. S. L. (2013) Wetland characteristics influence disease risk for a threatened amphibian. Ecological Applications, **24**: 650-662.

Hegyi, G. & Garamszegi, L. Z. (2011) Using information theory as a substitute for stepwise regression in ecology and behavior. Behav. Ecol. Sociobiol., **65**: 69-76.

Henderson, D. A. & Klepac, P. (2013) Lessons from the eradication of smallpox: an interview with D. A. Henderson. Philosophical Transactions of the Royal Society B-Biological Sciences, **368**: 7.

Heringstad, B., Klemetsdal, G. & Steine, T. (2007) Selection responses for disease resistance in two selection experiments with Norwegian red cows. Journal of Dairy Science, **90**: 2419-2426.

Hero, J. M., Gillespie, G., Lemckert, F., Robertson, P. & Littlejohn, M. (2011) *Litoria booroolongensis*. IUCN 2011 Red List of Threatened Species.

Hines, H., Mahony, M. & McDonald, K. (1999) An assessment of frog declines in wet subtropical Australia. In: Campbell, A. (Eds.) *Declines and disappearances of Australian frogs.* Canberra, ACT, Environment Australia.

Hodgkison, S. C. & Hero, J. M. (2002) Seasonal behaviour of *Litoria nannotis*, *Litoria rheocola* and *Nyctimystes dayi* in Tully Gorge, North Queensland, Australia. In: Nattrass, A. E. O. (Ed.) *Frogs in the Community: Proceedings of the Brisbane Symposium 13-14 February 1999.* Brisbane, The Queensland Frog Society Incorporated.

Hoegh-Guldberg, O., Hughes, L., McIntyre, S., Lindenmayer, D. B., Parmesan, C., Possingham, H. P. & Thomas, C. D. (2008) Assisted colonization and rapid climate change. Science, **321**: 345-346.

Holden, W. M. & Rollins-Smith, L. A. (2014) Skin bacteria protect newly metamorphosed *Rana sphenocephala* from the emerging fungal pathogen *Batrachochytrium dendrobatidis*. Integrative and Comparative Biology, **54**: E92-E92.

Holmala, K. & Kauhala, K. (2006) Ecology of wildlife rabies in Europe. Mammal Review, **36**: 17-36.

Houlahan, J. E., Findlay, C. S., Schmidt, B. R., Meyer, A. H. & Kuzmin, S. L. (2000) Quantitative evidence for global amphibian population declines. Nature, **404**: 752-755.

Hudson, P. J. & Dobson, A. P. (1998) Macroparasites: observed patterns in naturally fluctuating animal populations. In: Grenfell, B. T. & Dobson, A. P. (Eds.) *Ecology of Infectious Diseases in Natural Populations.* Cambridge, Cambridge University Press.

Hunter, D., Osborne, W., Marantelli, G. & Green, K. (1999) Implementation of a population augmentation project for remnant populations of the Southern Corroboree Frog (*Pseudophryne corroboree*). In: Campbell, A. (Eds.) *Declines and Disappearances of Australian Frogs.* Canberra, Environment Australia.

Hunter, D. A., Speare, R., Marantelli, G., Mendez, D., Pietsch, R. & Osborne, W. (2010) Presence of the amphibian chytrid fungus *Batrachochytrium dendrobatidis* in threatened corroboree frog populations in the Australian Alps. Diseases of Aquatic Organisms, **92**: 209-216.

Hurvich, C. M. & Tsai, C.-L. (1989) Regression and time series model selection in small samples. Biometrika, **76**: 297-307.

Hyatt, A. D., Boyle, D. G., Olsen, V., Boyle, D. B., Berger, L., Obendorf, D., Dalton, A., Kriger, K., Hero, M., Hines, H., Phillott, R., Campbell, R., Marantelli, G., Gleason, F. & Colling, A. (2007) Diagnostic assays and sampling protocols for the detection of *Batrachochytrium dendrobatidis*. Diseases of Aquatic Organisms, **73**: 175-192.

Ishii, A., Kawasaki, M., Matsumoto, M., Tochinai, S. & Seya, T. (2007) Phylogenetic and expression analysis of amphibian *Xenopus* Toll-like receptors. Immunogenetics, **59**: 281-293.

Ivosev, G., Burton, L. & Bonner, R. (2008) Dimensionality reduction and visualization in principal component analysis. Analytical Chemistry, **80**: 4933-4944.

Jabara, H. H., Weng, Y., Sannikova, T. & Geha, R. S. (2009) TRAF2 and TRAF3 independently mediate Ig class switching driven by CD40. International Immunology, **21**: 477-488.

Jackson, V. S., Huntley, S., Tomlinson, A., Smith, G. C., Taylor, M. A. & Delahay, R. J. (2009) Chapter 9 Risk assessment and contingency planning for exotic disease introductions. In: Delahay, R. J., Smith, G. C. & Hutchings, M. R. (Eds.) *Management of disease in wild mammals.* Tokyo, Springer.

James, T. Y., Litvintseva, A. P., Vilgalys, R., Morgan, J. A. T., Taylor, J. W., Fisher, M. C., Berger, L., Weldon, C., du Preez, L. & Longcore, J. E. (2009) Rapid global expansion of the fungal disease chytridiomycosis into declining and healthy amphibian populations. Plos Pathogens, **5**: e1000458.

Jeffrey, S. J., Carter, J. O., Moodie, K. B. & Beswick, A. R. (2001) Using spatial interpolation to construct a comprehensive archive of Australian climate data. Environ. Modell. Softw., **16**: 309-330.

Jennelle, C. S., Cooch, E. G., Conroy, M. J. & Senar, J. C. (2007) State-specific detection probabilities and disease prevalence. Ecological Applications, **17**: 154-167.

Joe, M. & Pollock, K. H. (2002) Separation of survival and movement rates in multi-state tag-return and capture-recapture models. Journal of Applied Statistics, **29**: 373-384.

Johnson, D. H. (1999) The insignificance of statistical significance testing. Journal of Wildlife Management, **63**: 763-772.

Johnson, M. L., Berger, L., Philips, L. & Speare, R. (2003) Fungicidal effects of chemical disinfectants, UV light, desiccation and heat on the amphibian chytrid *Batrachochytrium dendrobatidis*. Diseases of Aquatic Organisms, **57**: 255-260.

Johnson, M. L. & Speare, R. (2003) Survival of *Batrachochytrium dendrobatidis* in water: Quarantine and disease control implications. Emerging Infectious Diseases, **9**: 922-925.

Johnson, M. L. & Speare, R. (2005) Possible modes of dissemination of the amphibian chytrid *Batrachochytrium dendrobatidis* in the environment. Diseases of Aquatic Organisms, **65**: 181-186.

Johnson, P. T. J. & Hoverman, J. T. (2014) Heterogeneous hosts: how variation in host size, behaviour and immunity affects parasite aggregation. Journal of Animal Ecology, **83**: 1103-1112.

Jolly, G. M. (1965) Explicit estimates from capture-recapture data with both death and immigration-stochastic model. Biometrika, **52**: 225.

Jones, E. Y., Fugger, L., Strominger, J. L. & Siebold, C. (2006) MHC class II proteins and disease: a structural perspective. Nature Reviews Immunology, **6**: 271-282.

Jones, K. E., Patel, N. G., Levy, M. A., Storeygard, A., Balk, D., Gittleman, J. L. & Daszak, P. (2008) Global trends in emerging infectious diseases. Nature, **451**: 990-993.

Jones, M. E. B., Paddock, D., Bender, L., Allen, J. L., Schrenzel, M. S. & Pessier, A. P. (2012) Treatment of chytridiomycosis with reduced-dose itraconazole. Diseases of Aquatic Organisms, **99**: 243-249.

Jones, O. A. H. & Cheung, V. L. (2007) An introduction to metabolomics and its potential application in veterinary science. Comparative Medicine, **57**: 436-442.

Jones, P., Binns, D., Chang, H. Y., Fraser, M., Li, W. Z., McAnulla, C., McWilliam, H., Maslen, J., Mitchell, A., Nuka, G., Pesseat, S., Quinn, A. F., Sangrador-Vegas, A., Scheremetjew, M., Yong, S. Y., Lopez, R. & Hunter, S. (2014) InterProScan 5: genome-scale protein function classification. Bioinformatics, **30**: 1236-1240.

Joseph, L. N., Maloney, R. F. & Possingham, H. P. (2009) Optimal allocation of resources among threatened species: a project prioritization protocol. Conservation Biology, **23**: 328-338.

Joseph, M. B., Mihaljevic, J. R., Arellano, A. L., Kueneman, J. G., Preston, D. L., Cross, P. C. & Johnson, P. T. J. (2013) Taming wildlife disease: bridging the gap between science and management. Journal of Applied Ecology, **50**: 702-712.

Kalinowski, S. T., Taper, M. L. & Marshall, T. C. (2007) Revising how the computer program CERVUS accommodates genotyping error increases success in paternity assignment. Molecular Ecology, **16**: 1099-1106.

Kane, A. J. & Morley, P. S. (1999) How to investigate a disease outbreak. Proceedings of the Annual Convention of the AAEP, **45**: 137-141.

Kanehisa, M. & Goto, S. (2000) KEGG: Kyoto Encyclopedia of Genes and Genomes. Nucleic Acids Research, **28**: 27-30.

Karesh, W. B., Cook, R. A., Bennett, E. L. & Newcomb, J. (2005) Wildlife trade and global disease emergence. Emerging Infectious Diseases, **11**: 1000-1002.

Keesing, F., Belden, L. K., Daszak, P., Dobson, A., Harvell, C. D., Holt, R. D., Hudson, P., Jolles, A., Jones, K. E., Mitchell, C. E., Myers, S. S., Bogich, T. & Ostfeld, R. S. (2010) Impacts of biodiversity on the emergence and transmission of infectious diseases. Nature, **468**: 647-652.

Kell, D. B. & Goodacre, R. (2014) Metabolomics and systems pharmacology: why and how to model the human metabolic network for drug discovery. Drug Discovery Today, **19**: 171-182.

Kemere, P., Liddel, M. K., Evangelou, P., Slate, D. & Omsmek, S. (2000) Economic analysis of a large scale oral vaccination program to control raccoon rabies. *Human Conflicts with Wildlife: Economic Considerations.* Lincoln, University of Nebraska - Lincoln.

Kenta, T., Gratten, J., Haigh, N. S., Hinten, G. N., Slate, J., Butlin, R. K. & Burke, T. (2008) Multiplex SNP-SCALE: a cost-effective medium-throughput single nucleotide polymorphism genotyping method. Molecular Ecology Resources, **8**: 1230-1238.

Kiemnec-Tyburczy, K. M., Richmond, J. Q., Savage, A. E. & Zamudio, K. R. (2010) Selection, trans-species polymorphism, and locus identification of major histocompatibility complex class II beta alleles of New World ranid frogs. Immunogenetics, **62**: 741-751.

Kilburn, V. L., Ibanez, R. & Green, D. M. (2011) Reptiles as potential vectors and hosts of the amphibian pathogen *Batrachochytrium dendrobatidis* in Panama. Diseases of Aquatic Organisms, **97**: 127-134.

Kim, B. H., Shenoy, A. R., Kumar, P., Bradfield, C. J. & MacMicking, J. D. (2012) IFN-Inducible GTPases in Host Cell Defense. Cell Host & Microbe, **12**: 432-444.

Kindermann, C., Narayan, E. J. & Hero, J. M. (2012) Urinary corticosterone metabolites and chytridiomycosis disease prevalence in a free-living population of male Stony Creek frogs (*Litoria wilcoxii*). Comparative Biochemistry and Physiology a-Molecular & Integrative Physiology, **162**: 171-176.

King, J. D., Al-Ghaferi, N., Abraham, B., Sonnevend, A., Leprince, J., Nielsen, P. F. & Conlon, J. M. (2005) Pentadactylin: An antimicrobial peptide from the skin secretions of the South American bullfrog *Leptodactylus pentadactylus*. Comparative Biochemistry and Physiology C-Toxicology & Pharmacology, **141**: 393-397.

Kinney, V. C., Heemeyer, J. L., Pessier, A. P. & Lannoo, M. J. (2011) Seasonal pattern of *Batrachochytrium dendrobatidis* infection and mortality in *Lithobates areolatus*: Affirmation of Vredenburg's "10,000 zoospore rule". Plos One, **6**: 10.

Kirshtein, J. D., Anderson, C. W., Wood, J. S., Longcore, J. E. & Voytek, M. A. (2007) Quantitative PCR detection of *Batrachochytrium dendrobatidis* DNA from sediments and water. Diseases of Aquatic Organisms, **77**: 11-15.

Klamp, T., Boehm, U., Schenk, D., Pfeffer, K. & Howard, J. C. (2003) A giant GTPase, very large inducible GTPase-1, is inducible by IFNs. Journal of Immunology, **171**: 1255-1265.

Knowles, S. C. L., Wood, M. J. & Sheldon, B. C. (2010) Context-dependent effects of parental effort on malaria infection in a wild bird population, and their role in reproductive trade-offs. Oecologia, **164**: 87-97.

Kochs, G. & Haller, O. (1999) Interferon-induced human MxA GTPase blocks nuclear import of Thogoto virus nucleocapsids. Proceedings of the National Academy of Sciences of the United States of America, **96**: 2082-2086.

Kolby, J. E., Padgett-Flohr, G. E. & Field, R. (2010) Amphibian chytrid fungus *Batrachochytrium dendrobatidis* in Cusuco National Park, Honduras. Diseases of Aquatic Organisms, **92**: 245-251.

Kopp, J. & Schwede, T. (2006) The SWISS-MODEL repository: new features and functionalities. Nucleic Acids Research, **34**: D315-D318.

Koprivnikar, J., Gibson, C. H. & Redfern, J. C. (2011) Infectious personalities: behavioural syndromes and disease risk in larval amphibians. Proceedings of the Royal Society B-Biological Sciences, **279**: 1544-1550.

Kosakovsky Pond, S. L. & Frost, S. D. W. (2005) Not so different after all: a comparison of methods for detecting amino acid sites under selection. Molecular Biology and Evolution, **22**: 1208-22.

Kosakovsky Pond, S. L., Posada, D., Gravenor, M. B., Woelk, C. H. & Frost, S. D. W. (2006) Automated phylogenetic detection of recombination using a genetic algorithm. Molecular Biology and Evolution, **23**: 1891-1901.

Kosch, T. A. & Summers, K. (2013) Techniques for minimizing the effects of PCR inhibitors in the chytridiomycosis assay. Molecular Ecology Resources, **13**: 230-236.

Kouba, A. J., Lloyd, R. E., Houck, M. L., Silla, A. J., Calatayud, N., Trudeau, V. L., Clulow, J., Molinia, F., Langhorne, C., Vance, C., Arregui, L., Germano, J., Lermen, D. & Della Togna, G. (2013) Emerging trends for biobanking amphibian genetic resources: The hope, reality and challenges for the next decade. Biological Conservation, **164**: 10-21.

Kozubikova, E., Petrusek, A., Duris, Z., Martin, M. P., Dieguez-Uribeondo, J. & Oidtmann, B. (2008) The old menace is back: Recent crayfish plague outbreaks in the Czech Republic. Aquaculture, **274**: 208-217.

Kriger, K. M., Ashton, K. J., Hines, H. B. & Hero, J. M. (2007a) On the biological relevance of a single *Batrachochytrium dendrobatidis* zoospore: a reply to Smith (2007). Diseases of Aquatic Organisms, **73**: 257-260.

Kriger, K. M. & Hero, J. M. (2006a) Large-scale seasonal variation in the prevalence and severity of chytridiomycosis. Journal of Zoology, **271**: 352-359.

Kriger, K. M. & Hero, J. M. (2006b) Survivorship in wild frogs infected with chytridiomycosis. Ecohealth, **3**: 171-177.

Kriger, K. M. & Hero, J. M. (2009) Chytridiomycosis, Amphibian Extinctions, and Lessons for the Prevention of Future Panzootics. Ecohealth, **6**: 6-10.

Kriger, K. M., Hines, H. B., Hyatt, A. D., Boyle, D. G. & Hero, J. M. (2006) Techniques for detecting chytridiomycosis in wild frogs: comparing histology with real-time Taqman PCR. Diseases of Aquatic Organisms, **71**: 141-148.

Kriger, K. M., Pereoglou, F. & Hero, J. M. (2007b) Latitudinal variation in the prevalence and intensity of chytrid (*Batrachochytrium dendrobatidis*) infection in Eastern Australia. Conservation Biology, **21**: 1280-1290.

Kuiken, T., Leighton, F. A., Fouchier, R. A. M., LeDuc, J. W., Peiris, J. S. M., Schudel, A., Stohr, K. & Osterhaus, A. (2005) Public health - pathogen surveillance in animals. Science, **309**: 1680-1681.

Kuiken, T., Ryser-Degiorgis, M.-P., Gavier-Widen, D. & Gortazar, C. (2011) Establishing a European network for wildlife health surveillance. Rev Sci Tech, **30**: 755-761.

Kullback, S. & Leibler, R. A. (1951) On information and sufficiency. The Annals of Mathematical Statistics, **22**: 79-86.

Kurtz, J. & Scharsack, J. P. (2007) Resistance is skin-deep: innate immunity may help amphibians to survive a deadly fungus. Animal Conservation, **10**: 422-424.

La Marca, E., Lips, K. R., Lotters, S., Puschendorf, R., Ibanez, R., Rueda-Almonacid, J. V., Schulte, R., Marty, C., Castro, F., Manzanilla-Puppo, J., Garcia-Perez, J. E., Bolanos, F., Chaves, G., Pounds, J. A., Toral, E. & Young, B. E. (2005) Catastrophic population declines and extinctions in neotropical harlequin frogs (Bufonidae : Atelopus). Biotropica, **37**: 190-201.

Lafferty, K. D. & Gerber, L. R. (2002) Good medicine for conservation biology: The intersection of epidemiology and conservation theory. Conservation Biology, **16**: 593-604.

Lam, B. A., Walke, J. B., Vredenburg, V. T. & Harris, R. N. (2010) Proportion of individuals with anti-*Batrachochytrium dendrobatidis* skin bacteria is associated with population persistence in the frog *Rana muscosa*. Biological Conservation, **143**: 529-531.

Lam, B. A., Walton, D. B. & Harris, R. N. (2011) Motile zoospores of *Batrachochytrium dendrobatidis* move away from antifungal metabolites produced by amphibian skin bacteria. Ecohealth, **8**: 36-45.

Lamirande, E. W. & Nichols, D. K. (2002) Effects of host age on susceptibility to cutaneous chytridiomycosis in Blue-and-Yellow Poison Dart frogs (*Dendrobates tinctorius*). In: McKinnell, R. G. & Carlson, D. L. (Eds.) *Proceeding of the Sixth International Symposium on the Pathology of Reptiles and Amphibian.* Saint Paul, Minnesota, USA.

Langmead, B., Trapnell, C., Pop, M. & Salzberg, S. L. (2009) Ultrafast and memory-efficient alignment of short DNA sequences to the human genome. Genome Biology, **10**: 10.

Lauer, A., Simon, M. A., Banning, J. L., Andre, E., Duncan, K. & Harris, R. N. (2007) Common cutaneous bacteria from the eastern red-backed salamander can inhibit pathogenic fungi. Copeia: 630-640.

Laurenson, K., Sillero-Zubiri, C., Thompson, H., Shiferaw, F., Thirgood, S. & Malcolm, J. (1998) Disease as a threat to endangered species: Ethiopian wolves, domestic dogs and canine pathogens. Animal Conservation, **1**: 273-280.

Lebreton, J. D., Burnham, K. P., Clobert, J. & Anderson, D. R. (1992) Modeling survival and testing biological hypotheses using marked animals - a unified approach with case-studies. Ecological Monographs, **62**: 67-118.

Lebreton, J. D., Nichols, J. D., Barker, R. J., Pradel, R. & Spendelow, J. A. (2009) Modeling individual animal histories with multistate capture-recapture models. Adv. Ecol. Res., **41**: 87-173.

Lee, K. H., Wucherpfennig, K. W. & Wiley, D. C. (2001) Structure of a human insulin peptide-HLA-DQ8 complex and susceptibility to type I diabetes. Nature Immunology, **2**: 501-507.

Leeds, T. D., Silverstein, J. T., Weber, G. M., Vallejo, R. L., Palti, Y., Rexroad, C. E., Evenhuis, J., Hadidi, S., Welch, T. J. & Wiens, G. D. (2010) Response to selection for bacterial cold water disease resistance in rainbow trout. Journal of Animal Science, **88**: 1936-1946.

Lesbarreres, D., Fowler, M. S., Pagano, A. & Lode, T. (2010) Recovery of anuran community diversity following habitat replacement. Journal of Applied Ecology, **47**: 148-156.

Li, B. & Dewey, C. N. (2011) RSEM: accurate transcript quantification from RNA-Seq data with or without a reference genome. Bmc Bioinformatics, **12**: 16.

Li, G., Zhang, J. Y., Sun, Y., Wang, H. & Wang, Y. Q. (2009) The evolutionarily dynamic IFN-inducible GTPase proteins play conserved immune functions in vertebrates and cephalochordates. Molecular Biology and Evolution, **26**: 1619-1630.

Li, J., Barreda, D. R., Zhang, Y. A., Boshra, H., Gelman, A. E., LaPatra, S., Tort, L. & Sunyer, J. O. (2006) B lymphocytes from early vertebrates have potent phagocytic and microbicidal abilities. Nature Immunology, **7**: 1116-1124.

Liem, D. S. (1974) A review of the *Litoria nannotis* species group and a description of a new species of *Litoria* from northern Queensland Australia (*Anura: Hylidae*). Memoirs of the Queensland Museum, **17**: 151-168.

Lilley, J. H. & Inglis, V. (1997) Comparative effects of various antibiotics, fungicides and disinfectants on *Aphanomyces invaderis* and other saprolegniaceous fungi. Aquaculture Research, **28**: 461-469.

Lindberg, M. S. (2012) A review of designs for capture-mark-recapture studies in discrete time. Journal of Ornithology, **152 (Suppl 2)**: S355-S370.

Linden, A. & Knape, J. (2009) Estimating environmental effects on population dynamics: consequences of observation error. Oikos, **118**: 675-680.

Lindenmayer, D. & Hunter, M. (2010) Some Guiding Concepts for Conservation Biology. Conservation Biology, **24**: 1459-1468.

Link, W. A. & Barker, R. J. (2006) Model weights and the foundations of multimodel inference. Ecology, **87**: 2626-2635.

Lips, K. R. (1999) Mass mortality and population declines of anurans at an upland site in western Panama. Conservation Biology, **13**: 117-125.

Lips, K. R., Brem, F., Brenes, R., Reeve, J. D., Alford, R. A., Voyles, J., Carey, C., Livo, L., Pessier, A. P. & Collins, J. P. (2006) Emerging infectious disease and the loss of biodiversity in a Neotropical amphibian community. Proceedings of the National Academy of Sciences of the United States of America, **103**: 3165-3170.

Longcore, J. E., Pessier, A. P. & Nichols, D. K. (1999) *Batrachochytrium dendrobatidis* gen et sp nov, a chytrid pathogenic to amphibians. Mycologia, **91**: 219-227.

Longcore, J. R., Longcore, J. E., Pessier, A. P. & Halteman, W. A. (2007) Chytridiomycosis widespread in anurans of northeastern United States. Journal of Wildlife Management, **71**: 435-444.

Loudon, A. H., Woodhams, D. C., Parfrey, L. W., Archer, H., Knight, R., McKenzie, V. & Harris, R. N. (2014) Microbial community dynamics and effect of environmental microbial reservoirs on red-backed salamanders (*Plethodon cinereus*). Isme Journal, **8**: 830-840.

Lovitch, S. B. & Unanue, E. R. (2005) Conformational isomers of a peptide-class II major histocompatibility complex. Immunological Reviews, **207**: 293-313.

Lukacs, P. M., Burnham, K. P. & Anderson, D. R. (2010) Model selection bias and Freedman's paradox. Annals of the Institute of Statistical Mathematics, **62**: 117-125.

Lukacs, P. M., Thompson, W. L., Kendall, W. L., Gould, W. R., Doherty, P. F., Jr., Burnham, K. P. & Anderson, D. R. (2007) Concerns regarding a call for pluralism of information theory and hypothesis testing. Journal of Applied Ecology, **44**: 456-460.

Luong, L. T., Vigliotti, B. A. & Hudson, P. J. (2011) Strong density-dependent competition and acquired immunity constrain parasite establishment: Implications for parasite aggregation. International Journal for Parasitology, **41**: 505-511.

Maillard, J. C. & Gonzalez, J. P. (2006) Biodiversity and emerging diseases. Ann N Y Acad Sci, **1081**: 1-16.

Major, R. (2009) Southern Corroboree Frog *Pseudophryne corroboree* - critically endangered species listing. In: Department of the Environment, C. C. a. W. (Ed.). Canberra, Australian Government.

Mangoni, M. L., Miele, R., Renda, T. G., Barra, D. & Simmaco, M. (2001) The synthesis of antimicrobial peptides in the skin of *Rana esculenta* is stimulated by microorganisms. Faseb Journal, **15**: 1431-+.

Marioni, J. C., Mason, C. E., Mane, S. M., Stephens, M. & Gilad, Y. (2008) RNA-seq: An assessment of technical reproducibility and comparison with gene expression arrays. Genome Research, **18**: 1509-1517.

Marr, S., Morales, H., Bottaro, A., Cooper, M., Flajnik, M. & Robert, J. (2007) Localization and differential expression of Activation-Induced Cytidine Deaminase in the amphibian

Xenopus upon antigen stimulation and during early development. Journal of Immunology, **179**: 6783-6789.

Martel, A., Spitzen-van der Sluijs, A., Blooi, M., Bert, W., Ducatelle, R., Fisher, M. C., Woeltjes, A., Bosman, W., Chiers, K., Bossuyt, F. & Pasmans, F. (2013) *Batrachochytrium salamandrivorans* sp nov causes lethal chytridiomycosis in amphibians. Proceedings of the National Academy of Sciences of the United States of America, **110**: 15325-15329.

Martel, A., Van Rooij, P., Vercauteren, G., Baert, K., Van Waeyenberghe, L., Debacker, P., Garner, T. W. J., Woeltjes, T., Ducatelle, R., Haesebrouck, F. & Pasmans, F. (2011) Developing a safe antifungal treatment protocol to eliminate *Batrachochytrium dendrobatidis* from amphibians. Medical Mycology, **49**: 143-149.

May, R. M. & Anderson, R. M. (1979) Population biology of infectious diseases: Part II. Nature, **280**: 455-461.

May, S. & Beebee, T. J. C. (2009) Characterisation of major histocompatibility complex class II alleles in the natterjack toad, *Bufo calamita*. Conservation Genetics Resources, **1**: 415-417.

May, S., Zeisset, I. & Beebee, T. J. C. (2011) Larval fitness and immunogenetic diversity in chytrid-infected and uninfected natterjack toad (*Bufo calamita*) populations. Conservation Genetics, **12**: 805-811.

McCallum, H. (2012) Disease and the dynamics of extinction. Philosophical Transactions of the Royal Society B-Biological Sciences, **367**: 2828-2839.

McCallum, H., Barlow, N. & Hone, J. (2001) How should pathogen transmission be modelled? Trends in Ecology & Evolution, **16**: 295-300.

McClintock, B. T., Nichols, J. D., Bailey, L. L., MacKenzie, D. I., Kendall, W. L. & Franklin, A. B. (2010) Seeking a second opinion: uncertainty in disease ecology. Ecology Letters, **13**: 659-674.

McCrea, R. S. & Morgan, B. J. T. (2011) Multistate Mark-Recapture model selection using score tests. Biometrics, **67**: 234-241.

McDonald, K. & Alford, R. A. (1999) A review of declining frogs in northern Queensland. In: Campbell, A. (Eds.) *Declines and disappearances of Australian frogs.* Canberra, Environment Australia.

McDonald, K. R., Mendez, D., Muller, R., Freeman, A. B. & Speare, R. (2005) Decline in the prevalence of chytridiomycosis in frog populations in North Queensland, Australia. Pacific Conservation Biology, **11**: 114-120.

McKelvey, K. S., Aubry, K. B. & Schwartz, M. K. (2008) Using anecdotal occurrence data for rare or elusive species: The illusion of reality and a call for evidentiary standards. Bioscience, **58**: 549-555.

McLachlan, J. S., Hellmann, J. J. & Schwartz, M. W. (2007) A framework for debate of assisted migration in an era of climate change. Conservation Biology, **21**: 297-302.

McMahon, T. A., Brannelly, L. A., Chatfield, M. W. H., Johnson, P. T. J., Joseph, M. B., McKenzie, V. J., Richards-Zawacki, C. L., Venesky, M. D. & Rohr, J. R. (2013a) Chytrid fungus *Batrachochytrium dendrobatidis* has nonamphibian hosts and releases chemicals that cause pathology in the absence of infection. Proceedings of the National Academy of Sciences of the United States of America, **110**: 210-215.

McMahon, T. A., Romansic, J. M. & Rohr, J. R. (2013b) Nonmonotonic and monotonic effects of pesticides on the pathogenic fungus *Batrachochytrium dendrobatidis* in culture and on tadpoles. Environmental Science & Technology, **47**: 7958-7964.

McMahon, T. A., Sears, B. F., Venesky, M. D., Bessler, S. M., Brown, J. M., Deutsch, K., Halstead, N. T., Lentz, G., Tenouri, N., Young, S., Civitello, D. J., Ortega, N., Fites, J. S., Reinert, L. K., Rollins-Smith, L. A., Raffel, T. R. & Rohr, J. R. (2014) Amphibians acquire resistance to live and dead fungus overcoming fungal immunosuppression. Nature, **511**: 224-227.

Mechkarska, M., Meetani, M., Michalak, P., Vaksman, Z., Takada, K. & Conlon, J. M. (2012) Hybridization between the African clawed frogs *Xenopus laevis* and *Xenopus muelleri* (*Pipidae*) increases the multiplicity of antimicrobial peptides in skin secretions of female offspring. Comparative Biochemistry and Physiology D-Genomics & Proteomics, **7**: 285-291.

Mendelson, J. R., III, Lips, K. R., Gagliardo, R. W., Rabb, G. B., Collins, J. P., Diffendorfer, J. E., Daszak, P., Ibanez D, R., Zippel, K. C., Lawson, D. P., Wright, K. M., Stuart, S. N., Gascon, C., da Silva, H. R., Burrowes, P. A., Joglar, R. L., La Marca, E., Loetters, S., du Preez, L. H., Weldon, C., Hyatt, A., Rodriguez-Mahecha, J. V., Hunt, S., Robertson, H., Lock, B., Raxworthy, C. J., Frost, D. R., Lacy, R. C., Alford, R. A., Campbell, J. A., Parra-Olea, G., Bolanos, F., Calvo Domingo, J. J., Halliday, T., Murphy, J. B., Wake, M. H., Coloma, L. A., Kuzmin, S. L., Price, M. S., Howell, K. M., Lau, M., Pethiyagoda, R., Boone, M., Lannoo, M. J., Blaustein, A. R., Dobson, A., Griffiths, R. A., Crump, M. L., Wake, D. B. & Brodie, E. D., Jr. (2006) Biodiversity - Confronting amphibian declines and extinctions. Science, **313**: 48-48.

Merianos, A. (2007) Surveillance and response to disease emergence. Current Topics in Microbiology and Immunology: Wildlife and Emerging Zoonotic Diseases: The Biology, Circumstances and Consequences of Cross-Species Transmission, **315**: 477-509.

Meyer, D. & Thomson, G. (2001) How selection shapes variation of the human major histocompatibility complex: a review. Annals of Human Genetics, **65**: 1-26.

Micallef, L. & Rodgers, P. (2014) eulerAPE: Drawing Area-Proportional 3-Venn Diagrams Using Ellipses. Plos One, **9**: 18.

Miedaner, T. & Korzun, V. (2012) Marker-Assisted Selection for disease resistance in wheat and barley breeding. Phytopathology, **102**: 560-566.

Mills, J. N. (2006) Biodiversity loss and emerging infectious disease: An example from the rodent-borne hemorrhagic fevers. Biodiversity, **7**: 9-17.

Morens, D. M., Folkers, G. K. & Fauci, A. S. (2004) The challenge of emerging and re-emerging infectious diseases. Nature, **430**: 242-249.

Morgan, A. A. & Rubenstein, E. (2013) Proline: The distribution, frequency, positioning, and common functional roles of proline and polyproline sequences in the human proteome. Plos One, **8**.

Morgan, J. A. T., Vredenburg, V. T., Rachowicz, L. J., Knapp, R. A., Stice, M. J., Tunstall, T., Bingham, R. E., Parker, J. M., Longcore, J. E., Moritz, C., Briggs, C. J. & Taylor, J. W. (2007) Population genetics of the frog-killing fungus *Batrachochytrium dendrobatidis*. Proceedings of the National Academy of Sciences of the United States of America, **104**: 13845-13850.

Morner, T., Obendorf, D. L., Artois, M. & Woodford, M. H. (2002) Surveillance and monitoring of wildlife diseases. Rev Sci Tech, **21**: 67-76.

Morton, C. O., dos Santos, S. C. & Coote, P. (2007) An amphibian-derived, cationic, alpha-helical antimicrobial peptide kills yeast by caspase-independent but AIF-dependent programmed cell death. Molecular Microbiology, **65**: 494-507.

Moss, A. S., Carty, N. & Francisco, M. J. S. (2010) Identification and partial characterization of an elastolytic protease in the amphibian pathogen *Batrachochytrium dendrobatidis*. Diseases of Aquatic Organisms, **92**: 149-158.

Moss, A. S., Reddy, N. S., DortaJ, I. M. & Francisco, M. J. S. (2008) Chemotaxis of the amphibian pathogen *Batrachochytrium dendrobatidis* and its response to a variety of attractants. Mycologia, **100**: 1-5.

Muletz, C. R., Myers, J. M., Domangue, R. J., Herrick, J. B. & Harris, R. N. (2012) Soil bioaugmentation with amphibian cutaneous bacteria protects amphibian hosts from infection by *Batrachochytrium dendrobatidis*. Biological Conservation, **152**: 119-126.

Mundry, R. (2011) Issues in information theory-based statistical inference-a commentary from a frequentist's perspective. Behavioral Ecology and Sociobiology, **65**: 57-68.

Murphy, K. P. (2012) Janeway's Immunobiology, New York, Garland Science.

Murphy, P. J., St-Hilaire, S. & Corn, P. S. (2011) Temperature, hydric environment, and prior pathogen exposure alter the experimental severity of chytridiomycosis in boreal toads. Diseases of Aquatic Organisms, **95**: 31-42.

Murray, K. & Conner, M. M. (2009) Methods to quantify variable importance: implications for the analysis of noisy ecological data. Ecology, **90**: 348-355.

Murray, K. A., Retallick, R. W. R., McDonald, K., Mendez, D., Aplin, K., Kirkpatrick, P., Berger, L., Hunter, D., Hines, H. B., Campbell, R., Pauza, M., Driessen, M., Speare, R., Richards, S. J., Mahony, M., Freeman, A., Phillott, A. D., Hero, J. M., Kriger, K., Driscoll, D., Felton, A., Puschendorf, R. & Skerratt, L. F. (2010a) The distribution and host range of the pandemic disease chytridiomycosis in Australia, spanning surveys from 1956-2007. Ecology, **91**: 1557.

Murray, K. A., Retallick, R. W. R., Puschendorf, R., Skerratt, L. F., Rosauer, D., McCallum, H. I., Berger, L., Speare, R. & VanDerWal, J. (2011a) Assessing spatial patterns of disease risk to biodiversity: implications for the management of the amphibian pathogen, *Batrachochytrium dendrobatidis*. Journal of Applied Ecology, **48**: 163-173.

Murray, K. A., Rosauer, D., McCallum, H. & Skerratt, L. F. (2011b) Integrating species traits with extrinsic threats: closing the gap between predicting and preventing species declines. Proceedings of the Royal Society B-Biological Sciences, **278**: 1515-1523.

Murray, K. A. & Skerratt, L. F. (2012) Predicting wild hosts for amphibian chytridiomycosis: integrating host life-history traits with pathogen environmental requirements. Human and Ecological Risk Assessment, **18**: 200-224.

Murray, K. A., Skerratt, L. F., Garland, S., Kriticos, D. & McCallum, H. (2013) Whether the weather drives patterns of endemic amphibian chytridiomycosis: a pathogen proliferation approach. Plos One, **8**: 11.

Murray, K. A., Skerratt, L. F., Speare, R. & McCallum, H. (2009) Impact and dynamics of disease in species threatened by the amphibian chytrid fungus, *Batrachochytrium dendrobatidis*. Conservation Biology, **23**: 1242-1252.

Murray, K. A., Skerratt, L. F., Speare, R. & McCallum, H. (2010b) Evidence of effects of endemic chytridiomycosis on host survival, behavior, and emigration: Reply to Schmidt. Conservation Biology, **24**: 900-902.

Murrell, B., Wertheim, J. O., Moola, S., Weighill, T., Scheffler, K. & Pond, S. L. K. (2012) Detecting individual sites subject to episodic diversifying selection. Plos Genetics, **8**.

Muths, E., Scherer, R. D. & Pilliod, D. S. (2011) Compensatory effects of recruitment and survival when amphibian populations are perturbed by disease. Journal of Applied Ecology, **48**: 873-879.

Myers, J. M., Ramsey, J. P., Blackman, A. L., Nichols, A. E., Minbiole, K. P. C. & Harris, R. N. (2012) Synergistic inhibition of the lethal fungal pathogen *Batrachochytrium dendrobatidis*: The combined effect of symbiotic bacterial metabolites and antimicrobial peptides of the frog *Rana muscosa*. Journal of Chemical Ecology, **38**: 958-965.

Nakagawa, S. & Freckleton, R. P. (2011) Model averaging, missing data and multiple imputation: a case study for behavioural ecology. Behavioral Ecology and Sociobiology, **65**: 103-116.

Nakamura, T., Sekizawa, A., Fujii, T. & Katagiri, C. (1986) Cosegregation of the polymorphic-C4 with the MHC in the frog, *Xenopus laevis*. Immunogenetics, **23**: 181-186.

Newell, D. A., Goldingay, R. L. & Brooks, L. O. (2013) Population recovery following decline in an endangered stream-breeding frog (*Mixophyes fleayi*) from subtropical Australia. Plos One, **8**: 8.

Ni, Y., Xie, G. X. & Jia, W. (2014) Metabonomics of human colorectal cancer: new approaches for early diagnosis and biomarker discovery. Journal of Proteome Research, **13**: 3857-3870.

Nichols, D. K. & Lamirande, E. W. (2000) Treatment of cutaneous chytridiomycosis in blue-and-yellow poison dart frogs (*Dendrobates tinctorius*). (Eds.) *Getting the Jump! on Amphibian Disease: Conference and Workshop Compendium.* Cairns.

Nichols, D. K., Lamirande, E. W., Pessier, A. P. & Longcore, J. E. (2001) Experimental transmission of cutaneous chytridiomycosis in dendrobatid frogs. Journal of Wildlife Diseases, **37**: 1-11.

Nicolas, P. & Mor, A. (1995) Peptides as weapons against microorganisms in the chemical defense system of vertebrates. Annual Review of Microbiology, **49**: 277-304.

Niin, E., Laine, M., Guiot, A. L., Demerson, J. M. & Cliquet, F. (2008) Rabies in Estonia: Situation before and after the first campaigns of oral vaccination of wildlife with SAG2 vaccine bait. Vaccine, **26**: 3556-3565.

Normile, D. (2010) Convention on Biological Diversity: UN Biodiversity Summit Yields Welcome and Unexpected Progress. Science, **330**: 742-743.

Obendorf, D. (2005) Draft report for the Australian Government Department of the Environment and Heritage: Application of field and diagnostic methods to survey for chytridiomycosis in Tasmanian frogs. In: Department of the Environment and Heritage (Ed.). Hobart, Central North Field Naturalists Inc. Tasmania, Australia.

Ochman, H., Gerber, A. S. & Hartl, D. L. (1988) Genetic applications of an inverse polymerase chain-reaction. Genetics, **120**: 621-623.

Odds, F. C., Gow, N. A. R. & Brown, A. J. P. (2001) Fungal virulence studies come of age. Genome Biology, **2**: 1009.

Ohta, Y. & Flajnik, M. (2006) IgD, like IgM, is a primordial immunoglobulin class perpetuated in most jawed vertebrates. Proceedings of the National Academy of Sciences of the United States of America, **103**: 10723-10728.

OIE (2010) Training manual on wildlife diseases and surveillance. *Workshop for OIE national focal points for wildlife.* Paris, France, World Organisation for Animal Health (OIE).

Olson, D. H., Aanensen, D. M., Ronnenberg, K. L., Powell, C. I., Walker, S. F., Bielby, J., Garner, T. W. J., Weaver, G., Fisher, M. C. & Bd Mapping, G. (2013) Mapping the global emergence of *Batrachochytrium dendrobatidis*, the amphibian chytrid fungus. Plos One, **8**: 13.

Ostfeld, R. S. (2009) Biodiversity loss and the rise of zoonotic pathogens. Clinical Microbiology and Infection, **15**: 40-43.

Ostrovsky, D. S., Snyder, J. A., Iwata, T., Izaka, K. I., Maglott, D. S. & Nace, G. W. (1976) Frog lysozyme. I. Its identification, occurrence as isozymes, and quantitative distribution in tissues of the leopard frog, *Rana pipiens*. Journal of Experimental Zoology, **195**: 279-290.

Parker, J. M., Mikaelian, I., Hahn, N. & Diggs, H. E. (2002) Clinical diagnosis and treatment of epidermal chytridiomycosis in African clawed frogs (*Xenopus tropicalis*). Comparative Medicine, **52**: 265-268.

Parrish, C. R., Holmes, E. C., Morens, D. M., Park, E.-C., Burke, D. S., Calisher, C. H., Laughlin, C. A., Saif, L. J. & Daszak, P. (2008) Cross-species virus transmission and the emergence of new epidemic diseases. Microbiology and Molecular Biology Reviews, **72**: 457-70.

Pask, J. D., Cary, T. L. & Rollins-Smith, L. A. (2013) Skin peptides protect juvenile leopard frogs (*Rana pipiens*) against chytridiomycosis. Journal of Experimental Biology, **216**: 2908-2916.

Pask, J. D., Woodhams, D. C. & Rollins-Smith, L. A. (2012) The ebb and flow of antimicrobial skin peptides defends northern leopard frogs (*Rana pipiens*) against chytridiomycosis. Global Change Biology, **18**: 1231-1238.

Pavlidis, P. (2003) Using ANOVA for gene selection from microarray studies of the nervous system. Methods, **31**: 282-289.

Pech, R., Byrom, A., Anderson, D. R., Thomson, C. & Coleman, M. (2010) The effect of poisoned and notional vaccinated buffers on possum (*Trichosurus vulpecula*) movements: minimising the risk of bovine tuberculosis spread from forest to farmland. Wildlife Research, **37**: 283-292.

Pessier, A. P., Nichols, D. K., Longcore, J. E. & Fuller, M. S. (1999) Cutaneous chytridiomycosis in poison dart frogs (*Dendrobates spp.*) and White's tree frogs (*Litoria caerulea*). Journal of Veterinary Diagnostic Investigation, **11**: 194-199.

Peterson, J. D., Steffen, J. E., Reinert, L. K., Cobine, P. A., Appel, A., Rollins-Smith, L. & Mendonca, M. T. (2013) Host stress response is important for the pathogenesis of the deadly amphibian disease, chytridiomycosis, in *Litoria caerulea*. Plos One, **8**: 7.

Pettersen, E. F., Goddard, T. D., Huang, C. C., Couch, G. S., Greenblatt, D. M., Meng, E. C. & Ferrin, T. E. (2004) UCSF chimera - A visualization system for exploratory research and analysis. Journal of Computational Chemistry, **25**: 1605-1612.

Pham, C. T. N. (2006) Neutrophil serine proteases: specific regulators of inflammation. Nature Reviews Immunology, **6**: 541-550.

Phillott, A. D., Grogan, L. F., Cashins, S. D., McDonald, K. R., Berger, L. & Skerratt, L. F. (2013) Chytridiomycosis and seasonal mortality of tropical stream-associated frogs 15 years after introduction of *Batrachochytrium dendrobatidis*. Conservation Biology, **27**: 1058-1068.

Phillott, A. D., McDonald, K. R. & Skerratt, L. F. (2010a) Return rates of male hylid frogs *Litoria genimaculata*, *L. nannotis*, *L. rheocola* and *Nyctimystes dayi* after toe-tipping. Endangered Species Research, **11**: 183-188.

Phillott, A. D., Skerratt, L. F., McDonald, K. R., Lemckert, F. L., Hines, H. B., Clarke, J. M., Alford, R. A. & Speare, R. (2007) Toe-clipping as an acceptable method of identifying individual anurans in mark recapture studies. Herpetological Review, **38**: 305-308.

Phillott, A. D., Speare, R., Hines, H. B., Skerratt, L. F., Meyer, E., McDonald, K. R., Cashins, S. D., Mendez, D. & Berger, L. (2010b) Minimising exposure of amphibians to pathogens during field studies. Diseases of Aquatic Organisms, **92**: 175-185.

Picco, A. M. & Collins, J. P. (2008) Amphibian commerce as a likely source of pathogen pollution. Conservation Biology, **22**: 1582-1589.

Pilliod, D. S., Muths, E., Scherer, R. D., Bartelt, P. E., Corn, P. S., Hossack, B. R., Lambert, B. A., McCaffery, R. & Gaughan, C. (2010) Effects of amphibian chytrid fungus on individual survival probability in wild boreal toads. Conservation Biology, **24**: 1259-1267.

Piotrowski, J. S., Annis, S. L. & Longcore, J. E. (2004) Physiology of *Batrachochytrium dendrobatidis*, a chytrid pathogen of amphibians. Mycologia, **96**: 9-15.

Pioz, M., Loison, A., Gauthier, D., Gibert, P., Jullien, J. M., Artois, M. & Gilot-Fromont, E. (2008) Diseases and reproductive success in a wild mammal: example in the alpine chamois. Oecologia, **155**: 691-704.

Polkinghorne, A., Hanger, J. & Timms, P. (2013) Recent advances in understanding the biology, epidemiology and control of chlamydial infections in koalas. Veterinary Microbiology, **165**: 214-223.

Pollock, K. H., Nichols, J. D., Brownie, C. & Hines, J. E. (1990) Statistical-inference for capture-recapture experiments. Wildlife Monographs: 1-97.

Pongsiri, M. J., Roman, J., Ezenwa, V. O., Goldberg, T. L., Koren, H. S., Newbold, S. C., Ostfeld, R. S., Pattanayak, S. K. & Salkeld, D. J. (2009) Biodiversity loss affects global disease ecology. Bioscience, **59**: 945-954.

Porta, M., Greenland, S. & Last, J. M. (Eds.) (2008) *A Dictionary of Epidemiology,* Oxford, Oxford University Press.

Poulter, R. T. M., Busby, J. N., Bishop, P. J., Butler, M. I. & Speare, R. (2007) Chloramphenicol cures chytridiomycosis. *Amphibian Declines and Chytridiomycosis.* Tempe, Arizona, Translating Science into Urgent Action Conference.

Pradel, R. (1996) Utilization of capture-mark-recapture for the study of recruitment and population growth rate. Biometrics, **52**: 703-709.

Pradel, R., Wintrebert, C. M. A. & Gimenez, O. (2003) A proposal for a goodness-of-fit test to the Arnason-Schwarz multisite capture-recapture model. Biometrics, **59**: 43-53.

Pulliam, J. R. C. (2008) Viral host jumps: moving toward a predictive framework. EcoHealth, **5**: 80-91.

Puschendorf, R., Carnaval, A. C., VanDerWal, J., Zumbado-Ulate, H., Chaves, G., Bolanos, F. & Alford, R. A. (2009) Distribution models for the amphibian chytrid *Batrachochytrium dendrobatidis* in Costa Rica: proposing climatic refuges as a conservation tool. Diversity and Distributions, **15**: 401-408.

Puschendorf, R., Hodgson, L., Alford, R. A., Skerratt, L. F. & VanDerWal, J. (2013) Underestimated ranges and overlooked refuges from amphibian chytridiomycosis. Diversity and Distributions, **19**: 1313-1321.

Puschendorf, R., Hoskin, C. J., Cashins, S. D., McDonald, K., Skerratt, L. F., Vanderwal, J. & Alford, R. A. (2011) Environmental Refuge from Disease-Driven Amphibian Extinction. Conservation Biology, **25**: 956-964.

Rachowicz, L. J. & Briggs, C. J. (2007) Quantifying the disease transmission function: effects of density on *Batrachochytrium dendrobatidis* transmission in the mountain yellow-legged frog *Rana muscosa*. J. Anim. Ecol., **76**: 711-721.

Rachowicz, L. J. & Vredenburg, V. T. (2004) Transmission of *Batrachochytrium dendrobatidis* within and between amphibian life stages. Diseases of Aquatic Organisms, **61**: 75-83.

Raffel, T. R., Michel, P. J., Sites, E. W. & Rohr, J. R. (2010) What drives chytrid infections in newt populations? Associations with substrate, temperature, and shade. Ecohealth, **7**: 526-536.

Raffel, T. R., Rohr, J. R., Kiesecker, J. M. & Hudson, P. J. (2006) Negative effects of changing temperature on amphibian immunity under field conditions. Functional Ecology, **20**: 819-828.

Ragimekula, N., Varadarajula, N. N., Mallapuram, S. P., Gangimeni, G., Reddy, R. K. & Kondreddy, H. R. (2013) Marker assisted selection in disease resistance breeding. Journal of Plant Breeding and Genetics, **1**: 90-109.

Ramsey, J. P., Reinert, L. K., Harper, L. K., Woodhams, D. C. & Rollins-Smith, L. A. (2010) Immune defenses against *Batrachochytrium dendrobatidis*, a fungus linked to global

amphibian declines, in the South African Clawed Frog, *Xenopus laevis*. Infect. Immun., **78**: 3981-3992.

Real, L. A. & Biek, R. (2007) Infectious disease modeling and the dynamics of transmission. Wildlife and Emerging Zoonotic Diseases: The Biology, Circumstances and Consequences of Cross-Species Transmission, **315**: 33-49.

Reeder, N. M. M., Pessier, A. P. & Vredenburg, V. T. (2012) A reservoir species for the emerging amphibian pathogen *Batrachochytrium dendrobatidis* thrives in a landscape decimated by disease. Plos One, **7**: 7.

Reiner, G., Fresen, C., Bronnert, S. & Willems, H. (2009) Porcine Reproductive and Respiratory Syndrome Virus (PRRSV) infection in wild boars. Veterinary Microbiology, **136**: 250-258.

Relman, D. A. (2013) Metagenomics, infectious disease diagnostics, and outbreak investigations: Sequence first, ask questions later? Journal of the American Medical Association, **309**: 1531-1532.

Relyea, R. A. & Diecks, N. (2008) An unforeseen chain of events: Lethal effects of pesticides on frogs at sublethal concentrations. Ecological Applications, **18**: 1728-1742.

Retallick, R. W. R., McCallum, H. & Speare, R. (2004) Endemic infection of the amphibian chytrid fungus in a frog community post-decline. Plos Biology, **2**: 1965-1971.

Retallick, R. W. R. & Miera, V. (2007) Strain differences in the amphibian chytrid *Batrachochytrium dendrobatidis* and non-permanent, sub-lethal effects of infection. Diseases of Aquatic Organisms, **75**: 201-207.

Reznick, D., Bryant, M. J. & Bashey, F. (2002) r- and K-selection revisited: The role of population regulation in life-history evolution. Ecology, **83**: 1509-1520.

Ribas, L., Li, M. S., Doddington, B. J., Robert, J., Seidel, J. A., Kroll, J. S., Zimmerman, L. B., Grassly, N. C., Garner, T. W. J. & Fisher, M. C. (2009) Expression profiling the temperature-dependent amphibian response to infection by *Batrachochytrium dendrobatidis*. PLoS One, **4**: Article No.: e8408.

Ricardo, H. (2006) Distribution and ecology of chytrid in Tasmania (Honours Thesis). Hobart, University of Tasmania.

Richards-Zawacki, C. L. (2010) Thermoregulatory behaviour affects prevalence of chytrid fungal infection in a wild population of Panamanian golden frogs. Proceedings of the Royal Society B-Biological Sciences, **277**: 519-528.

Richards, S. A. (2005) Testing ecological theory using the information-theoretic approach: Examples and cautionary results. Ecology, **86**: 2805-2814.

Richards, S. A. (2008) Dealing with overdispersed count data in applied ecology. Journal of Applied Ecology, **45**: 218-227.

Richards, S. A., Whittingham, M. J. & Stephens, P. A. (2011) Model selection and model averaging in behavioural ecology: the utility of the IT-AIC framework. Behavioral Ecology and Sociobiology, **65**: 77-89.

Richards, S. J., McDonald, K. R. & Alford, R. A. (1993) Declines in populations of Australia's endemic tropical rainforest frogs. Pacific Conservation Biology, **1**: 66-77.

Richardson, L. & Loomis, J. (2009) The total economic value of threatened, endangered and rare species: An updated meta-analysis. Ecol Econ, **68**: 1535-1548.

Richmond, J. Q., Savage, A. E., Zamudio, K. R. & Rosenblum, E. B. (2009) Toward immunogenetic studies of amphibian chytridiomycosis: linking innate and acquired immunity. Bioscience, **59**: 311-320.

Rivas, L. R. (1964) A reinterpretation of the concepts "sympatric" and "allopatric" with proposal of the additional terms "syntopic" and "allotopic". Systematic Zoology, **13**: 42-43.

Robbins, A. H., Borden, M. D., Windmiller, B. S., Niezgoda, M., Marcus, L. C., O'Brien, S. M., Kreindel, S. M., McGuill, M. W., DeMaria, A., Rupprecht, C. E. & Rowell, S. (1998) Prevention of the spread of rabies to wildlife by oral vaccination of raccoons in Massachusetts. Journal of the American Veterinary Medical Association, **213**: 1407-1412.

Robert, J. & Ohta, Y. (2009) Comparative and Developmental Study of the Immune System in Xenopus. Developmental Dynamics, **238**: 1249-1270.

Robertson, L. S. & Cornman, R. S. (2014) Transcriptome resources for the frogs *Lithobates clamitans* and *Pseudacris regilla*, emphasizing antimicrobial peptides and conserved loci for phylogenetics. Molecular Ecology Resources, **14**: 178-183.

Robinson, M. D., McCarthy, D. J. & Smyth, G. K. (2010a) edgeR: a Bioconductor package for differential expression analysis of digital gene expression data. Bioinformatics, **26**: 139-140.

Robinson, R. A., Lawson, B., Toms, M. P., Peck, K. M., Kirkwood, J. K., Chantrey, J., Clatworthy, I. R., Evans, A. D., Hughes, L. A., Hutchinson, O. C., John, S. K., Pennycott, T. W., Perkins, M. W., Rowley, P. S., Simpson, V. R., Tyler, K. M. & Cunningham, A. A. (2010b) Emerging infectious disease leads to rapid population declines of common British birds. PLoS One, **5**: e12215.

Rocke, T. E., Smith, S., Marinari, P., Kreeger, J., Enama, J. T. & Powel, B. S. (2008) Vaccination with F1-V fusion protein protects black-footed ferrets (*Mustela nigripes*) against plague upon oral challenge with *Yersinia pestis*. Journal of Wildlife Diseases, **44**: 1-7.

Rohr, J. R., Raffel, T. R., Blaustein, A. R., Johnson, P. T., Paull, S. H. & Young, S. (2013) Using physiology to understand climate-driven changes in disease and their implications for conservation. Conservation Physiology, **1**: cot022.

Rollins-Smith, L. A. (1998) Metamorphosis and the amphibian immune system. Immunological Reviews, **166**: 221-230.

Rollins-Smith, L. A. (2009) The role of amphibian antimicrobial peptides in protection of amphibians from pathogens linked to global amphibian declines. Biochimica Et Biophysica Acta-Biomembranes, **1788**: 1593-1599.

Rollins-Smith, L. A., Carey, C., Conlon, J. M., Reinert, L. K., Doersam, J. K., Bergman, T., Silberring, J., Lankinen, H. & Wade, D. (2003) Activities of temporin family peptides against the chytrid fungus (*Batrachochytrium dendrobatidis*) associated with global amphibian declines. Antimicrobial Agents and Chemotherapy, **47**: 1157-1160.

Rollins-Smith, L. A., Carey, C., Longcore, J., Doersam, J. K., Boutte, A., Bruzgal, J. E. & Conlon, J. M. (2002a) Activity of antimicrobial skin peptides from ranid frogs against *Batrachochytrium dendrobatidis*, the chytrid fungus associated with global amphibian declines. Developmental and Comparative Immunology, **26**: 471-479.

Rollins-Smith, L. A., King, J. D., Nielsen, P. F., Sonnevend, A. & Conlon, J. M. (2005a) An antimicrobial peptide from the skin secretions of the mountain chicken frog *Leptodactylus fallax* (*Anura : Leptodactylidae*). Regulatory Peptides, **124**: 173-178.

Rollins-Smith, L. A., Ramsey, J. P., Pask, J. D., Reinert, L. K. & Woodhams, D. C. (2011) Amphibian immune defenses against chytridiomycosis: Impacts of changing environments. Integrative and Comparative Biology, **51**: 552-562.

Rollins-Smith, L. A., Ramsey, J. P., Reinert, L. K., Woodhams, D. C., Livo, L. J. & Carey, C. (2009) Immune defenses of *Xenopus laevis* against *Batrachochytrium dendrobatidis*. Frontiers in Bioscience, **S1**: 68-91.

Rollins-Smith, L. A., Reinert, L. K., Miera, V. & Conlon, J. M. (2002b) Antimicrobial peptide defenses of the Tarahumara frog, *Rana tarahumarae*. Biochemical and Biophysical Research Communications, **297**: 361-367.

Rollins-Smith, L. A., Reinert, L. K., O'Leary, C. J., Houston, L. E. & Woodhams, D. C. (2005b) Antimicrobial peptide defenses in amphibian skin. Integrative and Comparative Biology, **45**: 137-142.

Rollins-Smith, L. A. & Woodhams, D. C. (2012) Chapter 4 Amphibian Immunity Staying in tune with the environment. In: Demas, G. E. & Nelson, R. J. (Eds.) *Ecoimmunology*. New York, Oxford University Press.

Rollins-Smith, L. A., Woodhams, D. C., Reinert, L. K., Vredenburg, V. T., Briggs, C. J., Nielsen, P. F. & Conlon, J. M. (2006) Antimicrobial peptide defenses of the mountain

yellow-legged frog (*Rana muscosa*). Developmental and Comparative Immunology, **30**: 831-842.

Ron, E. Z. (2010) Distribution and evolution of virulence factors in septicemic *Escherichia coli*. International Journal of Medical Microbiology, **300**: 367-370.

Rosenblum, E. B., Poorten, T. J., Joneson, S. & Settles, M. (2012a) Substrate-specific gene expression in *Batrachochytrium dendrobatidis*, the chytrid pathogen of amphibians. Plos One, **7**: 10.

Rosenblum, E. B., Poorten, T. J., Settles, M. & Murdoch, G. K. (2012b) Only skin deep: shared genetic response to the deadly chytrid fungus in susceptible frog species. Molecular Ecology, **21**: 3110-3120.

Rosenblum, E. B., Poorten, T. J., Settles, M., Murdoch, G. K., Robert, J., Maddox, N. & Eisen, M. B. (2009) Genome-wide transcriptional response of *Silurana (Xenopus) tropicalis* to infection with the deadly chytrid fungus. PLOS One, **4**: e6494. doi:10.1371/journal.pone.0006494.

Rossi, S., Toigo, C., Hars, J., Pol, F., Hamann, J.-L., Depner, K. & Le Potier, M.-F. (2011) New insights on the management of wildlife diseases using multi-state recapture models: the case of classical swine fever in wild boar. PLoS One, **6**: e24257.

Rousset, F. (2008) GENEPOP ' 007: a complete re-implementation of the GENEPOP software for Windows and Linux. Molecular Ecology Resources, **8**: 103-106.

Rovito, S. M., Parra-Olea, G., Vasquez-Almazan, C. R., Papenfuss, T. J. & Wake, D. B. (2009) Dramatic declines in neotropical salamander populations are an important part of the global amphibian crisis. Proceedings of the National Academy of Sciences of the United States of America, **106**: 3231-3236.

Rowley, J. J. L. & Alford, R. A. (2007a) Behaviour of Australian rainforest stream frogs may affect the transmission of chytridiomycosis. Diseases of Aquatic Organisms, **77**: 1-9.

Rowley, J. J. L. & Alford, R. A. (2007b) Movement patterns and habitat use of rainforest stream frogs in northern Queensland, Australia: implications for extinction vulnerability. Wildlife Research, **34**: 371-378.

Rowley, J. J. L. & Alford, R. A. (2013) Hot bodies protect amphibians against chytrid infection in nature. Scientific Reports, **3**: 4.

Rowley, J. J. L., Skerratt, L. F., Alford, R. A. & Campbell, R. (2007) Retreat sites of rain forest stream frogs are not a reservoir for *Batrachochytrium dendrobatidis* in northern Queensland, Australia. Diseases of Aquatic Organisms, **74**: 7-12.

Ruthig, G. R. & DeRidder, B. P. (2012) Fast quantitative PCR, locked nucleic acid probes and reduced volume reactions are effective tools for detecting *Batrachochytrium dendrobatidis* DNA. Diseases of Aquatic Organisms, **97**: 249-253.

Ryser-Degiorgis, M.-P. (2013) Wildlife health investigations: needs, challenges and recommendations. Bmc Veterinary Research, **9**: 223-240.

Savage, A. E., Sredl, M. J. & Zamudio, K. R. (2011) Disease dynamics vary spatially and temporally in a North American amphibian. Biological Conservation, **144**: 1910-1915.

Savage, A. E. & Zamudio, K. R. (2011) MHC genotypes associate with resistance to a frog-killing fungus. Proceedings of the National Academy of Sciences of the United States of America, **108**: 16705-16710.

Scheele, B. C., Hunter, D. A., Grogan, L. F., Berger, L., Kolby, J. E., McFadden, M. S., Marantelli, G., Skerratt, L. F. & Driscoll, D. A. (2014) Interventions for reducing extinction risk in chytridiomycosis-threatened amphibians. Conservation Biology, **28**: 1195-1205.

Scheffler, K., Martin, D. P. & Seoighe, C. (2006) Robust inference of positive selection from recombining coding sequences. Bioinformatics, **22**: 2493-2499.

Schiesari, L., Grillitsch, B. & Grillitsch, H. (2007) Biogeographic biases in research and their consequences for linking amphibian declines to pollution. Conservation Biology, **21**: 465-471.

Schloegel, L. M., Ferreira, C. M., James, T. Y., Hipolito, M., Longcore, J. E., Hyatt, A. D., Yabsley, M., Martins, A., Mazzoni, R., Davies, A. J. & Daszak, P. (2010) The North American bullfrog as a reservoir for the spread of *Batrachochytrium dendrobatidis* in Brazil. Animal Conservation, **13**: 53-61.

Schloegel, L. M., Hero, J. M., Berger, L., Speare, R., McDonald, K. & Daszak, P. (2006) The decline of the sharp-snouted day frog (*Taudactylus acutirostris*): The first documented case of extinction by infection in a free-ranging wildlife species? Ecohealth, **3**: 35-40.

Schloegel, L. M., Picco, A. M., Kilpatrick, A. M., Davies, A. J., Hyatt, A. D. & Daszak, P. (2009) Magnitude of the US trade in amphibians and presence of *Batrachochytrium dendrobatidis* and ranavirus infection in imported North American bullfrogs (*Rana catesbeiana*). Biological Conservation, **142**: 1420-1426.

Schmidt, B. R. (2010) Estimating the impact of disease in species threatened by amphibian chytrid fungus: Comment on Murray et al. Conservation Biology, **24**: 897-899.

Scholes, R. J., Mace, G. M., Turner, W., Geller, G. N., Jurgens, N., Larigauderie, A., Muchoney, D., Walther, B. A. & Mooney, H. A. (2008) Toward a global biodiversity observing system. Science, **321**: 1044-1045.

Schwarz, G. (1978) Estimating the dimension of a model. Annals of Statistics, **6**: 461-464.

Schwinger, G., Zanger, K. & Greven, H. (2001) Structural and mechanical aspects of the skin of *Bufo marinus* (*Anura, Amphibia*). Tissue & Cell, **33**: 541-547.

Scott, M. E. (1988) The impact of infection and disease on animal populations: implications for conservation biology. Conservation Biology, **2**: 40-56.

Screaton, G. R., Xu, X. N., Olsen, A. L., Cowper, A. E., Tan, R. S., McMichael, A. J. & Bell, J. I. (1997) LARD: A new lymphoid-specific death domain containing receptor regulated by alternative pre-mRNA splicing. Proceedings of the National Academy of Sciences of the United States of America, **94**: 4615-4619.

Searle, C. L., Gervasi, S. S., Hua, J., Hammond, J. I., Relyea, R. A., Olson, D. H. & Blaustein, A. R. (2011) Differential host susceptibility to *Batrachochytrium dendrobatidis*, an emerging amphibian pathogen. Conservation Biology, **25**: 965-974.

Seber, G. A. F. (1965) A note on multiple-recapture census. Biometrika, **52**: 249.

Senar, J. C. & Conroy, M. J. (2004) Multi-state analysis of the impacts of avian pox on a population of Serins (*Serinus serinus*): the importance of estimating recapture rates. Anim. Biodivers. Conserv., **27**: 133-146.

Shoo, L. P., Olson, D. H., McMenamin, S. K., Murray, K. A., Van Sluys, M., Donnelly, M. A., Stratford, D., Terhivuo, J., Merino-Viteri, A., Herbert, S. M., Bishop, P. J., Corn, P. S., Dovey, L., Griffiths, R. A., Lowe, K., Mahony, M., McCallum, H., Shuker, J. D., Simpkins, C., Skerratt, L. F., Williams, S. E. & Hero, J. M. (2011) Engineering a future for amphibians under climate change. Journal of Applied Ecology, **48**: 487-492.

Skelly, D. K., Freidenburg, L. K. & Kiesecker, J. M. (2002) Forest canopy and the performance of larval amphibians. Ecology, **83**: 983-992.

Skerka, C., Chen, Q., Fremeaux-Bacchi, V. & Roumenina, L. T. (2013) Complement factor H related proteins (CFHRs). Molecular Immunology, **56**: 170-180.

Skerratt, L., Speare, R. & Berger, L. (2011a) Mitigating the impact of diseases affecting biodiversity - retrospective on the outbreak investigation for chytridiomycosis. Ecohealth, **7**: S26-S26.

Skerratt, L. F., Berger, L., Hines, H. B., McDonald, K. R., Mendez, D. & Speare, R. (2008) Survey protocol for detecting chytridiomycosis in all Australian frog populations. Diseases of Aquatic Organisms, **80**: 85-94.

Skerratt, L. F., Berger, L., Speare, R., Cashins, S., McDonald, K. R., Phillott, A. D., Hines, H. B. & Kenyon, N. (2007) Spread of chytridiomycosis has caused the rapid global decline and extinction of frogs. Ecohealth, **4**: 125-134.

Skerratt, L. F., Garner, T. W. J. & Hyatt, A. D. (2010) Determining causality and controlling disease is based on collaborative research involving multidisciplinary approaches. Ecohealth, **6**: 331-334.

Skerratt, L. F., Mendez, D., McDonald, K. R., Garland, S., Livingstone, J., Berger, L. & Speare, R. (2011b) Validation of diagnostic tests in wildlife: the case of chytridiomycosis in wild amphibians. Journal of Herpetology, **45**: 444-450.

Smith, G. L. & Chan, Y. S. (1991) Two Vaccinia virus proteins structurally related to the Interleukin-1 receptor and the immunoglobulin superfamily. Journal of General Virology, **72**: 511-518.

Smith, K. F., Acevedo-Whitehouse, K. & Pedersen, A. B. (2009a) The role of infectious diseases in biological conservation. Animal Conservation, **12**: 1-12.

Smith, K. F., Sax, D. F. & Lafferty, K. D. (2006) Evidence for the role of infectious disease in species extinction and endangerment. Conservation Biology, **20**: 1349-1357.

Smith, K. G. (2007) Use of quantitative PCR assay for amphibian chytrid detection: comment on Kriger et al. (2006a,b). Diseases of Aquatic Organisms, **73**: 253-255.

Smith, K. G., Lips, K. R. & Chase, J. M. (2009b) Selecting for extinction: nonrandom disease-associated extinction homogenizes amphibian biotas. Ecology Letters, **12**: 1069-1078.

Smith, K. G., Weldon, C., Conradie, W. & du Preez, L. H. (2007) Relationships among size, development, and *Batrachochytrium dendrobatidis* infection in African tadpoles. Diseases of Aquatic Organisms, **74**: 159-164.

Smith, K. L., Hale, J. M., Austin, J. J. & Melville, J. (2011) Isolation and characterization of microsatellite markers for the *Litoria ewingii* complex and their use in conservation and hybridization studies. Conservation Genetics Resources, **3**: 621-624.

Soorae, P. S. (2010) Global Re-introduction perspectives: additional case-studies from around the globe., Abu Dhabi, UAE, IUCN/SSC Re-introduction Specialist Group.

Soto-Azat, C., Clarke, B. T., Poynton, J. C. & Cunningham, A. A. (2010) Widespread historical presence of *Batrachochytrium dendrobatidis* in African pipid frogs. Diversity and Distributions, **16**: 126-131.

Spangenberg, J. H. & Settele, J. (2010) Precisely incorrect? Monetising the value of ecosystem services. Ecological Complexity, **7**: 327-337.

Speare, R. (2006) Background document for the threat abatement plan: infection of amphibians with chytrid fungus resulting in chytridiomycosis. . In: Department of the Environment and Heritage (Ed.). Canberra.

Stallknecht, D. E. (2007) Impediments to wildlife disease surveillance, research, and diagnostics. Current Topics in Microbiology and Immunology: Wildlife and Emerging Zoonotic Diseases: The Biology, Circumstances and Consequences of Cross-Species Transmission, **315**: 445-461.

Steenbergen, J. N. & Casadevall, A. (2003) The origin and maintenance of virulence for the human pathogenic fungus *Cryptococcus neoformans*. Microbes and Infection, **5**: 667-675.

Stephens, C. R., Heau, J. G., Gonzalez, C., Ibarra-Cerdena, C. N., Sanchez-Cordero, V. & Gonzalez-Salazar, C. (2009) Using biotic interaction networks for prediction in biodiversity and emerging diseases. Plos One, **4**: e5725.

Stephens, P. A., Buskirk, S. W. & del Rio, C. M. (2007) Inference in ecology and evolution. Trends in Ecology & Evolution, **22**: 192-197.

Stephens, P. A., Buskirk, S. W., Hayward, G. D. & Del Rio, C. M. (2005) Information theory and hypothesis testing: a call for pluralism. Journal of Applied Ecology, **42**: 4-12.

Stevenson, L. A., Alford, R. A., Bell, S. C., Roznik, E. A., Berger, L. & Pike, D. A. (2013) Variation in thermal performance of a widespread pathogen, the amphibian chytrid fungus *Batrachochytrium dendrobatidis*. Plos One, **8**: 14.

Stice, M. J. & Briggs, C. J. (2010) Immunization is ineffective at preventing infection and mortality due to the amphibian chytrid fungus *Batrachochytrium dendrobatidis*. Journal of Wildlife Diseases, **46**: 70-77.

Stockwell, M. P., Clulow, J. & Mahony, M. J. (2012) Sodium chloride inhibits the growth and infective capacity of the amphibian chytrid fungus and increases host survival rates. Plos One, **7**: 7.

Stockwell, M. P., Clulow, S., Clulow, J. & Mahony, M. (2008) The impact of the amphibian chytrid fungus *Batrachochytrium dendrobatidis* on a Green and Golden Bell Frog *Litoria aurea* reintroduction program at the Hunter Wetlands Centre Australia in the Hunter Region of NSW. Australian Zoologist, **34**: 379-386.

Stone, M. (1974) Cross-validatory choice and assessment of statistical predictions. Journal of the Royal Statistical Society, Series B (Methodological), **36**: 111-147.

Stuart, S. N., Chanson, J. S., Cox, N. A., Young, B. E., Rodrigues, A. S. L., Fischman, D. L. & Waller, R. W. (2004) Status and trends of amphibian declines and extinctions worldwide. Science, **306**: 1783-1786.

Symonds, E. P., Trott, D. J., Bird, P. S. & Mills, P. (2008) Growth characteristics and enzyme activity in *Batrachochytrium dendrobatidis* isolates. Mycopathologia, **166**: 143-147.

Symonds, M. R. E. & Moussalli, A. (2011) A brief guide to model selection, multimodel inference and model averaging in behavioural ecology using Akaike's information criterion. Behavioral Ecology and Sociobiology, **65**: 13-21.

Symons, J. A., Young, P. R. & Duff, G. W. (1995) Soluble type II interleukin 1 (IL-1) receptor binds and blocks processing of IL-1 beta precursor and loses affinity for IL-1 receptor agonist. Proceedings of the National Academy of Sciences of the United States of America, **92**: 1714-1718.

Sztatecsny, M. & Glaser, F. (2011) From the eastern lowlands to the western mountains: first records of the chytrid fungus *Batrachochytrium dendrobatidis* in wild amphibian populations from Austria. Herpetological Journal, **21**: 87-90.

Takeuchi, K. (1976) Distribution of informational statistics and a criterion of model fitting. Suri-Kagaku (Mathematical Sciences), **153**: 12-18.

Tambi, E. N., Maina, O. W., Mukhebi, A. W. & Randolph, T. F. (1999) Economic impact assessment of rinderpest control in Africa. Rev. Sci. Tech. OIE, **18**: 458-477.

Tamukai, K., Une, Y., Tominaga, A., Suzuki, K. & Goka, K. (2011) Treatment of spontaneous chytridiomycosis in captive amphibians using itraconazole. Journal of Veterinary Medical Science, **73**: 155-159.

Tan, K. C., Ipcho, S. V. S., Trengove, R. D., Oliver, R. P. & Solomon, P. S. (2009) Assessing the impact of transcriptomics, proteomics and metabolomics on fungal phytopathology. Molecular Plant Pathology, **10**: 703-715.

Taylor, L. H., Latham, S. M. & Woolhouse, E. J. (2001) Risk factors for human disease emergence. Philosophical Transactions of the Royal Society B-Biological Sciences, **356**: 983-989.

Taylor, S. K., Williams, E. S., Thorne, E. T., Mills, K. W., Withers, D. I. & Pier, A. C. (1999) Causes of mortality of the Wyoming toad. Journal of Wildlife Diseases, **35**: 49-57.

Thomas, S. R. & Elkinton, J. S. (2004) Pathogenicity and virulence. Journal of Invertebrate Pathology, **85**: 146-151.

Thompson, J. D., Higgins, D. G. & Gibson, T. J. (1994) CLUSTAL-W: Improving the sensitivity of progressive multiple sequence alignment through sequence weighting, position-specific gap penalties and weight matrix choice. Nucleic Acids Research, **22**: 4673-4680.

Thorne, E. T. & Williams, E. S. (1988) Disease and endangered species: The black-footed ferret as a recent example. Conservation Biology, **2**: 66-74.

Thulke, H. H., Eisinger, D., Freuling, C., Frohlich, A., Globig, A., Grimm, V., Muller, T., Selhorst, T., Staubach, C. & Zips, S. (2009) Situation-based surveillance: adapting investigations to actual epidemic situations. J Wildl Dis, **45**: 1089-1103.

Thurmond, M. C. (2003) Conceptual foundations for infectious disease surveillance. J Vet Diagn Invest, **15**: 501-514.

Tobler, U., Borgula, A. & Schmidt, B. R. (2012) Populations of a susceptible amphibian species can grow despite the presence of a pathogenic chytrid fungus. Plos One, **7**: 8.

Tobler, U. & Schmidt, B. R. (2010) Within- and among-population variation in chytridiomycosis-induced mortality in the toad *Alytes obstetricians*. *PLoS One.*

Tompkins, D. M., Dunn, A. M., Smith, M. J. & Telfer, S. (2011) Wildlife diseases: from individuals to ecosystems. Journal of Animal Ecology, **80**: 19-38.

Tong, J. C., Bramson, J., Kanduc, D., Chow, S., Sinha, A. A. & Ranganathan, S. (2006) Modeling the bound conformation of *Pemphigus vulgaris*-associated peptides to MHC Class II DR and DQ alleles. Immunome research, **2**: 1-1.

Tozer, C. R., Kiem, A. S. & Verdon-Kidd, D. C. (2011) On the uncertainties associated with using gridded rainfall data as a proxy for observed. Hydrology and Earth System Sciences Discussion, **8**: 8399-8433.

Tusher, V. G., Tibshirani, R. & Chu, G. (2001) Significance analysis of microarrays applied to the ionizing radiation response. Proceedings of the National Academy of Sciences of the United States of America, **98**: 5116-5121.

van den Berg, R. A., Hoefsloot, H. C. J., Westerhuis, J. A., Smilde, A. K. & van der Werf, M. J. (2006) Centering, scaling, and transformations: improving the biological information content of metabolomics data. Bmc Genomics, **7**: 142.

Van Ells, T., Stanton, J., Strieby, A., Daszak, P., Hyatt, A. D. & Brown, C. (2003) Use of immunohistochemistry to diagnose chytridiomycosis in dyeing poison dart frogs (*Dendrobates tinctorius*). Journal of Wildlife Diseases, **39**: 742-745.

Van Rooij, P., Martel, A., D'Herde, K., Brutyn, M., Croubels, S., Ducatelle, R., Haesebrouck, F. & Pasmans, F. (2012) Germ tube mediated invasion of *Batrachochytrium dendrobatidis* in amphibian skin is host dependent. Plos One, **7**: 8.

Vaz, V. C., D'Andrea, P. S. & Jansen, A. M. (2007) Effects of habitat fragmentation on wild mammal infection by *Trypanosoma cruzi*. Parasitology, **134**: 1785-1793.

Venesky, M. D., Mendelson, J. R., Sears, B. F., Stiling, P. & Rohr, J. R. (2012) Selecting for tolerance against pathogens and herbivores to enhance success of reintroduction and translocation. Conservation Biology, **26**: 586-592.

Venesky, M. D., Raffel, T. R., McMahon, T. A. & Rohr, J. R. (2013) Confronting inconsistencies in the amphibian-chytridiomycosis system: implications for disease management. Biological Reviews, **89**: 477-483.

Vieites, D. R., Wollenberg, K. C., Andreone, F., Kohler, J., Glaw, F. & Vences, M. (2009) Vast underestimation of Madagascar's biodiversity evidenced by an integrative amphibian inventory. Proc Natl Acad Sci U S A, **106**: 8267-8272.

Viggers, K. L., Lindenmayer, D. B. & Spratt, D. M. (1993) The importance of disease in reintroduction programs. Wildlife Research, **20**: 687-698.

Vogel, S. W. & Heyne, H. (1996) Rinderpest in South Africa - 100 years ago. Journal of the South African Veterinary Association (Tydskrif van die Suid-Afrikaanse Veterinere) **67**: 164-170.

Voyles, J. (2011) Phenotypic profiling of *Batrachochytrium dendrobatidis*, a lethal fungal pathogen of amphibians. Fungal Ecology, **4**: 196-200.

Voyles, J., Berger, L., Young, S., Speare, R., Webb, R., Warner, J., Rudd, D., Campbell, R. & Skerratt, L. F. (2007) Electrolyte depletion and osmotic imbalance in amphibians with chytridiomycosis. Diseases of Aquatic Organisms, **77**: 113-118.

Voyles, J., Johnson, L. R., Briggs, C. J., Cashins, S. D., Alford, R. A., Berger, L., Skerratt, L. F., Speare, R. & Rosenblum, E. B. (2012) Temperature alters reproductive life history patterns in *Batrachochytrium dendrobatidis*, a lethal pathogen associated with the global loss of amphibians. Ecology and Evolution, **2**: 2241-2249.

Voyles, J., Rosenblum, E. B. & Berger, L. (2011) Interactions between *Batrachochytrium dendrobatidis* and its amphibian hosts: a review of pathogenesis and immunity. Microbes and Infection, **13**: 25-32.

Voyles, J., Young, S., Berger, L., Campbell, C., Voyles, W. F., Dinudom, A., Cook, D., Webb, R., Alford, R. A., Skerratt, L. F. & Speare, R. (2009) Pathogenesis of chytridiomycosis, a cause of catastrophic amphibian declines. Science, **326**: 582-585.

Vrbova, L., Stephen, C., Kasman, N., Boehnke, R., Doyle-Waters, M., Chablitt-Clark, A., Gibson, B., FitzGerald, M. & Patrick, D. M. (2010) Systematic review of surveillance systems for emerging zoonoses. Transbound Emerg Dis, **57**: 154-161.

Vredenburg, V. T. (2004) Reversing introduced species effects: Experimental removal of introduced fish leads to rapid recovery of a declining frog. Proceedings of the National Academy of Sciences of the United States of America, **101**: 7646-7650.

Vredenburg, V. T., Briggs, C. J. & Harris, R. (2011) A18 Host-pathogen dynamics of amphibian chytridiomycosis: the role of the skin microbiome in health and disease. In: Olsen, L., Choffnes, E. R., Relman, D. A. & Pray, L. (Eds.) *Fungal Diseases: An emerging threat to human, animal, and plant health: Workshop summary.* Washington, D.C., The National Academies Press.

Vredenburg, V. T., Knapp, R. A., Tunstall, T. S. & Briggs, C. J. (2010) Dynamics of an emerging disease drive large-scale amphibian population extinctions. Proceedings of the National Academy of Sciences of the United States of America, **107**: 9689-9694.

Waddle, J. H., Rice, K. G., Mazzotti, F. J. & Percival, H. F. (2008) Modeling the effect of toe clipping on treefrog survival: Beyond the return rate. Journal of Herpetology, **42**: 467-473.

Wake, D. B. & Vredenburg, V. T. (2008) Are we in the midst of the sixth mass extinction? A view from the world of amphibians. Proceedings of the National Academy of Sciences of the United States of America, **105**: 11466-11473.

Wang, M. Q., Yang, X., Ren, L. H., Li, S. T., He, X., Wu, X. Y., Liu, T. T., Lin, L. Q., Li, Y. & Sun, C. H. (2014) Biomarkers identified by urinary metabonomics for noninvasive diagnosis of nutritional rickets. Journal of Proteome Research, **13**: 4131-4142.

Wang, Z., Gerstein, M. & Snyder, M. (2009) RNA-Seq: a revolutionary tool for transcriptomics. Nature Reviews Genetics, **10**: 57-63.

Waters, H. (2011) Malaria vaccine cuts risk in half in late-stage trial. Nature Medicine, **17**: 1329-1329.

Watson, R., Albon, S., Aspinall, R., Austen, M., Bardgett, R., Bateman, I., Berry, P., Bird, W., Bradbury, R., Brown, C., Bullock, J., Burgess, J., Church, A., Christie, S., Crute, I., Davies, L., Edwards-Jones, G., Emmett, B., Firbank, L., Fitter, A., Gibson, C., Hails, R., Haines-Young, R., Heathwaite, L., Hopkins, J., Jenkins, M., Jones, L., Mace, G., Malcolm, S., Maltby, E., Maskell, L., Norris, K., Ormerod, S., Osborne, J., Pretty, J., Quine, C., Russell, S., Simpson, L., Smith, P., Tierney, M., Turner, K., van der Wal, R., Vira, B., Walpole, M., Watkinson, A., Weighell, T., Winn, J. & Winter, M. (2011) The UK National Ecosystem Assessment: Synthesis of the Key Findings. Cambridge, UNEP-WCMC.

Weldon, C., du Preez, L. H., Hyatt, A. D., Muller, R. & Speare, R. (2004) Origin of the amphibian chytrid fungus. Emerging Infectious Diseases, **10**: 2100-2105.

Wells, K. D. (2007) The Ecology and Behavior of Amphibians, Chicago, The University of Chicago Press.

Whiles, M. R., Hall, R. O., Jr., Dodds, W. K., Verburg, P., Huryn, A. D., Pringle, C. M., Lips, K. R., Kilham, S. S., Colon-Gaud, C., Rugenski, A. T., Peterson, S. & Connelly, S. (2013) Disease-driven amphibian declines alter ecosystem processes in a tropical stream. Ecosystems, **16**: 146-157.

White, A. W. (2006) A trial using salt to protect green and golden bell frogs from chytrid infection. Herpetofauna, **36**: 93-96.

White, G. C. & Burnham, K. P. (1999) Program MARK: survival estimation from populations of marked animals. Bird Study, **46**: 120-139.

White, G. C., Kendall, W. L. & Barker, R. J. (2006) Multistate survival models and their extensions in Program MARK. Journal of Wildlife Management, **70**: 1521-1529.

Williams, E. S. (2005) Chronic wasting disease. Veterinary Pathology, **42**: 530-549.

Williams, E. S., Yuill, T., Artois, M., Fischer, J. & Haigh, S. A. (2002) Emerging infectious diseases in wildlife. Revue Scientifique Et Technique De L Office International Des Epizooties, **21**: 139-157.

Williams, J. & Crutzen, P. J. (2013) Perspectives on our planet in the Anthropocene. Environmental Chemistry, **10**: 269-280.

Williams, S. E. & Hoffman, E. A. (2009) Minimizing genetic adaptation in captive breeding programs: A review. Biological Conservation, **142**: 2388-2400.

Wilson, K., Bjornstad, O. N., Dobson, A. P., Merler, S., Poglayen, G., Randolph, S. E., Read, A. F. & Skorping, A. (2002) Heterogeneities in macroparasite infections: patterns and processes. In: Hudson, P. J., Rizzoli, A., Grenfell, B. T., Heesterbeek, H. & Dobson, A. P. (Eds.) *The ecology of wildlife diseases.* Oxford, UK, Oxford University Press.

Wobeser, G. (2002) Disease management strategies for wildlife. Revue Scientifique Et Technique De L Office International Des Epizooties, **21**: 159-178.

Wobeser, G. & Wobeser, A. G. (1992) Carcass disappearance and estimation of mortality in a simulated die-off of small birds. Journal of Wildlife Diseases, **28**: 548-554.

Wobeser, G. A. (2007) Disease in Wild Animals: Investigation and Management, New York, Springer.

Woodhams, D. C., Alford, R. A., Briggs, C. J., Johnson, M. & Rollins-Smith, L. A. (2008a) Life-history trade-offs influence disease in changing climates: Strategies of an amphibian pathogen. Ecology, **89**: 1627-1639.

Woodhams, D. C., Alford, R. A. & Marantelli, G. (2003) Emerging disease of amphibians cured by elevated body temperature. Diseases of Aquatic Organisms, **55**: 65-67.

Woodhams, D. C., Ardipradja, K., Alford, R. A., Marantelli, G., Reinert, L. K. & Rollins-Smith, L. A. (2007a) Resistance to chytridiomycosis varies among amphibian species and is correlated with skin peptide defenses. Animal Conservation, **10**: 409-417.

Woodhams, D. C., Bell, S. C., Kenyon, N., Alford, R. A. & Rollins-Smith, L. A. (2012a) Immune evasion or avoidance: Fungal skin infection linked to reduced defence peptides in Australian green-eyed treefrogs, *Litoria serrata*. Fungal Biology, **116**: 1203-1211.

Woodhams, D. C., Bigler, L. & Marschang, R. (2012b) Tolerance of fungal infection in European water frogs exposed to *Batrachochytrium dendrobatidis* after experimental reduction of innate immune defenses. Bmc Veterinary Research, **8**: 11.

Woodhams, D. C., Bosch, J., Briggs, C. J., Cashins, S., Davis, L. R., Lauer, A., Muths, E., Puschendorf, R., Schmidt, B. R., Sheafor, B. & Voyles, J. (2011) Mitigating amphibian disease: strategies to maintain wild populations and control chytridiomycosis. Frontiers in Zoology, **8**: 23.

Woodhams, D. C., Geiger, C. C., Reinert, L. K., Rollins-Smith, L. A., Lam, B., Harris, R. N., Briggs, C. J., Vredenburg, V. T. & Voyles, J. (2012c) Treatment of amphibians infected with chytrid fungus: learning from failed trials with itraconazole, antimicrobial peptides, bacteria, and heat therapy. Diseases of Aquatic Organisms, **98**: 11-25.

Woodhams, D. C., Kenyon, N., Bell, S. C., Alford, R. A., Chen, S., Billheimer, D., Shyr, Y. & Rollins-Smith, L. A. (2010) Adaptations of skin peptide defences and possible response to the amphibian chytrid fungus in populations of Australian green-eyed treefrogs, *Litoria genimaculata*. Diversity and Distributions, **16**: 703-712.

Woodhams, D. C., Kilburn, V. L., Reinert, L. K., Voyles, J., Medina, D., Ibanez, R., Hyatt, A. D., Boyle, D. G., Pask, J. D., Green, D. M. & Rollins-Smith, L. A. (2008b) Chytridiomycosis and Amphibian Population Declines Continue to Spread Eastward in Panama. Ecohealth, **5**: 268-274.

Woodhams, D. C., Rollins-Smith, L. A., Alford, R. A., Simon, M. A. & Harris, R. N. (2007b) Innate immune defenses of amphibian skin: antimicrobial peptides and more. Animal Conservation, **10**: 425-428.

Woodhams, D. C., Rollins-Smith, L. A., Carey, C., Reinert, L., Tyler, M. J. & Alford, R. A. (2006a) Population trends associated with skin peptide defenses against chytridiomycosis in Australian frogs. Oecologia, **146**: 531-540.

Woodhams, D. C., Voyles, J., Lips, K. R., Carey, C. & Rollins-Smith, L. A. (2006b) Predicted disease susceptibility in a panamanian amphibian assemblage based on skin peptide defenses. Journal of Wildlife Diseases, **42**: 207-218.

Woodhams, D. C., Vredenburg, V. T., Simon, M. A., Billheimer, D., Shakhtour, B., Shyr, Y., Briggs, C. J., Rollins-Smith, L. A. & Harris, R. N. (2007c) Symbiotic bacteria contribute to innate immune defenses of the threatened mountain yellow-legged frog, *Rana muscosa*. Biological Conservation, **138**: 390-398.

Woods, C. M., Hooper, D. N., Ooi, E. H., Tan, L. W. & Carney, A. S. (2011) Human lysozyme has fungicidal activity against nasal fungi. American Journal of Rhinology & Allergy, **25**: 236-240.

Woods, J. P. (2003) Knocking on the right door and making a comfortable home: *Histoplasma capsulatum* intracellular pathogenesis. Current Opinion in Microbiology, **6**: 327-331.

Xia, J. G., Mandal, R., Sinelnikov, I. V., Broadhurst, D. & Wishart, D. S. (2012) MetaboAnalyst 2.0-a comprehensive server for metabolomic data analysis. Nucleic Acids Research, **40**: W127-W133.

Yang, H., Baek, H., Speare, R., Webb, R., Park, S., Kim, T., Lasater, K. C., Shin, S., Son, S., Park, J., Min, M., Kim, Y., Na, K. & Lee, H. (2009) First detection of the amphibian chytrid fungus *Batrachochytrium dendrobatidis* in free-ranging populations of amphibians on mainland Asia: survey in South Korea. Diseases of Aquatic Organisms, **86**: 9-13.

Yang, Y. H. (2005) Can the strengths of AIC and BIC be shared? A conflict between model indentification and regression estimation. Biometrika, **92**: 937-950.

Yeoman, C. J., Thomas, S. M., Miller, M. E. B., Ulanov, A. V., Torralba, M., Lucas, S., Gillis, M., Cregger, M., Gomez, A., Ho, M. F., Leigh, S. R., Stumpf, R., Creedon, D. J., Smith, M. A., Weisbaum, J. S., Nelson, K. E., Wilson, B. A. & White, B. A. (2013) A multi-omic systems-based approach reveals metabolic markers of bacterial vaginosis and insight into the disease. Plos One, **8**: 18.

Young, S., Skerratt, L. F., Mendez, D., Speare, R., Berger, L. & Steele, M. (2012a) Using community surveillance data to differentiate between emerging and endemic amphibian diseases. Diseases of Aquatic Organisms, **98**: 1-10.

Young, S., Speare, R., Berger, L. & Skerratt, L. F. (2012b) Chloramphenicol with fluid and electrolyte therapy cures terminally ill green tree frogs (*Litoria caerulea*) with chytridiomycosis. Journal of Zoo and Wildlife Medicine, **43**: 330-337.

Young, S., Whitehorn, P., Berger, L., Skerratt, L. F., Speare, R., Garland, S. & Webb, R. (2014) Defects in host immune function in tree frogs with chronic chytridiomycosis. Plos One, **9**: 16.

Yule, J. V., Fournier, R. J. & Hindmarsh, P. L. (2013) Biodiversity, extinction, and humanity's future: The ecological and evolutionary consequences of human population and resource use. Humanities, **2**: 147-159.

Zeisset, I. & Beebee, T. J. C. (2009) Molecular characterization of major histocompatibility complex class II alleles in the common frog, *Rana temporaria*. Molecular Ecology Resources, **9**: 738-745.

Zeisset, I. & Beebee, T. J. C. (2013) *Bufo* MHC class II loci with conserved introns flanking exon 2: cross-species amplification with common primers. Conservation Genetics Resources, **5**: 211-213.

Zerbino, D. R. & Birney, E. (2008) Velvet: Algorithms for de novo short read assembly using de Bruijn graphs. Genome Research, **18**: 821-829.

Zhang, Z. Y., Cashins, S., Philips, A. & Burridge, C. P. (2014) Significant population genetic structuring but a lack of phylogeographic structuring in the endemic Tasmanian tree frog (*Litoria burrowsae*). Australian Journal of Zoology, **62**: 238-245.

Zhao, X. B. & Sandelin, A. (2012) GMD: measuring the distance between histograms with applications on high-throughput sequencing reads. Bioinformatics, **28**: 1164-1165.

Zhao, Y., Jin, Y., Lee, W. H. & Zhang, Y. (2006a) Purification of a lysozyme from skin secretions of *Bufo andrewsi*. Comparative Biochemistry and Physiology C-Toxicology & Pharmacology, **142**: 46-52.

Zhao, Y. F., Pan-Hammarstrom, Q., Yu, S. Y., Wertz, N., Zhang, X. F., Li, N., Butler, J. E. & Hammarstrom, L. (2006b) Identification of IgF, a hinge-region-containing Ig class, and IgD in *Xenopus tropicalis*. Proceedings of the National Academy of Sciences of the United States of America, **103**: 12087-12092.

Zhao, Y. Y., Cheng, X. L., Vaziri, N. D., Liu, S. M. & Lin, R. C. (2014) UPLC-based metabonomic applications for discovering biomarkers of diseases in clinical chemistry. Clinical Biochemistry, **47**: 16-26.

Zippel, K., Johnson, K., Gagliardo, R., Gibson, R., McFadden, M., Browne, R., Martinez, C. & Townsend, E. (2011) The amphibian ark: a global community for ex situ conservation of amphibians. Herpetological Conservation and Biology, **6**: 340-352.

Zucchini, W. (2000) An introduction to model selection. Journal of Mathematical Psychology, **44**: 41-61.

Co-author consent forms for jointly authored papers

This administrative form has been removed

Co-author consent to include jointly authored papers in the thesis

This administrative form
has been removed

Co-author consent to include jointly authored papers in the thesis

This administrative form has been removed

Co-author consent to include jointly authored papers in the thesis

This administrative form has been removed

Co-author consent to include jointly authored papers in the thesis

This administrative form
has been removed

Co-author consent to include jointly authored papers in the thesis

This administrative form has been removed

Co-author consent to include jointly authored papers in the thesis

This administrative form has been removed

Co-author consent to include jointly authored papers in the thesis

This administrative form has been removed

Co-author consent to include jointly authored papers in the thesis

This administrative form has been removed

Supporting Information

APPENDICES

associated with the thesis:

Understanding host and environmental factors in the immunology and epidemiology of chytridiomycosis in anuran populations in Australia

Thesis submitted by

Laura Frances GROGAN

BVSc (Hons) Uni Syd, BSc(Vet) (Hons) Uni Syd

November 2014

for the degree of

Doctor of Philosophy

in the School of Public Health, Tropical Medicine and Rehabilitation Sciences

James Cook University

APPENDIX A: Supporting information to CJS and Pradel modeling

A.1 Introduction

In this appendix I define in detail the estimable parameters and predictor variables that were used to populate the mark-recapture models, and briefly describe my rationale for their *a priori* inclusion. I follow this with some details regarding goodness of fit testing, and then my rationale for construction of the candidate model sets.

The full reference for the relevant published paper is:
Phillott, A. D., **Grogan, L. F.**, Cashins, S. D., McDonald, K. R., Berger, L., Skerratt, L. F. (2013) Chytridiomycosis and seasonal mortality of tropical stream-associated frogs 15 years after introduction of *Batrachochytrium dendrobatidis*. Conservation Biology 27:1058-1068.

A.2 Parameter probabilities

These are demographic parameters that we can estimate monthly probabilities for using standard mark-recapture methodologies.

- **φ** (phonetically 'phi'): local apparent monthly survival probability for adult male *Litoria rheocola* frogs, where φ_i is the probability of an individual surviving from occasion *i* to *i* + 1. It is important to note that the survival probability (φ) is confounded with the probability of permanent emigration from the study site with standard mark-recapture analyses.
- **ρ** (phonetically 'rho', otherwise represented as 'p'): monthly probability of capture for adult male *Litoria rheocola* frogs, where ρ_i is the probability of encounter on occasion *i* conditional on an individual being alive and remaining in the sampling region.
- **λ** (phonetically 'lambda'): Pradel modeled realized monthly population growth rate, $\lambda = \frac{N_{i+1}}{N_i}$, where *N* is population size of those individuals able to be encountered, and *i* is the encounter session. This is a measure of the rate of change of the age class from which the encounter histories were derived, and not necessarily the growth rate of the population itself. As the reproductive stage, however, adult frogs are expected to be the age class of greatest importance for population persistence.
- ***f***: Pradel modeled monthly recruitment probability, $f_i = \frac{B_i}{N_i}$; where B_i is the number of individuals entering the population between time *i* and *i+1*, and N_i is the number of individuals at risk of encounter already in the population at time *i*. Since this measure is based on the age class under study (adult male frogs), it represents individuals entering that age class, and as such is an indirect measure which includes *in situ* reproduction, survival of younger age classes and immigration to the study site. Recruitment f_i is related to population growth and survival in the following way $f_i = \lambda_i - \varphi_i$.

A.3 Predictor variables

We carefully chose predictor variables to test our hypotheses based on biological plausibility and *a priori* evidence in an attempt to avoid over-parameterization (Burnham and Anderson, 2002; Grueber et al., 2011; Guthery et al., 2005; Nakagawa and Freckleton, 2011). Below we describe these variables for pragmatic purposes as either grouping variables (entered in the input file in Program Mark), temporal structural variables including environmental and linear covariates (entered into the design matrix of Program Mark for individual models), or time independent individual covariates (entered in the input file). These variables are used to constrain the underlying structure of models that make up the candidate model set. The better a linear combination of such constraints *fits* the empirical data within a single model, and the smaller the included number of variables, the better that model will rank within the set using information theoretic criteria such as Akaike's Information Criterion ($QAIC_c$).

A.3.1 Grouping variable

- *g*: temporally independent, individual binary grouping variable defining infection status at first capture only (to eliminate recapture-associated biases within the single-state framework; determined via quantitative PCR where one well, one zoospore equivalent zse is considered positive for optimized sensitivity). Chytridiomycosis infection has been demonstrated to be an important determinant of survival even in endemically infected populations. Bd is an important cause of mortality in amphibians (Berger et al., 1998) and is capable of driving populations to extinction (Collins, 2010; Skerratt et al., 2007; Stuart et al., 2004; Vredenburg et al., 2010). Survival (and potentially site fidelity) in individuals that test positive for Bd in endemically infected populations has previously been demonstrated to be lower than in those that test negative (Murray et al., 2009; Pilliod et al., 2010). This is presumed because many subclinically infected frogs subsequently develop fatal disease. Infection status has not been found to have a detectable impact on recapture probability (ρ; Murray et al., 2009), however we suspect this may be biased by the predominant capture of subclinically infected individuals in typical mark-recapture field studies (likely the case here), leading to clinically diseased individuals being in an 'unobservable state' (Cooch et al., 2012). The incubation period for chytridiomycosis has commonly been reported to be around 3-4 weeks in optimal conditions (for example, see Berger et al., 2005b), and the clinical period is relatively short in comparison (around 2-3 days; Berger et al., 2009a; Berger et al., 1999a; Voyles et al., 2007). This means clinically diseased individuals with high infectious loads are less likely to be encountered due to both temporal distribution of infections, and the lower expected survival in clinically diseased individuals. Mark-recapture analyses can only draw inferences about the 'observable' population, so if this doesn't include the moribund class of individuals, we are unable to determine valid parameter estimates for them.

A.3.2 Environmental variables

- temp: temperature (mean of daily maximum temperatures in degrees Celcius over the 28 days preceding each trip start)
- rain: rainfall (sum of daily rainfall measurements in millimeters over the 28 days preceding each trip start)
- rh: relative humidity (mean of the relative humidity as % at daily maximum temperatures over the 28 days preceding each trip start)
- rad: radiation (mean radiation in MJ/m^2 of daily values over the 28 days preceding each trip start)

Environmental variables were obtained from the SILO climate database as spatially interpolated weather values (Jeffrey et al., 2001). Variables included in models were averages or sums over the 28 days preceding a trip to account for predefined trip intervals, the putative cumulative nature of their effects on the pathogenesis of chytridiomycosis, and to correspond roughly with the incubation period of chytridiomycosis (Berger et al., 2005b; Bureau of Meteorology, 2008). Rainfall was summed over the previous 28 days because interpolated rainfall data is subject to inherent uncertainties compared with observation data due to smoothing (Tozer et al., 2011), and the rainfall measure itself is typically erratic and non-parametric, rendering the arithmetic mean a poor summary measure of daily results.

Temporal environmental variables are hypothesized to play a role in driving annual patterns in adult frog **survival probability** (φ). Seasonality of population dynamics has demonstrable links to several causes, including through the mechanism of disease, and other host factors. These include *"seasonal changes in social behavior and contact rates, variation in encounters with infective stages in the environment, annual pulses of host births and deaths and changes in host immune defenses"* (Altizer et al., 2006). Environmental factors, particularly temperature, precipitation and syntopic diversity, have been demonstrated as important predictors of the spatial distribution of Bd, and its proliferation *in vitro* (Berger et al., 2004; Drew et al., 2006; Fisher et al., 2009b; Forrest and Schlaepfer, 2011; Johnson et al., 2003; Kriger et al., 2007b; Piotrowski et al., 2004; Richards-Zawacki, 2010). Field and laboratory evidence suggests that thermal immunomodulation may affect host ability to respond to infection (Andre et al., 2008; Raffel et al., 2006; Ribas et al., 2009), thermoregulatory behavior may influence the course of infection (Bradbury, 2009), and warm temperatures have been demonstrated to effectively cure infected frogs *in vitro* and replicating field conditions (Chatfield and Richards-Zawacki, 2011; Daskin et al., 2011; Murphy et al., 2011).

Recapture probability (ρ) is hypothesized to be influenced by seasonal weather variables. Observation via spotlighting relies on frog presence at perch sites on the stream transect after dusk. While adult male *L. rheocola* are commonly found on the stream year-round in tropical ecosystems depending on local

weather conditions (Liem, 1974), females are more likely to attend the stream for a narrowly defined breeding season, and post-metamorphic juveniles may favor terrestrial habitats until they are ready to breed (Hodgkison and Hero, 2002). Observed seasonal influences on breeding behaviors (Hodgkison and Hero, 2002) suggest likely interactions between weather variables and recapture probability. Anuran breeding behaviors are controlled by hormonal secretion from the adenohypophysis, and are stimulated directly by warm, wet weather conditions, and indirectly by other environmental factors such as nutritional status (Duellman and Trueb, 1994). In the context of our study, breeding behaviors such as presence and calling on the stream may thus be more visible to observers seasonally.

Climatic variables that cycle seasonally (and indeed, many other environmental variables in ecological studies; Johnson, 1999) are typically **correlated** (or collinear; Freckleton, 2011), hence it is often difficult to determine their independent effects, and this may lead to erroneous model selection and parameter estimates where environmental impacts are under- or over-estimated due to biased sampling variance (Linden and Knape, 2009). The usual recommendation is to combine collinear variables into a single parameter index, for instance through Principal Components Analysis (PCA; Grueber et al., 2011), however as exemplified by Freckleton (2011), this approach is inappropriate where the collinear variables have potentially differing mechanistic links with the response variable. In the context of chytridiomycosis, mechanistic interactions may be complex and counterbalanced as has been demonstrated with the temperature variable which acts differentially on host and pathogen (see above). Freckleton (2011) investigates the problem of collinearity with simulation comparing least squares analyses with the information theoretic approach (IT-AIC) and concludes that in the absence of measurement bias, and under low to moderate levels of collinearity, IT-AIC methods (including model averaging for parameter estimates) are generally robust.

Utilizing spatially interpolated climatic variables (Bureau of Meteorology, 2008) in our study context is subject to two types of **measurement error**; interpolation errors which are discussed in detail by Jeffrey et al. (2001), and microclimatic effects associated with small scale habitat factors (for example canopy cover and aspect). We assumed the first type of error to be minimal and consistent between variables and throughout our study period due to the interpolation techniques (Jeffrey et al., 2001). The second error is difficult to estimate without local observation data, but is assumed consistent because the site locations remained identical. It may, however, be impacted by temporal events such as tropical cyclone Larry (Category 4 cyclone at landfall), which passed through the region mid-late March, 2006, causing moderate damage to forest integrity.

We included the above-mentioned climatic variables in separate models (rather than within the same model; Mundry, 2011) in an attempt to determine, via model averaging, the best parameter estimates for the system (which may include the tapering effects of variables contained in less parsimonious models).

Mechanistic links between apparent survival, recapture and transition probabilities, and the various environmental covariates may be multifactorial and complex (as exemplified by the effects of temperature).

A.3.3 Linear variable

- prev: across-species apparent infection prevalence per trip was determined as a point based sampled prevalence per trip and site as the number of positive PCR results divided by the total number of PCR swab samples analyzed (where one well, one zse was considered positive, and the entire uninfected observable population is considered potentially susceptible).

During the course of this study we sampled three other species also present at the study sites (in an identical fashion to *Litoria rheocola*). These included the waterfall frog (*Litoria nannotis*), the Australian lacelid (*Nyctimystes dayi*) and the green-eyed tree frog (*Litoria genimaculata*, or more recently reclassified as *Litoria serrata*). All references to prevalence in the manuscript text refer to a combined cross-species prevalence measure for two reasons. Firstly, Bd is an indirectly transmitted pathogen with a motile environmental infectious stage (zoospore) meaning that infection abundance in syntopic host species potentially plays an important role in determining overall environmental burden of infectious zoospores at the study sites. Secondly, the precision of proportional measures, such as prevalence, is greatly improved by increased sample size which we were able to harness by utilizing total infection abundance data from each study site. *L. rheocola* prevalence measures were strongly positively correlated with across-species prevalence (Spearman's correlation coefficient 0.916, $p \leq 0.0005$, N = 26 trips), and also across-species prevalence excluding *L. rheocola* data (Spearman's correlation coefficient 0.793, $p \leq 0.0005$, N = 26 trips).

We included the variable prevalence to account for population-level transmission effects that are otherwise not encompassed by individual infection status. Apparent infection prevalence may influence survival and recapture probabilities in different ways. If greater infection prevalence leads to higher zoospore density in the creek environment, and/or wider geographic distribution, infection transmission may be increased, potentially leading to subsequent mortality (lower survival). Alternatively, if higher prevalence is related to more 'tolerant' (low infectious load) individuals, then rates of infection may be lower and survival higher than expected. This relationship may also be confounded by underlying levels of resistance in the population. Higher prevalence may be more a symptom of environmental covariates than transmission rates (particularly for endemic pathogens acting as macroparasites), and may thus correlate to survival through environmental factors. Associations between prevalence and recapture probability may be even more difficult to predict as they are presumably highly dependent on frog behavior and other factors related to visibility (Cooch et al., 2012). Clinically diseased frogs exhibit lethargy (Berger et al., 1999a) however this may lead either to increased visibility (if they are less likely

to hide), or decreased visibility (less likely to move to creek sites from daytime retreat sites). Similarly, behavior of subclinically infected individuals may be different to symptomatic frogs as well as potentially subtle differences between them and uninfected frogs. It may be difficult to separate whether behavioral change in subclinical frogs is a response to chytridiomycosis, or whether infection is more likely in frogs that already exhibit certain behavioral traits (the question of cause or effect).

- *d*: capture effort (measured in days per trip, where each capture day covered the identical stream transect once after dusk). Capture effort is expected to influence recapture probability by altering opportunities for observation.
- Ts *(*or just *T)*: annually cycling seasonal linear trend where autumn was assumed equivalent to spring (hence the annual cycle was summer = 1, autumn = 2, winter = 3, spring = 2)
- Tl: non-cycling linear trend based on seasons (hence over the study period, each season was given a consecutive number, the direction of the overall trend being flexible, either monotonically increasing or decreasing)
- *t*: time-dependence (indicates that there is no temporal linear constraint on the parameter)
- . (dot, or period): constant (indicates that the parameter is constrained to be temporally constant)

A.3.4 Individual variable

- sul: snout-urostyle length as a static individual covariate proxy for chronological age, for frogs > 24mm

Static individual covariates (such as the age proxy snout-urostyle length) may explain individual differences in survival (φ). Individuals and populations have been demonstrated to vary in susceptibility to chytridiomycosis induced mortality (Tobler and Schmidt, 2010) although the relative importance of the proximate causes of this variation is not yet clear. Putative determinants include innate or adaptive host immune responses including production of anti-microbial peptides, as well as age, life-stage, behavior, and presence of symbiotic skin bacteria (see for example Blaustein et al., 2005; Lam et al., 2010; Lamirande and Nichols, 2002; Murray et al., 2010b; Richards-Zawacki, 2010; Rollins-Smith et al., 2011; Rowley and Alford, 2007a; Savage et al., 2011; Smith et al., 2007; Woodhams et al., 2010; Woodhams et al., 2007c). In addition, marking methods such as toe-clipping have previously been associated with detrimental effects on survival (Waddle et al., 2008).

A.4 Specific details about Goodness Of Fit (GOF) testing and data exclusions

Programs RELEASE, U-CARE (which utilize chi-square tests) and examination of deviance residuals (Mundry, 2011) were used primarily to yield exploratory information regarding individual sources of heterogeneity (sparse recaptures yielding them less likely to provide valid c-hat values). Initial examination of goodness of fit testing suggested that a single frog (Lr210 at Tully) exhibited marked capture heterogeneity (making the overall 'trap-happiness' p-value marginally significant at 0.09, U-Care;

Choquet et al., 2009). Eliminating this frog from the data set improved capture homogeneity (p = 0.20). Possible reasons for 'capture-happiness' in this frog may include that it was larger, more distinctive, behaviorally easier to observe or may have had a well-defined territory or niche.

There appeared to be consistently higher capture deviance residuals (called from within Program Mark) in winter months in both 2006 and 2007, which is the breeding season for this species (as evidenced by when females were caught and presence of secondary sexual characteristics, consistent with Hodgkison and Hero [2002]). We suspect this may be due to either misidentified female frogs being included in the data set as males, or due to a temporarily immigrant group of male frogs (transients) that came to the stream coincident with the breeding season, before leaving again (or dying). Goodness of fit testing examination thus led to our exclusion of trip data from trips starting on 15/06/06, 29/06/2006, 12/07/2006, 13/06/2007, and 27/06/2007 and capture-happy frog Lr210 in the Tully data set for subsequent CMR analyses. The elimination of trip data precludes inference from those trip dates (and potentially excludes inference about temporarily immigrant individuals during the breeding season) however we believe that exclusion of this frog data does not constitute 'missing not at random' data which would systematically bias the data set analysis (Nakagawa and Freckleton, 2011). Trip dates are typically variable within the framework of mark-recapture studies, only trip capture data from an encounter history was eliminated unless the individual was only captured during those trips, trip-interval is accounted for when initiating analysis (and intervals weren't entirely even), and data are always analyzed in the context of trip date (so other trip parameter estimates are not affected).

Sparse recaptures precluded the use of the fully time and group-dependent model ($\varphi(g \times t)\rho(g \times t)$; where local apparent survival φ and recapture probability ρ are dependent on time *t*, infection status on first capture *g* and their interaction terms ×; additive models are represented by +). Hereafter we use this standard model notation, as described elsewhere (White and Burnham, 1999). The general model φ(g)ρ(g) with all parameters estimable was used for both study sites. At Tully, bootstrap GOF testing indicated no evidence for lack of fit, with p = 0.46 ($\hat{c}$ = 1.002; with 100 simulations). Corresponding median $\hat{c}$ with 1000 simulations yielded $\hat{c}$ = 1.145 (95% CI 1.005 - 1.284). The most conservative (highest) estimate of $\hat{c}$ = 1.145 was hence used for the analysis. Kirrama bootstrap GOF testing indicated no evidence for lack of fit with p = 0.78 ($\hat{c}$ = 1.098; with 100 simulations), and corresponding median c-hat with 1000 simulations yielded $\hat{c}$ = 0.948 (95% CI 0.713 - 1.183). The most conservative estimate of $\hat{c}$ = 1.098 was hence used for the analysis. Currently available GOF tests are inappropriate for Pradel models, hence $\hat{c}$ was left at one.

A.5 Rationale for the methodology used in construction of the candidate model sets

Within the framework of the two types of analyses we performed (CJS and Pradel) at two sites (Tully and Kirrama), candidate model sets were constructed *a priori* using a restricted form of the all subsets

approach and tested systematically (Doherty et al., 2012; Grueber et al., 2011; Hegyi and Garamszegi, 2011; Lukacs et al., 2010; Stephens et al., 2007; Symonds and Moussalli, 2011). Please see Appendix E of this thesis for more details and justification of approach. Following the reduction of predictor variables to only those with putative effects (described above), we also restricted the candidate model set to those combination types with biological plausibility (Dochtermann and Jenkins, 2011).

Bd infection status (*g*) was the variable of greatest interest for influencing the response parameters (survival φ and recapture ρ probability), hence it was tested both in isolation, and as an additive or multiplicative two-way interaction with the other variables. We did not restrict the model set to those models containing this infection status variable, however, because as discussed by Grueber et al. (2011), if infection status is a poor predictor, its relative importance may be inflated if it is present in all models, hence resulting inference may be biased. Thus the candidate model set also contained structural variables and individual covariates in isolation, as well as the null model for baseline comparison (constant or dot model; Burnham et al., 2011; Dochtermann and Jenkins, 2011) although its routine inclusion is not recommended by Burnham and Anderson (2002). Due to probable collinearities, other variables were not tested in combination or interaction with each other. Furthermore, capture effort (capture nights per trip; *d*) was presumed to only impact upon recapture probability, hence was excluded from testing with the other response parameters. Multiplicative interaction variables were not included on their own without their respective main variables (for example, 'g×prev' is an interaction variable) as this model type is not valid due to effect confounding (Mundry, 2011).

From the basis of these restrictions all variable combinations were tested (for example, this included models such as φ(g×prev)ρ(g×temp), φ(g)ρ(temp) and the null model φ(.)ρ(.)). Hence the number of variables (infection status *g*; environmental variables temp, rain, rh, rad; linear variables prev, Ts, Tl, ., *t*, *d*; individual covariates sul) was small relative to the sample size (for example, 285 individual adult male frogs in Tully CJS analysis) to avoid Freedman's paradox (Freedman, 1983; Lukacs et al., 2010) and data dredging (the discovery of spurious effects; Anderson et al., 2001). However, using the all subsets approach, the number of models tested in the candidate model set systematically included all feasible interactions in order to determine their relative importance (including additive and multiplicative variations).

Performing Pradel analyses necessitated the simultaneous estimation of a third parameter (population growth or recruitment), and hence increased the complexity of the model set. For this reason, only the variables that were best supported (based on the relative variable importance comparisons, see manuscript text results; Section 3.2.5), from the CJS analyses were included in the respective Pradel analyses for each site.

We constructed models using the intercept design matrix coding format and the logistic (logit) link function, and assessed them individually for estimable parameter count (Cooch et al., 2012; Lebreton et al., 2009). We used $QAIC_c$ (see Symonds and Moussalli, 2011) to rank model parsimony due to its performance for minimizing bias of estimated parameters in infinite-dimensional ecological space (Burnham and Anderson, 2002). We used model averaging to reduce selection bias while estimating parameters (Doherty et al., 2012), and we report their unconditional variances as 95% confidence intervals (95% CI; Burnham and Anderson, 2002). We used Akaike weights to determine relative variable importance (Doherty et al., 2012), and report evidence ratios and model averaged effect sizes (Burnham and Anderson, 2002).

APPENDIX B: Additional results for CJS and Pradel modeling

B.1 Introduction

In this appendix I present summarized tables (containing most parsimonious 100 models from the candidate model set) of results for CJS and Pradel recruitment/population growth candidate model sets for each site (Tully and Kirrama), together with an alternative visual presentation (heatmaps) of $QAIC_c$ values for all models in each candidate model set.

The full reference for the published paper is:
Phillott, A. D., **Grogan, L. F.**, Cashins, S. D., McDonald, K. R., Berger, L., Skerratt, L. F. (2013) Chytridiomycosis and seasonal mortality of tropical stream-associated frogs 15 years after introduction of *Batrachochytrium dendrobatidis*. Conservation Biology 27:1058-1068.

B.2 Summary tables

In the summary tables we have followed the model naming convention of White and Burnham (1999), whereby survival (φ) is represented by the ASCII text version 'phi', recapture (ρ) is represented by 'p', population growth (λ) is represented by 'lambda', and recruitment (*f*) is represented by 'f'. Predictor variables or variable interactions for each parameter are contained within parentheses (). Additive interactions are represented by + and multiplicative interactions are represented by *. Model names such as Phi(prev)p(d) are followed by the letters 'DM' to indicate that the model was built manually using the design matrix coding format.

- $QAIC_c$ represents the degree of model parsimony, and is the small sample size corrected Quasi Akaike's Information Criterion value for each model ('quasi' indicates that the AIC was adjusted to account for the variance inflation factor $\hat{c}$). The smaller this value, the more parsimonious the respective model within the candidate model set. These values cannot be compared between candidate model sets (separate analyses) however.
- Delta $QAIC_c$ is the subtractive difference between the $QAIC_c$ of the model in question, and that of the most parsimonious model of the set.
- AIC_c Weight is the model probability within the candidate model set. It is the weight of evidence in favor of the respective model being the actual best model in the set (minimizing the Kullback-Leibler distance)
- Model likelihood is the AIC_c Weight of the model of interest divided by the AIC_c Weight of the best model in the candidate set. It is the strength of evidence for this model relative to other models in the model set.
- 'Num par' is the number of estimable parameters of the respective model, and this differs depending on the nature of model variable constraints

- QDeviance is the Quasi model deviance (model deviance adjusted to account for the variance inflation factor $\hat{c}$). The lower this value, the better the model is estimated to fit the empirical data (this value doesn't take account of the number of parameters, hence is not equivalent to model parsimony)
- Cumulative sum of $QAIC_c$ Weights is a rank-order cumulative sum of Akaike weights which adds to one over the entire candidate model set.

The relative contribution of each variable (relative variable importance) is most readily interpreted from the second form of data presentation for each candidate model set (the heatmaps or coloured tables). For the purposes of displaying all models in the candidate model sets in two dimensions, variables and combinations of variables for representative estimable parameters have been represented separately (for example, the survival variable prev has been separated from models containing a combination of variables for survival such as *g*+prev or *g**prev, but the order of variables within these combinations is not important). In addition, for the three-parameter analyses (Pradel population growth and recruitment analyses), different variables for the third parameter (population growth or recruitment) have been separated into individual tables.

B.2.1 CJS Tully set

Table B.1. Ranking of most parsimonious models in CJS Tully set

Model (CJS Tully set)	$QAIC_c$	Delta $QAIC_c$	AIC_c Weights	Model Likelihood	NumPar	QDeviance	Cumulative sum of AIC_c Weight
Phi(prev) p(d) - DM	961.2068	0	0.06806	1	4	953.1099	0.06806
Phi(prev) p(rh) - DM	961.5770	0.3702	0.05656	0.831	4	953.4801	0.12462
Phi(prev) p(rad) - DM	962.4233	1.2165	0.03704	0.5442	4	954.3265	0.16166
Phi(prev) p(g+d) - DM	962.7880	1.5812	0.03087	0.4536	5	952.6424	0.19253
Phi(prev) p(g+rh) - DM	963.0464	1.8396	0.02713	0.3986	5	952.9008	0.21966
Phi(g+prev) p(d) - DM	963.0872	1.8804	0.02658	0.3905	5	952.9415	0.24624
Phi(prev) p(.) - DM	963.0971	1.8903	0.02645	0.3886	3	957.0391	0.27269
Phi(g+prev) p(rh) - DM	963.4201	2.2133	0.02250	0.3306	5	953.2745	0.29519
Phi(T) p(d) - DM	963.9983	2.7915	0.01685	0.2476	4	955.9015	0.31204
Phi(temp) p(d) - DM	964.0489	2.8421	0.01643	0.2414	4	955.952	0.32847
Phi(prev) p(g+rad) - DM	964.1527	2.9459	0.01560	0.2292	5	954.0071	0.34407
Phi(prev) p(g*d) - DM	964.2146	3.0078	0.01513	0.2223	6	952.0102	0.35920
Phi(g+prev) p(rad) - DM	964.2423	3.0355	0.01492	0.2192	5	954.0967	0.37412
Phi(g*prev) p(d) - DM	964.4229	3.2161	0.01363	0.2003	6	952.2185	0.38775
Phi(prev) p(g*rh) - DM	964.4825	3.2757	0.01323	0.1944	6	952.2782	0.40098
Phi(temp) p(rh) - DM	964.6053	3.3985	0.01244	0.1828	4	956.5085	0.41342
Phi(prev) p(sul) - DM	964.7116	3.5048	0.01180	0.1734	4	956.6147	0.42522
Phi(prev) p(prev) - DM	964.7346	3.5278	0.01166	0.1713	4	956.6378	0.43688
Phi(g*prev) p(rh) - DM	964.7469	3.5401	0.01159	0.1703	6	952.5426	0.44847
Phi(g+prev) p(g+d) - DM	964.8237	3.6169	0.01116	0.164	6	952.6193	0.45963
Phi(prev) p(g) - DM	964.8455	3.6387	0.01103	0.1621	4	956.7487	0.47066
Phi(prev) p(temp) - DM	964.8683	3.6615	0.01091	0.1603	4	956.7715	0.48157
Phi(g+prev) p(.) - DM	964.9798	3.773	0.01032	0.1516	4	956.8829	0.49189
Phi(g+prev) p(g+rh) - DM	965.0799	3.8731	0.00981	0.1441	6	952.8755	0.50170
Phi(prev) p(T) - DM	965.1056	3.8988	0.00969	0.1424	4	957.0087	0.51139
Phi(prev) p(rain) - DM	965.1354	3.9286	0.00955	0.1403	4	957.0386	0.52094
Phi(T) p(g+d) - DM	965.2280	4.0212	0.00911	0.1339	5	955.0823	0.53005
Phi(temp) p(.) - DM	965.3227	4.1159	0.00869	0.1277	3	959.2647	0.53874
Phi(temp) p(g+d) - DM	965.3241	4.1173	0.00869	0.1277	5	955.1785	0.54743
Phi(T) p(rh) - DM	965.4776	4.2708	0.00804	0.1181	4	957.3807	0.55547
Phi(g*prev) p(rad) - DM	965.5025	4.2957	0.00794	0.1167	6	953.2982	0.56341
Phi(temp) p(rad) - DM	965.6148	4.408	0.00751	0.1103	4	957.5179	0.57092
Phi(rain) p(T) - DM	965.6921	4.4853	0.00723	0.1062	4	957.5952	0.57815
Phi(g+T) p(d) - DM	965.7278	4.521	0.00710	0.1043	5	955.5822	0.58525
Phi(temp) p(g+rh) - DM	965.7852	4.5784	0.00690	0.1014	5	955.6396	0.59215
Phi(g+temp) p(d) - DM	965.8022	4.5954	0.00684	0.1005	5	955.6565	0.59899
Phi(prev) p(g*rad) - DM	965.9131	4.7063	0.00647	0.0951	6	953.7087	0.60546
Phi(g*prev) p(g+d) - DM	966.0088	4.802	0.00617	0.0907	7	951.7357	0.61163
Phi(g*prev) p(.) - DM	966.1066	4.8998	0.00587	0.0862	5	955.9609	0.61750
Phi(g+prev) p(g+rad) - DM	966.1321	4.9253	0.00580	0.0852	6	953.9277	0.62330
Phi(T) p(.) - DM	966.1407	4.9339	0.00577	0.0848	3	960.0827	0.62907
Phi(g+prev) p(g*d) - DM	966.2460	5.0392	0.00548	0.0805	7	951.9728	0.63455
Phi(g*prev) p(g+rh) - DM	966.2706	5.0638	0.00541	0.0795	7	951.9974	0.63996
Phi(rain) p(g+T) - DM	966.3050	5.0982	0.00532	0.0782	5	956.1594	0.64528
Phi(g+temp) p(rh) - DM	966.3300	5.1232	0.00525	0.0771	5	956.1844	0.65053

Phi(prev) p(g+sul) - DM	966.4237	5.2169	0.00501	0.0736	5	956.2781	0.65554
Phi(T) p(g*d) - DM	966.5311	5.3243	0.00475	0.0698	6	954.3267	0.66029
Phi(g+prev) p(g*rh) - DM	966.5451	5.3383	0.00472	0.0694	7	952.272	0.66501
Phi(prev) p(g+prev) - DM	966.5453	5.3385	0.00472	0.0694	5	956.3997	0.66973
Phi(rain) p(d) - DM	966.5628	5.356	0.00468	0.0688	4	958.466	0.67441
Phi(g+prev) p(sul) - DM	966.5934	5.3866	0.00460	0.0676	5	956.4478	0.67901
Phi(g+prev) p(prev) - DM	966.5978	5.391	0.00459	0.0674	5	956.4522	0.68360
Phi(T) p(rad) - DM	966.6231	5.4163	0.00454	0.0667	4	958.5262	0.68814
Phi(T) p(g+rh) - DM	966.6678	5.461	0.00444	0.0652	5	956.5222	0.69258
Phi(prev) p(g+temp) - DM	966.6899	5.4831	0.00439	0.0645	5	956.5443	0.69697
Phi(temp) p(g*d) - DM	966.6979	5.4911	0.00437	0.0642	6	954.4936	0.70134
Phi(g+prev) p(temp) - DM	966.7394	5.5326	0.00428	0.0629	5	956.5937	0.70562
Phi(temp) p(g) - DM	966.7667	5.5599	0.00422	0.062	4	958.6698	0.70984
Phi(temp) p(sul) - DM	966.7893	5.5825	0.00418	0.0614	4	958.6924	0.71402
Phi(prev) p(g+T) - DM	966.8368	5.63	0.00408	0.0599	5	956.6911	0.71810
Phi(g+prev) p(g) - DM	966.8536	5.6468	0.00404	0.0594	5	956.708	0.72214
Phi(prev) p(g+rain) - DM	966.8849	5.6781	0.00398	0.0585	5	956.7393	0.72612
Phi(prev) p(g*sul) - DM	966.8932	5.6864	0.00396	0.0582	6	954.6889	0.73008
Phi(g+prev) p(T) - DM	967.0015	5.7947	0.00375	0.0551	5	956.8559	0.73383
Phi(g+prev) p(rain) - DM	967.0280	5.8212	0.00371	0.0545	5	956.8823	0.73754
Phi(temp) p(g+rad) - DM	967.0476	5.8408	0.00367	0.0539	5	956.902	0.74121
Phi(g+temp) p(.) - DM	967.0503	5.8435	0.00366	0.0538	4	958.9534	0.74487
Phi(g*prev) p(g*d) - DM	967.0795	5.8727	0.00361	0.053	8	950.7274	0.74848
Phi(rain) p(temp) - DM	967.1007	5.8939	0.00357	0.0525	4	959.0038	0.75205
Phi(temp) p(temp) - DM	967.1076	5.9008	0.00356	0.0523	4	959.0107	0.75561
Phi(g+rain) p(T) - DM	967.1094	5.9026	0.00356	0.0523	5	956.9638	0.75917
Phi(temp) p(prev) - DM	967.1805	5.9737	0.00343	0.0504	4	959.0837	0.76260
Phi(g+T) p(rh) - DM	967.1933	5.9865	0.00341	0.0501	5	957.0477	0.76601
Phi(g*prev) p(g+rad) - DM	967.2312	6.0244	0.00335	0.0492	7	952.9581	0.76936
Phi(g+T) p(g+d) - DM	967.2315	6.0247	0.00335	0.0492	6	955.0271	0.77271
Phi(g+temp) p(rad) - DM	967.2912	6.0844	0.00325	0.0478	5	957.1456	0.77596
Phi(temp) p(T) - DM	967.3271	6.1203	0.00319	0.0469	4	959.2302	0.77915
Phi(temp) p(rain) - DM	967.3313	6.1245	0.00318	0.0467	4	959.2345	0.78233
Phi(g+temp) p(g+d) - DM	967.3341	6.1273	0.00318	0.0467	6	955.1297	0.78551
Phi(temp) p(g*rh) - DM	967.4233	6.2165	0.00304	0.0447	6	955.2189	0.78855
Phi(T) p(sul) - DM	967.5695	6.3627	0.00283	0.0416	4	959.4727	0.79138
Phi(T) p(g) - DM	967.5908	6.384	0.00280	0.0411	4	959.4939	0.79418
Phi(g*temp) p(d) - DM	967.6625	6.4557	0.00270	0.0397	6	955.4581	0.79688
Phi(rain) p(g+d) - DM	967.7027	6.4959	0.00264	0.0388	5	957.5571	0.79952
Phi(g*prev) p(sul) - DM	967.7130	6.5062	0.00263	0.0386	6	955.5087	0.80215
Phi(g*T) p(d) - DM	967.7135	6.5067	0.00263	0.0386	6	955.5091	0.80478
Phi(g*prev) p(prev) - DM	967.7147	6.5079	0.00263	0.0386	6	955.5103	0.80741
Phi(g*prev) p(g) - DM	967.7858	6.579	0.00254	0.0373	6	955.5814	0.80995
Phi(g+temp) p(g+rh) - DM	967.7962	6.5894	0.00252	0.037	6	955.5918	0.81247
Phi(g*prev) p(temp) - DM	967.8310	6.6242	0.00248	0.0364	6	955.6267	0.81495
Phi(rain) p(g+temp) - DM	967.8459	6.6391	0.00246	0.0361	5	957.7003	0.81741
Phi(g+T) p(.) - DM	967.8518	6.645	0.00245	0.036	4	959.755	0.81986
Phi(g+prev) p(g*rad) - DM	967.9151	6.7083	0.00238	0.035	7	953.642	0.82224
Phi(rain) p(prev) - DM	968.0139	6.8071	0.00226	0.0332	4	959.9171	0.82450
Phi(g+rain) p(d) - DM	968.0407	6.8339	0.00223	0.0328	5	957.8951	0.82673

Phi(T) p(g+rad) - DM	968.0570	6.8502	0.00222	0.0326	5	957.9114	0.82895
Phi(g*prev) p(g*rh) - DM	968.0648	6.858	0.00221	0.0325	8	951.7127	0.83116
Phi(T) p(temp) - DM	968.1002	6.8934	0.00217	0.0319	4	960.0033	0.83333
Phi(T) p(prev) - DM	968.1036	6.8968	0.00216	0.0317	4	960.0067	0.83549
Phi(g*prev) p(T) - DM	968.1436	6.9368	0.00212	0.0311	6	955.9392	0.83761
...							

Table B.2. AIC value and relative variable importance for CJS Tully set

Phi(↓) p(→)	d	rh	rad	g+d	g+rh	.	g+ rad	g*d	g*rh	SUL	prev	g	temp	T	rain	g* rad	g+ SUL	g+ prev	g+ temp	g+T	g+ rain	g* SUL	g* rain	g* prev	g* temp	g*T	t
prev	961.2	961.6	962.4	962.8	963.0	963.1	964.2	964.2	964.5	964.7	964.7	964.8	964.9	965.1	965.1	965.9	966.4	966.5	966.7	966.8	966.9	966.9	968.3	968.6	968.7	968.8	978.3
g+prev	963.1	963.4	964.2	964.8	965.1	965.0	966.1	966.2	966.5	966.6	966.6	966.9	966.7	967.0	967.0	967.9	968.4	968.5	968.7	968.9	968.9	969.0	970.3	970.6	970.7	970.8	980.3
T	964.0	965.5	966.6	965.2	966.7	966.1	968.1	966.5	968.3	967.6	968.1	967.6	968.1	968.2	968.2	970.0	968.9	969.6	969.6	969.6	969.6	969.1	971.1	971.6	971.6	971.6	981.6
temp	964.0	964.6	965.6	965.3	965.8	965.3	967.0	966.7	967.4	966.8	967.2	966.8	967.1	967.3	967.3	968.9	968.2	968.7	968.6	968.7	968.8	968.6	970.3	970.7	970.6	970.6	980.3
g*prev	964.4	964.7	965.5	966.0	966.3	966.1	967.2	967.1	968.1	967.7	967.7	967.8	967.8	968.1	968.2	969.0	969.3	969.5	969.6	969.8	969.9	969.0	971.7	971.4	971.0	971.3	981.4
g+T	965.7	967.2	968.3	967.2	968.7	967.9	970.0	968.5	970.4	969.3	969.8	969.5	969.8	969.9	969.9	972.0	970.9	971.5	971.5	971.6	971.6	971.1	973.1	973.6	973.6	973.6	983.5
g+temp	965.8	966.3	967.3	967.3	967.8	967.1	969.0	968.7	969.5	968.5	968.9	968.7	968.8	969.1	969.1	970.9	970.1	970.6	970.6	970.7	970.8	970.6	972.3	972.7	972.6	972.6	982.3
rain	966.6	969.0	970.8	967.7	970.1	968.7	972.0	969.5	971.8	970.4	968.0	970.0	967.1	965.7	970.7	974.0	971.7	968.9	967.8	966.3	971.9	970.3	973.5	971.0	969.9	968.3	984.0
g*temp	967.7	968.3	969.2	969.1	969.6	968.8	970.7	970.1	971.5	970.2	970.6	970.3	970.5	970.8	970.8	972.7	971.6	972.2	972.1	972.3	972.3	971.4	974.1	974.2	973.8	973.8	984.2
g*T	967.7	969.2	970.3	969.1	970.6	969.7	971.9	970.3	972.4	971.1	971.7	971.3	971.7	971.8	971.8	973.9	972.6	973.3	973.3	973.4	973.4	972.3	975.1	975.4	975.2	975.1	985.6
g+rain	968.0	970.5	972.2	969.6	972.0	970.2	973.9	971.3	973.8	971.9	969.5	971.9	968.5	967.1	972.2	975.9	973.5	970.8	969.8	968.2	973.8	972.3	975.5	972.9	971.8	970.2	985.8
g*rain	970.0	972.4	974.2	971.6	973.9	972.2	975.9	973.4	975.5	973.9	971.5	973.9	970.6	969.1	974.2	977.9	975.5	972.9	971.8	970.3	975.8	974.4	977.4	974.9	973.9	972.3	988.0
rh	970.9	972.5	976.3	972.2	973.8	974.3	977.8	974.0	975.3	976.1	972.5	975.7	971.2	970.1	975.6	979.6	977.5	973.5	972.0	970.7	976.9	976.7	978.4	975.5	974.0	972.7	987.0
g+rh	972.6	974.3	978.0	974.2	975.8	976.0	979.7	976.0	977.4	977.8	974.1	977.7	972.8	971.7	977.3	981.6	979.5	975.4	974.0	972.7	978.9	978.8	980.5	977.5	976.0	974.7	989.0
g*rh	974.6	976.1	979.9	976.2	977.7	977.9	981.7	978.0	978.8	979.7	976.1	979.6	974.8	973.7	979.2	983.3	981.4	977.5	976.0	974.8	980.8	980.9	982.3	979.5	978.0	976.7	991.1
rad	977.3	973.5	980.1	979.2	975.2	983.8	982.2	980.7	976.6	985.7	985.8	985.8	985.2	984.2	983.7	983.8	987.7	987.8	987.2	986.2	985.6	987.2	987.4	989.9	989.1	988.1	984.8
.	978.0	975.3	984.1	979.9	977.0	984.8	986.1	981.5	978.4	986.7	985.8	986.8	984.4	983.1	984.0	987.8	988.7	987.8	986.2	984.9	985.8	987.9	987.7	989.8	988.2	986.8	986.2
SUL	979.1	976.3	985.2	980.9	977.9	985.9	987.2	982.5	979.3	987.9	986.9	987.9	985.5	984.2	985.1	988.8	989.9	988.9	987.3	986.0	986.9	987.2	988.7	990.9	989.3	987.9	987.5
g+rad	979.4	975.5	982.1	981.2	977.2	985.8	984.1	982.7	978.5	987.7	987.8	987.8	987.2	986.3	985.7	985.7	989.7	989.8	989.1	988.1	987.5	989.0	989.3	991.8	991.1	990.0	987.0
g	980.1	977.4	986.2	981.9	979.0	986.8	988.1	983.5	980.3	988.7	987.8	988.8	986.4	985.1	986.1	989.8	990.7	989.7	988.2	986.9	987.8	989.8	989.6	991.8	990.1	988.8	988.4
g*rad	980.6	976.2	983.2	982.5	977.8	986.7	985.2	984.0	979.0	988.6	988.7	988.7	988.2	987.0	986.7	986.1	990.6	990.6	990.0	988.8	988.5	989.7	990.4	992.4	990.9	989.7	986.6
g+SUL	981.2	978.3	987.2	983.0	979.9	987.9	989.2	984.6	981.2	990.0	989.0	989.9	987.5	986.2	987.1	990.8	991.9	990.8	989.3	988.0	988.9	989.0	990.7	992.9	991.2	989.9	989.7
g*SUL	982.2	979.3	988.3	984.0	980.9	989.0	990.3	985.6	982.3	991.1	990.0	991.0	988.6	987.3	988.2	991.9	993.0	991.9	990.3	989.0	989.9	987.0	991.8	994.0	992.3	990.9	990.8

Each colored cell in this table represents a separate model in the respective candidate model set. Numbers within the cells represent the $QAIC_c$ value for the respective model, and cells have been colored according to $QAIC_c$ ranking (the more parsimonious the model, the lower its $QAIC_c$ value, and the closer towards the white end of the spectrum; red cells represent poorly parsimonious models).

Model variables in this depiction (survival φ variables are rows, recapture ρ variables are columns) have been ordered according to the most parsimonious model φ(prev)ρ(d). Borders around $QAIC_c$ top-ranking 23 models (depicted with white or pale yellow) cumulatively hold approximately 49% of total support within the candidate model set. Models displayed in orange and red are lower ranking based on $QAIC_c$ values.

B.2.2 CJS Kirrama set

Table B.3. Ranking of most parsimonious models in CJS Kirrama set

Model (CJS Kirrama set)	$QAIC_c$	Delta $QAIC_c$	AIC_c Weights	Model Likelihood	NumPar	QDeviance	Cumulative sum of AIC_c Weight
Phi(T) p(g*d) - DM	364.0165	0	0.09538	1	6	351.3498	0.09538
Phi(temp) p(g*d) - DM	364.7136	0.6971	0.06731	0.7057	6	352.0469	0.16269
Phi(.) p(g*d) - DM	365.2255	1.209	0.05211	0.5463	5	354.753	0.2148
Phi(rain) p(g*d) - DM	365.6194	1.6029	0.0428	0.4487	6	352.9528	0.2576
Phi(g+T) p(g*d) - DM	366.2046	2.1881	0.03194	0.3349	7	351.3086	0.28954
Phi(rad) p(g*d) - DM	366.2723	2.2558	0.03088	0.3238	6	353.6057	0.32042
Phi(g+T) p(d) - DM	366.6434	2.6269	0.02565	0.2689	5	356.1709	0.34607
Phi(g+temp) p(g*d) - DM	366.8682	2.8517	0.02292	0.2403	7	351.9722	0.36899
Phi(g+temp) p(d) - DM	366.8698	2.8533	0.0229	0.2401	5	356.3973	0.39189
Phi(sul) p(g*d) - DM	367.0955	3.079	0.02046	0.2145	6	354.4288	0.41235
Phi(prev) p(g*d) - DM	367.1036	3.0871	0.02038	0.2137	6	354.4369	0.43273
Phi(T) p(d) - DM	367.1059	3.0894	0.02035	0.2134	4	358.7934	0.45308
Phi(rain) p(d) - DM	367.3238	3.3073	0.01825	0.1913	4	359.0113	0.47133
Phi(.) p(d) - DM	367.3593	3.3428	0.01793	0.188	3	361.1733	0.48926
Phi(g*rh) p(d) - DM	367.3941	3.3776	0.01762	0.1847	6	354.7274	0.50688
Phi(g) p(g*d) - DM	367.419	3.4025	0.0174	0.1824	6	354.7524	0.52428
Phi(rh) p(g*d) - DM	367.4196	3.4031	0.0174	0.1824	6	354.7529	0.54168
Phi(temp) p(d) - DM	367.562	3.5455	0.0162	0.1698	4	359.2495	0.55788
Phi(g+rain) p(d) - DM	367.6541	3.6376	0.01547	0.1622	5	357.1816	0.57335
Phi(g) p(d) - DM	367.6939	3.6774	0.01517	0.159	4	359.3814	0.58852
Phi(T) p(g+d) - DM	367.7395	3.723	0.01483	0.1555	5	357.267	0.60335
Phi(g+rain) p(g*d) - DM	367.8462	3.8297	0.01406	0.1474	7	352.9502	0.61741
Phi(g*sul) p(g*d) - DM	368.1411	4.1246	0.01213	0.1272	8	350.9798	0.62954
Phi(temp) p(g+d) - DM	368.2284	4.2119	0.01161	0.1217	5	357.756	0.64115
Phi(g*T) p(g*d) - DM	368.3541	4.3376	0.0109	0.1143	8	351.1928	0.65205
Phi(.) p(g+d) - DM	368.3577	4.3412	0.01088	0.1141	4	360.0452	0.66293
Phi(g+rad) p(g*d) - DM	368.4957	4.4792	0.01016	0.1065	7	353.5997	0.67309
Phi(g*T) p(d) - DM	368.6379	4.6214	0.00946	0.0992	6	355.9713	0.68255
Phi(g+T) p(g+d) - DM	368.6623	4.6458	0.00935	0.098	6	355.9957	0.6919
Phi(prev) p(d) - DM	368.6888	4.6723	0.00922	0.0967	4	360.3763	0.70112
Phi(rain) p(g+d) - DM	368.6992	4.6827	0.00918	0.0962	5	358.2267	0.7103
Phi(sul) p(d) - DM	368.7829	4.7664	0.0088	0.0923	4	360.4704	0.7191
Phi(g+prev) p(d) - DM	368.7969	4.7804	0.00874	0.0916	5	358.3245	0.72784
Phi(g+temp) p(g+d) - DM	368.9535	4.937	0.00808	0.0847	6	356.2868	0.73592
Phi(g*rain) p(d) - DM	369.0177	5.0012	0.00782	0.082	6	356.351	0.74374
Phi(rad) p(d) - DM	369.0527	5.0362	0.00769	0.0806	4	360.7402	0.75143
Phi(g*temp) p(d) - DM	369.0626	5.0461	0.00765	0.0802	6	356.396	0.75908
Phi(g*prev) p(d) - DM	369.0656	5.0491	0.00764	0.0801	6	356.399	0.76672
Phi(g*rad) p(d) - DM	369.0862	5.0697	0.00756	0.0793	6	356.4196	0.77428
Phi(g*temp) p(g*d) - DM	369.1335	5.117	0.00738	0.0774	8	351.9722	0.78166
Phi(g*rh) p(g+d) - DM	369.1915	5.175	0.00717	0.0752	7	354.2955	0.78883
Phi(rh) p(d) - DM	369.251	5.2345	0.00696	0.073	4	360.9385	0.79579
Phi(g+rad) p(d) - DM	369.267	5.2505	0.00691	0.0724	5	358.7945	0.8027
Phi(g+sul) p(g*d) - DM	369.2931	5.2766	0.00682	0.0715	7	354.3971	0.80952

Phi(g+prev) p(g*d) - DM	369.3259	5.3094	0.00671	0.0703	7	354.4299	0.81623
Phi(g*sul) p(d) - DM	369.591	5.5745	0.00587	0.0615	6	356.9243	0.8221
Phi(g+rh) p(d) - DM	369.6277	5.6112	0.00577	0.0605	5	359.1553	0.82787
Phi(g+rh) p(g*d) - DM	369.6483	5.6318	0.00571	0.0599	7	354.7523	0.83358
Phi(rad) p(g+d) - DM	369.6852	5.6687	0.0056	0.0587	5	359.2128	0.83918
Phi(g) p(g+d) - DM	369.7269	5.7104	0.00549	0.0576	5	359.2545	0.84467
Phi(g+sul) p(d) - DM	369.7378	5.7213	0.00546	0.0572	5	359.2654	0.85013
Phi(g+rain) p(g+d) - DM	369.821	5.8045	0.00524	0.0549	6	357.1544	0.85537
Phi(prev) p(g+d) - DM	369.9788	5.9623	0.00484	0.0507	5	359.5063	0.86021
Phi(sul) p(g+d) - DM	370.0071	5.9906	0.00477	0.05	5	359.5346	0.86498
Phi(g*rain) p(g*d) - DM	370.0849	6.0684	0.00459	0.0481	8	352.9237	0.86957
Phi(rh) p(g+d) - DM	370.4807	6.4642	0.00377	0.0395	5	360.0083	0.87334
Phi(g*rad) p(g*d) - DM	370.706	6.6895	0.00336	0.0352	8	353.5448	0.8767
Phi(g*T) p(g+d) - DM	370.7602	6.7437	0.00327	0.0343	7	355.8642	0.87997
Phi(g*prev) p(g+d) - DM	370.8056	6.7891	0.0032	0.0335	7	355.9096	0.88317
Phi(g+prev) p(g+d) - DM	370.9603	6.9438	0.00296	0.031	6	358.2936	0.88613
Phi(g*rh) p(g*d) - DM	371.059	7.0425	0.00282	0.0296	8	353.8977	0.88895
Phi(g*rad) p(g+d) - DM	371.1127	7.0962	0.00275	0.0288	7	356.2167	0.8917
Phi(g*rain) p(g+d) - DM	371.1195	7.103	0.00274	0.0287	7	356.2235	0.89444
Phi(g*temp) p(g+d) - DM	371.1755	7.159	0.00266	0.0279	7	356.2795	0.8971
Phi(g+rad) p(g+d) - DM	371.189	7.1725	0.00264	0.0277	6	358.5224	0.89974
Phi(.) p(T) - DM	371.3091	7.2926	0.00249	0.0261	3	365.123	0.90223
Phi(g*sul) p(g+d) - DM	371.3463	7.3298	0.00244	0.0256	7	356.4503	0.90467
Phi(g*prev) p(g*d) - DM	371.5755	7.559	0.00218	0.0229	8	354.4142	0.90685
Phi(.) p(temp) - DM	371.7484	7.7319	0.002	0.021	3	365.5623	0.90885
Phi(g+rh) p(g+d) - DM	371.7662	7.7497	0.00198	0.0208	6	359.0996	0.91083
Phi(g+sul) p(g+d) - DM	371.768	7.7515	0.00198	0.0208	6	359.1013	0.91281
Phi(sul) p(T) - DM	372.3751	8.3586	0.00146	0.0153	4	364.0626	0.91427
Phi(.) p(g+T) - DM	372.4459	8.4294	0.00141	0.0148	4	364.1334	0.91568
Phi(g) p(T) - DM	372.6781	8.6616	0.00125	0.0131	4	364.3656	0.91693
Phi(sul) p(temp) - DM	372.8207	8.8042	0.00117	0.0123	4	364.5082	0.9181
Phi(.) p(g+temp) - DM	372.9355	8.919	0.0011	0.0115	4	364.623	0.9192
Phi(g) p(temp) - DM	373.0577	9.0412	0.00104	0.0109	4	364.7452	0.92024
Phi(g*sul) p(T) - DM	373.0809	9.0644	0.00103	0.0108	6	360.4142	0.92127
Phi(rain) p(T) - DM	373.0918	9.0753	0.00102	0.0107	4	364.7793	0.92229
Phi(temp) p(T) - DM	373.1274	9.1109	0.001	0.0105	4	364.8149	0.92329
Phi(g*sul) p(g*sul) - DM	373.1476	9.1311	0.00099	0.0104	8	355.9863	0.92428
Phi(prev) p(T) - DM	373.2076	9.1911	0.00096	0.0101	4	364.8951	0.92524
Phi(T) p(T) - DM	373.3451	9.3286	0.0009	0.0094	4	365.0326	0.92614
Phi(rad) p(T) - DM	373.4172	9.4007	0.00087	0.0091	4	365.1047	0.92701
Phi(rh) p(T) - DM	373.4246	9.4081	0.00086	0.009	4	365.1121	0.92787
Phi(rain) p(temp) - DM	373.5343	9.5178	0.00082	0.0086	4	365.2218	0.92869
Phi(prev) p(temp) - DM	373.6139	9.5974	0.00079	0.0083	4	365.3013	0.92948
Phi(.) p(rad) - DM	373.6229	9.6064	0.00078	0.0082	3	367.4369	0.93026
Phi(g*sul) p(temp) - DM	373.6384	9.6219	0.00078	0.0082	6	360.9718	0.93104
Phi(temp) p(temp) - DM	373.7643	9.7478	0.00073	0.0077	4	365.4518	0.93177
Phi(sul) p(g+T) - DM	373.8044	9.7879	0.00071	0.0074	5	363.332	0.93248
Phi(T) p(temp) - DM	373.807	9.7905	0.00071	0.0074	4	365.4945	0.93319
Phi(rh) p(temp) - DM	373.8747	9.8582	0.00069	0.0072	4	365.5622	0.93388
Phi(rad) p(temp) - DM	373.8748	9.8583	0.00069	0.0072	4	365.5623	0.93457

Phi(temp) p(rad) - DM	374.0831	10.0666	0.00062	0.0065	4	365.7706	0.93519
Phi(.) p(.) - DM	374.0907	10.0742	0.00062	0.0065	2	369.9984	0.93581
Phi(T) p(rad) - DM	374.1538	10.1373	0.0006	0.0063	4	365.8414	0.93641
Phi(temp) p(g+T) - DM	374.1602	10.1437	0.0006	0.0063	5	363.6878	0.93701
Phi(g+sul) p(T) - DM	374.2672	10.2507	0.00057	0.006	5	363.7947	0.93758
Phi(prev) p(g+T) - DM	374.2855	10.269	0.00056	0.0059	5	363.8131	0.93814
…							

Table B.4. AIC value and relative variable importance for CJS Kirrama set

Phi(↓) p(→)	g*d	d	g+d	T	temp	rad	g+T	rh	g+ rad	g+ temp	.	g+rh	prev	g*T	g	g+ prev	g* rad	g*rh	rain	g* temp	SUL	g* prev	g+ rain	g+ SUL	g* rain	g* SUL
T	364.0	367.1	367.7	373.3	373.8	374.2	374.4	374.6	374.8	375.0	375.1	375.2	375.5	376.4	376.4	376.6	376.7	376.8	377.0	377.1	377.2	378.1	378.2	378.5	380.3	380.7
temp	364.7	367.6	368.2	373.1	373.8	374.1	374.2	374.7	374.8	374.9	375.1	375.3	375.6	376.1	376.3	376.6	376.7	377.0	376.9	377.1	377.2	378.1	377.9	378.4	380.0	380.6
.	365.2	367.4	368.4	371.3	371.7	373.6	372.4	374.6	374.7	372.9	374.1	375.8	375.6	374.4	375.5	377.0	376.7	377.6	376.2	375.1	376.2	378.5	377.6	377.4	379.7	379.6
rain	365.6	367.3	368.7	373.1	373.5	374.8	374.4	375.8	376.1	374.9	375.9	377.1	377.2	376.3	377.5	378.8	378.1	378.9	378.0	377.0	378.0	380.3	379.5	379.4	381.7	381.6
g+T	366.2	366.6	368.7	374.6	375.0	375.2	376.5	375.4	376.8	377.0	376.2	377.1	376.3	378.4	378.2	378.3	378.7	378.8	378.0	379.1	378.3	380.1	380.0	380.4	382.1	382.6
rad	366.3	369.1	369.7	373.4	373.9	375.4	374.5	375.9	376.3	375.1	374.8	376.8	376.0	376.4	375.9	377.0	378.3	378.6	376.7	377.2	376.9	378.5	377.7	377.8	379.9	380.0
g+temp	366.9	366.9	369.0	374.3	375.0	374.8	376.2	375.2	376.6	376.9	376.0	377.0	376.1	378.0	378.0	378.1	378.5	378.8	377.6	379.1	378.1	379.9	379.6	380.2	381.7	382.4
SUL	367.1	368.8	370.0	372.4	372.8	374.8	373.8	375.9	376.2	374.3	375.2	377.3	376.8	375.7	376.9	378.5	378.2	379.2	377.4	376.5	374.8	380.0	379.0	375.0	381.2	376.3
prev	367.1	368.7	370.0	373.2	373.6	375.7	374.3	376.7	376.8	374.7	375.8	377.8	377.6	376.3	377.2	378.9	378.8	379.7	378.0	376.9	377.9	380.4	379.3	379.1	381.5	381.2
g	367.4	367.7	369.7	372.7	373.1	375.0	374.5	375.9	376.8	374.9	375.4	377.8	376.9	376.4	377.4	378.9	378.8	379.7	377.5	377.1	377.5	380.5	379.6	379.4	381.7	381.6
rh	367.4	369.3	370.5	373.4	373.9	375.7	374.5	376.7	376.8	375.1	375.6	377.7	377.2	376.5	376.8	378.4	378.8	379.6	377.7	377.2	377.7	379.8	378.9	378.7	381.1	380.9
g+rain	367.8	367.7	369.8	374.5	374.9	376.3	376.4	377.1	378.2	376.9	377.4	379.1	378.7	378.4	379.4	380.7	380.2	381.0	379.4	379.1	379.5	382.4	381.5	381.4	383.7	383.7
g*SUL	368.1	369.6	371.3	373.1	373.6	375.3	374.8	376.4	377.0	375.4	375.7	378.1	377.4	376.7	377.7	379.3	379.1	380.2	377.9	377.6	378.2	381.0	379.9	374.3	382.0	373.1
g*T	368.4	368.6	370.8	376.8	377.2	377.1	378.7	377.3	378.9	379.2	378.3	379.2	378.4	380.6	380.4	380.5	380.8	380.9	380.2	381.4	380.5	382.2	382.2	382.6	384.4	384.8
g+rad	368.5	369.3	371.2	374.8	375.2	376.6	376.6	377.1	378.4	377.1	375.9	378.8	377.0	378.5	377.8	378.9	380.4	380.7	377.9	379.3	378.1	380.6	379.7	379.8	381.9	382.0
g*temp	369.1	369.1	371.2	376.5	377.1	377.0	378.4	377.4	378.8	379.1	378.1	379.2	378.3	380.3	380.2	380.3	380.8	381.1	379.8	381.3	380.3	382.2	381.8	382.4	383.9	384.6
g+SUL	369.3	369.7	371.8	374.3	374.7	376.7	376.0	377.7	378.4	376.5	377.1	379.5	378.7	378.0	379.0	380.6	380.5	381.4	379.2	378.7	376.9	382.2	381.2	376.3	383.4	377.7
g+prev	369.3	368.8	371.0	374.6	375.0	377.1	376.4	378.0	378.9	376.8	377.3	379.9	379.0	378.4	379.2	381.0	380.9	381.8	379.4	379.0	379.3	382.5	381.4	381.1	383.6	383.3
g+rh	369.6	369.6	371.8	374.8	375.2	377.1	376.6	377.9	378.9	377.1	376.9	379.8	378.4	378.6	378.8	380.3	380.9	381.7	379.0	379.3	379.0	382.0	380.9	380.7	383.1	382.9
g*rain	370.1	369.0	371.1	376.6	377.0	378.1	378.6	379.0	379.9	379.0	379.4	380.8	380.7	380.6	381.5	382.9	382.1	383.1	381.5	381.3	381.6	384.7	383.7	383.6	385.6	385.9
g*rad	370.7	369.1	371.1	374.9	375.7	377.4	377.0	378.1	379.4	377.8	377.6	380.1	378.9	379.2	379.6	380.9	381.6	382.3	379.6	379.5	379.6	382.0	381.6	381.4	383.8	383.5
g*rh	371.1	367.4	369.2	374.4	375.1	376.7	376.5	377.7	378.6	377.2	377.8	379.6	379.4	378.7	379.8	381.3	380.7	381.4	379.9	379.3	379.9	383.1	381.9	381.7	383.9	383.9
g*prev	371.6	369.1	370.8	376.3	376.7	378.5	377.8	379.3	379.9	378.6	378.7	381.0	380.3	380.0	380.7	382.3	382.1	383.2	380.9	380.8	380.8	384.5	382.9	382.7	384.9	384.9

Each colored cell in this table represents a separate model in the respective candidate model set. Numbers within the cells represent the $QAIC_c$ value for the respective model, and cells have been colored according to $QAIC_c$ ranking (the more parsimonious the model, the lower its $QAIC_c$ value, and the closer towards the white end of the spectrum; red cells represent poorly parsimonious models).

Model variables in this depiction (survival φ variables are rows, recapture ρ variables are columns) have been ordered according to the most parsimonious model φ(T)ρ(g*d). Borders around $QAIC_c$ top-ranking 15 models (depicted with white or pale yellow) cumulatively hold approximately 51% of total support within the candidate model set. Models displayed in orange and red are lower ranking based on $QAIC_c$ values.

B.2.3 Pradel population growth Tully set

Table B.5. Ranking of most parsimonious models in Pradel population growth Tully set

Model (Pop growth Tully set)	$QAIC_c$	Delta $QAIC_c$	AIC_c Weights	Model Likelihood	NumPar	QDeviance	Cumulative sum of AIC_c Weight
Phi(prev)p(rh)lambda(rh) - DM	2544.797	0	0.40614	1	6	2532.596	0.40614
Phi(Ts)p(rh)lambda(rh) - DM	2546.097	1.2995	0.21208	0.5222	6	2533.896	0.61822
Phi(temp)p(rh)lambda(rh) - DM	2546.206	1.4085	0.20083	0.4945	6	2534.005	0.81905
Phi(prev)p(rad)lambda(prev) - DM	2547.719	2.9213	0.09426	0.2321	6	2535.518	0.91331
Phi(prev)p(rad)lambda(temp) - DM	2552.24	7.4424	0.00983	0.0242	6	2540.039	0.92314
Phi(temp)p(rad)lambda(prev) - DM	2552.547	7.7501	0.00843	0.0208	6	2540.346	0.93157
Phi(prev)p(rh)lambda(prev) - DM	2552.889	8.0915	0.00711	0.0175	6	2540.688	0.93868
Phi(.)p(rh)lambda(rh) - DM	2552.979	8.1816	0.00679	0.0167	5	2542.836	0.94547
Phi(prev)p(rh)lambda(temp) - DM	2553.092	8.2943	0.00642	0.0158	6	2540.891	0.95189
Phi(temp)p(rad)lambda(temp) - DM	2553.369	8.5712	0.00559	0.0138	6	2541.168	0.95748
Phi(prev)p(.)lambda(temp) - DM	2553.451	8.6538	0.00536	0.0132	5	2543.308	0.96284
Phi(prev)p(.)lambda(prev) - DM	2553.578	8.7808	0.00503	0.0124	5	2543.435	0.96787
Phi(temp)p(.)lambda(temp) - DM	2554.476	9.679	0.00321	0.0079	5	2544.333	0.97108
Phi(prev)p(d)lambda(temp) - DM	2554.719	9.9213	0.00285	0.007	6	2542.518	0.97393
Phi(temp)p(rh)lambda(temp) - DM	2555.024	10.2265	0.00244	0.006	6	2542.823	0.97637
Phi(prev)p(d)lambda(prev) - DM	2555.586	10.7883	0.00185	0.0046	6	2543.385	0.97822
Phi(prev)p(d)lambda(rh) - DM	2555.618	10.8203	0.00182	0.0045	6	2543.417	0.98004
Phi(prev)p(rad)lambda(rh) - DM	2555.853	11.0557	0.00161	0.004	6	2543.652	0.98165
Phi(prev)p(.)lambda(rh) - DM	2555.936	11.1385	0.00155	0.0038	5	2545.793	0.98320
Phi(temp)p(d)lambda(temp) - DM	2556.056	11.2586	0.00146	0.0036	6	2543.855	0.98466
Phi(Ts)p(rad)lambda(temp) - DM	2556.345	11.5479	0.00126	0.0031	6	2544.144	0.98592
Phi(Ts)p(.)lambda(rh) - DM	2556.365	11.5674	0.00125	0.0031	5	2546.222	0.98717
Phi(Ts)p(d)lambda(rh) - DM	2556.396	11.5988	0.00123	0.003	6	2544.195	0.98840
Phi(Ts)p(rad)lambda(rh) - DM	2556.448	11.6504	0.0012	0.003	6	2544.247	0.98960
Phi(Ts)p(rad)lambda(prev) - DM	2556.538	11.741	0.00115	0.0028	6	2544.337	0.99075
Phi(temp)p(rad)lambda(rh) - DM	2556.713	11.9159	0.00105	0.0026	6	2544.512	0.99180
Phi(temp)p(d)lambda(rh) - DM	2556.779	11.9817	0.00102	0.0025	6	2544.578	0.99282
Phi(prev)p(rad)lambda(Ts) - DM	2556.784	11.9866	0.00101	0.0025	6	2544.583	0.99383
Phi(temp)p(.)lambda(rh) - DM	2556.877	12.0792	0.00097	0.0024	5	2546.733	0.99480
Phi(prev)p(rh)lambda(Ts) - DM	2557.768	12.971	0.00062	0.0015	6	2545.567	0.99542
Phi(Ts)p(.)lambda(temp) - DM	2557.859	13.0621	0.00059	0.0015	5	2547.716	0.99601
Phi(Ts)p(rh)lambda(temp) - DM	2558.091	13.2933	0.00053	0.0013	6	2545.89	0.99654
Phi(temp)p(rad)lambda(Ts) - DM	2558.428	13.6304	0.00045	0.0011	6	2546.227	0.99699
Phi(temp)p(rh)lambda(prev) - DM	2558.644	13.847	0.0004	0.001	6	2546.443	0.99739
Phi(prev)p(d)lambda(Ts) - DM	2558.669	13.8714	0.00039	0.001	6	2546.468	0.99778
Phi(Ts)p(rad)lambda(Ts) - DM	2558.993	14.1958	0.00034	0.0008	6	2546.792	0.99812
Phi(temp)p(.)lambda(prev) - DM	2559.321	14.524	0.00028	0.0007	5	2549.178	0.99840
Phi(prev)p(.)lambda(Ts) - DM	2559.382	14.5847	0.00028	0.0007	5	2549.239	0.99868
Phi(Ts)p(d)lambda(temp) - DM	2559.432	14.6344	0.00027	0.0007	6	2547.231	0.99895
Phi(temp)p(rh)lambda(Ts) - DM	2560.033	15.2359	0.0002	0.0005	6	2547.832	0.99915
Phi(temp)p(d)lambda(Ts) - DM	2560.584	15.7862	0.00015	0.0004	6	2548.383	0.99930
Phi(Ts)p(rh)lambda(Ts) - DM	2560.759	15.9617	0.00014	0.0003	6	2548.558	0.99944
Phi(temp)p(.)lambda(Ts) - DM	2560.885	16.088	0.00013	0.0003	5	2550.742	0.99957
Phi(temp)p(d)lambda(prev) - DM	2561.374	16.5764	0.0001	0.0002	6	2549.173	0.99967

Phi(Ts)p(d)lambda(Ts) - DM	2561.392	16.5944	0.0001	0.0002	6	2549.191	0.99977
Phi(Ts)p(.)lambda(Ts) - DM	2561.442	16.6449	0.0001	0.0002	5	2551.299	0.99987
Phi(Ts)p(rh)lambda(prev) - DM	2562.77	17.9727	0.00005	0.0001	6	2550.569	0.99992
Phi(Ts)p(.)lambda(prev) - DM	2563.972	19.175	0.00003	0.0001	5	2553.829	0.99995
Phi(prev)p(rh)lambda(d) - DM	2565.491	20.6935	0.00001	0	6	2553.29	0.99996
Phi(.)p(d)lambda(rh) - DM	2565.715	20.9181	0.00001	0	5	2555.572	0.99997
Phi(.)p(rad)lambda(rh) - DM	2565.734	20.9366	0.00001	0	5	2555.591	0.99998
Phi(Ts)p(d)lambda(prev) - DM	2566.013	21.2161	0.00001	0	6	2553.812	0.99999
Phi(.)p(.)lambda(rh) - DM	2566.983	22.1857	0.00001	0	4	2558.888	1.00000
Phi(temp)p(rh)lambda(d) - DM	2567.8	23.0029	0	0	6	2555.599	1.00000
Phi(Ts)p(rh)lambda(d) - DM	2569.528	24.731	0	0	6	2557.327	1.00000
Phi(prev)p(rad)lambda(d) - DM	2573.069	28.2715	0	0	6	2560.868	1.00000
Phi(.)p(rh)lambda(temp) - DM	2573.148	28.3505	0	0	5	2563.005	1.00000
Phi(.)p(rad)lambda(prev) - DM	2574.249	29.4512	0	0	5	2564.105	1.00000
Phi(.)p(rad)lambda(temp) - DM	2574.402	29.6042	0	0	5	2564.258	1.00000
Phi(temp)p(rad)lambda(d) - DM	2574.53	29.7323	0	0	6	2562.329	1.00000
Phi(.)p(rh)lambda(Ts) - DM	2574.924	30.1266	0	0	5	2564.781	1.00000
Phi(.)p(rh)lambda(prev) - DM	2575.944	31.1471	0	0	5	2565.801	1.00000
Phi(Ts)p(rad)lambda(d) - DM	2576.16	31.3624	0	0	6	2563.959	1.00000
Phi(prev)p(.)lambda(d) - DM	2576.303	31.5057	0	0	5	2566.16	1.00000
Phi(.)p(rad)lambda(Ts) - DM	2576.694	31.8963	0	0	5	2566.55	1.00000
Phi(temp)p(.)lambda(d) - DM	2577.719	32.9212	0	0	5	2567.575	1.00000
Phi(.)p(rh)lambda(d) - DM	2577.904	33.1062	0	0	5	2567.76	1.00000
Phi(.)p(.)lambda(temp) - DM	2578.332	33.5345	0	0	4	2570.237	1.00000
Phi(prev)p(d)lambda(d) - DM	2578.357	33.5599	0	0	6	2566.156	1.00000
Phi(.)p(d)lambda(temp) - DM	2578.479	33.6817	0	0	5	2568.336	1.00000
Phi(temp)p(d)lambda(d) - DM	2579.728	34.9306	0	0	6	2567.527	1.00000
Phi(.)p(d)lambda(Ts) - DM	2580.046	35.2489	0	0	5	2569.903	1.00000
Phi(Ts)p(.)lambda(d) - DM	2580.252	35.4542	0	0	5	2570.108	1.00000
Phi(prev)p(rh)lambda(Tl) - DM	2580.659	35.8613	0	0	6	2568.458	1.00000
Phi(prev)p(rh)lambda(rad) - DM	2580.802	36.0044	0	0	6	2568.601	1.00000
Phi(Ts)p(rh)lambda(rad) - DM	2581.65	36.853	0	0	6	2569.449	1.00000
Phi(.)p(rh)lambda(rad) - DM	2581.742	36.9449	0	0	5	2571.599	1.00000
Phi(.)p(.)lambda(Ts) - DM	2581.947	37.1495	0	0	4	2573.852	1.00000
Phi(Ts)p(rh)lambda(Tl) - DM	2582.078	37.2806	0	0	6	2569.877	1.00000
Phi(temp)p(rh)lambda(rad) - DM	2582.155	37.3574	0	0	6	2569.954	1.00000
Phi(Ts)p(d)lambda(d) - DM	2582.307	37.5093	0	0	6	2570.106	1.00000
Phi(temp)p(rh)lambda(Tl) - DM	2582.718	37.9206	0	0	6	2570.517	1.00000
Phi(.)p(.)lambda(prev) - DM	2583.173	38.3755	0	0	4	2575.078	1.00000
Phi(.)p(rh)lambda(Tl) - DM	2583.632	38.8348	0	0	5	2573.489	1.00000
Phi(prev)p(rh)lambda(.) - DM	2583.828	39.0306	0	0	5	2573.685	1.00000
Phi(.)p(d)lambda(prev) - DM	2584.244	39.4471	0	0	5	2574.101	1.00000
Phi(temp)p(rh)lambda(.) - DM	2586.337	41.5397	0	0	5	2576.194	1.00000
Phi(Ts)p(rh)lambda(.) - DM	2586.383	41.5859	0	0	5	2576.24	1.00000
Phi(.)p(rad)lambda(d) - DM	2586.954	42.1567	0	0	5	2576.811	1.00000
Phi(.)p(rh)lambda(.) - DM	2588.095	43.2975	0	0	4	2580	1.00000
Phi(.)p(.)lambda(d) - DM	2591.53	46.7322	0	0	4	2583.434	1.00000
Phi(prev)p(rad)lambda(Tl) - DM	2591.861	47.0636	0	0	6	2579.66	1.00000
Phi(Ts)p(rad)lambda(Tl) - DM	2592.566	47.7689	0	0	6	2580.365	1.00000
Phi(.)p(d)lambda(d) - DM	2593.52	48.7227	0	0	5	2583.377	1.00000

Phi(prev)p(rad)lambda(.) - DM	2593.617	48.8192	0	0	5	2583.473	1.00000
Phi(temp)p(rad)lambda(Tl) - DM	2593.703	48.9052	0	0	6	2581.502	1.00000
Phi(Ts)p(rad)lambda(.) - DM	2595.161	50.3634	0	0	5	2585.018	1.00000
Phi(temp)p(rad)lambda(.) - DM	2595.633	50.8355	0	0	5	2585.49	1.00000
Phi(prev)p(rad)lambda(rad) - DM	2595.666	50.8686	0	0	6	2583.465	1.00000
Phi(.)p(rad)lambda(Tl) - DM	2596.382	51.5851	0	0	5	2586.239	1.00000
...							

Table B.6. AIC value and relative variable importance for Pradel population growth Tully set

Phi(↓) p(→) lambda(.)	.	rh	rad	d
.	2622.5	2588.1	2599.4	2620.0
prev	2616.7	2583.8	2593.6	2614.5
temp	2619.2	2586.3	2595.6	2617.3
Ts	2617.9	2586.4	2595.2	2616.4

Phi(↓) p(→) lambda(rh)	.	rh	rad	d
.	2567.0	2553.0	2565.7	2565.7
prev	2555.9	2544.8	2555.9	2555.6
temp	2556.9	2546.2	2556.7	2556.8
Ts	2556.4	2546.1	2556.4	2556.4

Phi(↓) p(→) lambda(prev)	.	rh	rad	d
.	2583.2	2575.9	2574.2	2584.2
prev	2553.6	2552.9	2547.7	2555.6
temp	2559.3	2558.6	2552.5	2561.4
Ts	2564.0	2562.8	2556.5	2566.0

Phi(↓) p(→) lambda(rad)	.	rh	rad	d
.	2620.7	2581.7	2600.9	2617.3
prev	2616.9	2580.8	2595.7	2614.2
temp	2618.8	2582.2	2597.7	2616.2
Ts	2617.2	2581.7	2597.1	2615.0

Phi(↓) p(→) lambda(temp)	.	rh	rad	d
.	2578.3	2573.1	2574.4	2578.5
prev	2553.5	2553.1	2552.2	2554.7
temp	2554.5	2555.0	2553.4	2556.1
Ts	2557.9	2558.1	2556.3	2559.4

Phi(↓) p(→) lambda(d)	.	rh	rad	d
.	2591.5	2577.9	2587.0	2593.5
prev	2576.3	2565.5	2573.1	2578.4
temp	2577.7	2567.8	2574.5	2579.7
Ts	2580.3	2569.5	2576.2	2582.3

Phi(↓) p(→) lambda(Ts)	.	rh	rad	d
.	2581.9	2574.9	2576.7	2580.0
prev	2559.4	2557.8	2556.8	2558.7
temp	2560.9	2560.0	2558.4	2560.6
Ts	2561.4	2560.8	2559.0	2561.4

Phi(↓) p(→) lambda(Tl)	.	rh	rad	d
.	2613.2	2583.6	2596.4	2607.6
prev	2608.6	2580.7	2591.9	2603.4
temp	2610.7	2582.7	2593.7	2605.7
Ts	2608.4	2582.1	2592.6	2603.9

These eight tables represent the different variables used to constrain the population growth parameter (λ, lambda). Survival (φ, phi) variables are rows, recapture (ρ, p) variables are columns. Each colored cell in these tables represents a separate model in the respective candidate model set. Numbers within the cells represent the $QAIC_c$ value for the respective model, and cells have been colored according to $QAIC_c$ ranking (the more parsimonious the model, the lower its $QAIC_c$ value, and the closer towards the white end of the spectrum; red cells represent poorly parsimonious models). Borders around $QAIC_c$ top-ranking 4 models (depicted with white or pale yellow) cumulatively hold approximately 91% of total support within the candidate model set. Models displayed in orange and red are lower ranking based on $QAIC_c$ values.

B.2.4 Pradel population growth Kirrama set

Table B.7. Ranking of most parsimonious models in Pradel population growth Kirrama set

Model (Pop growth Kirrama set)	$QAIC_c$	Delta $QAIC_c$	AIC_c Weights	Model Likelihood	NumPar	QDeviance	Cumulative sum of AIC_c Weight
Phi(.)p(g+d)lambda(Ts) - DM	845.3855	0	0.15706	1	6	832.7679	0.15706
Phi(temp)p(g+d)lambda(Ts) - DM	846.0411	0.6556	0.11316	0.7205	7	831.2115	0.27022
Phi(Ts)p(g+d)lambda(Ts) - DM	846.0614	0.6759	0.11202	0.7132	7	831.2318	0.38224
Phi(rain)p(g+d)lambda(Ts) - DM	847.1837	1.7982	0.06391	0.4069	7	832.3541	0.44615
Phi(.)p(g+d)lambda(temp) - DM	847.3888	2.0033	0.05768	0.3672	6	834.7712	0.50383
Phi(.)p(g*d)lambda(Ts) - DM	847.5754	2.1899	0.05255	0.3346	7	832.7458	0.55638
Phi(temp)p(g+d)lambda(temp) - DM	847.8733	2.4878	0.04527	0.2882	7	833.0437	0.60165
Phi(temp)p(g*d)lambda(Ts) - DM	848.2221	2.8366	0.03803	0.2421	8	831.1475	0.63968
Phi(Ts)p(g*d)lambda(Ts) - DM	848.2352	2.8497	0.03778	0.2405	8	831.1606	0.67746
Phi(Ts)p(g+d)lambda(temp) - DM	848.3085	2.923	0.03642	0.2319	7	833.4789	0.71388
Phi(rain)p(g+d)lambda(temp) - DM	849.2858	3.9003	0.02234	0.1422	7	834.4562	0.73622
Phi(rain)p(g*d)lambda(Ts) - DM	849.4119	4.0264	0.02098	0.1336	8	832.3373	0.7572
Phi(.)p(g*d)lambda(temp) - DM	849.5564	4.1709	0.01952	0.1243	7	834.7268	0.77672
Phi(.)p(g+d)lambda(rain) - DM	849.5655	4.18	0.01943	0.1237	6	836.9479	0.79615
Phi(temp)p(g*d)lambda(temp) - DM	850.001	4.6155	0.01563	0.0995	8	832.9264	0.81178
Phi(Ts)p(g*d)lambda(temp) - DM	850.445	5.0595	0.01251	0.0796	8	833.3704	0.82429
Phi(temp)p(d)lambda(Ts) - DM	850.9496	5.5641	0.00972	0.0619	6	838.332	0.83401
Phi(Ts)p(d)lambda(Ts) - DM	851.0126	5.6271	0.00942	0.06	6	838.395	0.84343
Phi(.)p(d)lambda(Ts) - DM	851.1144	5.7289	0.00895	0.057	5	840.6764	0.85238
Phi(rain)p(g+d)lambda(rain) - DM	851.2749	5.8894	0.00826	0.0526	7	836.4453	0.86064
Phi(rain)p(g*d)lambda(temp) - DM	851.4914	6.1059	0.00742	0.0472	8	834.4168	0.86806
Phi(Ts)p(g+d)lambda(rain) - DM	851.6888	6.3033	0.00672	0.0428	7	836.8592	0.87478
Phi(temp)p(g+d)lambda(rain) - DM	851.713	6.3275	0.00664	0.0423	7	836.8834	0.88142
Phi(.)p(g+d)lambda(rh) - DM	851.7322	6.3467	0.00658	0.0419	6	839.1146	0.888
Phi(.)p(g*d)lambda(rain) - DM	851.749	6.3635	0.00652	0.0415	7	836.9194	0.89452
Phi(rain)p(d)lambda(Ts) - DM	851.7505	6.365	0.00652	0.0415	6	839.1329	0.90104
Phi(.)p(g+d)lambda(.) - DM	851.8693	6.4838	0.00614	0.0391	5	841.4313	0.90718
Phi(temp)p(d)lambda(temp) - DM	852.4064	7.0209	0.00469	0.0299	6	839.7888	0.91187
Phi(.)p(d)lambda(temp) - DM	852.4919	7.1064	0.0045	0.0287	5	842.0539	0.91637
Phi(Ts)p(d)lambda(temp) - DM	852.8425	7.457	0.00377	0.024	6	840.2249	0.92014
Phi(.)p(d)lambda(rain) - DM	853.0364	7.6509	0.00343	0.0218	5	842.5984	0.92357
Phi(.)p(g+d)lambda(Tl) - DM	853.0837	7.6982	0.00335	0.0213	6	840.4661	0.92692
Phi(rain)p(d)lambda(temp) - DM	853.365	7.9795	0.00291	0.0185	6	840.7474	0.92983
Phi(.)p(g+d)lambda(d) - DM	853.4175	8.032	0.00283	0.018	6	840.7999	0.93266
Phi(rain)p(g*d)lambda(rain) - DM	853.5003	8.1148	0.00272	0.0173	8	836.4257	0.93538
Phi(.)p(d)lambda(.) - DM	853.5586	8.1731	0.00264	0.0168	4	845.2687	0.93802
Phi(rain)p(d)lambda(rain) - DM	853.7587	8.3732	0.00239	0.0152	6	841.1411	0.94041
Phi(rain)p(g+d)lambda(rh) - DM	853.7966	8.4111	0.00234	0.0149	7	838.967	0.94275
Phi(Ts)p(g*d)lambda(rain) - DM	853.898	8.5125	0.00223	0.0142	8	836.8234	0.94498
Phi(Ts)p(g+d)lambda(rh) - DM	853.9237	8.5382	0.0022	0.014	7	839.0941	0.94718
Phi(temp)p(g*d)lambda(rain) - DM	853.9239	8.5384	0.0022	0.014	8	836.8493	0.94938
Phi(temp)p(g+d)lambda(rh) - DM	853.9251	8.5396	0.0022	0.014	7	839.0955	0.95158
Phi(.)p(g*d)lambda(rh) - DM	853.9312	8.5457	0.00219	0.0139	7	839.1015	0.95377
Phi(temp)p(g+d)lambda(.) - DM	853.9435	8.558	0.00218	0.0139	6	841.3259	0.95595
Phi(Ts)p(g+d)lambda(.) - DM	853.9872	8.6017	0.00213	0.0136	6	841.3696	0.95808
Phi(.)p(g+d)lambda(rad) - DM	854.0204	8.6349	0.00209	0.0133	6	841.4028	0.96017

Phi(.)p(g*d)lambda(.) - DM	854.0392	8.6537	0.00207	0.0132	6	841.4216	0.96224
Phi(rain)p(g+d)lambda(.) - DM	854.0467	8.6612	0.00207	0.0132	6	841.4291	0.96431
Phi(.)p(d)lambda(rh) - DM	854.3583	8.9728	0.00177	0.0113	5	843.9203	0.96608
Phi(Ts)p(d)lambda(rain) - DM	854.784	9.3985	0.00143	0.0091	6	842.1664	0.96751
Phi(temp)p(d)lambda(rain) - DM	854.7934	9.4079	0.00142	0.009	6	842.1758	0.96893
Phi(.)p(d)lambda(Tl) - DM	854.9917	9.6062	0.00129	0.0082	5	844.5537	0.97022
Phi(Ts)p(g+d)lambda(Tl) - DM	855.2132	9.8277	0.00115	0.0073	7	840.3836	0.97137
Phi(temp)p(g+d)lambda(Tl) - DM	855.2269	9.8414	0.00115	0.0073	7	840.3973	0.97252
Phi(rain)p(g+d)lambda(Tl) - DM	855.2583	9.8728	0.00113	0.0072	7	840.4287	0.97365
Phi(.)p(d)lambda(d) - DM	855.2736	9.8881	0.00112	0.0071	5	844.8356	0.97477
Phi(.)p(g*d)lambda(Tl) - DM	855.2776	9.8921	0.00112	0.0071	7	840.448	0.97589
Phi(temp)p(d)lambda(.) - DM	855.2992	9.9137	0.0011	0.007	5	844.8612	0.97699
Phi(Ts)p(d)lambda(.) - DM	855.4022	10.0167	0.00105	0.0067	5	844.9642	0.97804
Phi(rain)p(d)lambda(.) - DM	855.458	10.0725	0.00102	0.0065	5	845.02	0.97906
Phi(temp)p(g+d)lambda(d) - DM	855.5649	10.1794	0.00097	0.0062	7	840.7353	0.98003
Phi(Ts)p(g+d)lambda(d) - DM	855.572	10.1865	0.00096	0.0061	7	840.7424	0.98099
Phi(.)p(g*d)lambda(d) - DM	855.6144	10.2289	0.00094	0.006	7	840.7848	0.98193
Phi(rain)p(g+d)lambda(d) - DM	855.6222	10.2367	0.00094	0.006	7	840.7926	0.98287
Phi(.)p(d)lambda(rad) - DM	855.7064	10.3209	0.0009	0.0057	5	845.2684	0.98377
Phi(rain)p(d)lambda(rh) - DM	855.7456	10.3601	0.00088	0.0056	6	843.128	0.98465
Phi(rain)p(g*d)lambda(rh) - DM	856.0322	10.6467	0.00077	0.0049	8	838.9576	0.98542
Phi(temp)p(g*d)lambda(.) - DM	856.1426	10.7571	0.00072	0.0046	7	841.313	0.98614
Phi(temp)p(g+d)lambda(rad) - DM	856.1465	10.761	0.00072	0.0046	7	841.3168	0.98686
Phi(Ts)p(g*d)lambda(rh) - DM	856.1538	10.7683	0.00072	0.0046	8	839.0792	0.98758
Phi(temp)p(g*d)lambda(rh) - DM	856.1554	10.7699	0.00072	0.0046	8	839.0808	0.9883
Phi(Ts)p(g+d)lambda(rad) - DM	856.1842	10.7987	0.00071	0.0045	7	841.3546	0.98901
Phi(Ts)p(g*d)lambda(.) - DM	856.1866	10.8011	0.00071	0.0045	7	841.357	0.98972
Phi(.)p(g*d)lambda(rad) - DM	856.2232	10.8377	0.0007	0.0045	7	841.3936	0.99042
Phi(rain)p(g+d)lambda(rad) - DM	856.232	10.8465	0.00069	0.0044	7	841.4023	0.99111
Phi(rain)p(g*d)lambda(.) - DM	856.2486	10.8631	0.00069	0.0044	7	841.419	0.9918
Phi(temp)p(d)lambda(rh) - DM	856.249	10.8635	0.00069	0.0044	6	843.6313	0.99249
Phi(Ts)p(d)lambda(rh) - DM	856.2792	10.8937	0.00068	0.0043	6	843.6615	0.99317
Phi(rain)p(d)lambda(Tl) - DM	856.6788	11.2933	0.00055	0.0035	6	844.0612	0.99372
Phi(temp)p(d)lambda(Tl) - DM	856.8741	11.4886	0.0005	0.0032	6	844.2565	0.99422
Phi(Ts)p(d)lambda(Tl) - DM	856.8766	11.4911	0.0005	0.0032	6	844.259	0.99472
Phi(rain)p(d)lambda(d) - DM	857.0844	11.6989	0.00045	0.0029	6	844.4668	0.99517
Phi(temp)p(d)lambda(d) - DM	857.1322	11.7467	0.00044	0.0028	6	844.5146	0.99561
Phi(Ts)p(d)lambda(d) - DM	857.1766	11.7911	0.00043	0.0027	6	844.559	0.99604
Phi(Ts)p(g*d)lambda(Tl) - DM	857.4353	12.0498	0.00038	0.0024	8	840.3607	0.99642
Phi(temp)p(g*d)lambda(Tl) - DM	857.4502	12.0647	0.00038	0.0024	8	840.3756	0.9968
Phi(temp)p(d)lambda(rad) - DM	857.4588	12.0733	0.00038	0.0024	6	844.8412	0.99718
Phi(rain)p(g*d)lambda(Tl) - DM	857.4869	12.1014	0.00037	0.0024	8	840.4123	0.99755
Phi(Ts)p(d)lambda(rad) - DM	857.5704	12.1849	0.00035	0.0022	6	844.9528	0.9979
Phi(rain)p(d)lambda(rad) - DM	857.6323	12.2468	0.00034	0.0022	6	845.0146	0.99824
Phi(temp)p(g*d)lambda(d) - DM	857.7919	12.4064	0.00032	0.002	8	840.7173	0.99856
Phi(Ts)p(g*d)lambda(d) - DM	857.7986	12.4131	0.00032	0.002	8	840.724	0.99888
Phi(rain)p(g*d)lambda(d) - DM	857.8529	12.4674	0.00031	0.002	8	840.7783	0.99919
Phi(temp)p(g*d)lambda(rad) - DM	858.3791	12.9936	0.00024	0.0015	8	841.3045	0.99943
Phi(Ts)p(g*d)lambda(rad) - DM	858.4173	13.0318	0.00023	0.0015	8	841.3427	0.99966
Phi(rain)p(g*d)lambda(rad) - DM	858.4676	13.0821	0.00023	0.0015	8	841.393	0.99989

Phi(.)p(g)lambda(Ts) - DM	865.4424	20.0569	0.00001	0.0001	5	855.0044	0.9999
Phi(.)p(g)lambda(.) - DM	865.8341	20.4486	0.00001	0.0001	4	857.5442	0.99991
Phi(.)p(g)lambda(d) - DM	865.9353	20.5498	0.00001	0.0001	5	855.4973	0.99992
Phi(.)p(.)lambda(d) - DM	865.9434	20.5579	0.00001	0.0001	4	857.6535	0.99993
...							

Table B.8. AIC value and relative variable importance for Pradel population growth Kirrama set

Phi(↓) p(→) lambda(.)	.	g	d	g+d	g*d
.	866.0	865.8	853.6	851.9	854.0
temp	867.8	867.8	855.3	853.9	856.1
rain	868.1	867.9	855.5	854.0	856.2
Ts	868.0	868.0	855.4	854.0	856.2

Phi(↓) p(→) lambda(Ts)	.	g	d	g+d	g*d
.	867.0	865.4	851.1	845.4	847.6
temp	868.1	867.0	850.9	846.0	848.2
rain	868.9	867.6	851.8	847.2	849.4
Ts	868.6	867.3	851.0	846.1	848.2

Phi(↓) p(→) lambda(rain)	.	g	d	g+d	g*d
.	868.1	867.7	853.0	849.6	851.7
temp	869.9	869.8	854.8	851.7	853.9
rain	870.1	869.9	853.8	851.3	853.5
Ts	870.1	869.9	854.8	851.7	853.9

Phi(↓) p(→) lambda(d)	.	g	d	g+d	g*d
.	865.9	865.9	855.3	853.4	855.6
temp	867.4	867.8	857.1	855.6	857.8
rain	868.1	868.0	857.1	855.6	857.9
Ts	867.8	868.1	857.2	855.6	857.8

Phi(↓) p(→) lambda(temp)	.	g	d	g+d	g*d
.	867.7	866.7	852.5	847.4	849.6
temp	869.1	868.3	852.4	847.9	850.0
rain	869.7	868.9	853.4	849.3	851.5
Ts	869.5	868.7	852.8	848.3	850.4

Phi(↓) p(→) lambda(Tl)	.	g	d	g+d	g*d
.	867.9	867.8	855.0	853.1	855.3
temp	869.6	869.8	856.9	855.2	857.5
rain	870.0	869.9	856.7	855.3	857.5
Ts	869.9	869.9	856.9	855.2	857.4

Phi(↓) p(→) lambda(rh)	.	g	d	g+d	g*d
.	868.1	868.0	854.4	851.7	853.9
temp	869.9	870.0	856.2	853.9	856.2
rain	870.2	870.1	855.7	853.8	856.0
Ts	870.1	870.1	856.3	853.9	856.2

Phi(↓) p(→) lambda(rad)	.	g	d	g+d	g*d
.	868.0	867.9	855.7	854.0	856.2
temp	869.6	869.9	857.5	856.1	858.4
rain	870.1	870.0	857.6	856.2	858.5
Ts	869.9	870.1	857.6	856.2	858.4

These eight tables represent the different variables used to constrain the population growth parameter (λ, lambda). Survival (φ, phi) variables are rows, recapture (ρ, p) variables are columns. Each colored cell in these tables represents a separate model in the respective candidate model set. Numbers within the cells represent the $QAIC_c$ value for the respective model, and cells have been colored according to $QAIC_c$ ranking (the more parsimonious the model, the lower its $QAIC_c$ value, and the closer towards the white end of the spectrum; red cells represent poorly parsimonious models). Borders around $QAIC_c$ top-ranking 5 models (depicted with white or pale yellow) cumulatively hold approximately 50% of total support within the candidate model set. Models displayed in orange and red are lower ranking based on $QAIC_c$ values.

B.2.5 Pradel recruitment Tully set

Table B.9. Ranking of most parsimonious models in Pradel recruitment Tully set

Model (recruitment Tully set)	$QAIC_c$	Delta $QAIC_c$	AIC_c Weights	Model Likelihood	NumPar	QDeviance	Cumulative sum of AIC_c Weight
Phi(prev) p(.) f(rh) - DM	2523.611	0	0.35329	1	5	2513.468	0.35329
Phi(prev) p(rh) f(rh) - DM	2524.496	0.885	0.22697	0.6424	6	2512.295	0.58026
Phi(prev) p(rad) f(rh) - DM	2525.003	1.3919	0.17615	0.4986	6	2512.802	0.75641
Phi(prev) p(d) f(rh) - DM	2525.031	1.4201	0.17369	0.4916	6	2512.83	0.9301
Phi(temp) p(.) f(rh) - DM	2529.008	5.3967	0.02378	0.0673	5	2518.864	0.95388
Phi(temp) p(rh) f(rh) - DM	2530.298	6.6875	0.01247	0.0353	6	2518.097	0.96635
Phi(temp) p(d) f(rh) - DM	2530.533	6.9218	0.01109	0.0314	6	2518.332	0.97744
Phi(temp) p(rad) f(rh) - DM	2530.855	7.2445	0.00944	0.0267	6	2518.654	0.98688
Phi(Ts) p(.) f(rh) - DM	2532.199	8.5882	0.00482	0.0136	5	2522.056	0.9917
Phi(Ts) p(d) f(rh) - DM	2532.946	9.3346	0.00332	0.0094	6	2520.745	0.99502
Phi(Ts) p(rh) f(rh) - DM	2533.271	9.6597	0.00282	0.008	6	2521.07	0.99784
Phi(Ts) p(rad) f(rh) - DM	2534.132	10.5206	0.00183	0.0052	6	2521.931	0.99967
Phi(prev) p(rh) f(rad) - DM	2542.288	18.6766	0.00003	0.0001	6	2530.087	0.9997
Phi(prev) p(rad) f(Tl) - DM	2542.723	19.1124	0.00002	0.0001	6	2530.522	0.99972
Phi(temp) p(rad) f(prev) - DM	2542.995	19.3836	0.00002	0.0001	6	2530.794	0.99974
Phi(prev) p(rad) f(rad) - DM	2543.149	19.5384	0.00002	0.0001	6	2530.948	0.99976
Phi(Ts) p(rad) f(prev) - DM	2543.522	19.911	0.00002	0.0001	6	2531.321	0.99978
Phi(prev) p(rad) f(prev) - DM	2543.728	20.1168	0.00002	0.0001	6	2531.527	0.9998
Phi(prev) p(rad) f(temp) - DM	2544.414	20.803	0.00001	0	6	2532.213	0.99981
Phi(temp) p(rad) f(temp) - DM	2544.586	20.9753	0.00001	0	6	2532.385	0.99982
Phi(Ts) p(.) f(prev) - DM	2544.731	21.1198	0.00001	0	5	2534.588	0.99983
Phi(prev) p(rad) f(Ts) - DM	2544.786	21.1753	0.00001	0	6	2532.585	0.99984
Phi(temp) p(.) f(prev) - DM	2545.12	21.5094	0.00001	0	5	2534.977	0.99985
Phi(temp) p(rad) f(Ts) - DM	2545.622	22.0106	0.00001	0	6	2533.421	0.99986
Phi(temp) p(.) f(temp) - DM	2545.653	22.0425	0.00001	0	5	2535.51	0.99987
Phi(temp) p(rad) f(d) - DM	2545.663	22.052	0.00001	0	6	2533.462	0.99988
Phi(prev) p(rh) f(Tl) - DM	2545.72	22.109	0.00001	0	6	2533.519	0.99989
Phi(Ts) p(rad) f(temp) - DM	2545.77	22.1592	0.00001	0	6	2533.569	0.9999
Phi(Ts) p(.) f(temp) - DM	2546.072	22.4611	0	0	5	2535.929	0.9999
Phi(temp) p(rad) f(Tl) - DM	2546.126	22.515	0	0	6	2533.925	0.9999
Phi(temp) p(rh) f(rad) - DM	2546.161	22.5505	0	0	6	2533.96	0.9999
Phi(temp) p(rad) f(rad) - DM	2546.192	22.581	0	0	6	2533.991	0.9999
Phi(Ts) p(rh) f(prev) - DM	2546.283	22.6716	0	0	6	2534.082	0.9999
Phi(prev) p(rad) f(d) - DM	2546.305	22.6944	0	0	6	2534.104	0.9999
Phi(Ts) p(rad) f(d) - DM	2546.334	22.7227	0	0	6	2534.133	0.9999
Phi(Ts) p(.) f(d) - DM	2546.335	22.7238	0	0	5	2536.192	0.9999
Phi(temp) p(.) f(d) - DM	2546.358	22.747	0	0	5	2536.215	0.9999
Phi(temp) p(rh) f(prev) - DM	2546.507	22.8962	0	0	6	2534.306	0.9999
Phi(Ts) p(d) f(prev) - DM	2546.579	22.9685	0	0	6	2534.378	0.9999
Phi(prev) p(rad) f(.) - DM	2546.843	23.2318	0	0	5	2536.7	0.9999
Phi(temp) p(rad) f(.) - DM	2546.931	23.3201	0	0	5	2536.788	0.9999
Phi(temp) p(rh) f(temp) - DM	2547.032	23.4208	0	0	6	2534.831	0.9999
Phi(temp) p(d) f(prev) - DM	2547.162	23.5508	0	0	6	2534.961	0.9999
Phi(temp) p(.) f(Ts) - DM	2547.311	23.7003	0	0	5	2537.168	0.9999
Phi(Ts) p(rh) f(d) - DM	2547.448	23.837	0	0	6	2535.247	0.9999

Phi(Ts) p(rh) f(temp) - DM	2547.485	23.8736	0	0	6	2535.284	0.9999
Phi(Ts) p(d) f(temp) - DM	2547.509	23.8981	0	0	6	2535.308	0.9999
Phi(temp) p(rh) f(d) - DM	2547.529	23.9182	0	0	6	2535.328	0.9999
Phi(temp) p(d) f(temp) - DM	2547.547	23.9365	0	0	6	2535.346	0.9999
Phi(temp) p(.) f(rad) - DM	2547.556	23.9452	0	0	5	2537.413	0.9999
Phi(prev) p(.) f(rad) - DM	2547.767	24.1562	0	0	5	2537.624	0.9999
Phi(prev) p(.) f(Tl) - DM	2547.974	24.3626	0	0	5	2537.83	0.9999
Phi(temp) p(rh) f(Tl) - DM	2548.062	24.4511	0	0	6	2535.861	0.9999
Phi(Ts) p(rad) f(Ts) - DM	2548.106	24.4949	0	0	6	2535.905	0.9999
Phi(temp) p(.) f(Tl) - DM	2548.142	24.5306	0	0	5	2537.998	0.9999
Phi(temp) p(rh) f(Ts) - DM	2548.292	24.681	0	0	6	2536.091	0.9999
Phi(temp) p(d) f(d) - DM	2548.312	24.701	0	0	6	2536.111	0.9999
Phi(prev) p(d) f(rad) - DM	2548.317	24.7064	0	0	6	2536.116	0.9999
Phi(Ts) p(d) f(d) - DM	2548.385	24.7742	0	0	6	2536.184	0.9999
Phi(prev) p(d) f(Tl) - DM	2548.46	24.8489	0	0	6	2536.259	0.9999
Phi(prev) p(rh) f(temp) - DM	2548.672	25.0608	0	0	6	2536.471	0.9999
Phi(prev) p(.) f(temp) - DM	2548.912	25.3013	0	0	5	2538.769	0.9999
Phi(temp) p(d) f(rad) - DM	2548.975	25.3639	0	0	6	2536.774	0.9999
Phi(temp) p(d) f(Ts) - DM	2549.004	25.3933	0	0	6	2536.803	0.9999
Phi(prev) p(rh) f(Ts) - DM	2549.213	25.6023	0	0	6	2537.012	0.9999
Phi(Ts) p(.) f(Ts) - DM	2549.224	25.6128	0	0	5	2539.081	0.9999
Phi(prev) p(rh) f(prev) - DM	2549.421	25.8098	0	0	6	2537.22	0.9999
Phi(temp) p(d) f(Tl) - DM	2549.437	25.8258	0	0	6	2537.236	0.9999
Phi(prev) p(rh) f(d) - DM	2549.663	26.0523	0	0	6	2537.462	0.9999
Phi(prev) p(.) f(prev) - DM	2550.002	26.3912	0	0	5	2539.859	0.9999
Phi(prev) p(.) f(Ts) - DM	2550.013	26.4023	0	0	5	2539.87	0.9999
Phi(Ts) p(rh) f(Ts) - DM	2550.015	26.4045	0	0	6	2537.814	0.9999
Phi(Ts) p(rh) f(rad) - DM	2550.016	26.4049	0	0	6	2537.815	0.9999
Phi(Ts) p(d) f(Ts) - DM	2550.177	26.566	0	0	6	2537.976	0.9999
Phi(temp) p(rh) f(.) - DM	2550.178	26.5666	0	0	5	2540.034	0.9999
Phi(Ts) p(rad) f(.) - DM	2550.288	26.6772	0	0	5	2540.145	0.9999
Phi(prev) p(d) f(temp) - DM	2550.61	26.999	0	0	6	2538.409	0.9999
Phi(Ts) p(rad) f(Tl) - DM	2550.667	27.0561	0	0	6	2538.466	0.9999
Phi(temp) p(.) f(.) - DM	2550.674	27.0635	0	0	4	2542.579	0.9999
Phi(prev) p(.) f(d) - DM	2550.92	27.3091	0	0	5	2540.777	0.9999
Phi(Ts) p(rad) f(rad) - DM	2550.942	27.3307	0	0	6	2538.741	0.9999
Phi(prev) p(d) f(Ts) - DM	2551.385	27.7744	0	0	6	2539.184	0.9999
Phi(Ts) p(rh) f(Tl) - DM	2551.765	28.1544	0	0	6	2539.564	0.9999
Phi(prev) p(rh) f(.) - DM	2551.94	28.3291	0	0	5	2541.797	0.9999
Phi(prev) p(d) f(prev) - DM	2551.951	28.3398	0	0	6	2539.75	0.9999
Phi(Ts) p(rh) f(.) - DM	2552.184	28.5732	0	0	5	2542.041	0.9999
Phi(temp) p(d) f(.) - DM	2552.552	28.9407	0	0	5	2542.408	0.9999
Phi(Ts) p(.) f(rad) - DM	2552.574	28.9634	0	0	5	2542.431	0.9999
Phi(Ts) p(.) f(Tl) - DM	2552.617	29.0059	0	0	5	2542.474	0.9999
Phi(Ts) p(d) f(rad) - DM	2552.866	29.2549	0	0	6	2540.665	0.9999
Phi(Ts) p(d) f(Tl) - DM	2552.916	29.3048	0	0	6	2540.715	0.9999
Phi(prev) p(d) f(d) - DM	2552.952	29.3409	0	0	6	2540.751	0.9999
Phi(Ts) p(.) f(.) - DM	2553.655	30.0436	0	0	4	2545.559	0.9999
Phi(Ts) p(d) f(.) - DM	2554.737	31.1258	0	0	5	2544.594	0.9999
Phi(.) p(rh) f(rh) - DM	2554.892	31.2808	0	0	5	2544.749	0.9999

Phi(prev) p(.) f(.) - DM	2556.734	33.1235	0	0	4	2548.639	0.9999
Phi(prev) p(d) f(.) - DM	2558.219	34.6085	0	0	5	2548.076	0.9999
Phi(.) p(d) f(rh) - DM	2566.447	42.8362	0	0	5	2556.304	0.9999
Phi(.) p(rad) f(rh) - DM	2567.495	43.884	0	0	5	2557.352	0.9999
Phi(.) p(.) f(rh) - DM	2568.411	44.7998	0	0	4	2560.316	0.9999
...							

Table B.10. AIC value and relative variable importance for Pradel recruitment Tully set

Phi(↓) p(→) f(.)	.	rh	rad	d
.	2622.5	2588.1	2599.4	2620.0
prev	2556.7	2551.9	2546.8	2558.2
temp	2550.7	2550.2	2546.9	2552.6
Ts	2553.7	2552.2	2550.3	2554.7

Phi(↓) p(→) f(rh)	.	rh	rad	d
.	2568.4	2554.9	2567.5	2566.4
prev	2523.6	2524.5	2525.0	2525.0
temp	2529.0	2530.3	2530.9	2530.5
Ts	2532.2	2533.3	2534.1	2532.9

Phi(↓) p(→) f(prev)	.	rh	rad	d
.	2586.6	2577.8	2577.3	2587.9
prev	2550.0	2549.4	2543.7	2552.0
temp	2545.1	2546.5	2543.0	2547.2
Ts	2544.7	2546.3	2543.5	2546.6

Phi(↓) p(→) f(rad)	.	rh	rad	d
.	2620.5	2582.1	2600.9	2616.7
prev	2547.8	2542.3	2543.1	2548.3
temp	2547.6	2546.2	2546.2	2549.0
Ts	2552.6	2550.0	2550.9	2552.9

Phi(↓) p(→) f(temp)	.	rh	rad	d
.	2587.2	2577.6	2580.9	2586.6
prev	2548.9	2548.7	2544.4	2550.6
temp	2545.7	2547.0	2544.6	2547.5
Ts	2546.1	2547.5	2545.8	2547.5

Phi(↓) p(→) f(d)	.	rh	rad	d
.	2593.9	2579.6	2586.4	2595.9
prev	2550.9	2549.7	2546.3	2553.0
temp	2546.4	2547.5	2545.7	2548.3
Ts	2546.3	2547.4	2546.3	2548.4

Phi(↓) p(→) f(Ts)	.	rh	rad	d
.	2596.1	2581.0	2585.5	2593.3
prev	2550.0	2549.2	2544.8	2551.4
temp	2547.3	2548.3	2545.6	2549.0
Ts	2549.2	2550.0	2548.1	2550.2

Phi(↓) p(→) f(Tl)	.	rh	rad	d
.	2613.7	2584.0	2596.8	2607.8
prev	2548.0	2545.7	2542.7	2548.5
temp	2548.1	2548.1	2546.1	2549.4
Ts	2552.6	2551.8	2550.7	2552.9

These eight tables represent the different variables used to constrain the recruitment parameter (*f*, or f). Survival (φ, phi) variables are rows, recapture (ρ, p) variables are columns. Each colored cell in these tables represents a separate model in the respective candidate model set. Numbers within the cells represent the $QAIC_c$ value for the respective model, and cells have been colored according to $QAIC_c$ ranking (the more parsimonious the model, the lower its $QAIC_c$ value, and the closer towards the white end of the spectrum; red cells represent poorly parsimonious models). Borders around $QAIC_c$ top-ranking 5 models (depicted with white or pale yellow) cumulatively hold approximately 95% of total support within the candidate model set. Models displayed in orange and red are lower ranking based on $QAIC_c$ values.

B.2.6 Pradel recruitment Kirrama set

Table B.11. Ranking of most parsimonious models in Pradel recruitment Kirrama set

Model (recruitment Kirrama set)	$QAIC_c$	Delta $QAIC_c$	AIC_c Weights	Model Likelihood	NumPar	QDeviance	Cumulative sum of AIC_c Weight
Phi(Ts) p(g+d) f(temp) - DM	846.4581	0	0.07961	0.9999	7	831.6285	0.07961
Phi(Ts) p(g+d) f(.) - DM	846.5326	0.0745	0.0767	0.9634	6	833.915	0.15631
Phi(Ts) p(g+d) f(rain) - DM	847.2517	0.7936	0.05354	0.6725	7	832.4221	0.20985
Phi(Ts) p(g+d) f(rh) - DM	847.7735	1.3154	0.04124	0.518	7	832.9439	0.25109
Phi(temp) p(g+d) f(Ts) - DM	847.9727	1.5146	0.03733	0.4689	7	833.143	0.28842
Phi(temp) p(g+d) f(temp) - DM	848.065	1.6069	0.03565	0.4478	7	833.2354	0.32407
Phi(Ts) p(g+d) f(Tl) - DM	848.0687	1.6106	0.03558	0.4469	7	833.2391	0.35965
Phi(Ts) p(g+d) f(d) - DM	848.2165	1.7584	0.03305	0.4151	7	833.3868	0.3927
Phi(.) p(g+d) f(temp) - DM	848.2686	1.8105	0.0322	0.4045	6	835.6509	0.4249
Phi(rain) p(g+d) f(temp) - DM	848.4576	1.9995	0.0293	0.368	7	833.628	0.4542
Phi(Ts) p(g*d) f(temp) - DM	848.5456	2.0875	0.02803	0.3521	8	831.471	0.48223
Phi(Ts) p(g*d) f(Ts) - DM	848.585	2.1269	0.02749	0.3453	8	831.5104	0.50972
Phi(Ts) p(g*d) f(.) - DM	848.6281	2.17	0.0269	0.3379	7	833.7985	0.53662
Phi(Ts) p(g+d) f(rad) - DM	848.7191	2.261	0.02571	0.3229	7	833.8894	0.56233
Phi(rain) p(g+d) f(Ts) - DM	848.7532	2.2951	0.02527	0.3174	7	833.9236	0.5876
Phi(.) p(g+d) f(Ts) - DM	848.956	2.4979	0.02283	0.2868	6	836.3384	0.61043
Phi(Ts) p(d) f(.) - DM	849.1164	2.6583	0.02107	0.2647	5	838.6784	0.6315
Phi(Ts) p(g*d) f(rain) - DM	849.357	2.8989	0.01869	0.2348	8	832.2823	0.65019
Phi(temp) p(g+d) f(Tl) - DM	849.5873	3.1292	0.01665	0.2091	7	834.7577	0.66684
Phi(Ts) p(g*d) f(rh) - DM	849.899	3.4409	0.01425	0.179	8	832.8244	0.68109
Phi(Ts) p(g*d) f(Tl) - DM	850.1686	3.7105	0.01245	0.1564	8	833.094	0.69354
Phi(temp) p(g*d) f(temp) - DM	850.1762	3.7181	0.01241	0.1559	8	833.1016	0.70595
Phi(Ts) p(d) f(Ts) - DM	850.3228	3.8647	0.01153	0.1448	6	837.7051	0.71748
Phi(Ts) p(g*d) f(d) - DM	850.3234	3.8653	0.01153	0.1448	8	833.2487	0.72901
Phi(.) p(g*d) f(temp) - DM	850.4327	3.9746	0.01091	0.137	7	835.6031	0.73992
Phi(Ts) p(d) f(rain) - DM	850.611	4.1529	0.00998	0.1254	6	837.9933	0.7499
Phi(Ts) p(d) f(temp) - DM	850.6117	4.1536	0.00998	0.1254	6	837.9941	0.75988
Phi(rain) p(g+d) f(.) - DM	850.6123	4.1542	0.00998	0.1254	6	837.9947	0.76986
Phi(temp) p(g+d) f(rad) - DM	850.6609	4.2028	0.00974	0.1223	7	835.8313	0.7796
Phi(rain) p(g*d) f(temp) - DM	850.6784	4.2203	0.00965	0.1212	8	833.6038	0.78925
Phi(.) p(g+d) f(rain) - DM	850.8103	4.3522	0.00903	0.1134	6	838.1926	0.79828
Phi(Ts) p(d) f(rh) - DM	850.8411	4.383	0.0089	0.1118	6	838.2235	0.80718
Phi(Ts) p(g*d) f(rad) - DM	850.8494	4.3913	0.00886	0.1113	8	833.7747	0.81604
Phi(Ts) p(d) f(Tl) - DM	850.8792	4.4211	0.00873	0.1097	6	838.2616	0.82477
Phi(Ts) p(d) f(d) - DM	850.9312	4.4731	0.0085	0.1068	6	838.3136	0.83327
Phi(rain) p(g*d) f(Ts) - DM	850.9875	4.5294	0.00827	0.1039	8	833.9129	0.84154
Phi(.) p(g*d) f(Ts) - DM	851.1437	4.6856	0.00765	0.0961	7	836.314	0.84919
Phi(Ts) p(d) f(rad) - DM	851.2959	4.8378	0.00709	0.0891	6	838.6782	0.85628
Phi(rain) p(d) f(Ts) - DM	851.311	4.8529	0.00703	0.0883	6	838.6933	0.86331
Phi(temp) p(g*d) f(rh) - DM	851.4444	4.9863	0.00658	0.0826	8	834.3698	0.86989
Phi(rain) p(d) f(temp) - DM	851.4738	5.0157	0.00648	0.0814	6	838.8561	0.87637
Phi(rain) p(d) f(.) - DM	851.4825	5.0244	0.00646	0.0811	5	841.0445	0.88283
Phi(rain) p(g+d) f(rain) - DM	851.6022	5.1441	0.00608	0.0764	7	836.7726	0.88891
Phi(temp) p(g*d) f(Tl) - DM	851.6925	5.2344	0.00581	0.073	8	834.6179	0.89472
Phi(temp) p(d) f(Ts) - DM	851.7962	5.3381	0.00552	0.0693	6	839.1786	0.90024

Phi(.) p(g+d) f(.) - DM	851.8693	5.4112	0.00532	0.0668	5	841.4313	0.90556
Phi(temp) p(d) f(temp) - DM	852.2602	5.8021	0.00438	0.055	6	839.6426	0.90994
Phi(.) p(g+d) f(rh) - DM	852.3247	5.8666	0.00424	0.0533	6	839.7071	0.91418
Phi(temp) p(d) f(rh) - DM	852.3924	5.9343	0.0041	0.0515	6	839.7748	0.91828
Phi(temp) p(d) f(Tl) - DM	852.4069	5.9488	0.00407	0.0511	6	839.7892	0.92235
Phi(rain) p(g+d) f(rh) - DM	852.4513	5.9932	0.00398	0.05	7	837.6217	0.92633
Phi(.) p(d) f(Ts) - DM	852.5935	6.1354	0.0037	0.0465	5	842.1556	0.93003
Phi(temp) p(d) f(d) - DM	852.6782	6.2201	0.00355	0.0446	6	840.0606	0.93358
Phi(rain) p(g+d) f(rad) - DM	852.6841	6.226	0.00354	0.0445	7	837.8545	0.93712
Phi(.) p(d) f(temp) - DM	852.6888	6.2307	0.00353	0.0443	5	842.2509	0.94065
Phi(rain) p(g+d) f(d) - DM	852.7615	6.3034	0.00341	0.0428	7	837.9319	0.94406
Phi(rain) p(g+d) f(Tl) - DM	852.7935	6.3354	0.00335	0.0421	7	837.9639	0.94741
Phi(temp) p(g*d) f(rad) - DM	852.8183	6.3602	0.00331	0.0416	8	835.7437	0.95072
Phi(rain) p(g*d) f(.) - DM	852.8208	6.3627	0.00331	0.0416	7	837.9912	0.95403
Phi(.) p(g*d) f(rain) - DM	852.998	6.5399	0.00303	0.0381	7	838.1683	0.95706
Phi(.) p(g+d) f(Tl) - DM	853.0129	6.5548	0.003	0.0377	6	840.3952	0.96006
Phi(temp) p(d) f(rad) - DM	853.1644	6.7063	0.00278	0.0349	6	840.5468	0.96284
Phi(rain) p(d) f(rain) - DM	853.2588	6.8007	0.00266	0.0334	6	840.6412	0.9655
Phi(rain) p(d) f(rad) - DM	853.3102	6.8521	0.00259	0.0325	6	840.6926	0.96809
Phi(.) p(d) f(.) - DM	853.5585	7.1004	0.00229	0.0288	4	845.2687	0.97038
Phi(rain) p(d) f(rh) - DM	853.6076	7.1495	0.00223	0.028	6	840.99	0.97261
Phi(.) p(d) f(rain) - DM	853.6468	7.1887	0.00219	0.0275	5	843.2089	0.9748
Phi(rain) p(d) f(d) - DM	853.6473	7.1892	0.00219	0.0275	6	841.0296	0.97699
Phi(.) p(g+d) f(d) - DM	853.6531	7.195	0.00218	0.0274	6	841.0355	0.97917
Phi(rain) p(d) f(Tl) - DM	853.6608	7.2027	0.00217	0.0273	6	841.0432	0.98134
Phi(rain) p(g*d) f(rain) - DM	853.8372	7.3791	0.00199	0.025	8	836.7625	0.98333
Phi(.) p(g+d) f(rad) - DM	854.0255	7.5674	0.00181	0.0227	6	841.4079	0.98514
Phi(.) p(g*d) f(.) - DM	854.0392	7.5811	0.0018	0.0226	6	841.4216	0.98694
Phi(.) p(g*d) f(rh) - DM	854.5248	8.0667	0.00141	0.0177	7	839.6952	0.98835
Phi(.) p(d) f(rh) - DM	854.6617	8.2036	0.00132	0.0166	5	844.2237	0.98967
Phi(rain) p(g*d) f(rh) - DM	854.6921	8.234	0.0013	0.0163	8	837.6175	0.99097
Phi(rain) p(g*d) f(rad) - DM	854.9251	8.467	0.00115	0.0144	8	837.8505	0.99212
Phi(.) p(d) f(Tl) - DM	854.9759	8.5178	0.00113	0.0142	5	844.5379	0.99325
Phi(rain) p(g*d) f(d) - DM	855.0031	8.545	0.00111	0.0139	8	837.9285	0.99436
Phi(rain) p(g*d) f(Tl) - DM	855.0344	8.5763	0.00109	0.0137	8	837.9598	0.99545
Phi(.) p(g*d) f(Tl) - DM	855.206	8.7479	0.001	0.0126	7	840.3764	0.99645
Phi(.) p(d) f(d) - DM	855.4393	8.9812	0.00089	0.0112	5	845.0013	0.99734
Phi(.) p(d) f(rad) - DM	855.7064	9.2483	0.00078	0.0098	5	845.2685	0.99812
Phi(.) p(g*d) f(d) - DM	855.8512	9.3931	0.00073	0.0092	7	841.0216	0.99885
Phi(.) p(g*d) f(rad) - DM	856.2282	9.7701	0.0006	0.0075	7	841.3986	0.99945
Phi(Ts) p(g+d) f(Ts) - DM	856.8965	10.4384	0.00043	0.0054	7	842.0669	0.99988
Phi(Ts) p(g) f(.) - DM	865.4608	19.0027	0.00001	0.0001	5	855.0229	0.99989
Phi(.) p(g) f(.) - DM	865.8341	19.376	0	0	4	857.5442	0.99989
Phi(Ts) p(.) f(.) - DM	865.9454	19.4873	0	0	4	857.6556	0.99989
Phi(Ts) p(g) f(d) - DM	865.9558	19.4977	0	0	6	853.3382	0.99989
Phi(temp) p(g) f(.) - DM	865.985	19.5269	0	0	5	855.547	0.99989
Phi(.) p(.) f(.) - DM	866.0233	19.5652	0	0	3	859.8506	0.99989
Phi(Ts) p(.) f(d) - DM	866.2909	19.8328	0	0	5	855.8529	0.99989
Phi(temp) p(g*d) f(Ts) - DM	866.3754	19.9173	0	0	8	849.3007	0.99989
Phi(.) p(g) f(d) - DM	866.4753	20.0172	0	0	5	856.0373	0.99989

Phi(temp) p(.) f(.) - DM	866.5381	20.08	0	0	4	858.2482	0.99989
Phi(.) p(.) f(d) - DM	866.5617	20.1036	0	0	4	858.2718	0.99989
Phi(.) p(g) f(Ts) - DM	866.6698	20.2117	0	0	5	856.2318	0.99989
Phi(temp) p(g) f(d) - DM	866.7302	20.2721	0	0	6	854.1125	0.99989
Phi(Ts) p(g) f(Tl) - DM	867.053	20.5949	0	0	6	854.4354	0.99989
...							

Table B.12. AIC value and relative variable importance for Pradel recruitment Kirrama set

Phi(↓) p(→) f(.)	.	g	d	g+d	g*d
.	866.0	865.8	853.6	851.9	854.0
temp	866.5	866.0	904.5	901.7	903.4
rain	868.0	867.9	851.5	850.6	852.8
Ts	865.9	865.5	849.1	846.5	848.6

Phi(↓) p(→) f(Ts)	.	g	d	g+d	g*d
.	867.5	866.7	852.6	849.0	851.1
temp	868.5	867.7	851.8	848.0	866.4
rain	869.5	868.8	851.3	848.8	851.0
Ts	868.0	867.3	850.3	856.9	848.6

Phi(↓) p(→) f(rain)	.	g	d	g+d	g*d
.	868.1	867.8	853.6	850.8	853.0
temp	908.6	906.6	906.6	903.9	905.6
rain	870.1	870.0	853.3	851.6	853.8
Ts	867.9	867.6	850.6	847.3	849.4

Phi(↓) p(→) f(d)	.	g	d	g+d	g*d
.	866.6	866.5	855.4	853.7	855.9
temp	867.1	866.7	852.7	903.7	905.4
rain	868.1	868.4	853.6	852.8	855.0
Ts	866.3	866.0	850.9	848.2	850.3

Phi(↓) p(→) f(temp)	.	g	d	g+d	g*d
.	867.8	867.1	852.7	848.3	850.4
temp	868.7	868.1	852.3	848.1	850.2
rain	869.9	869.3	851.5	848.5	850.7
Ts	868.1	867.5	850.6	846.5	848.5

Phi(↓) p(→) f(Tl)	.	g	d	g+d	g*d
.	867.9	867.7	855.0	853.0	855.2
temp	868.3	867.8	852.4	849.6	851.7
rain	869.5	869.7	853.7	852.8	855.0
Ts	867.5	867.1	850.9	848.1	850.2

Phi(↓) p(→) f(rh)	.	g	d	g+d	g*d
.	868.1	868.0	854.7	852.3	854.5
temp	868.6	868.2	852.4	903.7	851.4
rain	870.0	870.1	853.6	852.5	854.7
Ts	867.8	867.6	850.8	847.8	849.9

Phi(↓) p(→) f(rad)	.	g	d	g+d	g*d
.	867.9	867.9	855.7	854.0	856.2
temp	868.5	868.1	853.2	850.7	852.8
rain	869.8	870.0	853.3	852.7	854.9
Ts	867.9	867.6	851.3	848.7	850.8

These eight tables represent the different variables used to constrain the recruitment parameter (*f*, or f). Survival (φ, phi) variables are rows, recapture (ρ, p) variables are columns. Each colored cell in these tables represents a separate model in the respective candidate model set. Numbers within the cells represent the $QAIC_c$ value for the respective model, and cells have been colored according to $QAIC_c$ ranking (the more parsimonious the model, the lower its $QAIC_c$ value, and the closer towards the white end of the spectrum; red cells represent poorly parsimonious models). Borders around $QAIC_c$ top-ranking 12 models (depicted with white or pale yellow) cumulatively hold approximately 50% of total support within the candidate model set. Models displayed in orange and red are lower ranking based on $QAIC_c$ values.

APPENDIX C: Supporting information to MSMR modeling

C.1 Introduction

In this appendix I define in detail the estimable parameters and predictor variables that were used to populate the mark-recapture models, and briefly describe my rationale for their *a priori* inclusion. I follow this with my rationale for construction of the candidate model sets, describe goodness of fit testing, and describe my population dynamics simulation methodology.

The full reference for the manuscript is:
Grogan, L. F., Phillott, A. D., Scheele, B. C., Berger, L., Cashins, S. D., Bell, S. C., Puschendorf, R., Skerratt, L. F. (in prep) Parasite aggregation and its implications for the microparasitic disease, endemic chytridiomycosis.

C.2 Parameter probabilities

These are population demographic parameters that we can estimate monthly probabilities for using standard mark-recapture methodologies.

- ***S***: local apparent monthly survival probability for adult male *Litoria rheocola* frogs, where S_i is the probability of an individual surviving from occasion *i* to *i* + 1. It is important to note that the survival probability (S) is confounded with the probability of permanent emigration from the study site with standard mark-recapture analyses. This survival parameter (*S*) in multistate analyses has a different definition, and hence is symbolically differentiated from the survival parameter utilized in CJS analyses, φ, 'phi'.
- **ρ** (phonetically 'rho', otherwise represented as 'p'): monthly probability of recapture for adult male *Litoria rheocola* frogs, where ρ_i is the probability of encounter on occasion *i* conditional on an individual being alive and remaining in the sampling region.
- **ψ** (phonetically 'psi'): apparent infection state transition probability is the probability for an individual in a particular infection state to undergo each possible state transition. The state transition parameter ψ_i^{rs} defines the probability that an individual in state *r* at time *i* will be in state *s* at time *i + 1*. Importantly where there are more than two states, this includes the probability of transitions *from* each state and *to* each state in the MSMR Jolly-Movement Model (JMV; Lebreton et al., 2009), including the probability of remaining in the same state ψ_i^{rr}, and these probabilities must sum to one. States in this study represent discrete infection conditions (defined by zoospore equivalent [*zse*] infection intensities) in which the marked individual may potentially be encountered, conditional on being in that state and alive. Hence where three states are defined (for example, A, B and C), there are six possible state transitions (A to B, A to C, B to C, B to A, C to A, C to B), and nine total probabilities (to account for the additional probabilities of remaining in any one of the three states between subsequent occasions; A to A, B

to B, C to C). For three states, each directional group of three probabilities must sum to one (for example, the total probability of starting in state A, and either moving A to B, A to C or A to A must sum to one).

C.3 Predictor variables

We carefully chose predictor variables to test our hypotheses based on biological plausibility and *a priori* evidence in an attempt to avoid overparameterization (Burnham and Anderson, 2002; Grueber et al., 2011; Guthery et al., 2005; Nakagawa and Freckleton, 2011). Below we describe these variables, for pragmatic purposes, as grouping variables (entered in the input file in MARK) and temporal structural variables, including environmental and linear covariates (entered into the design matrix of MARK for individual models). These variables are used to constrain the underlying structure of models that make up the candidate model set. The better a linear combination of such constraints *fits* the empirical data within a single model, the better that model will rank within the set using information theoretic criteria such as Akaike's Information Criterion ($QAIC_c$). Please see Phillott et al. (2013) for further details about variables used in CJS and Pradel analyses.

C.3.1 Grouping variables

- *g*: time-varying individual categorical grouping variable (coded into the input file) defining infection status which is divided into either two or three states based on zoospore equivalent load (*zse*) at time of each capture. In two-state analysis A = Bd negative (uninfected) and B = Bd positive (infected). In three-state analysis, Bd load was discretized into groups: A = Bd negative, B = 1-4 *zse*, C > 4 *zse*. See the justification for this threshold in the manuscript text (Section 3.3.4.2 of this thesis). When infection state is used to describe the state transition parameter probability (ψ) in the three state analysis, the variables used require additional definition because there is more than one alternative for constraining this grouping variable:
    - *6g*: this state transition (ψ) variable implies that each possible state transition between the existing three states (not including the probabilities of remaining in each respective state) has been constrained to be separately defined, and hence yields a separate monthly probability.
    - *2g*: this state transition (ψ) variable alternatively defines transitions by the *direction* that the transition makes. 'Infection' transitions represent a gain of infection (from uninfected to either low or high infectious burden, or from low infectious burden to high burden), and 'recovery' transitions represent a reduction in infectious burden (low or high infectious burden to uninfected, or high infectious burden to low burden), making up two constraint groups. This constraint means that the monthly probability for a 'recovery' (a reduction in infectious burden) is constrained to be the same whether the transition made

is from the high to the low burden state, the high burden state to the uninfected state, or the low burden state to the uninfected state.

C.3.2 Environmental variables

Environmental variables were obtained from the SILO climate database as spatially interpolated weather values (Jeffrey et al., 2001). Variables included in models were averages or sums over the 28 days preceding a trip to account for predefined trip intervals, the putative cumulative nature of their effects on the pathogenesis of chytridiomycosis, and to correspond roughly with the incubation period of chytridiomycosis (Berger et al., 2005b; Bureau of Meteorology, 2008).

- *temp*: temperature (mean of daily maximum temperatures in degrees Celcius over the 28 days preceding each trip start).
- *rh*: relative humidity (mean of the relative humidity as % at daily maximum temperatures over the 28 days preceding each trip start).
- *rad*: radiation (mean radiation in MJ/m^2 of daily values over the 28 days preceding each trip start).

C.3.3 Linear variables

- *prev*: apparent infection prevalence per trip was determined as a point based sampled prevalence per trip and site as the number of positive PCR results divided by the total number of PCR swab samples analyzed (where one well, one zse was considered positive, and the entire uninfected observable population is considered potentially susceptible). For more details, please see Appendix A of this thesis.
- *d*: capture effort (measured in days per trip, where each capture day covered the identical stream transect once at dusk). Capture effort is expected to influence recapture probability by altering opportunities for observation.
- *T*: annually cycling seasonal linear trend where autumn was assumed equivalent to spring (hence the annual cycle was summer = 1, autumn = 2, winter = 3, spring = 2)
- . (dot, or period): constant (indicates that the parameter is constrained to be temporally constant)

C.4 Rationale for the methodology used in construction of the candidate model sets

Within the framework of the two types of analyses we performed (two and three state multistate), candidate model sets were constructed *a priori* using a restricted form of the all subsets approach and tested systematically (Doherty et al., 2012; Grueber et al., 2011; Hegyi and Garamszegi, 2011; Lukacs et al., 2010; Stephens et al., 2007; Symonds and Moussalli, 2011). Following the reduction of predictor variables to only those with putative effects (from *a priori* experience with the previous CJS/Pradel analyses, see Phillott et al. (2013), we also restricted the candidate model set to those combination types with biological plausibility (Dochtermann and Jenkins, 2011).

Bd infection status (*g*, *6g* and *2g*) was the variable of greatest interest for influencing the response parameters (survival S, recapture ρ and state transition ψ probability), hence it was tested both in isolation, and as an additive or multiplicative two-way interaction with the other variables. We did not restrict the model set to those models containing this infection status variable, however, as discussed by (Grueber et al., 2011), if infection status is a poor predictor, its relative importance may be inflated if it is present in all models, hence resulting inference may be biased. Thus, the candidate model set also contained structural variables and individual covariates in isolation, as well as the null model for baseline comparison (constant or dot model; Burnham et al., 2011; Dochtermann and Jenkins, 2011) although its routine inclusion is not recommended by (Burnham and Anderson, 2002). Due to probable collinearities, other variables were not tested in combination or interaction with each other. Furthermore, capture effort (capture nights per trip; *d*) was presumed to only impact upon recapture probability, hence was excluded from testing with the other response parameters. Multiplicative interaction variables were not included on their own without their respective main variables (for example, 'g×prev' is an interaction variable) as this model type is not valid due to effect confounding (Mundry, 2011).

From the basis of these restrictions all variable combinations were tested (for example, this included models such as S(g×prev)ρ(d)psi(g×prev), S(g)ρ(rad)psi(.) and the null model S(.)ρ(.)psi(.)). Hence the number of variables (infection status *g*, *6g*, *2g*; environmental variables *temp*, *rh*, *rad*; and linear variables *prev*, *T*, ., *d*) was small relative to the sample size to avoid Freedman's paradox (Freedman, 1983; Lukacs et al., 2010) and data dredging (the discovery of spurious effects; Anderson et al., 2001). However, using the all subsets approach, the number of models tested in the candidate model set systematically included all feasible interactions in order to determine their relative importance (including additive and multiplicative variations).

In the three state analysis, the least well supported variable of annually cycling seasonal linear trend (*T*) for survival (*S*) and state transition (ψ) parameters was excluded to reduce the overall candidate model set size and complexity, while necessarily accounting for the additional *6g* and *2g* variables for the state transition parameter (ψ).

C.5 Goodness Of Fit (GOF) testing

Multistate modeling involves several assumptions additional to the general CMR assumptions (Cooch et al., 2012; Lebreton et al., 2009; Lindberg, 2012; Phillott et al., 2013 for discussion). Firstly, states must be discrete, mutually exclusive, and absolute; respective state observations should be made simultaneously, and there should be no error in assignation of states. Secondly, the probability of state transition is dependent only on the previous state (assumed to be a first-order markov process). Lastly, the probability of survival during an interval is independent of the state to which the individual moves, all

state transition takes place at the same time during an interval, time between observations should be relevant to the biology of the species and/or disease, and all mortality occurs before state transition.

Under the first assumption, states are constrained to being categorical regardless of whether reliable continuous data are available (for example, infection intensity *zse* as determined by qPCR). This assumption is fulfilled within the limitations of the sensitivity and specificity of the qPCR diagnostic test (Hyatt et al., 2007; Skerratt et al., 2011b). There are potential caveats, however, with the use of categorical states for continuous data. For instance Briggs et al. (2010) were unable to demonstrate a difference in survival probability between infected and uninfected frogs. While this may be a true indication of infection tolerance, it may alternatively occur due to category definitions as a result of a positively skewed intensity-frequency curve (aggregated infectious burdens; Hudson and Dobson, 1998) where low-burden subclinically infected frogs detected through highly sensitive diagnostic tests show no differences in survival compared with uninfected frogs. Alternative current analytical methods for continuous data (such as integral projection models) rely on imputation of missing state values where recapture probabilities are less than one, or strong assumptions about the generating biological system which are inappropriate for most circumstances of disease analysis in wild animals (Bonner et al., 2010; Bonner and Schwarz, 2006; Bonner et al., 2009; Cooch et al., 2012; Ellner and Rees, 2007).

Regarding the second assumption, there is limited conclusive evidence for the presence of adaptive immunity against Bd that might constitute a higher order markov process (Cashins et al., 2013). Frogs are often observed to lose and gain infection multiple times in the field (this study and Briggs et al., 2010), and Bd appears to either evade (due to intracellular location of sporangia) or suppress an effective adaptive immune response in hosts (Berger et al., 1999a; Berger et al., 2009b; Ribas et al., 2009; Richmond et al., 2009; Rollins-Smith et al., 2009; Rosenblum et al., 2012b; Rosenblum et al., 2009; Stice and Briggs, 2010; Woodhams et al., 2006a). The third assumption may generally be violated in the modeling of infectious disease states, and its stringency is currently under investigation (Cooch et al., 2012). It implies that an individual cannot change state (for instance, become infected) and die prior to the subsequent capture session and is a problem particularly if the interval between sampling sessions varies and is not naturally discretized or consistent with some biological variable (such as seasonal migration). For this reason we attempted to space capture intervals in accordance with the expected incubation period for chytridiomycosis (roughly 28 days; Berger et al., 2005b). Despite this precaution, the potential rapidity of thermal cures (Chatfield and Richards-Zawacki, 2011; Daskin et al., 2011) may lead to multiple unobserved state transitions between captures. The problem of timing of state transition relative to captures is discussed by Joe and Pollock (2002), and may play a role in causing bias generally in multistate studies of chytridiomycosis in amphibians (K. Pollock, pers. comm.; Cooch et al., 2012).

Program U-CARE (which tests goodness of fit for the Arnason-Schwartz multistate model $S(g \times t)\rho(g \times t)\psi(g \times t)$ following standard notation (Pradel et al., 2003; White and Burnham, 1999) demonstrated no lack of fit for our data. Despite its previous use in the context of data sparseness (Lebreton et al., 2009), we were wary about the valid use of these tests with sparse data, as lack of fit may be obscured overall due to artificial shrinkage of the Chi squared test statistic. We hence applied the bootstrap and median $\hat{c}$ goodness of fit tests with the general model $S(g)\rho(g)\psi(g)$. Bootstrapping yielded p = 0.61 ($\hat{c}$ = 1.028), and median $\hat{c}$ yielded $\hat{c}$ = 1.110 (95% CI 0.925 - 1.295; 1000 simulations) for two state multistate data set, hence the most conservative estimate of $\hat{c}$ = 1.110 was used. Similarly for the three-state analysis, bootstrapping yielded p = 0.64 ($\hat{c}$ = 1.026), and median $\hat{c}$ gave $\hat{c}$ = 1.097 (95% CI 0.944 - 1.250; 1000 simulations), hence $\hat{c}$ = 1.097 was employed.

C.6 Population Dynamics Simulation

We performed a discrete time simulation for a population of adult frogs using an intuitive system dynamics approach employing the model-averaged trip-based parameter estimates from the three state multistate mark-recapture analysis over the study period (excluding the recapture parameter and unconditional confidence intervals). The purpose of this simulation was to demonstrate the impact of estimated state transition and survival parameters on actual population numbers (from the schematic illustrated in Appendix D, Fig. D.1). Three main scenarios were investigated in order to visually separate the unrelated, but important effect of recruitment within the population; these scenarios involved population dynamics 1) including mortalities and state transition but without recruitment; 2) including mortalities, state transition and recruitment values defined to constrain population size to remaining stable; and 3) mortalities, state transition and model-averaged recruitment estimates defined from Phillott et al., 2013). The latter scenario is likely to best represent actual population dynamics in the field. Each population was assumed to start at 1000 individual adult frogs which is the estimated upper population size of the nearby threatened armoured mist frog *Litoria lorica* (males and females were assumed to behave equivalently), iterations were performed in daily time steps, and hence parameter estimates were adjusted to their daily equivalent units. Newly recruited individuals (including immigrants) were assumed to be susceptible and infection naïve on introduction to the population, and recovered individuals were similarly assumed to return to a susceptible state. This assumption of a lack of adaptive immunity in chytridiomycosis is supported by a re-exposure experiment using *Litoria booroolongensis* (Cashins et al., 2013).

APPENDIX D: Additional results for MSMR modeling

D.1 Introduction

In this appendix I present summarized tables (containing most parsimonious 100 models from the candidate model set where applicable) of results for both two and three state multistate analysis candidate model sets, together with an alternative visual presentation (heatmaps) of $QAIC_c$ values for all models in each candidate model set. In addition I present the population dynamics simulation results with figures, and a brief explanation of the dependence of transition probabilities on the size of the state subpopulation.

The full reference for the manuscript is:
Grogan, L. F., Phillott, A. D., Scheele, B. C., Berger, L., Cashins, S. D., Bell, S. C., Puschendorf, R., Skerratt, L. F. (in prep) Parasite aggregation and its implications for the microparasitic disease, endemic chytridiomycosis.

D.2 Summary tables

In the summary tables we have followed the model naming convention of White and Burnham, 1999), whereby survival is represented by 'S', recapture (ρ) is represented by 'p' and state transition (ψ) is represented by 'psi'. Predictor variables or variable interactions for each parameter are contained within parentheses (). Additive interactions are represented by + and multiplicative interactions are represented by *. Model names such as S(prev)p(d)psi(prev) are followed by the letters 'DM' to indicate that the model was built manually using the design matrix coding format, or 'DMaltopt' where the alternative optimization routine was called from within MARK.

- $QAIC_c$ represents the degree of model parsimony, and is the small sample size corrected Quasi Akaike's Information Criterion value for each model ('quasi' indicates that the AIC was adjusted to account for the variance inflation factor $\hat{c}$). The smaller this value, the more parsimonious the respective model within the candidate model set. These values cannot be compared between candidate model sets (separate analyses) however.
- Delta $QAIC_c$ is the subtractive difference between the $QAIC_c$ of the model in question, and that of the most parsimonious model of the set.
- AIC_c Weight is the model probability within the candidate model set. It is the weight of evidence in favor of the respective model being the actual best model in the set (minimizing the Kullback-Leibler distance)
- Model likelihood is the AIC_c Weight of the model of interest divided by the AIC_c Weight of the best model in the candidate set. It is the strength of evidence for this model relative to other models in the model set.
- 'Num par' is the number of estimable parameters of the respective model, and this differs depending on the nature of model variable constraints

- QDeviance is the Quasi model deviance (model deviance adjusted to account for the variance inflation factor $\hat{c}$). The lower this value, the better the model is estimated to fit the empirical data (this value doesn't take account of the number of parameters, hence is not equivalent to model parsimony)
- Cumulative sum of $QAIC_c$ Weights is a rank-order cumulative sum of Akaike weights which adds to one over the entire candidate model set.

The relative contribution of each variable (relative variable importance) is most readily interpreted from the second form of data presentation for each candidate model set (the heatmaps or coloured tables). For the purposes of displaying all models in the candidate model sets in two dimensions, variables and combinations of variables for representative estimable parameters have been represented separately (for example, the survival variable *prev* has been separated from models containing a combination of variables for survival such as *g+prev* or *g*prev*, but the order of variables within these combinations is not important). The third parameter (state transition probability, ψ or psi) has been separated into individual tables for visualization in two dimensions.

D.2.1 MSMR 2 state set

Table D.1. Ranking of most parsimonious models in MSMR 2 state set

Model (MSMR 2 state Tully set)	$QAIC_c$	Delta $QAIC_c$	AIC_c Weights	Model Likelihood	Num Par	QDeviance	Cumulative sum of AIC_c Weight
S(g*prev)p(d)psi(g*prev) - DM	1159.146	0	0.09168	1	10	1138.603	0.09168
S(g*prev)p(rad)psi(g*prev) - DM	1159.829	0.6829	0.06516	0.7107	10	1139.286	0.15684
S(g*prev)p(rh)psi(g*prev) - DM	1160.096	0.9504	0.057	0.6217	10	1139.553	0.21384
S(g*temp)p(d)psi(g*prev) - DM	1160.216	1.0698	0.0537	0.5857	10	1139.672	0.26754
S(g*temp)p(rh)psi(g*prev) - DM	1160.493	1.3473	0.04674	0.5098	10	1139.95	0.31428
S(g*temp)p(rad)psi(g*prev) - DM	1160.559	1.4135	0.04522	0.4932	10	1140.016	0.3595
S(g*prev)p(g+d)psi(g*prev) - DM	1161.034	1.8884	0.03566	0.389	11	1138.381	0.39516
S(prev)p(d)psi(g*prev) - DM	1161.221	2.0752	0.03248	0.3543	8	1144.867	0.42764
S(g*prev)p(g*rad)psi(g*prev) - DM	1161.359	2.213	0.03032	0.3307	12	1136.585	0.45796
S(g*prev)p(g+rad)psi(g*prev) - DM	1161.593	2.4468	0.02698	0.2943	11	1138.939	0.48494
S(g*prev)p(.)psi(g*prev) - DM	1161.715	2.5688	0.02538	0.2768	9	1143.271	0.51032
S(prev)p(rh)psi(g*prev) - DM	1161.933	2.7872	0.02275	0.2481	8	1145.579	0.53307
S(g*temp)p(g*rad)psi(g*prev) - DM	1162	2.8537	0.02201	0.2401	12	1137.225	0.55508
S(g*temp)p(.)psi(g*prev) - DM	1162.101	2.9551	0.02092	0.2282	9	1143.658	0.576
S(g*prev)p(g+rh)psi(g*prev) - DM	1162.117	2.9715	0.02075	0.2263	11	1139.464	0.59675
S(g*temp)p(g+d)psi(g*prev) - DM	1162.147	3.0014	0.02044	0.2229	11	1139.494	0.61719
S(g*temp)p(g+rad)psi(g*prev) - DM	1162.239	3.0932	0.01953	0.213	11	1139.586	0.63672
S(g*temp)p(g+rh)psi(g*prev) - DM	1162.55	3.4042	0.01671	0.1823	11	1139.897	0.65343
S(prev)p(rad)psi(g*prev) - DM	1162.709	3.5627	0.01544	0.1684	8	1146.355	0.66887
S(g*prev)p(g*d)psi(g*prev) - DM	1162.743	3.5967	0.01518	0.1656	12	1137.968	0.68405
S(g+prev)p(d)psi(g*prev) - DM	1162.843	3.6972	0.01444	0.1575	9	1144.4	0.69849
S(prev)p(g+d)psi(g*prev) - DM	1163.082	3.9366	0.01281	0.1397	9	1144.639	0.7113
S(g+prev)p(rh)psi(g*prev) - DM	1163.32	4.1738	0.01137	0.124	9	1144.876	0.72267

S(prev)p(.)psi(g*prev) - DM	1163.565	4.4191	0.01006	0.1097	7	1149.29	0.73273
S(g*prev)p(g)psi(g*prev) - DM	1163.627	4.4809	0.00976	0.1065	10	1143.084	0.74249
S(g*prev)p(d)psi(g*temp) - DM	1163.815	4.669	0.00888	0.0969	10	1143.272	0.75137
S(temp)p(d)psi(g*prev) - DM	1163.929	4.7827	0.00839	0.0915	8	1147.575	0.75976
S(prev)p(g+rh)psi(g*prev) - DM	1163.946	4.8001	0.00832	0.0907	9	1145.503	0.76808
S(g+prev)p(rad)psi(g*prev) - DM	1163.992	4.8457	0.00813	0.0887	9	1145.548	0.77621
S(g*temp)p(g*d)psi(g*prev) - DM	1164.031	4.885	0.00797	0.0869	12	1139.257	0.78418
S(g*temp)p(g)psi(g*prev) - DM	1164.058	4.9124	0.00786	0.0857	10	1143.515	0.79204
S(g*prev)p(g*rh)psi(g*prev) - DM	1164.094	4.9479	0.00772	0.0842	12	1139.32	0.79976
S(prev)p(g*rad)psi(g*prev) - DM	1164.274	5.1277	0.00706	0.077	10	1143.73	0.80682
S(T)p(d)psi(g*prev) - DM	1164.318	5.172	0.00691	0.0754	8	1147.964	0.81373
S(g*prev)p(rad)psi(g*temp) - DM	1164.43	5.2845	0.00653	0.0712	10	1143.887	0.82026
S(g*temp)p(g*rh)psi(g*prev) - DM	1164.528	5.382	0.00622	0.0678	12	1139.754	0.82648
S(prev)p(g+rad)psi(g*prev) - DM	1164.615	5.4694	0.00595	0.0649	9	1146.172	0.83243
S(g+prev)p(g+d)psi(g*prev) - DM	1164.705	5.5593	0.00569	0.0621	10	1144.162	0.83812
S(prev)p(g*d)psi(g*prev) - DM	1164.76	5.6145	0.00553	0.0603	10	1144.217	0.84365
S(g*prev)p(rh)psi(g*temp) - DM	1164.774	5.6285	0.0055	0.06	10	1144.231	0.84915
S(temp)p(rh)psi(g*prev) - DM	1164.819	5.6736	0.00537	0.0586	8	1148.466	0.85452
S(g*temp)p(d)psi(g*temp) - DM	1165.163	6.0168	0.00453	0.0494	10	1144.619	0.85905
S(g+prev)p(.)psi(g*prev) - DM	1165.194	6.0485	0.00446	0.0486	8	1148.841	0.86351
S(g+prev)p(g+rh)psi(g*prev) - DM	1165.348	6.2019	0.00413	0.045	10	1144.805	0.86764
S(g*temp)p(rad)psi(g*temp) - DM	1165.457	6.3111	0.00391	0.0426	10	1144.914	0.87155
S(prev)p(g)psi(g*prev) - DM	1165.463	6.3176	0.00389	0.0424	8	1149.11	0.87544
S(g*temp)p(rh)psi(g*temp) - DM	1165.475	6.3296	0.00387	0.0422	10	1144.932	0.87931
S(g+prev)p(g*rad)psi(g*prev) - DM	1165.522	6.3764	0.00378	0.0412	11	1142.869	0.88309
S(temp)p(.)psi(g*prev) - DM	1165.583	6.4369	0.00367	0.04	7	1151.308	0.88676
S(g+temp)p(d)psi(g*prev) - DM	1165.586	6.44	0.00366	0.0399	9	1147.142	0.89042
S(temp)p(rad)psi(g*prev) - DM	1165.754	6.6086	0.00337	0.0368	8	1149.401	0.89379
S(g*prev)p(g+d)psi(g*temp) - DM	1165.823	6.6774	0.00325	0.0354	11	1143.17	0.89704
S(g+prev)p(g+rad)psi(g*prev) - DM	1165.841	6.6954	0.00322	0.0351	10	1145.298	0.90026
S(temp)p(g+d)psi(g*prev) - DM	1165.95	6.8039	0.00305	0.0333	9	1147.506	0.90331
S(prev)p(g*rh)psi(g*prev) - DM	1165.953	6.8067	0.00305	0.0333	10	1145.409	0.90636
S(g+T)p(d)psi(g*prev) - DM	1166.1	6.9537	0.00283	0.0309	9	1147.656	0.90919
S(g*prev)p(g+rad)psi(g*temp) - DM	1166.133	6.9871	0.00279	0.0304	11	1143.479	0.91198
S(T)p(rh)psi(g*prev) - DM	1166.184	7.0384	0.00272	0.0297	8	1149.83	0.9147
S(g+temp)p(rh)psi(g*prev) - DM	1166.307	7.1612	0.00255	0.0278	9	1147.864	0.91725
S(prev)p(d)psi(g*temp) - DM	1166.385	7.2395	0.00246	0.0268	8	1150.032	0.91971
S(T)p(g+d)psi(g*prev) - DM	1166.387	7.2412	0.00245	0.0267	9	1147.944	0.92216
S(g+prev)p(g*d)psi(g*prev) - DM	1166.407	7.2609	0.00243	0.0265	11	1143.753	0.92459
S(g*prev)p(.)psi(g*temp) - DM	1166.51	7.3642	0.00231	0.0252	9	1148.067	0.9269
S(g*prev)p(g+rh)psi(g*temp) - DM	1166.853	7.7068	0.00194	0.0212	11	1144.199	0.92884
S(temp)p(g+rh)psi(g*prev) - DM	1166.908	7.7619	0.00189	0.0206	9	1148.464	0.93073
S(T)p(.)psi(g*prev) - DM	1166.91	7.7637	0.00189	0.0206	7	1152.635	0.93262
S(temp)p(g*rad)psi(g*prev) - DM	1166.913	7.7674	0.00189	0.0206	10	1146.37	0.93451
S(g*temp)p(g+rad)psi(g*temp) - DM	1167.086	7.9398	0.00173	0.0189	11	1144.432	0.93624
S(g+prev)p(g)psi(g*prev) - DM	1167.087	7.9411	0.00173	0.0189	9	1148.644	0.93797
S(prev)p(rh)psi(g*temp) - DM	1167.097	7.9515	0.00172	0.0188	8	1150.744	0.93969
S(g*temp)p(.)psi(g*temp) - DM	1167.136	7.99	0.00169	0.0184	9	1148.692	0.94138
S(g+temp)p(rad)psi(g*prev) - DM	1167.148	8.0021	0.00168	0.0183	9	1148.705	0.94306
S(g*temp)p(g+d)psi(g*temp) - DM	1167.183	8.0368	0.00165	0.018	11	1144.529	0.94471

S(g+temp)p(.)psi(g*prev) - DM	1167.204	8.058	0.00163	0.0178	8	1150.85	0.94634
S(g*T)p(d)psi(g*prev) - DM	1167.213	8.0674	0.00162	0.0177	10	1146.67	0.94796
S(T)p(rad)psi(g*prev) - DM	1167.292	8.1465	0.00156	0.017	8	1150.938	0.94952
S(g+prev)p(g*rh)psi(g*prev) - DM	1167.365	8.2193	0.0015	0.0164	11	1144.712	0.95102
S(temp)p(g+rad)psi(g*prev) - DM	1167.544	8.3981	0.00138	0.0151	9	1149.101	0.9524
S(T)p(g*rad)psi(g*prev) - DM	1167.557	8.4108	0.00137	0.0149	10	1147.013	0.95377
S(g*temp)p(g+rh)psi(g*temp) - DM	1167.573	8.4267	0.00136	0.0148	11	1144.919	0.95513
S(temp)p(g)psi(g*prev) - DM	1167.614	8.4677	0.00133	0.0145	8	1151.26	0.95646
S(g+temp)p(g+d)psi(g*prev) - DM	1167.62	8.4742	0.00132	0.0144	10	1147.077	0.95778
S(temp)p(g*d)psi(g*prev) - DM	1167.711	8.5648	0.00127	0.0139	10	1147.167	0.95905
S(g+prev)p(d)psi(g*temp) - DM	1167.776	8.6299	0.00123	0.0134	9	1149.332	0.96028
S(prev)p(rad)psi(g*temp) - DM	1167.873	8.727	0.00117	0.0128	8	1151.519	0.96145
S(g+T)p(rh)psi(g*prev) - DM	1167.903	8.7572	0.00115	0.0125	9	1149.46	0.9626
S(g*prev)p(g*rad)psi(g*temp) - DM	1168	8.8543	0.0011	0.012	12	1143.226	0.9637
S(T)p(g*d)psi(g*prev) - DM	1168.142	8.9966	0.00102	0.0111	10	1147.599	0.96472
S(g+T)p(g+d)psi(g*prev) - DM	1168.172	9.0257	0.00101	0.011	10	1147.628	0.96573
S(g+temp)p(g*rad)psi(g*prev) - DM	1168.245	9.0987	0.00097	0.0106	11	1145.591	0.9667
S(T)p(g+rh)psi(g*prev) - DM	1168.26	9.1144	0.00096	0.0105	9	1149.817	0.96766
S(g+prev)p(rh)psi(g*temp) - DM	1168.271	9.125	0.00096	0.0105	9	1149.828	0.96862
S(prev)p(g+d)psi(g*temp) - DM	1168.382	9.2357	0.00091	0.0099	9	1149.938	0.96953
S(g+temp)p(g+rh)psi(g*prev) - DM	1168.407	9.2608	0.00089	0.0097	10	1147.863	0.97042
S(g*prev)p(g)psi(g*temp) - DM	1168.561	9.4149	0.00083	0.0091	10	1148.018	0.97125
S(g+T)p(.)psi(g*prev) - DM	1168.677	9.5312	0.00078	0.0085	8	1152.323	0.97203
S(prev)p(.)psi(g*temp) - DM	1168.729	9.5834	0.00076	0.0083	7	1154.455	0.97279
S(g+temp)p(g+rad)psi(g*prev) - DM	1168.843	9.6974	0.00072	0.0079	10	1148.3	0.97351
S(temp)p(g*rh)psi(g*prev) - DM	1168.855	9.7087	0.00071	0.0077	10	1148.311	0.97422
S(T)p(g+rad)psi(g*prev) - DM	1168.861	9.7151	0.00071	0.0077	9	1150.418	0.97493
...							

Table D.2. AIC value and relative variable importance for MSMR 2 state set

Psi(.)

S(rows)p(columns)	.	g	rh	g+rh	g*rh	rad	g+rad	g*rad	d	g+d	g*d
.	1225.9	1208.8	1216.0	1199.3	1200.7	1225.0	1206.9	1206.1	1218.3	1202.0	1203.6
g	1227.4	1210.7	1217.9	1200.6	1201.8	1226.7	1208.6	1207.9	1220.1	1203.7	1205.3
prev	1203.3	1186.7	1201.7	1185.2	1186.8	1202.4	1184.8	1184.0	1201.0	1184.7	1186.3
g+prev	1205.2	1187.4	1203.4	1185.4	1186.9	1204.2	1184.9	1184.8	1202.8	1185.3	1186.9
g*prev	1206.0	1189.5	1204.3	1187.5	1189.0	1205.1	1187.0	1186.9	1203.9	1187.4	1188.9
temp	1205.3	1188.7	1204.6	1188.1	1189.8	1205.5	1188.0	1187.2	1203.7	1187.4	1189.0
g+temp	1207.3	1189.9	1206.4	1188.8	1190.4	1207.4	1188.8	1188.4	1205.6	1188.5	1190.0
g*temp	1208.9	1186.2	1208.4	1184.6	1186.0	1209.2	1184.0	1183.7	1207.5	1184.2	1185.7
T	1206.7	1190.0	1205.9	1189.4	1191.1	1207.0	1189.6	1188.8	1204.1	1187.9	1189.4
g+T	1208.7	1191.5	1207.9	1190.5	1192.1	1209.0	1190.7	1190.2	1206.1	1189.2	1190.7
g*T	1210.1	1193.2	1209.9	1191.6	1193.0	1210.8	1192.2	1191.7	1207.9	1190.3	1191.7

Psi(g)

S(rows)p(columns)	.	g	rh	g+rh	g*rh	rad	g+rad	g*rad	d	g+d	g*d
.	1206.4	1206.2	1196.6	1196.5	1198.2	1205.6	1206.9	1206.1	1198.9	1197.9	1195.2
g	1208.2	1205.6	1198.6	1197.4	1198.7	1207.4	1207.2	1206.6	1200.9	1198.4	1195.4
prev	1183.9	1183.1	1182.2	1181.5	1183.6	1183.0	1183.8	1183.1	1181.5	1180.3	1177.6
g+prev	1185.6	1185.0	1183.8	1183.5	1185.3	1184.6	1185.9	1185.2	1183.2	1182.3	1179.5
g*prev	1187.6	1187.1	1185.9	1185.6	1185.2	1186.6	1188.0	1187.3	1185.2	1184.4	1179.2

temp	1185.9	1184.7	1185.1	1184.2	1186.2	1186.1	1186.3	1185.6	1184.2	1182.7	1182.3
g+temp	1187.7	1184.5	1186.8	1186.1	1187.6	1187.8	1188.4	1187.6	1186.0	1184.6	1182.0
g*temp	1185.2	1183.5	1183.6	1182.3	1185.4	1184.5	1185.9	1185.4	1182.9	1181.2	1182.3
T	1187.2	1186.2	1186.5	1185.6	1187.7	1187.6	1187.8	1187.1	1184.6	1183.1	1180.5
g+T	1189.1	1186.0	1188.3	1187.5	1189.2	1189.4	1189.9	1189.1	1186.5	1185.1	1182.3
g*T	1191.2	1188.1	1190.1	1189.5	1191.1	1191.4	1192.0	1191.1	1188.3	1187.1	1184.3

Psi(prev)

S(rows)p(columns)	.	g	rh	g+rh	g*rh	rad	g+rad	g*rad	d	g+d	g*d
.	1222.5	1208.9	1212.6	1199.3	1201.0	1221.6	1206.8	1206.8	1214.9	1202.4	1204.4
g	1221.1	1209.7	1213.1	1201.2	1203.0	1221.0	1207.9	1208.6	1214.5	1204.1	1206.1
prev	1199.9	1187.4	1198.3	1185.8	1187.6	1199.1	1185.3	1185.2	1197.6	1185.6	1187.4
g+prev	1202.0	1189.0	1200.3	1187.2	1188.7	1201.0	1186.7	1186.6	1199.6	1187.1	1188.8
g*prev	1202.3	1191.1	1200.7	1189.2	1190.8	1201.5	1188.8	1188.7	1200.2	1189.2	1190.9
temp	1202.0	1189.4	1201.2	1188.7	1190.4	1202.1	1188.5	1188.4	1200.3	1188.2	1190.1
g+temp	1204.0	1191.3	1203.2	1190.4	1192.1	1204.2	1190.3	1190.1	1202.3	1190.1	1191.8
g*temp	1205.6	1188.1	1205.0	1186.6	1188.1	1205.9	1185.9	1185.7	1204.2	1186.2	1187.7
T	1203.3	1190.5	1202.5	1189.9	1191.6	1203.6	1189.9	1189.9	1200.7	1188.6	1190.4
g+T	1205.3	1192.6	1204.6	1191.8	1193.5	1205.7	1191.9	1191.8	1202.7	1190.6	1192.4
g*T	1206.4	1194.6	1206.3	1193.4	1194.9	1207.2	1193.9	1193.6	1204.3	1192.1	1193.7

Psi(temp)

S(rows)p(columns)	.	g	rh	g+rh	g*rh	rad	g+rad	g*rad	d	g+d	g*d
.	1221.2	1208.5	1211.3	1198.9	1200.6	1220.3	1206.3	1206.3	1213.6	1202.2	1204.2
g	1221.0	1209.8	1212.5	1201.0	1202.7	1220.7	1207.9	1208.3	1214.2	1204.1	1206.2
prev	1198.6	1186.9	1197.0	1185.4	1187.2	1197.7	1184.8	1184.8	1196.3	1185.3	1187.3
g+prev	1200.6	1188.6	1198.9	1186.7	1188.4	1199.6	1186.3	1186.3	1198.2	1186.8	1188.6
g*prev	1201.6	1190.7	1200.0	1188.8	1190.5	1200.8	1188.3	1188.3	1199.4	1188.9	1190.7
temp	1200.6	1189.0	1199.9	1188.3	1190.1	1200.8	1188.2	1188.1	1199.0	1188.0	1190.0
g+temp	1202.6	1191.0	1201.8	1190.0	1191.8	1202.7	1190.0	1189.9	1201.0	1189.8	1191.7
g*temp	1204.7	1187.0	1203.9	1185.5	1187.0	1204.8	1184.7	1184.8	1203.1	1185.4	1187.1
T	1202.0	1190.2	1201.2	1189.6	1191.4	1202.3	1189.6	1189.6	1199.3	1188.4	1190.4
g+T	1204.0	1192.3	1203.3	1191.5	1193.2	1204.4	1191.6	1191.6	1201.4	1190.4	1192.3
g*T	1205.7	1194.1	1205.3	1192.6	1194.2	1206.3	1193.1	1193.1	1203.4	1191.6	1193.4

Psi(T)

S(rows)p(columns)	.	g	rh	g+rh	g*rh	rad	g+rad	g*rad	d	g+d	g*d
.	1227.0	1210.8	1217.1	1201.3	1202.8	1226.2	1208.9	1208.2	1219.5	1204.1	1205.7
g	1228.4	1212.7	1219.0	1202.6	1203.9	1227.7	1210.6	1209.9	1221.1	1205.6	1207.1
prev	1204.5	1188.7	1202.8	1187.3	1188.9	1203.6	1186.8	1186.1	1202.1	1186.8	1188.3
g+prev	1206.3	1189.4	1204.5	1187.4	1188.9	1205.3	1186.9	1186.8	1203.9	1187.2	1188.7
g*prev	1207.3	1191.5	1205.7	1189.5	1191.0	1206.4	1189.0	1188.9	1205.2	1189.3	1190.7
temp	1206.5	1190.8	1205.7	1190.2	1191.8	1206.6	1190.1	1189.3	1204.8	1189.5	1191.0
g+temp	1208.4	1191.9	1207.5	1190.8	1192.4	1208.5	1190.8	1190.3	1206.7	1190.4	1191.9
g*temp	1210.3	1188.2	1209.6	1186.7	1188.1	1210.5	1186.0	1185.7	1208.8	1186.2	1187.6
T	1207.8	1192.1	1207.1	1191.5	1193.2	1208.2	1191.7	1190.9	1205.2	1189.9	1191.5
g+T	1209.8	1193.5	1209.0	1192.5	1194.2	1210.1	1192.7	1192.2	1207.2	1191.1	1192.6
g*T	1211.4	1195.2	1211.0	1193.6	1195.1	1212.0	1194.2	1193.7	1209.2	1192.2	1193.6

Psi(g+prev)

S(rows)p(columns)	.	g	rh	g+rh	g*rh	rad	g+rad	g*rad	d	g+d	g*d
.	1203.2	1202.1	1193.3	1192.4	1193.1	1202.3	1203.6	1204.5	1195.7	1194.1	1191.9
g	1202.9	1199.6	1194.5	1193.3	1193.9	1202.5	1203.5	1204.7	1196.1	1194.6	1192.4
prev	1180.7	1174.4	1179.0	1175.4	1176.1	1179.8	1178.3	1179.5	1178.3	1174.2	1171.7

g+prev	1182.7	1176.4	1181.1	1177.4	1178.1	1181.8	1180.4	1181.5	1180.4	1176.2	1173.8
g*prev	1184.7	1178.2	1183.1	1179.4	1180.2	1183.9	1182.2	1183.5	1182.4	1178.2	1176.2
temp	1182.7	1176.5	1181.9	1178.4	1179.0	1182.8	1178.6	1182.1	1181.0	1177.0	1174.7
g+temp	1184.7	1178.4	1184.0	1180.3	1181.0	1184.9	1180.5	1184.1	1183.1	1178.9	1176.7
g*temp	1181.9	1178.0	1180.5	1177.3	1181.5	1181.0	1180.0	1184.3	1179.9	1176.2	1177.8
T	1184.0	1178.5	1183.3	1180.2	1181.0	1184.4	1180.5	1184.0	1181.4	1177.8	1175.4
g+T	1186.1	1180.4	1185.3	1182.2	1183.0	1186.5	1182.5	1186.0	1183.5	1179.8	1177.4
g*T	1188.1	1182.4	1187.3	1184.3	1185.1	1188.5	1184.5	1188.1	1185.5	1181.9	1179.5

Psi(g+temp)

S(rows)p(columns)	.	g	rh	g+rh	g*rh	rad	g+rad	g*rad	d	g+d	g*d
.	1202.6	1200.5	1192.8	1193.0	1194.0	1201.8	1203.8	1204.6	1195.1	1194.5	1191.7
g	1202.9	1200.1	1194.3	1193.9	1194.8	1202.5	1204.0	1204.9	1196.1	1195.0	1192.2
prev	1180.1	1173.7	1178.5	1175.1	1176.1	1179.2	1175.6	1178.9	1177.7	1173.8	1172.2
g+prev	1182.1	1175.8	1180.4	1177.2	1178.2	1181.2	1177.7	1181.0	1179.8	1175.8	1172.2
g*prev	1184.2	1177.6	1182.5	1179.2	1180.3	1178.0	1179.6	1183.1	1181.8	1177.9	1174.3
temp	1182.1	1175.7	1181.3	1178.0	1178.9	1182.3	1177.7	1181.4	1180.5	1176.4	1173.1
g+temp	1184.2	1177.6	1183.4	1179.9	1180.9	1184.3	1179.7	1183.4	1182.5	1178.4	1175.1
g*temp	1180.2	1179.1	1178.7	1176.7	1180.9	1179.2	1179.1	1181.2	1178.1	1175.4	1176.0
T	1183.4	1177.7	1182.7	1179.8	1180.9	1183.8	1179.7	1183.3	1180.8	1177.3	1173.8
g+T	1185.5	1179.7	1184.8	1181.8	1183.0	1185.9	1181.7	1185.4	1182.9	1179.3	1175.8
g*T	1187.5	1181.7	1186.4	1183.9	1185.0	1187.7	1183.8	1187.5	1184.7	1181.4	1177.9

Psi(g+T)

S(rows)p(columns)	.	g	rh	g+rh	g*rh	rad	g+rad	g*rad	d	g+d	g*d
.	1208.4	1207.7	1198.5	1198.2	1199.5	1207.5	1208.7	1208.2	1200.8	1199.6	1196.9
g	1210.0	1205.0	1200.5	1199.0	1200.1	1209.3	1208.9	1208.6	1202.7	1200.1	1197.2
prev	1185.8	1181.4	1184.2	1182.4	1183.6	1185.0	1185.1	1184.9	1183.5	1181.1	1178.2
g+prev	1187.5	1183.3	1185.8	1184.3	1185.6	1186.6	1187.2	1187.0	1185.2	1183.1	1180.2
g*prev	1189.6	1185.3	1187.9	1186.4	1185.7	1188.7	1189.3	1189.1	1187.2	1185.2	1180.1
temp	1187.8	1183.1	1187.1	1185.0	1186.1	1188.0	1185.1	1187.3	1186.2	1183.5	1180.9
g+temp	1189.7	1184.9	1188.8	1186.9	1188.0	1189.8	1187.0	1189.3	1188.0	1185.4	1182.7
g*temp	1186.9	1184.1	1185.3	1183.3	1183.3	1186.2	1186.1	1187.2	1184.6	1182.1	1183.3
T	1189.2	1184.5	1188.4	1186.4	1187.6	1189.5	1186.5	1188.8	1186.6	1183.9	1181.0
g+T	1191.1	1186.4	1190.3	1188.3	1189.5	1191.4	1188.4	1190.8	1188.5	1185.9	1183.0
g*T	1193.1	1188.4	1192.1	1190.3	1191.6	1193.4	1190.5	1192.8	1190.3	1187.9	1185.1

Psi(g*prev)

S(rows)p(columns)	.	g	rh	g+rh	g*rh	rad	g+rad	g*rad	d	g+d	g*d
.	1186.1	1187.0	1176.2	1177.3	1179.1	1185.3	1182.5	1181.2	1178.6	1179.8	1181.8
g	1185.1	1185.8	1177.4	1178.4	1180.2	1185.0	1183.1	1181.2	1178.6	1179.9	1181.8
prev	1163.6	1165.5	1161.9	1163.9	1166.0	1162.7	1164.6	1164.3	1161.2	1163.1	1164.8
g+prev	1165.2	1167.1	1163.3	1165.3	1167.4	1164.0	1165.8	1165.5	1162.8	1164.7	1166.4
g*prev	1161.7	1163.6	1160.1	1162.1	1164.1	1159.8	1161.6	1161.4	1159.1	1161.0	1162.7
temp	1165.6	1167.6	1164.8	1166.9	1168.9	1165.8	1167.5	1166.9	1163.9	1165.9	1167.7
g+temp	1167.2	1169.2	1166.3	1168.4	1170.4	1167.1	1168.8	1168.2	1165.6	1167.6	1169.4
g*temp	1162.1	1164.1	1160.5	1162.6	1164.5	1160.6	1162.2	1162.0	1160.2	1162.1	1164.0
T	1166.9	1169.0	1166.2	1168.3	1170.1	1167.3	1168.9	1167.6	1164.3	1166.4	1168.1
g+T	1168.7	1170.8	1167.9	1170.0	1171.8	1168.9	1170.4	1169.1	1166.1	1168.2	1170.0
g*T	1170.3	1172.4	1169.0	1171.1	1173.0	1170.2	1171.4	1170.3	1167.2	1169.3	1171.2

Psi(g*temp)

S(rows)p(columns)	.	g	rh	g+rh	g*rh	rad	g+rad	g*rad	d	g+d	g*d

.	1191.3	1191.2	1181.4	1182.1	1184.1	1190.4	1186.9	1188.2	1183.7	1184.6	1185.9
g	1191.4	1191.4	1183.0	1183.7	1185.8	1191.3	1188.5	1189.8	1184.7	1185.6	1193.1
prev	1168.7	1170.8	1167.1	1169.2	1171.1	1167.9	1169.7	1171.5	1166.4	1168.4	1168.9
g+prev	1170.1	1172.2	1168.3	1170.3	1172.3	1168.9	1170.7	1172.5	1167.8	1169.7	1171.0
g*prev	1166.5	1168.6	1164.8	1166.9	1168.9	1164.4	1166.1	1168.0	1163.8	1165.8	1170.6
temp	1170.7	1172.8	1170.0	1172.1	1174.1	1170.9	1172.7	1174.4	1169.1	1171.1	1171.9
g+temp	1172.2	1174.3	1171.3	1173.4	1175.4	1172.1	1173.9	1175.6	1170.6	1172.6	1173.9
g*temp	1167.1	1169.2	1165.5	1167.6	1169.6	1165.5	1167.1	1168.9	1165.2	1167.2	1172.5
T	1172.1	1174.1	1171.3	1173.4	1175.5	1172.5	1174.0	1175.5	1169.5	1171.6	1172.4
g+T	1173.7	1175.8	1172.9	1175.0	1177.1	1173.8	1175.5	1177.0	1171.1	1173.1	1175.0
g*T	1175.3	1177.4	1174.1	1176.1	1178.2	1175.1	1176.4	1177.9	1172.2	1174.4	1177.1

Psi(g*T)

S(rows)p(columns)	.	g	rh	g+rh	g*rh	rad	g+rad	g*rad	d	g+d	g*d
.	1203.6	1202.4	1193.7	1194.0	1196.0	1202.8	1197.1	1199.2	1196.1	1195.6	1197.7
g	1204.4	1208.0	1195.6	1196.0	1198.0	1204.0	1199.2	1201.3	1197.5	1200.7	1198.7
prev	1181.1	1182.2	1179.4	1180.6	1182.4	1180.2	1181.5	1183.4	1178.7	1179.8	1178.5
g+prev	1182.7	1184.3	1180.9	1182.7	1184.5	1181.7	1182.0	1184.1	1180.3	1181.9	1180.4
g*prev	1179.4	1181.1	1177.6	1179.4	1183.5	1177.7	1177.3	1179.3	1176.5	1178.2	1180.0
temp	1183.1	1183.9	1182.3	1183.4	1185.2	1183.3	1184.8	1186.7	1181.4	1182.4	1181.1
g+temp	1184.7	1186.0	1183.9	1185.5	1186.4	1184.8	1185.7	1188.3	1183.1	1184.5	1183.0
g*temp	1179.7	1181.7	1177.8	1179.7	1183.5	1178.2	1178.3	1180.3	1177.4	1179.3	1181.3
T	1184.4	1185.2	1183.7	1184.7	1186.5	1184.8	1186.5	1187.7	1181.8	1182.6	1183.3
g+T	1186.2	1187.3	1185.4	1186.8	1187.9	1186.5	1187.8	1189.8	1183.6	1184.7	1183.1
g*T	1187.7	1189.3	1186.2	1188.2	1190.1	1187.5	1185.6	1187.6	1184.3	1186.5	1185.2

These 11 tables (Table D.2) represent the different variables used to constrain the state transition probability parameter (ψ, psi). Survival (S) variables are rows, recapture (ρ, p) variables are columns. Each colored cell in these tables represents a separate model in the respective candidate model set. Numbers within the cells represent the $QAIC_c$ value for the respective model, and cells have been colored according to $QAIC_c$ ranking (the more parsimonious the model, the lower its $QAIC_c$ value, and the closer towards the white end of the spectrum; red cells represent poorly parsimonious models). Borders around $QAIC_c$ top-ranking 11 models (depicted with white or pale yellow) cumulatively hold approximately 51% of total support within the candidate model set. Models displayed in orange and red are lower ranking based on $QAIC_c$ values.

D.2.2 MSMR 3 state set

Table D.3. Ranking of most parsimonious models in MSMR 3 state set

Model (MSMR 3 state Tully set)	$QAIC_c$	Delta $QAIC_c$	AIC_c Weights	Model Likelihood	Num Par	QDeviance	Cumulative sum of AIC_c Weight
S(g*prev)p(g+rad)psi(6g*prev) - DMaltopt	1253.225	0	0.20439	1	22	1206.65	0.20439
S(g+prev)p(g+rad)psi(6g*prev) - DMaltopt	1254.204	0.9784	0.12532	0.6131	20	1212.077	0.32971
S(g+prev)p(g+rh)psi(6g*prev) - DMaltopt	1255.344	2.1182	0.07088	0.3468	20	1213.217	0.40059
S(g*prev)p(g+rh)psi(6g*prev) - DMaltopt	1256.025	2.7998	0.05041	0.2466	22	1209.45	0.451
S(g*prev)p(g*rad)psi(6g*prev) - DMaltopt	1256.946	3.7203	0.03181	0.1556	24	1205.877	0.48281
S(prev)p(d)psi(6g*prev) - DMaltopt	1257.104	3.8781	0.0294	0.1438	16	1223.74	0.51221
S(g+prev)p(g*rad)psi(6g*prev) - DMaltopt	1257.188	3.963	0.02818	0.1379	22	1210.613	0.54039
S(g+prev)p(g+d)psi(6g*prev) - DMaltopt	1257.309	4.0832	0.02653	0.1298	20	1215.182	0.56692
S(g*prev)p(g+d)psi(6g*prev) - DMaltopt	1257.442	4.2162	0.02483	0.1215	22	1210.867	0.59175
S(g+temp)p(g+rad)psi(6g*prev) - DMaltopt	1257.508	4.2822	0.02402	0.1175	20	1215.381	0.61577
S(g*temp)p(g+rad)psi(6g*prev) - DMaltopt	1257.8	4.5749	0.02075	0.1015	22	1211.225	0.63652
S(g+prev)p(d)psi(6g*prev) - DMaltopt	1257.92	4.6941	0.01955	0.0956	18	1220.197	0.65607
S(prev)p(rh)psi(6g*prev) - DMaltopt	1257.978	4.7521	0.01899	0.0929	16	1224.614	0.67506
S(g+temp)p(g+rh)psi(6g*prev) - DMaltopt	1258.211	4.9852	0.0169	0.0827	20	1216.084	0.69196
S(prev)p(g+rad)psi(6g*prev) - DMaltopt	1258.584	5.3581	0.01403	0.0686	18	1220.861	0.70599
S(g+prev)p(rh)psi(6g*prev) - DMaltopt	1258.604	5.3786	0.01388	0.0679	18	1220.881	0.71987
S(prev)p(rad)psi(6g*prev) - DMaltopt	1258.606	5.3806	0.01387	0.0679	16	1225.243	0.73374
S(prev)p(g+rh)psi(6g*prev) - DMaltopt	1258.647	5.422	0.01359	0.0665	18	1220.924	0.74733
S(g+prev)p(g)psi(6g*prev) - DMaltopt	1258.731	5.5058	0.01303	0.0638	19	1218.812	0.76036
S(g*prev)p(g)psi(6g*prev) - DMaltopt	1258.821	5.5954	0.01246	0.061	21	1214.476	0.77282
S(g*prev)p(d)psi(6g*prev) - DMaltopt	1258.903	5.6772	0.01196	0.0585	20	1216.776	0.78478
S(g+prev)p(g*rh)psi(6g*prev) - DMaltopt	1259.319	6.0939	0.00971	0.0475	22	1212.744	0.79449
S(g*prev)p(g*rh)psi(6g*prev) - DMaltopt	1259.369	6.1436	0.00947	0.0463	24	1208.3	0.80396
S(g*prev)p(g+rh)psi(6g*temp) - DM	1259.379	6.1534	0.00942	0.0461	22	1212.804	0.81338
S(prev)p(.)psi(6g*prev) - DM	1259.467	6.2414	0.00902	0.0441	15	1228.267	0.8224
S(prev)p(g+d)psi(6g*prev) - DMaltopt	1259.785	6.5594	0.00769	0.0376	18	1222.062	0.83009
S(g*prev)p(rh)psi(6g*prev) - DMaltopt	1259.794	6.5686	0.00766	0.0375	20	1217.667	0.83775
S(g+prev)p(rad)psi(6g*prev) - DMaltopt	1259.984	6.7588	0.00696	0.0341	18	1222.261	0.84471
S(g*temp)p(g+rh)psi(6g*prev) - DMaltopt	1260.145	6.9192	0.00643	0.0315	22	1213.57	0.85114
S(temp)p(d)psi(6g*prev) - DMaltopt	1260.203	6.978	0.00624	0.0305	16	1226.84	0.85738
S(g+temp)p(g+d)psi(6g*prev) - DMaltopt	1260.449	7.2236	0.00552	0.027	20	1218.322	0.8629
S(g+prev)p(.)psi(6g*prev) - DMaltopt	1260.49	7.2642	0.00541	0.0265	17	1224.952	0.86831
S(g+prev)p(g+rad)psi(6g*temp) - DMaltopt	1260.511	7.2856	0.00535	0.0262	20	1218.384	0.87366
S(g+prev)p(g*d)psi(6g*prev) - DMaltopt	1260.515	7.2893	0.00534	0.0261	22	1213.94	0.879
S(g+prev)p(g+rh)psi(6g*temp) - DM	1260.566	7.3408	0.00521	0.0255	20	1218.44	0.88421
S(g*prev)p(rad)psi(6g*prev) - DMaltopt	1260.709	7.4834	0.00485	0.0237	20	1218.582	0.88906
S(temp)p(rh)psi(6g*prev) - DM	1261.081	7.8554	0.00402	0.0197	16	1227.717	0.89308
S(g*prev)p(.)psi(6g*prev) - DMaltopt	1261.138	7.9124	0.00391	0.0191	19	1221.219	0.89699
S(g+temp)p(d)psi(6g*prev) - DM	1261.537	8.3114	0.0032	0.0157	18	1223.814	0.90019
S(temp)p(g+rh)psi(6g*prev) - DMaltopt	1261.569	8.3431	0.00315	0.0154	18	1223.846	0.90334
S(prev)p(d)psi(6g*temp) - DMaltopt	1261.638	8.4122	0.00305	0.0149	16	1228.274	0.90639
S(g+temp)p(rh)psi(6g*prev) - DMaltopt	1261.7	8.4742	0.00295	0.0144	18	1223.977	0.90934
S(g+prev)p(d)psi(6g*temp) - DMaltopt	1261.748	8.5221	0.00288	0.0141	18	1224.025	0.91222
S(g*temp)p(g*rad)psi(6g*prev) - DMaltopt	1261.844	8.6187	0.00275	0.0135	24	1210.775	0.91497
S(g*temp)p(g+d)psi(6g*prev) - DMaltopt	1261.897	8.6714	0.00268	0.0131	22	1215.322	0.91765

S(temp)p(rad)psi(6g*prev) - DMaltopt	1261.975	8.7498	0.00257	0.0126	16	1228.612	0.92022
S(prev)p(rh)psi(6g*temp) - DMaltopt	1262.129	8.9034	0.00238	0.0116	16	1228.765	0.9226
S(prev)p(g)psi(6g*prev) - DMaltopt	1262.186	8.9607	0.00232	0.0114	17	1226.648	0.92492
S(g+prev)p(g+d)psi(6g*temp) - DM	1262.299	9.074	0.00219	0.0107	20	1220.173	0.92711
S(prev)p(g*rad)psi(6g*prev) - DMaltopt	1262.309	9.0839	0.00218	0.0107	20	1220.183	0.92929
S(g+prev)p(rh)psi(6g*temp) - DMaltopt	1262.332	9.1068	0.00215	0.0105	18	1224.609	0.93144
S(temp)p(.)psi(6g*prev) - DMaltopt	1262.345	9.12	0.00214	0.0105	15	1231.145	0.93358
S(g*prev)p(g*rh)psi(6g*temp) - DM	1262.532	9.3069	0.00195	0.0095	24	1211.463	0.93553
S(prev)p(g*rh)psi(6g*prev) - DMaltopt	1262.642	9.4161	0.00184	0.009	20	1220.515	0.93737
S(g+temp)p(g*rad)psi(6g*prev) - DMaltopt	1262.649	9.4235	0.00184	0.009	22	1216.074	0.93921
S(g+temp)p(.)psi(6g*prev) - DM	1262.716	9.4902	0.00178	0.0087	17	1227.178	0.94099
S(prev)p(rad)psi(6g*temp) - DMaltopt	1262.728	9.503	0.00177	0.0087	16	1229.365	0.94276
S(g*temp)p(g)psi(6g*prev) - DMaltopt	1262.733	9.5077	0.00176	0.0086	21	1218.388	0.94452
S(g+prev)p(rad)psi(6g*temp) - DMaltopt	1262.834	9.6081	0.00168	0.0082	18	1225.111	0.9462
S(temp)p(g+d)psi(6g*prev) - DMaltopt	1262.85	9.625	0.00166	0.0081	18	1225.128	0.94786
S(g*prev)p(g+rad)psi(6g) - DM	1262.876	9.6505	0.00164	0.008	16	1229.513	0.9495
S(g+temp)p(rad)psi(6g*prev) - DMaltopt	1263.326	10.1005	0.00131	0.0064	18	1225.603	0.95081
S(g*temp)p(rh)psi(6g*prev) - DMaltopt	1263.497	10.2715	0.0012	0.0059	20	1221.37	0.95201
S(g*prev)p(d)psi(6g*temp) - DMaltopt	1263.604	10.3783	0.00114	0.0056	20	1221.477	0.95315
S(g+prev)p(g*rh)psi(6g*temp) - DM	1263.751	10.5254	0.00106	0.0052	22	1217.176	0.95421
S(prev)p(.)psi(6g*temp) - DMaltopt	1263.845	10.6198	0.00101	0.0049	15	1232.645	0.95522
S(g*temp)p(.)psi(6g*prev) - DMaltopt	1263.85	10.6246	0.00101	0.0049	19	1223.931	0.95623
S(g*prev)p(g+d)psi(6g*temp) - DMaltopt	1263.896	10.6704	0.00098	0.0048	22	1217.321	0.95721
S(g*temp)p(rad)psi(6g*prev) - DMaltopt	1263.921	10.6953	0.00097	0.0047	20	1221.794	0.95818
S(temp)p(g*rad)psi(6g*prev) - DMaltopt	1264.152	10.927	0.00087	0.0043	20	1222.026	0.95905
S(prev)p(g+rh)psi(6g*temp) - DM	1264.181	10.9555	0.00085	0.0042	18	1226.458	0.9599
S(g+temp)p(g*d)psi(6g*prev) - DMaltopt	1264.204	10.9783	0.00084	0.0041	22	1217.629	0.96074
S(g*prev)p(rh)psi(6g*temp) - DMaltopt	1264.229	11.0039	0.00083	0.0041	20	1222.103	0.96157
S(g*temp)p(d)psi(6g*prev) - DMaltopt	1264.237	11.0114	0.00083	0.0041	20	1222.11	0.9624
S(g*prev)p(g+rad)psi(2g) - DM	1264.444	11.219	0.00075	0.0037	12	1239.67	0.96315
S(g+prev)p(g+d)psi(6g+temp) - DMaltopt	1264.603	11.3775	0.00069	0.0034	15	1233.403	0.96384
S(prev)p(g+d)psi(6g+temp) - DMaltopt	1264.701	11.4755	0.00066	0.0032	13	1237.795	0.9645
S(temp)p(g)psi(6g*prev) - DMaltopt	1264.735	11.5094	0.00065	0.0032	17	1229.197	0.96515
S(g+prev)p(.)psi(6g*temp) - DMaltopt	1264.743	11.5176	0.00064	0.0031	17	1229.205	0.96579
S(g*prev)p(g+rad)psi(.) - DM	1264.754	11.529	0.00064	0.0031	11	1242.101	0.96643
S(g*prev)p(rad)psi(6g*temp) - DMaltopt	1264.813	11.5873	0.00062	0.003	20	1222.686	0.96705
S(g+temp)p(d)psi(6g*temp) - DMaltopt	1264.927	11.7019	0.00059	0.0029	18	1227.204	0.96764
S(g*temp)p(g+rad)psi(6g*temp) - DMaltopt	1264.933	11.7075	0.00059	0.0029	22	1218.358	0.96823
S(g*temp)p(g*d)psi(6g*prev) - DMaltopt	1264.955	11.7297	0.00058	0.0028	24	1213.886	0.96881
S(g*prev)p(g+rad)psi(6g+temp) - DM	1265.011	11.7853	0.00056	0.0027	17	1229.473	0.96937
S(temp)p(rh)psi(6g*temp) - DMaltopt	1265.041	11.8159	0.00056	0.0027	16	1231.678	0.96993
S(g*prev)p(g+rad)psi(6g+prev) - DM	1265.049	11.8236	0.00055	0.0027	17	1229.511	0.97048
S(g+prev)p(g+rad)psi(6g) - DM	1265.181	11.9558	0.00052	0.0025	14	1236.134	0.971
S(g*prev)p(g+rh)psi(6g) - DM	1265.222	11.9961	0.00051	0.0025	16	1231.858	0.97151
S(prev)p(d)psi(6g+temp) - DMaltopt	1265.233	12.0074	0.0005	0.0024	11	1242.579	0.97201
S(prev)p(g+d)psi(6g+prev) - DMaltopt	1265.244	12.0184	0.0005	0.0024	13	1238.338	0.97251
S(g*prev)p(.)psi(6g*temp) - DMaltopt	1265.26	12.0343	0.0005	0.0024	19	1225.341	0.97301
S(g+temp)p(g+rad)psi(6g*temp) - DMaltopt	1265.357	12.1314	0.00047	0.0023	20	1223.23	0.97348
S(prev)p(rh)psi(6g+temp) - DMaltopt	1265.429	12.2039	0.00046	0.0023	11	1242.776	0.97394
S(temp)p(d)psi(6g*temp) - DMaltopt	1265.466	12.2409	0.00045	0.0022	16	1232.103	0.97439

S(g+prev)p(g*rad)psi(6g*temp) - DMaltopt	1265.477	12.2518	0.00045	0.0022	22	1218.902	0.97484
S(prev)p(g+d)psi(6g*temp) - DMaltopt	1265.517	12.2916	0.00044	0.0022	18	1227.794	0.97528
S(temp)p(.)psi(6g*temp) - DMaltopt	1265.792	12.5665	0.00038	0.0019	15	1234.592	0.97566
S(prev)p(d)psi(6g+prev) - DMaltopt	1265.851	12.6257	0.00037	0.0018	11	1243.198	0.97603
S(g+prev)p(d)psi(6g+temp) - DMaltopt	1265.859	12.6332	0.00037	0.0018	13	1238.953	0.9764

…

Table D.4. AIC value and relative variable importance for MSMR 3 state set

Psi(.)

S(rows)p(columns)	.	g	rh	g+rh	g*rh	rad	g+rad	g*rad	d	g+d	g*d
.	1351.9	1293.8	1341.8	1285.1	1284.5	1350.9	1290.8	1291.0	1344.2	1287.9	1290.8
g	1347.8	1293.0	1339.1	1283.9	1283.4	1347.5	1290.0	1290.4	1341.0	1287.2	1290.2
prev	1329.0	1271.4	1327.3	1270.3	1270.7	1328.1	1268.4	1268.7	1326.6	1270.0	1273.0
g+prev	1327.0	1270.4	1325.5	1268.7	1269.0	1326.3	1266.7	1268.0	1324.8	1268.9	1271.9
g*prev	1322.0	1268.3	1321.6	1267.3	1267.9	1321.6	1264.8	1266.0	1320.8	1267.2	1270.2
temp	1331.0	1273.4	1330.2	1273.1	1273.7	1331.2	1271.8	1271.9	1329.3	1272.6	1275.6
g+temp	1329.3	1273.2	1328.6	1272.4	1272.8	1329.6	1271.0	1271.9	1327.8	1272.3	1275.4
g*temp	1324.3	1271.1	1324.8	1270.5	1271.0	1324.9	1268.4	1269.4	1323.8	1270.3	1273.3

Psi(6g)

S(rows)p(columns)	.	g	rh	g+rh	g*rh	rad	g+rad	g*rad	d	g+d	g*d
.	1294.7	1301.5	1284.7	1285.5	1288.4	1293.8	1293.2	1297.3	1287.0	1288.6	1290.9
g	1294.8	1289.7	1285.7	1277.7	1279.2	1294.3	1282.9	1287.0	1287.7	1285.3	1287.3
prev	1271.9	1273.1	1270.2	1271.0	1275.0	1271.0	1270.6	1274.7	1269.5	1270.7	1272.9
g+prev	1272.8	1272.0	1271.3	1266.4	1268.8	1272.1	1265.2	1269.3	1270.6	1270.3	1272.7
g*prev	1272.2	1268.9	1271.4	1265.2	1268.6	1271.8	1262.9	1266.8	1270.4	1267.3	1266.0
temp	1273.9	1279.0	1273.1	1275.9	1277.3	1274.1	1273.6	1276.1	1272.2	1273.1	1275.5
g+temp	1275.3	1275.0	1274.6	1270.2	1272.2	1275.6	1269.1	1273.2	1273.7	1272.7	1277.5
g*temp	1274.9	1271.2	1274.4	1267.3	1270.2	1275.1	1267.5	1270.0	1273.5	1269.9	1272.5

Psi(2g)

S(rows)p(columns)	.	g	rh	g+rh	g*rh	rad	g+rad	g*rad	d	g+d	g*d
.	1303.4	1295.0	1293.4	1287.1	1284.0	1302.5	1290.5	1292.6	1295.7	1289.9	1292.6
g	1300.9	1294.8	1292.0	1286.0	1283.3	1300.4	1290.1	1292.1	1294.0	1289.3	1292.2
prev	1280.6	1272.6	1278.9	1272.2	1270.6	1279.7	1268.1	1270.1	1278.2	1271.9	1274.4
g+prev	1279.4	1271.4	1277.8	1270.6	1268.9	1278.6	1266.3	1269.1	1277.2	1270.8	1273.3
g*prev	1276.9	1269.3	1276.4	1269.2	1268.1	1276.4	1264.4	1267.2	1275.5	1269.0	1271.5
temp	1282.6	1274.6	1281.8	1274.9	1273.0	1282.7	1271.4	1273.2	1280.9	1274.4	1277.1
g+temp	1281.5	1274.2	1280.8	1274.2	1272.2	1281.8	1270.5	1273.1	1280.0	1274.2	1276.8
g*temp	1279.9	1272.0	1279.8	1272.2	1270.7	1280.2	1268.2	1270.4	1278.9	1272.1	1274.7

Psi(prev)

S(rows)p(columns)	.	g	rh	g+rh	g*rh	rad	g+rad	g*rad	d	g+d	g*d
.	1343.2	1292.1	1333.2	1282.7	1282.8	1342.3	1287.9	1289.1	1335.6	1286.7	1290.4
g	1335.2	1290.2	1328.6	1282.4	1283.4	1335.9	1286.9	1287.5	1329.4	1285.9	1290.1
prev	1320.4	1271.4	1318.7	1270.0	1270.5	1319.5	1267.7	1268.6	1318.0	1270.2	1273.6
g+prev	1318.9	1271.7	1317.5	1269.9	1270.4	1318.3	1267.9	1269.1	1316.7	1270.3	1273.6
g*prev	1316.0	1270.0	1315.7	1269.0	1269.7	1315.8	1266.5	1267.6	1314.9	1268.9	1272.1
temp	1322.4	1273.3	1321.6	1272.7	1273.3	1322.5	1271.0	1271.9	1320.7	1272.6	1276.1
g+temp	1321.5	1274.2	1320.8	1273.4	1274.0	1321.9	1272.0	1272.9	1319.9	1273.5	1276.9
g*temp	1319.4	1272.5	1319.9	1271.9	1272.5	1320.1	1269.9	1270.8	1318.8	1271.8	1275.1

Psi(temp)

S(rows)p(columns)	.	g	rh	g+rh	g*rh	rad	g+rad	g*rad	d	g+d	g*d

.	1340.7	1291.9	1330.6	1282.7	1282.8	1339.8	1287.8	1289.0	1333.0	1286.9	1290.7
g	1334.6	1290.8	1327.6	1282.6	1283.4	1335.2	1287.6	1288.3	1328.6	1286.6	1290.7
prev	1317.8	1270.9	1316.1	1269.6	1270.1	1316.9	1267.2	1268.2	1315.4	1270.0	1273.5
g+prev	1316.7	1271.2	1315.2	1269.5	1270.0	1316.1	1267.4	1268.6	1314.5	1270.1	1273.5
g*prev	1314.8	1269.5	1316.7	1268.6	1269.3	1314.6	1265.9	1267.2	1313.6	1268.6	1272.0
temp	1319.8	1273.1	1319.0	1272.5	1273.2	1320.0	1270.8	1271.7	1318.1	1272.6	1276.2
g+temp	1319.2	1274.0	1318.5	1273.1	1273.8	1319.5	1271.7	1272.7	1317.6	1273.4	1276.9
g*temp	1318.3	1272.1	1318.6	1271.4	1272.0	1318.9	1270.7	1272.3	1317.6	1271.5	1274.9

Psi(6g+prev)

S(rows)p(columns)	.	g	rh	g+rh	g*rh	rad	g+rad	g*rad	d	g+d	g*d
.	1290.7	1293.1	1280.7	1285.3	1291.6	1290.1	1295.3	1294.9	1283.2	1285.5	1289.0
g	1287.0	1291.7	1279.3	1279.9	1281.4	1287.1	1285.1	1289.1	1280.9	1287.4	1289.4
prev	1267.8	1279.2	1266.3	1270.9	1278.0	1266.9	1276.4	1270.6	1265.9	1265.2	1268.0
g+prev	1268.1	1274.1	1266.7	1268.6	1271.0	1267.7	1267.3	1271.5	1266.2	1272.5	1274.8
g*prev	1269.2	1271.0	1268.8	1267.4	1270.3	1268.7	1265.0	1269.0	1267.9	1269.4	1271.9
temp	1270.8	1270.8	1270.7	1269.4	1280.3	1270.6	1274.3	1271.0	1268.4	1269.6	1272.2
g+temp	1271.2	1277.1	1270.0	1272.4	1274.4	1271.5	1271.3	1272.4	1269.4	1270.3	1279.2
g*temp	1272.8	1273.4	1272.1	1269.5	1273.8	1273.7	1268.1	1272.1	1271.6	1272.3	1274.6

Psi(6g+temp)

S(rows)p(columns)	.	g	rh	g+rh	g*rh	rad	g+rad	g*rad	d	g+d	g*d
.	1290.6	1293.2	1280.7	1281.9	1291.5	1290.2	1295.3	1294.8	1283.1	1285.5	1286.6
g	1287.9	1291.7	1280.2	1279.7	1281.4	1288.9	1285.1	1289.0	1281.8	1287.3	1289.4
prev	1268.0	1268.4	1265.4	1268.3	1267.8	1267.0	1272.3	1270.0	1265.2	1264.7	1266.9
g+prev	1268.3	1274.1	1266.3	1268.3	1270.9	1266.7	1267.3	1271.5	1265.9	1264.6	1266.8
g*prev	1269.1	1276.8	1268.5	1267.9	1274.8	1268.6	1265.0	1268.7	1267.4	1266.4	1268.8
temp	1269.6	1271.1	1269.2	1277.2	1273.2	1270.3	1275.4	1280.8	1267.9	1267.5	1268.9
g+temp	1271.0	1277.1	1270.2	1272.2	1274.3	1271.2	1271.2	1275.0	1269.2	1268.7	1269.6
g*temp	1272.9	1272.9	1271.1	1269.0	1273.3	1273.2	1271.2	1271.7	1271.7	1272.9	1274.2

Psi(6g*prev)

S(rows)p(columns)	.	g	rh	g+rh	g*rh	rad	g+rad	g*rad	d	g+d	g*d
.	1282.3	1284.7	1272.3	1271.1	1274.7	1281.6	1276.1	1283.9	1274.7	1277.3	1280.6
g	1278.6	1279.1	1272.1	1268.5	1274.5	1279.5	1275.5	1271.9	1272.3	1274.5	1276.9
prev	1259.5	1262.2	1258.0	1258.6	1262.6	1258.6	1258.6	1262.3	1257.1	1259.8	1273.7
g+prev	1260.5	1258.7	1258.6	1255.3	1259.3	1260.0	1254.2	1257.2	1257.9	1257.3	1260.5
g*prev	1261.1	1258.8	1259.8	1256.0	1259.4	1260.7	1253.2	1256.9	1258.9	1257.4	1270.9
temp	1262.3	1264.7	1261.1	1261.6	1267.6	1262.0	1266.7	1264.2	1260.2	1262.9	1266.2
g+temp	1262.7	1267.9	1261.7	1258.2	1266.8	1263.3	1257.5	1262.6	1261.5	1260.4	1264.2
g*temp	1263.9	1262.7	1263.5	1260.1	1270.2	1263.9	1257.8	1261.8	1264.2	1261.9	1265.0

Psi(6g*temp)

S(rows)p(columns)	.	g	rh	g+rh	g*rh	rad	g+rad	g*rad	d	g+d	g*d
.	1286.7	1287.2	1276.5	1277.5	1283.6	1285.5	1282.3	1282.9	1280.4	1285.3	1285.4
g	1283.4	1285.6	1276.1	1276.9	1278.3	1283.9	1278.5	1279.5	1277.2	1278.7	1284.6
prev	1263.8	1271.7	1262.1	1264.2	1277.7	1262.7	1267.1	1275.4	1261.6	1265.5	1269.3
g+prev	1264.7	1271.8	1262.3	1260.6	1263.8	1262.8	1260.5	1265.5	1261.7	1262.3	1272.4
g*prev	1265.3	1269.1	1264.2	1259.4	1262.5	1264.8	1274.9	1266.5	1263.6	1263.9	1271.6
temp	1265.8	1274.1	1265.0	1269.5	1276.2	1266.4	1268.4	1272.2	1265.5	1269.1	1271.0
g+temp	1266.6	1272.7	1266.0	1269.6	1274.2	1267.3	1265.4	1271.7	1264.9	1267.9	1270.8
g*temp	1268.7	1273.4	1267.9	1266.5	1269.0	1269.0	1264.9	1269.7	1267.7	1268.0	1270.8

These nine tables (Table D.4) represent the different variables used to constrain the state transition probability parameter (ψ, psi). The state transition variable '2g' means that 'infection' transitions that represent a gain of infection (from uninfected to either low or high infectious burden, or from low infectious burden to high burden) are one group, and 'recovery' transitions that represent a reduction in infectious burden (low or high infectious burden to uninfected, or high infectious burden to low burden) are the second group. The 'recovery' transition was defined as the intercept in the design matrix coding format. The state transition variable '6g' means that each of the six possible transition between infectious states (uninfected, low and high burden) is represented as its own group. Survival (S) variables are rows, recapture (ρ, p) variables are columns. Each colored cell in these tables represents a separate model in the respective candidate model set. Numbers within the cells represent the $QAIC_c$ value for the respective model, and cells have been colored according to $QAIC_c$ ranking (the more parsimonious the model, the lower its $QAIC_c$ value, and the closer towards the white end of the spectrum; red cells represent poorly parsimonious models). Borders around $QAIC_c$ top-ranking 6 models (depicted with white or pale yellow) cumulatively hold approximately 51% of total support within the candidate model set. Models displayed in orange and red are lower ranking based on $QAIC_c$ values.

D.2.3 MSMR Random and Sine curve set

In order to demonstrate that our most parsimonious models from the three state multistate analysis were not artifact, we also ran sets of models from two additional conditions, including a random number set (random), and a sine curve (sine) fitted to and replacing the prevalence curve. Both of these conditions were individually fitted to all six groups of state transitions ('6g'). The results below compare the top 100 of these models to the entire 3 state MSMR candidate model set (hence the reason why the 'top' AIC_c weight in the set is only 0.00114).

Table D.5. Ranking of most parsimonious models in Random and Sine curve set

Model (Random and Sine curve set)	$QAIC_c$	Delta $QAIC_c$	AIC_c Weights	Model Likelihood	Num Par	QDeviance
S(g*prev)p(g+rad)psi(6g*sine) - DMaltopt	1263.585	10.3599	0.00114	0.0056	22	1217.01
S(g+prev)p(g+rad)psi(6g*sine) - DMaltopt	1263.922	10.6967	0.00096	0.0047	20	1221.796
S(g*prev)p(g*d)psi(6g*sine) - DM	1264.334	11.1082	0.00078	0.0039	24	1213.265
S(prev)p(rh)psi(6g*sine) - DM	1264.518	11.2929	0.00071	0.0035	16	1231.155
S(prev)p(d)psi(6g*sine) - DM	1264.547	11.3216	0.0007	0.0035	16	1231.184
S(g+prev)p(d)psi(6g*sine) - DMaltopt	1264.797	11.572	0.00062	0.0031	18	1227.075
S(g+prev)p(g+rh)psi(6g*sine) - DMaltopt	1264.928	11.7028	0.00058	0.0029	20	1222.802
S(g*prev)p(d)psi(6g*sine) - DM	1265.232	12.0067	0.0005	0.0025	20	1223.106
S(prev)p(rad)psi(6g*sine) - DMaltopt	1265.309	12.0839	0.00048	0.0024	16	1231.946
S(g+prev)p(rh)psi(6g*sine) - DMaltopt	1265.61	12.3845	0.00041	0.002	18	1227.887
S(g+prev)p(g*rh)psi(6g*sine) - DMaltopt	1265.843	12.6179	0.00037	0.0018	22	1219.268
S(g+prev)p(g+d)psi(6g*sine) - DMaltopt	1265.936	12.711	0.00035	0.0017	20	1223.81
S(g*prev)p(g+d)psi(6g*sine) - DMaltopt	1266	12.7744	0.00034	0.0017	22	1219.425
S(prev)p(.)psi(6g*sine) - DM	1266.11	12.8845	0.00032	0.0016	15	1234.91

S(g+prev)p(rad)psi(6g*sine) - DMaltopt	1266.251	13.0256	0.0003	0.0015	18	1228.528
S(temp)p(d)psi(6g*sine) - DMaltopt	1266.917	13.6919	0.00022	0.0011	16	1233.554
S(g+prev)p(.)psi(6g*sine) - DM	1266.972	13.7465	0.00021	0.001	17	1231.434
S(g*prev)p(rh)psi(6g*sine) - DMaltopt	1267.008	13.7821	0.00021	0.001	20	1224.881
S(g+prev)p(g*d)psi(6g*sine) - DMaltopt	1267.027	13.8016	0.0002	0.001	22	1220.452
S(g*prev)p(g)psi(6g*sine) - DMaltopt	1267.301	14.0755	0.00018	0.0009	21	1222.956
S(g*prev)p(rad)psi(6g*sine) - DMaltopt	1267.333	14.108	0.00017	0.0008	20	1225.207
S(temp)p(rh)psi(6g*sine) - DM	1267.439	14.2133	0.00017	0.0008	16	1234.075
S(g*prev)p(g*rh)psi(6g*sine) - DMaltopt	1267.554	14.3287	0.00016	0.0008	24	1216.485
S(g+temp)p(g+rad)psi(6g*sine) - DMaltopt	1267.653	14.4278	0.00015	0.0007	20	1225.527
S(prev)p(g+rad)psi(6g*sine) - DMaltopt	1267.827	14.6016	0.00014	0.0007	18	1230.104
S(g+temp)p(d)psi(6g*sine) - DM	1267.859	14.6336	0.00013	0.0006	18	1230.136
S(g+prev)p(g*rad)psi(6g*sine) - DMaltopt	1267.863	14.6374	0.00013	0.0006	22	1221.288
S(g*prev)p(g*rad)psi(6g*sine) - DMaltopt	1267.929	14.7031	0.00013	0.0006	24	1216.86
S(prev)p(g+d)psi(6g*sine) - DMaltopt	1267.962	14.7364	0.00013	0.0006	18	1230.239
S(g*prev)p(g+rad)psi(6g*random) - DMaltopt	1268.061	14.8353	0.00012	0.0006	22	1221.486
S(g*prev)p(g+rh)psi(6g*sine) - DMaltopt	1268.061	14.8354	0.00012	0.0006	22	1221.486
S(g*prev)p(.)psi(6g*sine) - DMaltopt	1268.075	14.8498	0.00012	0.0006	19	1228.156
S(temp)p(.)psi(6g*sine) - DM	1268.152	14.9261	0.00012	0.0006	15	1236.952
S(temp)p(rad)psi(6g*sine) - DM	1268.385	15.1595	0.0001	0.0005	16	1235.022
S(g+temp)p(rh)psi(6g*sine) - DMaltopt	1269.124	15.8987	0.00007	0.0003	18	1231.401
S(g*temp)p(g+rh)psi(6g*sine) - DMaltopt	1269.226	16.0001	0.00007	0.0003	22	1222.651
S(prev)p(g*d)psi(6g*sine) - DMaltopt	1269.251	16.0254	0.00007	0.0003	20	1227.124
S(g+temp)p(.)psi(6g*sine) - DM	1269.406	16.1809	0.00006	0.0003	17	1233.869
S(g*temp)p(d)psi(6g*sine) - DMaltopt	1269.427	16.2017	0.00006	0.0003	20	1227.301
S(g+temp)p(rad)psi(6g*sine) - DM	1269.545	16.3197	0.00006	0.0003	18	1231.822
S(g+temp)p(g+d)psi(6g*sine) - DMaltopt	1269.571	16.3451	0.00006	0.0003	20	1227.444
S(prev)p(g)psi(6g*sine) - DMaltopt	1270.049	16.8237	0.00004	0.0002	17	1234.511
S(g+temp)p(g*d)psi(6g*sine) - DMaltopt	1270.477	17.2515	0.00004	0.0002	22	1223.902
S(g+prev)p(g+rh)psi(6g*random) - DM	1270.486	17.261	0.00004	0.0002	20	1228.36
S(g*temp)p(rh)psi(6g*sine) - DMaltopt	1270.671	17.4452	0.00003	0.0001	20	1228.544
S(g*temp)p(g)psi(6g*sine) - DMaltopt	1270.723	17.4975	0.00003	0.0001	21	1226.378
S(prev)p(g+rh)psi(6g*sine) - DMaltopt	1270.842	17.6169	0.00003	0.0001	18	1233.119
S(g*temp)p(g+rad)psi(6g*sine) - DMaltopt	1270.854	17.6284	0.00003	0.0001	22	1224.279
S(temp)p(g+rad)psi(6g*sine) - DMaltopt	1270.869	17.6433	0.00003	0.0001	18	1233.146
S(temp)p(g+rh)psi(6g*sine) - DMaltopt	1270.885	17.6596	0.00003	0.0001	18	1233.162
S(temp)p(g+d)psi(6g*sine) - DMaltopt	1270.996	17.7706	0.00003	0.0001	18	1233.273
S(g*temp)p(rad)psi(6g*sine) - DMaltopt	1271.352	18.1267	0.00002	0.0001	20	1229.226
S(temp)p(g)psi(6g*sine) - DMaltopt	1271.606	18.3801	0.00002	0.0001	17	1236.068
S(g+temp)p(g+rh)psi(6g*sine) - DM	1271.816	18.5904	0.00002	0.0001	20	1229.689
S(g*temp)p(.)psi(6g*sine) - DMaltopt	1271.94	18.7141	0.00002	0.0001	19	1232.02
S(prev)p(g*rad)psi(6g*sine) - DMaltopt	1271.953	18.7273	0.00002	0.0001	20	1229.826
S(g+prev)p(g)psi(6g*sine) - DM	1272.53	19.305	0.00001	0	19	1232.611
S(temp)p(g*rh)psi(6g*sine) - DMaltopt	1272.836	19.6101	0.00001	0	20	1230.709
S(temp)p(g*d)psi(6g*sine) - DMaltopt	1273.048	19.8222	0.00001	0	20	1230.921
S(g+temp)p(g)psi(6g*sine) - DMaltopt	1273.125	19.8998	0.00001	0	19	1233.206
S(prev)p(d)psi(6g*random) - DMaltopt	1273.227	20.0017	0.00001	0	16	1239.864
S(prev)p(rh)psi(6g*random) - DMaltopt	1273.239	20.014	0.00001	0	16	1239.876
S(g+prev)p(g+d)psi(6g*random) - DMaltopt	1273.395	20.1698	0.00001	0	20	1231.269
S(g*temp)p(g*rad)psi(6g*sine) - DMaltopt	1274.05	20.8246	0.00001	0	24	1222.981

S(g*temp)p(g+d)psi(6g*sine) - DMaltopt	1274.298	21.0729	0.00001	0	22	1227.723
S(prev)p(rad)psi(6g*random) - DMaltopt	1274.316	21.0907	0.00001	0	16	1240.953
S(prev)p(.)psi(6g*random) - DMaltopt	1274.374	21.1486	0.00001	0	15	1243.174
S(prev)p(g+d)psi(6g*random) - DMaltopt	1274.402	21.1768	0.00001	0	18	1236.679
S(g+prev)p(d)psi(6g*random) - DMaltopt	1274.418	21.1924	0.00001	0	18	1236.695
S(prev)p(g+rh)psi(6g*random) - DMaltopt	1274.598	21.3729	0	0	18	1236.875
S(g+prev)p(rh)psi(6g*random) - DMaltopt	1274.646	21.4204	0	0	18	1236.923
S(prev)p(g+rad)psi(6g*random) - DM	1274.692	21.4661	0	0	18	1236.969
S(temp)p(g*rad)psi(6g*sine) - DMaltopt	1274.715	21.4894	0	0	20	1232.588
S(g*prev)p(.)psi(6g*random) - DM	1275.22	21.9945	0	0	19	1235.301
S(temp)p(d)psi(6g*random) - DMaltopt	1275.278	22.0528	0	0	16	1241.915
S(g+prev)p(rad)psi(6g*random) - DMaltopt	1275.329	22.1036	0	0	18	1237.606
S(g*prev)p(d)psi(6g*random) - DMaltopt	1275.332	22.1061	0	0	20	1233.205
S(g+temp)p(g*rh)psi(6g*random) - DMaltopt	1275.347	22.1213	0	0	22	1228.772
S(g+temp)p(g*rad)psi(6g*random) - DMaltopt	1275.527	22.3013	0	0	22	1228.952
S(g*prev)p(rh)psi(6g*random) - DMaltopt	1275.971	22.746	0	0	20	1233.845
S(temp)p(g+d)psi(6g*random) - DMaltopt	1276.131	22.9056	0	0	18	1238.408
S(g*prev)p(rad)psi(6g*random) - DMaltopt	1276.193	22.9671	0	0	20	1234.066
S(prev)p(g)psi(6g*random) - DMaltopt	1276.549	23.3239	0	0	17	1241.012
S(g+prev)p(.)psi(6g*random) - DMaltopt	1276.61	23.3847	0	0	17	1241.072
S(g+temp)p(g*rad)psi(6g*sine) - DMaltopt	1276.8	23.5743	0	0	22	1230.225
S(g*prev)p(.)psi(6g*random) - DMaltopt	1277.037	23.8117	0	0	19	1237.118
S(temp)p(rad)psi(6g*random) - DMaltopt	1277.115	23.8897	0	0	16	1243.752
S(g+prev)p(g*d)psi(6g*random) - DMaltopt	1277.136	23.9106	0	0	22	1230.561
S(g+temp)p(d)psi(6g*random) - DMaltopt	1277.241	24.016	0	0	18	1239.519
S(g+temp)p(g*rh)psi(6g*sine) - DMaltopt	1277.261	24.0357	0	0	22	1230.686
S(prev)p(g*rad)psi(6g*random) - DMaltopt	1277.277	24.0516	0	0	20	1235.15
S(temp)p(g+rh)psi(6g*random) - DMaltopt	1277.342	24.1168	0	0	18	1239.619
S(g*prev)p(g+rh)psi(6g*random) - DMaltopt	1277.41	24.1846	0	0	22	1230.835
S(temp)p(.)psi(6g*random) - DMaltopt	1277.43	24.2046	0	0	15	1246.23
S(g*prev)p(g+d)psi(6g*random) - DMaltopt	1277.457	24.2319	0	0	22	1230.882
S(g)p(g+rh)psi(6g*sine) - DMaltopt	1277.573	24.348	0	0	19	1237.654
S(g+prev)p(g*rad)psi(6g*random) - DMaltopt	1277.715	24.4899	0	0	22	1231.14
S(g+temp)p(g+rh)psi(6g*random) - DMaltopt	1277.756	24.5309	0	0	20	1235.63
S(g*prev)p(g)psi(6g*random) - DMaltopt	1277.764	24.5381	0	0	21	1233.418
S(g+prev)p(g+rad)psi(6g*random) - DMaltopt	1277.817	24.5915	0	0	20	1235.69
…						

Table D.6. AIC value and relative variable importance for the Random and Sine curve set

Psi(6g*random)

S(rows)p(columns)	.	g	rh	g+rh	g*rh	rad	g+rad	g*rad	d	g+d	g*d
.	1297.4	1301.1	1287.8	1289.6	1291.9	1296.2	1296.1	1299.6	1289.5	1292.6	1296.8
g	1297.7	1295.7	1288.4	1284.1	1284.2	1299.2	1283.8	1287.3	1290.5	1290.1	1289.2
prev	1274.4	1276.5	1273.2	1274.6	1278.2	1274.3	1274.7	1277.3	1273.2	1274.4	1278.5
g+prev	1276.6	1278.3	1274.6	1270.5	1277.9	1275.3	1277.8	1277.7	1274.4	1273.4	1277.1
g*prev	1277.0	1277.8	1276.0	1277.4	1279.2	1276.2	1268.1	1280.8	1275.3	1277.5	1278.5
temp	1277.4	1279.6	1277.9	1277.3	1281.0	1277.1	1280.4	1280.9	1275.3	1276.1	1279.6
g+temp	1279.7	1280.9	1278.8	1277.8	1275.3	1279.5	1280.8	1275.5	1277.2	1278.1	1279.2
g*temp	1281.3	1283.1	1279.9	1280.4	1286.8	1281.1	1282.5	1283.7	1279.2	1280.9	1280.0

Psi(6g*sine)

S(rows)p(columns)	.	g	rh	g+rh	g*rh	rad	g+rad	g*rad	d	g+d	g*d
.	1288.9	1288.7	1278.9	1280.1	1280.6	1288.4	1281.6	1282.8	1281.3	1283.0	1283.4
g	1285.7	1283.9	1278.7	1277.6	1281.1	1286.4	1281.4	1282.4	1279.8	1280.7	1282.9
prev	1266.1	1270.0	1264.5	1270.8	1279.7	1265.3	1267.8	1272.0	1264.5	1268.0	1269.3
g+prev	1267.0	1272.5	1265.6	1264.9	1265.8	1266.3	1263.9	1267.9	1264.8	1265.9	1267.0
g*prev	1268.1	1267.3	1267.0	1268.1	1267.6	1267.3	1263.6	1267.9	1265.2	1266.0	1264.3
temp	1268.2	1271.6	1267.4	1270.9	1272.8	1268.4	1270.9	1274.7	1266.9	1271.0	1273.0
g+temp	1269.4	1273.1	1269.1	1271.8	1277.3	1269.5	1267.7	1276.8	1267.9	1269.6	1270.5
g*temp	1271.9	1270.7	1270.7	1269.2	1278.2	1271.4	1270.9	1274.1	1269.4	1274.3	1278.8

These two tables (Table D.6) represent the different variables used to constrain the state transition probability parameter (ψ, psi) similar to above, but in this case, the two conditions used were firstly a random number set (random), and secondly, a sine curve (sine) fitted to and replacing the prevalence curve. Both of these conditions were individually fitted to all six groups of state transitions ('6g'). Survival (S) variables are rows, recapture (ρ, p) variables are columns. Each colored cell in these tables represents a separate model (these models were not included in the final candidate model set used to estimate parameter probabilities). Numbers within the cells represent the $QAIC_c$ value for the respective model (from amongst the entire 3 state MSMR set), and cells have been colored according to $QAIC_c$ ranking (the more parsimonious the model, the lower its $QAIC_c$ value, and the closer towards the white end of the spectrum; red cells represent poorly parsimonious models). Borders have been placed around $QAIC_c$ top-ranking 6 models (depicted with white or pale yellow). Models displayed in orange and red are lower ranking based on $QAIC_c$ values.

D.3 Simulation Results

The three simulation scenarios performed consistently with our expectations. Low annual survival probabilities (as discussed in Phillott et al., 2013) led to rapid reduction in population size in the scenario where recruitment was not included as a source variable (Fig. D.1a). In the second scenario, where recruitment values were defined to maintain stable population size, clearly cyclical population dynamics emerged as a direct result of seasonal state transition dynamics (described above; Fig. D.1b). In the third scenario, total population size exhibited annual fluctuations consistent with the use of model-averaged recruitment estimates (Phillott et al., 2013), and the performance of this scenario is thus most likely to represent real-world population dynamics for our *L. rheocola* system (Fig. D.1c). We hypothesize that size peaks are associated with recruitment of newly metamorphosed individuals into the adult population, and the influx of transient immigrant individuals during the breeding season which occurs from May-August (Phillott et al., 2013). Altering starting numbers of individuals in each state did not affect population size outcomes of the simulation, and variations in state size trajectory were negligible by six months of iterations in each scenario (Fig. D.1 represents starting values of A = 900, B = 50 and C = 50 individuals). Simulations are illustrated to start in November because the model-averaged parameter

estimates for survival are monthly mean probabilities for the interval between trip sessions, and the initial trip was conducted in November 2005 (Fig. D.1).

Figure D.1. Outcomes from the demographic simulation without recruitment (a); with recruitment to force population stability (b); with recruitment as model-averaged estimates from Phillott et al. (2013) (c).

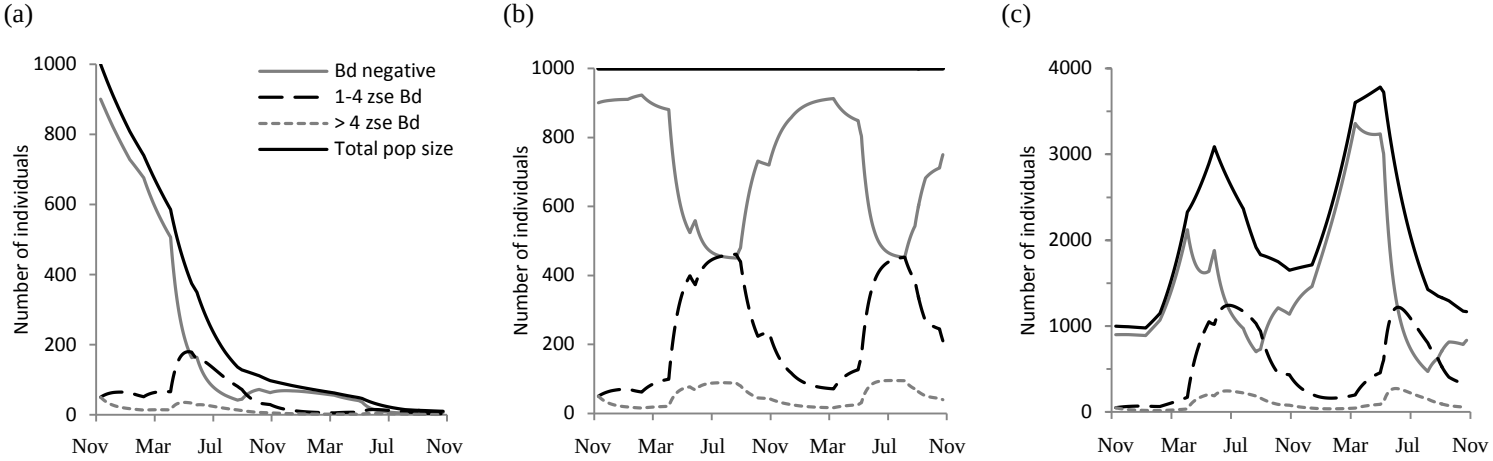

Figure D.2. Model averaged monthly state transition probabilities depicted as stacked area charts for transitions from each of the three states, from state A (a), state B (b), and state C (c).

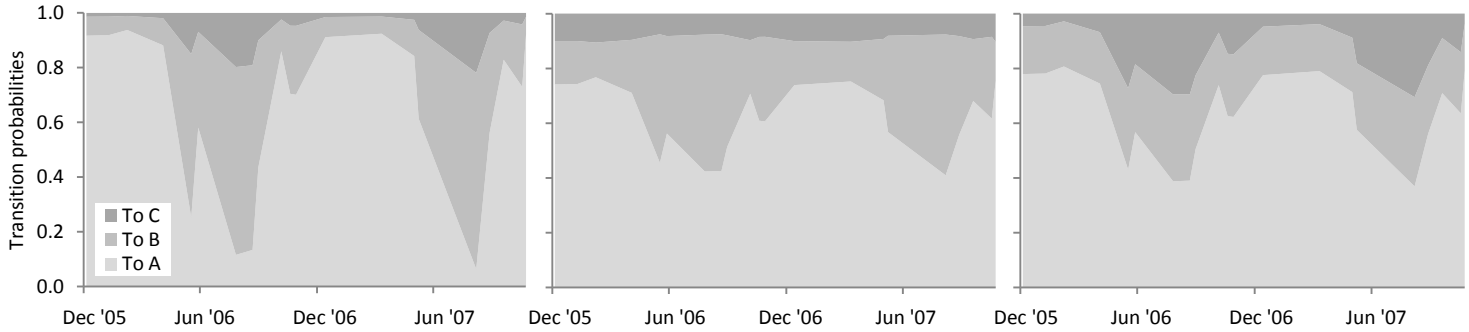

(a) From State A (uninfected) (b) From State B (low burden) (c) From State C (higher burden)

D.4 Transition probabilities as a function of state subpopulation size

The observed high recovery transition probability estimates compared with infection transitions (main manuscript text Figs. 3.8c and 3.8d) are the result of low to moderate Bd infection prevalence (Phillott et al., 2013), and because transition probabilities are a function of the size of the subpopulation from which the individuals move. To illustrate this phenomenon, consider a population with 100 frogs, 10 of which are currently infected. If we sample the population again two weeks later, and if five of those infected frogs have recovered, then recovery probability is 50%. If during that period two infected frogs die and a further seven frogs become infected, then in that time interval, the prevalence remains the same at 10%, the survival of infected frogs is 80%, and the probability of becoming infected is 7/90 = 8% (despite very similar numbers of frogs both recovering and becoming infected as observed from our summary statistics).

APPENDIX E: Capture-Mark-Recapture methodological review

E.1 Introduction

This appendix contains a detailed methodological review justifying the approach taken for the capture-mark-recapture analyses reported in Chapter 3 of this thesis.

The full references for the published paper and prepared manuscript are:

Phillott, A. D., **Grogan, L. F.**, Cashins, S. D., McDonald, K. R., Berger, L., Skerratt, L. F. (2013) Chytridiomycosis and seasonal mortality of tropical stream-associated frogs 15 years after introduction of *Batrachochytrium dendrobatidis*. Conservation Biology 27:1058-1068.

Grogan, L. F., Phillott, A. D., Scheele, B. C., Berger, L., Cashins, S. D., Bell, S. C., Puschendorf, R., Skerratt, L. F. (in prep) Parasite aggregation and its implications for the microparasitic disease, endemic chytridiomycosis.

E.2 Overview of capture-mark-recapture methodologies and best practices

Capture-Mark-Recapture (CMR) modeling aims to find good approximating models to empirical data as the basis for statistical inference. CMR analyses assume that the chance of encountering an individual on a particular occasion is a product of one or more apparent probabilities (survival φ, recapture ρ, population growth λ, and recruitment f) which may be influenced by predictor variables (such as infection status, environmental, linear or individual covariates).

Capture-mark-recapture analyses involve a number of steps including a) defining biological questions, *a priori* hypotheses and estimable parameters, b) determining biologically plausible predictor variables, c) goodness of fit testing based on general mark-recapture assumptions for the most parameterized models to determine an overdispersion parameter $\hat{c}$, d) data preparation, e) specification of candidate model sets, f) selection for parsimonious models via small sample size and overdispersion-corrected Quasi-Akaike's Information Criterion ($QAIC_c$), g) multi-model inference via model averaging to determine h) parameter and unconditional precision estimates (95% Confidence Intervals) as well as i) relative factor importance based on Akaike weights, j) the evidence ratios of support between models for inference about certain hypotheses, and k) the model averaged effect sizes of infection status groupings where applicable.

This outline was prompted by the recent methodological controversy especially surrounding the specification of candidate model sets, the history of frequent reporting problems with mark-recapture studies (Lebreton et al., 1992; Lindberg, 2012), as well as the new and expanding context of studying wildlife disease using capture-mark-recapture (Cooch et al., 2012). The following sections will outline current controversies and best practice approaches for CMR analyses.

E.2.1 Confirmatory versus exploratory analyses

The terms 'confirmatory' and 'exploratory' have been widely used with reference to the type of analytical approach employed for investigating ecological data. A 'confirmatory' approach has been advocated by information-theoretic Akaike's Information Criterion (IT-AIC) proponents such as Burnham and Anderson (2002), and is typically taken to mean hypothetico-deductive inference (hypothesis testing) for prediction or extrapolation, whereas 'exploratory' data analysis (EDA) involves identification of patterns within a data set and hypothesis generation (Symonds and Moussalli, 2011). Despite its proponents (Grueber et al., 2011; Stephens et al., 2005), EDA is typically considered in a derogatory light as non-rigorous, poorly replicable, and subject to inference of spurious results according to Freedman's Paradox (Freedman, 1983). Both approaches are necessary, however, as explained by Hegyi and Garamszegi (2011) and Symonds and Moussalli (2011) for the generation and testing of biological hypotheses in complex ecological systems where *a priori* evidence is sparse and predictors are often correlated. The question remains as to whether IT-AIC approaches should be restricted to the confirmatory stage due to the propensity for post hoc model creation (Burnham and Anderson, 2002; Grueber et al., 2011; Guthery et al., 2005). We reject this view on the grounds of the numerous advantages conferred by the IT-AIC approach for exploratory analysis (for example, multi model inference; Stephens et al., 2007). The 'exploratory' approach may pertain to two quite different aspects of data analysis according to the context in which it is invoked, however. Firstly, studies have been criticized as exploratory if they include biologically implausible variables in the explanatory variable set (see Appendices A and C for discussion of our inclusion of predictor variables; Dochtermann and Jenkins, 2011; Stephens et al., 2007). Secondly, 'exploratory' may refer to the model specification approach; most often this refers to the use of a large number of models to describe patterns from a study of relatively small sample size (Lukacs et al., 2007).

E.2.2 Specification of candidate model sets

The candidate model set refers to the collection of models that will be investigated, and should include only biologically plausible combinations of putative predictor variables (McCrea and Morgan, 2011). There is considerable contention in the literature regarding the appropriate method for specifying candidate model sets (Burnham and Anderson, 2002; Dochtermann and Jenkins, 2011; Doherty et al., 2012; Hegyi and Garamszegi, 2011; Symonds and Moussalli, 2011). This is a critical issue because both the nature and number of models being tested plays an important role in resulting model selection and parameter estimation. Clearly, the higher the number of parameters being estimated (for example, the extension of CJS models to multistate analysis increases the number of simultaneous parameters to three; S, ρ and, ψ), the more variable combinations being tested, and the addition of interaction terms will greatly increase the number of potential models for a given system (Hegyi and Garamszegi, 2011).

The main controversy of model specification surrounds the problem of model selection bias and Freedman's paradox (Burnham and Anderson, 2002; Freedman, 1983; Zucchini, 2000). Model selection bias occurs because firstly we must *estimate* from the data which is the best approximating model for the data (never knowing 'full truth'), and secondly, depending on model specification methods, this 'best selected model' may appear to fit the data better than it actually does due to residual variance being underestimated (Zucchini, 2000). Indeed, when fitting models with many explanatory variables, particularly if they are weak or unrelated to the response variable, Freedman (1983) showed that selection bias will occur leading to apparent 'significance' of these unrelated variables in best approximating models. This problem is often quoted as occurring where either the number of variables (Lukacs et al., 2010; Mundry, 2011), or the number of models (Anderson and Burnham, 2002; Burnham et al., 2011; Guthery et al., 2005; Lukacs et al., 2010) being tested exceeds the effective sample size.

Several different model specification approaches have been used in the last couple of decades to minimize the effect of selection bias and increase the ease of analysis, although none are ideal and therein lies the contention (Dochtermann and Jenkins, 2011; Stephens et al., 2007; Symonds and Moussalli, 2011). Ad hoc methods for reducing the size of the candidate model set include stepwise, arbitrary selection or *a priori* elimination of predictor variables. Stepwise approaches have long been used in regression analyses, and numerous different forms have been developed including for instance, forwards selection and backwards

elimination (sequentially eliminating variables from a fully parameterized global model; Hegyi and Garamszegi, 2011). There is mounting criticism of stepwise approaches, however, and the shortcomings of these methods have been summarized by several groups (Burnham and Anderson, 2002; Grueber et al., 2011; Hegyi and Garamszegi, 2011; Lukacs et al., 2010; Mundry, 2011). Shortcomings include model uncertainty (different methods give different solutions, small changes in data can grossly change final model, variances are deflated, and resulting model set is poorly representative of whole model space because only some of the possible models are fit; Anderson and Burnham, 2002; Lukacs et al., 2010), uncertainty surrounding importance of variables (predictor variables cannot be reliably ranked by importance, stepwise methods promote nuisance variables and often exclude important predictors), and shortcomings associated with arbitrary thresholds, α levels, and multiple testing problems where null hypothesis significance testing (NHST) is used (Lukacs et al., 2010). These issues are particularly of concern with small data sets and interrelated predictors (as expected in ecological studies and discussed above; Freckleton, 2011). A recent example of a stepwise approach utilizing NHST score tests in the context of multistate models is presented by McCrea and Morgan (2011). Stepwise approaches have also been used in the context of IT-AIC for mark-recapture analyses whereby one parameter (for example, survival) is fixed first, followed by the others (an approach recommended by Lebreton et al., 1992 and utilized frequently thereafter; Murray et al., 2009; Pilliod et al., 2010). Importantly, this approach assumes that the parameter initially fixed is the most inherently variable (once it is fixed it imparts unaccounted variation to the remaining unconstrained parameters inflating estimated process variance for parameters investigated later in the stepwise process), and this is difficult to assume without prior knowledge. For example, all models with constant recapture ($\rho_.$) may not be more parsimonious than all models with time-varying recapture (ρ_t) despite an initially favourable comparison of the models $\varphi_.\rho_.$ with $\varphi_.\rho_t$. This strategy is also subject to the shortcomings of stepwise approaches in general, hence its use with IT-AIC is similarly not recommended (Burnham et al., 2011; Doherty et al., 2012; Hegyi and Garamszegi, 2011; Mundry, 2011).

Where stepwise approaches are not used, but a small candidate set is obtained, either an extremely limited set of *a priori* explanatory variables must be employed, or the model specification method must be somewhat arbitrary in selecting models to test, leading inevitably to bias and model selection uncertainty (Guthery et al., 2005; Hegyi and Garamszegi, 2011; Stephens et al., 2005). A small data set where a single 'best' model has 95% of the support of the data may misleadingly imply that this model is close to 'full truth', a

phenomenon described more appropriately by Guthery et al. (2005) as the discovery of a 'best' model "in a set of outrageously bad models". To illustrate how limited an *a priori* set of variables must be to allow all possible combinations still retaining a small candidate model set (see Dochtermann and Jenkins, 2011; Hegyi and Garamszegi, 2011), four variables in estimation of one parameter (for example, survival probability) leads to 65 possible combinations considering only two-way interactions. When simultaneously estimating survival and recapture probability (two parameters), this value is squared. Burnham and Anderson (2002) and Lukacs et al. (2007) stress the importance of 'hard thinking' in eliminating less plausible variables and subset models, but Hegyi and Garamszegi (2011) and Guthery et al. (2005) point out that it is rare that we have sufficient information to exclude or include variables and models, in which case reduction of the candidate model set becomes somewhat inconsistent ('tantamount to the use of "silly nulls"'; Stephens et al., 2007).

An alternative to ad hoc reduction of the candidate model set is the all subsets approach, whereby all biologically plausible variations of a set of putative explanatory variables are tested sequentially (Doherty et al., 2012; Grueber et al., 2011; Hegyi and Garamszegi, 2011; Lukacs et al., 2010; Stephens et al., 2007; Symonds and Moussalli, 2011). There are two main criticisms of this approach. Firstly as touched on above, testing all possible combinations of predictor variables can lead to an overwhelming number of models being tested (as illustrated above), potentially leading to selection bias, spurious inferences and the fitting of biologically implausible models (Anderson and Burnham, 2002; Burnham and Anderson, 2002; Freedman, 1983; Lukacs et al., 2010). Secondly, generating a large number of models can make analysis logistically burdensome due to time, computing power and expertise required (Doherty et al., 2012; Lukacs et al., 2010).

Proponents of the all subsets approach recommend its use particularly for exploratory analyses to counter the arbitrary nature of the ad hoc approaches (Hegyi and Garamszegi, 2011), to improve predictive properties (Symonds and Moussalli, 2011), and to reliably identify weak and strong variable effects and determine relative importance of predictor variables via multi model inference using model averaging providing estimates of model uncertainty (Doherty et al., 2012; Lukacs et al., 2010; Stephens et al., 2007). Doherty et al. (2012) uses simulation to compare ad hoc and all subsets approaches and their implications for parameter estimates and variable selection, concluding that ad hoc approaches were less robust. Hegyi and Garamszegi (2011) and Mundry (2011) additionally suggest two further improvements to overcome model selection bias and improve predictive qualities; replication

(repeated independent analysis) and bootstrap resampling. Moreover, refuting criticisms associated with model selection bias, Stephens et al. (2007) highlights that most statistical procedures are capable of fitting biologically implausible models in the absence of due *a priori* consideration. Hegyi and Garamszegi (2011) unify these disparate views by claiming that 'restricted candidate sets are not a requirement in IT exercises but a suggestion that may improve our inferences in a limited number of cases'. Indeed, K.P. Burnham, a previous critic of 'unthoughtful' all subsets approaches (Burnham and Anderson, 2002) is an author on Doherty et al. (2012) which states 'in terms of variable selection [...] model sets based on ad hoc strategies did not perform as well as those based on all combinations, as less important variables often had higher weights with the former than with the all possible combinations strategy'. Whichever approach taken, and despite pitfalls of differing model specification strategies, Mundry (2011) recommends that it is crucial the strategy used should be 'well-founded, carefully developed and clearly stated'.

E.2.3 Model selection, multi-model inference (MMI) and analytical outputs

E.2.3.1 Model selection

Model selection is the choice of a model (or models) of optimal complexity given the data, from which to make formal inference, and it pertains to the principle of parsimony and the compromise between model bias and variance (Burnham and Anderson, 2002). Model selection has been a controversial area in the literature for decades, and numerous different methods have been utilized including ad hoc approaches (where only one model is used, or selection is data independent) and empirical strategies such as stepwise approaches (for example stepwise regression, see discussion above), cross-validation and bootstrapping (Efron, 1979; Stone, 1974). With the recent expansion of information theoretic (IT) and Bayesian methods, the fundamental search for the ideal ranking criterion (optimally balancing bias and variance) has flourished, resulting in development of numerous information criteria such as Akaike's Information Criterion (AIC;Akaike, 1973), Bayesian Information Criterion (BIC; Link and Barker, 2006; Schwarz, 1978) and Takeuchi's Information Criterion (TIC; Takeuchi, 1976). AIC is the criterion to have received most widespread attention (Hegyi and Garamszegi, 2011), particularly in the ecological sciences due firstly to its strong theoretical underpinnings and resultant inferential properties, and secondly due to the advocacy and accessibility of the seminal text, Burnham and Anderson (2002).

E.2.3.2 Akaike's Information Criterion (AIC)

The **AIC measure** is not one of 'significance', but rather a comparative estimate of the parsimony of the models in question with the unknown and infinitely complex 'full reality'. $AIC = -2log\left(\mathcal{L}(\hat{\theta}|y)\right) + 2K$ and is an estimator of the *fundamental quantity* of the Kullback-Leibler discrepancy (Kullback and Leibler, 1951) based on Fisher's maximized log-likelihood which contains the penalty term *+2K* to account for the increased bias with an increase in parameters (*K*) usually associated with reduced model deviance (Burnham and Anderson, 2002). Unlike multiple comparisons in classical null hypothesis testing necessitating use of conservative 'significance' measures such as the Bonferroni correction, information theoretic methods for ranking model parsimony such as AIC do not suffer from multiple testing problems. It is thus correct to use AIC to make formal inference from many models (Burnham et al., 2011), although it is incorrect to compare AIC values for models between different data sets (despite identical model structure). Subsequent to its development, several further modifications were made, notably to correct for small sample size (AICc; Hurvich and Tsai, 1989), and to incorporate the overdispersion parameter $\hat{c}$ (Quasi-AICc or QAICc; Lebreton et al., 1992; see Grueber et al., 2011 for summary equations). It is recommended that AICc be used where the effective sample size is less than 40 (Burnham and Anderson, 2002). AICc is asymptotically equivalent to AIC and can be used for studies of any sample size (Lukacs et al., 2010), although there is contention regarding its performance under all scenarios (Richards, 2005). While there are a couple of methods for modeling overdispersion, additive (Browne et al., 2005) and multiplicative; the latter is in wide use as the approach employed in QAIC (Grueber et al., 2011). The primary criticism of the AIC and derivative criteria is a propensity for overfitting, leading to overly complex models with numerous parameters (Hegyi and Garamszegi, 2011; Link and Barker, 2006). Additionally, AIC is not *consistent* in that as sample size tends to infinity, probability of selecting full truth does not necessarily tend to 1 (Yang, 2005). Alternatively, when full truth is finite-dimensional (and the generating model exists in the candidate set), BIC which aims to maximize posterior model probability, has been proposed to perform better (Burnham and Anderson, 2002; Link and Barker, 2006; Yang, 2005). Given studies performed within infinite-dimensional ecological space, where the purpose of model selection is to estimate predictors with minimal error rather than select a single correct model, we favour the use of AIC (and hence QAICc) over BIC or other criteria (Burnham and Anderson, 2002; Burnham and Anderson, 2004; Cubaynes et al., 2012).

E.2.3.3 Model selection bias and model averaging

Model selection bias (as introduced above) is also an important consideration when choosing models for inference. Multi-model inference (specifically model averaging) has been proven to consistently reduce selection bias compared with single model approaches; reducing spurious results, improving stability of parameter estimates (lowering bias) and providing nominal level confidence interval coverage (Burnham and Anderson, 2002; Burnham and Anderson, 2004; Lukacs et al., 2010). **Model averaging** improves inference where model uncertainty is high, which may occur particularly in complex ecological systems, where the candidate model set is large (relevant for the use of all subsets approaches; Doherty et al., 2012), predictor variables have weak and potentially correlated effects, and sample size is relatively small (Lukacs et al., 2010). Model averaging involves obtaining parameter estimates from a group of models rather than just one, and weighting these estimates according to the Akaike weight (w_i for model i) of each respective model. Akaike weights (see equation below) quantify the relative likelihood of each model given the data and conditional on a particular candidate set (Burnham and Anderson, 2002; Lukacs et al., 2007). They do not represent absolute model probabilities which is a common misconception where small model sets are used.

$$w_i = \frac{exp\left(-\frac{1}{2}\Delta_i\right)}{\sum_{r=1}^{R} exp\left(-\frac{1}{2}\Delta_r\right)}$$

where Δ_i is the difference between AIC values for the best model and model i in a set of R models. With regards to problems involving regression (as relevant here), there are two forms of model averaging; the 'natural average' involves only models in which the predictor variable/s of interest are present, whereas the 'zero method' refers to inference from all models, substituting a zero value where a predictor variable is absent from a particular model (Burnham and Anderson, 2002; Grueber et al., 2011; Nakagawa and Freckleton, 2011). Burnham and Anderson (2002), Hegyi and Garamszegi (2011) and Nakagawa and Freckleton (2011) recommend the latter, inference based on all models; and indeed substitution of zero for absent variables has the effect of shrinking the respective model parameter estimate towards zero which reduces model selection bias associated with spuriously included variables (Lukacs et al., 2010). Reporting precision of model averaged estimates involves two variance components, the conditional sampling variance (weighted average of the variance of each model) and the variation in estimates across models (accounting for model selection uncertainty); together they comprise the unconditional variance which is reported in Chapter 3 (Anderson and Burnham, 2002; Burnham and Anderson, 2002; Lukacs et al., 2010).

E.2.3.4 Post-hoc restriction of the candidate model set

For the purposes of multi-model inference and hypothesis testing, some groups have advocated **post hoc restriction of the candidate model set** based on either 'rules of thumb' from ΔAIC (Bolker et al., 2009; Burnham and Anderson, 2002; Burnham et al., 2011; Guthery et al., 2005; Richards, 2008; Richards et al., 2011; Symonds and Moussalli, 2011) or a 'confidence set' of cumulative Akaike weights in an attempt to minimise 'false positives' (or artificial inflation of variable importance; Mundry, 2011; Symonds and Moussalli, 2011). Rules of thumb tend to be subjective, and suggestions have varied through the years from including only models with $\Delta AIC < 2$ (Burnham and Anderson, 2002) to $\Delta AIC < 10$ (Bolker et al., 2009), to $\Delta AIC < 20$ (Burnham et al., 2011). In a NHST twist, the 'confidence set' is often chosen to include models whose Akaike weights sum to 0.95 (hence 95% of support and the somewhat arbitrary 0.05 α level; Mundry, 2011). An alternative approach removes overparameterized models where a nested version has lower ΔAIC (Richards et al., 2011), although this technique has not yet been widely applied (Symonds and Moussalli, 2011). Hegyi and Garamszegi (2011) argue that restricting the *a priori* candidate set introduces additional uncertainty based on inconsistent model set delimitation, particularly if the cutoff is varied according to whether the null model, or a variable of interest are present (Grueber et al., 2011; Mundry, 2011). Since model averaging over the entire candidate set leads to shrinkage of potentially spurious variables, and low weighting of estimates from redundant models, there appears little justification for post hoc candidate set reduction (Anderson and Burnham, 2002; Hegyi and Garamszegi, 2011).

E.2.3.5 Relative importance of variables

An additional benefit of the all subsets approach is the ability to determine **relative importance of different variables** using model Akaike weights summed across the entire candidate set, rather than relying on variables present in a single 'best' model, an approach of particular concern where there is high model selection uncertainty (Burnham and Anderson, 2002). This method utilizes both the number of models and the weight of those models in which a particular variable is present (Burnham and Anderson, 2002; Murray and Conner, 2009). Determining relative variable importance is biased with reduced candidate sets because the different variables must be equally represented throughout the set, which is generally not the case, particularly where ad hoc stepwise approaches are used (Burnham and Anderson, 2002). Murray and Conner (2009) compare the use of several techniques with simulation, and criticizes the use of Akaike weights for quantifying variable importance, particularly in the case of spurious variables and partial correlations. Doherty et al. (2012)

highlights, however their use of an unrealistic infinite sample size, whereby the Akaike weights method performs poorly by defaulting all variables with any relationship to the response parameter to a likelihood of one, hence a relative importance of $\frac{1}{\#\ of\ variables}$. This is an area of active investigation, however we consider the use of Akaike weights to be appropriate for determining relative variable importance in finite samples given the current evidence (Doherty et al., 2012).

E.2.3.6 Evidence ratios

Evidence ratios allow the comparative quantification of the support for one model over another model in the candidate set and are hence useful for testing hypotheses associated with relative likelihoods (where NHST significance thresholds are inappropriate in the context of IT-AIC; Burnham and Anderson, 2002; Lukacs et al., 2007). Lukacs et al. (2007) provide a useful 'rule of thumb' table for interpreting evidence ratios, for instance where a ratio of 1-10 indicates limited support, and > 100 indicates strong support. Strength of evidence is ultimately open to interpretation, and rules of thumb are just that (Anderson and Burnham, 2002). Confusion often arises, however, when there is more than one possible combination of models (and thus more than one evidence ratio result) related to a specific hypothesis. This occurs because we test more than one parameter simultaneously (for instance, φ and ρ), and parameter constraints lead to differing distribution of variance residuals between parameters. An example leading into this was provided above in discussion of stepwise model specification approaches. When testing whether temporal variation in recapture probability is important (as compared with constant recapture), an evidence ratio comparing $\varphi_{.}\rho_{.}$ with $\varphi_{.}\rho_{t}$ may not be equivalent to one comparing $\varphi_{t}\rho_{.}$ with $\varphi_{t}\rho_{t}$, even though both comparisons theoretically test the same hypothesis. Where this problem occurs it has been recommended not to constrain parameters that are not of immediate interest (use φ_{t} in this case). A commonly employed, but unrecommended approach (see Anderson et al., 2001; Burnham and Anderson, 2002; Burnham et al., 2011) is to rank models with AIC then 'significance test' them with likelihood ratio tests (NHST).

E.2.3.7 Effect size

The term **'effect size'** is generally used to denote a comparison (a subtractive difference, although both estimates should be reported) in estimates of the respective parameter between the levels of a grouping variable (group effect) within a model (for example, effect size of Bd infection status on survival), or between the presence and absence of a variable between two models (effect of the variable; Burnham and Anderson, 2002). Model averaged effect sizes

can alternatively be reported for both group and variable comparisons, and represent weighted average comparisons using Akaike weights over the candidate model set as above (Lukacs et al., 2007). In Chapter 3 of this thesis we use model averaged effect sizes due to model selection uncertainty.

APPENDIX F: Lva clinical manuscript supporting information

F.1 Introduction

This supporting information contains additional supporting figures and a table to supplement the data presented in the main text (Section 5.2 of this thesis).

The full reference for the manuscript is:
Cashins, S. D., **Grogan, L. F.**, McFadden, M., Hunter, D., Harlow, P. S., Berger, L., Skerratt, L. F. (in prep) Alpine tree frogs have variable innate immunity against chytridiomycosis with potential evolution of disease resistance.

F.2 Additional figures

Figure F.1. Individual enclosure set up for exposure experiment (with an uninfected alpine tree frog), including drainage holes and pebble substrate.

Figure F.2. Detail of individual frog enclosures.

Individual frog tubs had a permeable gauze window in the lid, and were held at a mild angle to facilitate water drainage (whilst still retaining a pool down one end). Tubs were supported on an egg crate floor suspended within large glass trays with high sides (to prevent splashing).

Figure F.3. A system of closed drainage pipes was used to remove waste water.

Figure F.4. Differences in mean body mass (g) between populations of exposed *L. v. alpina* at commencement of the experiment.

Error bars show standard deviation; Bonferroni-corrected two-tailed T-test [a]Eucumbene < Grey Mare, $p < 0.001$, [b]Eucumbene < Kiandra, $p < 0.01$; [c]Ogilvies < Grey Mare, $p < 0.001$.

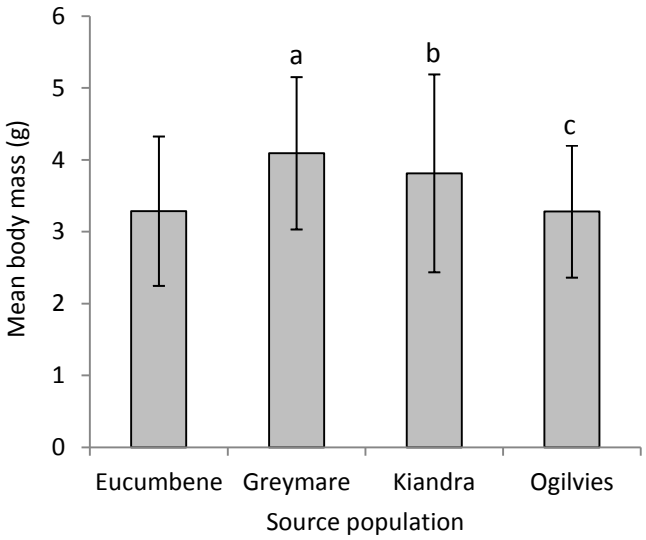

Figure F.5. Correlation scatter-plot between body mass (g) and snout-vent length (mm) of exposed *L. v. alpina* at the commencement of the experiment; Pearson correlation coefficient $r = 0.81$.

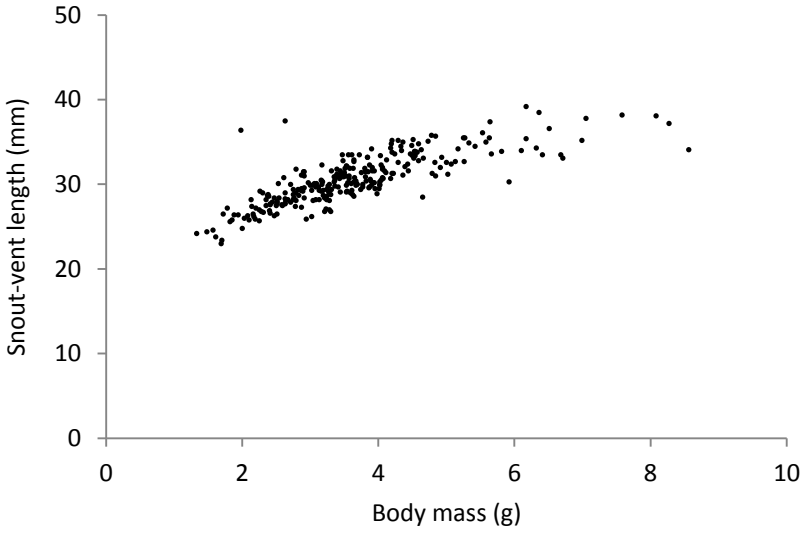

Figure F.6. Correlation scatter-plot between body mass (g) and days survived (days) of exposed *L. v. alpina* throughout the experiment (total length of the experiment = 86 days); Pearson correlation coefficient r = -0.03.

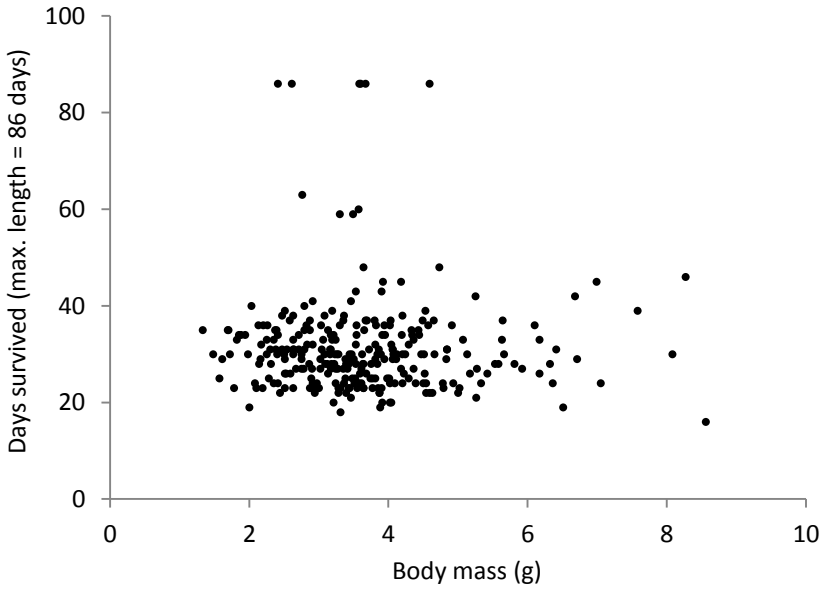

F.3 Additional table

Table F.1. Experimental design and results. Numbers of frogs from each population and clutch, details of blind randomized block design used for allocation of treatment groups (exposed frogs versus sham-exposed negative control frogs), and summary results.

Population (total number frogs)[a]	Clutch (total number frogs)[a]	Exposure group[b]	Total number of frogs	Number of males[f]	Number of females[f]	Number with undetermined gender	Mass average (g) at exp start	SVL average (mm) at exp start	Number survived to exp end	Number of days survived average (exclu died pre-exp & anasarca frog)	ZSE average at death or exp end	ZSE median at death or exp end
Eucumbene (99)	A (30)	E	20	7	13	0	3.41	28.8	0	29	651634	455267
		C	10	6	4	0	2.83	28.2	8	82	143196	0
	B (19)	E	19	10	9	0	2.83	29.0	0	30	912876	421145
		C	0	0	0	0	-	-	-	-	-	-
	C (29)	E	20	10	10	0	3.28	29.2	0	31	309014	84643
		C	9	4	5	0	3.44	29.4	7	80	56822	0
	D (21)	E	19	11	8	0	3.61	29.5	0	28	1594079	804084
		C	2[c]	0	1	1	4.65	31.8	0	66	66288	66288
Grey Mare (80)	A (14)	E	14	7	6	1	3.95	31.2	0	25	1203220	525252
		C	0	0	0	0	-	-	-	-	-	-
	B (26)	E	20	10	10	0	3.70	32.1	0	27	1209047	554631
		C	6	3	3	0	3.43	32.3	5	85	710563	0
	C (29)	E	20	11	9	0	4.54	33.6	1	36	1059128	526776
		C	9	6	3	0	4.24	33.6	5	69	234574	0
	D (11)	E	11	9	2	0	4.17	31.0	0	25	845406	1152590
		C	0	0	0	0	-	-	-	-	-	-
Kiandra (100)	A (25)	E	20	9	11	0	4.05	32.4	2	39	464597	142610
		C	5	1	4	0	3.94	32.7	3	73	368264	0
	B (25)	E	20	12	8	0	3.19	29.6	1	38	399876	188194

	C (25)	C	5	1	4	0	3.40	30.7	3	80	17429	0
		E	20[d]	8	10	2	3.63	30.9	1	39	857940	621014
	D (25)	C	5	3	2	0	3.45	34.6	3	79	486842	0
		E	20	11	9	0	4.62	31.9	1	36	958319	816608
		C	5	1	4	0	5.03	33.6	2	70	965848	411190
Ogilvies (76)	A (19)	E	19	13	6	0	3.09	30.0	0	25	961606	640914
		C	0	0	0	0	-	-	-	-	-	-
	B (40)	E	20	7	13	0	3.81	31.0	0	26	1772309	1246682
		C	20	6	14	0	3.90	30.7	9	71	892735	536875
	C (17)	E	16	9	7	0	2.95	28.8	0	31	943121	581168
		C	1[e]	0	0	1	4.01	31.9	-	-	-	-

[a]Total number of frogs in parentheses for each group; [b]E represents exposed frogs, C represents control frogs; [c]Includes one frog died pre-exposure and was excluded from further analyses; [d]This number includes the frog that died of anasarca post-exposure, unrelated to chytridiomycosis; [e]This frog died pre-exposure and was excluded from analyses; [f]Gender as determined by post-mortem coelomic examination.

APPENDIX G: Transcriptomics manuscript supporting information

G.1 Introduction

This appendix contains additional supporting figures and tables to supplement the data presented in the main text (Section 5.3 of this thesis). Tables G.2-G.5 can be found in the Microsoft Excel spreadsheet file: Appendix G Tables G2-G5.xlsx.

The full reference for the manuscript is:

Grogan, L. F., Cashins, S. D., Berger, L., Skerratt, L. F., Mulvenna, J. P. (in prep) Evolution of resistance to chytridiomycosis is associated with a robust early immune response in a wild amphibian.

G.2 Additional tables

Table G.1. Minimum numbers of read counts per million (cpm).

Minimum cpm were used to filter out and remove low expression tags for the various EdgeR differential gene expression analyses. I filtered transcripts (genes) with fewer than at least one count per million in at least the minimum number of samples in the smallest group included in the comparison. For example, in the Kiandra spleen comparison of 'controls versus 14 DPE' samples, the filter was set at three rather than four due to a missing sample; this means that I retained genes that achieved at least one count per million in at least three samples (the minimum number of samples from the smallest group in the comparison).

Population	Comparisons in EdgeR	Liver	Skin	Spleen
Controls	Sample session batch comparison	5	5	5
All	Controls versus Exposed	15	15	15
Eucumbene	Controls versus Exposed	6	6	6
	Controls versus 4 DPE	4	4	4
	Controls versus 8 DPE	4	4	4
	Controls versus 14 DPE	4	4	4
Grey Mare	Controls versus Exposed	3	3	3
	Controls versus 4 DPE	3	3	3
	Controls versus 8 DPE	3	3	3
	Controls versus 14 DPE	3	3	3
Kiandra	Controls versus Exposed	6	6	6
	Controls versus 4 DPE	4	4	4
	Controls versus 8 DPE	4	4	4
	Controls versus 14 DPE	4	4	3

Table G.2. Liver immune genes.

Immune-associated genes found to be differentially expressed among treatment groups in the liver of *Litoria verreauxii alpina*. Where a gene had more than one search term assigned to it, the most relevant term was assigned manually. PLEASE NOTE: **Table G.2.** can be found in the Microsoft Excel spreadsheet file: Appendix G Tables G2-G5.xlsx.

Table G.3. Skin immune genes.

Immune-associated genes found to be differentially expressed among treatment groups in the skin of *Litoria verreauxii alpina*. Where a gene had more than one search term assigned to it, the most relevant term was assigned manually. PLEASE NOTE: **Table G.3.** can be found in the Microsoft Excel spreadsheet file: Appendix G Tables G2-G5.xlsx.

Table G.4. Spleen immune genes.

Immune-associated genes found to be differentially expressed among treatment groups in the skin of *Litoria verreauxii alpina*. Where a gene had more than one search term assigned to it, the most relevant term was assigned manually. PLEASE NOTE: **Table G.4.** can be found in the Microsoft Excel spreadsheet file: Appendix G Tables G2-G5.xlsx.

Table G.5. Enriched Gene Ontology (GO) terms for skin samples.

Enriched GO terms for differentially expressed gene group comparisons comparing test sets with *Xenopus (Silurana) tropicalis* (Gotz et al., 2011). Only GO terms with a p-value < 0.05 are show, and only the 'reduced' set of GO terms (as defined in BLAST2GO; Conesa et al., 2005) are shown, including only the most specific GO term supported. PLEASE NOTE: **Table G.5.** can be found in the Microsoft Excel spreadsheet file: Appendix G Tables G2-G5.xlsx.

G.3 Additional figures

Figure G.1. Venn diagrams (non proportional) comparing numbers of differentially expressed genes shared between control samples (pooled between populations) taken at different times post exposure in the batch effect comparison.

Red, blue and yellow colours represent genes differentially expressed between 4 and 8 DPE, 4 and 14 DPE and 8 and 14 DPE, respectively, amongst tissues (A) liver, (B) skin, and (C) spleen.

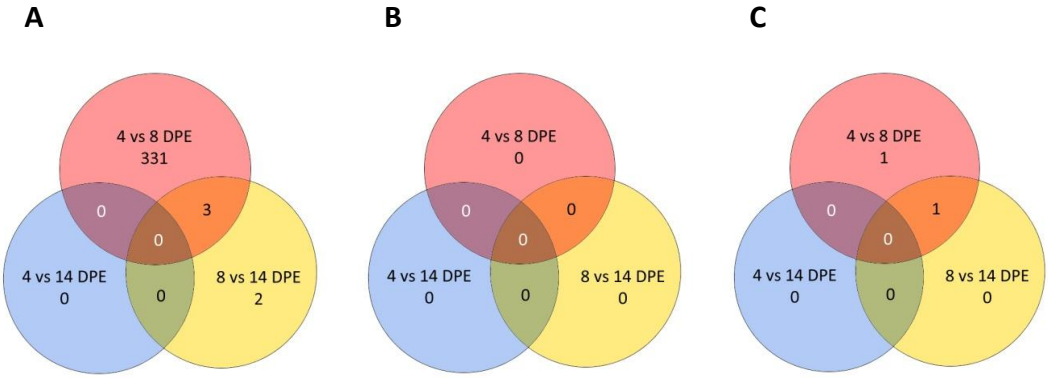

Figure G.2. Proportional Venn diagrams comparing numbers of differentially expressed genes between controls and sampling times post exposure in the liver tissue samples.

Yellow, red and blue colours represent genes differentially expressed between control samples and samples obtained at 4, 8 and 14 days post exposure, respectively, amongst populations (A) Eucumbene, (B) Grey Mare, and (C) Kiandra.

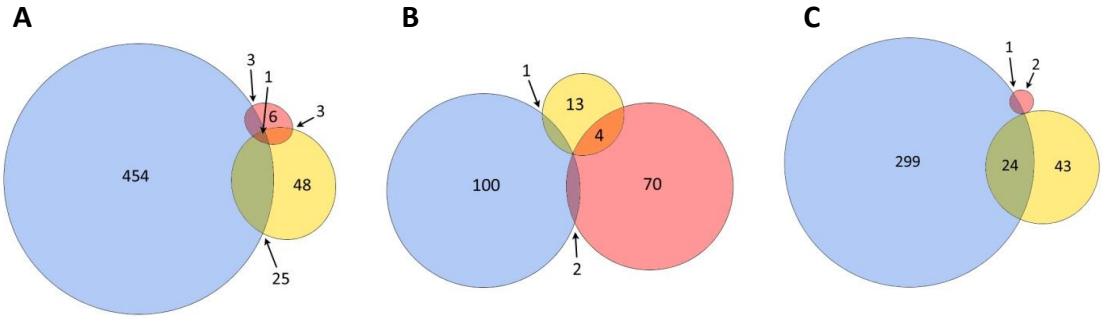

Figure G.3. Proportional Venn diagrams comparing numbers of differentially expressed genes between controls and sampling times post exposure in the skin tissue samples. Yellow, red and blue colours represent genes differentially expressed between control samples and samples obtained at 4, 8 and 14 days post exposure, respectively, amongst populations (A) Eucumbene, (B) Grey Mare, and (C) Kiandra.

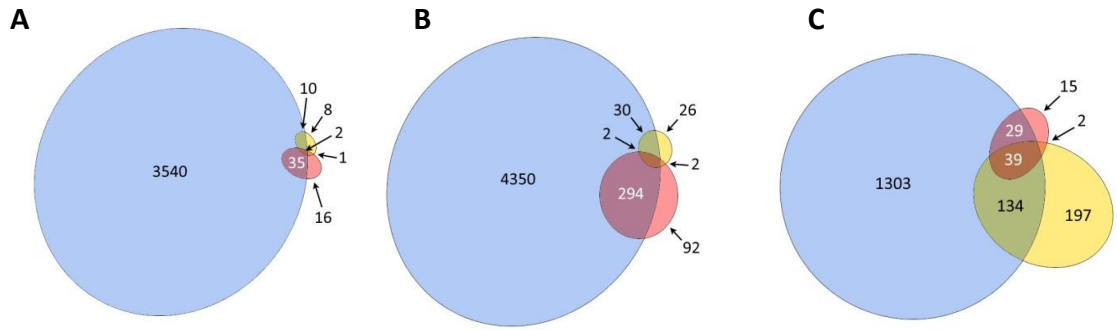

Figure G.4. Proportional Venn diagrams comparing numbers of differentially expressed genes between controls and sampling times post exposure in the spleen tissue samples. Yellow, red and blue colours represent genes differentially expressed between control samples and samples obtained at 4, 8 and 14 days post exposure, respectively, amongst populations (A) Eucumbene, (B) Grey Mare, and (C) Kiandra.

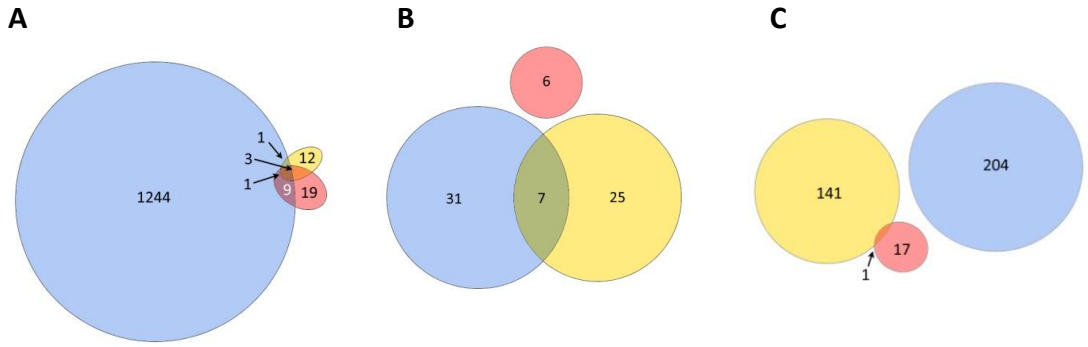

APPENDIX H: Metabolomics manuscript supporting information

H.1 Introduction

This appendix contains additional supporting figures and tables to supplement the data presented in the main text (Section 5.4 of this thesis).

The full reference for the manuscript is:
Grogan, L. F., Berger, L., Skerratt, L. F., Cashins, S. D., Trengove, R. D., Gummer, J. P. A. (in prep) Using a non-targeted metabolomics approach to investigate amphibian host responses to chytridiomycosis.

H.2 Additional figures

Figure H.1. Principal Components Analysis (PCA) score plot for liver and skin tissue samples grouping samples by batch (extraction processing date). The distinct horizontal clusters are a separation associated with tissue type (liver samples on the left, skin samples on the right).

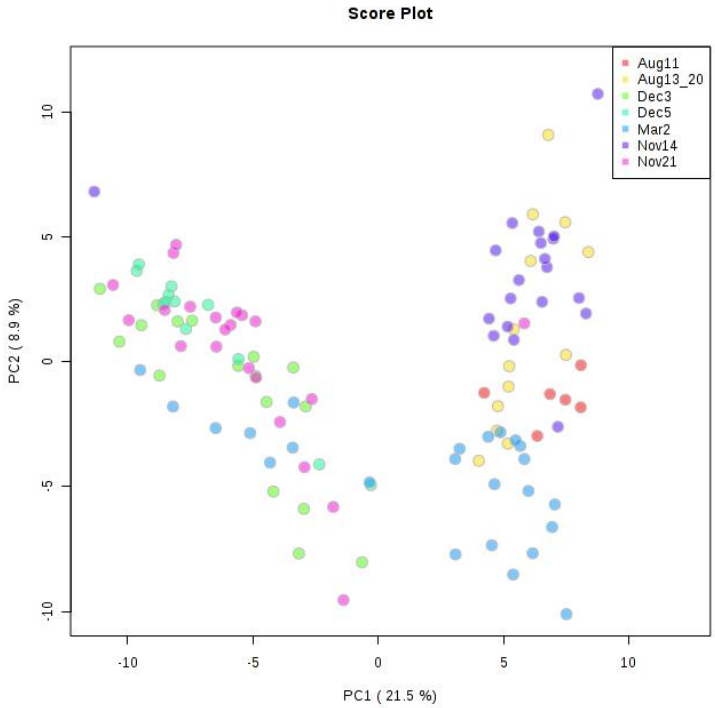

Figure H.2. Sum metabolite concentrations for samples grouped by batch (metabolite extraction processing date), with outliers labeled.

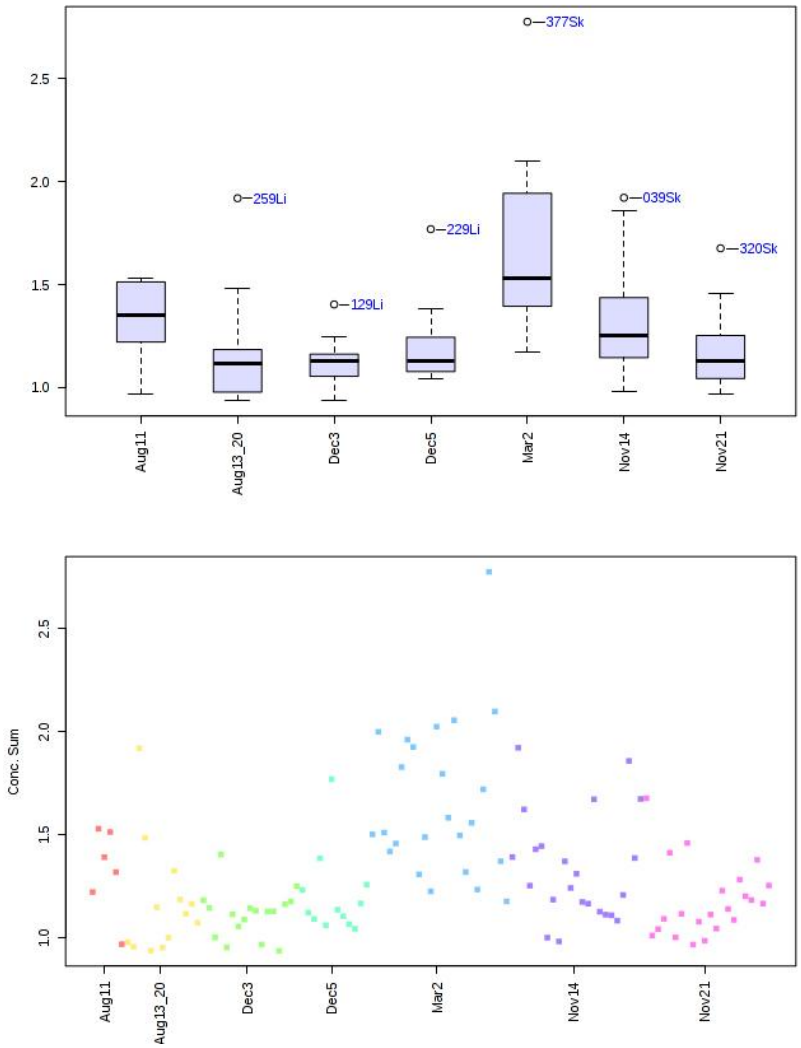

Figure H.3. Principal Components Analysis (PCA) scores plot (PC1 vs PC2) for liver tissue data grouped by site (frog population) demonstrating the outlier frog sample Lva259.

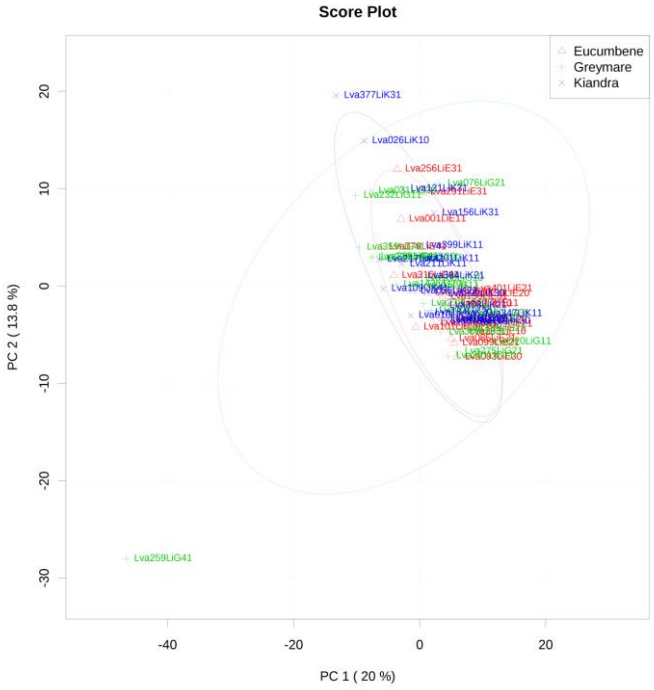

Figure H.4. Principal Components Analysis (PCA) scores plot (PC1 vs PC2) for skin tissue data grouped by site (frog population) demonstrating the outlier frog sample Lva259.

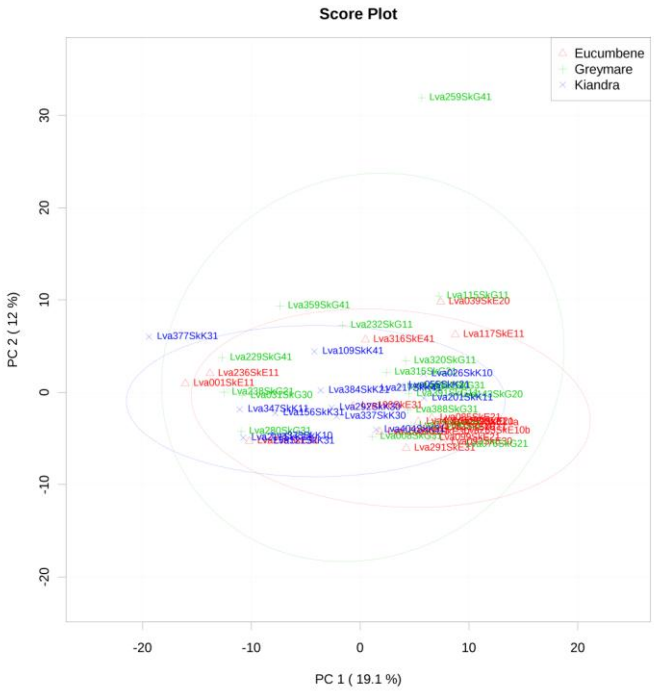

Figure H.5. Liver versus skin tissue samples cluster markedly, with a couple of exceptions, on Principal Components Analysis (PCA) scores plot.

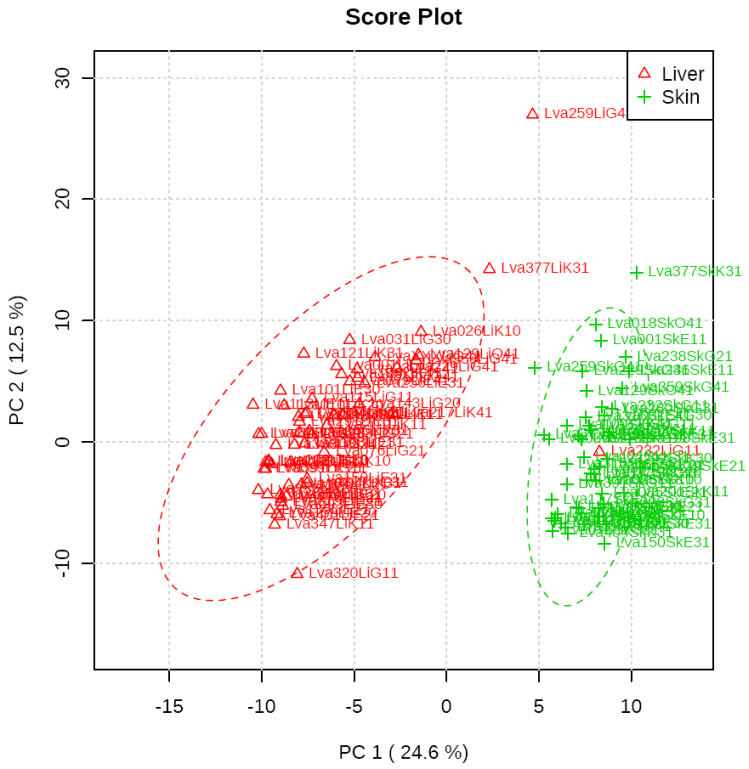

Figure H.6. Projection to Latent Structures - Discriminant Analysis (PLS-DA) Variable Importance in Projection (VIP) scores of the top 20 metabolites differentiating between **sampling periods** in **skin** samples, including heatmaps indicating the relative direction of metabolite expression between sampling periods.

Control frogs have been pooled and labeled group 0, and sampling periods at 4, 8, 14 days post exposure and moribund frogs have been labeled groups 1, 2, 3 and 4 respectively.

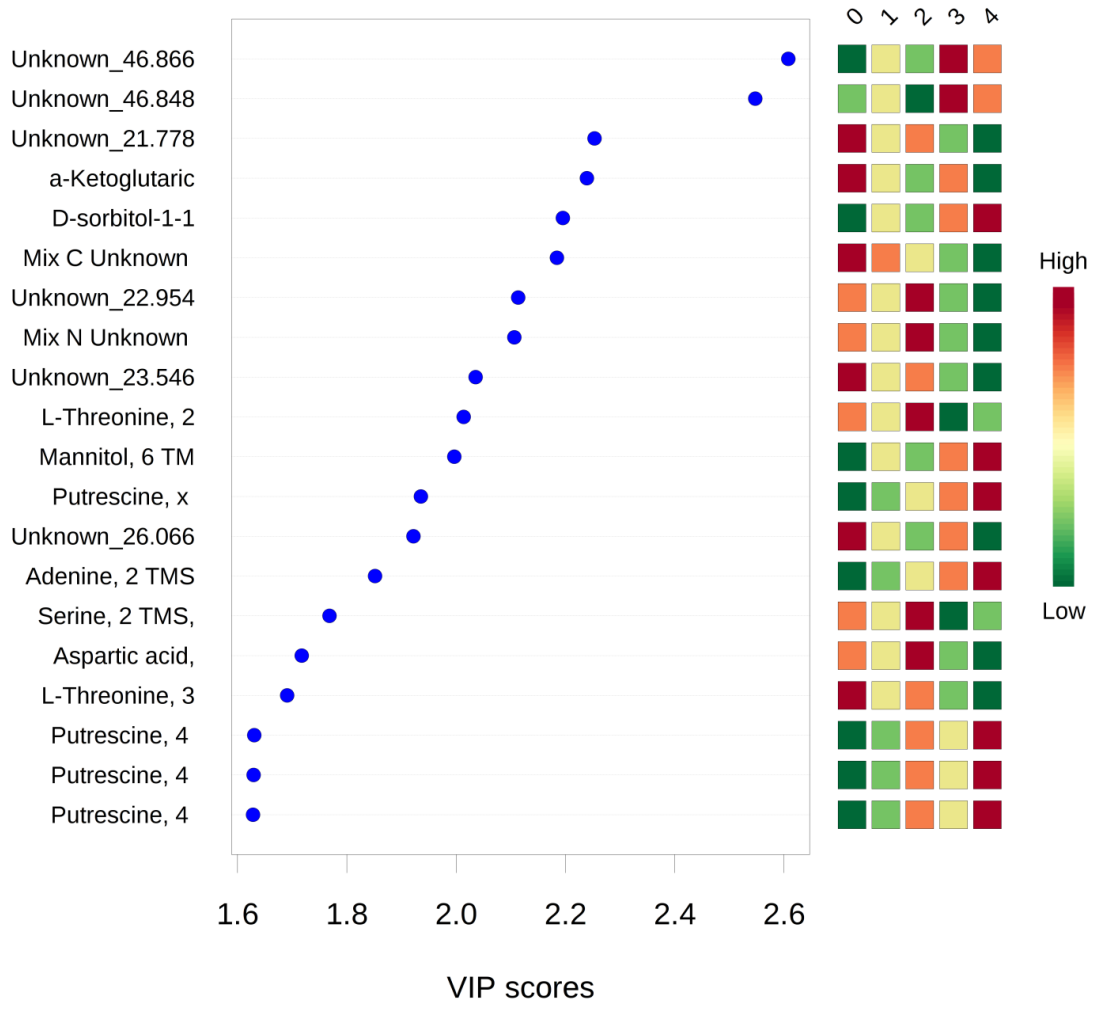

Figure H.7. Projection to Latent Structures - Discriminant Analysis (PLS-DA) Variable Importance in Projection (VIP) scores of the top 20 metabolites differentiating between **sampling periods** in **liver** samples, including heatmaps indicating the relative direction of metabolite expression between sampling periods.

Control frogs have been pooled and labeled group 0, and sampling periods at 4, 8, 14 days post exposure and moribund frogs have been labeled groups 1, 2, 3 and 4 respectively.

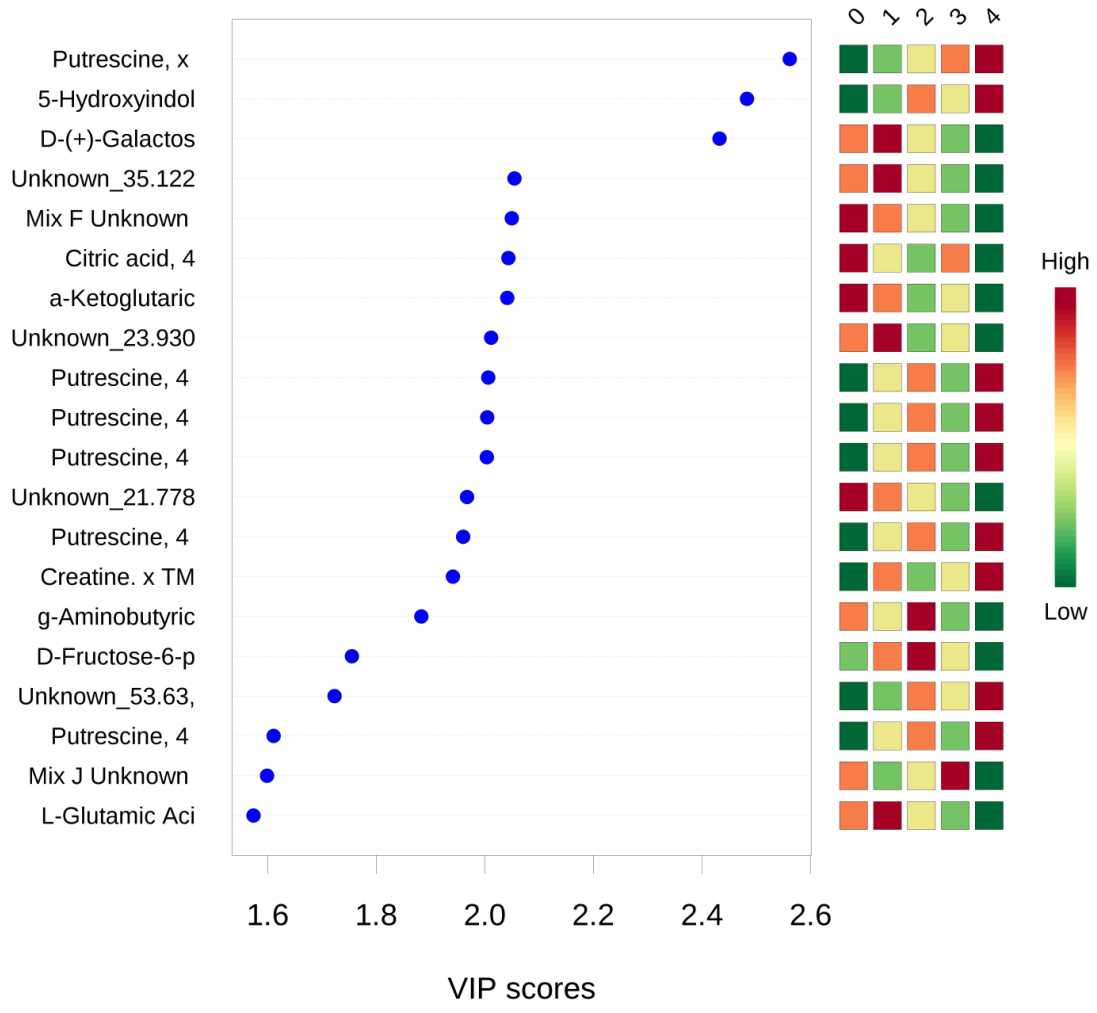

Figure H.8. Projection to Latent Structures - Discriminant Analysis (PLS-DA) Variable Importance in Projection (VIP) scores of the top 20 metabolites differentiating between **populations** in **skin** samples, including heatmaps indicating the relative direction of metabolite expression between populations.

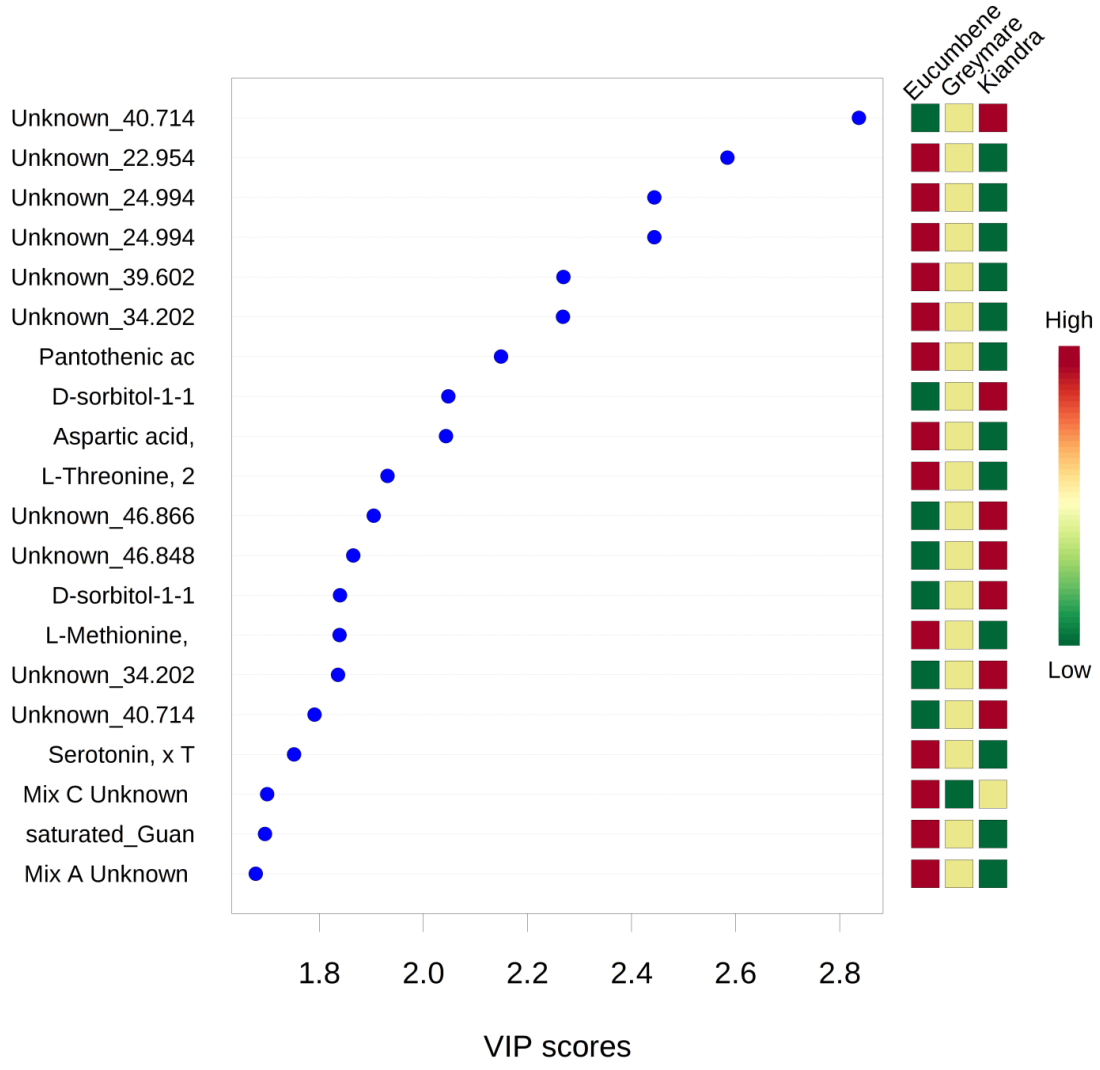

Figure H.9. Projection to Latent Structures - Discriminant Analysis (PLS-DA) Variable Importance in Projection (VIP) scores of the top 20 metabolites differentiating between **populations** in **liver** samples, including heatmaps indicating the relative direction of metabolite expression between populations.

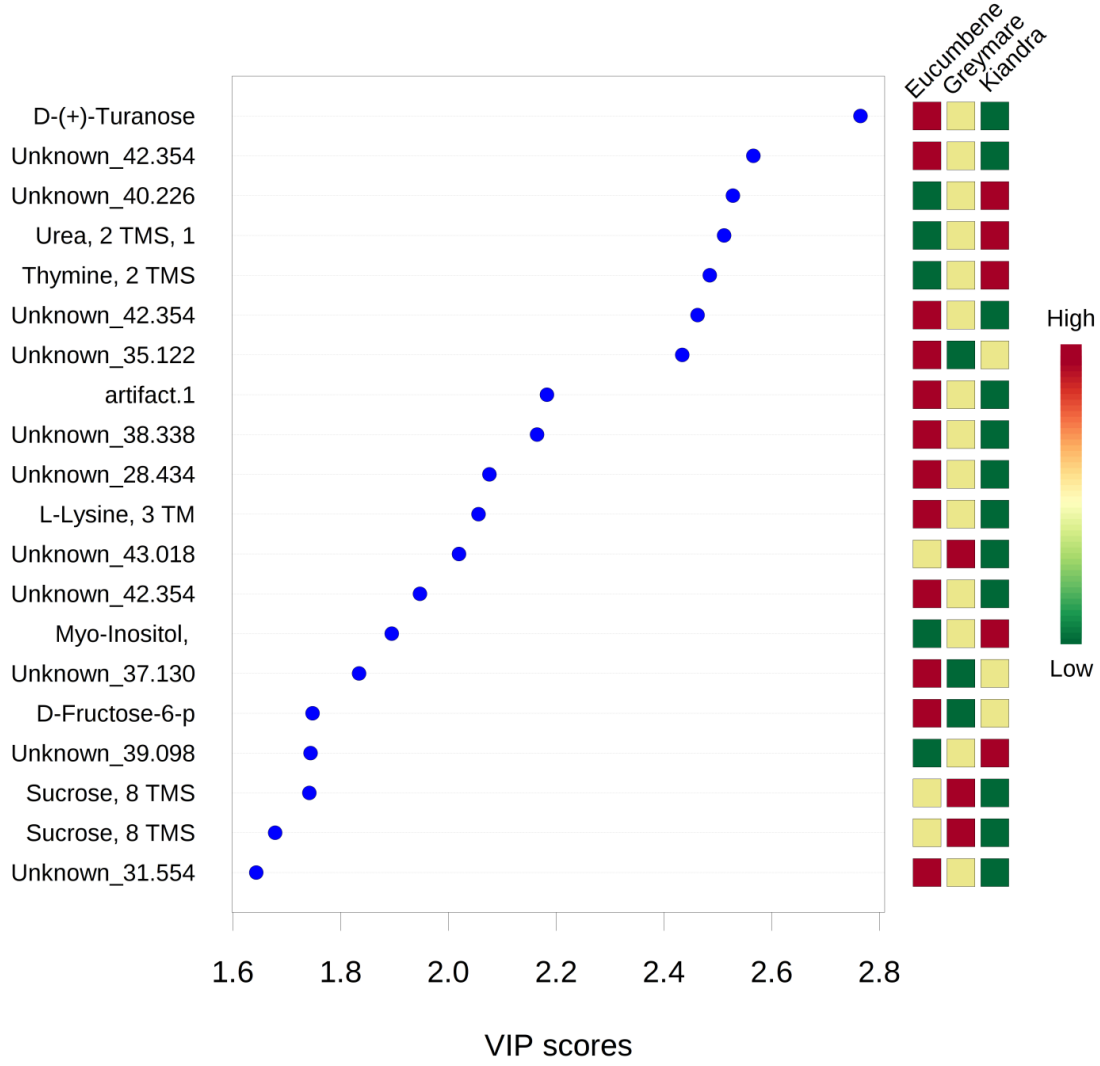

H.3 Additional tables

Table H.1. One-way ANOVA Tukey's honestly significant difference post-hoc tests on **skin** samples to determine significant comparisons between **sampling periods**.

The last column (Tukey's HSD) represents the sample period comparisons that yielded significant results; 0 represents the control group, 1 represents samples taken at 4 days post-exposure, 2 represents samples taken at 8 days post exposure, 3 represents samples taken at 14 days post exposure and 4 represents moribund frogs (roughly at 21+ days post exposure) (only showing metabolites with FDR < 0.05). Metabolites with differences between sampling groups excluding the moribund group (group 4) are highlighted in blue.

#	Metabolite name	p.value	-log10(p)	FDR	Tukey's HSD
1	a-Ketoglutaric acid, x TMS, 23.95, 1578	3.21E-08	7.4936	6.51E-06	4-0; 4-1; 4-2; 4-3
2	Unknown_21.778, 1476, m/z234_arabino-hexos-2-ulose-like	8.89E-06	5.051	0.000818	4-0; 4-1; 4-2; 4-3
3	Mix J Unknown 3, 21.95, 1484_malic acid-like	1.21E-05	4.9174	0.000818	4-0; 4-1; 4-2; 4-3
4	Mix C Unknown 3, 24.71, 1617	4.28E-05	4.3685	0.002042	4-0; 4-1; 4-2; 4-3
5	Serotonin, x TMS, 39.11, 2470	5.21E-05	4.283	0.002042	4-0; 4-1; 4-2; 4-3
6	5-Hydroxyindole-3-acetic acid, 3 TMS, 35.49, 2212	6.04E-05	4.2193	0.002042	4-0; 4-1; 4-2; 4-3
7	Unknown_23.546, 1558, m/z 292-threonic acid-like	0.000105	3.9775	0.003054	4-0; 4-1; 4-2; 4-3
8	L-Isoleucine, 2 TMS, 17.32, 1295	0.000125	3.9036	0.003168	4-0; 4-1; 4-2; 4-3
9	Glutamic acid, 3 TMS, 24.79, 1623	0.000163	3.7871	0.003682	4-0; 4-1; 4-2; 4-3
10	Serotonin, x TMS, 39.11, 2470_saturated	0.000199	3.7022	0.003701	4-0; 4-1; 4-2; 4-3
11	Glutamic acid, 3 TMS, 24.79, 1623_saturated.1	0.00021	3.6775	0.003701	4-0; 4-1; 4-2; 4-3
12	Glutamic acid, 3 TMS, 24.79, 1623_saturated	0.000219	3.6601	0.003701	4-0; 4-1; 4-2; 4-3
13	DL-Ornithine, 3 TMS, 24.71, 1623	0.000594	3.226	0.00928	2-1; 3-2; 4-2
14	Unknown_39.602, 2501, m/z174-serotonin-like	0.000841	3.0752	0.012195	4-0; 4-1; 4-2; 4-3
15	DL-Tartaric acid 4TMS-like	0.001161	2.9353	0.015706	4-0; 4-1; 4-2
16	Urea, 2 TMS, 16.14, 1249	0.001717	2.7652	0.021784	1-0; 3-1
17	L-Glutamic acid, 2 TMS, 22.7, 1519_saturated.1	0.001921	2.7164	0.022225	4-0; 4-2
18	Serine, 2 TMS, 16.43, 1260	0.001971	2.7054	0.022225	3-0; 3-2
19	Mix N Unknown 1, 22.98, 1532	0.002311	2.6363	0.02274	4-0; 4-2
20	L-Glutamic acid, 2 TMS, 22.7, 1519_saturated	0.002476	2.6062	0.02274	4-0; 4-2
21	Fumaric acid, 2 TMS, 18.29, 1357	0.002554	2.5928	0.02274	4-0; 4-3
22	L-Threonine, 2 TMS, 17.37, 1298	0.002605	2.5842	0.02274	3-0; 3-2
23	L-Threonine, 3 TMS, 19.59, 1387	0.00268	2.5719	0.02274	3-0
24	Gallic acid, x TMS, 22.73, 1520_saturated	0.002742	2.5619	0.02274	4-0; 4-2
25	saturated_L-Pyroglutamic acid, 2 TMS, 22.76, 1520	0.002952	2.5299	0.02274	4-0; 4-2
26	L-Glutamic Acid, 2 TMS, 22.75, 1519_saturated	0.003023	2.5196	0.02274	4-0; 4-2
27	L-Pyroglutamic acid, 2 TMS, 22.76, 1520_saturated	0.003025	2.5193	0.02274	4-0; 4-2
28	Mix F Unknown 1, 19.28, 1377	0.003332	2.4773	0.024159	4-0; 4-1; 4-2
29	g-Aminobutyric acid, 3 TMS, 22.9, 1526	0.004636	2.3338	0.032454	4-0; 4-1; 4-3
30	L-Lysine, 4 TMS, 30.54, 1915	0.005241	2.2806	0.035461	2-1; 3-1; 4-1
31	Uridine, 3 TMS, 38.98, 2462	0.006828	2.1657	0.044709	4-0; 4-1; 4-2

32	Unknown_24.994, 1631, m/z174	0.007974	2.0983	0.04905	4-0; 4-2; 4-3
33	Unknown_24.994, 1631, m/z174.1	0.007974	2.0983	0.04905	4-0; 4-2; 4-3

Table H.2. Pattern searching template matching approach (negative control-1-2-3-moribund) on **skin** samples to determine analytes with significant comparisons between **sampling periods** (only showing metabolites with FDR < 0.05).

#	Metabolite name	correlation	t-stat	p-value	FDR
1	Unknown_21.778, 1476, m/z234_arabino-hexos-2-ulose-like	-0.52544	-4.4534	4.51E-05	0.005576
2	Unknown_23.546, 1558, m/z 292-threonic acid-like	-0.51112	-4.2882	7.83E-05	0.005576
3	a-Ketoglutaric acid, x TMS, 23.95, 1578	-0.50977	-4.2729	8.24E-05	0.005576
4	Putrescine, x TMS, 22.45, 1506_putative	0.48387	3.987	0.00021	0.01065
5	Adenine, 2 TMS, 29.74, 1869	0.47166	3.8572	0.000318	0.010911
6	Mix C Unknown 3, 24.71, 1617	-0.47123	-3.8527	0.000322	0.010911
7	L-Threonine, 3 TMS, 19.59, 1387	-0.46134	-3.7497	0.000446	0.012941
8	DL-Tartaric acid 4TMS-like	-0.44113	-3.5445	0.000841	0.021352
9	L-Glutamic acid, 2 TMS, 22.7, 1519_saturated.1	-0.42832	-3.4181	0.001233	0.026337
10	L-Glutamic acid, 2 TMS, 22.7, 1519_saturated	-0.41981	-3.3355	0.001577	0.026337
11	Mix F Unknown 1, 19.28, 1377	-0.41882	-3.3259	0.001622	0.026337
12	Gallic acid, x TMS, 22.73, 1520_saturated	-0.41624	-3.3011	0.001745	0.026337
13	L-Glutamic Acid, 2 TMS, 22.75, 1519_saturated	-0.41308	-3.2709	0.001907	0.026337
14	L-Pyroglutamic acid, 2 TMS, 22.76, 1520_saturated	-0.41254	-3.2658	0.001935	0.026337
15	saturated_L-Pyroglutamic acid, 2 TMS, 22.76, 1520	-0.41235	-3.2639	0.001946	0.026337
16	Mix N Unknown 1, 22.98, 1532	-0.40792	-3.2218	0.0022	0.027913
17	L-Threonine, 2 TMS, 17.37, 1298	-0.39804	-3.1288	0.002875	0.034335
18	Unknown_46.866, 3064, m/z169	0.39111	3.0644	0.003453	0.035524
19	Glutamic acid, 3 TMS, 24.79, 1623	-0.38507	-3.0088	0.004037	0.035524
20	Adenosine, 4 TMS, 41.49, 2642	0.38269	2.987	0.004291	0.035524
21	likely artifact-glucose-like	-0.38259	-2.9861	0.004301	0.035524
22	likely artifact-glucose-like.1	-0.38259	-2.9861	0.004301	0.035524
23	Unknown_46.848, 3063, m/z169	0.38217	2.9822	0.004348	0.035524
24	Cellobiose, x TMS, 42.19, 2962	0.38001	2.9625	0.004592	0.035524
25	Unknown_22.954, 1529, m/z 160	-0.37837	-2.9476	0.004786	0.035524
26	Glutamic acid, 3 TMS, 24.79, 1623_saturated	-0.37547	-2.9213	0.005146	0.035524
27	Glutamic acid, 3 TMS, 24.79, 1623_saturated.1	-0.37493	-2.9164	0.005216	0.035524
28	Putrescine, 4 TMS, 27.09, 1739_saturated	0.37157	2.886	0.005668	0.035524
29	Putrescine, 4 TMS, 27.09, 1739_saturated.2	0.3714	2.8846	0.005692	0.035524
30	Putrescine, 4 TMS, 27.09, 1739	0.37121	2.8828	0.005719	0.035524
31	Putrescine, 4 TMS, 27.09, 1739_saturated.1	0.37121	2.8828	0.005719	0.035524
32	Putrescine, 4 TMS, 27.13, 1738_saturated	0.37121	2.8828	0.005719	0.035524
33	Myo-Inositol, 6 TMS, 33.38, 2081	-0.37081	-2.8792	0.005775	0.035524
34	Serine, 2 TMS, 16.43, 1260	-0.36268	-2.8064	0.007034	0.041999

Table H.3. Significance Analysis of Microarrays on **skin** samples to determine analytes with significant differences between **sampling periods** (only showing metabolites with FDR < 0.05). D-sorbitol (spike-in) has been highlighted in pink.

#	Metabolite name	d.value	stdev	rawp	FDR
1	a-Ketoglutaric acid, x TMS, 23.95, 1578	9.1435	0.81626	0	0
2	Unknown_21.778, 1476, m/z234_arabino-hexos-2-ulose	6.0858	0.98763	9.85E-05	0.0005
3	Serotonin, x TMS, 39.11, 2470	6.0485	1.7967	9.85E-05	0.0005
4	Mix C Unknown 3, 24.71, 1617	5.5787	1.2348	9.85E-05	0.0005
5	5-Hydroxyindole-3-acetic acid, 3 TMS, 35.49, 2212	5.3891	1.2476	9.85E-05	0.0005
6	Serotonin, x TMS, 39.11, 2470_saturated	5.313	2.0116	9.85E-05	0.0005
7	Unknown_23.546, 1558, m/z 292-threonic acid-like	4.6078	0.94778	0.000394	0.001333
8	Unknown_39.602, 2501, m/z174-serotonin-like	4.5319	2.3341	0.000394	0.001333
9	Mix J Unknown 3, 21.95, 1484_malic acid-like	4.4953	0.52878	0.000394	0.001333
10	Urea, 2 TMS, 16.14, 1249	4.3822	3.6252	0.000493	0.001499
11	Mix N Unknown 1, 22.98, 1532	3.6981	1.8259	0.001133	0.002558
12	Serine, 2 TMS, 16.43, 1260	3.6799	1.616	0.001232	0.002558
13	Glutamic acid, 3 TMS, 24.79, 1623	3.6739	0.62565	0.001232	0.002558
14	Glutamic acid, 3 TMS, 24.79, 1623_saturated.1	3.602	0.64049	0.001379	0.002558
15	L-Threonine, 2 TMS, 17.37, 1298	3.5974	1.762	0.001379	0.002558
16	Glutamic acid, 3 TMS, 24.79, 1623_saturated	3.5903	0.64287	0.001379	0.002558
17	DL-Ornithine, 3 TMS, 24.71, 1623	3.5129	0.82385	0.001429	0.002558
18	L-Isoleucine, 2 TMS, 17.32, 1295	3.328	0.48252	0.002266	0.003832
19	L-Lysine, 4 TMS, 30.54, 1915	3.104	1.5686	0.002956	0.004735
20	g-Aminobutyric acid, 3 TMS, 22.9, 1526	2.9491	1.2181	0.004187	0.005306
21	DL-Tartaric acid 4TMS-like	2.9487	0.68177	0.004187	0.005306
22	L-Threonine, 3 TMS, 19.59, 1387	2.9419	0.92576	0.004286	0.005306
23	Unknown_46.866, 3064, m/z169	2.9337	3.3164	0.004286	0.005306
24	Unknown_24.994, 1631, m/z174.1	2.8912	1.606	0.004434	0.005306
25	Unknown_24.994, 1631, m/z174	2.8912	1.606	0.004434	0.005306
26	Mix F Unknown 1, 19.28, 1377	2.8855	0.96771	0.004532	0.005306
27	Unknown_46.848, 3063, m/z169	2.8425	3.3375	0.005025	0.005664
28	Unknown_26.066, 1685, m/z159	2.7046	2.2557	0.006453	0.007015
29	Unknown_22.954, 1529, m/z 160	2.6057	2.3582	0.007734	0.007997
30	Putrescine, x TMS, 22.45, 1506_putative	2.5926	1.1631	0.007882	0.007997
31	Unknown_35.898, 2236, m/z188-putative phosphoric a	2.4853	1.3183	0.010246	0.009922
32	Aspartic acid, 2 TMS, 20.54, 1428	2.4525	2.1339	0.010788	0.009922
33	Unknown_38.398, 2421, m/z387-myo-inositol-like	2.4508	1.4139	0.010837	0.009922
34	L-Glutamic acid, 2 TMS, 22.7, 1519_saturated.1	2.4403	0.53816	0.011084	0.009922
35	Adenine, 2 TMS, 29.74, 1869	2.4078	1.1378	0.011773	0.010239
36	L-Glutamic acid, 2 TMS, 22.7, 1519_saturated	2.361	0.54559	0.012808	0.010683
37	Gallic acid, x TMS, 22.73, 1520_saturated	2.3304	0.54931	0.013744	0.010683
38	saturated_L-Pyroglutamic acid, 2 TMS, 22.76, 1520	2.3153	0.5554	0.013842	0.010683
39	L-Pyroglutamic acid, 2 TMS, 22.76, 1520_saturated	2.3032	0.55398	0.014039	0.010683

40	L-Glutamic Acid, 2 TMS, 22.75, 1519_saturated	2.3023	0.55342	0.014039	0.010683
41	Uridine, 3 TMS, 38.98, 2462	2.2249	0.69504	0.016847	0.012428
42	Unknown_37.130, 2142, m/z315-myo-inositol-2-phosph	2.2032	1.2742	0.017635	0.012428
43	DL-Ornithine, 4 TMS, 28.65, 1815	2.1919	0.77577	0.01803	0.012428
44	Unknown_39.274, 2478, m/z204	2.1838	1.6353	0.018374	0.012428
45	D-(+)-Galactose, 5 TMS, MEOX, 29.94, 1880	2.1808	1.6078	0.018374	0.012428
46	Glycine, 2 TMS, 12.72, 1110	2.1106	2.0145	0.022266	0.014733
47	Unknown_36.722, 2295, m/z318-myo-inositol-like?	2.0221	1.3252	0.025764	0.016684
48	Pantothenic acid, O,O,O-TMS-putative	1.9658	1.1486	0.02867	0.01818
49	Fumaric acid, 2 TMS, 18.29, 1357	1.9441	0.38632	0.03	0.018635
50	Unknown_20.426, 1421, m/z 172	1.9034	0.99269	0.032512	0.019492
51	D-Fructose-6-phosphate 6TMS, MEOX, 36.72, 2300-put	1.8857	1.5781	0.033695	0.019492
52	Unknown_29.466, 1855, m/z217	1.8716	0.86424	0.034631	0.019492
53	Unknown_41.866, 2664, m/z204	1.858	1.2453	0.035665	0.019492
54	Putrescine, 4 TMS, 27.09, 1739_saturated	1.8389	1.5254	0.037044	0.019492
55	Putrescine, 4 TMS, 27.09, 1739_saturated.2	1.8354	1.525	0.03734	0.019492
56	Putrescine, 4 TMS, 27.13, 1738_saturated	1.8336	1.5249	0.037488	0.019492
57	Putrescine, 4 TMS, 27.09, 1739_saturated.1	1.8336	1.5249	0.037488	0.019492
58	Putrescine, 4 TMS, 27.09, 1739	1.8336	1.5249	0.037488	0.019492
59	D-sorbitol-1-13C m/z_320	1.8286	3.683	0.037783	0.019492
60	Myo-Inositol, 6 TMS, 33.38, 2081	1.7882	0.74805	0.040788	0.020691
61	Unknown_31.242, 1953, m/z361-cellobiose-like	1.7164	1.0693	0.046946	0.023425
62	Ribose-5-phosphate, 5 TMS, MEOX, 33.65, 2100	1.7037	0.92234	0.048621	0.023869
63	Cellobiose, x TMS, 42.19, 2962	1.6754	1.1626	0.051182	0.024728
64	Unknown_42.354, 2698, m/z289.1	1.6239	1.6517	0.056404	0.026825
65	L-Lysine, x TMS, 29.32, 1852	1.5951	0.96907	0.060049	0.028119
66	L-Methionine, 1 TMS, 20.27, 1416_putative.2	1.5828	2.3746	0.061232	0.028238
67	D-Fructose-1-phosphate, x TMS, 36.58, 2290	1.5696	1.3306	0.063399	0.028801
68	Unknown_18.090, 1327, m/z 315	1.5491	0.48499	0.066256	0.029066
69	likely artifact-glucose-like.1	1.5439	1.1858	0.066847	0.029066
70	likely artifact-glucose-like	1.5439	1.1858	0.066847	0.029066
71	Unknown_34.202, 2129, m/z352-putative guanine	1.5307	5.9674	0.068719	0.029459
72	Citric acid, 4 TMS, 28.69, 1817	1.5173	1.1693	0.070837	0.029946
73	L-Tyrosine, 3 TMS, 30.86, 1934	1.4981	1.3166	0.07335	0.030583
74	Unknown_53.63, 3702, m/z311-stearic acid-like	1.487	1.9196	0.074778	0.030757
75	Unknown_30.49, 1908, m/z 174-dopamine-like	1.4684	1.1295	0.077044	0.031267
76	Unknown_42.354, 2704, m/z217	1.4409	1.6512	0.082759	0.033144
77	Unknown_44.002, 2820, m/z131	1.4161	2.9211	0.086995	0.034388
78	D-(+)-Galactose, 5 TMS, MEOX, 29.94, 1880_saturate	1.3934	1.5623	0.091675	0.035773
79	Adenosine, 4 TMS, 41.49, 2642	1.366	0.77269	0.097438	0.036635
80	L-Proline, 2 TMS, 17.43, 1300	1.3637	0.78493	0.098227	0.036635
81	L-Methionine, 1 TMS, 20.27, 1416_putative.1	1.3594	2.3046	0.098818	0.036635
82	L-Methionine, 1 TMS, 20.27, 1416_putative	1.3594	2.3046	0.098818	0.036635
83	D-(+)-Galactose, 5 TMS, MEOX, 29.94, 1880_too over	1.3555	1.04	0.099901	0.036635
84	Unknown_21.586, 1468, m/z 218_amino malonic acid-l	1.3356	1.6814	0.10473	0.037696
85	D-sorbitol-1-13C m/z_319	1.333	2.9625	0.10527	0.037696
86	Mannitol, 6 TMS, 30.6, 1915_saturated	1.3193	3.8887	0.10818	0.038286

87	Unknown_28.434, 1803, m/z204	1.3072	1.0883	0.11138	0.038714
88	Unknown_40.714, 2581, m/z217.1	1.2999	1.6433	0.11281	0.038714
89	Unknown_20.61, 1428, m/z 158_tentative glycine	1.2991	0.99118	0.1132	0.038714
90	L-Leucine, 2 TMS, 16.74, 1274	1.266	0.78852	0.12079	0.04076
91	ISTD D-sorbitol 13C6	1.2551	2.7739	0.1231	0.04076
92	D-sorbitol 13C6 m/z_323	1.2547	2.7739	0.1232	0.04076
93	Unknown_37.770, 2370, m/z397	1.2324	1.7047	0.12995	0.042531
94	Unknown_44.010, 2820, m/z169-5'-uridine monophosph	1.223	2.0551	0.13187	0.0427
95	Unknown_32.634, 2082, m/z179	1.198	2.0204	0.13946	0.043976
96	Unknown_36.242, 2261, m/z315	1.1978	1.3111	0.13946	0.043976
97	Unknown_23.930, 1578, m/z129	1.1953	0.66095	0.14015	0.043976
98	Sucrose, 8 TMS, 41.32, 2630.1	1.1572	1.2856	0.15	0.046588
99	Mix D Unknown 5, 42.68, 2722.1	1.1356	0.94092	0.15724	0.048343

Table H.4. One-way ANOVA Tukey's honestly significant difference post-hoc tests on **liver** samples to determine significant comparisons between **sampling periods**.

The last column (Tukey's HSD) represents the sample period comparisons that yielded significant results; 0 represents the control group, 1 represents samples taken at 4 days post-exposure, 2 represents samples taken at 8 days post exposure, 3 represents samples taken at 14 days post exposure and 4 represents moribund frogs (roughly at 21+ days post exposure) (only showing metabolites with FDR < 0.05). Metabolites with differences between sampling groups excluding the moribund group (4) are highlighted in blue. D-sorbitol (spike-in) has been highlighted in pink.

#	Metabolite name	p.value	-log10(p)	FDR	Tukey's HSD
1	L-Isoleucine, 2 TMS, 17.32, 1295	3.81E-13	12.419	7.66E-11	4-0; 2-1; 4-1; 3-2; 4-2; 4-3
2	L-Glutamic acid, 2 TMS, 22.7, 1519_saturated	3.68E-12	11.435	1.56E-10	4-0; 4-1; 4-2; 4-3
3	Gallic acid, x TMS, 22.73, 1520_saturated	4.30E-12	11.366	1.56E-10	4-0; 4-1; 4-2; 4-3
4	L-Glutamic Acid, 2 TMS, 22.75, 1519_saturated	4.38E-12	11.359	1.56E-10	4-0; 4-1; 4-2; 4-3
5	L-Pyroglutamic acid, 2 TMS, 22.76, 1520_saturated	4.46E-12	11.35	1.56E-10	4-0; 4-1; 4-2; 4-3
6	saturated_L-Pyroglutamic acid, 2 TMS, 22.76, 1520	4.66E-12	11.331	1.56E-10	4-0; 4-1; 4-2; 4-3
7	L-Glutamic acid, 2 TMS, 22.7, 1519_saturated.1	9.04E-12	11.044	2.60E-10	4-0; 4-1; 4-2; 4-3
8	L-Leucine, 2 TMS, 16.74, 1274	1.22E-09	8.9143	2.96E-08	4-0; 4-1; 3-2; 4-2; 4-3
9	Mix J Unknown 3, 21.95, 1484_malic acid-like	1.32E-09	8.878	2.96E-08	4-0; 4-1; 4-2; 4-3
10	Putrescine, 4 TMS, 27.09, 1739	2.38E-08	7.6239	4.78E-07	4-0; 4-1; 4-2; 4-3
11	Glutamic acid, 3 TMS, 24.79, 1623	3.05E-08	7.5152	5.14E-07	4-0; 4-1; 4-2; 4-3
12	Putrescine, 4 TMS, 27.09, 1739_saturated.2	3.07E-08	7.5128	5.14E-07	4-0; 4-1; 4-2; 4-3
13	Putrescine, 4 TMS, 27.09, 1739_saturated	3.82E-08	7.4177	5.91E-07	4-0; 4-1; 4-2; 4-3
14	Citric acid, 4 TMS, 28.69, 1817	5.08E-08	7.2943	7.29E-07	4-0; 4-1; 4-2; 4-3

15	Unknown_38.802, 2301, m/z387-D-mannose-6-phosphate-like	6.50E-08	7.1872	8.71E-07	4-0; 4-1; 4-2; 4-3
16	Fumaric acid, 2 TMS, 18.29, 1357	6.94E-08	7.1589	8.71E-07	4-0; 4-1; 4-2; 4-3
17	Glutamic acid, 3 TMS, 24.79, 1623_saturated	1.14E-07	6.9443	1.29E-06	4-0; 4-1; 4-2; 4-3
18	Glutamic acid, 3 TMS, 24.79, 1623_saturated.1	1.15E-07	6.9385	1.29E-06	4-0; 4-1; 4-2; 4-3
19	D-Fructose-6-phosphate 6TMS, MEOX, 36.72, 2300-putative.2	2.89E-07	6.539	3.06E-06	4-0; 4-1; 4-2; 4-3
20	Unknown_21.778, 1476, m/z234_arabino-hexos-2-ulose-like	3.87E-07	6.4124	3.89E-06	4-0; 4-1; 4-2; 4-3
21	Putrescine, x TMS, 22.45, 1506_putative	4.19E-07	6.3774	4.01E-06	4-0; 4-1; 4-2; 4-3
22	D-Glucose-6-phosphate, 6 TMS, MEOX, 37.23, 2332	1.89E-06	5.723	1.73E-05	4-0; 4-1; 4-2; 4-3
23	D-Fructose-6-phosphate 6TMS, MEOX, 36.72, 2300-putative.1	3.30E-06	5.4817	2.82E-05	4-0; 4-1; 4-2; 4-3
24	D-Glucose-6-phosphate, 6 TMS, MEOX, 36.95, 2312	3.36E-06	5.4733	2.82E-05	4-0; 4-1; 4-2; 4-3
25	g-Aminobutyric acid, 3 TMS, 22.9, 1526	3.73E-06	5.4287	3.00E-05	3-0; 4-0; 4-1; 3-2; 4-2
26	a-Ketoglutaric acid, x TMS, 23.95, 1578	8.76E-06	5.0573	6.63E-05	4-0; 4-1; 4-2; 4-3
27	Unknown_40.226, 2546, m/z387-glucose-6-phosphate-like	9.21E-06	5.0359	6.63E-05	4-0; 4-1; 4-2; 4-3
28	Unknown_23.930, 1578, m/z129	9.24E-06	5.0345	6.63E-05	4-0; 2-1; 3-1; 4-1; 4-2; 4-3
29	Creatine. x TMS, 23.39, 1551	1.42E-05	4.848	9.84E-05	4-0; 4-1; 4-2; 4-3
30	L-Lysine, x TMS, 29.32, 1852	1.90E-05	4.7214	0.000127	4-0; 4-1; 4-2; 4-3
31	Putrescine, 4 TMS, 27.09, 1739_saturated.1	2.42E-05	4.6171	0.000157	4-0; 4-1; 4-2; 4-3
32	Mix F Unknown 1, 19.28, 1377	4.98E-05	4.3027	0.000313	4-0; 4-1; 4-2; 4-3
33	D-Fructose-6-phosphate 6TMS, MEOX, 36.72, 2300-putative	7.10E-05	4.1486	0.000431	4-0; 4-1; 4-2; 4-3
34	Unknown_31.554, 1971, m/z191-glucose, pentakis-O-TMS-like_Mix A Unknown 11, 31.54, 1971	7.29E-05	4.137	0.000431	4-0; 4-1; 4-2; 4-3
35	Unknown_35.122, 2184, m/z357	0.000147	3.8321	0.000845	4-0; 4-1; 4-2; 4-3
36	5-Hydroxyindole-3-acetic acid, 3 TMS, 35.49, 2212	0.000169	3.7726	0.000929	4-0; 4-1; 4-2; 4-3
37	Unknown_39.306, 2480, m/z315-D-fructose-6-phosphate-like	0.000171	3.7669	0.000929	4-0; 4-1; 4-2; 4-3
38	Unknown_35.898, 2236, m/z188-putative phosphoric acid	0.000332	3.4786	0.001739	4-0; 4-1; 4-2; 4-3
39	Unknown_22.674, 1515, m/z 176	0.000346	3.4608	0.001739	4-0; 4-1; 4-2; 4-3
40	Unknown_22.674, 1515, m/z 176.1	0.000346	3.4608	0.001739	4-0; 4-1; 4-2; 4-3
41	Putrescine, 4 TMS, 27.13, 1738_saturated	0.000375	3.4254	0.001841	4-0; 4-1; 4-2; 4-3
42	Ascorbic acid, x TMS, 29.19, 1844	0.000413	3.3844	0.001975	4-0; 4-1; 4-2; 4-3
43	artifact.1	0.000724	3.1405	0.003383	4-0; 4-1; 4-2
44	Serine, 3 TMS, 18.98, 1363	0.00081	3.0918	0.003698	3-0; 4-0; 4-1; 4-2
45	Unknown_38.338, 2411, m/z217-uridine-3TMS-like	0.000839	3.0764	0.003747	4-0; 4-2; 4-3
46	Unknown_23.546, 1558, m/z 292-threonic acid-like	0.0009	3.046	0.003931	4-0; 4-1; 4-3
47	Unknown_26.066, 1685, m/z159	0.000967	3.0148	0.004134	3-0; 3-2; 4-2
48	Unknown_34.074, 2121, m/z319-galactose-like	0.001031	2.9866	0.004319	2-0; 4-1; 4-2
49	Unknown_42.354, 2698, m/z289	0.001292	2.8889	0.005298	2-1; 4-2
50	DL-Ornithine, 3 TMS, 24.71, 1623	0.001475	2.8311	0.005931	4-0; 4-1; 4-3
51	Sucrose, 8 TMS, 41.32, 2630.1	0.001543	2.8117	0.00608	2-0; 3-1; 3-2
52	Unknown_24.994, 1631, m/z174	0.001624	2.7893	0.006161	4-0; 4-1; 4-2; 4-3
53	Unknown_24.994, 1631, m/z174.1	0.001624	2.7893	0.006161	4-0; 4-1; 4-2; 4-3
54	Unknown_17.908, 1332, m/z247_succinic acid-like	0.002099	2.6781	0.007811	4-0; 4-2; 4-3
55	Unknown_39.098, 2465, m/z285, m/z285	0.002266	2.6447	0.008281	1-0; 4-0; 3-1; 4-3
56	Unknown_37.130, 2142, m/z315-myo-inositol-2-phosphate-like.1	0.002634	2.5793	0.009338	4-0; 4-1; 4-2; 4-3
57	Unknown, 20.834, 1437, m/z 158	0.002648	2.5771	0.009338	4-0; 4-2; 4-3

58	Unknown_42.674, 2721, m/z361	0.002825	2.5489	0.009791	2-0; 4-2
59	Unknown_42.354, 2698, m/z289.1	0.002987	2.5248	0.010174	4-1; 4-2
60	Unknown_21.714, 1437, m/z 68_hydroxy proline-like	0.003093	2.5096	0.010361	4-0; 4-3
61	Cellobiose, x TMS, 42.19, 2962	0.003516	2.454	0.011586	2-0; 3-2; 4-2
62	Pantothenic acid, O,O,O-TMS-putative	0.003903	2.4086	0.012603	4-0; 4-2; 4-3
63	Mannitol, 6 TMS, 30.6, 1915_saturated	0.00395	2.4034	0.012603	4-0; 4-2; 4-3
64	Adenine, 2 TMS, 29.74, 1869	0.004858	2.3136	0.015256	4-0; 4-1; 4-2; 4-3
65	Unknown_34.17, 2127, m/z319-galactose-like	0.00557	2.2541	0.017224	4-2
66	D-(+)-Turanose, 7 TMS, 42.29, 2702	0.007358	2.1332	0.022408	4-2
67	Unknown_37.130, 2142, m/z315-myo-inositol-2-phosphate-like	0.007511	2.1243	0.022532	4-0; 4-1; 4-2; 4-3
68	Unknown_21.482, 1464, m/z 204	0.009184	2.037	0.027147	
69	Unknown_22.370, 1500, m/z 115	0.010574	1.9758	0.030802	4-0; 4-2
70	Ribulose-5-phosphate, 5 TMS, MEOX, 33.83, 2111	0.010737	1.9691	0.03083	4-1; 4-2; 4-3
71	Unknown_20.61, 1428, m/z 158_tentative glycine	0.011846	1.9264	0.033536	3-1
72	Unknown_20.426, 1421, m/z 172	0.01248	1.9038	0.034841	3-0; 3-2
73	Glycine, 3 TMS, 17.63, 1308	0.013935	1.8559	0.038368	4-0
74	Unknown_44.002, 2820, m/z131	0.016584	1.7803	0.044801	4-0
75	ISTD D-sorbitol 13C6	0.016936	1.7712	0.044801	3-1; 4-3
76	D-sorbitol 13C6 m/z_323	0.01694	1.7711	0.044801	3-1; 4-3
77	D-Fructose-1-phosphate, x TMS, 36.58, 2290	0.017856	1.7482	0.045665	4-0; 4-1; 4-2
78	Potential artifact	0.017918	1.7467	0.045665	1-0
79	Unknown_28.042, 1784, m/z174	0.017948	1.746	0.045665	4-0; 4-3
80	D-(+)-Galactose, 5 TMS, MEOX, 29.94, 1880	0.019223	1.7162	0.048298	4-0; 4-1

Table H.5. Pattern searching template matching approach (negative control-1-2-3-moribund) on **liver** samples to determine analytes with significant comparisons between **sampling periods** (only showing metabolites with FDR < 0.05).

#	Metabolite name	correlation	t-stat	p-value	FDR
1	L-Glutamic Acid, 2 TMS, 22.75, 1519_saturated	-0.64101	-6.415	2.62E-08	1.26E-06
2	L-Pyroglutamic acid, 2 TMS, 22.76, 1520_saturated	-0.6409	-6.4132	2.64E-08	1.26E-06
3	saturated_L-Pyroglutamic acid, 2 TMS, 22.76, 1520	-0.64034	-6.4037	2.74E-08	1.26E-06
4	Gallic acid, x TMS, 22.73, 1520_saturated	-0.64029	-6.4027	2.75E-08	1.26E-06
5	L-Glutamic acid, 2 TMS, 22.7, 1519_saturated	-0.63829	-6.3689	3.13E-08	1.26E-06
6	L-Glutamic acid, 2 TMS, 22.7, 1519_saturated.1	-0.61514	-5.993	1.33E-07	4.45E-06
7	Putrescine, x TMS, 22.45, 1506_putative	0.60632	5.8566	2.23E-07	6.42E-06
8	Putrescine, 4 TMS, 27.09, 1739	0.56301	5.2328	2.32E-06	5.68E-05
9	Putrescine, 4 TMS, 27.09, 1739_saturated.2	0.56119	5.208	2.54E-06	5.68E-05
10	Putrescine, 4 TMS, 27.09, 1739_saturated	0.55796	5.1644	2.99E-06	6.00E-05
11	L-Isoleucine, 2 TMS, 17.32, 1295	0.55359	5.1059	3.70E-06	6.69E-05
12	L-Leucine, 2 TMS, 16.74, 1274	0.55202	5.0852	3.99E-06	6.69E-05
13	Mix F Unknown 1, 19.28, 1377	-0.54465	-4.9884	5.68E-06	8.79E-05
14	g-Aminobutyric acid, 3 TMS, 22.9, 1526	-0.52173	-4.6975	1.62E-05	0.000229
15	Unknown_21.778, 1476, m/z234_arabino-hexos-2-ulose-like	-0.52054	-4.6828	1.71E-05	0.000229

16	Glutamic acid, 3 TMS, 24.79, 1623	-0.51368	-4.5988	2.30E-05	0.000289
17	Unknown_23.930, 1578, m/z129	-0.50309	-4.4714	3.59E-05	0.000425
18	Putrescine, 4 TMS, 27.09, 1739_saturated.1	0.49762	4.4066	4.50E-05	0.000502
19	Glutamic acid, 3 TMS, 24.79, 1623_saturated	-0.49588	-4.3862	4.83E-05	0.000507
20	Glutamic acid, 3 TMS, 24.79, 1623_saturated.1	-0.49482	-4.3738	5.04E-05	0.000507
21	Citric acid, 4 TMS, 28.69, 1817	-0.48927	-4.3092	6.30E-05	0.000603
22	Mix J Unknown 3, 21.95, 1484_malic acid-like	-0.48808	-4.2954	6.60E-05	0.000603
23	Fumaric acid, 2 TMS, 18.29, 1357	-0.48676	-4.2802	6.96E-05	0.000608
24	Serine, 3 TMS, 18.98, 1363	0.48474	4.2569	7.53E-05	0.000631
25	Creatine. x TMS, 23.39, 1551	0.46729	4.0598	0.000147	0.001148
26	Unknown_35.122, 2184, m/z357	-0.46696	-4.0561	0.000148	0.001148
27	Unknown_23.546, 1558, m/z 292-threonic acid-like	-0.46317	-4.0143	0.000171	0.001271
28	a-Ketoglutaric acid, x TMS, 23.95, 1578	-0.44826	-3.8518	0.000291	0.002092
29	Glycine, 3 TMS, 17.63, 1308	0.44285	3.7939	0.000352	0.002438
30	5-Hydroxyindole-3-acetic acid, 3 TMS, 35.49, 2212	0.43288	3.6885	0.000493	0.003305
31	Unknown_38.802, 2301, m/z387-D-mannose-6-phosphate-like	-0.40395	-3.3919	0.001244	0.008069
32	L-Lysine, x TMS, 29.32, 1852	0.40261	3.3784	0.001297	0.008144
33	D-Fructose-6-phosphate 6TMS, MEOX, 36.72, 2300-putative	-0.40072	-3.3595	0.001373	0.008363
34	D-Fructose-6-phosphate 6TMS, MEOX, 36.72, 2300-putative.2	-0.38862	-3.2397	0.001968	0.011633
35	Unknown_26.066, 1685, m/z159	-0.3844	-3.1983	0.002224	0.012772
36	Unknown_22.674, 1515, m/z 176	0.38204	3.1754	0.00238	0.012927
37	Unknown_22.674, 1515, m/z 176.1	0.38204	3.1754	0.00238	0.012927
38	Putrescine, 4 TMS, 27.13, 1738_saturated	0.38075	3.1628	0.002469	0.013058
39	Pantothenic acid, O,O,O-TMS-putative	0.36494	3.0108	0.003831	0.019532
40	Unknown_22.370, 1500, m/z 115	0.3644	3.0057	0.003887	0.019532
41	Unknown_44.002, 2820, m/z131	0.36194	2.9824	0.004153	0.020362
42	Mix N Unknown 1, 22.98, 1532	-0.3537	-2.9046	0.005168	0.024735
43	Unknown_40.226, 2546, m/z387-glucose-6-phosphate-like	-0.35072	-2.8767	0.005586	0.026109
44	D-Glucose-6-phosphate, 6 TMS, MEOX, 37.23, 2332	-0.34723	-2.8441	0.006111	0.027918
45	D-Fructose-6-phosphate 6TMS, MEOX, 36.72, 2300-putative.1	-0.34244	-2.7996	0.006904	0.030339
46	D-Glucose-6-phosphate, 6 TMS, MEOX, 36.95, 2312	-0.34222	-2.7975	0.006943	0.030339
47	DL-Ornithine, 3 TMS, 24.71, 1623	0.34098	2.7861	0.007164	0.030638
48	D-(+)-Galactose, 5 TMS, MEOX, 29.94, 1880	-0.33519	-2.7327	0.008276	0.034657
49	D-Fructose-1-phosphate, x TMS, 36.58, 2290	-0.33004	-2.6856	0.009387	0.038479
50	Unknown_38.338, 2411, m/z217-uridine-3TMS-like	-0.32924	-2.6783	0.009572	0.038479
51	L-Phenylalanine, 1 TMS, 23.37, 1550	0.32285	2.6202	0.011156	0.042915
52	Unknown_24.994, 1631, m/z174	-0.32226	-2.6148	0.011316	0.042915
53	Unknown_24.994, 1631, m/z174.1	-0.32226	-2.6148	0.011316	0.042915
54	Unknown_31.554, 1971, m/z191-glucose, pentakis-O-TMS-like_Mix A Unknown 11, 31.54, 1971	-0.31949	-2.5898	0.01208	0.044963
55	Unknown_28.530, 1808, m/z 357-ribulose 5-phosphate-like	-0.31708	-2.568	0.012781	0.046709

Table H.6. Significance Analysis of Microarrays on **liver** samples to determine analytes with significant differences between **sampling periods** (only showing metabolites with FDR < 0.05). D-sorbitol (spike-in) has been highlighted in pink.

#	Metabolite name	d.value	stdev	rawp	FDR
1	5-Hydroxyindole-3-acetic acid, 3 TMS, 35.49, 2212	1.9505	2.2745	0	0
2	Citric acid, 4 TMS, 28.69, 1817	1.9392	0.88996	0	0
3	Putrescine, x TMS, 22.45, 1506_putative	1.7977	0.98476	0	0
4	a-Ketoglutaric acid, x TMS, 23.95, 1578	1.7176	1.2817	9.95E-05	0.00097
5	Unknown_38.802, 2301, m/z387-D-mannose-6-phosphate	1.6512	0.75575	9.95E-05	0.00097
6	Mannitol, 6 TMS, 30.6, 1915_saturated	1.6224	3.3272	9.95E-05	0.00097
7	Unknown_40.226, 2546, m/z387-glucose-6-phosphate-l	1.6062	1.1876	9.95E-05	0.00097
8	Putrescine, 4 TMS, 27.09, 1739	1.5086	0.6288	0.000199	0.001359
9	Putrescine, 4 TMS, 27.09, 1739_saturated.2	1.505	0.64012	0.000199	0.001359
10	Putrescine, 4 TMS, 27.09, 1739_saturated	1.504	0.65107	0.000199	0.001359
11	Unknown_21.778, 1476, m/z234_arabino-hexos-2-ulose	1.4887	0.78566	0.000249	0.001544
12	artifact.1	1.465	1.9745	0.000299	0.001598
13	Mix J Unknown 3, 21.95, 1484_malic acid-like	1.4328	0.47877	0.000398	0.001598
14	Creatine. x TMS, 23.39, 1551	1.4303	1.0862	0.000398	0.001598
15	D-(+)-Galactose, 5 TMS, MEOX, 29.94, 1880	1.4126	4.3866	0.000398	0.001598
16	D-Fructose-6-phosphate 6TMS, MEOX, 36.72, 2300-put	1.4069	0.71765	0.000398	0.001598
17	Unknown_35.898, 2236, m/z188-putative phosphoric a	1.4027	1.6303	0.000398	0.001598
18	D-Fructose-6-phosphate 6TMS, MEOX, 36.72, 2300-put	1.3896	1.2833	0.000448	0.001617
19	Unknown_42.354, 2698, m/z289	1.3801	2.033	0.000498	0.001617
20	Unknown_23.930, 1578, m/z129	1.3788	0.99012	0.000498	0.001617
21	D-Glucose-6-phosphate, 6 TMS, MEOX, 37.23, 2332	1.3609	0.82494	0.000498	0.001617
22	Unknown_35.122, 2184, m/z357	1.3186	1.3315	0.000597	0.001853
23	L-Isoleucine, 2 TMS, 17.32, 1295	1.3016	0.25981	0.000647	0.001902
24	D-Fructose-6-phosphate 6TMS, MEOX, 36.72, 2300-put	1.2836	0.81599	0.000697	0.001902
25	D-Glucose-6-phosphate, 6 TMS, MEOX, 36.95, 2312	1.2819	0.8164	0.000697	0.001902
26	Putrescine, 4 TMS, 27.09, 1739_saturated.1	1.2613	0.99624	0.000896	0.002351
27	g-Aminobutyric acid, 3 TMS, 22.9, 1526	1.2201	0.77971	0.001144	0.002893
28	L-Lysine, x TMS, 29.32, 1852	1.2137	0.92575	0.001194	0.002911
29	Unknown_39.306, 2480, m/z315-D-fructose-6-phosphat	1.1961	1.2071	0.001244	0.002928
30	Unknown_31.554, 1971, m/z191-glucose, pentakis-O-T	1.1774	1.0541	0.001542	0.003506
31	Fumaric acid, 2 TMS, 18.29, 1357	1.1746	0.5201	0.001592	0.003506
32	Putrescine, 4 TMS, 27.13, 1738_saturated	1.1371	1.2763	0.001791	0.003821
33	Unknown_21.714, 1437, m/z 68_hydroxy proline-like	1.1151	1.8265	0.002139	0.004426
34	Mix F Unknown 1, 19.28, 1377	1.1079	0.93459	0.002338	0.004695
35	Sucrose, 8 TMS, 41.32, 2630.1	1.0505	1.4709	0.002935	0.005725
36	Adenine, 2 TMS, 29.74, 1869	1.0163	1.7853	0.003184	0.005781
37	ISTD D-sorbitol 13C6	1.0077	2.454	0.003333	0.005781
38	D-sorbitol 13C6 m/z_323	1.0077	2.454	0.003333	0.005781
39	D-(+)-Turanose, 7 TMS, 42.29, 2702	1.0012	1.9317	0.003383	0.005781
40	Ascorbic acid, x TMS, 29.19, 1844	0.98812	1.0924	0.003582	0.005781
41	Glutamic acid, 3 TMS, 24.79, 1623	0.98442	0.40255	0.003582	0.005781

42	Unknown, 20.834, 1437, m/z 158	0.97514	1.4865	0.003781	0.005781
43	Gallic acid, x TMS, 22.73, 1520_saturated	0.96362	0.21818	0.00398	0.005781
44	L-Glutamic Acid, 2 TMS, 22.75, 1519_saturated	0.96342	0.21835	0.00398	0.005781
45	L-Pyroglutamic acid, 2 TMS, 22.76, 1520_saturated	0.96276	0.21844	0.00398	0.005781
46	L-Glutamic acid, 2 TMS, 22.7, 1519_saturated	0.96188	0.21577	0.00398	0.005781
47	saturated_L-Pyroglutamic acid, 2 TMS, 22.76, 1520	0.96172	0.21875	0.00398	0.005781
48	Potential artifact	0.95522	2.3134	0.004179	0.005944
49	Glutamic acid, 3 TMS, 24.79, 1623_saturated	0.93993	0.42527	0.004577	0.006249
50	Glutamic acid, 3 TMS, 24.79, 1623_saturated.1	0.9373	0.42445	0.004577	0.006249
51	L-Glutamic acid, 2 TMS, 22.7, 1519_saturated.1	0.93109	0.21994	0.004925	0.006541
52	Unknown_34.074, 2121, m/z319-galactose-like	0.92798	1.1745	0.005174	0.006541
53	Unknown_42.674, 2721, m/z361	0.92767	1.4142	0.005174	0.006541
54	Unknown_42.354, 2698, m/z289.1	0.92484	1.4246	0.005174	0.006541
55	Unknown_38.338, 2411, m/z217-uridine-3TMS-like	0.91242	1.1115	0.005423	0.006731
56	Unknown_40.714, 2581, m/z217.2	0.89466	2.2395	0.00597	0.007144
57	Urea, 2 TMS, 16.14, 1249	0.89419	5.5806	0.00602	0.007144
58	Cellobiose, x TMS, 42.19, 2962	0.89045	1.4046	0.00607	0.007144
59	Unknown_41.866, 2664, m/z204	0.88339	2.1891	0.006219	0.007196
60	Unknown_39.098, 2465, m/z285, m/z285	0.87922	1.2674	0.006468	0.007359
61	L-Leucine, 2 TMS, 16.74, 1274	0.86174	0.27685	0.007114	0.007962
62	Unknown_26.066, 1685, m/z159	0.83377	1.0221	0.008309	0.009148
63	Unknown_40.714, 2581, m/z217	0.82612	2.0522	0.008856	0.009446
64	Unknown_37.130, 2142, m/z315-myo-inositol-2-phosph	0.8261	1.2088	0.008856	0.009446
65	Unknown_34.17, 2127, m/z319-galactose-like	0.77847	1.3102	0.011095	0.011652
66	Unknown_24.994, 1631, m/z174.1	0.75572	0.9943	0.012687	0.012927
67	Unknown_24.994, 1631, m/z174	0.75572	0.9943	0.012687	0.012927
68	Unknown_37.130, 2142, m/z315-myo-inositol-2-phosph	0.73612	1.3071	0.01393	0.01378
69	Unknown_21.482, 1464, m/z 204	0.73347	1.3638	0.01403	0.01378
70	Unknown_42.354, 2704, m/z217	0.73276	2.2488	0.014129	0.01378
71	Unknown_44.002, 2820, m/z131	0.70213	1.5	0.016866	0.016217
72	likely artifact-glucose-like.1	0.68067	3.2962	0.019502	0.018238
73	likely artifact-glucose-like	0.68067	3.2962	0.019502	0.018238
74	Unknown_43.018, 2746, m/z361	0.67852	1.9545	0.019801	0.018267
75	Unknown_23.546, 1558, m/z 292-threonic acid-like	0.65716	0.76669	0.021891	0.019925
76	Unknown_20.61, 1428, m/z 158_tentative glycine	0.64809	1.2449	0.023234	0.02064
77	Unknown_40.226, 2546, m/z387-glucose-6-phosphate-l	0.64569	1.7039	0.023483	0.02064
78	DL-Ornithine, 3 TMS, 24.71, 1623	0.64455	0.81299	0.023582	0.02064
79	L-Threonine, 2 TMS, 17.37, 1298	0.62563	1.419	0.025821	0.022313
80	Pantothenic acid, O,O,O-TMS-putative	0.59988	0.89215	0.030448	0.025745
81	D-(+)-Glucose, 5 TMS, MEOX, 30.38, 1902_saturated	0.59916	3.4665	0.030547	0.025745
82	L-Methionine, 1 TMS, 20.27, 1416_putative.2	0.5923	2.0672	0.031642	0.026343
83	Unknown_36.242, 2261, m/z315	0.59003	1.614	0.03209	0.026394
84	D-sorbitol-1-13C m/z_320	0.58555	2.6505	0.033035	0.026848
85	Ribulose-5-phosphate, 5 TMS, MEOX, 33.83, 2111	0.58004	1.0637	0.034428	0.027527
86	D-(+)-Galactose, 5 TMS, MEOX, 29.94, 1880_saturate	0.57876	1.5635	0.034677	0.027527
87	Unknown_22.370, 1500, m/z 115	0.56684	1.0313	0.037363	0.029041
88	L-Methionine, 1 TMS, 20.27, 1416_putative.1	0.56487	2.0638	0.037861	0.029041

89	L-Methionine, 1 TMS, 20.27, 1416_putative	0.56487	2.0638	0.037861	0.029041
90	Unknown_28.530, 1808, m/z 357-ribulose 5-phosphate	0.54319	1.248	0.042836	0.032492
91	Serine, 2 TMS, 16.43, 1260	0.53775	1.6998	0.044229	0.03318
92	Serine, 3 TMS, 18.98, 1363	0.53331	0.59679	0.045572	0.033816
93	Unknown_17.908, 1332, m/z247_succinic acid-like	0.52843	0.68918	0.046866	0.034402
94	Unknown_53.63, 3702, m/z311-stearic acid-like	0.51827	3.4229	0.048657	0.035337
95	Mix N Unknown 1, 22.98, 1532	0.51505	1.3557	0.049453	0.035537
96	D-Fructose-1-phosphate, x TMS, 36.58, 2290	0.5104	1.0352	0.050896	0.036193
97	Unknown_40.714, 2581, m/z217.1	0.50194	1.5246	0.053234	0.037465
98	Unknown_22.674, 1515, m/z 176.1	0.49891	0.49074	0.054478	0.037566
99	Unknown_22.674, 1515, m/z 176	0.49891	0.49074	0.054478	0.037566
100	Unknown_24.53, 1608, m/z 156	0.49262	1.431	0.056617	0.038651
101	Hypoxanthine, 2 TMS, 28.53, 1812, purine derivativ	0.47941	2.6727	0.061294	0.041429
102	Unknown_51.603, 3505, m/z283-palmitic acid-like	0.46872	3.0233	0.065522	0.043853
103	Mannitol, 6 TMS, 30.6, 1915 / D-Sorbitol, 6 TMS,	0.4521	1.0577	0.073831	0.048934

Table H.7. Variable Importance in Projection measures of the top 20 ranked analytes (sorted by component one) from PLS-DA of **skin** samples, grouping by **sample period**. D-sorbitol (spike-in) has been highlighted in pink.

#	Metabolite name	Comp. 1	Comp. 2	Comp. 3	Comp. 4	Comp. 5
1	Unknown_46.866, 3064, m/z169	2.6077	2.1017	2.0228	2.043	2.0316
2	Unknown_46.848, 3063, m/z169	2.5473	2.0512	1.9575	1.9911	1.9812
3	Unknown_21.778, 1476, m/z234_arabino-hexos-2-ulose-like	2.2531	1.8961	1.7875	1.7486	1.7108
4	a-Ketoglutaric acid, x TMS, 23.95, 1578	2.2391	2.0479	1.8545	1.7767	1.7584
5	D-sorbitol-1-13C m/z_320	2.1952	2.0519	2.0143	1.9344	1.888
6	Mix C Unknown 3, 24.71, 1617	2.1843	1.9059	1.7035	1.7289	1.694
7	Unknown_22.954, 1529, m/z 160	2.1134	1.9259	1.7215	1.6556	1.6242
8	Mix N Unknown 1, 22.98, 1532	2.1063	1.8852	1.7077	1.6393	1.6028
9	Unknown_23.546, 1558, m/z 292-threonic acid-like	2.0355	1.7542	1.5918	1.5966	1.5912
10	L-Threonine, 2 TMS, 17.37, 1298	2.0136	1.6289	1.4761	1.4195	1.4862
11	Mannitol, 6 TMS, 30.6, 1915_saturated	1.9965	1.9687	1.9404	1.8707	1.8246
12	Putrescine, x TMS, 22.45, 1506_putative	1.9353	1.6905	1.5114	1.4719	1.4402
13	Unknown_26.066, 1685, m/z159	1.9217	1.5554	1.4016	1.3915	1.3572
14	Adenine, 2 TMS, 29.74, 1869	1.8514	1.6316	1.4988	1.4342	1.404
15	Serine, 2 TMS, 16.43, 1260	1.7681	1.4334	1.3723	1.3128	1.3063
16	Aspartic acid, 2 TMS, 20.54, 1428	1.7173	1.7316	1.5481	1.4904	1.4551
17	L-Threonine, 3 TMS, 19.59, 1387	1.6906	1.639	1.6158	1.5639	1.5267
18	Putrescine, 4 TMS, 27.09, 1739_saturated	1.6304	1.4625	1.317	1.2632	1.2336

19	Putrescine, 4 TMS, 27.09, 1739_saturated.2	1.6292	1.4626	1.3167	1.2629	1.2333
20	Putrescine, 4 TMS, 27.09, 1739	1.6282	1.4618	1.316	1.2621	1.2326

Table H.8. Variable Importance in Projection measures of the top 20 ranked analytes (sorted by component one) from PLS-DA of **liver** samples, grouping by **sample period**.

#	Metabolite name	Comp. 1	Comp. 2	Comp. 3	Comp. 4	Comp. 5
1	Putrescine, x TMS, 22.45, 1506_putative	2.5617	2.3126	2.1257	2.0383	1.9892
2	5-Hydroxyindole-3-acetic acid, 3 TMS, 35.49, 2212	2.4829	2.2033	2.0312	1.9855	1.9379
3	D-(+)-Galactose, 5 TMS, MEOX, 29.94, 1880	2.4324	2.0264	1.9417	1.9981	1.9536
4	Unknown_35.122, 2184, m/z357	2.0546	1.7031	1.6363	1.5831	1.5692
5	Mix F Unknown 1, 19.28, 1377	2.0497	1.7884	1.6763	1.6085	1.5703
6	Citric acid, 4 TMS, 28.69, 1817	2.0435	1.7606	1.731	1.6574	1.6193
7	a-Ketoglutaric acid, x TMS, 23.95, 1578	2.0414	1.7016	1.6363	1.5934	1.5583
8	Unknown_23.930, 1578, m/z129	2.0117	1.7324	1.5925	1.5242	1.4905
9	Putrescine, 4 TMS, 27.09, 1739_saturated.2	2.0064	1.6893	1.5581	1.4961	1.4612
10	Putrescine, 4 TMS, 27.09, 1739	2.0045	1.689	1.558	1.4963	1.4612
11	Putrescine, 4 TMS, 27.09, 1739_saturated	2.0037	1.6847	1.5539	1.4918	1.4573
12	Unknown_21.778, 1476, m/z234_arabino-hexos-2-ulose-like	1.9673	1.6645	1.5424	1.4892	1.4532
13	Putrescine, 4 TMS, 27.09, 1739_saturated.1	1.9601	1.6591	1.5486	1.49	1.4549
14	Creatine. x TMS, 23.39, 1551	1.9413	1.6129	1.4819	1.5126	1.4805
15	g-Aminobutyric acid, 3 TMS, 22.9, 1526	1.8831	1.7769	1.6834	1.6129	1.5731
16	D-Fructose-6-phosphate 6TMS, MEOX, 36.72, 2300-putative	1.7552	1.5008	1.395	1.3557	1.3294
17	Unknown_53.63, 3702, m/z311-stearic acid-like	1.7233	1.6161	1.505	1.6404	1.6358
18	Putrescine, 4 TMS, 27.13, 1738_saturated	1.6111	1.3445	1.3323	1.2821	1.259
19	Mix J Unknown 3, 21.95, 1484_malic acid-like	1.5989	1.33	1.327	1.2699	1.2388
20	L-Glutamic Acid, 2 TMS, 22.75, 1519_saturated	1.574	1.3558	1.2531	1.2151	1.1868

Table H.9. One-way ANOVA Tukey's honestly significant difference post-hoc tests on **skin** samples to determine significant comparisons between populations (only showing metabolites with FDR < 0.05).

#	Metabolite name	p.value	-log10(p)	FDR	Tukey's HSD
1	Pantothenic acid, O,O,O-TMS-putative	5.14E-05	4.2892	0.010429	Grey Mare-Eucumbene; Kiandra-Eucumbene
2	Myo-Inositol, 6 TMS, 33.38, 2081	0.000211	3.6762	0.018693	Kiandra-Eucumbene; Kiandra-Grey Mare
3	Unknown_40.714, 2581, m/z217.2	0.000288	3.5404	0.018693	Grey Mare-Eucumbene; Kiandra-Eucumbene
4	Unknown_35.234, 2190, m/z200-	0.000431	3.3651	0.018693	Grey Mare-Eucumbene; Kiandra-Grey Mare

	sperimine-like				
5	Unknown_24.994, 1631, m/z174	0.000553	3.2577	0.018693	Grey Mare-Eucumbene; Kiandra-Eucumbene
6	Unknown_24.994, 1631, m/z174.1	0.000553	3.2577	0.018693	Grey Mare-Eucumbene; Kiandra-Eucumbene
7	L-Leucine, 2 TMS, 16.74, 1274	0.000717	3.1446	0.020789	Kiandra-Eucumbene; Kiandra-Grey Mare
8	Unknown_40.714, 2581, m/z217	0.000938	3.0277	0.023248	Kiandra-Eucumbene
9	L-Isoleucine, 2 TMS, 17.32, 1295	0.001031	2.9869	0.023248	Kiandra-Eucumbene
10	Unknown_22.370, 1500, m/z 115	0.001294	2.8881	0.026268	Kiandra-Eucumbene; Kiandra-Grey Mare

Table H.10. Pattern searching template matching approach (Eucumbene-Grey Mare-Kiandra) on **skin** samples to determine analytes with significant comparisons between **populations** (only showing metabolites with FDR < 0.05).

#	Metabolite name	correlation	t-stat	p-value	FDR
1	Pantothenic acid, O,O,O-TMS-putative	-0.52519	-4.364	6.40E-05	0.009059
2	Unknown_40.714, 2581, m/z217	0.49659	4.0455	0.000181	0.009059
3	L-Isoleucine, 2 TMS, 17.32, 1295	0.49353	4.0125	0.000201	0.009059
4	L-Leucine, 2 TMS, 16.74, 1274	0.4929	4.0058	0.000205	0.009059
5	Unknown_24.994, 1631, m/z174	-0.48471	-3.9185	0.000271	0.009059
6	Unknown_24.994, 1631, m/z174.1	-0.48471	-3.9185	0.000271	0.009059
7	Unknown_40.714, 2581, m/z217.2	0.48011	3.8701	0.000316	0.009059
8	Unknown_22.370, 1500, m/z 115	0.47638	3.8312	0.000357	0.009059
9	Unknown_22.954, 1529, m/z 160	-0.44351	-3.499	0.000991	0.022351
10	Unknown_22.674, 1515, m/z 176	0.41667	3.2411	0.002121	0.039146
11	Unknown_22.674, 1515, m/z 176.1	0.41667	3.2411	0.002121	0.039146
12	L-Proline, 2 TMS, 17.43, 1300	0.40588	3.1403	0.002832	0.044236
13	Creatine. x TMS, 23.39, 1551	0.40588	3.1403	0.002833	0.044236
14	D-(-)-Ribose, 4 TMS, MEOX, 25.89, 1678	0.39998	3.0859	0.003305	0.047918

Table H.11. Significance Analysis of Microarrays on **skin** samples to determine analytes with significant differences between **populations** (only showing metabolites with FDR < 0.05).

#	Metabolite name	d.value	stdev	rawp	FDR
1	Unknown_40.714, 2581, m/z217.2	6.7004	2.0135	4.93E-05	0.00693
2	Unknown_35.234, 2190, m/z200-sperimine-like	6.1609	1.8633	0.000148	0.00693
3	Pantothenic acid, O,O,O-TMS-putative	6.1058	0.90007	0.000148	0.00693
4	Unknown_24.994, 1631, m/z174.1	5.5084	1.5054	0.000493	0.013861

5	Unknown_24.994, 1631, m/z174	5.5084	1.5054	0.000493	0.013861
6	Unknown_22.954, 1529, m/z 160	4.5218	2.1662	0.001379	0.032342
7	Myo-Inositol, 6 TMS, 33.38, 2081	4.2248	0.64096	0.00202	0.040593
8	Mix C Unknown 3, 24.71, 1617	4.1242	1.5832	0.002365	0.041583

Table H.12. Variable Importance in Projection measures of the top 20 ranked analytes (sorted by component one) from PLS-DA of **skin** samples, grouping by **population**. D-sorbitol (spike-in) has been highlighted in pink.

#	Metabolite name	Comp. 1	Comp. 2	Comp. 3	Comp. 4	Comp. 5
1	Unknown_40.714, 2581, m/z217.2	2.8368	2.7978	2.4585	2.4545	2.4382
2	Unknown_22.954, 1529, m/z 160	2.5842	2.1158	1.825	1.7727	1.7405
3	Unknown_24.994, 1631, m/z174	2.4437	2.1692	1.8725	1.8932	1.8573
4	Unknown_24.994, 1631, m/z174.1	2.4437	2.1692	1.8725	1.8932	1.8573
5	Unknown_39.602, 2501, m/z174-serotonin-like	2.2691	1.7841	1.6262	1.5834	1.5867
6	Unknown_34.202, 2129, m/z352-putative guanine.1	2.2682	1.8505	1.596	1.6716	1.6319
7	Pantothenic acid, O,O,O-TMS-putative	2.1491	1.7224	1.5514	1.5112	1.4951
8	D-sorbitol-1-13C m/z_319	2.0479	1.8761	1.6474	1.6005	1.5909
9	Aspartic acid, 2 TMS, 20.54, 1428	2.0434	1.8142	1.5647	1.5286	1.4928
10	L-Threonine, 2 TMS, 17.37, 1298	1.931	1.5261	1.3817	1.3418	1.3345
11	Unknown_46.866, 3064, m/z169	1.9045	1.5931	1.4148	1.3746	1.4237
12	Unknown_46.848, 3063, m/z169	1.8652	1.5709	1.3868	1.3481	1.4099
13	D-sorbitol-1-13C m/z_320	1.8397	2.104	1.8204	1.769	1.7367
14	L-Methionine, 1 TMS, 20.27, 1416_putative.2	1.8389	1.6526	1.4914	1.4521	1.4176
15	Unknown_34.202, 2129, m/z352-putative guanine	1.8359	1.9768	1.8298	1.7972	1.7688
16	Unknown_40.714, 2581, m/z217	1.7907	2.0696	1.7951	1.7442	1.716
17	Serotonin, x TMS, 39.11, 2470_saturated	1.7514	1.3821	1.5227	1.4974	1.5077
18	Mix C Unknown 3, 24.71, 1617	1.6997	1.4054	1.2922	1.3179	1.3295
19	saturated_Guanine manual	1.6956	1.3427	1.1698	1.2964	1.2758
20	Mix A Unknown 12, 32.38, 2022	1.6778	1.3215	1.1575	1.1347	1.1546

Table H.13. Variable Importance in Projection measures of the top 20 ranked analytes (sorted by component one) from PLS-DA of **liver** samples, grouping by **population**.

#	Metabolite name	Comp. 1	Comp. 2	Comp. 3	Comp. 4	Comp. 5
1	D-(+)-Turanose, 7 TMS, 42.29, 2702	2.7651	1.8088	1.712	1.6658	1.633
2	Unknown_42.354, 2704, m/z217	2.5663	1.6496	1.6234	1.6032	1.5837
3	Unknown_40.226, 2546, m/z387-glucose-6-phosphate-like.1	2.5283	3.1682	2.9468	2.8493	2.8099

4	Urea, 2 TMS, 16.14, 1249	2.512	2.1668	2.0347	2.0796	2.041
5	Thymine, 2 TMS, 19.94, 1403	2.4853	1.6039	1.4932	1.4801	1.4534
6	Unknown_42.354, 2698, m/z289	2.4627	1.8655	1.7593	1.7017	1.6778
7	Unknown_35.122, 2184, m/z357	2.4343	1.5472	1.5001	1.459	1.4296
8	artifact.1	2.1831	1.6636	1.6518	1.5985	1.6239
9	Unknown_38.338, 2411, m/z217-uridine-3TMS-like	2.1648	1.4203	1.3225	1.3065	1.2985
10	Unknown_28.434, 1803, m/z204	2.0763	1.349	1.3479	1.3086	1.2898
11	L-Lysine, 3 TMS, 26.54, 1712	2.0561	1.3538	1.2482	1.2148	1.2128
12	Unknown_43.018, 2746, m/z361	2.0199	1.5578	1.5603	1.5189	1.4932
13	Unknown_42.354, 2698, m/z289.1	1.9474	1.3039	1.2962	1.2536	1.2467
14	Myo-Inositol, 6 TMS, 33.38, 2081.1	1.895	1.7153	1.5798	1.5424	1.5208
15	Unknown_37.130, 2142, m/z315-myo-inositol-2-phosphate-like	1.8344	1.1931	1.1746	1.136	1.1297
16	D-Fructose-6-phosphate 6TMS, MEOX, 36.72, 2300-putative	1.7481	1.2631	1.1665	1.1282	1.1099
17	Unknown_39.098, 2465, m/z285, m/z285	1.7444	1.4582	1.4481	1.4527	1.4258
18	Sucrose, 8 TMS, 41.32, 2630.1	1.7421	1.1166	1.1544	1.1396	1.1509
19	Sucrose, 8 TMS, 41.32, 2630	1.6786	1.1362	1.0682	1.0383	1.0182
20	Unknown_31.554, 1971, m/z191-glucose, pentakis-O-TMS-like_Mix A Unknown 11, 31.54, 1971	1.6435	1.1227	1.0426	1.0102	0.99119

Table H.14. Important metabolites (from manuscript Table 5.7) and associated Gene Ontology (GO) terms identified from GO term enrichment analysis on differentially expressed gene sets from the associated transcriptomics study.

Only the most specific GO terms for each pathway have been assigned. For more information about GO enrichment analyses, refer to Section 5.3 of this thesis, and Supplementary Information Appendix G, Table G.5.

Search term (metabolite)	Gene Ontology (GO) term	GO ID
Adenine	flavin adenine dinucleotide binding	GO:0050660
Adenine	pyrimidine- and adenine-specific:sodium symporter activity	GO:0015389
Adenine	adenine salvage	GO:0006168
Adenine	tRNA (adenine-N1-)-methyltransferase activity	GO:0016429
Alanine	D-alanine catabolic process	GO:0055130
Alanine	alanine metabolic process	GO:0006522
Aspartic acid	aspartic endopeptidase activity, intramembrane cleaving	GO:0042500
Creatine	phosphocreatine biosynthetic process	GO:0046314
Fructose	fructose 1,6-bisphosphate 1-phosphatase activity	GO:0042132
Fructose	fructose-2,6-bisphosphate 2-phosphatase activity	GO:0004331
Galactose	fucosylgalactoside 3-alpha-galactosyltransferase activity	GO:0004381
Galactose	glycoprotein-fucosylgalactoside alpha-N-acetylgalactosaminyltransferase activity	GO:0004380
Galactose	UDP-N-acetylgalactosamine metabolic process	GO:0019276
Galactose	beta-N-acetylglucosaminylglycopeptide beta-1,4-galactosyltransferase activity	GO:0003831
Galactose	galactose metabolic process	GO:0006012
Galactose	acetylgalactosaminyltransferase activity	GO:0008376
Galactose	procollagen galactosyltransferase activity	GO:0050211
Galactose	UDP-galactose transmembrane transporter activity	GO:0005459
Galactose	UDP-galactose:glucosylceramide beta-1,4-galactosyltransferase activity	GO:0008489
Galactose	UDP-galactose transmembrane transport	GO:0072334
Galactose	galactosylceramide biosynthetic process	GO:0006682
Galactose	N-acetylgalactosaminyl-proteoglycan 3-beta-glucuronosyltransferase activity	GO:0050510
Galactose	2-hydroxyacylsphingosine 1-beta-galactosyltransferase activity	GO:0003851
Galactose	N-acetyl-beta-glucosaminyl-glycoprotein 4-beta-N-acetylgalactosaminyltransferase activity	GO:0033842
Galactose	galactose catabolic process	GO:0019388
Galactose	UDP-galactosyltransferase activity	GO:0035250
Galactose	beta-galactosyl-N-acetylglucosaminylgalactosylglucosyl-ceramide beta-1,3-acetylglucosaminyltransferase activity	GO:0008457
Galactose	alpha-galactosidase activity	GO:0004557
g-aminobutyric	negative regulation of gamma-aminobutyric acid secretion	GO:0014053
g-aminobutyric	gamma-aminobutyric acid metabolic process	GO:0009448
Glucose	UTP:glucose-1-phosphate uridylyltransferase activity	GO:0003983
Glucose	UDP-glucose metabolic process	GO:0006011
Glucose	glucose 6-phosphate metabolic process	GO:0051156

Glucose	cellular glucose homeostasis	GO:0001678
Glucose	glucose binding	GO:0005536
Glucose	UDP-glucose 4-epimerase activity	GO:0003978
Glucose	UDP-glucose 6-dehydrogenase activity	GO:0003979
Glucose	D-glucose transmembrane transporter activity	GO:0055056
Glucose	glucose homeostasis	GO:0042593
Glucose	negative regulation of insulin secretion involved in cellular response to glucose stimulus	GO:0061179
Glutamic acid	glutamate decarboxylase activity	GO:0004351
Glutamic acid	glutamine biosynthetic process	GO:0006542
Glutamic acid	glutamate-ammonia ligase activity	GO:0004356
Glutamic acid	cystine:glutamate antiporter activity	GO:0015327
Glutamic acid	positive regulation of glutamate secretion	GO:0014049
Glutamic acid	glutamate-5-semialdehyde dehydrogenase activity	GO:0004350
Glutamic acid	asparagine synthase (glutamine-hydrolyzing) activity	GO:0004066
Glutamic acid	glutamate 5-kinase activity	GO:0004349
Glutamic acid	N-formylglutamate deformylase activity	GO:0050129
Glutamic acid	gamma-glutamyl-peptidase activity	GO:0034722
Glutamic acid	gamma-glutamyltransferase activity	GO:0003840
Glutamic acid	glutamine metabolic process	GO:0006541
Glutamic acid	protein-glutamine gamma-glutamyltransferase activity	GO:0003810
Glutamic acid	tetrahydrofolylpolyglutamate biosynthetic process	GO:0046901
Glutamic acid	glutamine family amino acid metabolic process	GO:0009064
Guanine	guanine salvage	GO:0006178
Guanine	tRNA (guanine(37)-N(1))-methyltransferase activity	GO:0052906
Inositol	positive regulation of 1-phosphatidylinositol 4-kinase activity	GO:0043128
Inositol	phosphatidylinositol phosphate binding	GO:1901981
Inositol	1-phosphatidylinositol-4-phosphate 3-kinase, class IB complex	GO:0005944
Inositol	phosphatidylinositol 3-kinase regulator activity	GO:0035014
Inositol	regulation of phosphatidylinositol 3-kinase activity	GO:0043551
Inositol	1-phosphatidylinositol-4-phosphate 3-kinase, class IA complex	GO:0005943
Inositol	1-phosphatidylinositol binding	GO:0005545
Inositol	phosphatidylinositol 3-kinase cascade	GO:0014065
Inositol	positive regulation of phosphatidylinositol 3-kinase activity	GO:0043552
Inositol	inositol biosynthetic process	GO:0006021
Inositol	inositol-3-phosphate synthase activity	GO:0004512
Inositol	phosphatidylinositol kinase activity	GO:0052742
Inositol	phosphatidylinositol-mediated signaling	GO:0048015
Isoleucine	isoleucine-tRNA ligase activity	GO:0004822
Lysine	peptidyl-lysine deacetylation	GO:0034983
Lysine	peptidyl-lysine trimethylation	GO:0018023
Methionine	peptide-methionine (R)-S-oxide reductase activity	GO:0033743
Methionine	L-methionine biosynthetic process from S-adenosylmethionine	GO:0019284
Methionine	L-methionine transmembrane transporter activity	GO:0015191
Methionine	L-methionine salvage from methylthioadenosine	GO:0019509
Methionine	S-adenosyl-L-methionine transmembrane transport	GO:1901962
Ornithine	ornithine carbamoyltransferase activity	GO:0004585

Ornithine	ornithine metabolic process	GO:0006591
Ornithine	putrescine biosynthetic process from ornithine	GO:0033387
Ornithine	ornithine decarboxylase activity	GO:0004586
Putrescine	putrescine catabolic process	GO:0009447
Serine	serine-type endopeptidase inhibitor activity	GO:0004867
Serine	serine-type endopeptidase activity	GO:0004252
Serine	L-serine biosynthetic process	GO:0006564
Serine	positive regulation of cyclin-dependent protein serine/threonine kinase activity involved in G2/M transition of mitotic cell cycle	GO:0031662
Serine	phosphatidylserine catabolic process	GO:0006660
Serine	regulation of peptidyl-serine phosphorylation	GO:0033135
Serine	L-serine transport	GO:0015825
Serine	L-serine transmembrane transporter activity	GO:0015194
Serine	negative regulation of Rho-dependent protein serine/threonine kinase activity	GO:2000299
Serine	D-serine catabolic process	GO:0036088
Serine	phosphatidylserine acyl-chain remodeling	GO:0036150
Serine	serine-type carboxypeptidase activity	GO:0004185
Serine	cyclin-dependent protein serine/threonine kinase activity	GO:0004693
Serine	serine C-palmitoyltransferase activity	GO:0004758
Serine	serine C-palmitoyltransferase complex	GO:0017059
Serine	negative regulation of cyclin-dependent protein serine/threonine kinase activity	GO:0045736
Serotonin	serotonin metabolic process	GO:0042428
Serotonin	serotonin secretion, neurotransmission	GO:0060096
Threonine	threonine-type endopeptidase activity	GO:0004298
Threonine	threonine-tRNA ligase activity	GO:0004829
Threonine	threonine metabolic process	GO:0006566
Threonine	positive regulation of peptidyl-threonine phosphorylation	GO:0010800
Threonine	L-threonine 3-dehydrogenase activity	GO:0008743
Threonine	L-threonine catabolic process to glycine	GO:0019518
Urea	urea cycle	GO:0000050
Urea	sulfonylurea receptor activity	GO:0008281
Urea	urea transmembrane transport	GO:0071918
Urea	urea transport	GO:0015840

APPENDIX I: Major Histocompatibility Complex (MHC) study

I.1 Introduction

This appendix has been included in supplement to the study performed in Section 5.2 of this thesis, which has been abbreviated and incorporated into the manuscript below for the purposes of publication.

I.2 PAPER 1: Susceptibility of amphibians to chytridiomycosis is associated with MHC class II conformation

This manuscript submitted to the journal Proceedings of the National Academy of Sciences journal, represents original research led by Arnaud Bataille, the primary investigator. My role in the manuscript involved collection and shipping of tissue samples from the frog exposure experiment (in which I was involved in assisting with experimental study design, I performed the majority of animal husbandry work, conducted the experiment proper, collected data, and wrote up the experimental methodology), and I also contributed substantial editorial input to this manuscript.

The full reference for the manuscript is:
Bataille, A., Cashins, S. D., **Grogan, L. F.**, Skerratt, L. F., Hunter, D., McFadden, M., Scheele, B., Brannelly, L. A., Macris, A., Harlow, P. S., Bell, S., Berger, L., Waldman, B. (submitted) Susceptibility of amphibians to chytridiomycosis is associated with MHC class II conformation.

The following text is a word for word copy of the manuscript submitted to the Proceedings of the National Academy of Sciences journal. Section, table and figure numbering has been added or reformatted for this thesis for ease of reference. Since the journal uses American English, the spelling follows this convention.

I.2.1 Front matter

Susceptibility of amphibians to chytridiomycosis is associated with MHC class II conformation

Arnaud Bataille[1], Scott D. Cashins[2], Laura Grogan[2], Lee F. Skerratt[2], David Hunter[3], Michael McFadden[4], Benjamin Scheele[5], Laura A. Brannelly[2], Amy Macris[5], Peter S. Harlow[4], Sara Bell[2], Lee Berger[2], Bruce Waldman[1*]

[1]School of Biological Sciences, Seoul National University, Seoul 151-747, South Korea.
[2]School of Public Health, Tropical Medicine and Rehabilitation Sciences, James Cook University, Townsville, QLD 4811, Australia.
[3]New South Wales Office of Environment and Heritage, Biodiversity Conservation Section, Queanbeyan, NSW 2620, Australia.
[4]Taronga Conservation Society Australia, Herpetofauna Division, Mosman, NSW 2088, Australia.
[5]Fenner School of Environment and Society, Australian National University, Acton, ACT 2601, Australia

[*] To whom correspondence should be addressed. E-mail: waldman@snu.ac.kr.

Keywords: major histocompatibility complex, chytridiomycosis, evolution, conservation, emerging infectious disease, peptide-binding domain, pocket residue, disease resistance

I.2.2 Abstract

The pathogenic chytrid fungus *Batrachochytrium dendrobatidis* (Bd) causes precipitous population declines in its amphibian hosts around the world. Determining the genetic basis for and immunologic mechanisms that underlie the capability of certain individuals to survive catastrophic epizootics is a necessary step toward saving species from extinction. Some alleles of the major histocompatibility (MHC) may confer on infected frogs effective adaptive immune responses against chytridiomycosis. In wild populations of 11 amphibian species across four continents, we identified specific amino acids of the MHC class II antigen-binding β1 domain (MHCIIβ1) associated with resistance to Bd. Those residues define the binding properties of one pocket of the binding groove critical for antigen recognition (pocket 9). In the laboratory, we experimentally inoculated Australian tree frogs with a virulent Bd culture. Subjects from historically infected populations survived longer and in higher numbers than those from Bd-naïve populations. MHCIIβ1 peptide-binding pocket conformations of individuals that survived matched those prevalent in wild populations living with Bd. Strong signals of selection acting on 5 amino acids comprising pocket 9, as well as on the entire MHC class II β1 domain, are evident among all amphibian species surveyed. Thus, the MHCIIβ1 domain conformation predicts, and may determine, amphibian resistance to chytridiomycosis. Rescuing amphibian biodiversity will depend on our understanding of

amphibian immune defence mechanisms against Bd. The identification of adaptive genetic markers for Bd resistance represents an important step forward toward that goal.

I.2.3 Significance statement

The region of the MHC that binds antigens and presents them to immune cells is highly variable, changing its capacity to recognize and induce immune responses against specific pathogens. In this study, we identified in worldwide amphibian species five amino acid residues forming a specific binding pocket within the MHC molecule that are associated with resistance to a fungal disease causing catastrophic declines in global amphibian populations. With this knowledge, vulnerable species should be readily identifiable before the disease spreads. Furthermore, recovery programmes can be planned to breed disease-resistant amphibians for release.

I.2.4 Introduction

The emerging infectious skin disease chytridiomycosis, induced by the chytrid fungus *Batrachochytrium dendrobatidis* (Bd) (Berger et al., 1998; Longcore et al., 1999), is a leading cause of global amphibian population declines and species extinctions (Fisher et al., 2009b; Skerratt et al., 2007). Efforts are underway around the world to develop strategies to control the disease in the wild and mitigate its effect on susceptible amphibians (McMahon et al., 2014; Woodhams et al., 2011), especially for species that are believed to be extinct in the wild and whose very survival, until reintroduction is plausible, depends on captive management (Griffiths and Pavajeau, 2008). A key step towards disease mitigation is to further our understanding of the evolution and mechanism of amphibian immune defense against Bd and identify specific immunologic characters associated with disease resistance (Rollins-Smith et al., 2011; Woodhams et al., 2011).

The major histocompatibility complex (MHC) encodes receptors at the cell surface that induce and regulate acquired immune responses against pathogens in all vertebrates (Bernatchez and Landry, 2003). In amphibians, MHC allele-specific disease resistance has been identified against *Aeromonas* bacteria (Barribeau et al., 2008), and, importantly, against Bd (Savage and Zamudio, 2011), suggesting that particular features of the MHC molecules can improve their capacity to bind Bd antigens and induce adaptive immune response. However, it has not yet been determined if the level of susceptibility to Bd can be associated with the evolution and selection for MHC variants in global amphibian populations.

Many variable amino acid residue positions associated with disease susceptibility in humans and other studied species are situated in the antigen-binding β1 segment encoded by the exon 2 of the MHC class II B gene (Jones et al., 2006; Tong et al., 2006). Indeed, amino acid changes in this segment can lead to important structural modifications in the binding groove and change the affinity of the MHC molecule for different antigens (Jones et al., 2006; Tong et al., 2006). The MHC class II β1 domain (MHCIIβ1) has been characterized in various amphibian species (Hauswaldt et al., 2007; Kiemnec-Tyburczy et al., 2010; Savage and Zamudio, 2011; Zeisset and Beebee, 2009; Zeisset and Beebee, 2013), with several of the residue positions identified in humans also highly variable and under selection in the species tested (Kiemnec-Tyburczy et al., 2010; Savage and Zamudio, 2011). Notably, the residue β56 was identified as potentially important for Bd peptide binding in the lowland leopard frog, *Rana [Lithobates] yavapaiensis* (Savage and Zamudio, 2011) (designated as codon 46 in the study), although no structural explanation was proposed for this result. Analysis of the amino acid composition and structure of the MHC class II β1 domain in amphibian populations with

different histories of Bd infection could help identify specific conformations of the MHC molecule that would predict resistance to chytridiomycosis.

Here, we use a combination of comparative and experimental analyses to demonstrate selection for MHC conformations that foster the survival of individuals infected by Bd in amphibians across four continents. Amphibian species less susceptible to Bd present very similar conformations at the pocket 9 of the MHCII binding groove and these are lacking in susceptible individuals and species. We find strong signals of selection acting on the amino acids comprising pocket 9 among all amphibian species. We show that these residues have an important role in peptide binding affinity and conformation of the binding groove. This conclusion is supported by results of a laboratory experiment that we conducted in which only subjects sharing the same pocket 9 conformation survived infection. We also demonstrate that protective alleles are undergoing positive selection after Bd invades naïve amphibian populations.

I.2.5 Results and discussion

I.2.5.1 MHCIIβ1-associated Bd resistance in worldwide amphibian species

If specific MHC class IIβ1 alleles are associated with increased resistance to Bd, such alleles would be expected to be frequent in global amphibian populations, especially those with histories of infection by Bd. These alleles should present similar composition at codon positions important for peptide binding and immune response during Bd infection.

We used intron-specific primers to genotype the β1 domain of one MHC class II locus in two amphibian species that historically have been infected by endemic Bd strains in Korea, the oriental fire-bellied toad *Bombina orientalis* (20 individuals, two populations) and the common toad *Bufo gargarizans* (60 individuals, two populations). Neither morbidity nor mortality attributable to chytridiomycosis have been recorded in those two species, despite extensive fieldwork having been undertaken (Bataille et al., 2013). The sequences obtained were aligned with publicly available MHC class IIβ1 sequences from 17 amphibian species with variable susceptibility to Bd (Fig. I.1, and supplementary information Fig. I.5). We examined the amino acid residue composition at 16 codon positions known in humans to affect the properties of the P4, P6, and P9 pockets of the MHC class II peptide-binding groove (Jones et al., 2006; Tong et al., 2006).

The MHCIIβ1 alleles of amphibian species least affected by Bd infection (Bosch and Martinez-Solano, 2006; Daszak et al., 2004; Davidson et al., 2003; Ramsey et al., 2010; Sztatecsny and Glaser, 2011) consistently presented similar residue composition at 4 codon positions associated with the P9 pocket binding groove (β37, β56, β57 and β60; Fig. I.1, Table I.1, and supplementary information Fig. I.5). Alleles most frequently coded for aromatic Pheβ37 or Tyrβ37, acidic residue Aspβ57, aromatic Tyrβ60, and proline at residue 56β (Fig. I.1, Table I.1, and supplementary information Fig. I.5). In contrast, species susceptible to Bd (Savage and Zamudio, 2011; Searle et al., 2011) were more variable at these positions. The *R. yavapaiensis* allele most strongly associated with Bd resistance (*Raya*-Q; Savage and Zamudio, 2011) uniquely encoded valine at residue 56β.

We assessed the selection pressures acting on the MHC class IIβ1 locus by estimating the ratio of non-synonymous to synonymous nucleotide substitutions (ω = dN/dS; positive selection: ω >1). We detected signatures of site-specific positive selection acting on the β1 domain of MHC class II locus B in all amphibian groups tested, including positions 37β, β57 and β60 of the P9 pocket (Table I.2). Importantly, codon positions 37β and 56β were identified as under purifying selection in Korean *Bufo* and *Bombina* spp. (Table I.2), which suggests that alleles presenting the most frequent residues Phe37β and Pro56β confer a strong fitness advantage over other alleles in these genera.

I.2.5.2 Characterization of the MHC class IIβ P9 pocket residues

The differences in P9 pocket residue composition between alleles of resistant and susceptible amphibians may influence binding properties of the pocket peptide (Fig. I.1, Table I.1). Acidic residue Aspβ57, present frequently in alleles of amphibians with low susceptibility to Bd, has been shown to be especially important in human MHC II P9 pocket because it forms a hydrogen bond to an anchor residue of epitopes and a salt bridge with P9 pocket residue Arg76α of the MHCII α1 domain (Jones et al., 2006). We tested whether specific biochemical properties were driving substitutions at the peptide binding sites using property-informed model of evolution (PRIME; Delport et al., 2010). Results confirmed that variation at position β57 was associated with a change in the chemical composition (property α1 in Conan-Stadler set of amino acid properties; Conant et al., 2007) at this site (weight property α1 = -3.496, P = 0.048).

Residue β56 is not usually considered to be important for human MHC II peptide binding (Jones et al., 2006; Tong et al., 2006), but it has been shown to cause conformational changes

that influence binding properties of β57 and an association with type 1 diabetes (Lee et al., 2001). Importantly, this residue has been shown to be under positive selection in various amphibian species (Kiemnec-Tyburczy et al., 2010; Savage and Zamudio, 2011), and to be associated with evolution of Bd resistance in *R. yavapaiensis* (Savage and Zamudio, 2011).

The codon β56 of the vast majority of amphibians less susceptible to Bd coded for proline, the only such amino acid within the peptide binding region of this MHCIIβ locus (Table I.1, Fig. I.5). Proline is an amino acid with a unique conformational rigidity created by the covalent bond of its nitrogen atom within a five atoms ring, strongly affecting protein secondary structure such as alpha helices (Morgan and Rubenstein, 2013). Modeling of the MHCIIβ1 three-dimensional structure positioned the Proβ56 in the middle and the outside of the MHCIIβ1 alpha helix (Fig. I.2), which is a rare position for this residue, usually excluded from alpha helices and beta sheets, or positioned at the ends of these motifs (Morgan and Rubenstein, 2013). The model shows that, by its location, the Proβ56 may directly influence how the peptide-binding, acidic Aspβ57 is positioned within the P9 pocket (Fig. I.2) (Morgan and Rubenstein, 2013). Further exploration of codon 56β variation across model vertebrate taxa demonstrates that Pro56β is widely present in vertebrates, supporting its adaptive advantage and conformational role in the MHC II binding groove (Supplementary Information Fig. I.6).

I.2.5.3 MHCIIβ1 P9 conformation predicts higher survival in experimental infection

We challenged endangered Australian alpine tree frogs (*Litoria verreauxii alpina*) originating from two sites (A and B) with long histories of Bd infection and a third that had never been infected by Bd (C). After inoculating frogs with Bd, site A subjects survived significantly longer than those from the other two sites (Kaplan-Meier $p = 0.001$, Fig. I.3, Supplementary Information Table I.3). Selection for resistance to Bd thus presumably occurs over time but differentially among sites. Many individuals presented high infection intensity and died within 5 weeks (Fig. I.3). Infection loads in some individuals from sites A and C stabilized after 5 weeks but increased afterwards, leading to morbidity and mortality after 8 weeks. Six of 178 frogs (5 from site A, 1 from site C) demonstrated greatly reduced loads after 3 weeks, allowing survival until the end of the experiment (Fig. I.3). These results suggest adaptive immune system-mediated recovery.

We genotyped the β1 domain of one MHC class II locus in alpine tree frogs (*L. v. alpina*) experimentally exposed to Bd. Twenty-two MHC class IIβ1 alleles were recovered, with 8

alleles identified among the 6 surviving individuals (*Livea*-1, 2, 3b, 5a, 5b, 11, 13, and 14; Fig. I.4, and Supplementary Information Table I.3, Fig. I.5). These eight alleles had identical residues at the 5 codon positions associated with the P9 pocket, corresponding to the conformation identified in worldwide amphibians. The other 11 codon positions associated with P1, P4, and P6 pockets were variable among these alleles (Fig. I.1, and Supplmentary Information Fig. I.5). Another 6 alleles (*Livea*-3a, 5c, 12, 16, 17, and 21) were characterized by the same P9 pocket residue composition as alleles of the survivors, while the remaining 9 alleles recovered from individuals that died showed various levels of variation from this configuration (Figs. I.1 and I.4, Table I.1, and Supplementary Information Fig. I.5).

We used Cox proportional hazards model to determine whether, among other parameters, P9 pocket residue composition and MHC heterozygosity affected the survivorship of subjects during the experiment. The model that best fit the data included P9 pocket residue composition, the clutch and site of origin, and the interaction between P9 composition and the maximum Bd infection load (LRT=45.37, df = 10, $P < 0.0001$). Having the specific P9 pocket composition associated with Bd resistance in both MHCII alleles significantly increased the chance of survival of the subjects ($P = 0.02$, Fig. I.4). Having only one allele with this P9 composition did not significantly improve survival ($P = 0.82$). MHC alleles are codominantly expressed (Nakamura et al., 1986), so two doses of MHC molecules binding preferentially to Bd peptides may be required to offset the pathogen's mechanism of attack on the adaptive immune system (Fites et al., 2013). Alternatively, MHC alleles with the protective P9 conformation may interact more efficiently with the specific repertoire of T-cell receptors or T-cell subsets that respond to Bd antigens (Lovitch and Unanue, 2005). Contrary to results from an earlier infection study with the lowland leopard frog *Rana* [*Lithobates*] *yavapaiensis* (Savage and Zamudio, 2011), we did not observe any significant effect of MHC heterozygosity on survival ($P = 0.30$), although 5 out of 6 surviving individuals had heterozygote MHC genotypes (Table I.3). This result may be due to the small number of survivors in our study.

The MHC class IIβ1 genotype of an additional 29 individuals also exclusively contained alleles with the same residue composition at positions β9, β37, β56, β57 and β60 of the pocket P9 as the 6 survivors (Fig. I.4, Table I.3). This small number of survivors suggests that the advantage conferred by the presence of MHC class IIβ1 molecules with this specific P9 pocket configuration for the resistance against Bd infection is dependent on other factors, such as individual variation in other components of the innate and adaptive immune systems.

The very high infection loads observed during the experiment (over 1 million zoospore equivalents [ZSE] in many subjects; Fig. I.3, Table I.3) indicates the high virulence of the Bd strain to *L. v. alpina* which may have resulted in effective inhibition of adaptive immunity (Fites et al., 2013).

I.2.5.4 Positive selection at P9 pocket residues and in wild L. v. alpina populations

We assessed the selection pressures acting on the *L. v. alpina* MHC class IIβ1 locus. A selection model allowing for site-specific positive selection fit better to the MHC data (ω = 3.14, LRT = 6.58, P = 0.04). Along with other peptide binding residues, residues β37 and β57 of the P9 pocket were identified as being under positive selection using random-effects likelihood analysis (REL; Kosakovsky Pond and Frost, 2005; Posterior Probability > 0.99 for both residues), and residue β57 using mixed-effects model of episodic diversifying selection analysis (MEME; Murrell et al., 2012; P = 0.002; Table I.2).

If some alleles indeed associated with increased resistance to Bd in *L. v. alpina*, we should also have observed signs of selection pressure on this locus in wild *L. v. alpina* exposed to this pathogen. We sampled 30 individuals from the 3 sites used as source populations for the infection experiment, and genotyped them for the MHC class IIβ1 domain and 9 microsatellite markers. We found that genetic variation among populations (measured as F_{ST}) was significantly higher at the MHC class II locus than the microsatellite loci when considering data from the three populations (F_{ST} = 0.147, Posterior Probability > 0.99, Supplementary Information Table I.3), confirming that directional selection is affecting the MHC class II locus (Bernatchez and Landry, 2003).

I.2.5.5 P9 pocket residues as adaptive markers of Bd resistance in amphibians

Several lines of evidence thus point to the selection for properties of the MHC class II molecule P9 pocket that may confer resistance to chytridiomycosis in worldwide amphibians. We have demonstrated that protective alleles are undergoing positive selection after Bd enters naïve amphibian populations. Results of some studies suggest that levels of MHC heterozygosity may be more important than specific alleles for disease resistance (Bernatchez and Landry, 2003; Savage and Zamudio, 2011). The variation at the P9 pocket residues in amphibian populations long-exposed to Bd is consistent with this view. Still, we identified many MHCIIβ1 alleles with the resistance-associated P9 residue composition, with high level of heterozygosity among individuals with those alleles. Amphibian populations with high levels of MHC heterozygosity and high frequencies of resistance-associated alleles should be

more likely to recover from Bd infection. The results of our infection experiment support this idea, although the high mortality observed during exposure even in individuals with advantageous P9 pocket conformation suggests that other mechanisms are involved.

Presence in the P9 pocket of an acidic Aspβ57 associated with a Proβ56/Valβ56, an aromatic β37, and an aromatic/hydrophobic β60 residue seems to confer a selective advantage on amphibian populations infected by Bd by binding Bd peptides or activating a more efficient immune response. The importance of β9, another P9 peptide binding residue, could not be thoroughly explored because this position was missing in many sequences of worldwide amphibians we gathered. The limited results obtained suggest that this residue may have more variable biochemical properties compared with other residues within the pocket 9.

Our results demonstrate that the residue β56 may be of special importance for efficient Bd antigen binding, probably because of its conformational role within P9. The association of this residue with resistance to Bd is supported by a previous *R. yavapaiensis* infection study (Savage and Zamudio, 2011). Residue Proβ56 seemed more advantageous for all species included in this study, whereas Valβ56 was selected in *R. yavapaiensis*. The exact composition of the P9 pocket peptide binding residues associated with Bd resistance may vary depending on host, Bd strain, and environmental characteristics. However, our data include a wide variety of amphibians, Bd strains, and environmental contexts, and all converged in pointing to the P9 pocket peptide binding residues of the MHCIIβ1 as strong candidate adaptive markers of amphibian resistance against the pathogenic chytrid fungus.

The adaptive markers that we have identified may facilitate the identification of wild amphibian populations most susceptible to Bd. For those species now dependent on *ex situ* management for their very survival, selective breeding of Bd-resistant individuals may be possible and would make reintroduction strategies practical. The molecular bases of resistance may also be critical to the development of immunization strategies. But much remains to be learned before these actions become practicable.

For most species included in our study, we have compared MHC class IIβ1 sequences obtained from one specific locus. Yet the MHC complex of many amphibians consists of at least two class II loci (Kiemnec-Tyburczy et al., 2010; Zeisset and Beebee, 2013). The structure and role of those additional loci in conferring disease resistance need to be further studied. In addition, the capacity of Bd to produce factors inhibiting amphibian adaptive

immune response represents a major issue for any mitigation strategy based on adaptive immunity (Fites et al., 2013) that needs to be further elucidated.

Many studies have shown the importance of innate and adaptive immune defense mechanisms against Bd (McMahon et al., 2014; Rollins-Smith et al., 2011; Woodhams et al., 2011), but this is the first time that susceptibility to chytridiomycosis could be associated with the selection for specific immunogenetic traits across a wide variety of amphibians. Rescuing amphibian biodiversity will depend on our understanding of amphibian innate and adaptive immune defense mechanisms against Bd. The identification of adaptive markers for Bd resistance is an important step forward towards that goal.

I.2.6 Methods

I.2.6.1 Experimental infection

Alpine tree frogs (*Litoria verreauxii alpina*) were collected as 15 clutches from three similar but geographically separate populations in Kosciuszko National Park, New South Wales, Australia, in 2010. Two of the three populations have been long exposed to the pathogen (Site A, Kiandra, 35°52.335'S 148°29.994'E; Site B, Ogilvies Creek, 36°2.175'S 148°19.327'E), and a third had never been infected by Bd (Site C, Grey Mare Range, 36°19.010'S 148°15.567'E). Frogs were reared in Bd-free quarantine conditions to adulthood. Frogs were confirmed negative to Bd (via qPCR, see below) prior to the commencement of the exposure experiment.

A subset of 200 adults was randomly chosen from each clutch and population, and assigned to treatments that were inoculated with 750,000 infective Bd zoospores (strain AbercrombieNP-L.booroolongensis-09-LB-P7). As a control, 56 frogs were sham-infected with Bd-free culture medium in dilute salts solution. The experimental design, involving the utilization of frogs from each population and clutch together with details of the blind randomized block design used for allocation of treatment groups, is outlined in Table I.6. Numbers of frogs available for utilization were subject to actual clutch sizes and natural attrition during growth and development.

Frogs were maintained in a quarantine room at temperatures between 18 and 20°C under a 12:12 LD regimen. Subjects were housed individually in small plastic tubs on an angled rack with drainage holes, a loose pebble floor, and a gauze-covered top. They were fed twice

weekly with vitamin-dusted (calcium and herptivite alternately) crickets, and tubs were cleaned daily by flushing with fresh filtered water.

Subjects were monitored daily for clinical signs of infection (dullness, lethargy, peripheral erythema and increased skin shedding). Bd infection intensity data (in zoospore equivalents, ZSE) were collected weekly by swabbing each time with fresh gloves and a new sterile dry swab (MW100; Medical Wire and Equipment, Corsham, UK) for each subject. We subsequently analyzed swabs for Bd by qPCR (Hyatt et al., 2007). The experiment was terminated after three months. Frogs showing marked clinical signs of chytridiomycosis were euthanized throughout the experiment using tricaine methanesulfonate (MS-222). Immediately prior to euthanasia, frogs were swabbed to confirm infection status and to quantify Bd infection intensity (by qPCR as above). Foot or toe-clip samples for MHC analysis were collected post-mortem soon after euthanasia of individual frogs and placed into 90% ethanol.

Frog husbandry and experimental work was covered under permits issued by the Taronga Conservation Society and James Cook University ethics committees (4c/01/10).

I.2.6.2 Sample collection

In South Korea, we collected toe-clip samples from wild-caught Asiatic toads (*Bufo gargarizans*) in Geumsan (36°8.249'N 127°22.876E) and Jeonju (35°47.241'N 127°8.348E), and from wild-caught oriental fire-bellied toads (*Bombina orientalis*) in Chuncheon (37°58.664'N 127°36.146'E) and Chiaksan (37°23.676'N 128°03.221'E) under permits issued by the local Korean government authorities (Table I.4). We selected toe-clip samples preserved in ethanol from 100 alpine tree frogs (*L. v. alpina*) that we had infected with Bd. This selection included the only 6 individuals that survived the experiment and 94 individuals encompassing all the clutches collected from the three populations (Table I.3). In addition, to study MHC genetic variation in natural populations, toe-clip samples were collected from 30 wild *L. v. alpina* individuals in each of the three sites used for the infection experiment under permits issued by the New South Wales Government and Australian National University.

I.2.6.3 Isolation and characterization of MHC class II β1 domain

We collected fresh road-kills of *B. orientalis* and dissected out liver tissue which we kept at -80 °C for subsequent RNA extraction. RNA was extracted from liver samples using RNeasy kit (Qiagen) following the manufacturer's instructions. We also obtained liver samples from

10 *L. v. alpina* subjects that did not survive the experiment and were preserved in RNAlater for subsequent RNA extraction.

RNA was used to synthesize complementary DNA (cDNA) by reverse transcription reaction using ProtoScript® AMV First Strand cDNA Synthesis Kit (New England BioLabs). The cDNA was used to amplify expressed MHC class II β1 alleles of *L. v. alpina* and *B. orientalis* by PCR using exonic primers BC6F and BobomSR (May and Beebee, 2009), and BobomMHCIIEXON2F2 and BobomEXON2R1 (Hauswaldt et al., 2007), respectively. The resulting sequences were used to design primers to recover locus-specific intronic sequences flanking the MHC class II β1 domain using a genome walking technique (Cottage et al., 2001) for *L. v. alpina* and an inverse PCR protocol (Ochman et al., 1988) for *B. orientalis*. The 5' intronic sequence of one MHCII β1 locus was obtained for *L. v. alpina* (GenBank accession number KJ679286) and the 3' intronic sequence was isolated for *B. orientalis* (GenBank accession number KJ679287). Using these sequences, we designed intronic primers (MHC-LVAintF1 and MHC-BOintR) that we used in combination with exonic reverse primer BobomSR (for *L. v. alpina*) and newly designed forward primer MHC-BOexF (for *B. orientalis*) to amplify by PCR locus-specific MHC class II β1 alleles for both species. Full details of primer sequences and PCR protocols are given in Table I.7.

I.2.6.4 MHCIIβ1 isolation, genotyping and structure characterization

DNA was extracted from toe clips using a salting-out extraction method with ammonium acetate (Aljanabi and Martinez, 1997). We used locus-specific primers to genotype *L. v. alpina*, *B. gargarizans*, and *B. orientalis* samples at the β1 domain of one MHC class II locus. Full details of primer sequences and PCR protocols are given in Table I.7. All PCR products were purified and sent for sequencing to the National Instrumentation Center for Environmental Management (NICEM, Seoul National University, South Korea). MHCII β1 amplicons were purified and cloned using the RBC A&T cloning kit and accompanying HIT-DH5alpha competent cells (RC001 and RH617, RBC Bioscience) following the manufacturer's protocol.

Between 8 and 20 clones were amplified and sequenced using M13 primers. Allelic identity was confirmed when the corresponding DNA sequence was found in at least two clones. Only one or two alleles were recovered from any of our samples, confirming that our primers targeted one single MHC class II locus in all species. Sequences obtained were aligned with publicly available MHCII β1 sequences of other amphibians (complete list in Supplementary

Information Fig. I.5, GenBank accession numbers KJ679288-KJ679331) using Clustal W (Thompson et al., 1994), and translated into amino acids using BioEdit (Hall, 1999). The three-dimensional structure of the MHCII β1 domain was predicted by homology modeling using the SWISS-MODEL beta server (Bordoli et al., 2009). The template model (HLA Class II histocompatibility antigen DRB1-15 beta chain, PDB entry: 2wbj.1.B) was selected from the SWISS-MODEL Repository (Kopp and Schwede, 2006) using BLAST (Altschul et al., 1997). The modeled structures were visualized with the UCSF Chimera package v1.8.1 (Pettersen et al., 2004), developed by the Resource for Biocomputing, Visualization, and Informatics at the University of California, San Francisco.

I.2.6.5 Microsatellite markers isolation and data analysis

A *L. v. alpina* partial genomic DNA library generating by 454-Roche pyrosequencing (unpublished data) was mined for tandem repeat regions using MSATCOMMANDER (Faircloth, 2008). Primers were designed for 20 potential microsatellite markers, of which 7 gave single, scorable, polymorphic bands. In addition, we tested the cross-amplification of microsatellite markers isolated from the *Litoria ewingii* complex (Smith et al., 2011) on *L. v. alpina*, and identified 2 markers (Le2 and Le4) that amplified well.

The panel of 9 microsatellite markers was organized in two fluorescently-labeled multiplexes, and multiplex PCR were performed with Qiagen multiplex PCR Master Mix following the method described in Table I.7 (Kenta et al., 2008). Details of microsatellite primers, GenBank accession numbers, and PCR protocols are given in Table I.8. Allele sizes were assigned using an ABI3730 DNA Analyzer at NICEM (Seoul National University, South Korea) and Peak Scanner v.1.0 (Applied Biosystems). Conformity to Hardy–Weinberg equilibrium and linkage disequilibrium was determined with GENEPOP 4.0 (Rousset, 2008). Heterozygosity values and frequency of null alleles were estimated by CERVUS (Kalinowski et al., 2007).

Frequency of null alleles was high (F > 0.100) for four markers (*Livea*-GT1, *Livea*-AG3, Le2, and Le4) in the three populations genotyped, so we generated a new genotyping data set corrected for null alleles using FreeNA (Chapuis and Estoup, 2007). Subsequent analyses were run both with the 5-markers data set and the full 9-markers data set corrected for null alleles.

I.2.6.6 Survival statistical analysis

We used Cox proportional hazard models (Cox, 1972) to identify variables that affected the chance of survival of *L. v. alpina* during the experiment (*7*). Parameters included as variables in the initial model were site of origin, clutch, maximum Bd infection load, mass at start of experiment, mass at end of experiment, mass difference, MHC heterozygosity, P9 pocket residue composition, and the interaction between maximum infection load and the other parameters. We used likelihood ratio tests to calculate the predictive power of each variable. Independent variables that did not show a significant association with length of survival were excluded from the model. The model that best fit the data included P9 pocket residue composition, the clutch and the site of origin, and the interaction between P9 composition and the maximum Bd infection load (LRT=45.37, df = 10, $P < 0.0001$). Analyses were performed using the package 'survival' in the statistical platform R v3.0.2.

I.2.6.7 Detection of selection pressure

Genetic variation among populations (F_{ST}) at MHC and microsatellite markers was calculated and compared to simulated expected F_{ST} values using Fdist (Beaumont and Nichols, 1996) implemented in Lositan (Antao et al., 2008). Markers with F_{ST} values significantly higher than the simulated distribution (posterior probability > 0.95) were considered to be under positive selection. Analyses were done on the full data set including the three populations, and on pairs of populations, to identify population-specific differences in selection pressure.

Selection pressure on the MHCII β1 domain of *L. v. alpina*, *Bufo* spp., and *Bombina* spp. was investigated by estimating the ratio of non-synonymous to synonymous nucleotide substitutions using multiple methods available on the Datamonkey website (Delport et al., 2010). First, we confirmed the absence of recombination in our sequences using single breakpoint recombination (SBR) and genetic algorithms for recombination detection (GARD) approaches (Kosakovsky Pond et al., 2006). We used the partitioning approach for robust inference of selection (PARRIS) (Scheffler et al., 2006) to estimate the ratio of non-synonymous to synonymous nucleotide substitutions (ω = dNu/dS; positive selection: $\omega > 1$) across the MHCII β1 sequence alignments and identify the selection model best fitting our data. Positively selected sites were detected using single likelihood ancestor counting (SLAC)**,** fixed effects likelihood (FEL), random effects likelihood analysis (REL) (Kosakovsky Pond and Frost, 2005), and mixed effects model of episodic diversifying selection (MEME) (Murrell et al., 2012).

I.2.7 Acknowledgments

Martin Flajnik provided helpful comments to improve the manuscript. This study was conducted with approval by the Taronga Conservation Society Australia Animal Ethics Committee (4c/01/10). The research was supported by the National Research Foundation of Korea (NRF), funded by the government of the Republic of Korea (MSIP) (grants 2010-0002767, 2012R1A1A2044449 and 2012K1A2B1A03000496 to B.W.), by Seoul National University (Brain Fusion Program, Brain Korea 21 Program, and New Faculty Resettlement Fund grants to B.W.), and by the Australian Biosecurity CRC for Emerging Infectious Diseases and the Australian Research Council (grants FT100100375, LP110200240 and DP120100811 to L.S. and L.B). Thanks to Rick Speare and Rebecca Spindler for advice and support. All data reported in this study are presented in the main text and the supplementary material. DNA sequences are archived in GenBank and genotyping data in Dryad.

Figure I.1. Alignment of the β1 domain of the MHC class II in amphibians illustrating peptide binding residues.

Each sequence in the alignment represents a consensus sequence grouping alleles isolated in a species, or subgroup within species. Susceptibility of each was determined by experimental infections or field observation of Bd-associated population declines. Positions encoding amino acids similar to Bd-resistant *L. v. alpina* are represented by a dot. Variable positions in consensus sequences are represented by the most frequent amino acid in the group (lower-case letters). Dashes indicate missing data. Peptide binding residues are highlighted in colors, as indicated, to indicate their association with pockets of the MHC peptide binding groove. Species groups and their abbreviations: Bd-resistant *Litoria verreauxii alpina* (*Livea*-R), Bd-susceptible *L. v. alpina* (*Livea*-S), *Bufo gargarizans* (*Buga*), *Bombina orientalis* (*Boor*), *Bombina bombina* (*Bobo*), *Bombina variegate* (*Bova*), *Bombina pachypus* (*Bopa*), *Bufo bufo* (*Bubu*), *Bufo* [*Epidalea*] *calamita* (*Buca*), *Rana [Lithobates] yavapaiensis* (*Raya*), *R. catesbeiana* (*Raca*), susceptibles *Rana* spp. (s*Rana*) including *R. clamitans*, *R. pipiens*, *R. sylvatica*, *R. warszewitschii*, and *Rana temporaria*, *Alytes obstetricans* (*Alob*), *Xenopus laevis* (*Xela*), *Andrias davidianus* (*Anda*), *Ambystoma mexicanum* and *tigrinum* (*Anme/Amti*). *Raya*-Q, allele from *R yavapaiensis* associated with *Bd* resistance. The complete alignment with all MHCIIβ1 included in the study is presented in the supplementary materials.

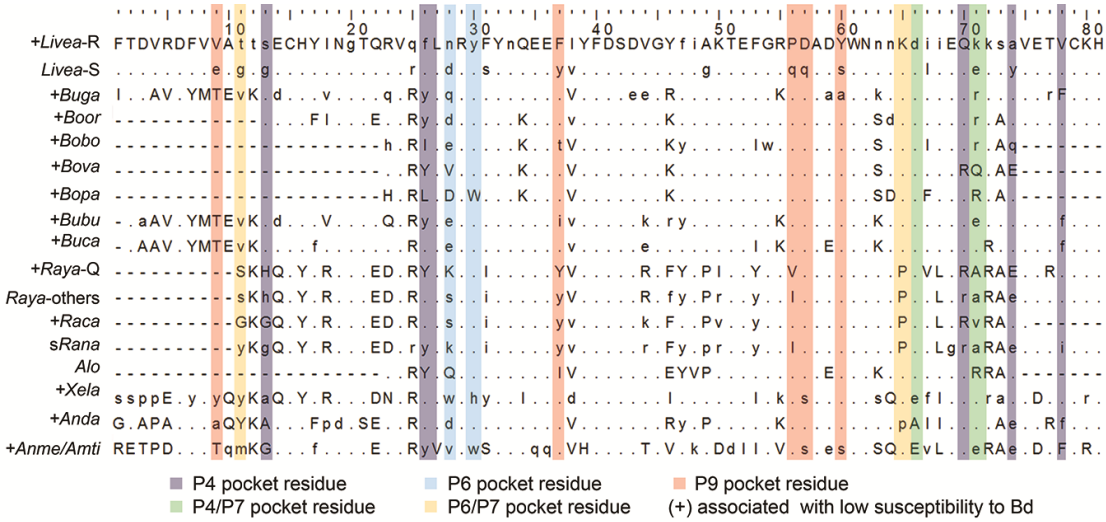

Figure I.2. Homology modeling of MHC class II β1 domain allele *Buga-1*.

Display of the typical three-dimensional structure of the vertebrate MHC class II β1 domain, with α-helices represented as red helical ribbons and β-sheets as purple thick arrows. The peptide binding residues of the P9 pocket are indicated, with atomic structure for residues 56β and 57β.

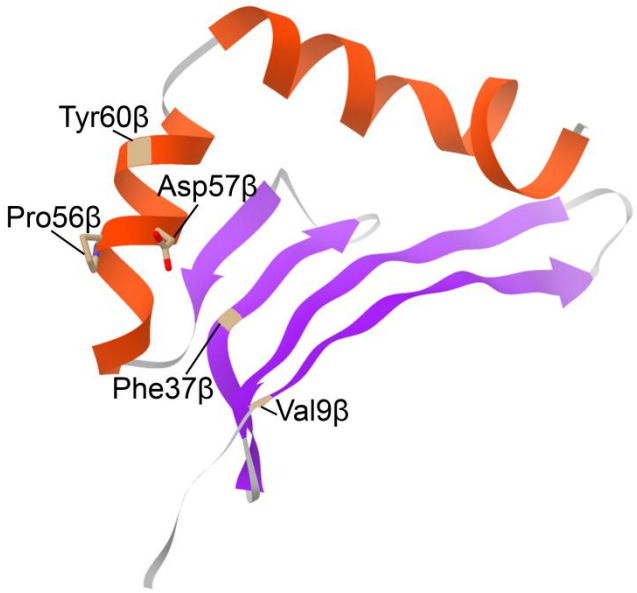

Figure I.3. Experimental infection of *L. v. alpina* frogs from populations with varied Bd infection histories.

(A) Survival curves for captive-reared frogs from two historically infected sites (sites A and B) and an uninfected site C in Kosciuszko National Park, Australia, experimentally infected with a virulent Bd culture. (B) Mean infection intensity as a function of time since Bd inoculation for those subjects that survived 5 weeks or less, 8 weeks, or through the duration of the 12-week experiment. These results include the weekly swabs from up to 30 frogs from each site, selected by stratified random sampling based on days survived. Infection intensity is given in log-transformed zoospore equivalents (ZSE). Error bars represent 95% confidence intervals.

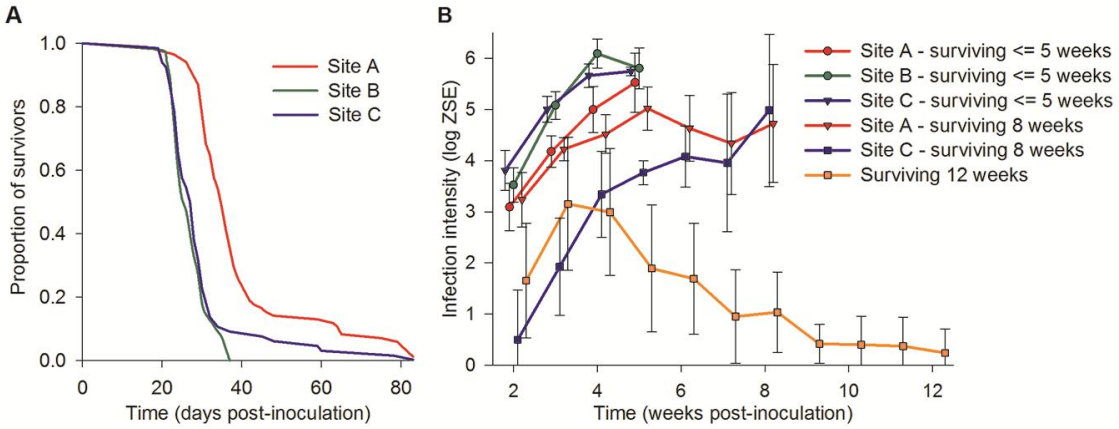

Figure I.4. Association of the MHC class II β1 domain with survival to Bd in *L. v. alpina.* (A) Frequency of MHC class II β1 alleles (*Livea*) in subjects that survived (red) and succumbed (blue) to experimental infection by Bd, indicating alleles encoding the specific P9 pocket residue Val9β-Phe37β-Pro56β-Asp57β-Tyr60β; Frequency of individuals with two (2/2), one (1/2), or no (0/2) MHCII β1 alleles with the specific P9 residue composition. (B) Survival curves for individuals during the course of the Bd infection experiment with respect to the presence of the specific P9 pocket residue composition in two (2/2), one (1/2), or none (0/2) of their two MHCIIβ1 domains.

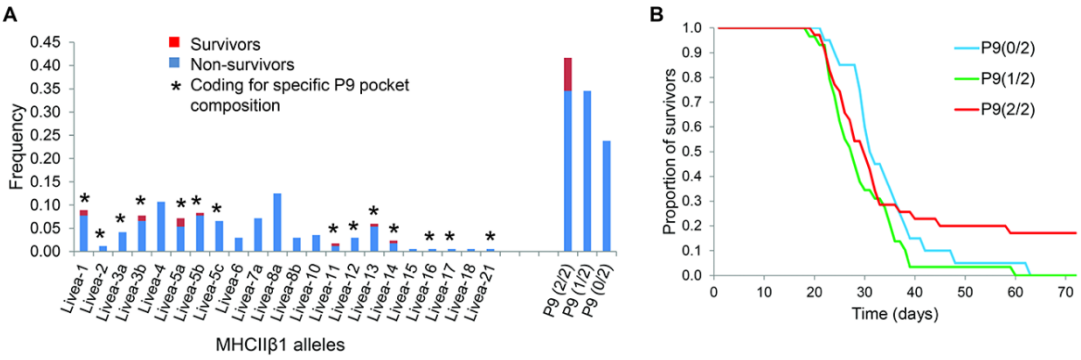

Table I.1. Amino acid residues of the P9 pocket of the MHC class II peptide binding groove associated with resistance to infection by *Batrachochytrium dendrobatidis* (Bd).

MHC Class IIβ1 alleles	9β	37β	56β	57β	60β
Worldwide amphibians					
Buga 1-8	Thr	Ile/Leu/**Phe**	Pro	**Asp**/Ser	**Ala**/Tyr
Boor 1-7	-	**Phe**/Tyr/Thr	Pro	**Asp**/Glu	Asp/Ser/**Tyr**
Bombina spp.	-	Phe	Pro	**Asp**/Glu/ser	Tyr
Bufo locus B	Thr	Ile/Leu/**Phe**/Tyr	Pro	Ala/**Asp**/Ser/Val	Ala/**Tyr**
Rana spp.	-	Leu/Phe/**Tyr**	Leu/Pro/Val	Asn/**Asp**	Ser/**Tyr**
Raya-Q	-	Tyr	Val	Asp	Tyr
Alob	-	Ile	Pro	Asp	Tyr
Anda	**Ala**/Thr	Ile/**Phe**	**Pro**/Thr	**Asp**/Thr	Tyr
Xela	Tyr/Phe	Ile/Leu/**Thr**/Tyr	Pro/Val	**Asp**/Asn/His	Tyr
***Livea* Bd infection experiment**					
Livea survivors	Val	Phe	Pro	Asp	Tyr
Livea non-survivors	Glu/Asp	Asn/Asp/Tyr	Cys/Gln/Ser/Tyr	Asp/Gln/Thr	**Ser**/Tyr

Buga, *Bufo gargarizans* MHC class II locus B alleles; *Boor*, locus-specific *Bombina orientalis* alleles; *Bombina* spp., locus non-specific alleles from *Bombina bombina*, *B. variegata*, and *B. pachypus*; *Bufo*, orthologous MHC class II locus B alleles isolated from *Bufo bufo* and *B.* [*Epidalea*] *calamita*; *Rana [Lithobates]* spp., alleles from *R. yavapaiensis*, *R. catesbeiana*, *R. clamitans*, *R. pipiens*, *R. sylvatica*, *R. warszewitschii*, *Alytes obstetricans* (*Alob*), Xenopus *laevis* (*Xela*), *Andrias davidianus* (*Anda*), *Ambystoma mexicanum* and *tigrinum* (*Anme/Amti*) ; *Raya*-Q, allele from *R yavapaiensis* associated with *Bd* resistance; *Livea*, *Litoria verreauxii alpina* individuals experimentally infected by Bd. Residues most frequent (frequency > 0.5) among alleles within each species are in bold.

Table I.2. Evidence of positive and purifying selection among potential peptide binding residues of amphibian MHC class II β1 domain.

Method	Pocket 4	Pocket 6	Pocket 4/7	Pocket 6/7	Pocket 9
Bufo					
SLAC			67β*		*(-)37β***
			71β*		*(-)56β**
REL	13β**	11β**	67β**	30β**	57β**
	26β**	66β**	71β**		60β**
	74β**				*(-)37β**
	78β**				*(-)56β***
FEL	13β*	11β**	67β**	28β**	57β**
	26β*	66β*	71β*	30β*	*(-)37β**
	74β*				*(-)56β***
MEME	13β**	11β**	67β*	28β*	57β**
	74β**		71β*		60β**
Bombina					
SLAC	*(-)26β**				
REL	*(-)26β**		67β*		37β**
					57β*
					60β*
FEL	*(-)26β**				37β*
MEME			67β*		37β**
			71β*		57β*
Xenopus					
REL			67β**		37β**
			71β*		
MEME			71β*		57β**
Ambystoma					
REL	13β**	11β**	67β**	28β**	37β**
	26β**		71β**	30β**	57β**
	74β**				
	78β**				
MEME	13β*		71β*		57β*
Rana					
SLAC					56β**
REL	26β**			28β**	37β**
				30β**	56β**
FEL	26β*			28β*	56β**
MEME	26β*			28β*	56β*
				30β*	
Anda					
REL	78β**	11β**	67β**	28β**	57β**
			71β**		
Livea					
REL	13β**	11β**	67β**	28β**	37β**

		66β**			57β**
FEL	13β*	11β*	67β*		
MEME	13β*	11β*	67β*	28β*	57β**

Bufo, orthologous MHC classII locus B alleles isolated from *Bufo bufo*, *B. calamita*, and *B. gargarizans; Bombina*, locus non-specific alleles from *Bombina bombina, B. variegata*, and *B. pachypus*; *Xenopus*, MHCIIβ1 alleles isolated from *Xenopus laevis; Anda*, *Andrias davidianus*; *Ambystoma*, *A. mexicanum* and *A. tigrinum; Rana*, *R. yavapaiensis*, *R. catesbeiana*, *R. clamitans*, *R. pipiens*, *R. sylvatica*, *R. warszewitschii*, *R. temporaria; Livea*, *Litoria verreauxii alpina* individuals experimentally infected by *Bd*; MHCIIβ1 alleles isolated from SLAC, single likelihood ancestor counting; REL, random-effects likelihood; FEL, fixed-effects likelihood; MEME, mixed-effects model of episodic diversifying selection; (*) 0.05> P > 0.01, posterior probability > 0.95 (for REL analysis); (**) P < 0.01, posterior probability > 0.99 (for REL analysis). All residues listed were identified as being under positive selection, except residues in italic and preceded by a negative sign.

I.2.8 Supplementary Information

This section contains additional supporting figures and tables to supplement the data presented in the main text.

Figure I.5. Alignment of the β1 domain of the MHC class II in amphibians illustrating peptide binding residues.

Species represented include *Litoria verreauxii alpina* (Livea), *Bufo gargarizans* (Buga), *Bombina orientalis* (Boor), *Bombina bombina* (Bobo), *Bombina variegate* (Bova), *Bombina pachypus* (Bopa), *Bufo bufo* (Bubu), *Bufo* [*Epidalea*] *calamita* (Buca), *Rana* [*Lithobates*] *yavapaiensis* (Raya), *R. catesbeiana* (Raca), *R. clamitans* (Racl), *R. pipiens* (Rapi), *R. sylvatica* (Rasy), *R. warszewitschii* (Rawa), *Alytes obstetricans* (*Alob*), *Xenopus laevis* (*Xela*), *Andrias davidianus* (*Anda*), *Ambystoma mexicanum* and *tigrinum* (*Anme/Amti*). GenBank accession numbers are indicated for each sequence beside the name of the allele. *Livea* alleles in bold were associated with individuals surviving Bd infection. *Livea* alleles in italics were isolated from wild animals only. Peptide binding residues are classified according to their association with specific pockets of the binding groove: P4 (#), P4/P7 ($), P6 (^), P6/P7 (+), and P9 (*).

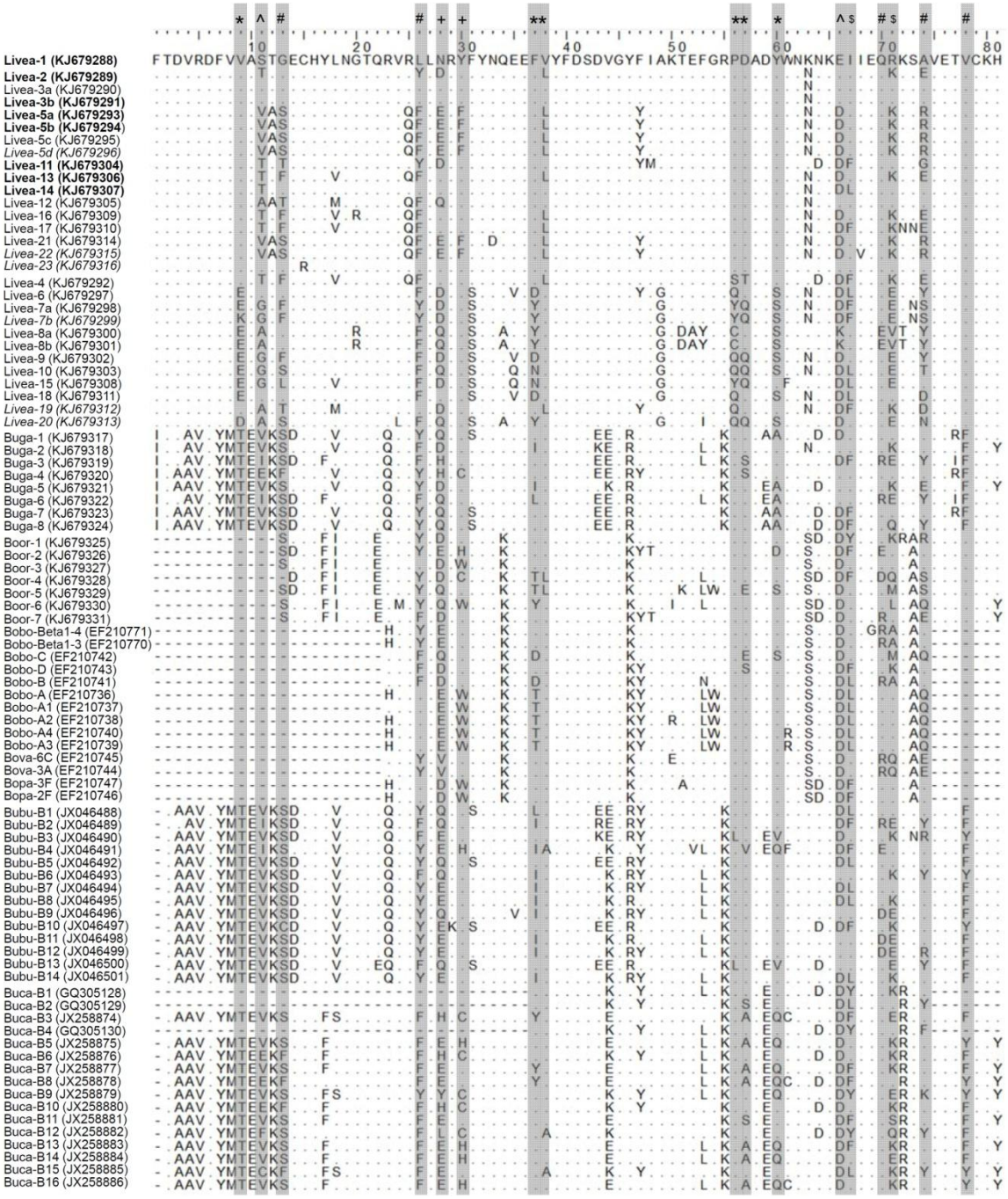
Livea-1 (KJ679288)
Livea-2 (KJ679289)
Livea-3a (KJ679290)
Livea-3b (KJ679291)
Livea-5a (KJ679293)
Livea-5b (KJ679294)
Livea-5c (KJ679295)
Livea-5d (KJ679296)
Livea-11 (KJ679304)
Livea-13 (KJ679306)
Livea-14 (KJ679307)
Livea-12 (KJ679305)
Livea-16 (KJ679309)
Livea-17 (KJ679310)
Livea-21 (KJ679314)
Livea-22 (KJ679315)
Livea-23 (KJ679316)
Livea-4 (KJ679292)
Livea-6 (KJ679297)
Livea-7a (KJ679298)
Livea-7b (KJ679299)
Livea-8a (KJ679300)
Livea-8b (KJ679301)
Livea-9 (KJ679302)
Livea-10 (KJ679303)
Livea-15 (KJ679308)
Livea-18 (KJ679311)
Livea-19 (KJ679312)
Livea-20 (KJ679313)
Buga-1 (KJ679317)
Buga-2 (KJ679318)
Buga-3 (KJ679319)
Buga-4 (KJ679320)
Buga-5 (KJ679321)
Buga-6 (KJ679322)
Buga-7 (KJ679323)
Buga-8 (KJ679324)
Boor-1 (KJ679325)
Boor-2 (KJ679326)
Boor-3 (KJ679327)
Boor-4 (KJ679328)
Boor-5 (KJ679329)
Boor-6 (KJ679330)
Boor-7 (KJ679331)
Bobo-Beta1-4 (EF210771)
Bobo-Beta1-3 (EF210770)
Bobo-C (EF210742)
Bobo-D (EF210743)
Bobo-B (EF210741)
Bobo-A (EF210736)
Bobo-A1 (EF210737)
Bobo-A2 (EF210738)
Bobo-A4 (EF210740)
Bobo-A3 (EF210739)
Bova-6C (EF210745)
Bova-3A (EF210744)
Bopa-3F (EF210747)
Bopa-2F (EF210746)
Bubu-B1 (JX046488)
Bubu-B2 (JX046489)
Bubu-B3 (JX046490)
Bubu-B4 (JX046491)
Bubu-B5 (JX046492)
Bubu-B6 (JX046493)
Bubu-B7 (JX046494)
Bubu-B8 (JX046495)
Bubu-B9 (JX046496)
Bubu-B10 (JX046497)
Bubu-B11 (JX046498)
Bubu-B12 (JX046499)
Bubu-B13 (JX046500)
Bubu-B14 (JX046501)
Buca-B1 (GQ305128)
Buca-B2 (GQ305129)
Buca-B3 (JX258874)
Buca-B4 (GQ305130)
Buca-B5 (JX258875)
Buca-B6 (JX258876)
Buca-B7 (JX258877)
Buca-B8 (JX258878)
Buca-B9 (JX258879)
Buca-B10 (JX258880)
Buca-B11 (JX258881)
Buca-B12 (JX258882)
Buca-B13 (JX258883)
Buca-B14 (JX258884)
Buca-B15 (JX258885)
Buca-B16 (JX258886)

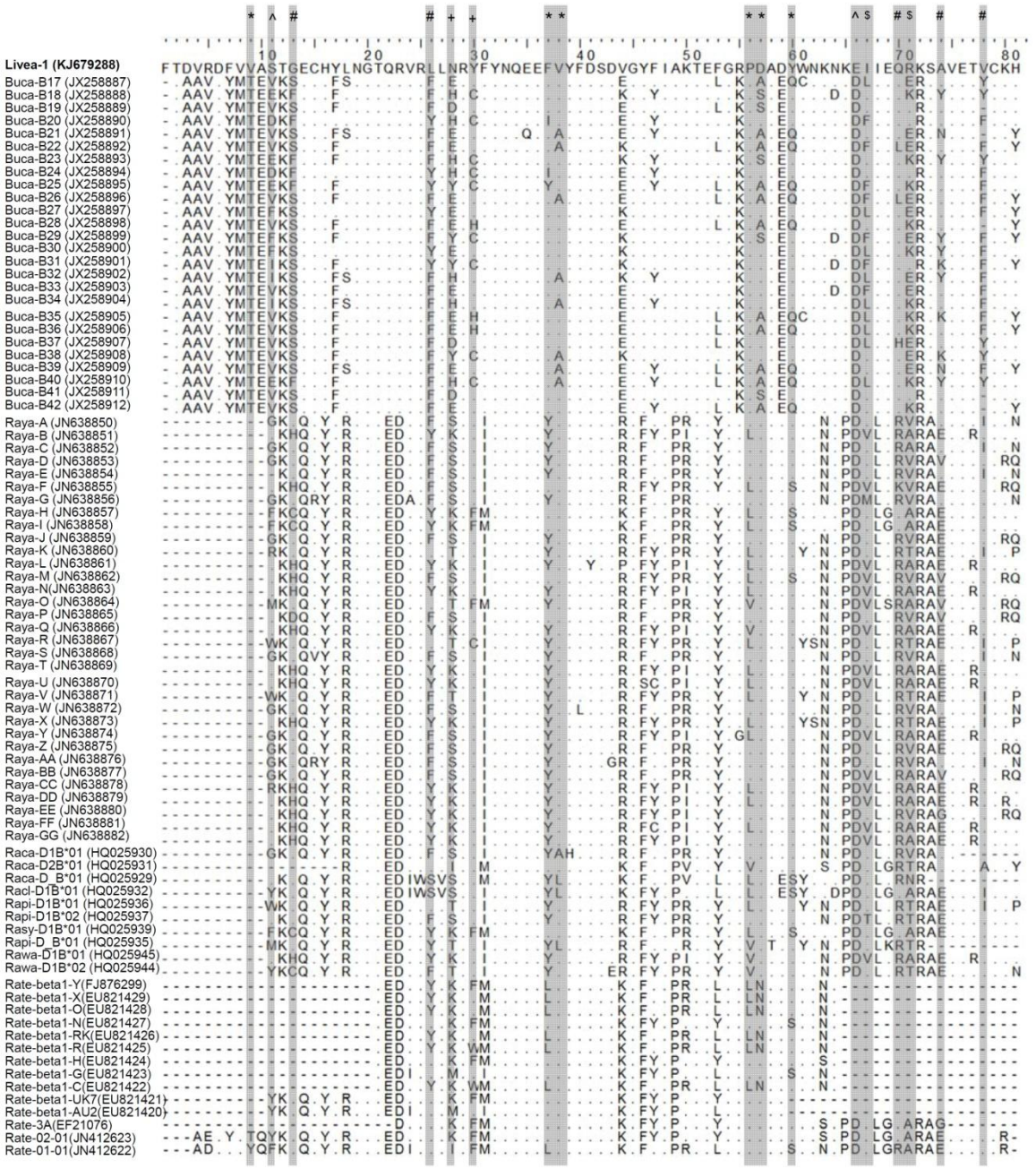
Livea-1 (KJ679288)
Buca-B17 (JX258887)
Buca-B18 (JX258888)
Buca-B19 (JX258889)
Buca-B20 (JX258890)
Buca-B21 (JX258891)
Buca-B22 (JX258892)
Buca-B23 (JX258893)
Buca-B24 (JX258894)
Buca-B25 (JX258895)
Buca-B26 (JX258896)
Buca-B27 (JX258897)
Buca-B28 (JX258898)
Buca-B29 (JX258899)
Buca-B30 (JX258900)
Buca-B31 (JX258901)
Buca-B32 (JX258902)
Buca-B33 (JX258903)
Buca-B34 (JX258904)
Buca-B35 (JX258905)
Buca-B36 (JX258906)
Buca-B37 (JX258907)
Buca-B38 (JX258908)
Buca-B39 (JX258909)
Buca-B40 (JX258910)
Buca-B41 (JX258911)
Buca-B42 (JX258912)
Raya-A (JN638850)
Raya-B (JN638851)
Raya-C (JN638852)
Raya-D (JN638853)
Raya-E (JN638854)
Raya-F (JN638855)
Raya-G (JN638856)
Raya-H (JN638857)
Raya-I (JN638858)
Raya-J (JN638859)
Raya-K (JN638860)
Raya-L (JN638861)
Raya-M (JN638862)
Raya-N(JN638863)
Raya-O (JN638864)
Raya-P (JN638865)
Raya-Q (JN638866)
Raya-R (JN638867)
Raya-S (JN638868)
Raya-T (JN638869)
Raya-U (JN638870)
Raya-V (JN638871)
Raya-W (JN638872)
Raya-X (JN638873)
Raya-Y (JN638874)
Raya-Z (JN638875)
Raya-AA (JN638876)
Raya-BB (JN638877)
Raya-CC (JN638878)
Raya-DD (JN638879)
Raya-EE (JN638880)
Raya-FF (JN638881)
Raya-GG (JN638882)
Raca-D1B*01 (HQ025930)
Raca-D2B*01 (HQ025931)
Raca-D_B*01 (HQ025929)
Racl-D1B*01 (HQ025932)
Rapi-D1B*01 (HQ025936)
Rapi-D1B*02 (HQ025937)
Rasy-D1B*01 (HQ025939)
Rapi-D_B*01 (HQ025935)
Rawa-D1B*01 (HQ025945)
Rawa-D1B*02 (HQ025944)
Rate-beta1-Y(FJ876299)
Rate-beta1-X(EU821429)
Rate-beta1-O(EU821428)
Rate-beta1-N(EU821427)
Rate-beta1-RK(EU821426)
Rate-beta1-R(EU821425)
Rate-beta1-H(EU821424)
Rate-beta1-G(EU821423)
Rate-beta1-C(EU821422)
Rate-beta1-UK7(EU821421)
Rate-beta1-AU2(EU821420)
Rate-3A(EF21076)
Rate-02-01(JN412623)
Rate-01-01(JN412622)

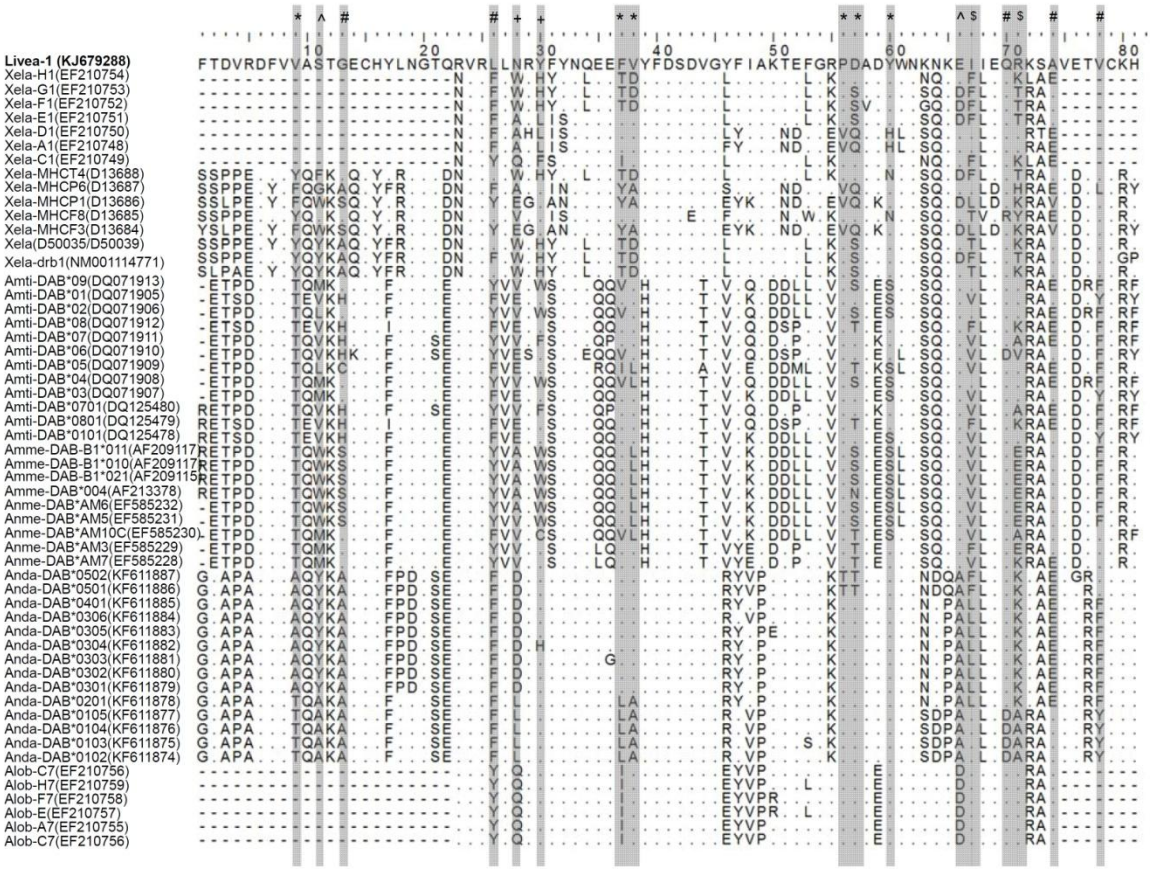
Livea-1 (KJ679288)
Xela-H1(EF210754)
Xela-G1(EF210753)
Xela-F1(EF210752)
Xela-E1(EF210751)
Xela-D1(EF210750)
Xela-A1(EF210748)
Xela-C1(EF210749)
Xela-MHCT4(D13688)
Xela-MHCP6(D13687)
Xela-MHCP1(D13686)
Xela-MHCF8(D13685)
Xela-MHCF3(D13684)
Xela(D50035/D50039)
Xela-drb1(NM001114771)
Amti-DAB*09(DQ071913)
Amti-DAB*01(DQ071905)
Amti-DAB*02(DQ071906)
Amti-DAB*08(DQ071912)
Amti-DAB*07(DQ071911)
Amti-DAB*06(DQ071910)
Amti-DAB*05(DQ071909)
Amti-DAB*04(DQ071908)
Amti-DAB*03(DQ071907)
Amti-DAB*0701(DQ125480)
Amti-DAB*0801(DQ125479)
Amti-DAB*0101(DQ125478)
Amme-DAB-B1*011(AF209117)
Amme-DAB-B1*010(AF209117)
Amme-DAB-B1*021(AF209115)
Amme-DAB*004(AF213378)
Anme-DAB*AM6(EF585232)
Anme-DAB*AM5(EF585231)
Anme-DAB*AM10C(EF585230)
Anme-DAB*AM3(EF585229)
Anme-DAB*AM7(EF585228)
Anda-DAB*0502(KF611887)
Anda-DAB*0501(KF611886)
Anda-DAB*0401(KF611885)
Anda-DAB*0306(KF611884)
Anda-DAB*0305(KF611883)
Anda-DAB*0304(KF611882)
Anda-DAB*0303(KF611881)
Anda-DAB*0302(KF611880)
Anda-DAB*0301(KF611879)
Anda-DAB*0201(KF611878)
Anda-DAB*0105(KF611877)
Anda-DAB*0104(KF611876)
Anda-DAB*0103(KF611875)
Anda-DAB*0102(KF611874)
Alob-C7(EF210756)
Alob-H7(EF210759)
Alob-F7(EF210758)
Alob-E(EF210757)
Alob-A7(EF210755)
Alob-C7(EF210756)

Figure I.6. Importance of Pro56β in model vertebrate organisms.

Frequency of the residue proline at codon 56 in MHC class II beta1 alleles in model vertebrate organisms. Alleles were compared using EMBL IPD-MHC databases, except for (*) chicken, mouse, and rat, for which alleles were obtained from GenBank.

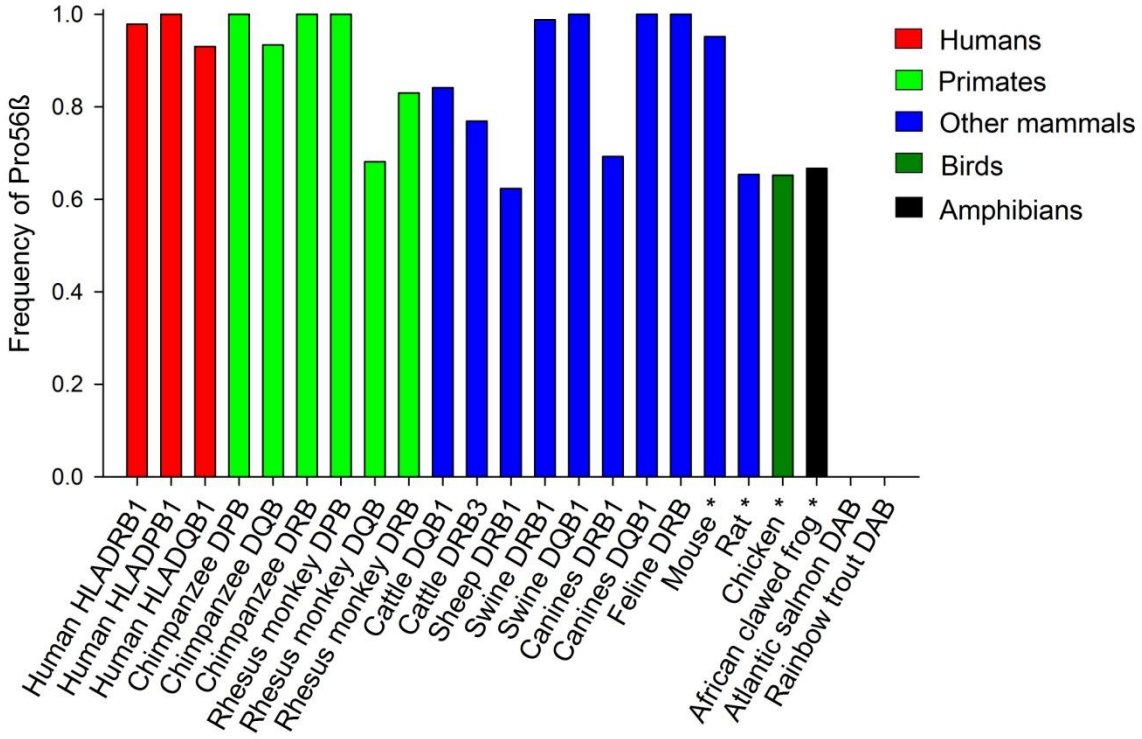

Table I.3. List of *Litoria verreauxii alpina* individuals from Bd infection experiment genotyped at the β1 domain of one MHC class II locus.

ID	Site	Clutch	Tank	Start Mass (g)	End Mass (g)	Mass Diff (g)	SVL (mm)	Max Inf (ZSE)	Sex	Survived	Survival Time (days)	P9+ Het	MHC IIβ1 Allele1	MHC IIβ1 Allele2
9	A	C	1	2.61	3.11	-0.5	30.8	112736	f	Yes	72	2/2 ho	5a	5a
12	A	C	1	2.79	2.04	0.75	29	350862	m	No	40	2/2 ho	5a	5a
30	A	D	2	7.58	5.56	2.02	38.2	787576	f	No	39	1/2 he	5b	8b
36	A	A	1	3.72	3.69	0.03	33.5	116102	f	No	31	0/2 ho	8a	8a
67	A	A	2	5.53	5.69	-0.16	36.1	76648	f	No	28	1/2 he	21	10
74	A	D	4	6.17	4.93	1.24	35.4	3285076	f	No	26	2/2 ho	14	14
100	A	C	4	2.3	2.62	-0.32	29	37471	m	No	31	2/2 ho	5a	5a
109	A	C	1	3.44	2.94	0.5	31.6	5612799	f	No	30	0/2 he	4	8a
118	A	B	2	4.18	3.54	0.64	34.3	36534	f	No	45	2/2 he	1	14
148	A	B	4	3.17	3.49	-0.32	32.3	57519	f	No	34	1/2 he	7a	13
170	A	A	1	6.1	5.75	0.35	34	2431749	f	No	36	1/2 he	8a	11
187	A	D	1	3.19	2.66	0.53	29.3	127486	m	No	39	1/2 he	5b	8b
199	A	B	2	2.16	2.11	0.05	26.5	322260	m	No	29	0/2 he	7a	8a
210	A	C	4	4.33	3.29	1.04	34.5	1665650	f	No	35	0/2 he	7a	8a
215	A	C	2	2.37	2.46	-0.09	28.7	577810	f	No	35	1/2 he	5a	8a
249	A	D	2	5.66	4.58	1.08	33.6	1264450	f	No	30	2/2 ho	5b	5b
260	A	B	3	3.26	2.75	0.51	29.8	18517	m	No	30	0/2 he	7a	8a
277	A	D	1	5.17	4.99	0.18	34.2	2463656	f	No	26	1/2 he	5b	8b
297	A	C	1	2.63	2.78	-0.15	27.8	184012	f	No	38	0/2 he	7a	8a
300	A	B	1	2.47	2.18	0.29	28.4	187494	f	No	38	1/2 he	5a	8a
330	A	B	1	3.81	3.74	0.07	30.9	663235	m	No	32	0/2 he	6	15
336	A	C	2	6.41	7.3	-0.89	33.5	664218	f	No	31	0/2 he	7a	8a
341	A	C	2	4.07	4.11	-0.04	30.7	447596	f	No	30	0/2 he	7a	8a
352	A	D	1	4.36	3.19	1.17	35	929209	f	No	33	2/2 ho	5b	5b
354	A	A	2	4.73	4.28	0.45	35.1	147473	f	No	48	0/2 he	6	7a
368	A	B	4	5.25	3.95	1.3	35.5	2149610	f	No	42	0/2 he	7a	8a
372	A	B	2	3.6	3.28	0.32	30.1	3228	f	Yes	72	2/2 he	1	13
383	A	C	4	2.76	2.32	0.44	28.4	712933	m	No	63	0/2 he	7a	8a
385	A	A	1	4.79	4.27	0.52	31.3	51733	m	No	23	1/2 he	2	7a
387	A	A	3	4.53	4.55	-0.02	33.9	529909	f	No	39	0/2 he	6	7a
394	A	A	3	4.59	3.91	0.68	32.8	8582	f	Yes	72	2/2 he	5b	11
397	A	D	1	2.41	3.25	-0.84	26.6	44137	f	Yes	72	2/2 he	2	14
400	A	A	3	3.67	3.49	0.18	29.9	853	m	Yes	72	2/2 he	3b	5a
2	B	C	1	2.2	2.25	-0.05	27.2	412545	m	No	36	0/2 ho	4	4
17	B	B	4	3.87	3.63	0.24	29.7	855307	m	No	22	0/2 he	8a	18
18	B	A	1	3.43	2.97	0.46	31.1	399523	m	No	28	1/2 he	3b	4
20	B	C	1	1.61	1.31	0.3	23.8	1163310	m	No	29	1/2 he	3a	4
45	B	B	3	4.5	4.23	0.27	33.4	828342	f	No	24	2/2 he	5c	12
47	B	B	1	3.46	3.8	-0.34	30.9	1241178	f	No	21	1/2 he	8a	12
72	B	C	1	4.49	4.22	0.27	34.6	492805	f	No	37	0/2 ho	4	4
89	B	A	1	2.1	1.81	-0.29	25.8	366371	m	No	23	1/2 he	4	5a
106	B	C	1	2.79	2.02	-0.77	28.1	387068	m	No	35	1/2 he	3a	4
120	B	A	3	2.51	2.18	-0.33	27.8	640914	m	No	29	0/2 ho	10	10

129	B	B	3	4.66	3.61	-1.05	33.1	830377	f	No	30	2/2	he	5b	12
136	B	A	1	2.17	1.33	-0.84	26.2	380071	m	No	32	1/2	he	3b	10
151	B	C	1	3.64	3.65	0.01	30.3	620529	f	No	28	2/2	ho	3a	3a
196	B	B	3	3.85	4.43	0.58	31.5	562288	f	No	23	2/2	ho	5b	5b
227	B	C	1	1.57	1.58	0.01	24.6	1413768	f	No	25	2/2	ho	3a	3a
248	B	B	4	5.42	4.72	-0.7	34.5	5970139	f	No	26	1/2	he	8a	13
258	B	A	3	3.81	3.28	-0.53	31.6	2291061	f	No	25	1/2	he	4	5a
261	B	B	2	4.91	3.77	-1.14	32	2512094	f	No	36	1/2	he	4	12
263	B	A	3	3	3.14	0.14	29.9	277552	m	No	23	1/2	he	4	5a
281	B	B	2	3.59	3.36	-0.23	29	2815366	m	No	26	2/2	he	5b	12
295	B	A	3	1.78	1.69	-0.09	27.2	1992837	m	No	23	1/2	he	3b	4
324	B	A	1	3.61	3.8	0.19	33.5	800314	f	No	24	1/2	he	3b	10
331	B	A	3	3.43	3.21	-0.22	30.7	829177	f	No	23	1/2	he	3b	10
333	B	C	1	3.54	3.13	-0.41	32.1	733436	f	No	34	0/2	ho	4	5a
335	B	B	1	2.78	2.5	-0.28	27.4	1387106	m	No	27	1/2	he	5b	4
339	B	A	1	4.01	3.27	-0.74	29.5	1947171	m	No	25	0/2	he	4	10
350	B	C	1	3.36	3.33	-0.03	29.8	552079	f	No	24	0/2	he	4	12
19	C	B	4	3.38	3.26	0.12	31	460153	f	No	25	1/2	he	5c	10
23	C	D	1	3.74	4	-0.26	29.4	1152590	m	No	25	1/2	he	1	3a
25	C	B	3	3.91	4.6	-0.69	31.6	45778	f	No	20	2/2	he	5c	5b
35	C	C	1	5.27	3.89	1.38	35.5	1289907	f	No	27	2/2	ho	1	3a
52	C	B	1	3.53	3.75	-0.22	32.2	538548	m	No	32	2/2	he	5c	13
53	C	C	3	3.84	3.65	0.19	33.2	2162675	m	No	28	2/2	he	1	5a
54	C	A	1	3.68	3.45	0.23	30.1	675129	m	No	26	2/2	he	1	12
96	C	A	1	5.81	5.78	0.03	33.9	67862	f	No	28	2/2	he	1	5a
111	C	C	2	3.49	2.88	0.61	30.9	489031	m	No	59	2/2	he	1	12
126	C	B	1	4.59	4.18	0.41	34.8	1838958	f	No	22	2/2	ho	13	4
131	C	A	1	3.28	2.82	0.46	28.1	6179549	m	No	23	2/2	ho	5c	10
154	C	B	4	4.84	5.2	-0.36	35.7	554706	f	No	31	2/2	ho	13	10
216	C	C	2	3.57	3.46	0.11	31	551506	m	No	60	1/2	he	3b	4
219	C	A	1	4.93	3.95	0.98	33.2	967513	f	No	24	2/2	ho	5c	6
222	C	D	1	7.05	6.24	0.81	37.8	1161688	f	No	24	1/2	he	5c	8a
225	C	C	3	3.64	3.41	0.23	32.7	652888	m	No	23	2/2	ho	3b	6
226	C	C	1	3.39	3.67	-0.28	31.2	584615	m	No	22	2/2	he	1	8b
230	C	A	1	4.83	3.4	1.43	32.6	316548	NA	No	29	1/2	he	3a	8a
239	C	C	2	3.58	3.83	-0.25	31.9	27	m	Yes	72	2/2	he	1	13
287	C	C	3	6.17	4.97	1.2	39.2	609344	f	No	33	2/2	ho	1	1
290	C	C	2	5.64	5.04	0.6	37.4	2531427	f	No	37	2/2	ho	1	13
344	C	B	3	4.29	4.41	-0.12	32.6	707072	f	No	32	2/2	he	13	3b
366	C	D	1	3.88	5.42	-1.54	30.6	329202	m	No	19	1/2	he	5b	5c
403	C	D	1	4.04	3.58	0.46	30.5	13660	m	No	32	2/2	he	11	5c

ID, frog individual number; Site, sampling site; Start Mass, mass at day=0 of experiment; End Mass, mass at death of day=72 of experiment; Mass Diff, difference in mass between day=0 and day=72; SVL, snout-vent length; Max Inf, maximum Bd infection load during the course of infection in zoospore genomic equivalent; Sex, m= male, f= female; P9, presence of 1 (1/2) or 2 (2/2) alleles with the residue composition at the pocket 9 of the peptide-binding groove of MHC IIβ1 associated with increased resistance to Bd; Het, heterozygosity, he= heterozygote, ho= homozygote.

Table I.4. Detection of loci under positive selection in pairs of *L. v. alpina* populations.

	All sites			Site A-B			Site A-C			Site B-C		
Locus	Het	Fst	*PP*	Het	Fst	*PP*	Het	Fst	*PP*	Het	Fst	*PP*
LVmGT1	0.90	0.06	0.39	0.91	0.06	0.63	0.91	0.07	0.60	0.87	0.05	0.44
LVmAG1a	0.68	0.04	0.28	0.73	0.04	0.49	0.66	0.01	0.27	0.67	0.07	0.68
LVmAG1b	0.78	0.02	0.03	0.81	0.02	0.28	0.79	0.03	0.29	0.74	0.00	0.04
LVmAG3	**0.96**	**0.32**	**1.00**	**0.93**	**0.28**	**1.00**	**0.99**	**0.33**	**1.00**	**0.96**	**0.34**	**1.00**
Le2	0.91	0.09	0.71	0.88	0.05	0.51	0.90	0.08	0.71	0.95	0.14	0.96
LVmAC4	0.77	0.08	0.52	0.77	0.09	0.78	0.75	0.06	0.52	0.78	0.08	0.69
LVmAG4	0.49	0.09	0.66	0.55	0.15	0.85	0.57	0.07	0.61	0.34	0.02	0.43
LVmCCT1	**0.40**	**0.26**	**0.97**	0.13	-0.01	0.18	0.54	0.27	0.97	**0.53**	**0.31**	**0.99**
Le4	0.87	0.13	0.90	0.87	0.14	0.95	0.89	0.16	0.94	0.84	0.10	0.78
MHCIIβ1	**0.96**	**0.15**	**0.99**	**0.94**	**0.16**	**0.99**	**0.98**	**0.19**	**1.00**	0.94	0.09	0.85

	All sites			Site A-B			Site A-C			Site B-C		
Locus	Het	Fst	*PP*	Het	Fst	*PP*	Het	Fst	*PP*	Het	Fst	*PP*
AG1a	0.68	0.04	0.36	0.73	0.04	0.54	0.66	0.01	0.31	0.67	0.07	0.73
AG1b	0.76	0.01	0.06	0.79	0.02	0.34	0.77	0.02	0.30	0.71	0.00	0.12
AC4	0.73	0.10	0.75	0.74	0.12	0.89	0.70	0.08	0.73	0.74	0.09	0.79
AG4	0.49	0.09	0.73	0.55	0.15	0.89	0.57	0.07	0.63	0.34	0.02	0.47
CCT1	**0.40**	**0.26**	**0.98**	0.13	-0.01	0.16	0.54	0.27	0.97	**0.53**	**0.31**	**0.99**
MHCIIβ1	**0.95**	**0.16**	**1.00**	**0.94**	**0.17**	**0.99**	**0.98**	**0.20**	**1.00**	0.94	0.11	0.94

Genetic variation among populations (F_{ST}) at MHC and microsatellite markers was calculated and compared to simulated expected F_{ST} values using Fdist implemented in Lositan. In the first section, microsatellite markers corrected for null alleles are included. In the second section, analysis was done only with loci with frequency of null alleles < 0.1. Markers with F_{ST} values significantly higher than the simulated distribution (*PP* > 0.95) were considered to be under positive selection (rows in bold). Het; expected heterozygosity.

Table I.5. Genotyping results at β1 domain of MHC classII locus B of *Bufo gargarizans* and of one MHC class II locus of *Bombina orientalis.*

ID	Site	Sampling date	MHCIIb1 allele1	MHCIIb1 allele 2
Bufo gargarizans				
BG143	Jeonju	3/5/2012	2	3
BG144	Jeonju	3/5/2012	1	3
BG145	Jeonju	3/5/2012	3	6
BG168	Jeonju	3/8/2012	1	3
BG169	Jeonju	3/8/2012	2	3
BG172	Jeonju	3/9/2012	3	5
BG173	Jeonju	3/9/2012	1	3
BG194	Jeonju	3/11/2012	3	6
BG195	Jeonju	3/11/2012	1	5
BG196	Jeonju	3/11/2012	3	3
BG197	Jeonju	3/11/2012	6	6
BG198	Jeonju	3/11/2012	1	3
BG199	Jeonju	3/11/2012	2	6
BG200	Jeonju	3/11/2012	2	3
BG201	Jeonju	3/11/2012	1	3
BG202	Jeonju	3/11/2012	5	6
BG203	Jeonju	3/11/2012	3	6
BG204	Jeonju	3/11/2012	1	4
BG205	Jeonju	3/11/2012	1	2
BG206	Jeonju	3/11/2012	1	2
BG208	Jeonju	3/11/2012	3	6
BG209	Jeonju	3/11/2012	3	3
BG210	Jeonju	3/11/2012	2	3
BG211	Jeonju	3/11/2012	1	1
BG212	Jeonju	3/11/2012	3	5
BG213	Jeonju	3/11/2012	6	6
BG214	Jeonju	3/11/2012	7	7
BG215	Jeonju	3/11/2012	1	6
BG217	Jeonju	3/11/2012	2	3
BG218	Jeonju	3/11/2012	2	3
BG229	Geunsam	3/17/2012	1	5
BG230	Geunsam	3/17/2012	1	1
BG244	Geunsam	3/17/2012	4	5
BG245	Geunsam	3/17/2012	1	3
BG246	Geunsam	3/17/2012	5	5
BG247	Geunsam	3/17/2012	1	8
BG249	Geunsam	3/17/2012	1	3
BG251	Geunsam	3/20/2012	1	4
BG252	Geunsam	3/20/2012	1	3
BG253	Geunsam	3/20/2012	1	1
BG257	Geunsam	3/20/2012	3	5
BG258	Geunsam	3/20/2012	1	2
BG259	Geunsam	3/20/2012	1	2

BG260	Geunsam	3/20/2012	1	5
BG261	Geunsam	3/20/2012	4	5
BG262	Geunsam	3/20/2012	3	3
BG263	Geunsam	3/20/2012	3	3
BG264	Geunsam	3/20/2012	3	4
BG272	Geunsam	3/20/2012	1	1
BG273	Geunsam	3/20/2012	1	1
BG275	Geunsam	3/20/2012	1	4
BG276	Geunsam	3/20/2012	1	1
BG277	Geunsam	3/20/2012	2	4
BG278	Geunsam	3/20/2012	1	1
BG279	Geunsam	3/20/2012	1	1
BG280	Geunsam	3/20/2012	3	4
BG281	Geunsam	3/20/2012	1	3
BG282	Geunsam	3/20/2012	1	3
BG284	Geunsam	3/20/2012	3	4
BG285	Geunsam	3/20/2012	3	3
Bombina orientalis				
BO060	Chuncheon	7/1/2011	1	2
BO061	Chuncheon	7/1/2011	6	2
BO064	Chuncheon	7/1/2011	3	1
BO065	Chuncheon	7/1/2011	2	2
BO066	Chuncheon	7/1/2011	3	1
BO067	Chuncheon	7/1/2011	7	1
BO068	Chuncheon	7/1/2011	3	3
BO069	Chuncheon	7/1/2011	1	1
BO070	Chuncheon	7/1/2011	4	1
BO071	Chuncheon	7/1/2011	1	1
BO272	Chiak	9/30/2011	3	3
BO273	Chiak	9/30/2011	3	3
BO274	Chiak	9/30/2011	1	2
BO275	Chiak	9/30/2011	3	3
BO276	Chiak	9/30/2011	2	1
BO277	Chiak	9/30/2011	3	1
BO278	Chiak	9/30/2011	3	1
BO279	Chiak	9/30/2011	5	2
BO280	Chiak	9/30/2011	3	1
BO281	Chiak	9/30/2011	3	3

Allele numbers correspond to *Buga*- and *Boor*- allele numbers in Supplementary Information Figure I.5.

Table I.6. Experimental design.

Numbers of *L. v. alpina* frogs from each population and clutch, and details of blind randomized block design used for allocation of treatment groups (exposed frogs versus sham-exposed negative control frogs).

Population (total number frogs)[a]	Clutch (total number frogs)[a]	Exposure group[b]	Total number of frogs	Number of males[g]	Number of females[g]	Number with undetermined gender
Grey Mare (80)	A (14)	E	14	7	6	1
		C	0	0	0	0
	B (26)	E	20	10	10	0
		C	6	3	3	0
	C (29)	E	20	11	9	0
		C	9	6	3	0
	D (11)	E	11	9	2	0
		C	0	0	0	0
Kiandra (100)	A (25)	E	20	9	11	0
		C	5	1	4	0
	B (25)	E	20	12	8	0
		C	5	1	4	0
	C (25)	E	20[d]	8	10	2
		C	5	3	2	0
	D (25)	E	20	11	9	0
		C	5	1	4	0
Ogilvies (76)	A (19)	E	19	13	6	0
		C	0	0	0	0
	B (40)	E	20	7	13	0
		C	20	6	14	0
	C (17)	E	16	9	7	0
		C	1[e]	0	0	1
Total	256		E (200) C (56)[f]	127	125	4

[a]Total number of frogs in parentheses for each group; [b]E represents exposed frogs, C represents control frogs; [c]Includes one frog died pre-exposure and was excluded from further analyses; [d]This number includes the frog that died of anasarca post-exposure, unrelated to chytridiomycosis; [e]This frog died pre-exposure and was excluded from analyses; [f]Total frogs grouped by exposure (E) and control (C); [g]Gender as determined by post-mortem coelomic examination.

Table I.7. List of primers and PCR protocols used for MHC isolation and genotyping.

Primer	sequence (5'-3')	Target	Reference	Conc (uM)	PCR cycling protocol
Litoria verreauxii alpina					
BCF6	CATTGTACAATCAGGAGGAG	MHCII exon2	May and Beebee, 2009	0.4	(94C for 40 sec, 54C for 40 sec, 72C for 1mi n)x35
bobomSR	CCATAGTTGTGTTTACAGACTGTTTCCAC	MHCII exon2	May and Beebee, 2009	0.4	
ADAPL	CTAATACGACTCACTATAGGGCTCGAGCGGC CGCCCGGGCAGGT	genome walking-adaptor	Cottage et al., 2001		
ADPS	P-ACCTGCCC	genome walking-adaptor	Cottage et al., 2001		
AP1	GGATCCTAATACGACTCACTATAGGGC	genome walking-1stPCR	Cottage et al., 2001	0.2	(94C for 30 sec, 60C for 30 sec, 72C for 2 min)x35
LvaWP3	CTGTTCTATGATATCCTTATTGTTGT	genome walking-1stPCR-3'direction	this study	0.2	
LvaWP5	TATTTCATAGCGAAGACCGAGT	genome walking-1stPCR-5'direction	this study	0.2	
NAP1	TATAGGGCTCGAGCGGC	genome walking-2ndPCR	Cottage et al., 2001	0.2	(94C for 30 sec, 60C for 30 sec, 72C for 2 min)x35*
LvaNWP3	CGCTGTCAAAGTAAAGAAACTC	genome walking-2ndPCR-3'direction	this study	0.2	
LvaNWP5	GAAACAGTCTGTAAACACAACTAT	genome walking-2ndPCR-5'direction	this study	0.2	
MHC-LVAintF1	GCTCTGGTCAGGGGAAATATT	Locus-specific MHCIIb1	this study	0.4	(94C for 30 sec, 58C for 30 sec, 72C for 1 min)x35
Bombina orientalis					
BobomMHCIIEXON2F2	CTGASTGTCACTTTATAAACGGCACTGA	MHCII exon2	Hauswaldt et al., 2007	0.4	(94C for 40 sec, 50C for 40 sec, 72C for 1 min)x35
BobomMHCIIEXON2R1	CCATAGTTGTRTTTACAGACTGTTTCCAC	MHCII exon2	Hauswaldt et al., 2007	0.4	

BOinvF	ACAGTRATAAGGACWWCATAGAG	inverse PCR	this study	0.2	(94C for 30 sec, 52C for 30 sec, 72C for 2 min)x35
BOinvR	ACCRACATCACTGTCAAAGT	inverse PCR	this study	0.2	
MHC-BOexF	TTTGACAGTGATGTYGGTAAAT	Locus-specific MHCIIb1	this study	0.2	(94C for 30 sec, 52C for 30 sec, 72C for 40 sec)x35
MHC-BOintR	GAAGGGTCATATAATGATATAGT	Locus-specific MHCIIb1	this study	0.2	
Bufo gargarizans					
2F347	GTGACCCTCTGCTCTCCATT	MHC classIIb1 Locus B	May et al., 2011	0.2	(94C for 30 sec, 58C for 30 sec, 72C for 40 sec)x35
2R307b	ATAATTCAGTATATACAGGGTCTCACC	MHC classIIb1 Locus B	May et al., 2011	0.2	

All PCR was performed in 20 ul volumes with 1 ul of DNA, 0.2 mM of each dNTP and 0.5 unit of TaKaRa Ex Taq polymerase, and started with a denaturation step at 94C for 5min and ended with an elongation step at 72C for 10min. (*) Second PCR starts with PCR product from first PCR diluted 1:100

Table I.8. Characteristics of the 9 microsatellites markers used to genotype *Litoria verreauxii alpina* populations.

Locus name	Primer sequences (5'-3')	MP set	Ta	Repeat motif	Na	Allele size range (bp)	Freq NA	He	Ho	Accession number
LVmGT1	F: FAM-TAGACCGTATTTAACTAATGGGA	M1	52	(GT)9	14	166-192	0.150-0.342*	0.778-0.851	0.393-0.625	KJ679332
	R: ACGTTGAGCCTGATATCGC									
LVmAG1a	F: FAM-CTGCCCACTGCTCTGATAGTT	M1	52	(AG)9	6	212-226	(-)0.023-0.07	0.570-0.725	0.583-0.889	KJ679333
	R: GTGGGCGAAGACTAGCTGTT									
LVmAG1b	(same primers)	M1	52		9	227-247	0.059-0.098	0.695-0.812	0.600-0.692	KJ679333
LVmAG3	F: HEX-ACGTCACTTGTTGCTGGGAG	M1	52	(AG)8	9	236-266	0.039-0.700*	0.503-0.629	0.095-0.600	KJ679334
	R: TTCAAGCAAGAGCTTCGGCG									
LVmAG4	F: FAM-ATCCAGACTGACGCATGGCA	M2	55	(AG)6	7	357-373	(-)0.081-0.079	0.267-0.669	0.310-0.586	KJ679335
	R: AGAACCGTAAACCATTCAAGGC									
LVmAC4	F: HEX-CTGTAGTGACTGTAGGGTCATA	M2	55	(AC)10	7	218-232	0.047-0.068	0.620-0.693	0.591-0.621	KJ679336
	R: TGGTCTGTATCTTGGCCTGC									
LVmCCT1	F: FAM-CCGTGTGATTACTGGCTGCG	M2	55	(CCT)5	4	154-172	(-)0.03-0.014	0.100-0.625	0.103-0.615	KJ679337
	R:TGCCTGTCCTCTGACCATCC									
Le2*	F: HEX-TCTCCAGGACACAACACAGG	M1	52	(GT)11	10	189-208	0.063-0.273*	0.800-0.820	0.444-0.880	JF772865
	R: TTCCCTCTAGTGCCAACTGC									
Le4*	F: HEX-AATCCATCTCCGGGAATCTC	M2	55	(CA)11	6	155-169	0.062-0.269*	0.641-0.741	0.370-0.655	JF772868
	R: CTCGATCTTCGGTCTTGTGG									

MP set, multiplex set to each locus belongs; Ta, annealing temperature; Na, number of alleles; Freq NA, frequency of null alleles; He, expected heterozygosity; Ho, observed heterozygosity. Values encompass the three populations genotyped. (*) Loci with high frequency of null alleles (F > 0.100) also deviated from Hardy–Weinberg equilibrium. There was no linkage disequilibrium between loci.

Multiplex PCRs were performed in a 2-ul volume, containing approximately 10 ng of dried down DNA, 0.2–0.3 mM of each primer and 1 ml of QIAGEN Multiplex PCR Master Mix. The PCR program used was 95C for 15 min, followed by 35 cycles of 94C for 30 sec, Ta for 90 sec, 72C for 60 sec, and finally 60C for 30 min. (*) Loci isolated and described in[40]